SYNTHETIC OLIGOMERS WITH HETEROGENEOUS BACKBONES FEATURING α/β-CONJUGATED BUILDING BLOCKS

A THESIS TO BE SUBMITTED TO THE

UNIVERSITY OF PUNE

FOR THE DEGREE OF

DOCTOR OF PHILOSOPHY

(IN CHEMISTRY)

By

ROSHNA V.

Dr. G. J. SANJAYAN
Research Guide

DIVISION OF ORGANIC CHEMISTRY
NATIONAL CHEMICAL LABORATORY
PUNE 411008
INDIA

DECEMBER 2013

CERTIFICATE

Certified that the work incorporated in the thesis entitled **"*Synthetic Oligomers with Heterogeneous Backbones Featuring α/β-Conjugated Building Blocks*"**, submitted by **Ms. Roshna V.** for the Degree of **Doctor of Philosophy** was carried out by the candidate under my supervision in the Division of Organic Chemistry, National Chemical Laboratory, Pune, India. Materials obtained from other sources have been duly acknowledged in the thesis.

Date:

Place: Pune

Dr. G. J. Sanjayan

(Research Guide)

DECLARATION

I hereby declare that the thesis entitled **"*Synthetic Oligomers with Heterogeneous Backbones Featuring α/β-Conjugated Building Blocks*"**, submitted for the Degree of Doctor of Philosophy in Chemistry to the University of Pune, has not been submitted by me to any other university or institution. This work has been carried out at Division of Organic Chemistry, National Chemical Laboratory, Pune under the supervision of Dr. G. J. Sanjayan (Research guide).

Date:

Roshna V.
(Research student)
Division of Organic Chemistry
National Chemical Laboratory
Pune-411008

CONTENTS

SECTION II

Formation of Pseudo-β-hairpin Motif Utilizing Ant-Pro Reverse Turn

CHAPTER 2: *Conformational Pre-Disposition of -α/$β_n$- Oligomers*

SECTION I

Synthesis and Conformational Evaluation of Homo-chiral -(^{L}Pro-Ant-Ant)$_n$- Oligomers

SECTION II

(Thio)urea mediated benzoxazinone opening: Mild Approach Towards Synthesis of 2-(acylamido)benzamides

SECTION III

Conformational Predilection of Orthanilic Acid in Peptide Sequences

ABBREVIATIONS

A

Å	Angström
AA	Amino acid
Ac	Acyl
AcOH	Acetic acid
AcOEt	Ethyl acetate
Aib	α-amino isobutyric acid
Ala	Alanine
Anal.	Analysis
Ant	Anthranilic acid
Ani-Br	4-bromoaniline

B

β	beta
Boc	tert.- butyloxycarbonyl
Bn	Benzyl

C

Calcd	Calculated
$CDCl_3$	Chloroform-d
COSY	Correlated spectroscopy

D

d	doublet (NMR)
δ	Chemical shift (NMR)
DBU	1,8-Diazabicycloundec-7-ene
DCC	*N,N'*-dicyclohexylcarbodimide
DCM	Dichloromethane
DMF	Dimethyl formamide
DIPEA	Diisopropyl ethylamine
DMSO	Dimethylformamide
4-DMAP	4-dimethyl aminopyridine

E

ESI	Electron spray ionization
Et	Ethyl
EtOH	Ethanol

G

Gly	Glycine

H

H-bond	Hydrogen bond
HMBC	Hetero Multiple-Bond Correlation
HBTU	O-benzotriazol-1-yl-N,N, N',N'-tetramethyluronium hexafluorophosphate
HOBt	1-hydroxybenzotriazole
HSQC	Hetero Nuclear Single Quantum Coherence
Hz	Hertz

M

MALDI	Matrix-Assisted Laser Desorption Ionization
m	Multiplet (NMR)
Me	Methyl
MHz	Megahertz
mp	Melting point
MS	Mass Spectrometry

N

NMR	Nuclear Magnetic Resonanace
NOESY	Nuclear Overhauser and Exchange Spectroscopy

P

Piv	Pivaloyl
Pd/C	palladium 10 % on activated Carbon
$Pd(OH)_2$	Palladium hydroxide
Ph	Phenyl
Pro	Proline

S

s	Singlet (NMR)
^{S}Ant	2-aminobenzenesulfonic acid
SEM	Scanning Electon Microscopy

T

t	Triplet (NMR)
TFA	Trifluroacetic acid
TEA	Triethyl amine
THF	Tetrahydrofuran
TBAB	Tetrabutyl ammonium bromide
TOCSY	Total Correlation Spectroscopy
TOF	Time of Flight
Tyr	Tyrosine

ABSTRACT

Intricate arrangements of biopolymers lead to versatile processes to support and sustain life. Polypeptides/proteins form a major class of biopolymers, which participate in myriad of the cellular events like cellular signaling to catalysis, in addition to its role as chief structural units in biology. Understanding the origin and development of their sophisticated structural and functional aspects led to emergence of the research area called '*foldamers*'. In this connection, the dissertation entitled "***Synthetic Oligomers with Heterogeneous Backbones Featuring α/β-Conjugated Building Blocks***" attempts the design and creation of assorted assemblies featuring natural-unnatural α/β-conjugated (specifically aliphatic-aromatic) building blocks. The work undertaken herein, is oriented towards understanding the interplay of non-covalent interactions in governing the structural preferences of compact three-dimensional assemblies that emanate from the permutation and combination of these building blocks. The broad objective of the work is directed towards comprehending the folding behavior of biopolymers.

Section I of **Chapter 1** deals with investigations of the folding propensity of aliphatic-aromatic amino acid conjugate *Ant-Pro* motif (Pro = $^{L/D}$proline and Ant = anthranilic acid), which is known to exhibit a nine-membered hydrogen-bonding pattern. Significance of both the units has been assessed and was found to be equally crucial for the creation of the turn motif. Our next objective was to appraise the robustness of Ant-Pro motif as a reverse turn mimic. Hence, a number of structural modulations around the turn segment by altering chiralities of the amino acid residues were undertaken, using N- and C-terminal amidated peptides (Figure 1).

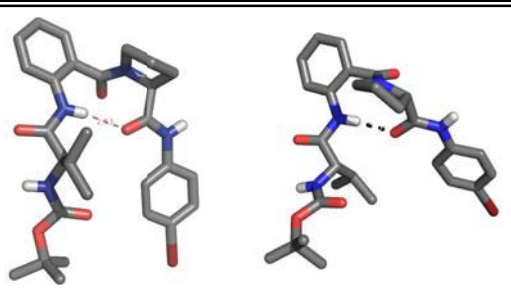

Figure 1. Crystal structures of Boc-^{D}Val-Ant-^{L}Pro-p(C_6H_4)Br (left) and Boc-^{L}Val-Ant-^{L}Pro-p(C_6H_4)Br (right) revealing stable reverse turn architecture. (Hydrogens have been removed for clarity).

In order to determine its sensitivity towards the structural perturbation, beta-branched amino acid like valine was substituted at N-terminal of the motif. Solid and solution state studies revealed the insensitivity of the turn segment towards structural and chirality modulation, establishing its potential as a robust reverse turn mimetic. This section also discusses the synthesis of Fmoc-Ant-Pro-OH scaffold meant for incorporation into peptides *via* solid phase, in order to facilitate rigidity of the bioactive peptide for enhanced proteolytic stability.

Section II of the chapter focuses on determination the *β*-hairpin nucleation propensity of the *Ant-Pro* motif. With the intention to establish the minimum criteria for *β*-hairpin formation, different "*α-β-α-α*" tetramer sequences were synthesized with alternating chirality comprising both natural (L) and unnatural (D) analogues of Val, Pro and Leu residues. Four sequences of R_1-$^{L/D}$Val-Ant-$^{L/D}$Pro-$^{L/D}$Leu-R_2 (R_1 = Piv and R_2 = NHMe) were designed *i.e.* LLL, DLL, LDL and DLD with varying chirality pattern at α-amino acids. Their folding propensities were explored using solid and extensive solution state studies. The studies revealed that *hetero*-chiral analogues with alternate chirality exhibits best hairpin nucleation tendency (Figure 2).

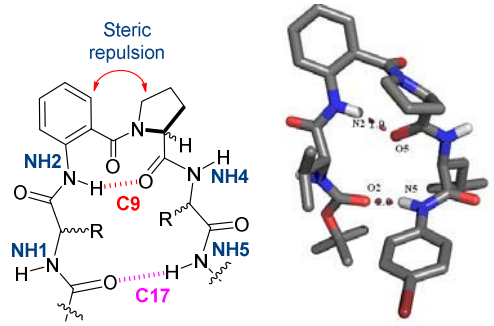

Figure 2. Schematic representation of *intramolecular* H-bonding pattern of the plausible *β*-hairpin featuring Ant-Pro reverse turn (left) and crystal structure of Boc-^{D}Val-Ant-^{L}Pro-^{L}Leu-p(C_6H_4)Br (right) (Hydrogens have been removed for clarity).

Chapter 2 *"Investigations of conformational pre-disposition of -α/β$_n$-oligomers (α = $^{L/D}$proline and β = anthranilic acid)"* is an attempt to investigate the effect of constitutional ratio variation of residues on the conformational disposition of the oligomers. **Section I** describes the effect of stoichiometric variation of α:β residues (α = Pro and β = anthranilic acid), from the structural studies of sequentially repeating *homo-* chiral and *hetero*-chiral -Pro-Ant-Ant-[α/β/β] units. Ant-Pro 1:1 sequential repeats are known to adopt a compact, rigid right-handed helical secondary structure displaying 1→2 forward turns. On the other hand, Ant-Ant repeats are well established sheet inducers due to the

hybridization induced planarity of the aromatic rings and constant amide dihedral angles (ω).

Also, the chirality of amino acids induces severe effects on the structure formulation. Structural studies revealed a helical disposition for the *homo*-chiral repeats R_1-($^{L}\alpha\beta_2)_n$-R_2 (n=2) (Figure 3a); whereas, the *hetero*-chiral R_1-($^{L}\alpha\beta_2{}^{D}\alpha\beta_2)_n$-$R_2$ (n=2) *i.e.* Piv-^{L}Pro-$(Ant)_2$-^{D}Pro-$(Ant)_2$-NHMe exhibited a unique zipper like folded architecture featuring a large inter-residual hydrogen bond spanning 26 atoms (Figure 3b).

In order to explore and establish the non-covalent forces responsible for the remote hydrogen-bond, further studies were undertaken. Thus, we synthesized and investigated structural characteristics of corresponding analogues of zipper motif devoid of hydrogen-bond donor and the acceptor sites. Solution-state NMR structure obtained for its corresponding *hetero*-chiral ester derivative Piv-^{L}Pro-$(Ant)_2$-^{D}Pro-$(Ant)_2$-OMe revealed that in the absence of donor atom at C-terminal, the termini fray apart. So was the result obtained for the pentapeptide Br-Aib-$(Ant)_2$-^{D}Pro-$(Ant)_2$-NHMe devoid of acceptor atom at N-terminus, where the solid-state structure revealed absence of folding. Solution state studies also vindicated fair amount of *edge-to-face* aromatic stacking effect between the aromatic rings. These observations led to an inference that the co-operative interplay of the non-covalent interactions namely H-bonding and aromatic stacking drive the assembly along with the stereochemical control.

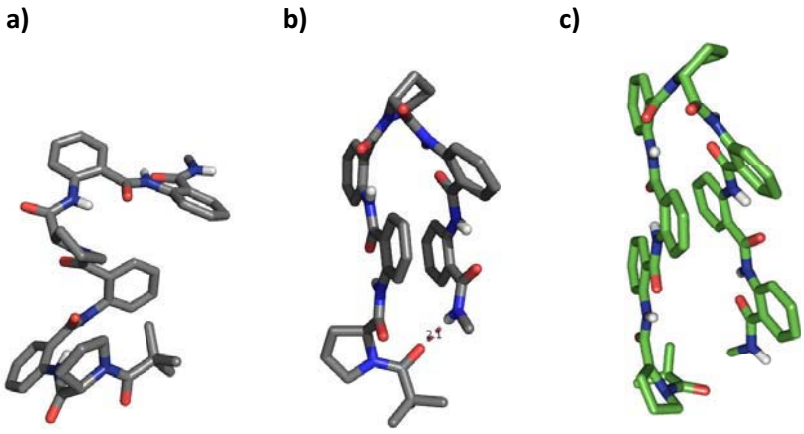

Figure 3. Crystal structures of *homo*-chiral analogue Piv-^{L}Pro-$(Ant)_2$-^{L}Pro-$(Ant)_2$-NHMe (a), *hetero*-chiral analogue Piv-^{L}Pro-$(Ant)_2$-^{D}Pro-$(Ant)_2$-NHMe (b) and PyMOL generated model of Piv-^{L}Pro-$(Ant)_3$-^{D}Pro-$(Ant)_3$-NHMe (c). (Hydrogens are removed for clarity).

To evaluate the effect of further constitutional variation of residues, oligomers featuring -Pro-Ant-Ant-Ant- [α/β/β/β] repeats were synthesized and their folding propensities were explored in **Section II** of the chapter. Solution-state studies substantiated the folded architecture even in the absence of remote H-bonding interaction, supporting the co-operative effect of the participating non-covalent forces (Figure 3c).

Chapter 3 discusses few instances where the local constraints of individual amino acids largely contribute towards the conformational bias of the peptides.

Section I describes the synthesis and investigations of oligomer based on -Aib-Ant-^{L}Pro- repeats. The motif was designed with the purpose to understand the influence of individual torsional preference of amino acid on the overall conformational disposition. Along these lines, we attempted to understand the structural influence of a constrained amino acid like Aib at the N-terminus of Ant-^{L}Pro motif and its repeats. Sequential repeat of -Aib-Ant-^{L}Pro- unit is anticipated to reveal one or more type of hydrogen-bonding patterns i.e. either C9- / C10-hydrogen bonding pattern or both concurrently by strategically placing the residues adjacent to each other. But, NMR studies of the hexamer derivatives posed serious challenges due to the poor solubility, possibly due to aggregation. However, the solution-state NMR studies of hexamer (Figure 4) indicated existence of multiple conformations, which can be attributed to exposed amide NHs associated *inter*-molecularly and/or absence of any specific *intra*-molecular hydrogen bonding network in the peptide motif.

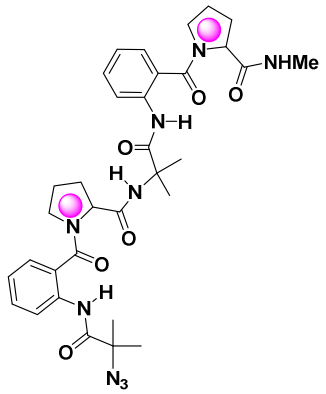

Figure 4. Molecular structure hexapeptide analogue N_3-Aib-Ant-^{L}Pro-Aib-Ant-^{L}Pro-NHMe.

Monomer unit synthesis posed lots of challenges because of benzoxazinone formation as the major side product obtained on C-terminal activation of N_3-Aib-Ant-OH segment during coupling with H-^{L}Pro-OBn. As several coupling strategies were unrewarding, different Lewis acid catalysed carbonyl activation of corresponding benzoxazinone moiety was attempted. However, Schreiner's

(thio)urea provided best results. Using Schreiner's (thio)urea in reaction provided a mild means for opening of azlactone moiety with amines without exploiting harsh conditions successfully facilitated amide bond formation (Figure 5).

Optimization revealed 10 mol% of Schreiner's (thio)urea in DMSO to be the best condition. Reaction was also found to proceed considerably well in water. Different sets of primary and secondary amines were reacted with the benzoxazinones isolated by activation of corresponding beta-aromatic amino acids. Amino acids with less steric bulk reacted readily, also sterically constrained acyclic amino acid like aminoisobutyric acid, cyclic amino acid like proline reacted well providing good yields of coupled product.

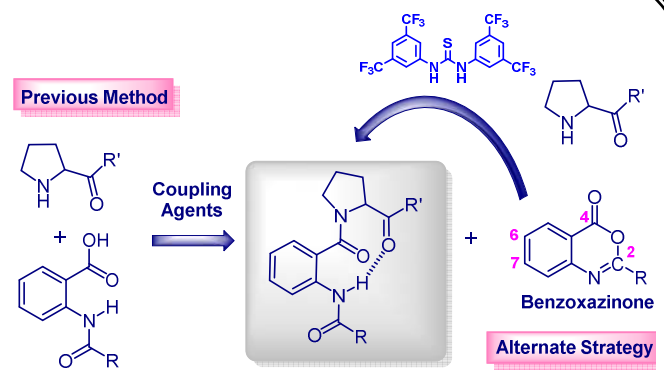

Figure 5: Organocatalytic ring opening of 4H-benzo[d][1,3]oxazin-4-one derivatives with different primary and secondary amines.

Section III of chapter 3 demonstrates the utilization of ^{S}Ant-Pro motif as a reverse turn inducer which is also known to feature nine-membered H-bonding network. Sequences containing ^{S}Ant-Pro at centre with orthanilic acid as a connecting entity were designed and developed. In order to assess the influence of substitution of constrained amino acid like Aib on the turn at both N- and C- termini sequence Boc-^{L}Leu(1)-Aib(2)-^{S}Ant(3)-Pro(4)-Aib(5)-^{L}Leu(6)-NHMe was synthesized and its structural propensity was evaluated (Figure 6). Elucidated structure revealed that substitution of constrained amino acid like Aib at both N- and C-termini around the ^{S}Ant-Pro segment did not perturb the folding pattern. The oligomer revealed the long range 15- and 10- membered H-bonded ring. These results further supported the strong reverse-turn inducing ability of orthanilic acid.

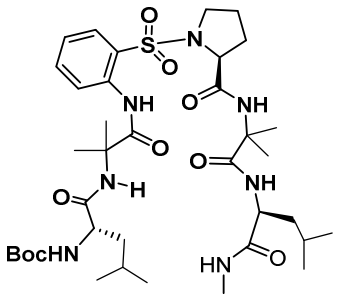

Figure 6. Designed hexapeptide hexamer possessing ^{S}Ant-Pro at the turn region.

GENERAL REMARKS

- Unless otherwise stated, all the chemicals and reagents were obtained commercially
- Required Dry solvents and reagents were prepared using the standard procedures.
- Dry reactions were performed under argon atmosphere.
- All the reactions were monitored by thin layer chromatography (TLC) on precoated silica gel plates (Kieselgel $60F_{254}$, Merck) with UV, I_2 or Ninhydrin solution, anisaldehyde solution, as the developing reagents in the concerned cases.
- Column chromatographic purifications were done with 100-200 Mesh Silica gel or with Flash silica gel (230-400) mesh in special cases.
- Distilled solvents were used as eluents in the column chromatography
- All evaporations were carried out under reduced pressure on Buchi rotary evaporator below 50 °C, unless otherwise stated.
- Melting points were determined on a Buchi Melting Point B-540 and are un corrected.
- Optical rotations were measured on JASCO-P2000 polarimeter.
- IR spectra were recorded in nujol or $CHCl_3$ using Shimadzu FTIR-8400 spectrophotometer.
- NMR spectra were recorded in $CDCl_3$ on AC 200 MHz, AV 400 MHz and AV 500 MHz Bruker NMR spectrometers. All chemical shifts are reported in δ ppm downfield to TMS and peak multiplicities as singlet (s), doublet (d), quartet (q), broad (br), broad singlet (bs) and multiplet (m).
- Elemental analyses were performed on a Elmentar-Vario- EL (Heraeus Company Ltd., Germany).
- Electron Scattered Ionization (ESI) Mass Spectrometric measurements were done with API QSTAR Pulsar mass Spectrometer.
- MALDI-TOF/TOF mass spectrometric measurements were done on ABSCIEX TOF/TOF^{TM} 5800 mass spectrometer.

List of Publications

1. A Synthetic Zipper Peptide Motif Orchestrated *via* Co-operative Interplay of Hydrogen Bonding, Aromatic Stacking and Backbone Chirality.
Nair, R. V.; Kheria, S.; Rayavarapu, S.; Kotmale, A. S.; Jagadeesh, B.; Gonnade, R. G.; Puranik, V. G.; Rajamohanan, P. R.; Sanjayan, G. J. *J. Am. Chem. Soc.* **2013**, *135*, 11477-11480.

2. The Ant-Pro Reverse-Turn Motif: Structural Features and Conformational Characteristics.
Thorat, V. H.; Ingole, T. S.; Vijayadas, K. N.; **Nair**, **R**. **V**.; Kale, S. S.; Ramesh, V. V. E.; Davis, H. C.; Prabhakaran, P.; Gonnade, R. G.; Gawade, R. L.; Puranik, V. G.; Rajamohanan, P. R.; Sanjayan, G. J. *Eur. J. Org. Chem.* **2013**, 3529-3542. (*Invited article for special issue on foldamer*)

3. Formation of Pseudo-β-hairpin Motif Utilizing Ant-Pro Reverse Turn: Consequences of Stereochemical Reordering.
Nair, R. V.; Kotmale, A. S.; Dhokale. S.A.; Gawade, R. L.; Puranik, V. G.; Rajamohanan, P. R.; Sanjayan, G. J. (*Org. Biomol. Chem.* **2014**, Advance Article, **DOI:** 10.1039/C3OB42016G)

4. (Thio)urea-Mediated Benzoxazinone Opening: Mild Approach Towards Synthesis of *o*-(substituted amido)benzamides.
Nair, R. V.; Sanjayan, G. J. (*RSC Adv.* **2013**, **DOI:** 10.1039/C3RA45903A)

5. Heterogenous Foldamers from Aliphatic-Aromatic Amino Acid Building Blocks: Current Trends and Future Prospects.
Nair, R. V.; Vijayadas, K. N.; Arup Roy; Sanjayan, G. J. (*Manuscript under preparation*)

Symposia Attended

1. Delivered oral presentation at *National Conference on Chirality* [NCC-2013], Vadodara held during Dec 7-8, 2013, organised by Faculty of Science, The Maharaja Sayajirao University of Baroda, India.

2. Participated and presented poster in the *International Meeting on Chemical Biology* (IMCB-2013) Pune held during May 26-28, 2013, organized by Indian Institute of Science Education and Research, Pune, India.

3. Participated in the *Indo-Korean symposium* in Organic Chemistry entitled 'Contemporary organic chemistry and its future directions' held during January 12-13, 2009, at National Chemical Laboratory, Pune, India.

Posters Presented

1. *Diversifying the Structural Architecture of Synthetic Oligomers: The Hetero Foldamer Approach*. **Roshna V. Nair**, Vijaykumar H. Thorat, Vijayadas K. N., Vedavati G. Puranik, Pattuparambil R. Rajamohanan and Gangadhar J. Sanjayan. Poster presented during the 1st CRSI-Zonal Meeting function held at National Chemical Laboratory, Pune, May 2011, India. ***(Won the best poster award)***

2. *Conformational Characteristics of the Ant-Pro Reverse Turn*. **Roshna V. Nair**, Vijaykumar H .Thorat, Tukaram Ingole, Vijayadas K. N., Vedavati G. Puranik, Pattuparambil R. Rajamohanan and Gangadhar J. Sanjayan. Poster presented during the *National Science Day* function held at National Chemical Laboratory, Pune, Feb 2012, India.

3. *Formation of Pseudo-β-hairpin Motif Utilizing Ant-Pro Reverse Turn: Consequences of Stereochemical Reordering*. **Roshna V. Nair**, Amol S. Kotmale, Snehal A. Dhokale, Rupesh L. Gawade, Vedavati G. Puranik, Pattuparambil R. Rajamohanan and Gangadhar J. Sanjayan. Poster presented during the *National Science Day* function held at National Chemical Laboratory, Pune, Feb 2013, India.

4. *Studies on a Synthetic Zipper Peptide Motif Orchestrated via Co-operative Interplay of Hydrogen Bonding, Aromatic Stacking and Backbone Chirality*. **Roshna V. Nair**, Sanjeev B. Kheria, Suresh Rayavarapu, Amol S. Kotmale, B. Jagadeesh, R.G. Gonnade, V.G. Puranik, P. R. Rajamohanan and G. J. Sanjayan. Poster presented during the *National Magnetic Resonance Society-2013 Symposium*, held at IIT Bombay, Feb 2013, India.

CHAPTER 1

Ant-Pro Motif as a Potent Turn and Hairpin Nucleator

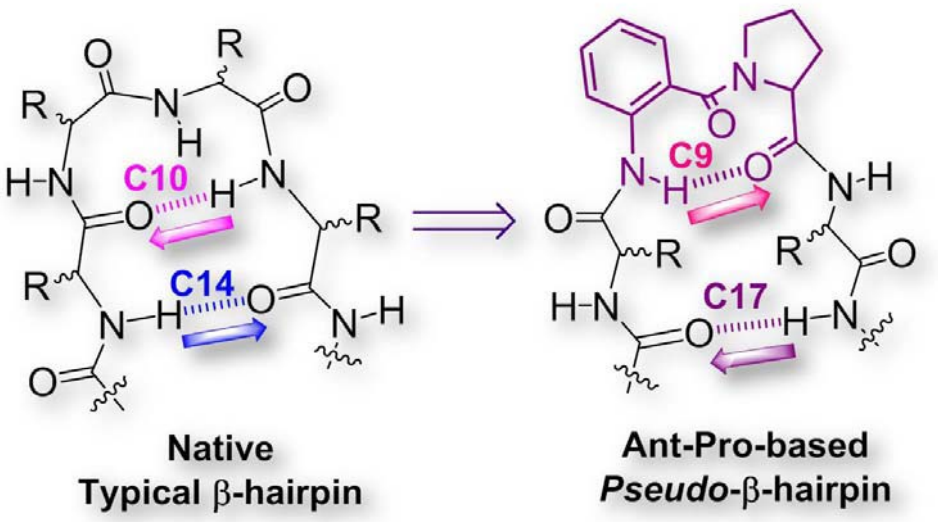

This chapter exclusively deals with investigations of the folding propensity of Ant-Pro motif (Pro = $^{L/D}$proline and Ant = anthranilic acid). Section I discusses about Ant-Pro motif as a potent reverse turn mimic and its modification meant for its utilization in biomedical application. Section II describes the investigations on hairpin nucleation propensity of Ant-Pro motif. The conformational pre-disposition has been thoroughly explored using NMR spectroscopy and single crystal X-ray diffraction studies.

It has been recognized that hydrogen bonds restrain protein molecules to their native configurations, and I believe that as the methods of structural chemistry are further applied to physiological problems, it will be found that the significance of the hydrogen bond for physiology is greater than that of any other single structural feature.

— Linus Pauling

1.0 Preamble

To identify the structure and function of biopolymers, probing and understanding their conformational features in solution as well as in solid-state becomes indispensable. Amongst different biopolymers, proteins perform key functions in cellular communication, biocatalysis, molecular transportation *etc*., where the spatial arrangement of its residues holds the key to their properties. Last two decades have witnessed growth of peptides as preferred drug candidates with escalating demand for bio-compatible drugs. But, as they still suffer from poor bioavailability due to rapid proteolysis and limited shelf life, an efficient method of constructing bio-compatible structures and 3D- pharmacokinetic profiling presents tricky challenge to future drug development.

Field of foldamers[1] - a branch of peptidomimetics – which deals with the thorough analyses of the structural aspects of *de novo* generated secondary structural motifs, exploits this understanding in development of peptide-derived therapeutics. This area of study has been evolving and flourishing since the advent of unnatural amino acids-based replication of the topology of natural peptide components. Conformationally constrained amino acids and molecules derived from the unnatural analogues satisfactorily mimic the natural shape of the target molecule and can be tethered rather effortlessly into peptide backbones. The combinations that arise by the virtue of these unnatural residues (heterogeneous backbones) quite often successfully duplicate the structure and function of native functional entities and also increase stability.[2] Mimicking specific protein secondary structure elements, specifically the turn motifs, using a hybrid aliphatic-aromatic amino acid conjugate is the primary motivation of the work carried out in this chapter.

1.1 Turns in biology

Turns in proteins are irregular secondary structure elements and are the sites, where the polypeptide chain totally folds back on itself causing proteins to adopt a globular shape.[3] Folding of the peptide chains are preferentially caused by amino acids like Asn, Gly and Pro (about 50% of turns found in proteins) *etc*, because of their torsional characteristics. They are mostly located at the surface of proteins providing means for the interaction with receptors, and thus they are involved in various biological events and pathways.[4] Reverse turns exhibit multi-faceted functions in biological systems

like *β*-turns, which act as recognition sites for the initiation of complex immunological, metabolic, hematological, and endocrinological reactions. Fairlie and co-worker's extensive coverage on protein-protein interaction depict that over hundred peptide-activated GPCR ligands recognise turn structures.[5]

Unlike α-helices or *β*-sheet secondary structures, turns are termed as irregular structures due to lack of clearly defined torsion angle preferences. In proteins, reverse turns are generally classified into different types on a virtual basis of the number of residues that participate in the formation of *intra*-turn hydrogen bond between the main-chain carbonyl group from the first residue and the main-chain amide group from the last residue of the turn. A peptide turn may be categorized by 7-, 10-, and 13-membered hydrogen bonded rings formed by participation of 3 residues (*γ*-turn), 4 residues (*β*-turn), and 5 residues (α-turn), respectively (Figure 1A). The most common turn-type found in proteins is the *β*-turn (≈ 25% of overall turns), which was first recognised in the 1960s by Venkatachalam. *β*-turns revert the total direction of the polypeptide chain and the chain progresses in the overturned direction to construct *β*-hairpin/sheet secondary structure (Figure 1B).

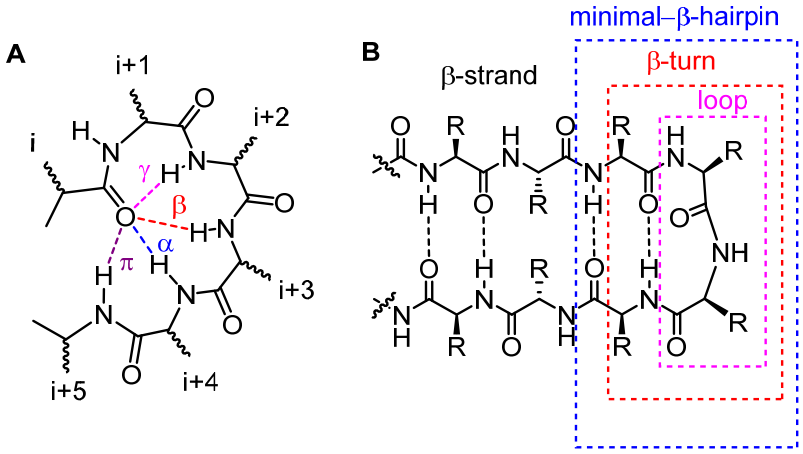

Figure 1: Types of reverse turns (A), and schematic representation of a typical *β*-hairpin secondary structure detailing the components of its structure: *β*-strand, *β*-turn, and loop (B).

β-turns can be further sub-categorised into types based on their dihedral angle values. The consecutive repeats of *β*-turns produce 3_{10}-helices and the usual α-helices are created by multiple α-turns. In current perception, turns also include 'open' turn conformation lacking a hydrogen bond, whose C_α-C_α distance <10 Å of the first and last residue that participates in peptide chain direction reversal. [6,7]

1.2 Reverse turn mimics

Reverse turns are common motifs in biomolecules and a range of bioactive peptide sequences mediate their function through the interaction of the side chains of amino acids situated at the turn units with different receptor sites. Various synthetic three-dimensionally (3D) ordered reverse turn mimics lucratively imitate the structural topology of such peptides but, interfere in their biological pathways. Their incorporation into functional bioactive core increasingly meliorates the understanding of interactions of small molecules with biological targets such as enzymes or receptors, besides tackling different 'peptides as drugs' related concerns. Rigidification or stabilisation of reverse turn can be accomplished by use of various backbone modifications or by making reverse turn mimics.

1.2.1 Cyclisation mediated reverse turn mimics

In order to obtain selective protein inhibitors, Freidinger introduced the idea of local backbone cyclization meant to limit the local mobility of an oligopeptide.[8] Several scaffolds employing chimeric amino acids to develop reverse-turn mimics have been formulated in the past three decades.[9] Different exercises include head-to-tail covalently linked cyclization through click chemistry,[10] alkyne bond formation, ring-closing olefin metathesis,[11] disulphide brigding[12] *etc* to render rigidified systems.

Integrating constrained moieties saw use of dipeptide lactams,[13] proline derivatives,[14] spirolactam bicyclic and tricyclic systems based on proline,[15] functionalized dibenzofurans,[16] substitution by dehydroamino acids,[17] benzodiazepines,[18] diketopiperazines,[19] sugars,[20] benzodiazepinones,[21] (S)-aminobicyclo- [2.2.2]octane-2-carboxylic acid (ABOC),[22] and metal complexes of linear peptides[23] or chiral pentaazacrowns and so on (Figure 2).[24] In order to retain biological activity, cyclic constraints must influence the backbone conformation without compromising crucial side chain interactions with the receptor.[25-28]

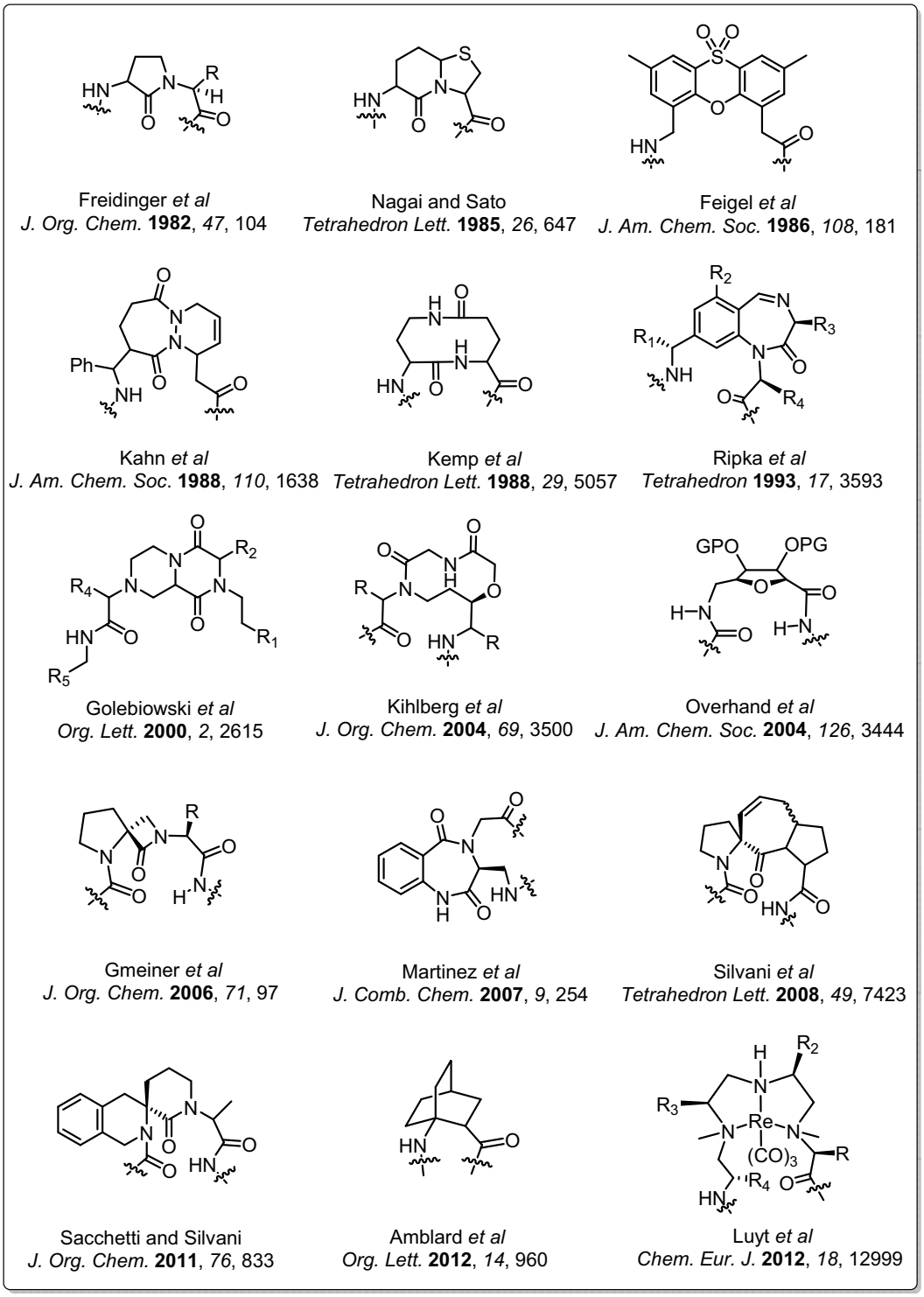

Figure 2: Selected examples of *β*-turn mimetics.

1.2.2 Reverse turn mimics based on unnatural amino acid residues

To restrict the reverse turn architecture, one of the easiest ways is to integrate torsionally constrained amino acids into the peptide backbone (Figure 3). The common choices include germinal constraints, such as α - amino acids like α-amino

butyric acid (Aib) (gem-dimethyl substituted open amino acid) [29] and *N*-aminoproline (cyclically constrained).[30] Another important category is insertion of modified *homo*-analogues i.e. *β*-amino acids like 2-aminocyclopropanecarboxylic acid (ACC),[31] 2-aminocyclopentanecarboxylic acid (ACPC),[32] 2-aminocyclohexanecarboxylic acid (ACHC),[33] and 2-aminobenzoic acid (anthranilic acid, Ant)[34] or γ- amino acids like nipecotic acid (*hetero*-chiral dinipecotic acid segment promotes antiparallel sheet secondary structure),[35] 1-aminomethylcyclohexaneacetic acid (gabapentin, Gpn),[36] δ-amino acids like C-linked carbo-γ(4)-amino acids and γ-aminobutyric acid *etc*. [37,38]

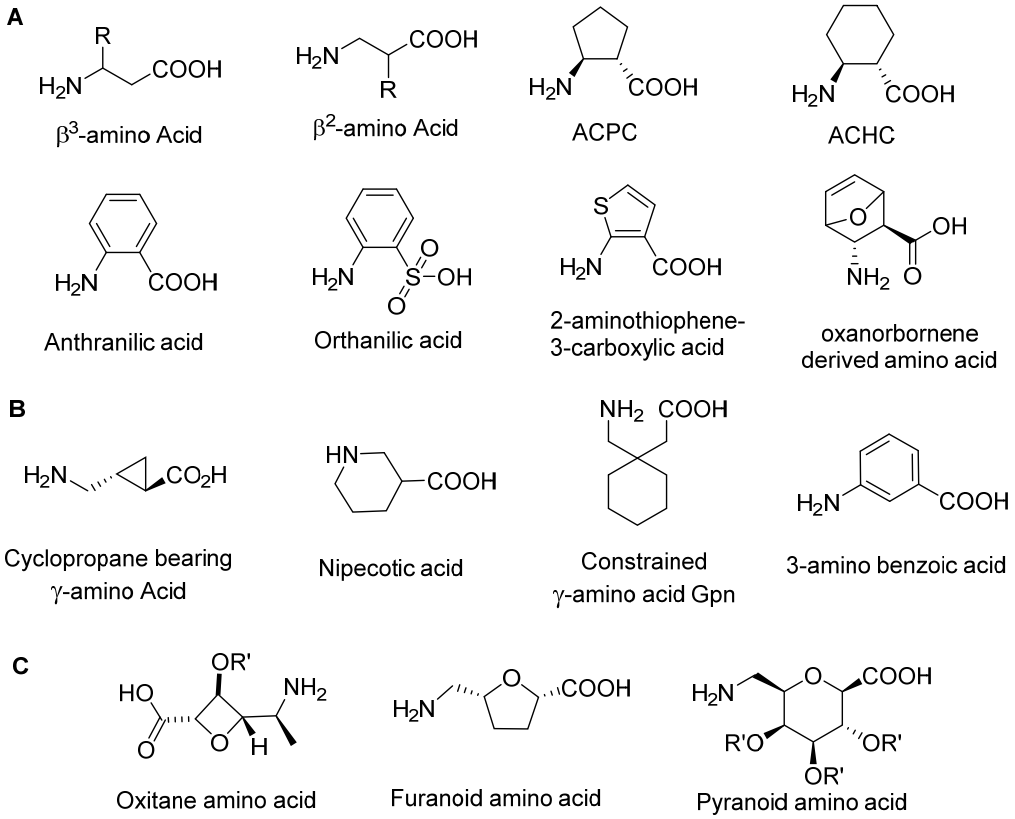

Figure 3: Selected examples peptide building blocks: *β*-amino acids(A), γ-amino acids (B), and δ–amino acids (C).

The use of aliphatic-aromatic hybrids is a recent practise in the locale of heterogeneous peptide design. They also often deliver turn structures, owing to the combined local conformational preferences of the α-amino acid and rigidity of the conjoining aromatic residue. The constrained torsions of aromatic residues enforce linear structural design on the plane. A very coherent design of a reverse turn motif by Smith *et al*, involves amino acid derived alcohol conjoining aromatic amine which was found to promote parallel sheet structure (Figure 4).[39, 40]

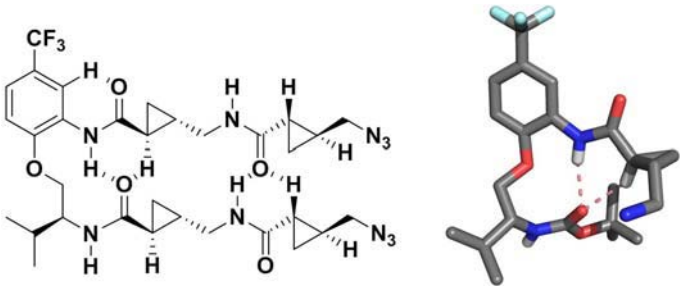

Figure 4: Molecular structure of Smith's reverse turn structure that stabilizes sheet-like structural architecture (left) and crystal structure of turn motif (right).

Another remarkable aliphatic-aromatic amino acid based reverse turn motif reported from our group is the anthranilic acid-proline conjugated pseudo beta turn mimic (Figure 5). [41] The effect of the steric and dihedral angle constraints offered by proline on the anthranilic acid residue evades the formation of much anticipated 6-membered H-bond (which causes the Ant repeats to adopt sheet structure[42]) to establish a 9-membered H-bond between Ant-NH and Pro-CO (Figure 5A). Extensive studies confirmed that the proline and six-membered constrained ring structure of Ant are essential for the formation of pseudo-β-turn structure.[43a] Interestingly, we observed an unusual conformational similarity of two peptide folds featuring sulfonamide and carboxamide on the backbone (Figure 5B).[43b] Further analysis of the robustness of this motif will be discussed in this chapter.

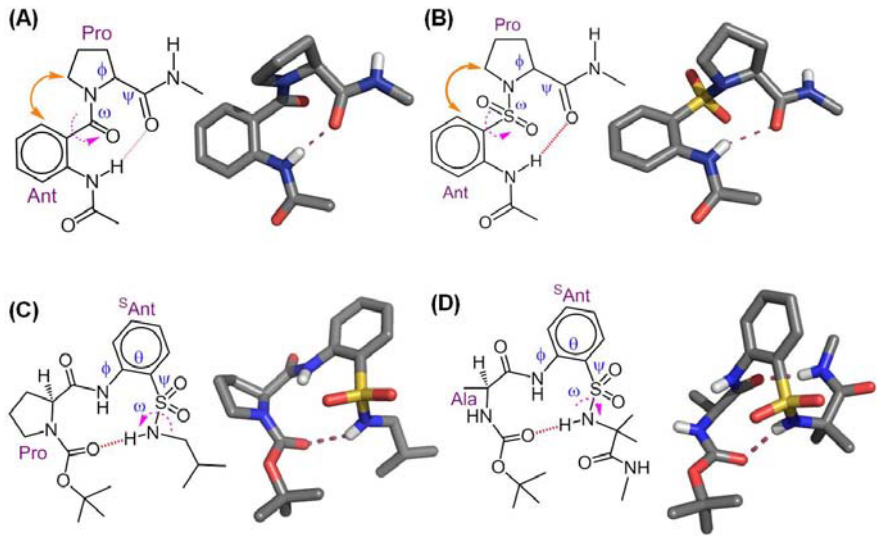

Figure 5: Molecular structures and corresponding crystal structures of: Ant-Pro motifs linked *via* carboxamide and sulphonamide (A and B, respectively), Xaa-^{S}Ant-Yaa peptide sequences Boc-Pro-^{S}Ant-NH^{i}Bu and Boc-Gly-^{S}Ant-Aib-OMe (C and D, respectively). Non polar hydrogens have been removed for clarity.

In recent times, use of 2-aminobenzenesulfonic acid (orthanilic acid, ^{S}Ant) at the C-terminal of any flexible or constrained amino acids with peptide sequences (Xaa-^{S}Ant-Yaa), has also been found to induce a strong reverse-turn featuring 11-membered-ring hydrogen bonding network formed in the backward direction (Figure 5C,D).

Slight variation in the Ant- residue substitution pattern from (*o*- to *m*-) furnishes 3-amino-5-bromo-2-methoxy benzoic acid (Amb), which on combination with Pro (proline) unfolds a well-defined, compact, three-dimensional helix with periodic γ-turns (Figure 6). An additional conformational restriction offered by methoxy group orients the NH of Amb in close proximity to the prolyl carbonyl, resulting in the formation of S(7)-type 7-membered γ-turn stabilised by an *intra*-molecular bifurcated S(5)-type hydrogen bond with the Amb methoxy group.[44] Several designer amino acids are being developed to create such intriguing assemblies and this area is ever-growing with the intent of coming up with better and stronger reverse turn mimics.

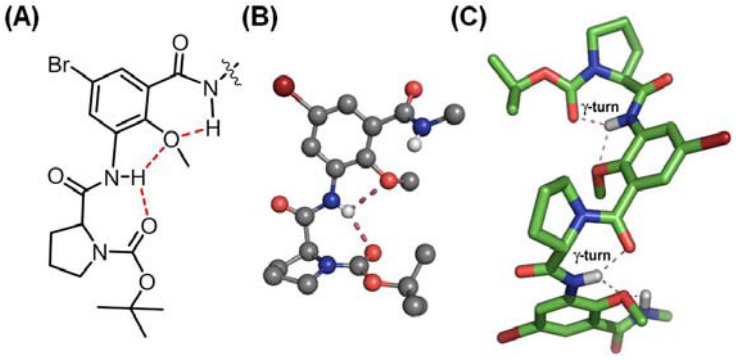

Figure 6: Molecular structure of -(Pro-Amb)- dipeptide unit (A), its corresponding crystal structure (B), and conformation of the tetrapeptide at the HF/6-31G* level of *ab initio* MO theory (C).[44]

1.3 Significance of foldamer based mimics

Peptides face an inherent problem of large degree of conformational freedom rendering the biologically active conformations to be feebly populated in solution state. Also, they possess the tendency to form unintended hydrogen bonds, thus they face difficulties in crossing membranes leading to poor transportation into cells. However, the modified bioactive peptides are one of the most preferred drug candidates because of their high potency, specificity and biological & chemical diversity. They are better than the peptide based therapeutics which possess short

half-life (prone to rapid proteolysis), poor solubility or aggregate and cumbersome synthesis. Peptide-based drugs are biocompatible to greater extents with lesser toxicity, reaching the site of action after an easy administration with minimized drug-drug interactions and reduced accumulation in tissues. There has been great development in the area of peptide based drug research, with various technologies meant for improvement in their activity and bioavailability. Different techniques involve methods like glycosylation, amino acid modification, *intra*-molecular cyclisation *etc*.

1.4 Application of reverse turn mimics

Foldamer-based mimics maintain stable three-dimensional compact architecture in both solid- and solution state. These robust turn mimics successfully retain the desired conformation for biological receptor recognition by enzymes or peptides. Besides medicinal relevance, it also has established its forte in organic asymmetric synthesis by providing the proper orientation and site selectivity over long distances meant to bring reactants closer or activate the functional groups.

1.4.1 Reverse turn mimics in therapeutics

Bioactive peptides are ubiquitous in all forms of life and a large number of physiological processes in living systems is an outcome of their interactions with the receptor molecules. Several peptides have been identified carrying out specific functions for *eg*. octapeptide angiotensin that causes vasoconstrictor effects, vasopressin that brings vasodilator effects, enkephalins and neurotensin that directs central nervous mechanisms like respiratory, cardiovascular, temperature pain and sensory controls *etc*. This knowledge significantly stimulated the development of peptide emulating drugs or structural analogs in form of their agonists (which mimic the parent peptide) and antagonists (that occupies peptide receptor) as they are non-toxic.

Reverse turns form an integral part in many antibiotics, toxins, antitoxins, ionophores, antimicrobial decapeptide sequences like gramicidin S and tyrocidines A-E, antibiotic viomycin and cyclic dodecadepsipeptide valinomycin, octapeptide amatoxins and the heptapeptide phallotoxins,

Many of these bioactive peptides possess turn structure at the site of molecular recognition. Even a small peptide can acquire the turn conformation, triggering

physiological process through peptide-receptor interaction. Turn mimics are one of the most thoroughly investigated secondary structure mimics. These motifs are having implications in recognition of elements in structure-activity studies of the peptide hormones, angiotensin II, bradykinin, GnRH, somatostatin, and many others.

Various groups have been working on incorporating turn mimics into these peptides. Seebach and group replaced (Phe-Trp-Lys-Thr) sequence that binds to somatostatin receptor with a cyclic *β*-tetrapeptide (Figure 7).[45] The cyclic *β*-peptide showed binding affinity at micromolar concentration (KD = 3.3 - 186 μM).

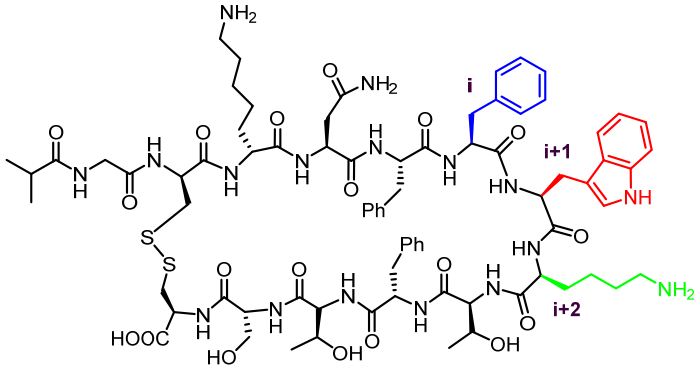

Figure 7: Cyclic peptidomimetic of somatostatin reported by Seebach *et al.*[45]

Gramicidin S, a cyclic decapeptide containing two type II *β*-turns was found to have antibiotic properties, which can kill the bacterium by interrupting the synthesis of Adenosin-triphosphate (ATP) from ADP. Introduction of azabicycloalkane amino acids (*β*-turn dipeptide/ BTD) into GS resulted in antibiotic analogues with similar activity as the parent peptide.[45] Hruby and co-workers developed a bicycle leu-enkephalin analogue incorporating 4-phenyl indolizidinone.[46] Similarly, Jurzak and group used (2*S*,6*S*,8*S*)-indolidin-9-one amino ester as BTD.[47] Sugar-based reverse turn mimetic has been shown to mimic GS structure (Figure 8).[48]

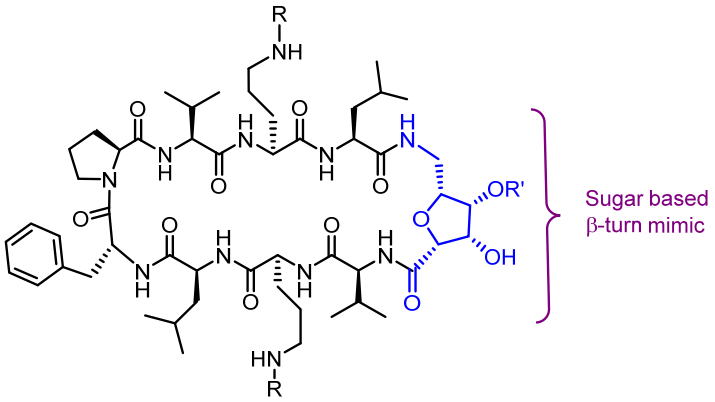

Figure 8: Sugar based *β*-turn mimic of Gramicidin S designed by Overhand *et al.*[48]

Angiotensin II (Ang II) is a linear octapeptide with sequence Asp-Arg-Val-Tyr-Ile-His-Pro-Phe and it is the active component of rennin-angiotensin system, which plays important role in regulation of blood pressure, body fluid and electrolyte homeostasis. It is produced by the stepwise cleavage of angiotensinogen (decapeptide) by rennin and angiotensin converting enzyme. Several ACE inhibitors/blockers have been developed so as to avert the vasoconstriction effect caused due to the interaction between AT_1 receptor and Ang II (Figure 9), but they stand to face problems like their interference in bradykinin metabolism or enhanced prostaglandin synthesis.

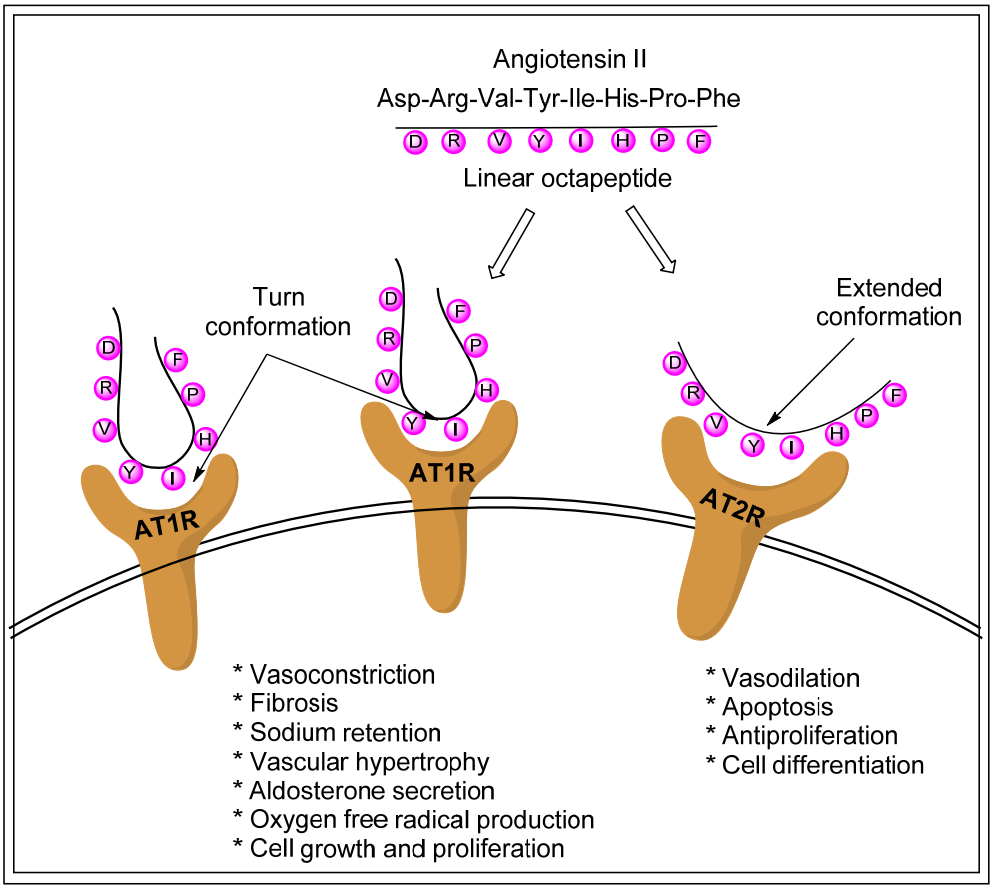

Figure 9: Mode of interaction of AngII with receptors AT1 and AT2 and its effects.

Also, few of the side effects known are dry & excessive nonproductive cough, dizziness *etc*. This led to the advancement of angiotensin receptor blockers (ARB), which are primarily used to treat high blood pressure, cardiac diseases such as stroke, heart attack and congestive heart failure (CHF). Unlike ACE inhibitors, Ang II receptor antagonists do not inhibit bradykinin metabolism or enhance prostaglandin synthesis. They do not adversely affect lipid profiles or cause rebound hypertension

after discontinuation and have beneficial effect on the kidney, particularly the kidneys of people with diabetes, making them the more effective and relatively safe in the treatment of hypertension. Two Ang II receptor antagonists have been commercialised losartan (Cozaar) and valsartan (Diovan). Peptide-derived drugs also could be safely used for the treatment of heart failure in patients intolerant of ACE inhibitor therapy, particularly Candesartan (Diovan).

Several analogs comprising turn mimics replacing Tyr^4-Ile^5 residues have been synthesized and studied. Replacement of Tyr^4-Ile^5 residues with benzodiazepine-derived *β*-turn mimic revealed high binding affinity towards AT_2 receptor at (K_i = 1.8 nM) concentration (Figure 10). [12]

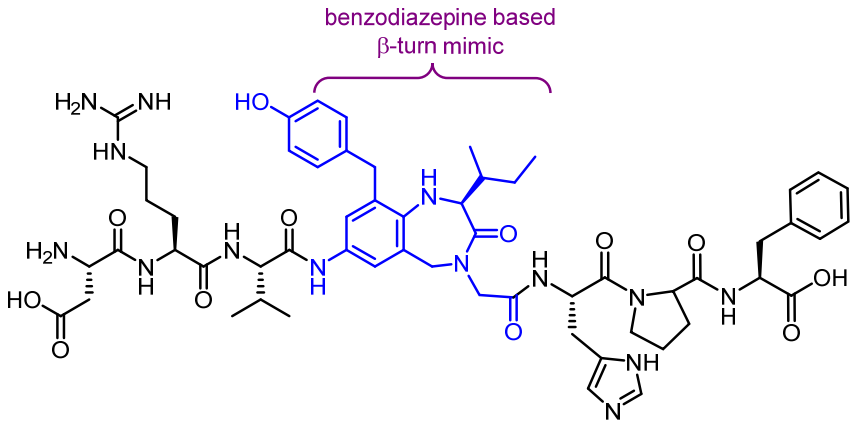

Figure 10: Angiotensin II analog featuring benzodiazepine as reverse turn mimic designed by Hallberg *et al.* [12]

1.4.2 Reverse turn mimics in catalysis

General points usually considered for the development of catalysts include economy, availability, stability while handling, moisture sensitivity (serious issue for chiral metal complexes) and better enantioselectivity, conversion and catalyst loading. Peptides as catalysts fulfil many of these criteria and thus have found great applications in organocatalytic chemistry as they offer high chemoselectivity, wide substrate scope, chemical robustness and catalyst reusability. In the early 1980s, simple peptide like polyalanine (upto >10 residues) was productively utilised for Julia-Colonna epoxidation. Later, Berkessel *et al* employed poly-leucine (upto >4 residues) was employed for the epoxidation with low catalyst loading with better enantioselectivity.[50] Peptides have been exploited greatly in asymmetric catalysts for *eg*. in acylation reactions, oxidations, hydrolytic reactions, and C–C bond formations.[51]

Miller's group extensively explored *p*-methyl-histidine-containing peptides for group transfer chemistry. Previous work from the Miller group has accomplished selective transfer of groups like acyl, phosphoryl, sulfinyl and thiocarbonyl to alcohols,[52] enantioselective mono (sulfonylation)-mediated desymmetrization of meso-1,3-diols,[53] site- and enantioselective oxidation of certain positions of various isoprenols-polyene epoxidation,[54] kinetic resolution of alcohols[55] amongst various other reactions. Selected examples of synthetic peptides used as organocatalysts are depicted in figure 11. Qu *et al.* modified amide into thioamide and utilised the modified tetrapeptide analogue synthesised by Miller and co-workers to successfully carry out acyl transfer reactions (Figure 11A).[56] Wennemer's group introduced peptides of the category Pro-Pro-Xaa for enamine catalysis, where Xaa is an acidic amino acid (Figure 11B). They utilized tripeptide H-Pro-Pro-Asp-NH_2 with a well-defined turn conformation, which was found to be crucial for the high catalytic activity and selectivity of direct asymmetric aldol reactions and asymmetric catalysts for 1,4-addition reactions of aldehydes to nitroolefins.[57] In an elegant example, thiourea catalyst with a aliphatic-aromatic hybrid backbone ten-membered *β*-turn-like structure that catalyzes Mukaiyama–Mannich reaction with high enantioselectivity (Figure 11D) was reported by Smith *et al.*

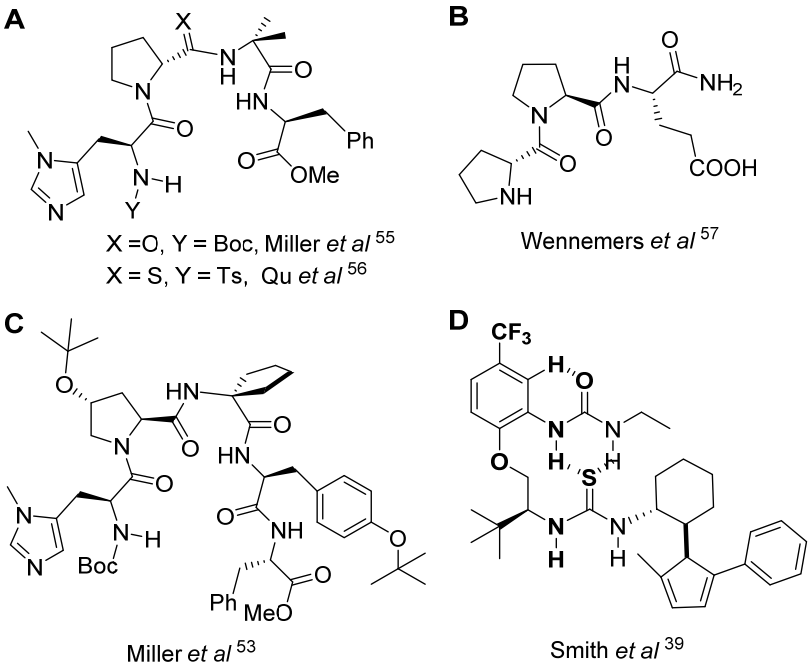

Figure 11: Selected examples of peptides used as organocatalysts having turn conformation.

Section I
Investigations on Ant-Pro Motif as a Potent Reverse Turn Mimic

1.5 Objective of the work

As described in **Section 1.2.2**, aliphatic-aromatic amino acid conjugate Ant-Pro motif features a nine-membered H-bonding pattern connecting the amide NH of the Ant residue and the carbonyl of the Pro residue. Significance of both the units has been assessed and was found to be equally crucial for the creation of the turn motif. Therefore, our objective was to appraise the robustness of Ant-Pro motif as a reverse turn mimic. Thus, extensive structural modulations around the turn segment of the N- and C-terminal amidated peptides by altering chiralities of the amino acid residues were undertaken. A part of this study has been described in this section.

1.6 Design strategy

Mutual influence of the conformational constraints of L-proline and anthranilic acid fabricates a completely novel secondary structure element (pseudo *β*-turn). Modifications around the turn segment have been carried out in order to determine its sensitivity towards the structural perturbations employing beta-branched amino acid like valine at N-terminal of Ant-Pro motif. The functionalization of the C- terminus with 4(Br)-anilide was carried out considering the relative ease of crystal formation observed by bromo compounds.[58]

1.7 Synthesis

The functionalized tripeptides **3a** and **3b**, with alternating chirality at valine required for the present study were synthesized as depicted in Scheme 2.1. Boc-^{L}Val-OH on coupling with anthranilic methyl ester using DCC in DCM afforded **2a**. Similarly, **2c** was obtained from Boc^{D}Val-OH. Methyl ester cleavage with LiOH in THF:H_2O furnished acids **2b** and **2d**. The final Ant-Pro reverse-turn analogs **3a** and **3b** were accessed by the direct coupling of Boc-^{L}Val-Ant-OH and Boc-^{D}Val-Ant-OH with HN-^{L}Pro-NH(*p*-C_6H_4-Br) **2f**, respectively, aided by HBTU as coupling agent in DCM in considerable yields.

Scheme 1.1. Synthesis of reverse turn analogs **3a** and **3b**

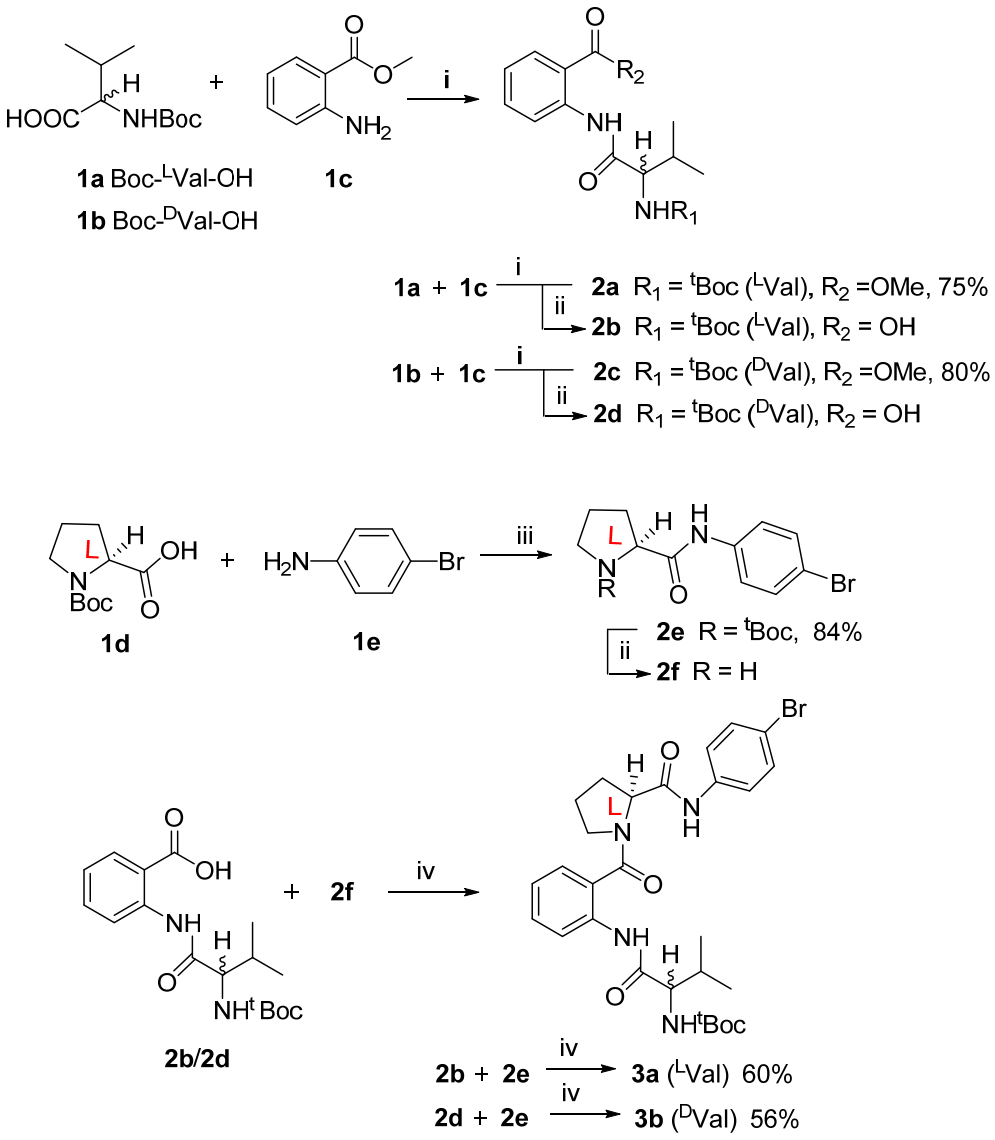

Reagents and conditions: (i) DCC, cat. HOBt, DCM, 0 °C-rt, overnight; (ii) LiOH, THF, H_2O; (iii) EDC.HCl, DMAP, CH_3CN; (iv) HBTU, DIEA, DCM, 0 °C-rt, 12h.

1.8 Conformational analyses

The reverse-turn conformational architecture was examined using X-ray crystallography, solution state NMR and CD studies.

1.8.1 Single crystal X-ray diffraction studies

The solid-state conformation of both tripeptides **3a** and **3b** revealed that the unusual nine-membered hydrogen-bonding pattern of Ant-Pro reverse-turn clearly

prevails in both the cases, regardless of structural and chirality modulations, around the turn segment. The Ant and the Pro rings evidently maintained an *anti-periplanar* arrangement perfectly, causing the otherwise strong 6-membered-ring hydrogen-bonding to collapse, facilitating a folded conformation (Figure 12).

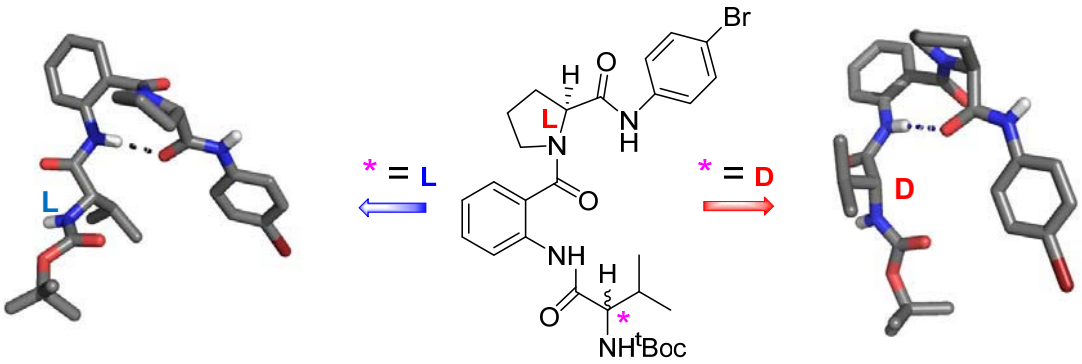

Figure 12: Crystal structures of Ant-Pro reverse turn analogues **3a** and **3b**. Hydrogens, other than the polar amide hydrogens have been removed for clarity.

The $C\alpha_i$-$C\alpha_{i+3}$ distance of an ideal *β*-turn was observed to be <7Å and both the pseudo-*β*-turn mimics **3a** and **3b** reveal a distance ≈ 5.6 Å, with the H-bonding distance [d(N-H..O=C)] = 2.1 Å, suggesting the robustness of C9-H-bonded network. In stark contrast to the normal anthranilamides where the ψ value appears about ± 150°, it differs substantially and appears about -75° and -95°, respectively for **3a** and **3b**, which is presumably due to the *antiperiplanar* pre-disposition of the Ant and Pro rings. The torsion angle θ = 7.43° for the constrained *β*-amino acid Ant in **3a**, due to the *cis*-disposition of the carboxyl and amino groups appended on the rigid aromatic framework. It is noteworthy that the distinctive cyclic structure imparts proline an exceptional conformational rigidity with a restricted N-Cα torsion angle of about ≈ ± 60° allowing it to seek spaces in the "turn" regions of proteins.[34a]

Table 1: Backbone torsion angles and hydrogen bonding parameters observed in crystals of **3a** and **3b**.

	Torsion (deg.)[b]						Hydrogen Bonding Parameters					
	Ant			Pro			Distances (Å)			Angles (deg.)		
	φ	θ	ψ	φ	ψ	NH...O=C	d($C\alpha_{i-1}$-$C\alpha_{i+2}$)	O...H	N...O	C=O..H	C=O..N	NH..O
3a	158.7	7.43	-75.6	-53.4	156.7	-95.6	5.76	2.12	2.97	130.29	130.52	168.89
3b	-168.7	2.09	-95.1	-52.4	160.3	171.1	5.54	2.13	2.99	132.76	135.12	171.67

In the Ant-Pro reverse turns reported herein, Pro adopts values that range from 52.36 (**3b**) and the torsion φ ranging between 156.66 (**3a**).

1.8.2 NMR studies

In order to investigate the solution-state conformation of the Ant-Pro two-residue reverse turns, we performed 2D NOESY NMR study of analogue **3b** in solution ($CDCl_3$, 400 MHz). The signal assignments were carried out with a combination of 2D COSY, TOCSY and HMBC. The characteristic strong nOes which supported the folded architecture were NH_1 *vs* $P2_\delta H$ and NH_1 *vs* C24H/C21H (Figure 13).

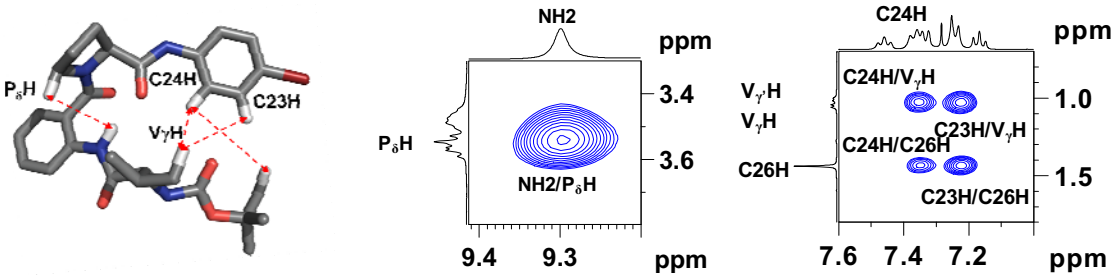

Figure 13: 2D NOESY excerpts of tripeptide **3b** (Boc-^{D}Val-Ant-^{L}Pro-AniBr) (400 MHz, $CDCl_3$).

Also, the characteristic chemical shifts of the Ant amide NHs involved in the 9-membered ring hydrogen-bonded network (δ 9-9.5 ppm) provides a good reference to the possibilities of 9-membered ring hydrogen-bonding compared to 6-membered ring hydrogen-bonding, which appears between δ 10-13 ppm.

1.8.3 CD studies

Circular dichroism (CD) spectra provide characteristic signatures for the conformational features of ordered chiral molecules (Figure 14).[59] The Ant-Pro reverse turn structures **3a** and **3b** both displayed similar pattern with maxima at around 195 nm, zero crossing at 200 nm and minima at 209 nm. A strong negative cotton effect was also observed (second minima) around 240 nm, consistently in both the cases, owing to the backbone aromatic groups/aromatic electronic transitions in the oligomers.[60] It is noteworthy that the typical cotton effects observed for these systems suggest the onset of helical architecture.

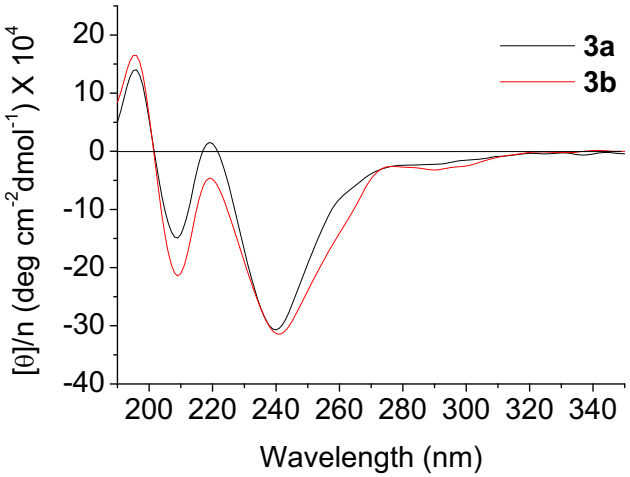

Figure 14. Representative CD spectra tripeptides **3a** and **3b** recorded in acetonitrile. All spectra were recorded at 298 K with a concentration of 0.04 mM.

Preparation of Suitably Protected Ant-Pro Motif for Solid Phase Peptide Synthesis

1.9 Objective of the work

An exhaustive analysis led to the understanding about Ant-Pro motif as a strong reverse turn inducer, which is significantly insensitive to structural and chirality perturbation in-and-around the turn segment. This inspired us to utilise it in the conformational rigidification of bioactive peptides (for *eg*. Angiotensin-II peptide).[60] The inflexibility and tolerance of the Ant-Pro motifs might ensure conformational rigidity to the peptide core. Our objective was oriented towards incorporation of this reverse turn mimic into diverse bioactive peptides to impart conformational rigidity.

1.10 Design strategy

Selected bioactive peptides that mediate their function through reverse turn architectures (selected few examples have been discussed in **Section 1.4.1**) are comprised of a variable peptide length of 6 to 20 amino acid residues. Solid phase peptide synthesis (SPPS) allows an easy access towards incorporation of modified

peptide units into these large peptides. Thus we chose to prepare protect N-terminus of -Ant-^{L}Pro- dipeptide, suitable for SPPS using Fmoc- strategy.

1.11 Synthesis

Several attempts to couple Fmoc-Ant-OH **1f** with HN-^{L}Pro-OBn **1g** were attempted but led to only meagre yields of the product. Different coupling reagents like DCC, EDC.HCl, HBTU were used in varied solvents like DCM, DMF *etc*. Even the acid chloride mediated coupling reaction produced sparse yield of the product. After several trials, THF was found to be the best solvent in which coupling with EDC.HCl fetched 48% of coupled product **4a.** Using HBTU in THF, the product was isolated with highest yield 74%. Later, to generate free acid Fmoc-Ant-^{L}Pro-OH, acid-mediated deprotection was attempted and the desired product **4b** was obtained after using 33% HBr in AcOH.

Scheme 1.2: Synthesis of dipeptide **4b**

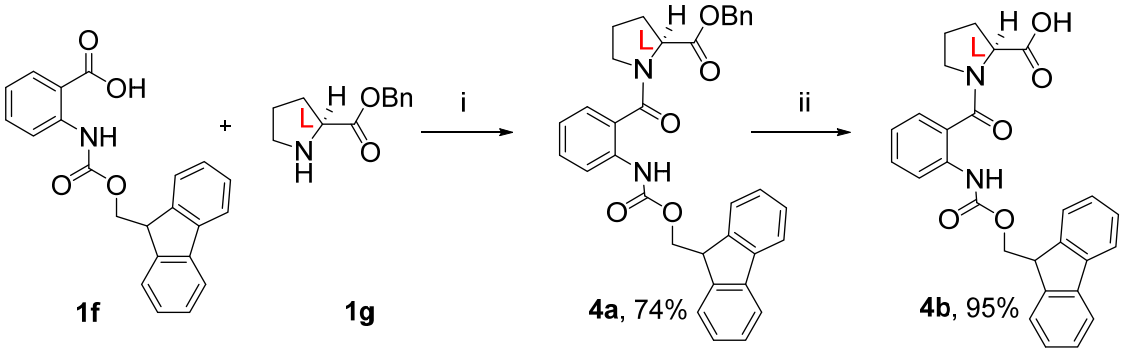

Reagents and conditions: (i) HBTU, DIEA, THF, 0 ^{o}C-rt, 12h; (ii) HBr, AcOH.

1.12 Conclusions

Conformational investigations of both L and D- valine substitutions at the N-terminus of Ant-Pro segment, i.e. -$^{L/D}$Val-Ant-^{L}Pro- reveal that Ant-Pro turn is robust and is highly insensitive towards chirality modulation and substitution effects around the turn segment. The robustness of the Ant-Pro motif towards structural modulations around the turn segment has a great bearing in practical utility - particularly in rigidifying flexible peptide backbones of bioactive peptides.

Section II

Formation of Pseudo-β-hairpin Motif Utilizing Ant-Pro Reverse Turn

1.13 Foldamers as *β*-hairpin mimics

β-hairpin structures form the smallest structural units for the augmentation of a *β*-sheet secondary structure in biopolymers.[61] They are one of the most preferred motifs/ candidates for 'protein epitope mimetic' design due to their involvement in various molecular recognition events. Robinson J. A. has summarised a broad assortment of *β*-hairpin mimics of key epitopes involved in protein-protein and protein-nucleic acid interactions.[62] The idea of mimicking these motifs commenced with the objective of inducing proteolytic stability into different bio-active peptides. Incorporation of unnatural residues in the peptide backbone and designed reverse-turn analogues extend to further nucleate hairpin formation and various such mimics have been found to successfully exhibit wide variety of applications in the area of peptide based drugs to catalysis.

Pro-Xaa where Xaa= Pro/Gly/Asn *etc*. is the prominent combination found in naturel proteins. Balaram's group experimented alternating chirality of proline unit and confirmed that heterochirality strengthens turn induction capability.[63] Other hairpin nucleating combinations using cyclic α,α-disubstituted amino acids developed by the same group are Gpn and 1-Aminocycloalkane-1-carboxylic Acid (Ac_6c).[64] Also Overhand's sugar mimic successfully stabilised Gramicidin S cyclic hairpin architecture.[65] Several reviews earlier illustrated the principles behind the design and application of *β*-sheet templates and *β*-turn mimics.[66] Most of the *β*-hairpin templates were designed spanning four peptide residues like dibenzofuran-based and *cis* azobenzene based templates reported by Kelly and co-workers.[67] Several bicyclic and tricyclic diketopiperazine-based mimics have been designed by Robinson *et al*.[62] The category of bicyclic lactams are also one of the important candidates (Figure 15). Further development in this area witnessed rather rigidified strands that stabilise hairpin structures like 1,6-dehydro-3(2H) pyridinone ring (@-tides) developed by Bartlett and co.,[68] Nowick's Hao units,[69] alkene isosteres by Kelly *et al*,[70] Chakraborthy *et al*'s triazole units[71] *etc*.[72]

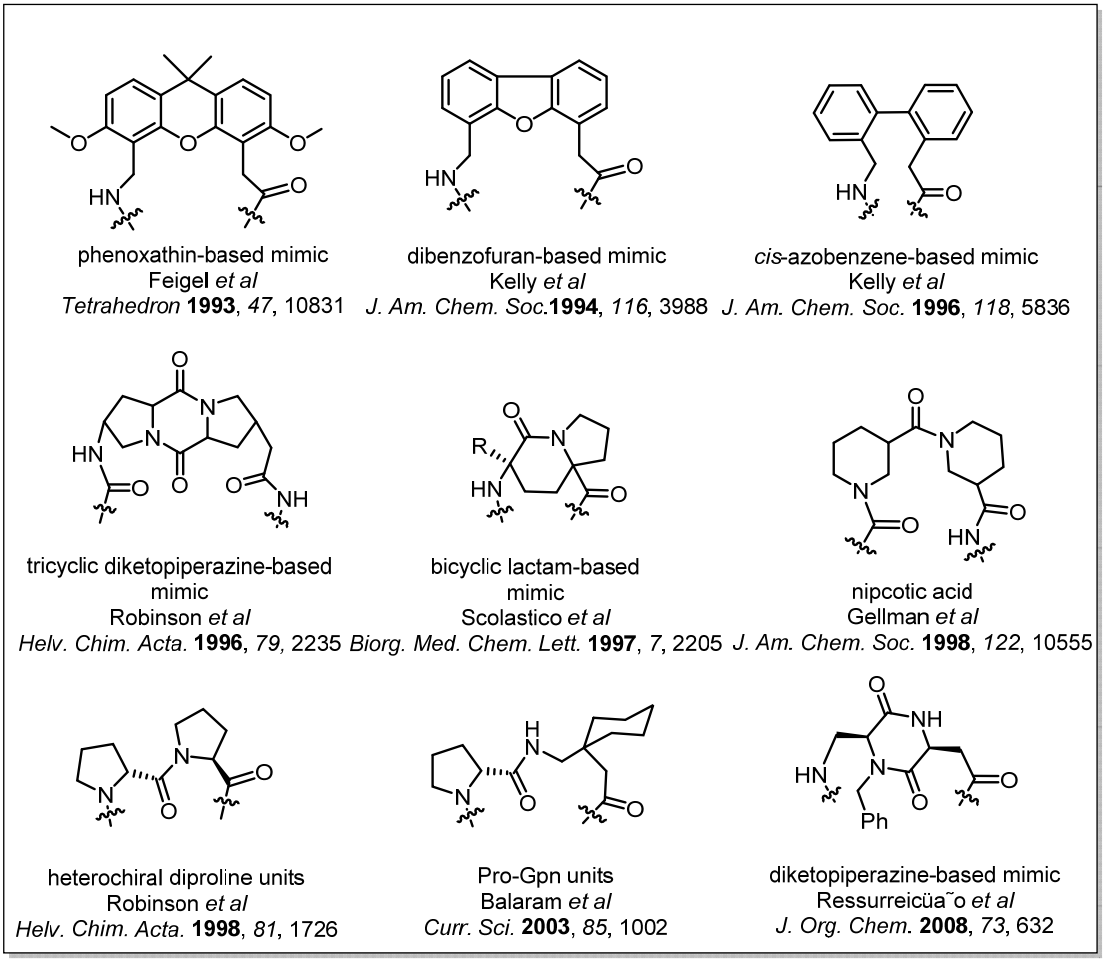

Figure 15: Set of synthetic turn motifs that render hairpin structure.

1.14 Consequences of stereochemical reordering in conformation of peptides

Stereochemistry provides an excellent tool to tune secondary structures. Modulation of chirality and substitution pattern of the amino acid residues in any secondary structure mimic affects the hydrogen-bonding interactions and hence the stability of the structure as exemplified in a number of cases.[73,74]

Demizu's group has comprehensively explored the chirality alteration effect of different diastereomeric -Leu-Leu-Aib-Leu-Leu-Aib- hexapeptide sequences. Homo-chiral sequence adopted a 3_{10}-helical architecture, whereas stereochemical variation of even a single residue caused backbones to fold into entirely different conformations (Figure 16).[75] Diastereomeric hexapeptide with D-Leu at 4th and 5th positions retained the right-handed (*P*) 3_{10}-helix, while alternating chiality sequence having D-Leu at 2nd and 5th position adopted a hairpin like folded architecture. Most surprisingly, on

incorporating D-Leu at 2nd and 4th positions, the S-shaped folded arrangement featured two types of β-turns (Type II and III) simultaneously.

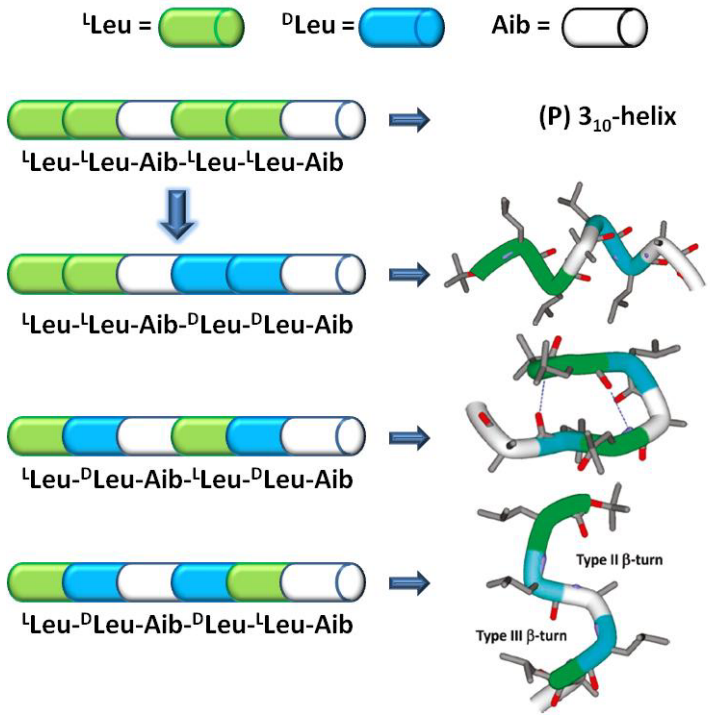

Figure 16: Consequences of stereochemical reordering in peptides.

Stereochemical alteration studies by Gellman (JACS 1996) points out that the conformational proclivity of the backbone arises from a combination of the torsional preferences of the covalent bonds, steric repulsions experienced in alternative folding patterns, and the entropic factors. Ramachandran and co-workers, in the early 1970s, predicted that the turn nucleation propensity of LD-segments are better than LL-segments in natural peptide sequences.[76] Balaram's (*hetero*-chiral Pro-Pro segment) and Gellman's group also compared (D)Pro-Xxx and (L)Pro-Xxx containing sequences and reassured the finding.[77] Several such studies have been undertaken by different research groups that highlight the importance of stereochemical patterning approach to design peptide based foldamers.[78]

1.15 Objective of the work

Broad investigations about the Ant-Pro motif established its credibility as a potent mimic of native β-turns. β-turns in biology display a backward hydrogen-bonding

pattern (1←4)-type involving four residues and are the candidates that preorganize the two polypeptide chains in a favorable geometry to render the *β*-hairpin/sheet secondary structure. The unusual pseudo-*β*-turn mimic is expected to nucleate inter-residual hydrogen-bonding *viz*. (i→i+1)-type C9- and (i-2←i+3)-type C17-networks, between the central and terminal residues, respectively, and it is anticipated to promote antiparallel beta sheet formation (Figure 17). Stereochemical variation is known to cause conformational modulation in different secondary structures.[78] Hence we also sought out to evaluate the competence of Ant-Pro reverse turn motif as a promoter of *β*-hairpin structure by means of chirality modulation in-and-around the turn segment in a tetrapeptide sequence.

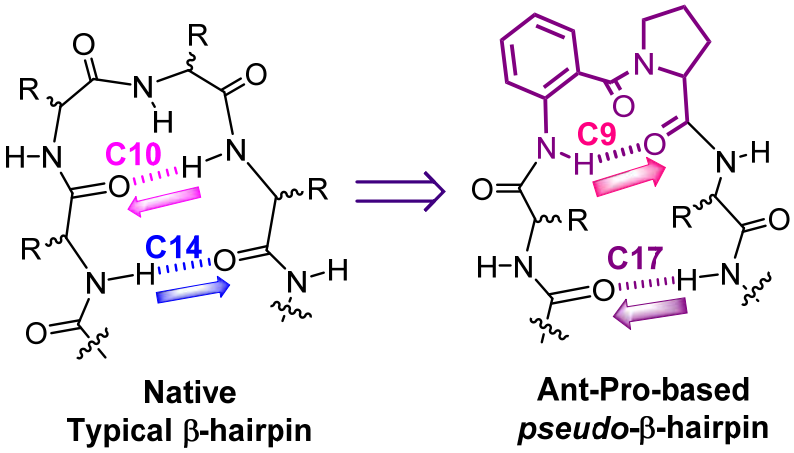

Figure 17: Schematic representation with *intramolecular* H-bonding patterns of a typical *β*-hairpin motif found in proteins (left) and plausible *pseudo-β*-hairpin featuring Ant-Pro reverse turn (right).

1.16 Design strategy

Configurational variation serves as good means for the assessment of stability and conformational pre-organisation of different peptide sequences. In this work, we have utilised stereochemically reordered amino acids in order to evaluate the hairpin nucleation tendency of the Ant-Pro *pseudo-β*-turn unit. We compared the structural features of a series of protected tetrapeptide sequences R_1CO-$^{L/D}$Val-Ant-$^{L/D}$Pro-$^{L/D}$Leu-NHR_2, comprising Ant-Pro turn motif at the loop region (Figure 18). Valine and leucine residues were selected on basis of their sheet promoting dihedral preferences. In order to carry out the solution phase investigations, pivaloyl-

protection was preferred so as to confer structural rigidity at the N-terminus and methylamide protection at C-terminus for a dispersed and distinct non-overlapping signal. Derivatives with varying stereochemical patterns of α-amino acids were synthesized such as LLL (homochiral) and DLL (*hetero*-chiral), LDL and DLD (alternate *hetero*-chiral) and their structural pre-disposition were expounded by means of solid and solution-state studies.

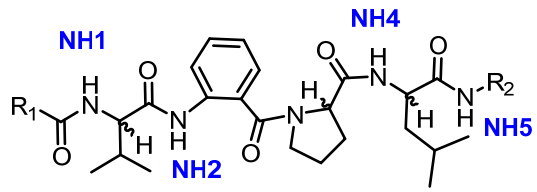

5 R_1= ^{t}Bu, R_2 =Me, {Piv-^{L}Val-Ant-^{L}Pro-^{L}Leu-NHMe}
6 R_1= ^{t}Bu, R_2 =Me, {Piv-^{D}Val-Ant-^{L}Pro-^{L}Leu-NHMe}
7 R_1= ^{t}Bu, R_2 =Me, {Piv-^{L}Val-Ant-^{D}Pro-^{L}Leu-NHMe}
8 R_1= ^{t}Bu, R_2 =Me, {Piv-^{D}Val-Ant-^{L}Pro-^{D}Leu-NHMe}

Figure 18: Designed Ant–Pro tetramers with chirality modulation.

1.17 Synthesis

Syntheses of all the tetrapeptide analogues **5-8** were carried out using conventional solution phase peptide synthesis under standard coupling conditions (scheme 2.3). Coupling reactions were carried out from N-terminus, in order to avert the formation of the benzoxazinone intermediate obtained on activation of anthranilic carboxylic group. After synthesizing dipeptides **11a**, **11c** and **11e**, the amine terminated dipeptides were coupled with Boc- protected anthranilic acid **12**, using HBTU as coupling agent and DIEA as base. The tripeptide analogue **13a** was deprotected and was coupled with Boc-^{L}Val-OH and Boc-^{D}Val-OH to afford **5a** and **6a**, respectively.

The N-terminus of tetrapeptide analogues were converted into their corresponding pivaloyl analogs **5c** and **6c**, which were then subjected to amidation using methylamine solution in methanol to afford **5** and **6**, respectively. Analogue **6f** was obtained by coupling acid counterpart **6e** with 4-bromoaniline.

Scheme 1.3: Synthesis of dipeptide and tripeptide units

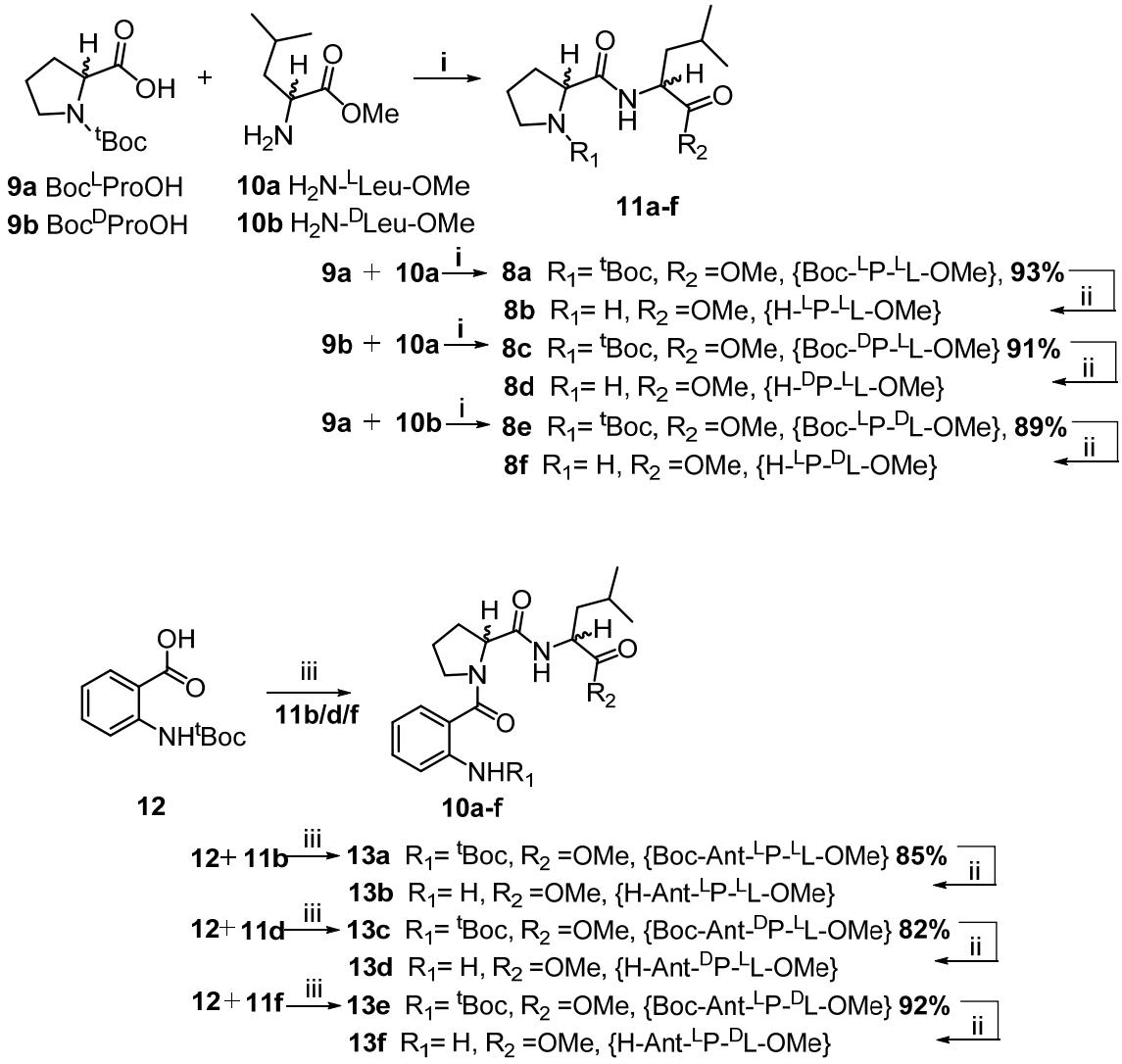

Reagents and conditions: (i) DCC, DMAP, DCM, 12h; (ii) TFA:DCM, 1:1, 2h; (iii) HBTU, DIEA, ACN, overnight.

For analogues **7** and **8**, the free amines **13d** and **13e** were subjected to coupling with phthalimide protected valine, the tetramers thus obtained were treated with methylamine solution in methanol for simultaneous phthalimide deprotection and methylamide conversion.

Scheme 1.4: Synthesis of tetrapeptide analogues **5** – **8**

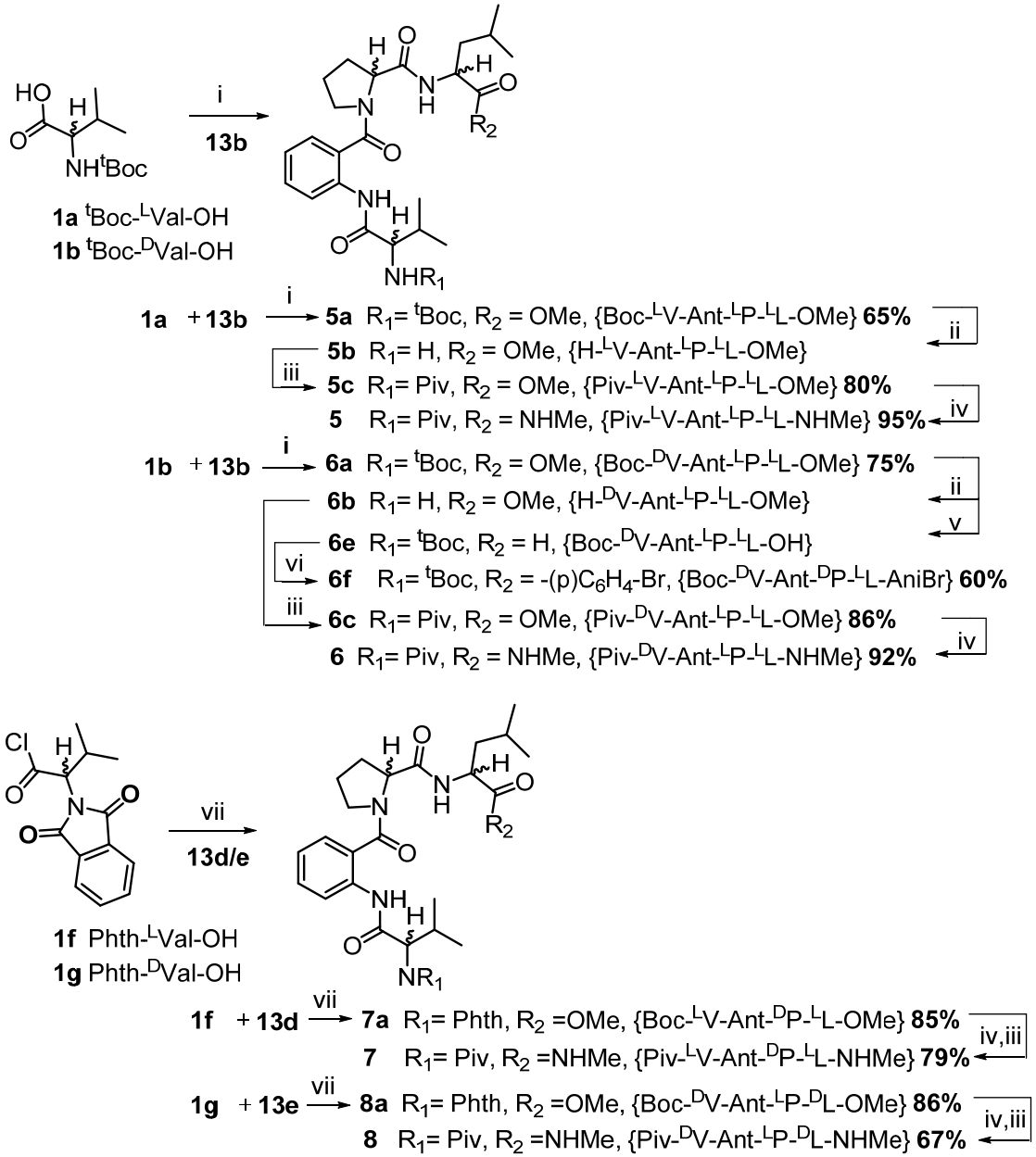

Reagents and conditions: (i) HBTU, DIEA, ACN, overnight; (ii) TFA:DCM, 1:1, 2h; (iii) Piv-Cl, Et_3N, dry DCM, rt, 4 h; (iv) methanolic methylamine, rt 2h; (v) LiOH, MeOH, rt, 12 h; (vi) H_2N-(p)C_6H_4-Br, HBTU, DIEA, DCM, 12h; (vii) TEA, DCM, 0 °C-rt, 1h.

1.18 Conformational analyses

Secondary structural analyses were accomplished by extensive solution state 2D NMR and CD studies and solid state X-ray diffraction studies.

1.18.1 Single crystal X-ray diffraction studies

Extensive efforts culminated in crystals of *hetero*-chiral DLL derivative **6f** (Figure 19). Crystal structure revealed presence of strong C9-turn between anthranilamide -NH3 and C=O of ^{L}Pro residue in i→i+1 forward direction supporting the earlier observations. Strikingly, it revealed presence of a 17-membered H-bonded ring between the C=O of ^{t}Boc- functionality of Val and the methylamide functionality of the Leu residue in i-2←i+3 reverse direction. The observed H-bond distances [d(N-H···O=C)] = 2.1 Å and H- bonding geometry of the C9- and C17- membered H-bonds are characterized by the angles (N-H···O) = 165° and 168°, respectively confirming equal strength for both the interactions.

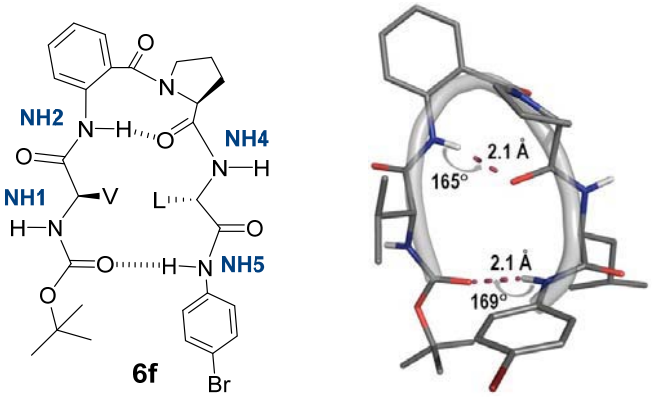

Figure 19: Molecular structure (left) and crystal structure (right) of analogue **6f** (Boc-^{D}Val-Ant-^{L}Pro-^{L}Leu-NH-(p)C_6H_4-Br).

1.18.2 NMR studies

The interactions arising from the folding pattern of peptide were explicitly evaluated by solution state NMR studies, which were undertaken for all the tetramer analogues **5-8**. First glimpse at the ^{1}H-NMR spectra ($CDCl_3$, 298 K) of all the anlogues unequivocally confirmed the presence of nine-membered H-bonding network from the appearance of anthranilamide protons about 9-9.5 ppm (Figure 20). Also a vague estimation of the presence of 17-membered H-bonding interaction could be gained from the chemical shift values of amide proton -NH5. The *homo*-chiral tetrapeptide **5** NH5 appears relatively upfield and broad revealing concentration dependence at 7.4 δ, clearly suggested the absence of terminal H-bonding interaction. The downfield chemical shifts exhibited by NH5 of all other

hetero-chiral analogues **6-8** appeared >7.9 ppm with consistant chemical shift values at different concentrations were indicating terminal H-bonding interaction.

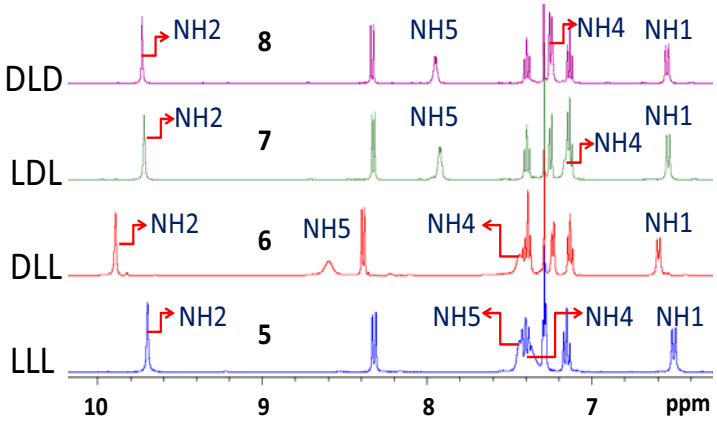

Figure 20. Comparison of chemical shift values of amide protons of all tetramer analogues.

To validate these interpretations, we carried out structural elucidation *via* solution state NMR studies (see experimental section, pages 87-97) to accrue further evidences. 2D NOESY experiments of all tetrapeptide sequences explicitly suggested the presence of C9- turn from the prominent NOE cross-peaks observed between the amide NH2 *vs* $P_{\delta}H$ protons (C17/17'H) and NH2 *vs* $P_{\alpha}H$ (C14H) due to the folding induced by the 9-membered H-bonding formation (Figure 21 c,e,h,k, respectively). Confirmatory diagnostic long-range dipolar coupling interactions resulting from 17- membered H-bonding network were validated by NOE cross-peaks arising spatial proximity between Piv- (C27H) *vs* methylamide NH5 and methyl (C25H) protons (Figure 21). The alternate *hetero*-chiral analogues **7** and **8** displayed intense cross-peaks owing to both these terminal contacts. But, in case of *homo*-chiral analogue **5** and *hetero*-chiral tetrapeptide **6**, corresponding long range NOEs were very weak in intensity. Contradictory to the expectations from the downfield shift in NMR spectrum, the 2D spectral interpretation of compound **6** revealed the partially bound state of NH5 with carbonyl of Piv- group. However, another medium dipolar coupling observed between NH5 and $Val_{\alpha}H$ confirmed the induction of a folded architecture in **6**. Examination of the strength of these H-bonded contacts from MeOD exchange studies caused differential solvation of amide NHs and caused protons to shift downfield that resisted NH/D exchange (see experimental section, page 79, Figure 24).[79]

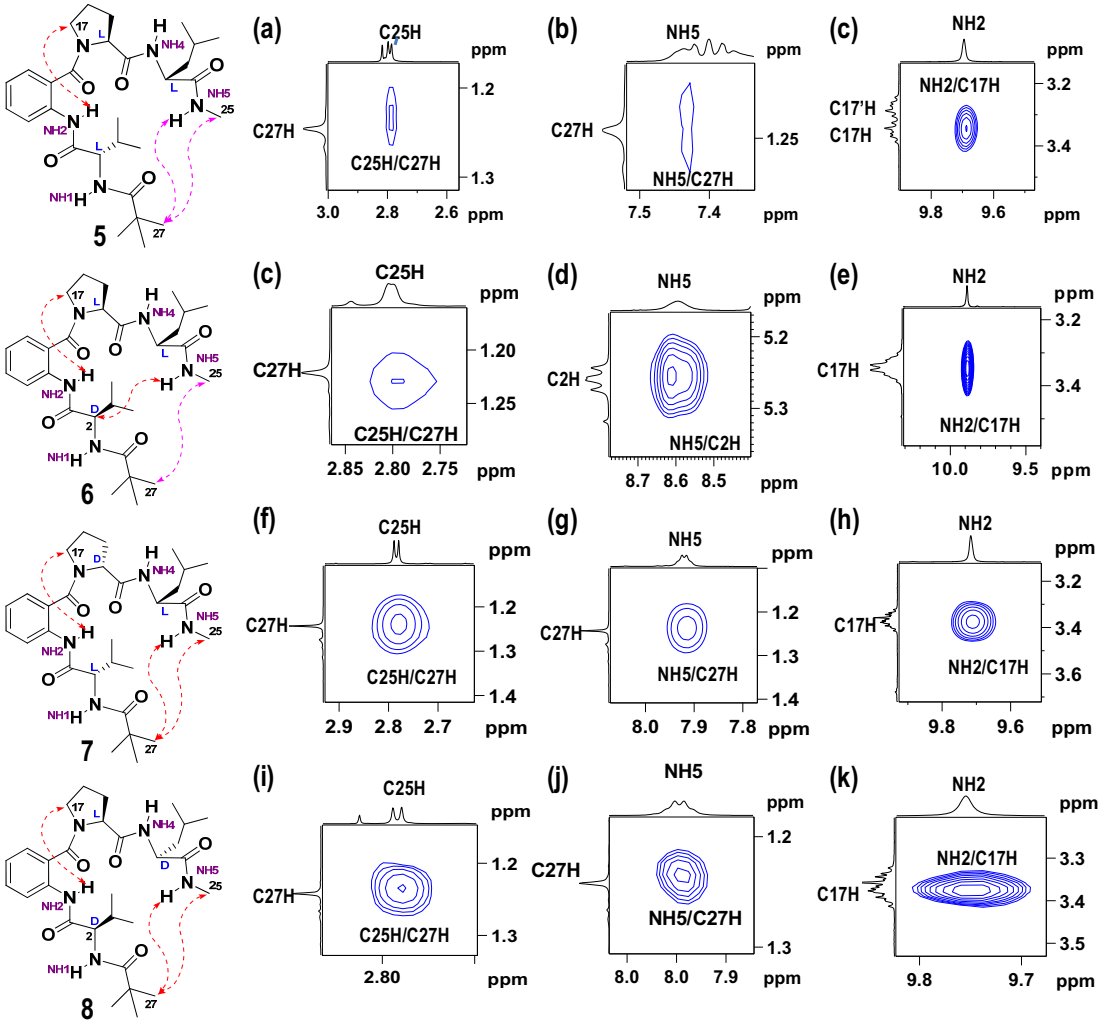

Figure 21. Selected NOE extracts from the 2D NOESY data of **5** ($CDCl_3$, 400 MHz), **6, 7** and **8** ($CDCl_3$, 500 MHz (a), (d), (f) & (i) Piv *vs* NH-$\underline{CH_3}$; (b), (g) & (j) NH_5 *vs* Piv; (c), (e), (h) & (k) NH_2 *vs* $Pro_{\delta}H$; (d) NH_5 *vs* $Val_{\alpha}H$.

Thus variable temperature NMR experiments for all tetrapeptide sequences were undertaken, from which strength of the H-bonds was evaluated (see experimental section, pages 83-84, Tables 6-9).[80] Especially, comparison of chemical shift values of –NH2 (anthranilamide involved in C9- turn formation) and –NH5 (methylamide proton that participates in C17- H-bonding network) were thoroughly examined. Strikingly, a considerably lower temperature coefficient ($\Delta\delta HN/\Delta T$) of ≈ -2.5 ppb/K was observed for NH2 of tetrapeptides **5** and **6**, but a poor value > -7.5 ppb/K for NH5 indicated solvent exposition of terminal amide proton. It is noteworthy that ($\Delta\delta HN/\Delta T$) lower than -4 ppb/K is indicative of strong *intra*-molecular hydrogen bonding. Strangely for **7** and **8**, comparable values of about -5 ppb/K for both NH2 and NH5 were obtained, revealing both amide protons in

equilibrium between hydrogen-bonded and non-hydrogen-bonded states. These observations indicated the fact that alternate *hetero*-chiral analogues **7** and **8** exhibit a better stereochemistry, with respect to compounds **5** and **6**, for possible hairpin nucleation.

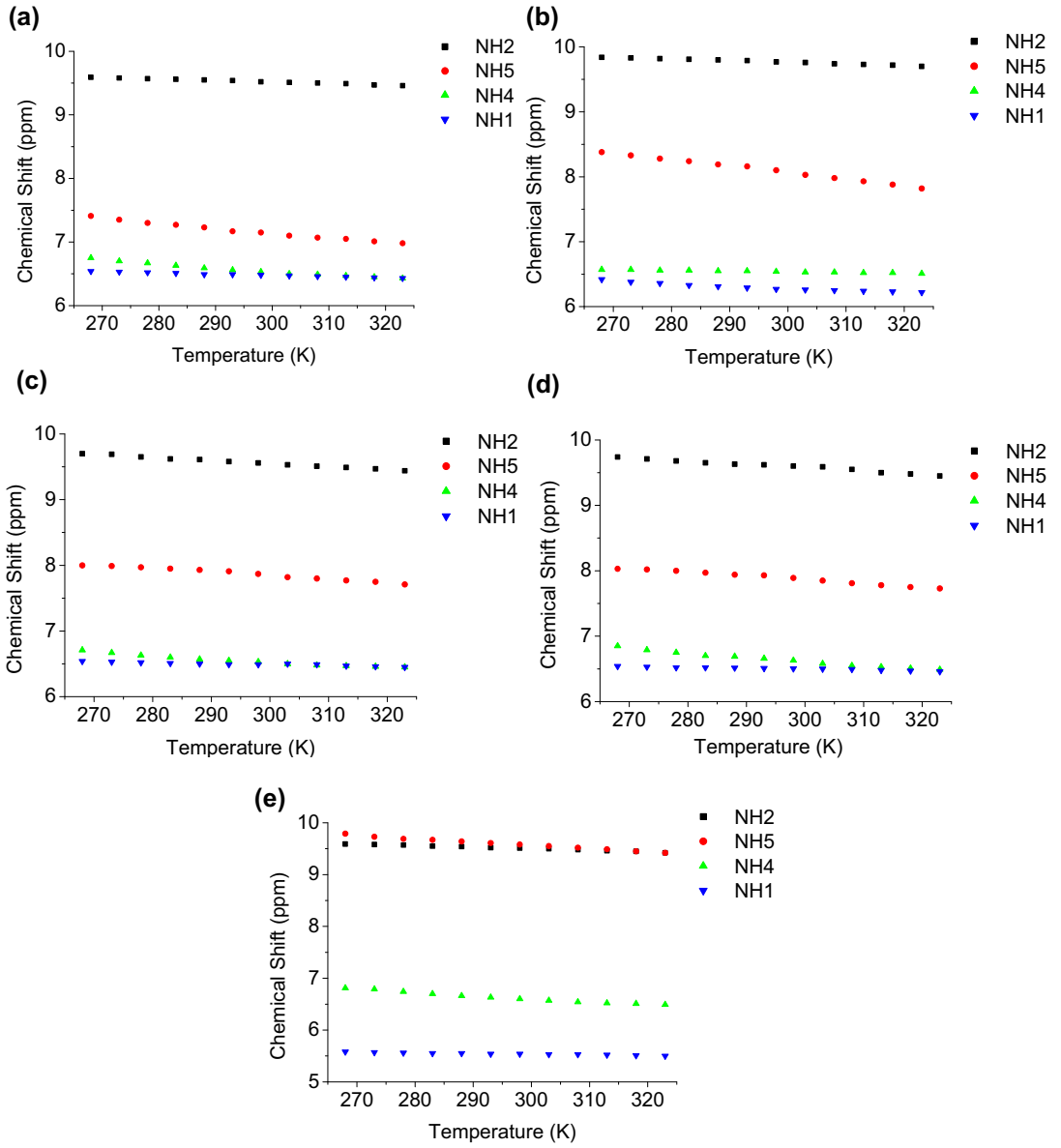

Figure 22: Variable temperature studies of tetrapeptides **5**-**8** (2 mM) and **6f** (15 mM).

Variable temperature study was undertaken for tetrapeptide **6f**, which strangely revealed temperature coefficient of -5.9 ppb/K, contradicting the observations of the strong terminal *intra*-molecular H-bonding contact apparent from its crystal structure (Figure 19). These observations presumably suggest the

predominance of packing effects in crystals. However, the collective interpretation of solution-state NMR studies suggest that though the *hetero*-chiral tetrapeptides **6f** and **6** reveal the sign of hairpin nucleation, the orientation of NH5 poorly drives the chains in parallel fashion.

Strangely, DMSO titration studies revealed no chemical shift dependence of the amide protons on addition of DMSO-d_6 except for amide proton NH4 (see experimental section, pages 78-79, Tables 2-5). The negligible ^{1}H NMR chemical shifts ($\Delta\delta$ NH: <0.15 ppm) observed for tetrapeptides **5** - **8** up on DMSO-d_6 titration studies (up to 10% of DMSO-d_6 in $CDCl_3$) (Figure 23) strongly supported the *intra*-molecular nature of hydrogen bonds in solution-state, suggesting polar solvent induced folding. This observation was further validated by CD spectra recorded in acetonitrile, in which tetrapeptide **5** revealed partial conformational ordering.

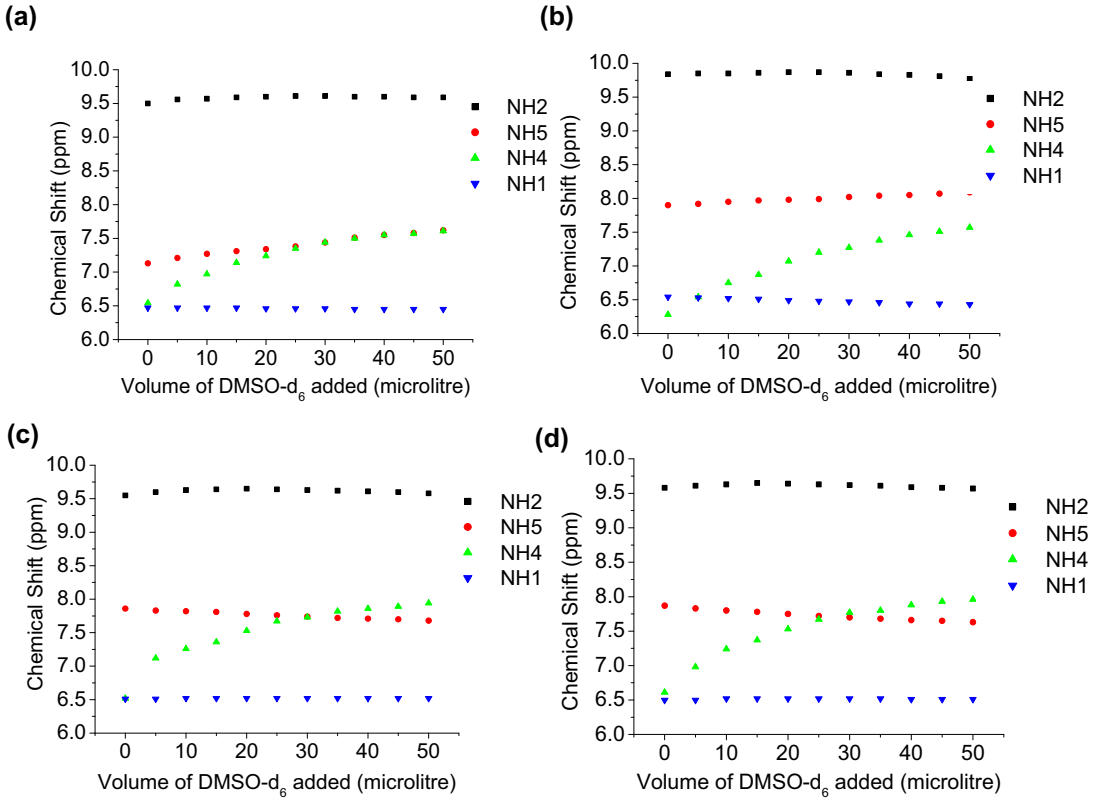

Figure 23: ^{1}H NMR DMSO-d_6 titration study of tetrapeptides **5** – **8** (2mM).

1.18.3 IR and CD studies

IR spectra of **7** and **8** displayed only one strong N-H stretch band about ≈ 3312 cm^{-1}, supporting all intramolecularly H- bonded amide protons. But, in case of both

tetrapeptides **5** and **6**, an additional intense absorption band about 3439 cm^{-1} confirms the availability of amide protons for intermolecular contacts (see experimental section, pages 81-82).[78a] Unlike tetrapeptide **5**, which exhibits no sharp bands representing NH stretching, analogue **6** features strong absorption band at 3314 cm^{-1}, confirming a partially bound state. CD spectra were recorded in non-polar solvent like 2,2,2-triflouroethanol (TFE) and a polar competing solvent like acetonitrile (Figure 24). A maxima *ca.* 218 nm revealing conformational ordering was observed for analogues **6**-**8** in both solvents, with alternate *hetero*-chiral analogues **7** and **8** featuring exact mirror image of the absorption peaks. But, analogue **5** displayed totally dissimilar CD signatures on solvent variation showing no defined cotton effect. Intense absorbance peaks around 250 nm appeared due to backbone aromatic groups/aromatic electronic transitions.

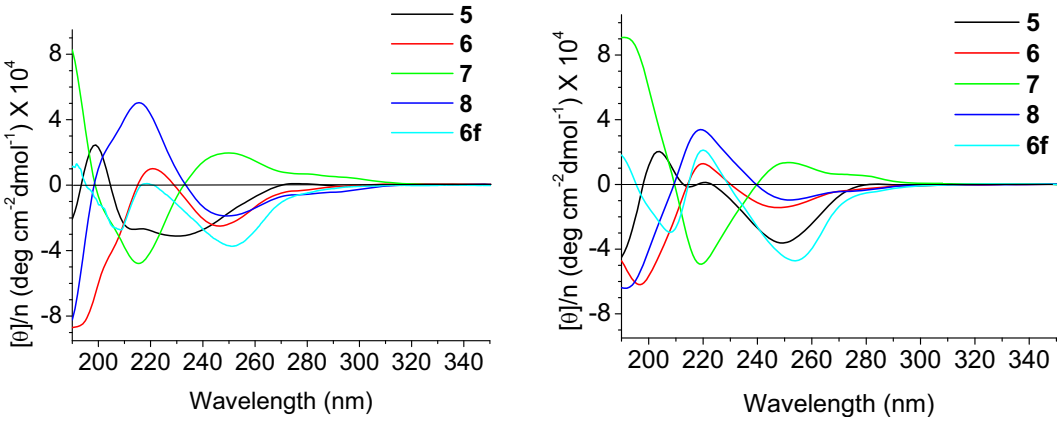

Figure 24. Comparison of CD spectra of tetramer analogues **5**-**8** and **6f** in TFE (left) and acetonitrile (right), respectively.

1.19 Conclusions

In conclusion, we have successfully evaluated the fundamental requisites for the design of a novel *pseudo*-*β*-hairpin mimic. Even though *hetero*-chiral tetrapeptides **6** and **6f** reveal the sign of hairpin nucleation, the observations demonstrated that alternate *hetero*-chiral sequences **7** and **8** exhibit the best hairpin nucleation propensity. We anticipate that this understanding will deeply benefit in development and expansion in the locale of *β*-hairpin mimetics.

1.20 Experimental section

Crystal Data: Data for the compounds were collected at T = 296 K, on SMART APEX CCD Single Crystal X-ray diffractometer using Mo-Kα radiation (λ = 0.7107 Å) to a maximum θ range of 25.00°. The structures were solved by direct methods using SHELXTL. All the data were corrected for Lorentzian, polarization and absorption effects. SHELX-97 (ShelxTL) was used for structure solution and full matrix least squares refinement on F^2. Hydrogen atoms were included in the refinement as per the riding model. The refinements were carried out using SHELXL-97.

Crystal data for 3a: Single crystals of **3a** were grown by slow evaporation of the solution mixture of ethyl acetate and pet-ether. Colorless needle type crystal of approximate size 0.45 x 0.12 x 0.07 mm^3, was used for data collection, Quadrant data acquisition, Total scans = 4, total frames = 2424, θ range = 1.72 to 25.00°, completeness to θ of 24.99 º is 99.9 %, $C_{28}H_{35}BrN_4O_5$, M = 587.51. Crystals belong to Orthorhombic, space group $P2_12_12_1$, a = 7.7067(3), b = 12.9597(6), c = 29.2017(12) Å, V = 2916.6(2) $Å^3$, Z = 4, Dc = 1.338 g/cc, μ (Mo–Kα) = 1.452 mm^{-1}, 28137 reflections measured, 5117 unique [I>2σ(I)], R value 0.0414, wR_2 = 0.1026, largest diff. peak and hole 0.484 and -0.335 e. $Å^{-3}$.

Crystal data for 3b: Single crystals of **3b** were grown by slow evaporation of the solution mixture of ethyl acetate and pet-ether. Colorless needle type crystal of approximate size 0.25 x 0.09 x 0.01 mm_3, was used for data collection, Hemisphere data acquisition. Total scans = 3, total frames = 1271, θ range = 2.07 to 25.00°, completeness to θ of 25.00 º is 99.7 %, $C_{28}H_{35}BrN_4O_5$, M = 587.51. Crystals belong to Monoclinic, space group $P2_1$, a = 11.7520(7), b = 9.1568(6), c = 13.7591(9) Å, V = 1445.55(16) Å3, Z = 2, Dc = 1.350 g/cc, μ (Mo–Kα) = 1.464 mm^{-1}, 7234 reflections measured, 4793 unique [I>2σ(I)], R value 0.0314, wR_2 = 0.0693, largest diff. peak and hole 0.489 and -0.207 e. $Å^{-3}$.

Crystal data of 6f. Single crystals of **6f** were grown by slow evaporation of the solution mixture of ethyl acetate and pet-ether. Colorless needle-type crystal of approximate size 0.26 x 0.21 x 0.03 mm^3, was used for data collection. Total runs = 3,

total frames = 1265, θ range = 2.13 to 25.00°, completeness to θ of 25.00 º is 99.9 %, $C_{34}H_{46}BrN_5O_5$, M = 702.69. Crystals system: Orthorhombic, space group $P2_12_12_1$, a = 9.6704(5), b = 9.8238(6), c = 38.263(2) Å, V = 3634.9(3) Å^3, Z = 4, D_c = 1.280 g/cc, μ (Mo–Kα) = 1.179 mm^{-1}, 46085 reflections measured, 6400 unique reflections, 5166 observed [I>2σ(I)], R value 0.0447, wR_2 = 0.1143, largest diff. peak and hole 0.45 and -0.21 e. Å^{-3}.

2-(2-*tert*-Butoxycarbonylamino-3-methyl-butyrylamino)-benzoic acid methyl ester 2a:

A solution containing Boc ^{L}Valine (4 g, 18.34 mmol) and 2-methyl anthranilate (2.22 mL, 14.67 mmol) in DCM was cooled to 0 ^{o}C. DCC (4.54 g, 22 mmol) and a catalytic amount of HOBt were added to the reaction mixture, and stirred at 0 °C for 10 min and then at room temperature for 12 h. The solvent was stripped off under reduced pressure and the residue was taken in ether and subjected to filtration to remove the insoluble DCU. The organic layer was washed sequentially with sat. $NaHCO_3$ solution followed by sat. $KHSO_4$ solution, water and brine. The organic layer was dried over anhydrous Na_2SO_4, and the crude product obtained on the removal of solvent under reduced pressure was purified by column chromatography (93:7 pet. ether/ethyl acetate, *Rf*: 0.3) to afford **2a** (4.85 g, 75%) as a white solid. mp: 146-147 °C; $[\alpha]^{27}_D$:-36.396° (c = 1, $CHCl_3$); IR ($CHCl_3$) ν (cm^{-1}): 3442, 3019, 2935, 2400, 1698, 1650, 1590, 1524, 1501, 1395, 1394, 1215, 1045; ^{1}H NMR (200 MHz, $CDCl_3$) δ: 11.51 (s, 1H), 8.77-8.72 (dd, J = 8.59, 0.89 Hz, 1H), 8.06-8.01 (dd, J = 7.96, 1.51 Hz, 1H), 7.59-7.5 (m, 1H), 7.14-7.06 (m, 1H), 5.22-5.17 (d, J = 8.33 Hz, 1H), 4.29-4.20 (m, 1H), 3.93 (s, 3H), 2.43-2.27 (m, 2H), 1.48 (s, 9H), 1.07-1.03 (d, J = 6.83 Hz, 3H), 0.97-0.94 (d, J = 6.83 Hz, 3H); ^{13}C NMR (50 MHz, $CDCl_3$) δ: 170.8, 168.4, 155.7, 140.9, 134.5, 130.8, 122.7, 120.2, 115.2, 79.8, 60.9, 52.3, 30.9, 28.2, 19.3, 17.3; ESI-MS: 351.4256 $(M+H)^+$; 373.4204 $(M+Na)^+$; Elemental analysis calculated for $C_{18}H_{26}N_2O_5$: C, 61.70; H, 7.48; N, 7.99; Found: C, 61.59; H, 7.62; N, 7.84.

General method for Boc deprotection

A solution containing the Boc-peptide (3 mmol) was subjected to deprotection using DCM/TFA (50%, 10 mL) at 0°C. After completion of the reaction (~2 h), the reaction

mixture was stripped off the solvent, neutralized with saturated sodium bicarbonate solution, diluted with DCM and the product was repeatedly extracted into dichloromethane (3 x 10 mL). The organic layer was dried over anhydrous Na_2SO_4. The crude product, obtained after evaporating the solvent under reduced pressure, was used for the next step without further purification.

General method for methyl ester hydrolysis:

To the solution of ester (10 mmol) in methanol, $LiOH \cdot H_2O$ (40 mmol) was added in water (12 mL) at 0°C, and the reaction mixture was stirred for 4 h. After the complete consumption of the starting material, the solvent was evaporated under reduced pressure, and the free acid was liberated by treating with sat. $KHSO_4$ solution followed by extraction with DCM (2 X 25 mL). The corresponding crude acid derivatives obtained after evaporation of the solvent under reduced pressure were carried forward for the next reaction, without further purification.

(S)-*tert*-butyl2-(4-bromophenylcarbamoyl)pyrrolidine-1-carboxylate 2e:

To a solution of Boc ^{L}Proline (5g, 23.2 mmol) in dry MeCN, 4-bromo aniline (4.39 g, 25.5 mmol), EDC.HCl (5.34 g, 27.9 mmol), DMAP (3.4 g, 27.9 mmol), and catalytic amount of HOBt were added at 0 ^{o}C and stirred for 15 min. The reaction mixture was then stirred at room temperature for 12 h. The solvent was evaporated and the residue was dissolved in DCM (25 mL) and washed with sat. $NaHCO_3$ solution followed by sat. $KHSO_4$ solution, water and brine. The organic layer was dried over anhydrous Na_2SO_4 and evaporated under reduced pressure to get the crude product which on purification by column chromatography, (eluent: pet. ether/ethyl acetate 80:20, *Rf*: 0.6) afforded **2e** as a white solid (7.2 g, 84%); mp: 197-198 °C; $[\alpha]^{25}_{D}$: -94° (*c* = 1, $CHCl_3$); IR ($CHCl_3$) ν (cm^{-1}): 3318, 3122, 2977, 1668, 1591, 1539, 1490, 1397, 1366, 1302, 1289, 1247, 1162, 1127, 1073; ^{1}H NMR (200 MHz, $CDCl_3$) δ: 9.66 (s, 1H), 7.42 -7.38 (m, 4H), 4.47 (bs, 1H), 3.45 (bs, 2H), 2.46-1.93 (m, 1H), 1.49 (m, 1H); ^{13}C NMR (50 MHz, $CDCl_3$) δ: 170.4, 156.0, 137.5, 131.5, 120.8, 116.0, 80.7, 60.3, 47.1, 28.3, 24.4; ESI-MS: 369.2641 $(M+H)^+$; 391.2549 $(M+Na)^+$; 409.2371 $(M+K)^+$; Elemental analysis calculated for $C_{16}H_{21}N_2O_3Br$: C, 52.04; H, 5.73; N, 7.59; Found: C, 52.14; H, 5.77; N, 7.45.

2-(2-*tert*-Butoxycarbonylamino-3-methyl-butyrylamino)-benzoic acid methyl ester 2c:

Compound **2c** was synthesized by similar way as that of **2a**. The product **2c** was obtained as white solid (80%); mp: 97- 98 °C; $[\alpha]^{27}_{D}$: 27.50° (*c* = 1, $CHCl_3$); IR ($CHCl_3$) ν (cm^{-1}): 3442, 3019, 2935, 2400, 1698, 1650, 1590, 1524, 1501, 1395, 1394, 1215, 1045; ^{1}H NMR (200 MHz, $CDCl_3$) δ: 11.5 (s, 1H), 8.76-8.72 (d, *J* = 8.05 Hz, 1H), 8.05-8.01 (dd, *J* = 8.04, 0.93 Hz, 1H), 7.57-7.50 (m, 1H), 7.13-7.05 (m, 1H), 5.22-5.18 (m, 1H), 4.28-4.2 (m, 1H), 3.92 (s, 3H), 2.39-2.30 (m, 1H), 1.47 (s, 9H), 1.06-1.03 (d, *J* = 6.88 Hz, 3H), 0.97-0.93 (d, *J* = 6.92 Hz, 3H); ^{13}C NMR (100 MHz, $CDCl_3$) δ: 170.8, 168.4, 155.7, 140.9, 134.5, 130.8, 122.7, 120.2, 115.2, 79.8, 60.9, 52.3, 30.9, 28.3, 19.4, 17.3; ESI-MS: 351.2807 $(M+H)^+$; 373.2709 $(M+Na)^+$; 389.2405 $(M+K)^+$; Elemental analysis calculated for $C_{18}H_{26}N_2O_5$: C, 61.70; H, 7.48; N, 7.99; Found: C, 62.32; H, 7.37; N, 7.89.

(1-{2-[2-(4-Bromo-phenylcarbamoyl)-pyrrolidine-1-carbonyl]-phenylcarbamoyl} -2-methyl-propyl)-carbamic acid *tert*-butyl ester 3a:

To a solution of **2a** (0.1g, 29.7 mmol) and **2f** (0.079 g, 0.2976 mmol) in DCM maintained at 0 °C, DIEA (0.052 mL, 0.3571 mmol) and HBTU (0.135 g, 0.3571 mmol) were added. The reaction mixture was stirred at 0 °C for 10 min and then at room temperature for 12 h. The organic layer was washed sequentially with sat. $NaHCO_3$ solution followed by sat. $KHSO_4$ solution, water and brine. The organic layer was dried over anhydrous Na_2SO_4 and the crude product was subjected to column purification (60:40 pet. ether/ethyl acetate, *Rf*: 0.3) to furnish **3a** as a white solid (0.104 g, 60%); mp:198-199 °C; $[\alpha]^{25}_{D}$: -285.68° (*c* = 1, $CHCl_3$); IR ($CHCl_3$) ν (cm^{-1}): 3303, 3121, 2932, 2876, 1676, 1617, 1543, 1490, 1427, 1397, 1366, 1301, 248, 1163, 1163; ^{1}H (200 MHz, $CDCl_3$) δ: 9.71 (s, 1H), 9.57 (s, 1H), 8.52-8.48 (d, *J* = 8.21 Hz, 1H), 7.49-7.4 (m, 1H), 7.35-7.29 (m, 3H), 7.19-7.12 (m, 3H), 5.33-5.29 (d, *J* = 9.22 Hz, 1H), 4.99-4.92 (m, 1H), 4.51-4.44 (m, 1H), 3.66- 3.54 (m, 1H), 3.42-3.31 (m, 1H), 2.41-1.82 (m, 7H), 1.40 (s, 9H), 1.08-1.05 (d, *J* = 6.69 Hz, 3H), 1.0-0.96 (d, *J* =6.70 Hz, 3H); ^{13}C NMR (50 MHz, $CDCl_3$) δ: 171.8, 170.4, 168.7, 165.7, 155.8, 137.1, 135.0, 131.3, 130.8, 126.4, 126, 123.8, 121.4, 121.2, 116.4, 60.9, 59.9, 31.4, 29.7, 28.2, 25.1, 19.4, 17.5; ESI-MS: 609.8739 $(M+Na)^+$; Elemental analysis calculated for $C_{28}H_{35}BrN_4O_5$: C, 57.24; H, 6.00; N, 9.54; Found: 57.39; H, 5.88; N, 9.76.

(1-{2-[2-(4-Bromo-phenylcarbamoyl)-pyrrolidine-1-carbonyl]-phenylcarbamoyl} -2-methyl-propyl)-carbamic acid *tert*-butyl ester 3b:

Compound **3b** was synthesized by similar way as that of **3a**. White solid (56%); mp: 197-198 °C, $[\alpha]^{25}_{D}$: -105.3° (*c* = 0.11, $CHCl_3$); IR ($CHCl_3$) ν (cm^{-1}): 3303, 3121, 2932, 2876, 1676, 1617, 1543, 1490, 1427, 1397, 1366, 1301, 248, 1163, 1163; ^1H NMR (200 MHz, $CDCl_3$) δ: 9.78 (s, 1H), 9.29 (s, 1H), 8.54-8.50 (d, *J* = 8.21 Hz, 1H), 7.47-7.39 (m, 4H), 7.18-7.14 (m, 3H), 5.9-5.86 (d, *J* = 9.1 Hz, 1H), 4.98-4.91 (m, 1H), 4.44-4.36 (t, *J* = 7.58 Hz, 1H), 3.57-3.42 (m, 2H), 2.44-1.79 (m, 7H), 1.41 (s, 9H), 1.04-0.98 (m, 6H); ^{13}C NMR (50 MHz, $CDCl_3$) δ: 171.5, 170.4, 168.6, 165.7, 155.6, 136.8, 134.7, 131.3, 130.6, 125.9, 125.8, 123.7, 121.1, 116.6, 79.4, 61.0, 60.8, 49.5, 38.5, 31.3, 29.9, 28.2, 24.9, 19.2, 17.9; ESI-MS: 588.0416 $(M+H)^+$; 590.0733 $(M+H)^+$, 610.0925 $(M+Na)^+$; 612.0887 $(M+Na)^+$; Elemental analysis calculated for $C_{28}H_{35}BrN_4O_5$: C, 57.24; H, 6.00; N, 9.54; Found: C, 57.38; H, 6.21; N, 9.23.

benzyl (2-((((9H-fluoren-9-yl)methoxy)carbonyl)amino)benzoyl)-L-prolinate 4a:

To a solution of Fmoc-Ant-OH **1f** (0.4g, 1.138 mmol, 1equiv.) and HN-^{L}Pro-OBn **1g** (0.28 g, 1.366 mmol, 1.2 equiv.) in THF maintained at 0 °C, DIEA (0.256 mL, 1.479 mmol, 1.3 equiv.) and HBTU (0.517 g, 1.3658 mmol, 1.2 equiv.) were added. The reaction mixture was stirred at 0 °C for 10 min and then at room temperature for 12 h. The organic layer was washed sequentially with sat. $NaHCO_3$ solution followed by sat. $KHSO_4$ solution, water and brine. The organic layer was dried over anhydrous Na_2SO_4 and the crude product was subjected to column purification (80:20 pet. ether/ethyl acetate, *Rf*: 0.3) to furnish **4a** as a sticky solid (0.46 g, 74%); $[\alpha]^{25}_{D}$: -29.848° (*c* = 0.5, $CHCl_3$); IR ($CHCl_3$) ν (cm^{-1}): 3362, 3020, 2400.6, 1733, 1624, 1598, 1524, 1422, 1045, 929; ^1H (200 MHz, $CDCl_3$) δ: 8.73 (s, 1H, amide), 8.24-8.20 (d, *J* = 8.08 Hz, 1H), 7.79-7.69 (m, 4H), 7.46-7.31 (m, 11H), 7.12-7.05 (d, *J* = 7.33 Hz, 1H), 5.26 (s, 1H), 4.84-4.77 (m, 1H), 4.47-4.43 (m, 2H), 4.32-4.25 (m, 1H), 3.66-3.44 (m, 2H), 2.48-2.30 (m, 1H), 2.15-1.87 (m, 1H); ^{13}C NMR (50 MHz, $CDCl_3$) δ: 172.0, 168.6, 153.7, 143.9, 143.8, 141.2, 136.4, 135.5, 131.0, 128.6, 128.3, 128.1, 127.7, 127.1, 125.3, 124.2, 122.4, 120.2, 119.9, 67.3, 37.2, 59.1, 49.7, 47.0, 29.3, 25.2; LC-MS: 546.91 $(M+H)^+$, 568.89 $(M+Na)^+$, 584.93 $(M+K)^+$; Elemental analysis

calculated for $C_{34}H_{30}N_2O_5$: C, 74.71; H, 5.53; N, 5.12; Found: C, 74.69; H, 5.69; N, 5.04.

(2-((((9H-fluoren-9-yl)methoxy)carbonyl)amino)benzoyl)-L-proline 4b:

Compound **4a** (0.1g) was dissolved in 33% w/w HBr in AcOH (2 mL) under anhydrous conditions and stirred in an inert atmosphere. After completion of the reaction, HBr and AcOH were removed in vacuo. The reaction mixture was dissolved in EtOAc and was washed sequentially with sat. $NaHCO_3$ solution followed by sat. $KHSO_4$ solution, water and brine. The organic layer was dried over anhydrous Na_2SO_4 and the crude product was subjected to column purification (55:45 pet. ether/ethyl acetate, *Rf*: 0.3) to furnish **4b** as a white fluffy solid (0.07 g, 72%); mp:73-75 °C; $[\alpha]^{25}_D$: -43.4° (*c* = 0.5, $CHCl_3$); IR ($CHCl_3$) ν (cm^{-1}): 3431 (broad), 3020, 2400, 2090, 1635, 1526, 1452, 1419, 1301, 1218, 1113, 1041; ^1H (200 MHz, $CDCl_3$) δ: 9.47 (s, 1H, amide), 8.57 (s, 1H, amide), 8.02-7.98 (d, *J* = 7.33 Hz, 1H), 7.85-7.62 (d, *J* = 7.33 Hz, 1H), 7.54-7.50 (m, 2H), 7.31-7.11 (m, 7H), 6.91-6.83 (d, *J* = 7.45 Hz, 1H), 4.62-4.55 (m, 1H), 4.3-4.26 (m, 2H), 4.18-4.11 (m, 1H), 3.27- 3.21 (m, 2H), 2.25-2.11 (m, 1H), 1.91-1.63 (m, 3H); ^{13}C NMR (50 MHz, $CDCl_3$) δ: 175.4, 168.8, 153.9, 143.7, 143.6, 141.1, 136.0, 130.9, 127.6, 127.0, 126.9, 125.3, 124.3, 122.6, 120.4, 119.8, 67.3, 58.9, 49.6, 46.8, 29.1, 25.0; LC-MS/MS: 457.20 $(M+H)^+$, 479.18 $(M+Na)^+$, 495.14 $(M+K)^+$; Elemental analysis calculated for $C_{27}H_{24}N_2O_5$: C, 71.04; H, 5.30; N, 6.14; Found: C, 71.24; H, 5.05; N, 6.10.

General method for the synthesis of compounds 11a, 11c and 11e.

(*R*)-*tert*-butyl 2-(((*S*)-1-methoxy-4-methyl-1-oxopentan-2-yl)carbamoyl) pyrrolidine-1-carboxylate 11c.

Compound **11c** was synthesized by the reported procedure. Purification by column chromatography (eluent: 10:90 ethyl acetate/pet. ether, R_f: 0.5) afforded **11c** as a colorless white solid (91%). mp: 124-125 ^oC; $[\alpha]^{26.4}_D$: 58.488° (*c* = 0.5, $CHCl_3$); IR ($CHCl_3$, ν (cm^{-1}): 3422, 3307, 3083, 2959, 2932. 1741, 1690, 1537, 1453, 1392, 1245, 1216, 1124, 1090, 1017, 980; ^1H NMR ($CDCl_3$/200MHz): δ ppm $7.02_{rotamer}$ (b, 0.4H, amide), $6.38_{rotamer}$ (b, 0.6H, amide), 4.63 (b, 1H), 3.72 (s, 3H), 3.49 (b, 2H), 2.16 (b, 1H), 1.94-1.86 (m, 3H), 1.71-1.60 (m, 4H), 1.46 (s, 9H), $0.94\text{-}0.92_{rotamer}$ (m, 4H), $0.85\text{-}0.82_{rotamer}$ (m, 2H); ^{13}C NMR ($CDCl_3$,50MHz): δ ppm 173.7, 173.3, 153.4, 80.5, 52.2, 50.5, 47.1, 41.5, 33.9, 28.3, 24.9, 24.7, 22.9, 21.7; LC-MS: 364.93 $(M+Na)^+$, 380.90

$(M+K)^+$; Elemental Analysis calculated for $C_{17}H_{30}N_2O_5$: C, 59.63; H, 8.83; N, 8.18; Found: C, 59.60; H, 8.70; N, 8.10.

General method for the synthesis of compounds 13a, 13c and 13e.

(*S*)-methyl 2-((*S*)-1-(2-((*tert*-butoxycarbonyl)amino)benzoyl) pyrrolidine-2-carboxamido)-4-methylpentanoate 13a.

To a solution of compound **11b** (1.8 g, 7.258 mmoles) and Boc-Ant-OH (1.37 g, 5.806 mmoles, 0.8 equiv) in DCM (30 mL), DIPEA (1.89 mL, 10.887 mmol, 1.5 equiv) and HBTU (3.3 g, 8.709 mmol, 1.2 equiv) were added at 0 ^oC. After 12 h, the reaction mixture was diluted with DCM (30 mL) and washed sequentially with saturated solutions of $NaHCO_3$ (20 mL), water (20 mL) and $KHSO_4$ (20 mL). The washings were extracted with DCM (10 mL x 3) and the combined organic layer was dried over anhydrous Na_2SO_4 and evaporated under reduced pressure to obtain the crude residue, which was purified by column chromatography (eluent: 30% AcOEt/pet. Ether, R_f: 0.3) to afford **13a** as a waxy solid (2.3 g, 85%). $[\alpha]^{25.3}_D$: -121.10° (*c* = 1, $CHCl_3$); IR ($CHCl_3$, ν (cm^{-1}): 3364, 3020, 2977, 2401, 1725, 1683, 1624, 1521, 1417, 1159, 1046, 929; ^1H NMR ($CDCl_3$/200MHz): δ ppm 8.35 (s, 1H, amide), 8.17-8.13 (d, *J* = 8.34Hz, 1H), 7.41-7.31 (m, 2H), 7.04-6.92 (m, 2H), 4.81-4.74 (m, 1H), 4.66-4.54 (m, 1H), 3.73 (s, 3H), 3.57-3.47 (m, 2H), 2.33-1.78 (m, 4H), 1.71-1.60 (m, 2H), 1.50 (s, 9H), 0.93-0.88 (m, 6H); ^{13}C NMR ($CDCl_3$, 50MHz): δ ppm 173.2, 170.9, 168.9, 153.0, 137.2, 131.0, 127.4, 123.6, 121.8, 120.4, 80.4, 59.6, 52.2, 50.9, 50.6, 41.2, 28.3, 27.7, 25.3, 24.8, 22.7, 21.9; MALDI-TOF/TOF: 484.8722 $(M+Na)^+$; 500.8892 $(M+K)^+$; Elemental Analysis calculated for $C_{24}H_{35}N_3O_6$: C, 62.45; H, 7.64; N, 9.10; Found: C, 62.36; H, 7.56; N, 9.18.

(*S*)-methyl 2-((*R*)-1-(2-((*tert*-butoxycarbonyl)amino)benzoyl) pyrrolidine-2-carboxamido)-4-methylpentanoate 13c.

Compound **13c** was synthesized following the procedure for **13a**. The crude product was purified by column chromatography (eluent: 30% AcOEt/pet. Ether, Rf: 0.3) to furnish **13c** (82%) as a waxy solid. $[\alpha]^{25.9}_D$: 111.728° (*c* = 1, $CHCl_3$); IR ($CHCl_3$, ν (cm^{-1}): 3355, 3017, 2975, 2897, 2401, 1724, 1683, 1625, 1590,1521, 1413, 1158, 1050, 928; ^1H NMR ($CDCl_3$/200MHz): δ ppm 8.23 (s, 1H, amide), 8.11-8.07 (d, *J*=8.34Hz, 1H), 7.42-7.27 (m, 3H), 7.08-7.01 (m, 1H), 4.90-4.84 (m, 1H), 4.67-4.58 (m, 1H), 3.70 (s, 3H), 3.60-3.48 (m, 2H), 2.46-2.38 (m, 1H), 2.15-1.82 (m, 4H), 1.70-1.60 (m, 2H), 1.50 (s, 9H), 0.95-0.93 (m, 6H); ^{13}C NMR ($CDCl_3$, 50MHz): δ ppm

173.3, 170.9, 170.2, 153.1, 136.9, 131.0, 127.5, 124.3, 122.2, 121.1, 80.4, 59.2, 52.3, 50.9, 50.3, 49.0, 41.2, 28.3, 27.0, 25.2, 24.9, 22.8, 21.7; MALDI-TOF/TOF: 485.0148 $(M+Na)^+$; 501.0496 $(M+K)^+$; Elemental Analysis calculated for $C_{24}H_{35}N_3O_6$: C, 62.45; H, 7.64; N, 9.10; Found: C, 62.36; H, 7.56; N, 9.18.

(*S*)-methyl 2-((*R*)-1-(2-((*tert*-butoxycarbonyl)amino)benzoyl) pyrrolidine-2-carboxamido)-4-methylpentanoate 13e.

Compound **13e** was synthesized following the procedure for **13a**. The crude product was purified by column chromatography (eluent: 30% AcOEt/pet. Ether, Rf: 0.3) to furnish **13e** (92%) as a waxy solid. $[\alpha]^{26.1}_D$: -112.868° (*c* = 1, $CHCl_3$); IR ($CHCl_3$, ν (cm^{-1}): 3348, 3018, 2897, 2401, 1724, 1682, 1625, 1590,1520, 1412, 1369, 1158, 1052, 928; ^1H NMR ($CDCl_3$/200MHz): δ ppm 8.23 (s, 1H, amide), 8.10-8.06 (d, *J*=8.34Hz, 1H), 7.41-7.27 (m, 3H), 7.07-7.00 (m, 1H), 4.89-4.80 (m, 1H), 4.66-4.55 (m, 1H), 3.69 (s, 3H), 3.53-3.44 (m, 2H), 2.45-2.32 (m, 1H), 2.15-1.82 (m, 4H), 1.69-1.55 (m, 2H), 1.49 (s, 9H), 0.94-0.91 (m, 6H); ^{13}C NMR ($CDCl_3$, 50MHz): δ ppm 173.3, 170.9, 170.1, 153.1, 136.9, 131.0, 127.5, 124.2, 122.2, 121.0, 80.4, 59.2, 52.3, 50.8, 50.3, 41.2, 28.3, 27.0, 25.2, 24.8, 22.8, 21.7; MALDI-TOF/TOF: 484.8722 $(M+Na)^+$; 500.8892 $(M+K)^+$; Elemental Analysis calculated for $C_{24}H_{35}N_3O_6$: C, 62.45; H, 7.64; N, 9.10; Found: C, 62.43; H, 7.69; N, 8.98.

General method for the synthesis of compounds 5a and 6a.

(*S*)-methyl 2-((*S*)-1-(2-((*S*)-2-((*tert*-butoxycarbonyl)amino)-3-methylbutanamido) benzoyl) pyrrolidine-2-carboxamido)-4-methylpentanoate 5a.

To a solution of compound **13b** (0.4 g, 1.108 mmoles, 1 equiv) and Boc-^{L}Val-OH (0.29 g, 1.329 mmoles, 1.2 equiv) in DCM (5mL), HBTU (0.546 g, 1.44 mmol, 1.3 equiv) and DIEA (0.287 mL, 1.662 mmol, 1.5 equiv) were added. After 12 h, the reaction mixture was diluted with DCM (30 mL) and washed sequentially with saturated solutions of $NaHCO_3$ (20 mL), water (20 mL) and $KHSO_4$ (20 mL). The washings were extracted with DCM (10 mL x 3) and the combined organic layer was dried over anhydrous Na_2SO_4 and evaporated under reduced pressure to obtain the crude residue, which was purified by column chromatography (eluent: 40% AcOEt/pet. Ether, Rf: 0.4) to afford **5a** (0.40 g, 65%) as a sticky liquid. $[\alpha]^{26.9}_D$: -44.216° (*c* = 1, $CHCl_3$); IR ($CHCl_3$, ν (cm^{-1}): 3280, 3069, 2963, 2931, 2875, 1745, 1715, 1668, 1589, 1541, 1457, 1421, 1391, 1370, 1275, 1247, 1162, 1092, 1016, 987, 873; ^1H NMR ($CDCl_3$/200MHz): δ ppm 9.39 (s, 1H), 8.26-8.28 (d, *J* = 7.96 Hz, 1H),

7.37-7.21 (m, 2H), 7.09-7.02 (m, 1H), 6.78-6.74 (d, *J* = 7.96 Hz, 1H), 5.34-5.30 (d, *J* = 8.97 Hz, 1H), 4.68-4.53 (m, 2H), 4.28-4.21 (m, 1H), 3.68 (s, 3H), 3.48-3.17 (m, 2H), 2.21-2.11 (m, 3H), 1.98-1.5 (m, 5H), 1.36 (s, 9H), 0.97-0.94 (d, *J* = 6.69 Hz, 3H), 0.88-0.84 (m, 9H); ^{13}C NMR ($CDCl_3$, 50MHz): δ ppm 173.6, 171.6, 168.5, 165.6, 155.9, 134.8, 130.4, 126.6, 124.0, 121.9, 79.4, 68.6, 60.2, 59.9, 52.3, 51.0, 49.1, 43.9, 41.2, 31.3, 29.2, 28.2, 25.1, 24.7, 22.7, 21.8, 19.3, 17.5; MALDI-TOF/TOF: 584.1642 $(M+Na)^+$; 600.1794 $(M+K)^+$; Elemental Analysis calculated for $C_{29}H_{44}N_4O_7$: C, 62.12; H, 7.91; N, 9.99; Found: C, 62.15; H, 7.69; N, 9.88.

(*S*)-methyl 2-((*S*)-1-(2-((*R*)-2-((*tert*-butoxycarbonyl)amino)-3-methylbutanamido) benzoyl) pyrrolidine-2-carboxamido)-4-methylpentanoate 6a.

Compound **6a** was synthesized following the procedure for **5a.** The crude product was purified by column chromatography (eluent: 40% AcOEt/pet. Ether, Rf: 0.4) to furnish **6a** (75%) as a sticky liquid. $[\alpha]^{26.9}_D$: -66.352° (*c* = 1, $CHCl_3$); IR ($CHCl_3$, ν (cm^{-1}): 3300, 2960, 2925, 1747, 1667, 1626, 1514, 1456, 1414, 1368, 1246, 1204, 1160, 1017, 875; IR ($CHCl_3$, ν (cm^{-1}): 3280, 3069, 2963, 2931, 2875, 1745, 1715, 1668, 1589, 1541, 1457, 1421, 1391, 1370, 1275, 1247, 1162, 1092, 1016, 987, 873; ^{1}H NMR ($CDCl_3$/200MHz): δ ppm 9.22 (s, 1H), 8.39-8.35 (d, *J* = 8.21 Hz, 1H), 7.41-7.26 (m, 2H), 7.11-7.03 (m, 1H), 6.97-6.93 (bs, 1H), 5.82-5.77 (d, *J* = 8.84 Hz, 1H), 4.71-4.54 (m, 2H), 4.19-4.12 (m, 1H), 3.72 (s, 3H), 3.42-3.37 (m, 2H), 2.26-2.19 (m, 4H) 2.02-1.51 (m, 4H), 1.40 (s, 9H), 0.99-0.87 (m, 12H); ^{13}C NMR ($CDCl_3$, 50MHz): δ ppm 173.1, 171.5, 171.0, 168.6, 165.6, 155.6, 135.3, 130.6, 126.8, 125.3, 123.4, 121.3, 79.3, 61.2, 59.7, 52.1, 51.1, 49.6, 41.0, 31.1, 28.7, 28.2, 25.2, 24.6, 22.6, 21.7, 19.2, 17.8; MALDI-TOF/TOF: 584.0563 $(M+Na)^+$; 600.0703 $(M+K)^+$; Elemental Analysis calculated for $C_{29}H_{44}N_4O_7$: C, 62.12; H, 7.91; N, 9.99; Found: C, 62.20; H, 7.72; N, 9.91.

***tert*-butyl ((*R*)-1-((2-((*S*)-2-(((*S*)-1-((4-bromophenyl)amino)-4-methyl-1-oxopentan-2-yl) carbamoyl)pyrrolidine-1-carbonyl) phenyl)amino)-3-methyl-1-oxobutan-2-yl)carbamate 6f:**

To a solution of acid **6e** (0.1g, 0.183 mmol, 1 equiv) and 4-bromoaniline (0.031 g, 0.183 mmol, 1 equiv) in dry DCM (10 mL), HBTU (0.083g, 0.219 mmol, 1.2 equiv) and DIEA (0.041 mL, 0.238 mmol, 1.3 equiv) were added and reaction was maintained at 0 ^oC. The mixture was stirred at room temperature for an additional 12 h. DCM (10 mL) was added to the reaction mixture and the combined organic layers were washed sequentially with solutions of $KHSO_4$, $NaHCO_3$ and brine. Organic

layer was then dried over Na_2SO_4 and was evaporated *in vacuo*. The crude product was purified by column chromatography (eluent: 40% AcOEt/pet. Ether, Rf: 0.4) to furnish **6f** (0.75 g, 60%). as a white crystalline solid. mp: 229-231 $^{\circ}$C; $[\alpha]^{27.1}_{D}$: -73.588° (*c* 1, $CHCl_3$); IR ($CHCl_3$) *v* (cm^{-1}): 3272, 2962, 2930, 2403, 1682.4, 1621, 1538, 1490, 1457, 1394, 1302, 1246, 1163, 1075, 1010, 828; ^{1}H NMR ($CDCl_3$,500MHz): δ ppm 9.64 (s, 1H, amide), 9.58 (s, 1H, amide), 8.34-8.32 (d, *J* = 8.24 Hz, 1H), 7.59-7.57 (m, 2H), 7.39-7.37 (m, 3H), 7.24-7.22 (m, 3H), 7.14-7.09 (m, 2H), 5.56-5.54 (d, *J* = 9.46 Hz, 1H), 4.96-4.88 (dd, *J* = 6.71Hz, *J* = 9.16 Hz, 1H), 4.72-4.69 (m, 1H), 4.60-4.56 (m, 1H), 3.39-3.31 (m, 2H), 2.30-2.24 (m, 1H), 2.07-1.84 (m, 4H), 1.74-1.64 (m, 3H), 1.46 (s, 9H), 0.98-0.96 (d, *J* = 6.10 Hz, 3H), 0.91-0.86 (m, 9H); ^{13}C NMR ($CDCl_3$, 125MHz): δ ppm 173.1, 171.6, 171.0, 168.6, 156.1, 137.6, 134.5, 131.6, 130.0, 127.0, 125.3, 123.9, 121.3, 121.25, 116.5, 79.9, 59.8, 58.9, 54.0, 49.2, 40.9, 33.3, 29.6, 28.5, 24.8, 22.6, 22.3, 18.9, 18.4; MALDI-TOF/TOF: 725.4464 $(M+Na)^+$; 741.5165 $(M+K)^+$; Anal. calcd for $C_{34}H_{46}BrN_5O_6$: C, 58.28; H, 6.62; Br, 11.40; N, 10.00; Found: C, 58.36; H, 6.69; Br, 11.41; N, 9.94.

General method for the synthesis of compounds 7a and 8a.

(*S*)-methyl 2-((*R*)-1-(2-((*S*)-2-(1,3-dioxoisoindolin-2-yl)-3-methylbutanamido) benzoyl) pyrrolidine-2-carboxamido)-4-methylpentanoate 7a.

To a solution of Phth-^{L}Val-OH (0.576g, 2.333 mmol, 1.2 equiv) in dry DCM (10 mL) and catalytic amount of DMF, oxalyl chloride (0.20 mL, 2.527 mmol, 1.3equiv) was added dropwise at 0 ^{o}C, later reaction was allowed to continue at rt for 1h. DCM was then stripped off *in vacuo*. To the solution containing **13d** (0.7g, 1.944 mmol, 1 equiv) and Et_3N (0.394 mL, 2.916 mmol, 1.5 equiv) in dry DCM (15 mL) was cooled in an ice bath with stirring. A solution of Phth-^{L}Val-COCl in DCM (10 mL) was added dropwise for 15 min to the reaction mixture. The mixture was stirred at room temperature for an additional 1 h. DCM (10 mL) was added to the mixture which was then washed with $KHSO_4$ solution (10 mL), saturated aqueous $NaHCO_3$ (10 mL), and brine (10 mL). The organic layer was dried over Na_2SO_4 and evaporated *in vacuo*. The crude product was purified by column chromatography (eluent: 40% AcOEt/pet. Ether, Rf: 0.4) to furnish **7a** (0.96 g, 85%) as a white crystalline solid. mp: 157-160 $^{\circ}$C; $[\alpha]^{26.9}_{D}$: -117.856° (*c* 1, $CHCl_3$); IR ($CHCl_3$) *v* (cm^{-1}): 3063, 2959, 2927, 2874, 1722, 1622, 1532, 1453, 1417, 1384, 1247, 1153, 1071, 988; ^{1}H NMR (200 MHz, $CDCl_3$) δ: 9.54 (1H, amide), 8.08-8.04 (d, *J* = 8.08 Hz, 1H), 7.91-7.85 (m, 2H), 7.78-

7.74 (m, 2H), 7.43-7.33 (m, 2H), 7.17-7.10 (m, 2H), 4.63-4.52 (m, 3H), 3.69 (s, 3H), 3.50-3.42 (m, 2H), 3.04-2.92 (m, 1H), 2.46-2.35 (m, 1H), 2.1-1.92 (m, 2H), 1.85-1.46 (m, 4H), 1.19-1.16 (d, J = 6.57 Hz, 3H), 0.93-0.90 (m, 9H); ^{13}C NMR (50 MHz, $CDCl_3$) δ: 173.1, 170.6, 170.2, 168.0, 166.8, 135.2, 134.3, 131.6, 130.9, 127.5, 126.2, 124.0, 123.5, 123.2, 61.6, 59.0, 52.2, 50.8, 50.4, 41.0, 38.6, 29.6, 27.5, 26.8, 25.2, 24.8, 22.8, 21.8, 20.5, 19.4; MALDI-TOF: 613.3940 ($M+Na^+$), 629.4184 ($M+K^+$); Anal. calcd for $C_{32}H_{38}N_4O_7$: C, 64.85; H, 6.80; N, 9.45; Found: C, 64.98; H, 6.69; N, 9.49.

(*R*)-methyl 2-((*S*)-1-(2-((*R*)-2-(1,3-dioxoisoindolin-2-yl)-3-methylbutanamido) benzoyl) pyrrolidine-2-carboxamido)-4-methylpentanoate 8a.

Compound **8a** was synthesized following the procedure for **7a.** The crude product was purified by column chromatography (eluent: 40% AcOEt/pet. Ether, Rf: 0.4) to furnish **8a** (86%) as a white solid. mp: 151-153 °C; $[\alpha]^{26.2}{}_D$: -107.592° (*c* 1, $CHCl_3$); IR ($CHCl_3$) *v* (cm^{-1}): 3062, 2959, 2923, 2873, 2951, 1721, 1623, 1532, 1456, 1428, 1383, 1249, 1153, 1071; ^{1}H NMR (200 MHz, $CDCl_3$) δ: 9.55 (1H, amide), 8.08-8.04 (d, J = 7.96 Hz, 1H), 7.91-7.87 (m, 2H), 7.79-7.75 (m, 2H), 7.44-7.34 (m, 2H), 7.17-7.10 (m, 2H), 4.63-4.53 (m, 3H), 3.69 (s, 3H), 3.51-3.42 (m, 2H), 3.04-2.93 (m, 1H), 2.49-2.32 (m, 1H), 2.07-1.93 (m, 2H), 1.86-1.47 (m, 4H), 1.19-1.16 (d, J = 6.69 Hz, 3H), 0.94-0.90 (m, 9H); ^{13}C NMR (50 MHz, $CDCl_3$) δ: 173.1, 170.6, 170.2, 168.0, 166.9, 135.2, 134.32, 131.6, 130.9, 127.5, 126.3, 124.0, 123.5, 123.3, 61.6, 59.1, 52.2, 50.9, 50.4, 41.0, 38.6, 27.6, 26.8, 25.2, 24.8, 22.8, 21.8, 20.5, 19.5; MALDI-TOF: 613.7018 ($M+Na^+$), 629.7104 ($M+K^+$); Anal. calcd for $C_{32}H_{38}N_4O_7$: C, 64.85; H, 6.80; N, 9.45; Found: C, 64.97; H, 6.71; N, 9.51.

General method for the synthesis of compounds 5c and 6c:

(*S*)-methyl 4-methyl-2-((*S*)-1-(2-((*S*)-3-methyl-2-pivalamido butanamido)benzoyl) pyrrolidine-2-carboxamido)pentanoate 5c.

To a solution of **5b** (0.33 g, 0.713 mmol, 1 equiv) in dry DCM (5 mL), Et_3N (0.145 mL, 1.071 mmol, 1.5 equiv) was added. Reaction was kept under N_2 atmosphere and the temperature was maintained at 0 °C in ice. Piv-Cl (0.1 mL, 0.855 mmol, 1.2 equiv) was added drop wise slowly into the reaction mixture. After 15 min, reaction was allowed to continue at rt for 1 hr. DCM (10 mL) was added to the reaction mixture and DCM layer was washed with $NaHCO_3$ solution followed by water and brine. DCM layer was dried over Na_2SO_4 and was concentrated *in vacuo*. The crude product

was purified by column chromatography (eluent: 45% AcOEt/pet. Ether, Rf: 0.4) to furnish **5c** (0.30 g, 80%) as a sticky liquid. $[\alpha]^{25.7}_{D}$: -53.748° (*c* 1, $CHCl_3$); IR ($CHCl_3$) *v* (cm^{-1}): 3408, 3020, 2400, 1635, 1420, 1318, 1079; ^1H NMR ($CDCl_3$/200MHz): δ ppm 9.44 (s, 1H), 8.25-8.21 (d, *J* = 7.96 Hz, 1H), 7.42-7.26 (m, 2H), 7.16-7.11 (m, 1H), 7.0-6.96 (d, *J* = 8.46 Hz, 1H), 6.43-6.39 (d, *J* = 8.59 Hz, 1H), 4.76-4.55 (m, 3H), 3.73 (s, 3H), 3.46-3.21 (m, 2H), 2.28-2.12 (m, 2H), 2.03-1.51 (m, 6H), 1.22 (s, 9H), 1.02-0.98 (d, *J* = 6.69 Hz, 3H), 0.93-0.85 (m, 9H); ^{13}C NMR ($CDCl_3$, 50MHz): δ ppm 178.6, 173.8, 171.7, 171.3, 168.4, 134.6, 130.4, 127.0, 126.7, 124.1, 122.1, 60.5, 58.3, 52.3, 50.8, 49.1, 41.2, 38.8, 31.2, 29.6, 29.2, 27.4, 25.1, 24.9, 22.7, 21.7, 19.3, 17.8; MALDI-TOF/TOF: 570.2427 $(M+K)^+$; Anal. calcd for $C_{29}H_{44}N_4O_6$: C, 63.95; H, 8.14; N, 10.29; Found: C, 63.88; H, 8.20; N, 10.25.

(*S*)-methyl 4-methyl-2-((*S*)-1-(2-((*R*)-3-methyl-2-pivalamido butanamido) benzoyl)pyrrolidine-2-carboxamido)pentanoate 6c.

Compound **6c** was synthesized following the procedure for **5c** from **6b.** The crude product was purified by column chromatography (eluent: 45% AcOEt/pet. Ether, Rf: 0.4) to furnish **2c** (86%) as a sticky liquid. mp: 58-60 °C; $[\alpha]^{26.3}_{D}$: -89.084° (*c* 1, $CHCl_3$); IR ($CHCl_3$) *v* (cm^{-1}): 3283, 3073, 2960, 2873, 1747, 1667, 1626, 1588, 1524, 1455, 1417, 1370, 1301, 1201, 1155, 1025, 986, 914; ^1H NMR ($CDCl_3$/200MHz): δ ppm 9.53 (s, 1H), 8.32-8.28 (d, *J* = 8.21 Hz, 1H), 7.44-7.32 (m, 2H), 7.15-7.07 (m, 1H), 6.82-6.79 (d, *J* = 7.83 Hz, 1H), 6.51-6.47 (d, *J* = 8.21 Hz, 1H), 4.80-4.73 (m, 1H), 4.63-4.49 (m, 2H), 3.74 (s, 3H), 3.58-3.42 (m, 2H), 2.31-2.16 (m, 3H), 2.04-1.6 (m, 5H), 1.23 (s, 9H), 1.02-0.89 (m, 12H); ^{13}C NMR ($CDCl_3$, 50MHz): δ ppm 178.4, 173.3, 171.1, 170.4, 169.2, 135.9, 131.0, 127.3, 124.8, 123.4, 121.9, 59.7, 58.6, 52.3, 51.1, 50.5, 41.1, 38.9, 31.8, 29.6, 28.1, 27.5, 25.3, 24.8, 22.7, 21.9, 19.3, 17.7; MALDI-TOF/TOF: 570.1554 $(M+K)^+$; Anal. calcd for $C_{29}H_{44}N_4O_6$: C, 63.95; H, 8.14; N, 10.29; Found: C, 63.88; H, 8.20; N, 10.25.

(*S*)-N-((*S*)-4-methyl-1-(methylamino)-1-oxopentan-2-yl)-1-(2-((*S*)-3-methyl-2-pivalamidobutanamido)benzoyl)pyrrolidine-2-carboxamide 5.

Compound **5c** (0.2g, 0.25 mmol) was stirred in saturated solution of methanolic methylamine for 2h at rt. Solvent was evaporated *in vacuo* and the crude product was purified by column chromatography (eluent: 45% AcOEt/pet. Ether, Rf: 0.4) to furnish **5** (95%) as a white fluffy solid. mp: 100-102 °C; $[\alpha]^{27.10d}$: -50.672° (*c* 0.5, $CHCl_3$); IR ($CHCl_3$) *v* (cm^{-1}): 3318, 3020, 2967, 2401, 1648, 1589, 1509, 1457, 1420,

1369; ^{1}H NMR (400 MHz, $CDCl_3$) δ: 9.68 (1H, amide), 8.32-8.29 (d, *J* = 8.28 Hz, 1H), 7.42-7.35 (m, 3H), 7.28-7.26 (m, 1H), 7.16-7.12 (t, *J* = 7.53 Hz, 1H), 6.50-6.48 (d, *J* = 8.28 Hz, 1H), 4.98-4.94 (m, 1H), 4.74-4.71 (dd, *J* = 5.27 Hz, *J* = 8.03 Hz, 1H), 4.64-4.58 (m, 1H), 3.37-3.23 (m, 2H), 2.78-2.77 (d, *J* = 4.52 Hz, 3H), 2.35-2.26 (m, 1H), 2.17-1.07 (m, 3H), 1.85-1.80 (m, 1H), 1.70-1.57 (m, 3H), 1.23 (s, 9H), 1.02-1.0 (d, *J* = 6.78 Hz, 3H), 0.96-0.91 (m, 9H); ^{13}C NMR (100 MHz, $CDCl_3$) δ: 178.4, 173.9, 171.8, 171.3, 168.6, 134.5, 130.1, 127.7, 125.9, 124.1, 121.6, 60.5, 58.0, 52.2, 48.9, 40.4, 38.8, 32.3, 29.8, 29.7, 27.5, 26.4, 24.7, 24.6, 22.7, 22.3, 19.3, 18.2; MALDI-TOF: 567.2104 ($M+Na^+$), 583.2536 ($M+K^+$); Anal. calcd for $C_{29}H_{45}N_5O_5$: C, 64.06; H, 8.34; N, 12.88; Found: C, 64.17; H, 8.44; N, 12.87.

(*S*)-N-((*S*)-4-methyl-1-(methylamino)-1-oxopentan-2-yl)-1-(2-((*R*)-3-methyl-2-pivalamidobutanamido)benzoyl)pyrrolidine-2-carboxamide 6.

Compound **6** was synthesized following the procedure for **5** from **6c.** The crude product was purified by column chromatography (eluent: 45% AcOEt/pet. Ether, Rf: 0.4) to furnish **6** (67%) as a sticky liquid. $[\alpha]^{27.1}_{D}$: -79.944° (*c* 0.5, $CHCl_3$); IR ($CHCl_3$) *v* (cm^{-1}): 3314, 3020, 2965, 2874, 2401, 1646, 1589, 1550, 1515, 1456, 1417, 1370, 1296; ^{1}H NMR (500 MHz, $CDCl_3$) δ: 9.89 (1H, amide), 8.59 (m, 1H, amide), 8.40-8.38 (d, *J* = 8.54 Hz, 1H), 7.44-7.37 (m 2H), 7.24-7.23 (d, *J* = 7.32 Hz, 1H), 7.14-7.11 (m, 1H), 6.60-6.58 (d, *J* = 8.54 Hz, 1H), 5.27-5.24 (dd, *J* = 6.71 Hz, *J* = 8.54 Hz, 1H), 4.78-4.77 (m, 1H), 4.48-4.47 (m, 1H), 3.37-3.32 (m, 2H), 2.8-2.8 (d, *J* = 2.75 Hz, 3H), 2.33 (m, 1H), 2.08-1.96 (m, 3H), 1.98-1.88 (m, 1H), 1.79-1.63 (m, 3H), 1.22 (s, 9H), 0.99-0.96 (m, 9H), 0.93-0.92 (d, *J* = 6.1 Hz, 3H); ^{13}C NMR (125 MHz, $CDCl_3$) δ: 178.3, 174.0, 172.9, 171.0, 168.4, 134.5, 129.9, 127.2, 125.4, 123.9, 121.0, 59.7, 57.3, 53.3, 49.2, 40.6, 38.9, 33.4, 28.8, 27.6, 26.4, 24.84, 24.82, 22.7, 22.2, 18.9, 18.3; MALDI-TOF: 566.9368 ($M+Na^+$), 583.1334 ($M+K^+$); Anal. calcd for $C_{29}H_{45}N_5O_5$: C, 64.06; H, 8.34; N, 12.88; Found: C, 64.09; H, 8.39; N, 12.77.

(*R*)-N-((*S*)-4-methyl-1-(methylamino)-1-oxopentan-2-yl)-1-(2-((*S*)-3-methyl-2-pivalamidobutanamido)benzoyl)pyrrolidine-2-carboxamide 7.

Compound **7** was synthesized following the procedure for **5** to afford the free amine which was further protected with pivaloyl group following the procedure for **5c.** The crude product was purified by column chromatography (eluent: 45% AcOEt/pet. Ether, Rf: 0.4) to furnish **7** (79%) as a white solid. mp: 80-82 °C; $[\alpha]^{26.10d}$: 22.608° (*c* 0.5, $CHCl_3$); IR ($CHCl_3$) *v* (cm^{-1}): 3312, 3019, 2966, 2874, 2401, 1648, 1588, 1518,

1456, 1420, 1369, 1297; ^{1}H NMR (500 MHz, $CDCl_3$) δ: 9.7 (1H, amide), 8.32-8.30 (dd, *J* = 1.53 Hz, *J* = 8.54 Hz, 1H), 7.91-7.90 (m, 1H, amide), 7.39-7.36 (dd, *J* = 1.53 Hz, *J* = 8.54 Hz, 1H), 7.24-7.22 (dd, *J* = 1.53 Hz, *J* = 7.32 Hz, 1H), 7.15-7.10 (m, 2H), 6.53-6.51 (d, *J* = 9.16 Hz, 1H), 5.09-5.06 (dd, *J* = 7.02 Hz, *J* = 8.85 Hz, 1H), 4.94-4.90 (m, 1H), 4.72-4.69 (m, 1H), 3.40-3.31 (m, 2H), 2.77-2.76 (d, *J* = 4.58 Hz, 3H), 2.36-2.29 (m, 1H), 2.12-1.86 (m, 4H), 1.7-1.61 (m, 3H), 1.23 (s, 9H), 1.03-1.02 (d, *J* = 6.71 Hz, 3H), 0.98-0.95 (m, 9H); ^{13}C NMR (125 MHz, $CDCl_3$) δ: 178.2, 172.5, 172.2, 171.1, 168.4, 134.7, 129.8, 127.5, 125.2, 123.8, 121.7, 60.1, 57.4, 51.9, 49.2, 42.0, 38.9, 33.2, 30.1, 29.7, 27.7, 26.3, 25.0, 24.6, 22.8, 22.4, 19.3, 18.0; MALDI-TOF: 566.7384 ($M+Na^+$), 583.7939 ($M+K^+$); Anal. calcd for $C_{29}H_{45}N_5O_5$: C, 64.06; H, 8.34; N, 12.88; Found: C, 64.09; H, 8.39; N, 12.77.

(*R*)-N-((*S*)-4-methyl-1-(methylamino)-1-oxopentan-2-yl)-1-(2-((*S*)-3-methyl-2-pivalamidobutanamido)benzoyl)pyrrolidine-2-carboxamide 8.

Compound **8** was synthesized following the procedure for **5** to afford the free amine which was further protected with pivaloyl group following the procedure for **5c.** The crude product was purified by column chromatography (eluent: 45% AcOEt/pet. Ether, Rf: 0.4) to furnish **8** (67%) as a white solid. mp: 75-77 °C; $[\alpha]^{26.4}_{D}$: -23.68° (*c* 0.5, $CHCl_3$); IR ($CHCl_3$) *v* (cm^{-1}): 3312, 3018, 2966, 2874, 2401, 1648, 1588, 1551, 1513, 1456, 1420, 1369, 1297; ^{1}H NMR (500 MHz, $CDCl_3$) δ: 9.71 (1H, amide), 8.32-8.31 (d, *J* = 8.24 Hz, 1H), 7.93-7.92 (m, 1H, amide), 7.39-7.36 (dd, *J* = 1.53 Hz, *J* = 8.54 Hz, 1H), 7.24-7.22 (m, 2H), 7.13-7.10 (m, 1H), 6.53-6.51 (d, *J* = 9.16 Hz, 1H), 5.10-5.06 (dd, *J* = 6.71 Hz, *J* = 9.16 Hz, 1H), 4.94-4.89 (m, 1H), 4.72-4.69 (m, 1H), 3.40-3.31 (m, 2H), 2.77-2.76 (d, *J* = 4.88 Hz, 3H), 2.37-2.30 (m, 1H), 2.11-1.88 (m, 4H), 1.7-1.61 (m, 3H), 1.22 (s, 9H), 1.03-1.02 (d, *J* = 6.71 Hz, 3H), 0.98-0.95 (m, 9H); ^{13}C NMR (125 MHz, $CDCl_3$) δ: 178.2, 172.6, 172.2, 171.1, 168.4, 134.6, 129.8, 127.5, 125.2, 123.8, 121.6, 60.1, 57.4, 51.8, 49.1, 42.0, 38.9, 33.1, 30.1, 27.6, 26.3, 25.0, 24.6, 22.7, 22.3, 19.2, 18.0; MALDI-TOF: 566.8729 ($M+Na^+$), 583.0687 ($M+K^+$); Anal. calcd for $C_{29}H_{45}N_5O_5$: C, 64.06; H, 8.34; N, 12.88; Found: C, 64.09; H, 8.39; N, 12.77.

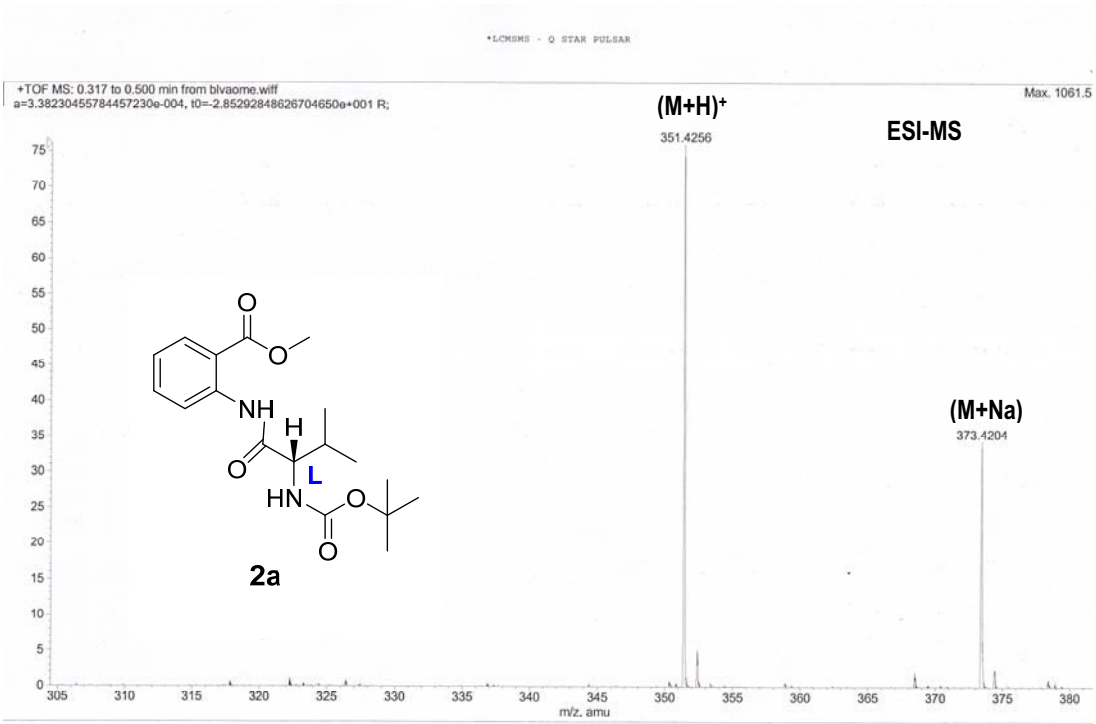
+LCMSMS - Q STAR PULSAR
+TOF MS: 0.317 to 0.500 min from blvaome.wiff
a=3.38230455784457230e-004, t0=-2.85292848626704650e+001 R;
Max. 1061.5
(M+H)+
351.4256
ESI-MS
(M+Na)
373.4204
L
2a
m/z, amu

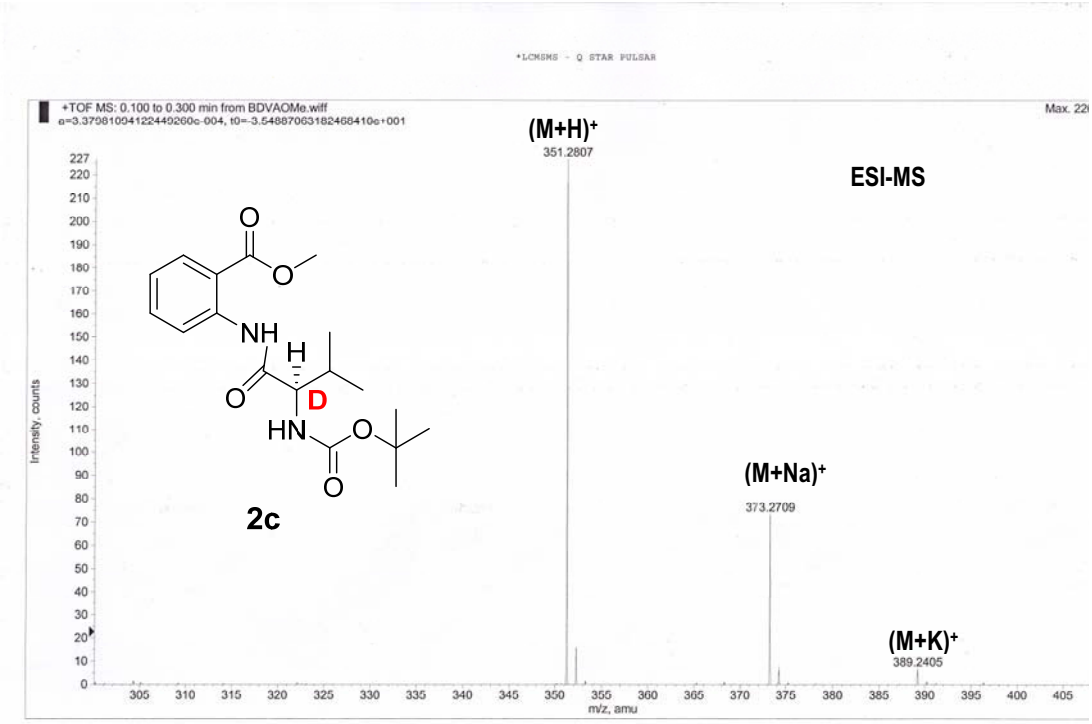
+LCMSMS - Q STAR PULSAR
+TOF MS: 0.100 to 0.300 min from BDVAOMe.wiff
a=3.37981094122449260e-004, t0=-3.54887063182468410e+001
(M+H)+
351.2807
ESI-MS
(M+Na)+
373.2709
(M+K)+
389.2405
D
2c
Intensity, counts
m/z, amu

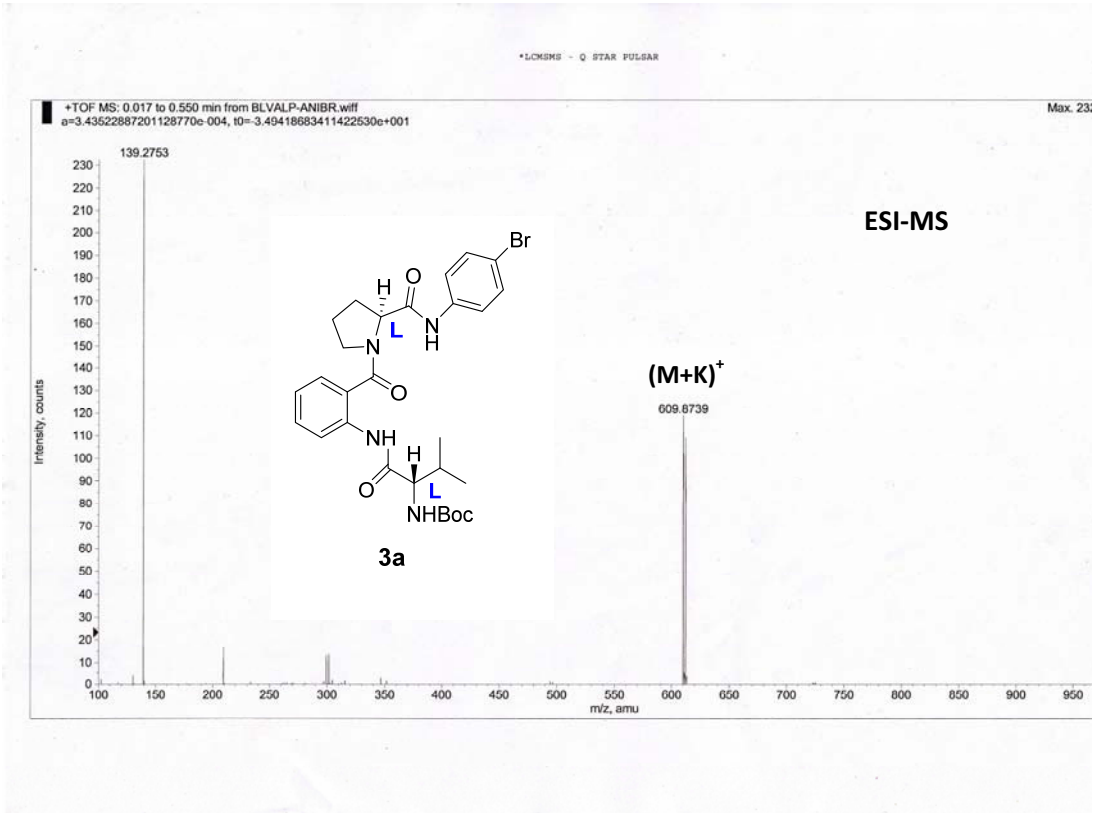
*LCMSMS - Q STAR PULSAR
+TOF MS: 0.017 to 0.550 min from BLVALP-ANIBR.wiff
a=3.4352288720112877 0e-004, t0=-3.4941868341142253 0e+001
Max. 23
139.2753
ESI-MS
(M+K)+
609.8739
Intensity, counts
m/z, amu
Br
H
O
L
N
H
N
O
NH
H
O
L
NHBoc
3a

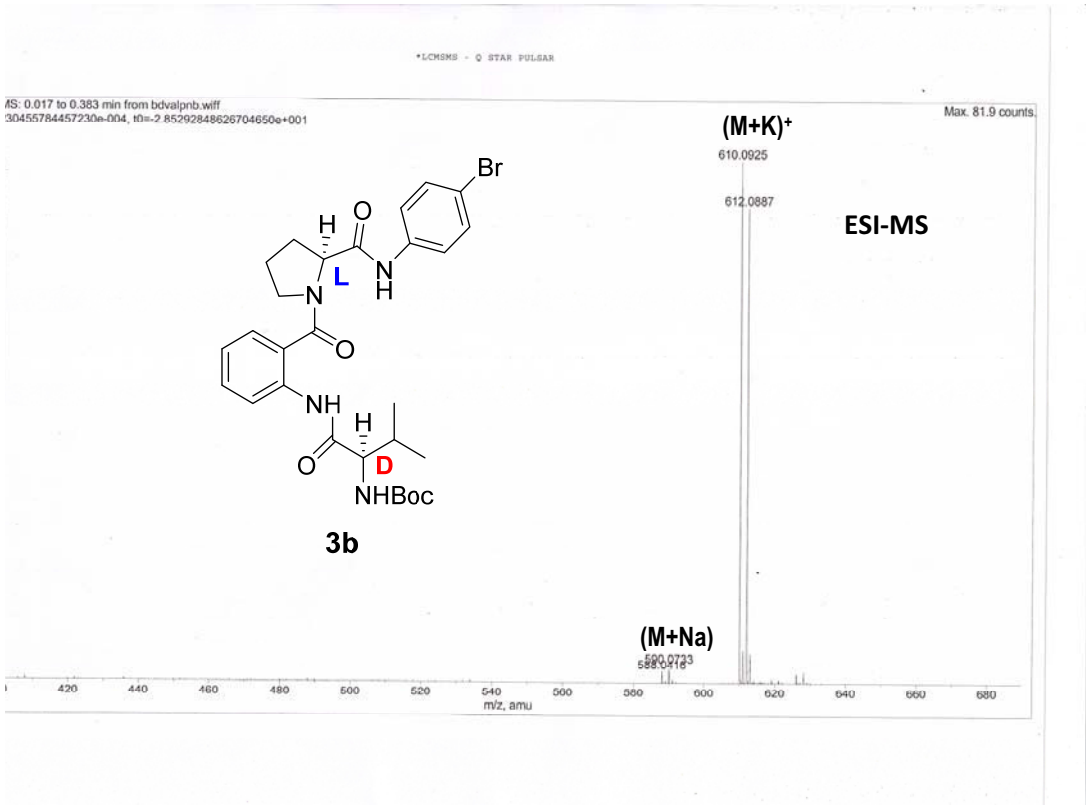
*LCMSMS - Q STAR PULSAR
MS: 0.017 to 0.383 min from bdvalpnb.wiff
Max. 81.9 counts.
(M+K)+
610.0925
612.0887
ESI-MS
(M+Na)
590.0733
588.0418
m/z, amu
Br
H
O
L
N
H
N
O
NH
H
O
D
NHBoc
3b

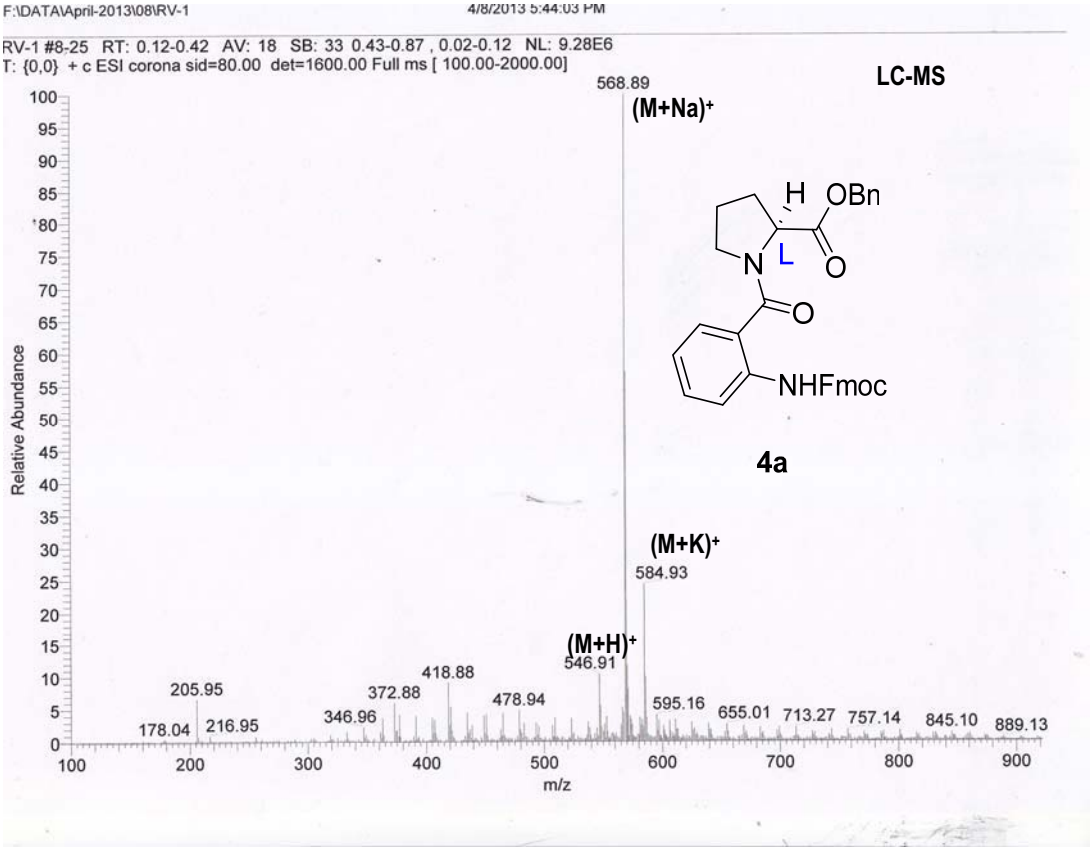
F:\DATA\April-2013\08\RV-1
4/8/2013 5:44:03 PM
RV-1 #8-25 RT: 0.12-0.42 AV: 18 SB: 33 0.43-0.87 , 0.02-0.12 NL: 9.28E6
T: {0,0} + c ESI corona sid=80.00 det=1600.00 Full ms [100.00-2000.00]
LC-MS
568.89
(M+Na)+
H OBn
N L O
O
NHFmoc
4a
(M+K)+
584.93
(M+H)+
546.91
418.88
372.88
205.95
478.94
595.16
655.01
713.27
757.14
845.10
889.13
178.04
216.95
346.96
Relative Abundance
m/z

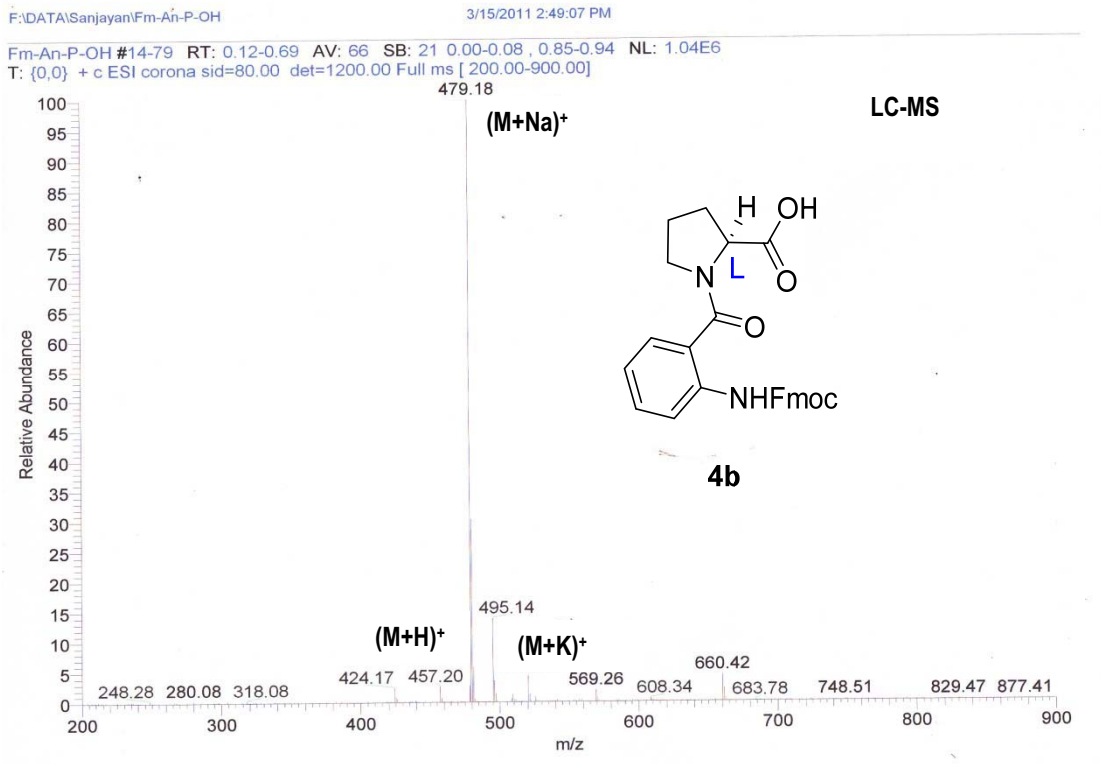
F:\DATA\Sanjayan\Fm-An-P-OH
3/15/2011 2:49:07 PM
Fm-An-P-OH #14-79 RT: 0.12-0.69 AV: 66 SB: 21 0.00-0.08 , 0.85-0.94 NL: 1.04E6
T: {0,0} + c ESI corona sid=80.00 det=1200.00 Full ms [200.00-900.00]
LC-MS
479.18
(M+Na)+
H OH
N L O
O
NHFmoc
4b
495.14
(M+H)+
(M+K)+
660.42
424.17
457.20
569.26
608.34
683.78
748.51
829.47
877.41
248.28
280.08
318.08
Relative Abundance
m/z

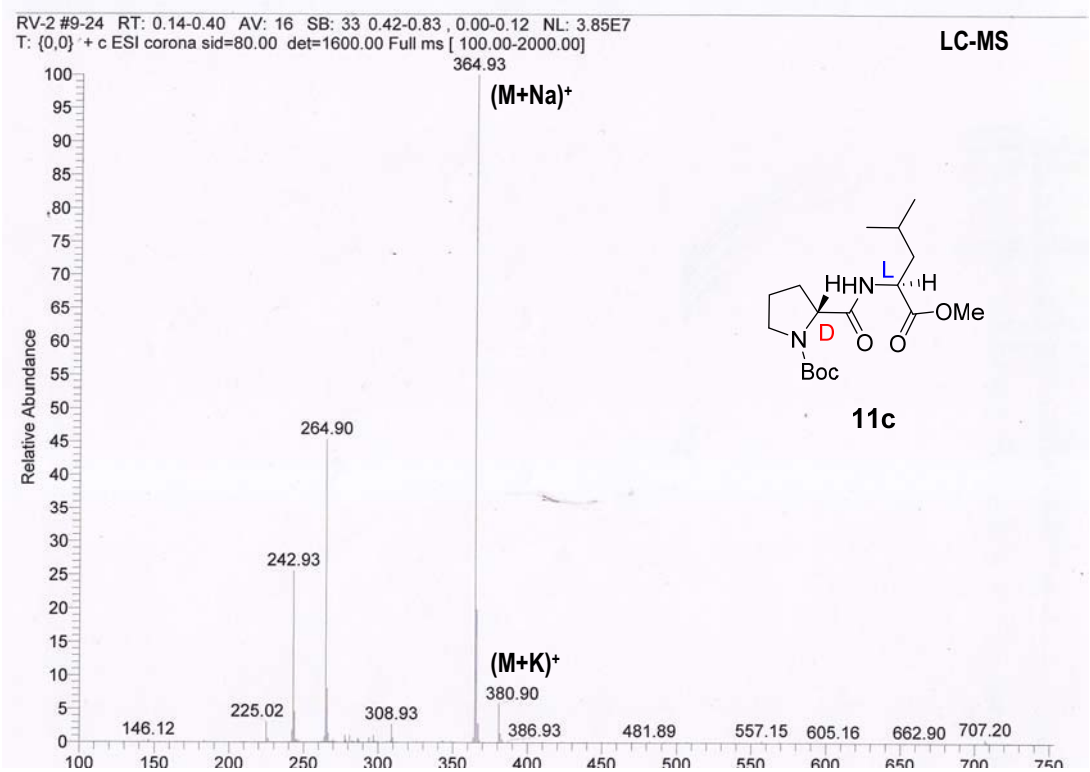
RV-2 #9-24 RT: 0.14-0.40 AV: 16 SB: 33 0.42-0.83 , 0.00-0.12 NL: 3.85E7
T: {0,0} + c ESI corona sid=80.00 det=1600.00 Full ms [100.00-2000.00]
LC-MS
364.93
(M+Na)+
264.90
242.93
(M+K)+
380.90
146.12
225.02
308.93
386.93
481.89
557.15
605.16
662.90
707.20
Relative Abundance
HHN
L
H
OMe
N
D
O
O
Boc
11c

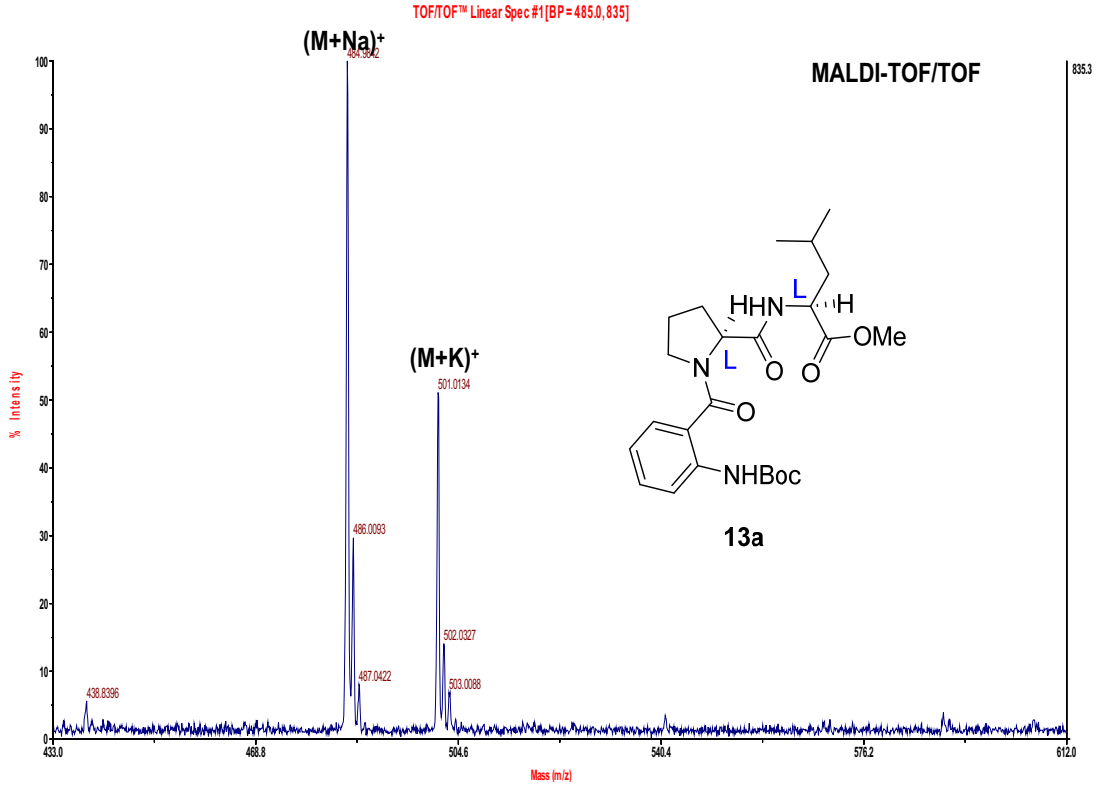
TOF/TOF™ Linear Spec #1 [BP = 485.0, 835]
(M+Na)+
MALDI-TOF/TOF
(M+K)+
501.0134
486.0093
502.0327
487.0422
503.0088
438.8396
% Intensity
Mass (m/z)
HHN
L
H
OMe
N
L
O
O
O
NHBoc
13a

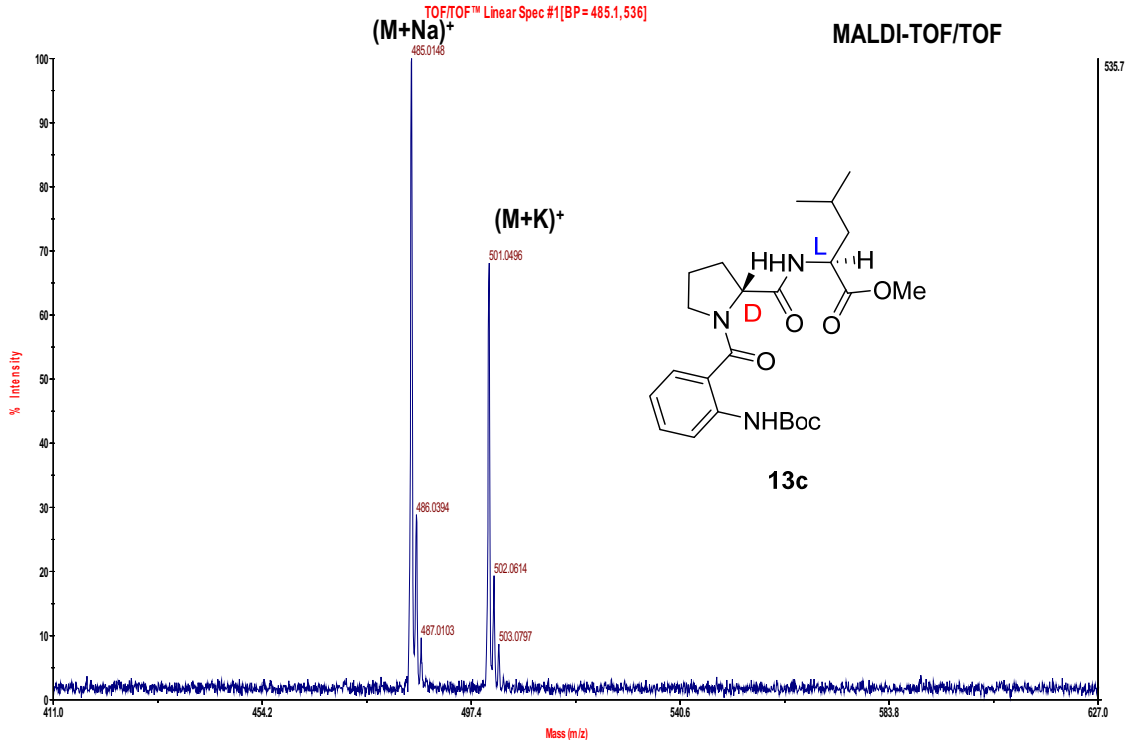
TOF/TOF™ Linear Spec #1[BP = 485.1,536]
(M+Na)+
485.0148
MALDI-TOF/TOF
(M+K)+
501.0496
486.0394
502.0614
487.0103
503.0797
% Intensity
Mass (m/z)
HHN
L
H
OMe
N
D
O
O
O
NHBoc
13c

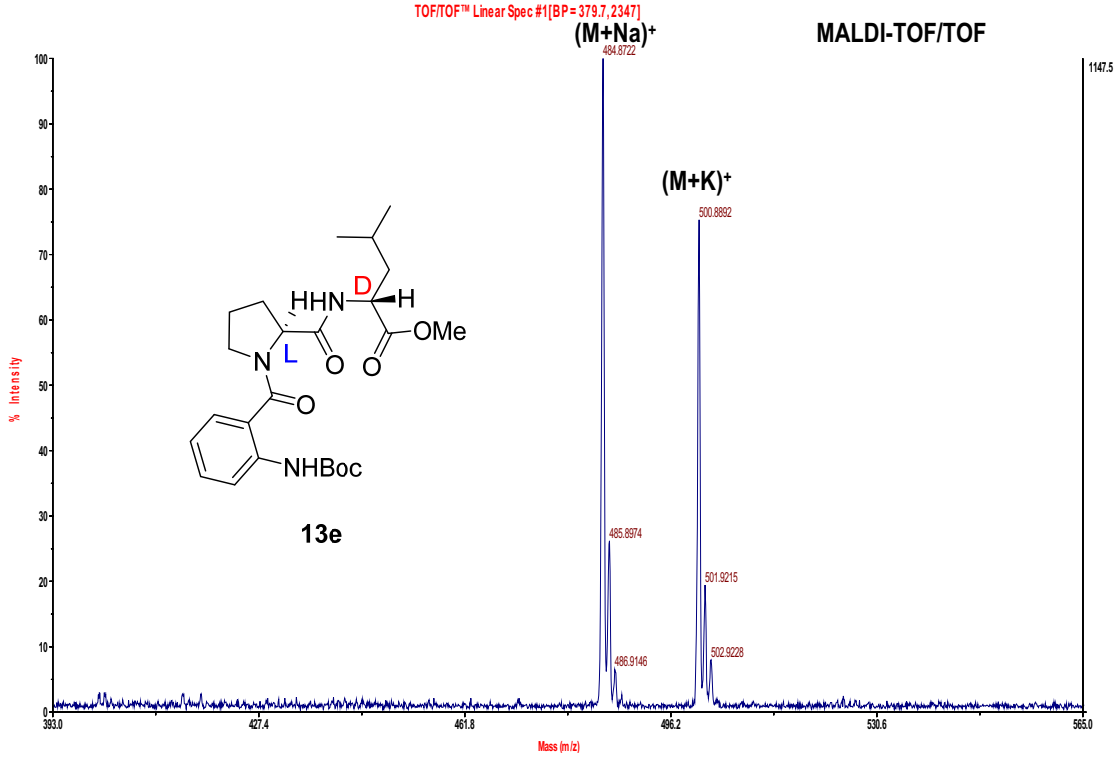
TOF/TOF™ Linear Spec #1[BP = 379.7,2347]
(M+Na)+
484.8722
MALDI-TOF/TOF
(M+K)+
500.8892
485.8974
501.9215
486.9146
502.9228
% Intensity
Mass (m/z)
HHN
D
H
OMe
N
L
O
O
O
NHBoc
13e

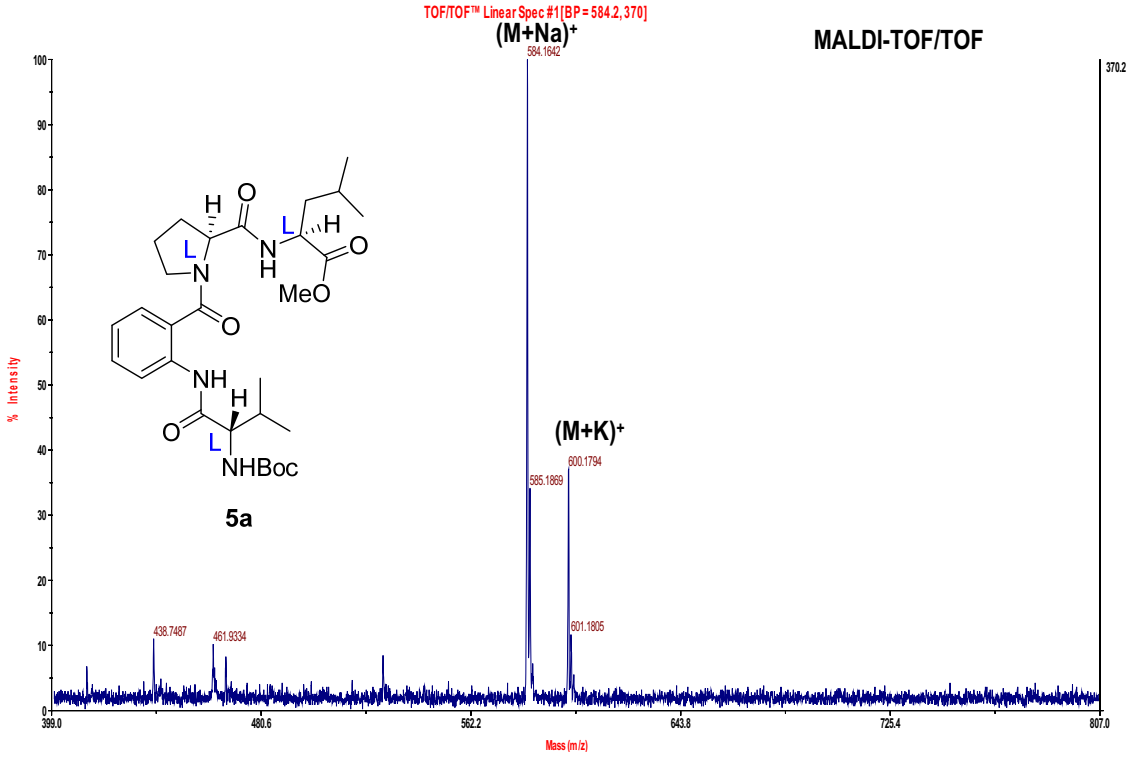
TOF/TOF™ Linear Spec #1[BP = 584.2, 370]
(M+Na)+
MALDI-TOF/TOF
584.1642
370.2
(M+K)+
600.1794
585.1869
601.1805
438.7487
461.9334
% Intensity
Mass (m/z)
399.0
480.6
562.2
643.8
725.4
807.0
MeO
NHBoc
5a

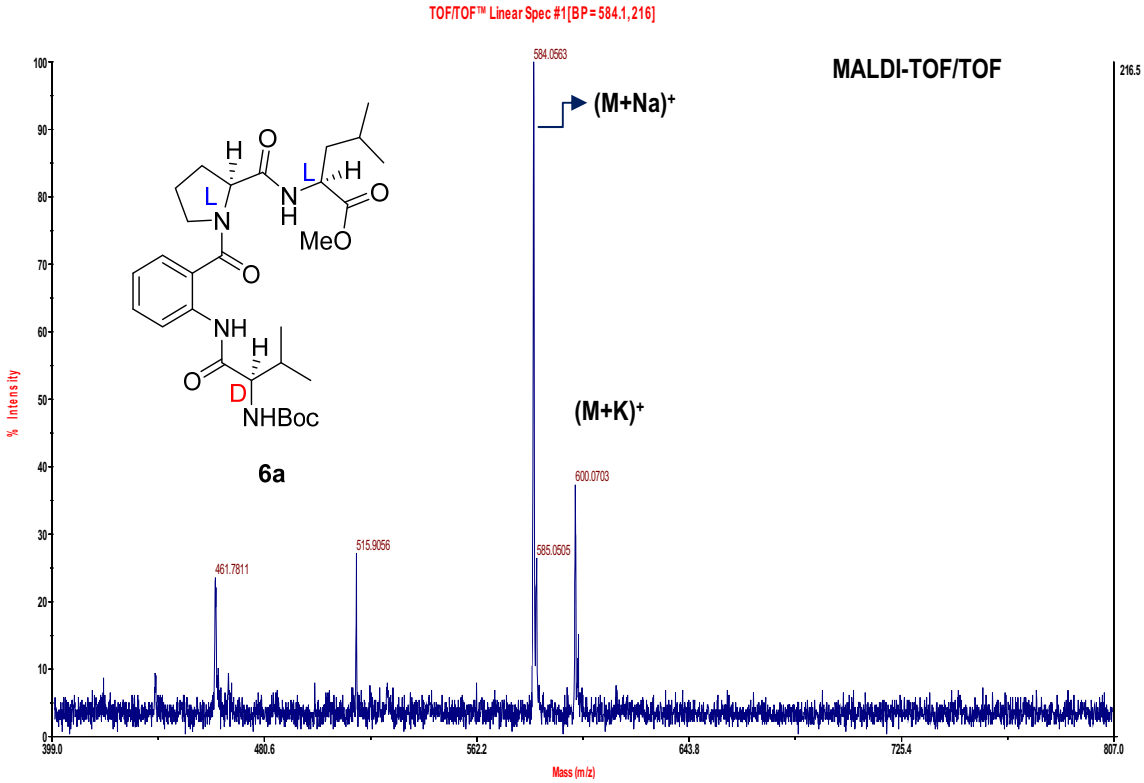
TOF/TOF™ Linear Spec #1[BP = 584.1, 216]
584.0563
MALDI-TOF/TOF
216.5
(M+Na)+
(M+K)+
600.0703
585.0505
515.9056
461.7811
% Intensity
Mass (m/z)
399.0
480.6
562.2
643.8
725.4
807.0
MeO
NHBoc
6a

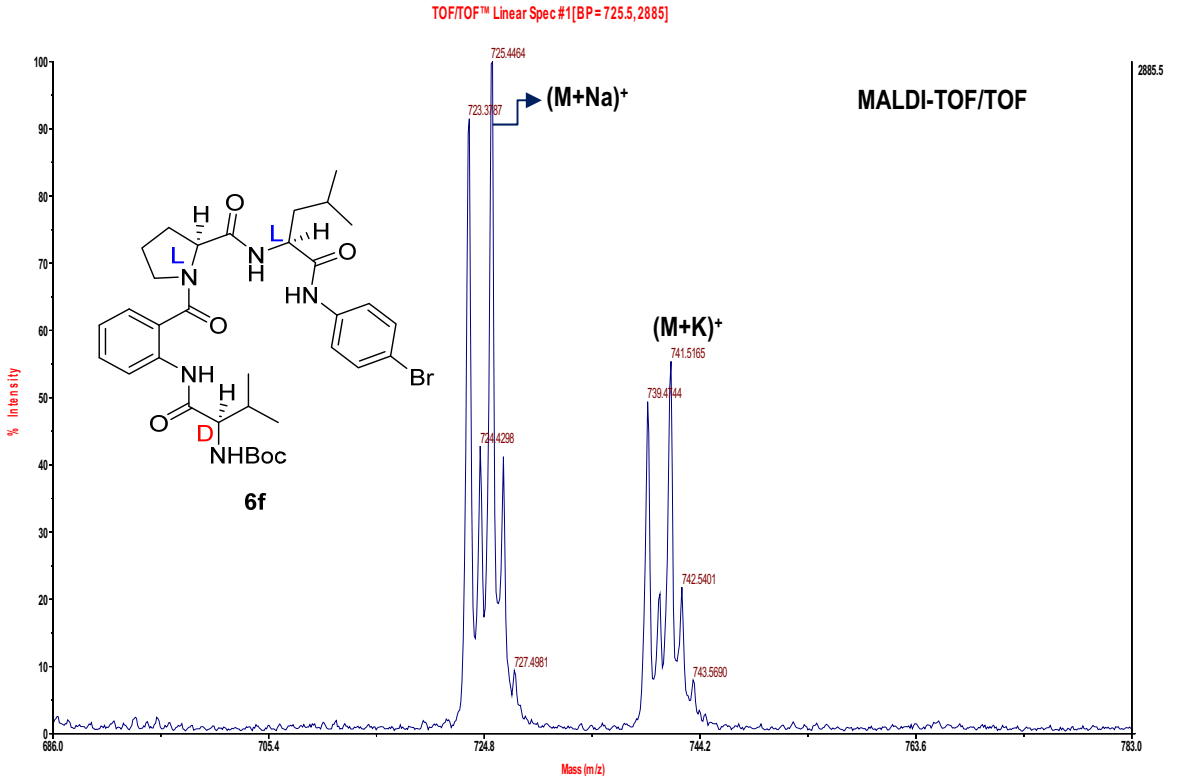
TOF/TOF™ Linear Spec #1[BP = 725.5, 2885]
725.4464
(M+Na)+
723.3787
MALDI-TOF/TOF
2885.5
(M+K)+
741.5165
739.4744
724.4298
742.5401
727.4981
743.5690
% Intensity
Mass (m/z)
6f

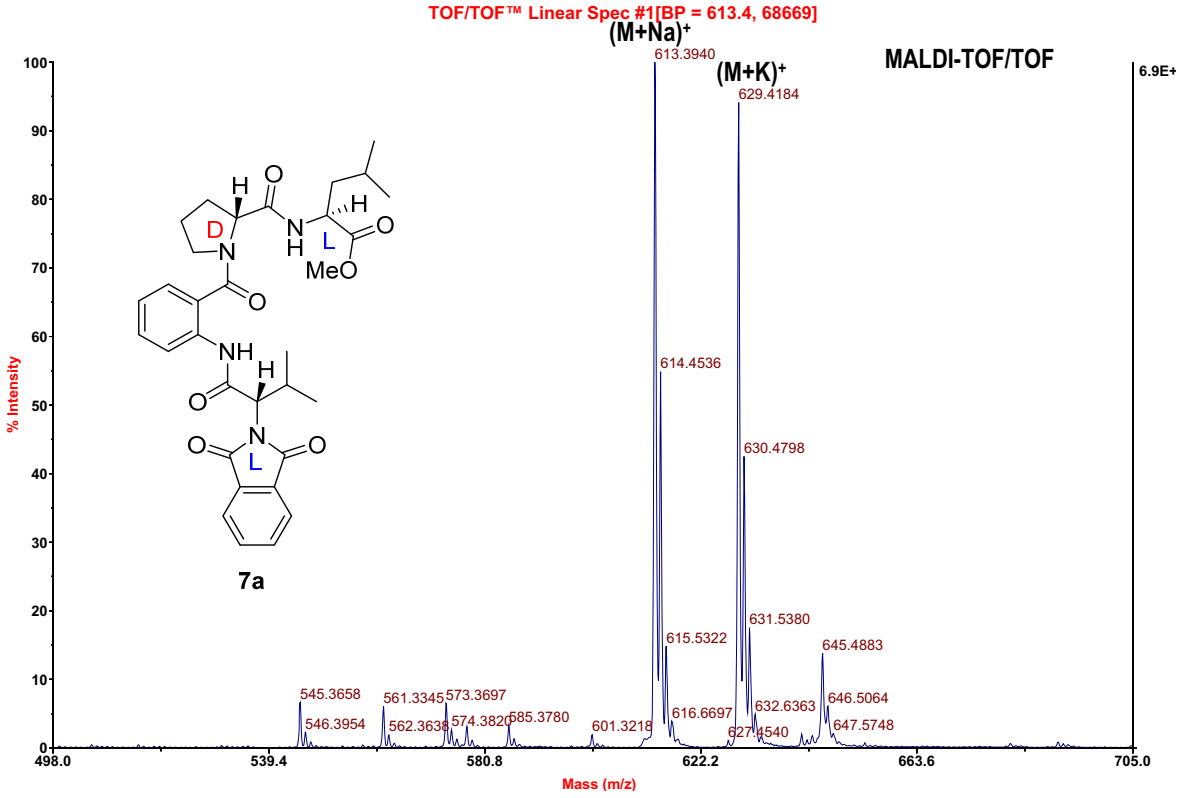
TOF/TOF™ Linear Spec #1[BP = 613.4, 68669]
(M+Na)+
613.3940
(M+K)+
629.4184
MALDI-TOF/TOF
6.9E+
614.4536
630.4798
631.5380
615.5322
645.4883
545.3658
561.3345
573.3697
546.3954
562.3638
574.3820
585.3780
601.3218
616.6697
632.6363
646.5064
627.4540
647.5748
% Intensity
Mass (m/z)
7a

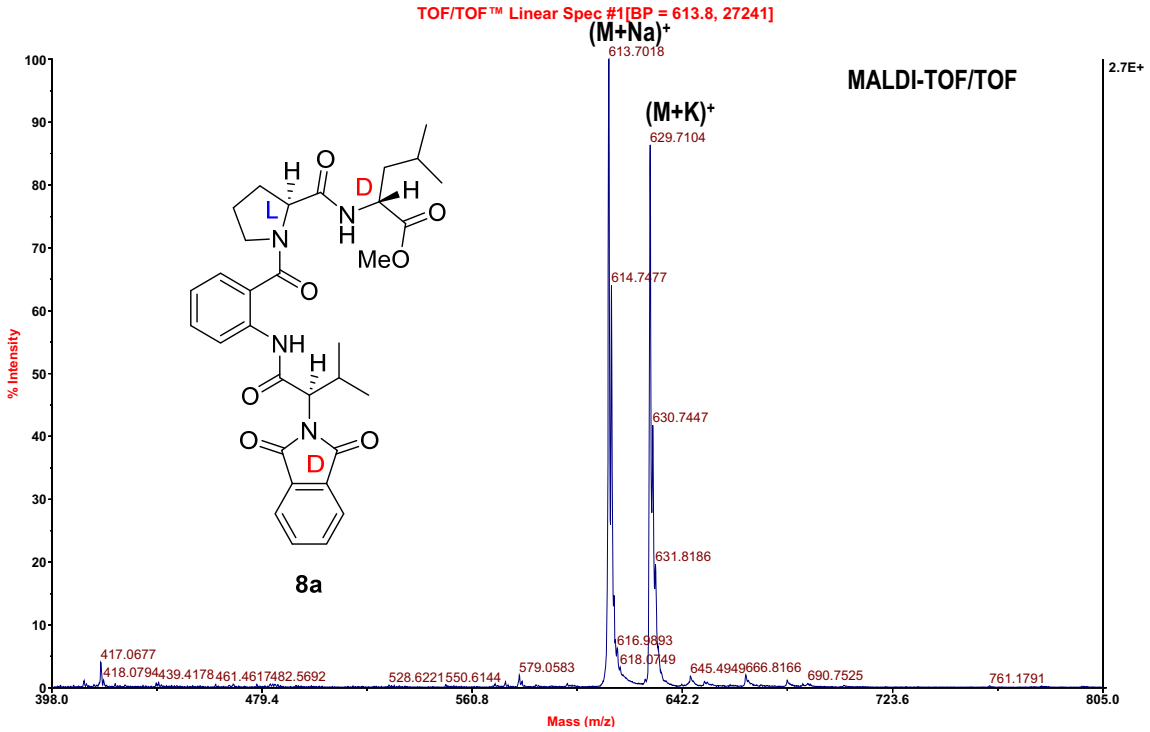
TOF/TOF™ Linear Spec #1[BP = 613.8, 27241]
(M+Na)+
613.7018
MALDI-TOF/TOF
2.7E+
(M+K)+
629.7104
614.7477
630.7447
631.8186
616.9893
618.0749
417.0677
418.0794
439.4178
461.4617
482.5692
528.6221
550.6144
579.0583
645.4949
666.8166
690.7525
761.1791
% Intensity
Mass (m/z)
8a

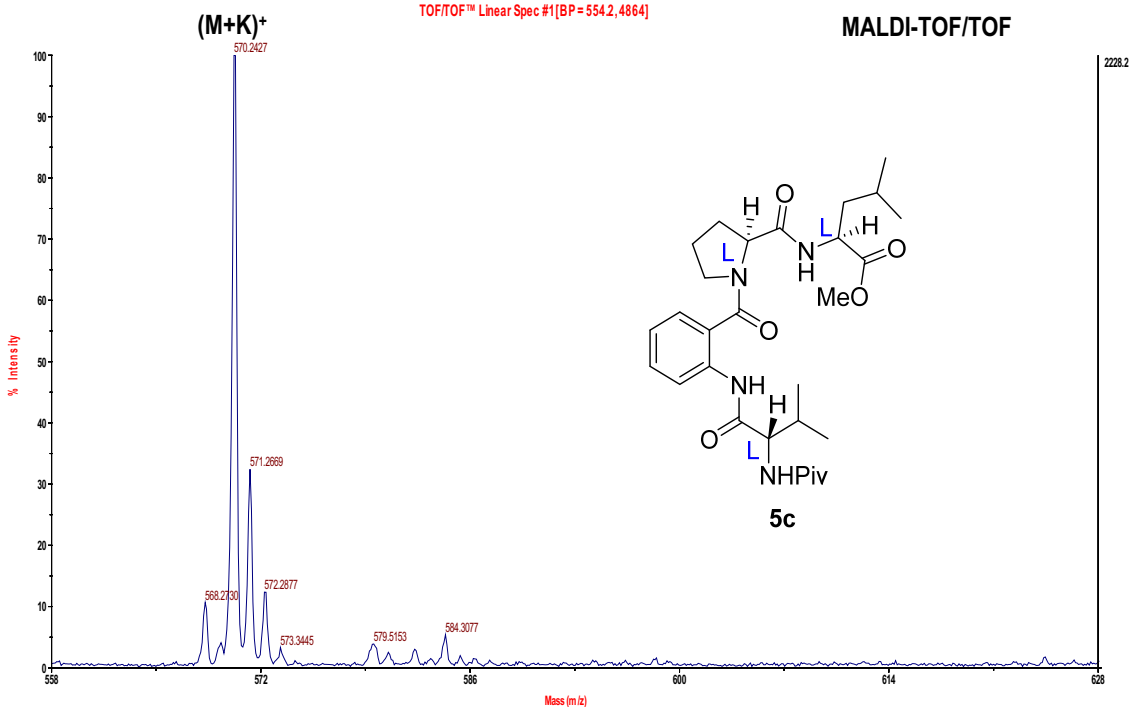
TOF/TOF™ Linear Spec #1[BP = 554.2, 4864]
(M+K)+
570.2427
MALDI-TOF/TOF
2228.2
571.2669
572.2877
568.2730
573.3445
579.5153
584.3077
% Intensity
Mass (m/z)
5c

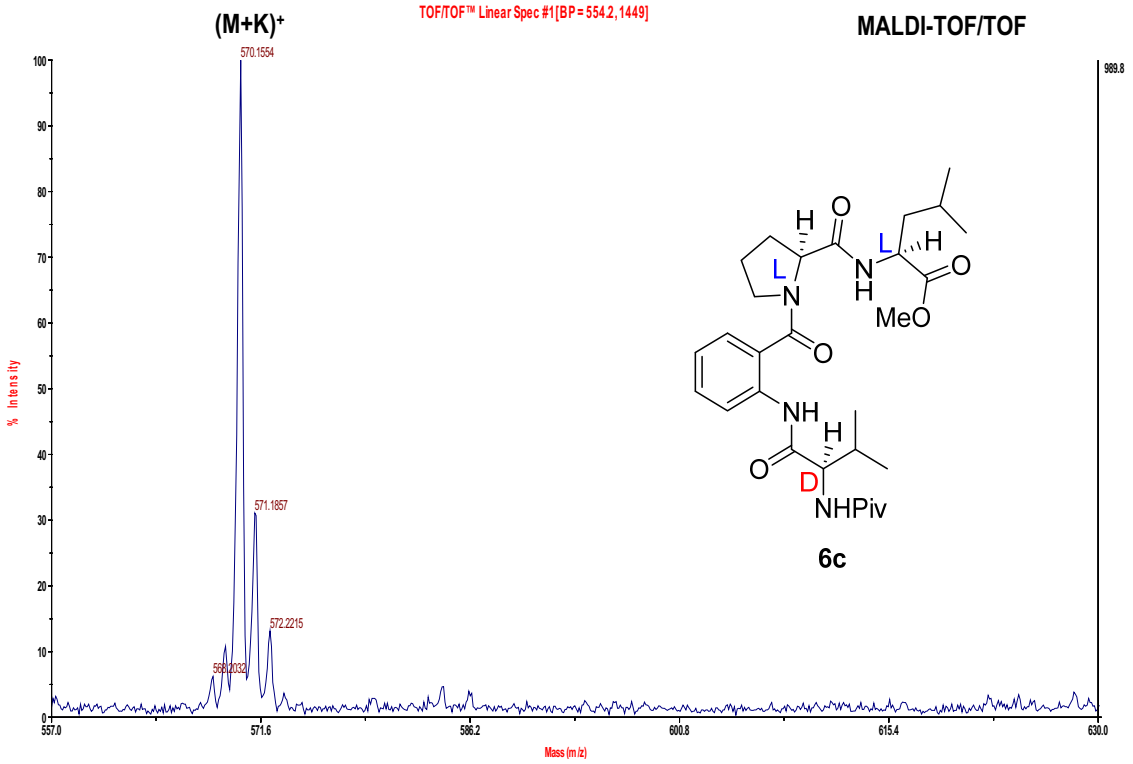
TOF/TOF™ Linear Spec #1[BP = 554.2, 1449]
(M+K)+
MALDI-TOF/TOF
570.1554
571.1857
572.2215
568.2032
989.8
% Intensity
Mass (m/z)
MeO
NHPiv
6c

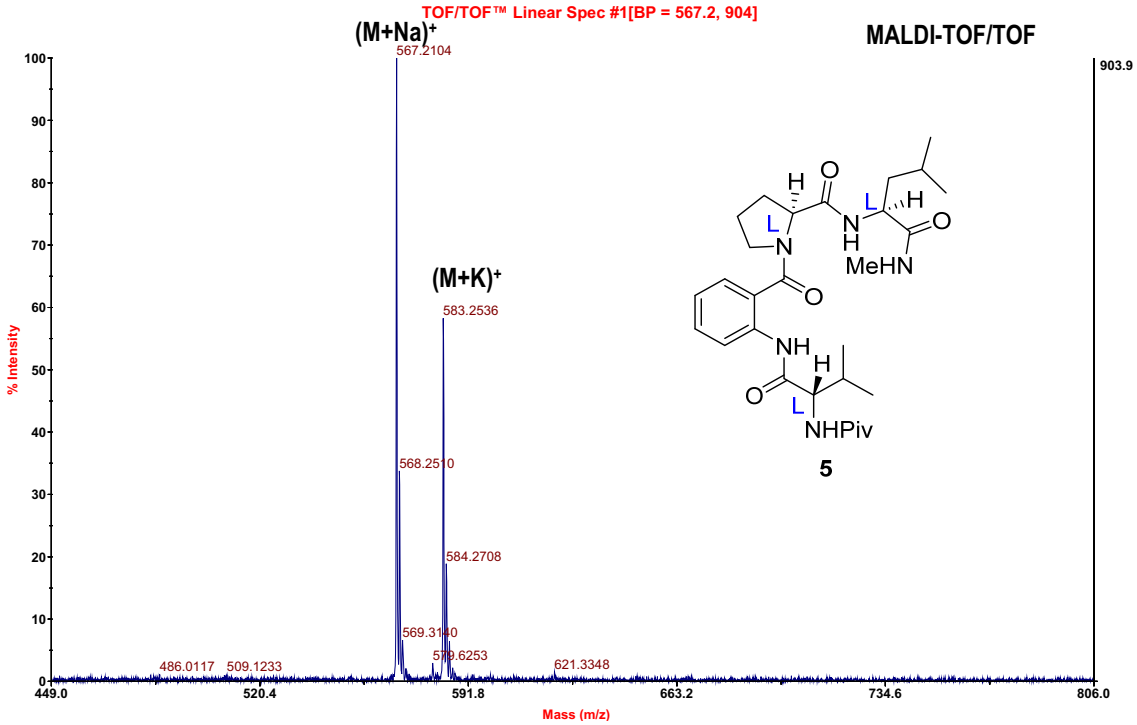
TOF/TOF™ Linear Spec #1[BP = 567.2, 904]
(M+Na)+
MALDI-TOF/TOF
567.2104
(M+K)+
583.2536
568.2510
584.2708
569.3140
579.6253
486.0117
509.1233
621.3348
903.9
% Intensity
Mass (m/z)
MeHN
NHPiv
5

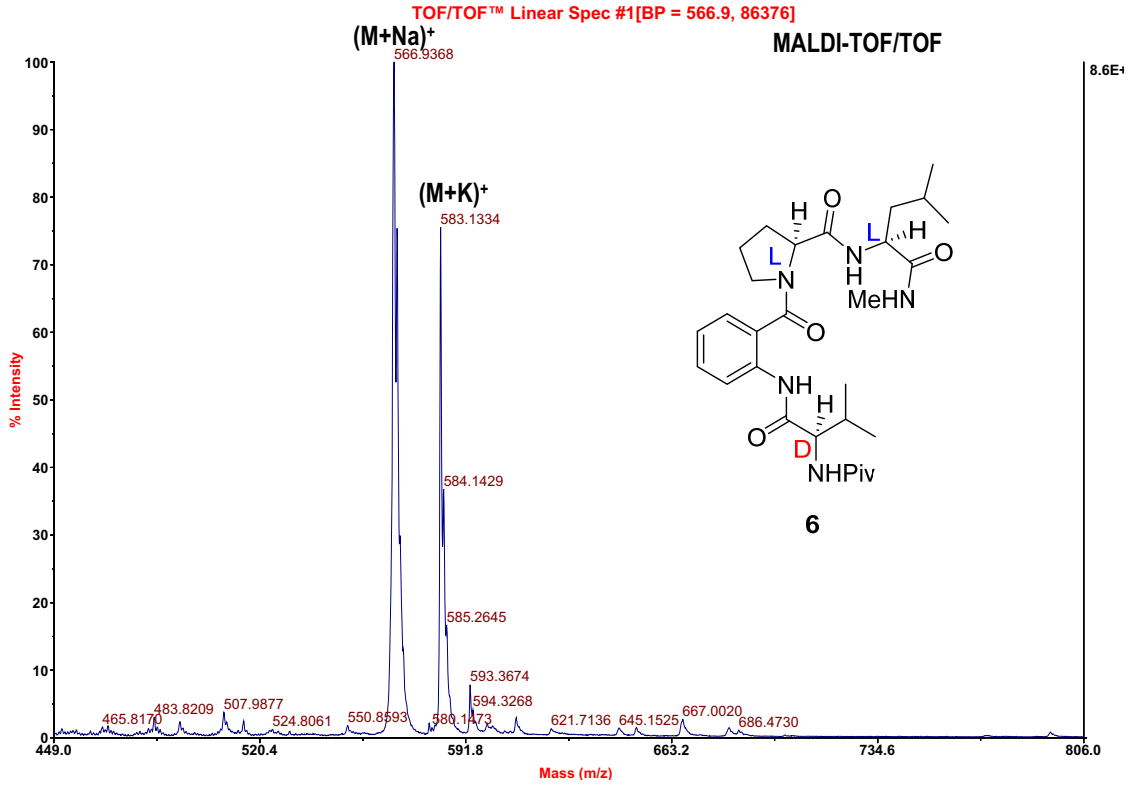
TOF/TOF™ Linear Spec #1[BP = 566.9, 86376]
MALDI-TOF/TOF
(M+Na)+
566.9368
(M+K)+
583.1334
584.1429
585.2645
593.3674
594.3268
465.8170
483.8209
507.9877
524.8061
550.8593
580.1473
621.7136
645.1525
667.0020
686.4730
% Intensity
Mass (m/z)
MeHN
NHPiv
6

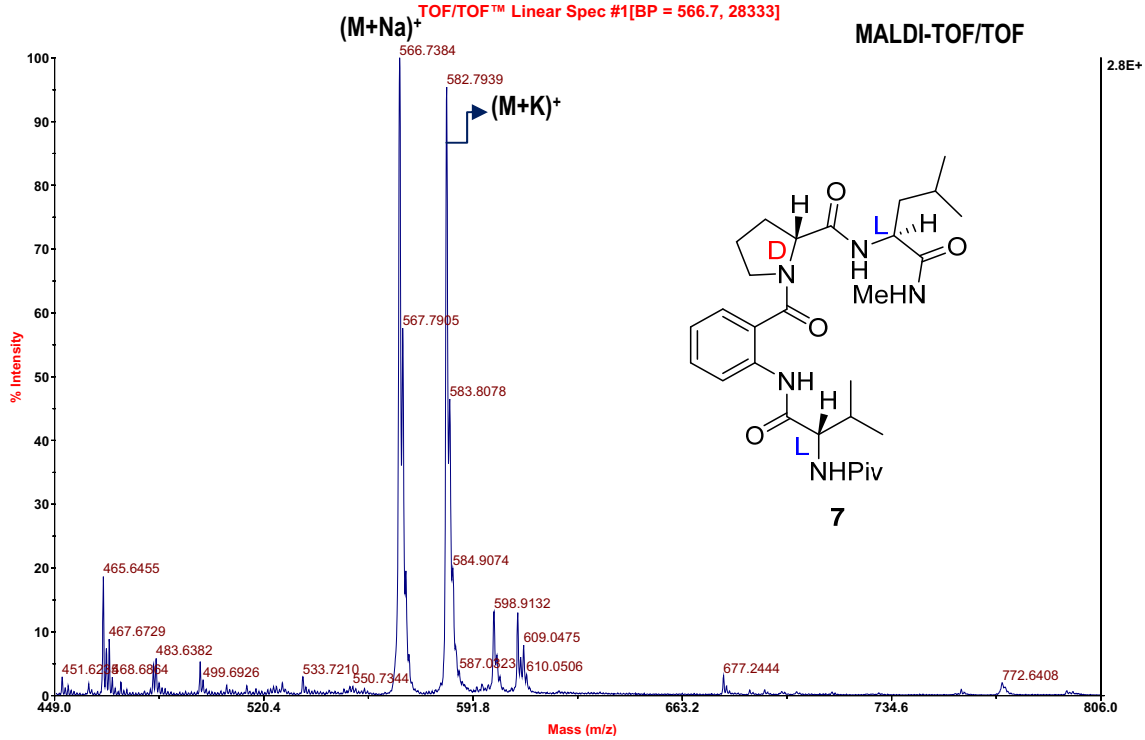
TOF/TOF™ Linear Spec #1[BP = 566.7, 28333]
MALDI-TOF/TOF
(M+Na)+
566.7384
582.7939
(M+K)+
567.7905
583.8078
584.9074
598.9132
609.0475
465.6455
467.6729
483.6382
499.6926
533.7210
550.7344
587.0123
610.0506
677.2444
772.6408
% Intensity
Mass (m/z)
MeHN
NHPiv
7

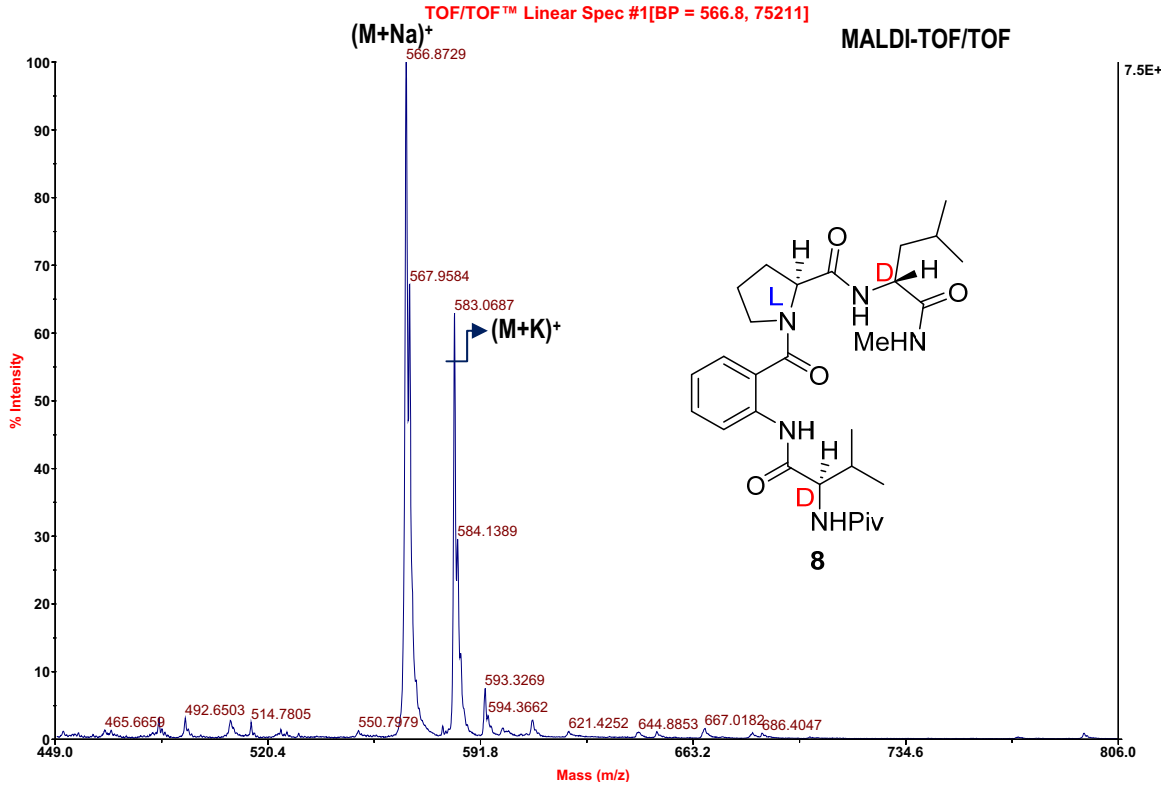
TOF/TOF™ Linear Spec #1[BP = 566.8, 75211]
MALDI-TOF/TOF
(M+Na)+
566.8729
567.9584
583.0687
(M+K)+
584.1389
593.3269
594.3662
465.6659
492.6503
514.7805
550.7979
621.4252
644.8853
667.0182
686.4047
% Intensity
Mass (m/z)
7.5E+
MeHN
NHPiv
8

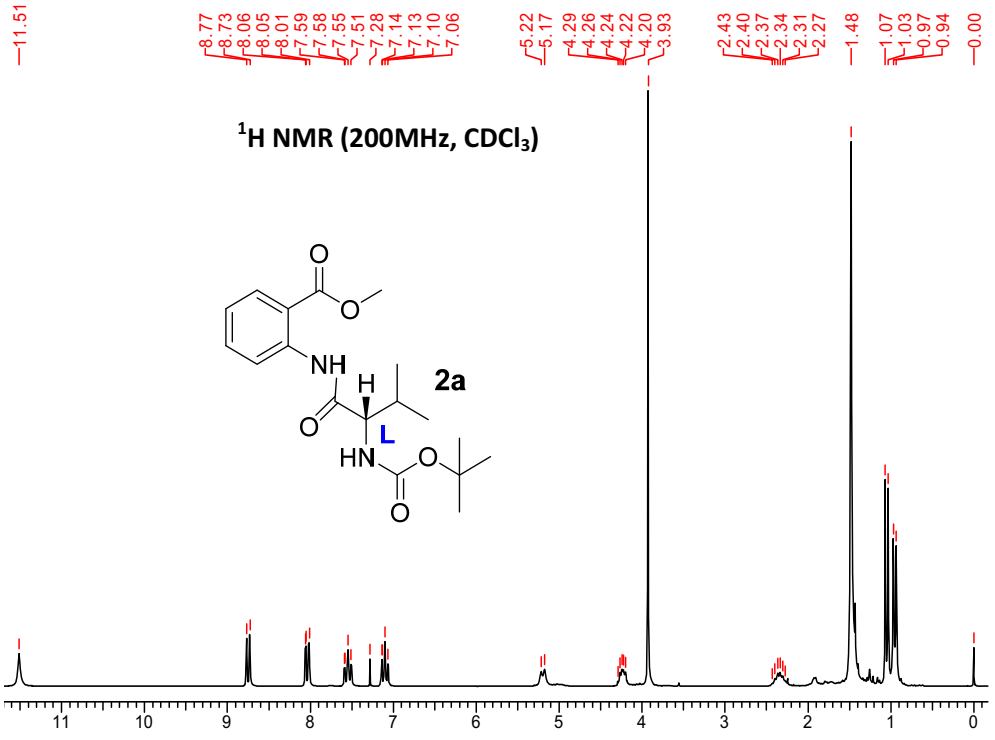
11.51
8.77
8.73
8.06
8.05
8.01
7.59
7.58
7.55
7.51
7.28
7.14
7.13
7.10
7.06
5.22
5.17
4.29
4.26
4.24
4.22
4.20
3.93
2.43
2.40
2.37
2.34
2.31
2.27
1.48
1.07
1.03
0.97
0.94
0.00
^{1}H NMR (200MHz, CDCl$_3$)
2a
L
NH
H
HN
O
11
10
9
8
7
6
5
4
3
2
1
0

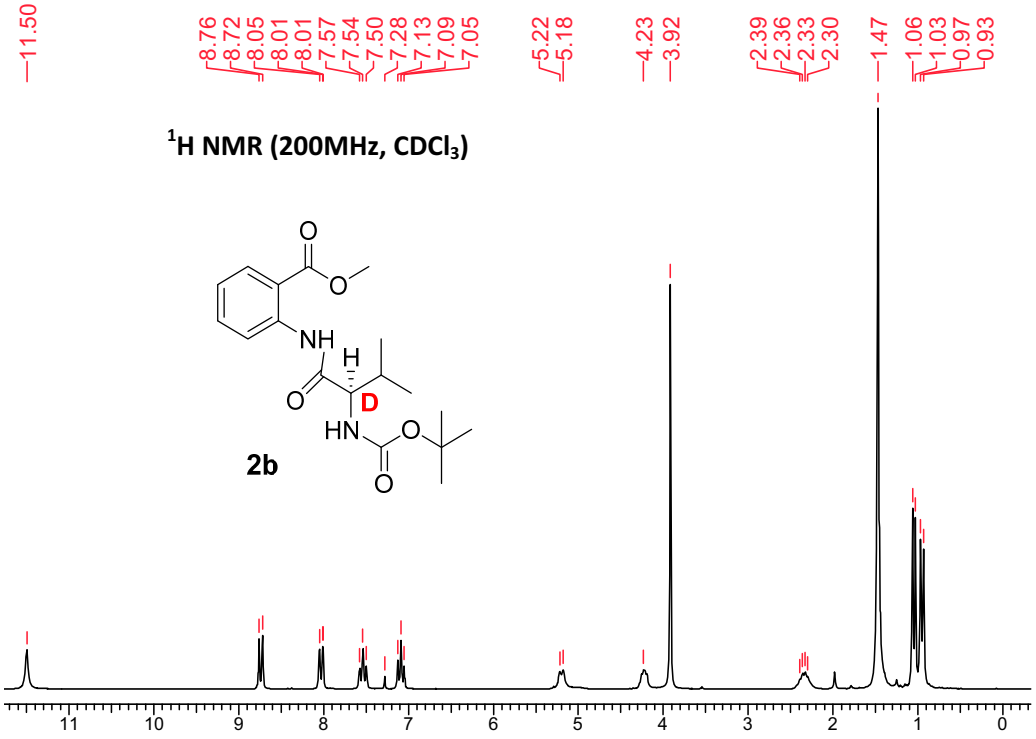
11.50
8.76
8.72
8.05
8.01
8.01
7.57
7.54
7.50
7.28
7.13
7.09
7.05
5.22
5.18
4.23
3.92
2.39
2.36
2.33
2.30
1.47
1.06
1.03
0.97
0.93
^{1}H NMR (200MHz, CDCl$_3$)
2b
D
NH
H
HN
O
11
10
9
8
7
6
5
4
3
2
1
0

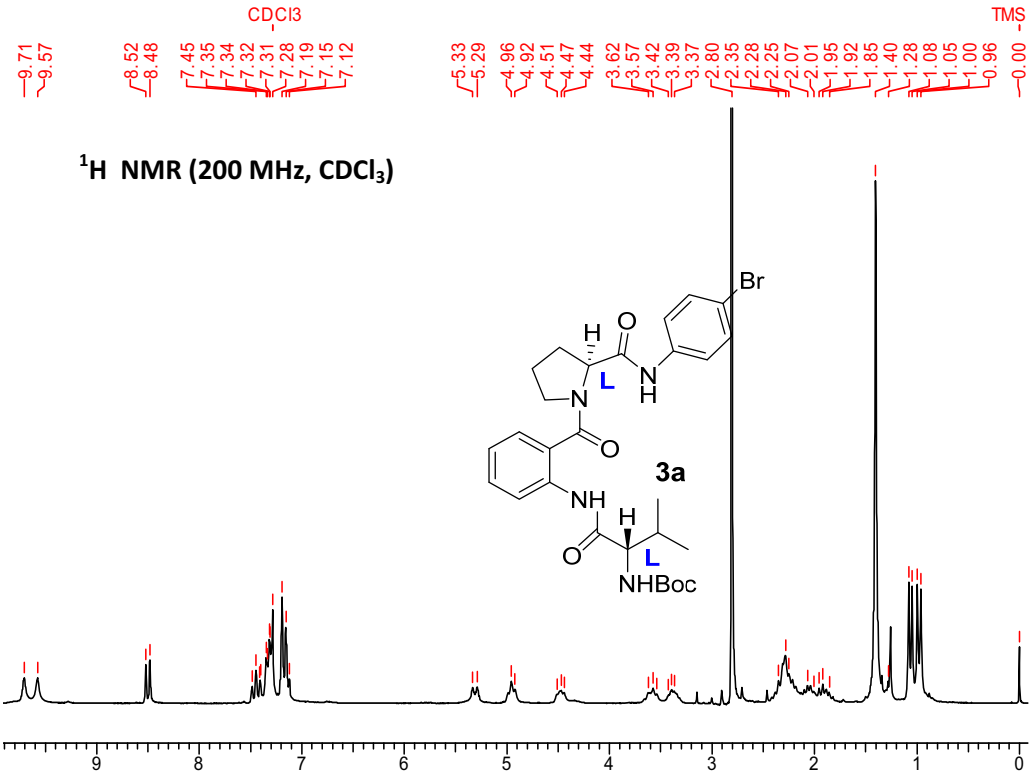
CDCl3
TMS
9.71
9.57
8.52
8.48
7.45
7.35
7.34
7.32
7.31
7.28
7.19
7.15
7.12
5.33
5.29
4.96
4.92
4.51
4.47
4.44
3.62
3.57
3.42
3.39
3.37
2.80
2.35
2.28
2.25
2.07
2.01
1.95
1.92
1.85
1.40
1.28
1.08
1.05
1.00
0.96
0.00
^{1}H NMR (200 MHz, CDCl$_3$)
Br
H
O
N
H
L
N
O
3a
NH
H
O
L
NHBoc
9
8
7
6
5
4
3
2
1
0

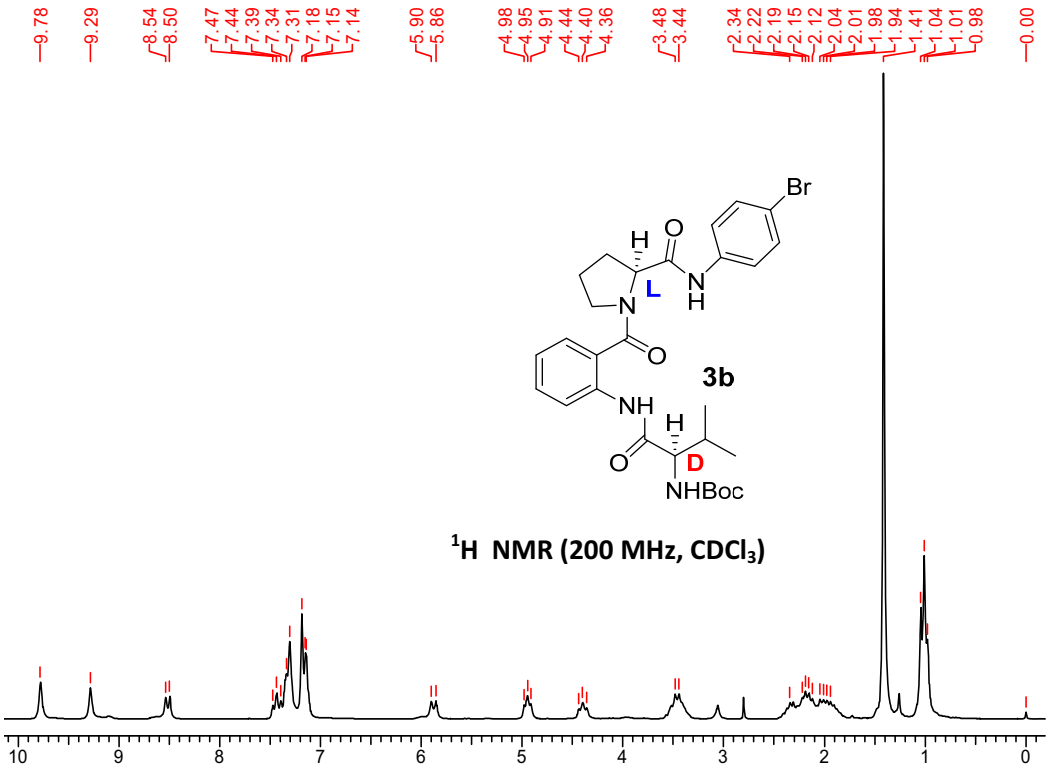
9.78
9.29
8.54
8.50
7.47
7.44
7.39
7.34
7.31
7.18
7.15
7.14
5.90
5.86
4.98
4.95
4.91
4.44
4.40
4.36
3.48
3.44
2.34
2.22
2.19
2.15
2.12
2.04
2.01
1.98
1.94
1.41
1.04
1.01
0.98
0.00
Br
H
O
N
H
L
N
O
3b
NH
H
O
D
NHBoc
^{1}H NMR (200 MHz, CDCl$_3$)
10
9
8
7
6
5
4
3
2
1
0

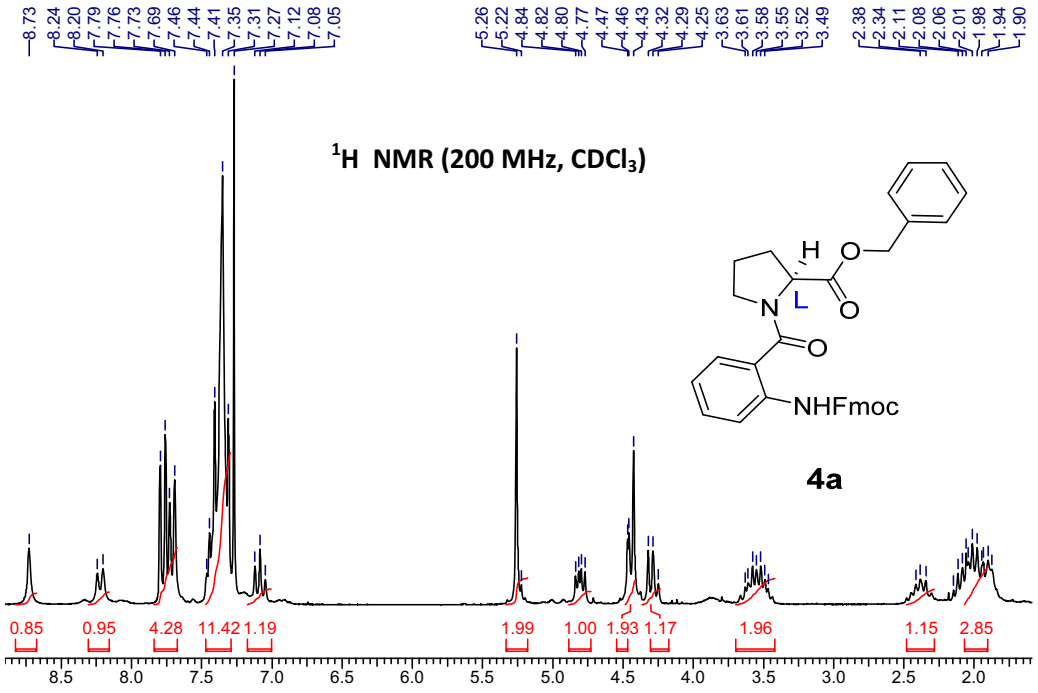
8.73 8.24 8.20 7.79 7.76 7.73 7.69 7.46 7.44 7.41 7.35 7.31 7.27 7.12 7.08 7.05
5.26 5.22 4.84 4.82 4.80 4.77 4.47 4.46 4.43 4.32 4.29 4.25 3.63 3.61 3.58 3.55 3.52 3.49
2.38 2.34 2.11 2.08 2.06 2.01 1.98 1.94 1.90
^{1}H NMR (200 MHz, CDCl$_3$)
H
O
N
L
O
O
NHFmoc
4a
0.85 0.95 4.28 11.42 1.19 1.99 1.00 1.93 1.17 1.96 1.15 2.85
8.5 8.0 7.5 7.0 6.5 6.0 5.5 5.0 4.5 4.0 3.5 3.0 2.5 2.0

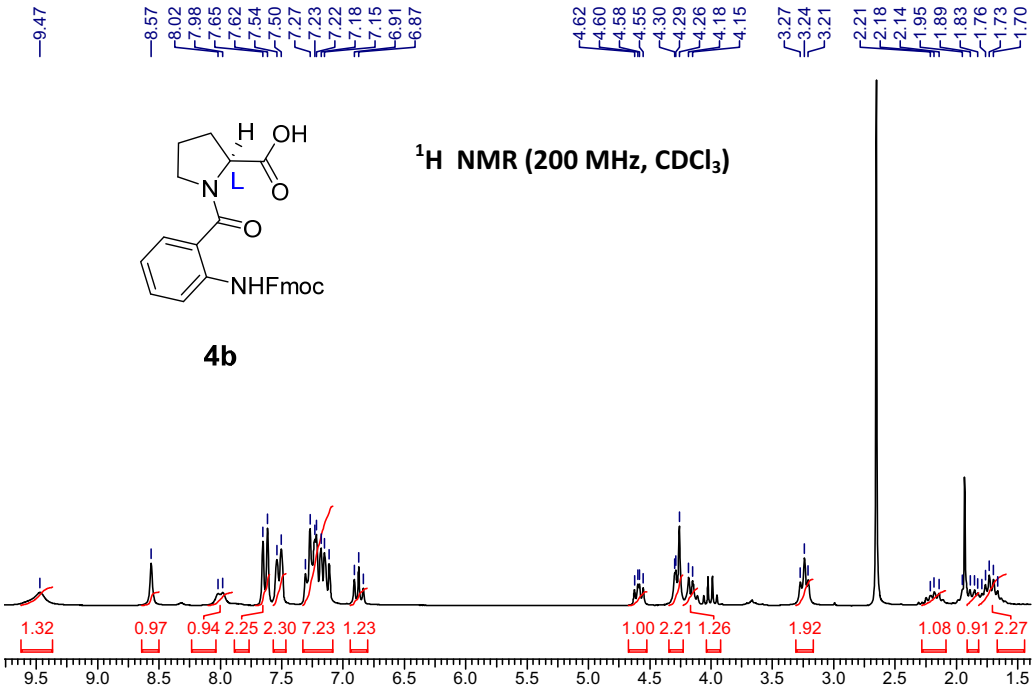
9.47
8.57 8.02 7.98 7.65 7.62 7.54 7.50 7.27 7.23 7.22 7.18 7.15 6.91 6.87
4.62 4.60 4.58 4.55 4.30 4.29 4.26 4.18 4.15
3.27 3.24 3.21
2.21 2.18 2.14 1.95 1.89 1.83 1.76 1.73 1.70
H
OH
N
L
O
O
NHFmoc
4b
^{1}H NMR (200 MHz, CDCl$_3$)
1.32 0.97 0.94 2.25 2.30 7.23 1.23 1.00 2.21 1.26 1.92 1.08 0.91 2.27
9.5 9.0 8.5 8.0 7.5 7.0 6.5 6.0 5.5 5.0 4.5 4.0 3.5 3.0 2.5 2.0 1.5

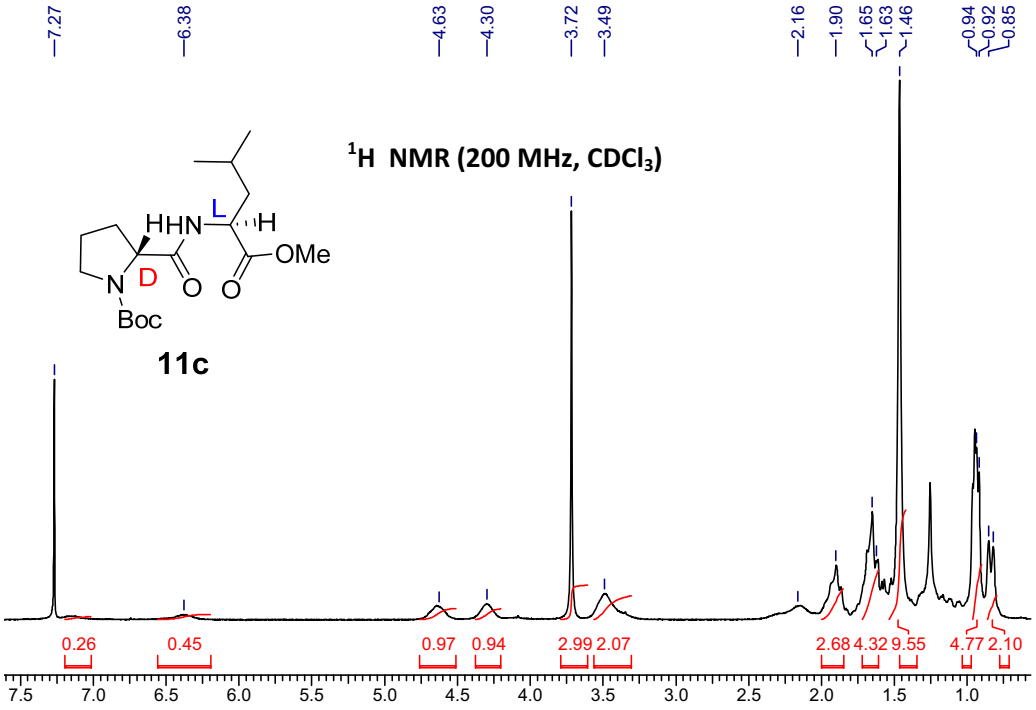
7.27
6.38
4.63
4.30
3.72
3.49
2.16
1.90
1.65
1.63
1.46
0.94
0.92
0.85
^{1}H NMR (200 MHz, CDCl$_3$)
HHN
L
H
OMe
N
D
O
O
Boc
11c
0.26
0.45
0.97
0.94
2.99
2.07
2.68
4.32
9.55
4.77
2.10
7.5
7.0
6.5
6.0
5.5
5.0
4.5
4.0
3.5
3.0
2.5
2.0
1.5
1.0

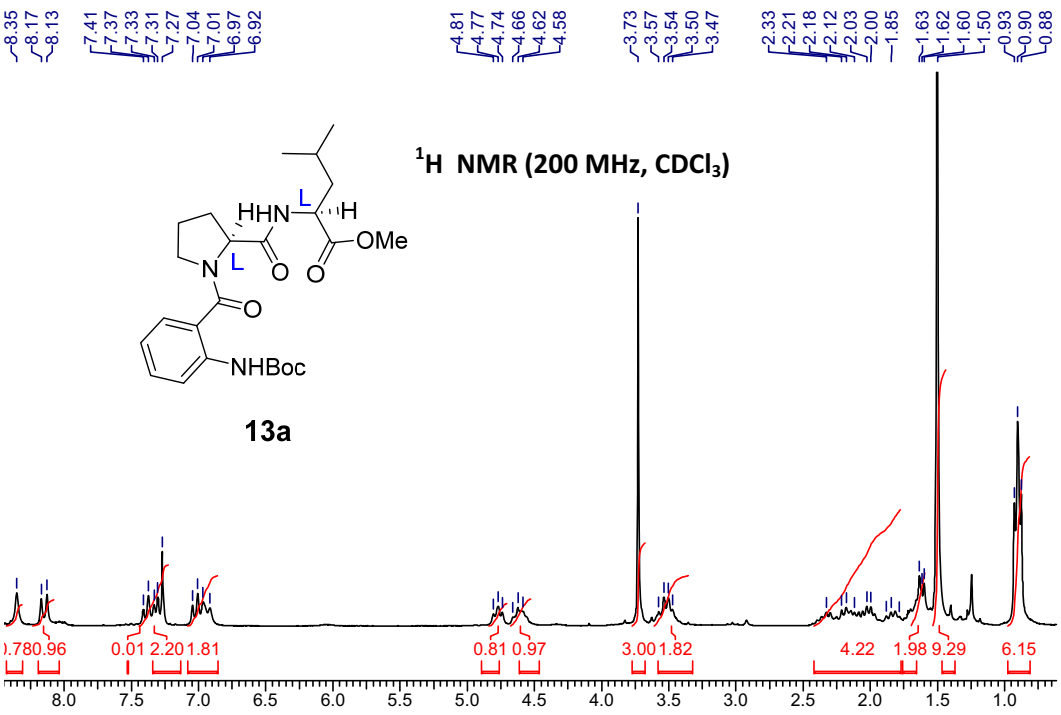
8.35
8.17
8.13
7.41
7.37
7.33
7.31
7.27
7.04
7.01
6.97
6.92
4.81
4.77
4.74
4.66
4.62
4.58
3.73
3.57
3.54
3.50
3.47
2.33
2.21
2.18
2.12
2.03
2.00
1.85
1.63
1.62
1.60
1.50
0.93
0.90
0.88
^{1}H NMR (200 MHz, CDCl$_3$)
HHN
L
H
OMe
N
L
O
O
O
NHBoc
13a
0.78
0.96
0.01
2.20
1.81
0.81
0.97
3.00
1.82
4.22
1.98
9.29
6.15
8.0
7.5
7.0
6.5
6.0
5.5
5.0
4.5
4.0
3.5
3.0
2.5
2.0
1.5
1.0

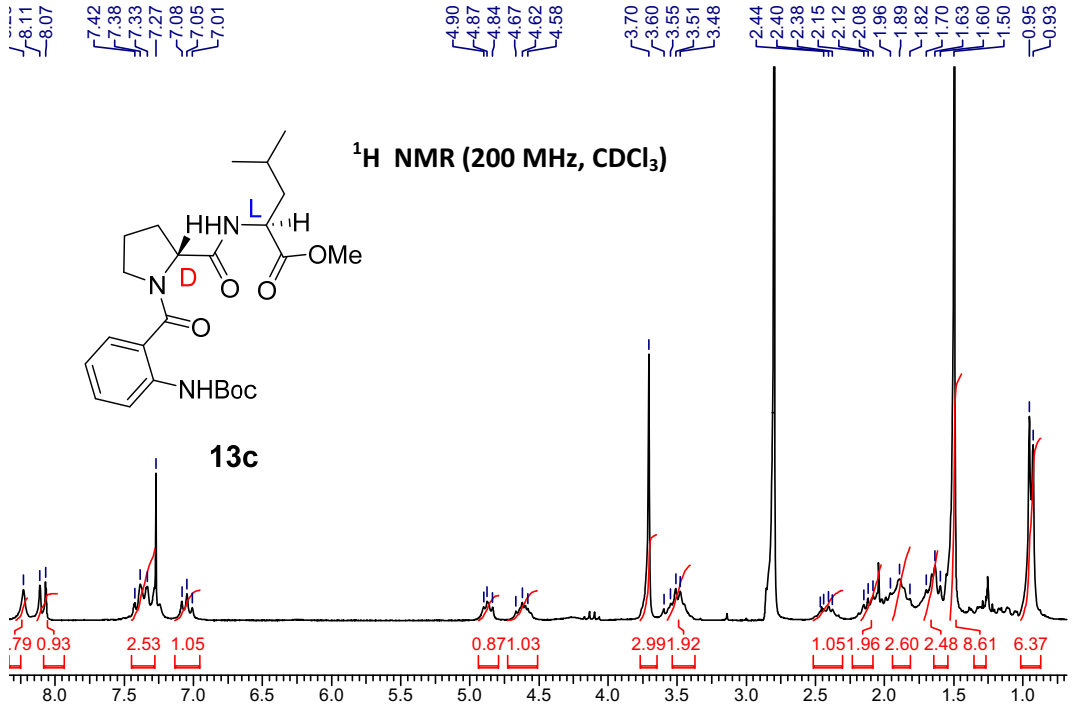
^{1}H NMR (200 MHz, CDCl$_3$)
HHN
L
H
OMe
N
D
O
O
O
NHBoc
13c

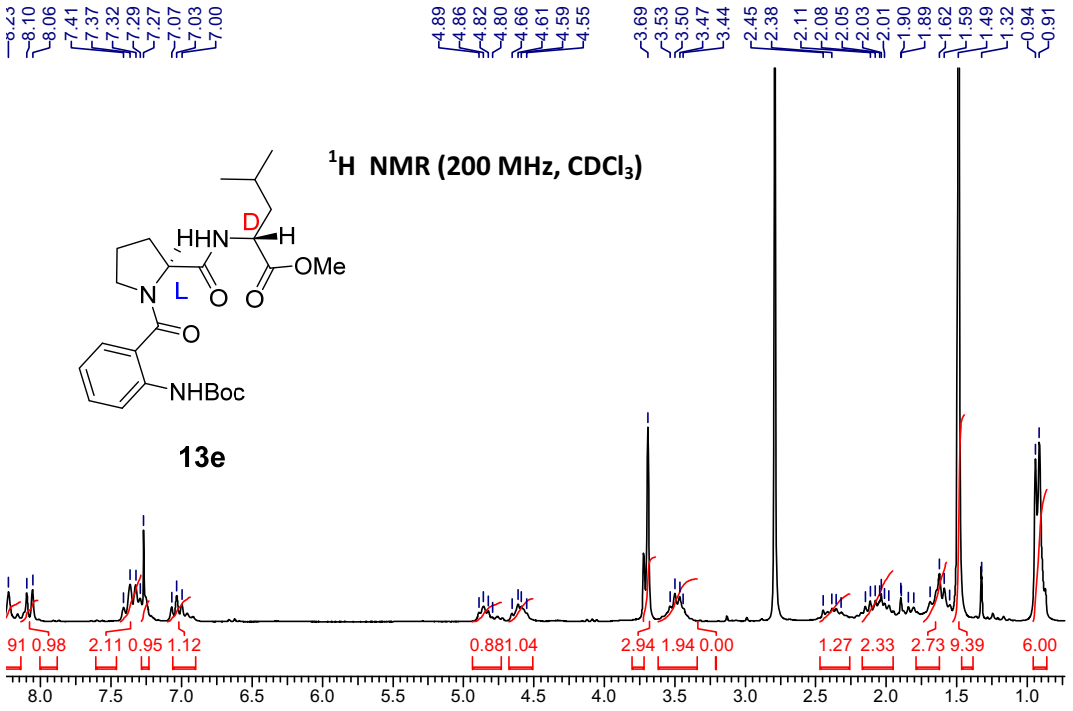
^{1}H NMR (200 MHz, CDCl$_3$)
HHN
D
H
OMe
N
L
O
O
O
NHBoc
13e

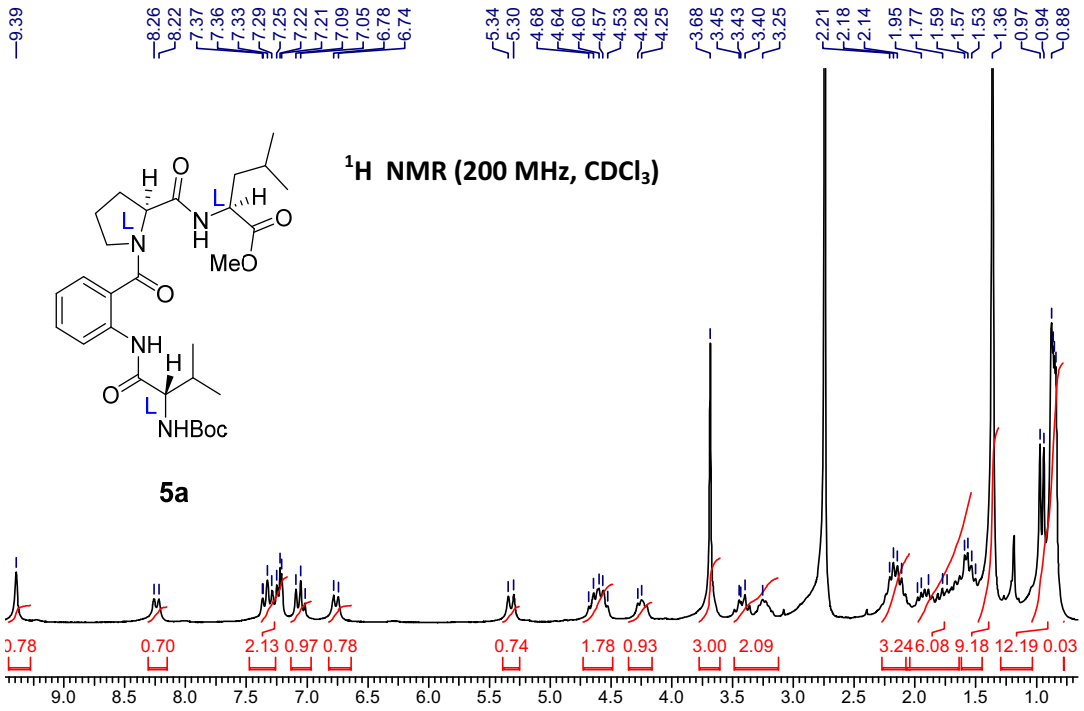
^{1}H NMR (200 MHz, CDCl$_3$)
5a
MeO
NHBoc

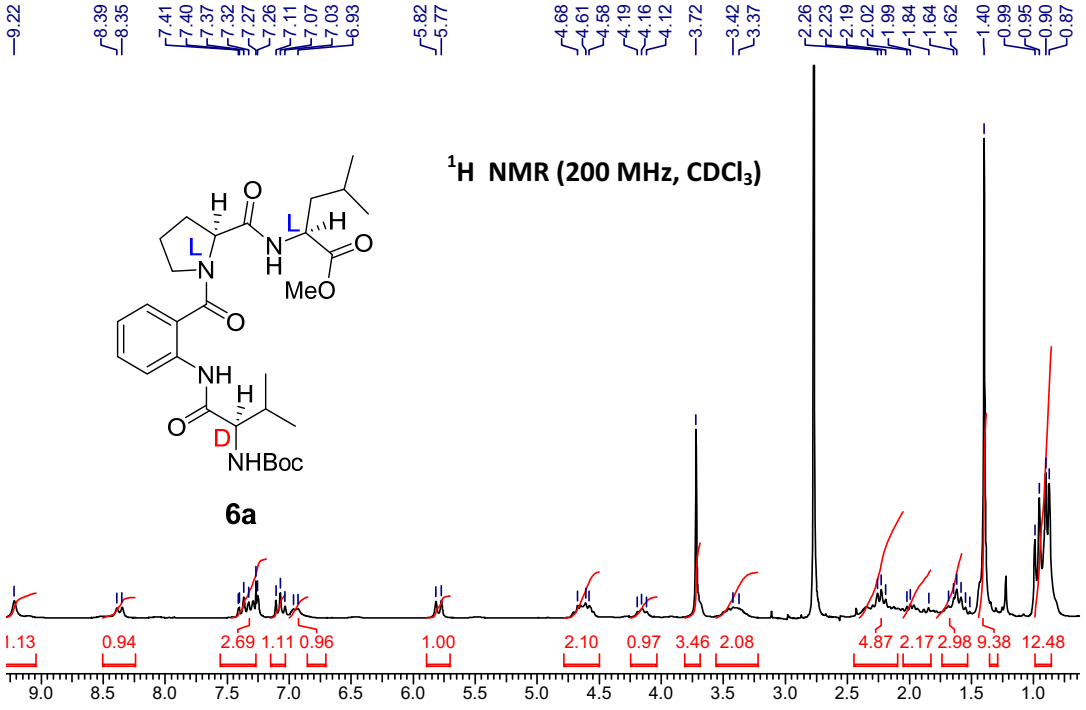
^{1}H NMR (200 MHz, CDCl$_3$)
6a
MeO
NHBoc

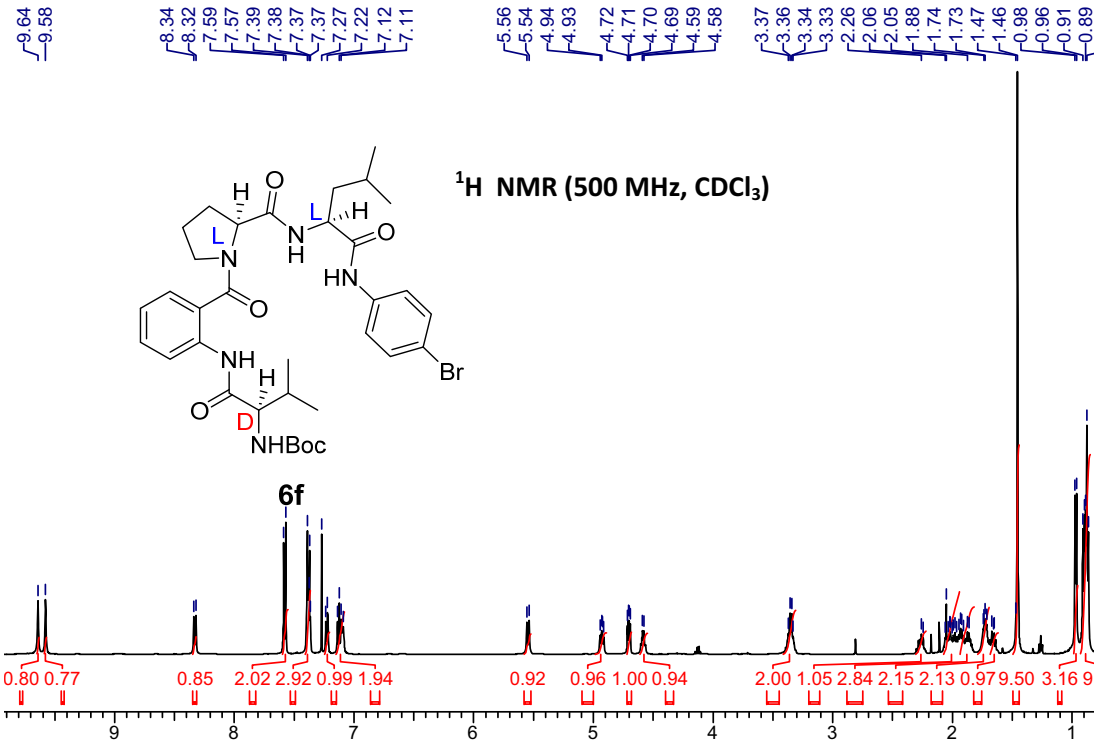
^{1}H NMR (500 MHz, CDCl$_3$)
6f
NHBoc
Br

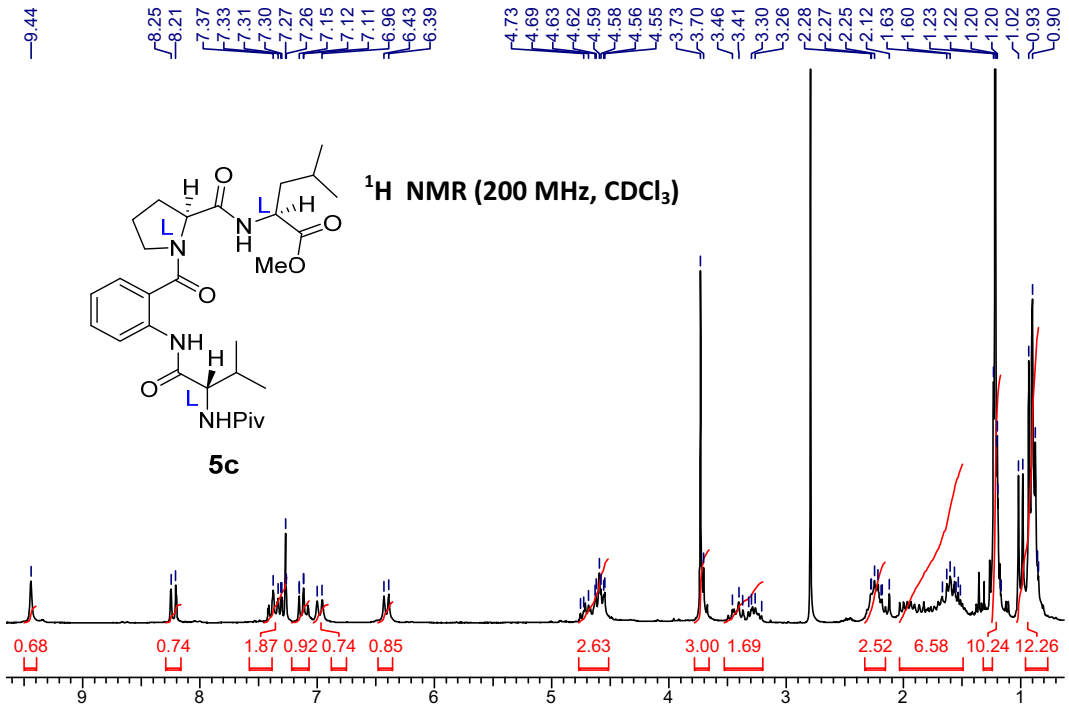
^{1}H NMR (200 MHz, CDCl$_3$)
MeO
NHPiv
5c

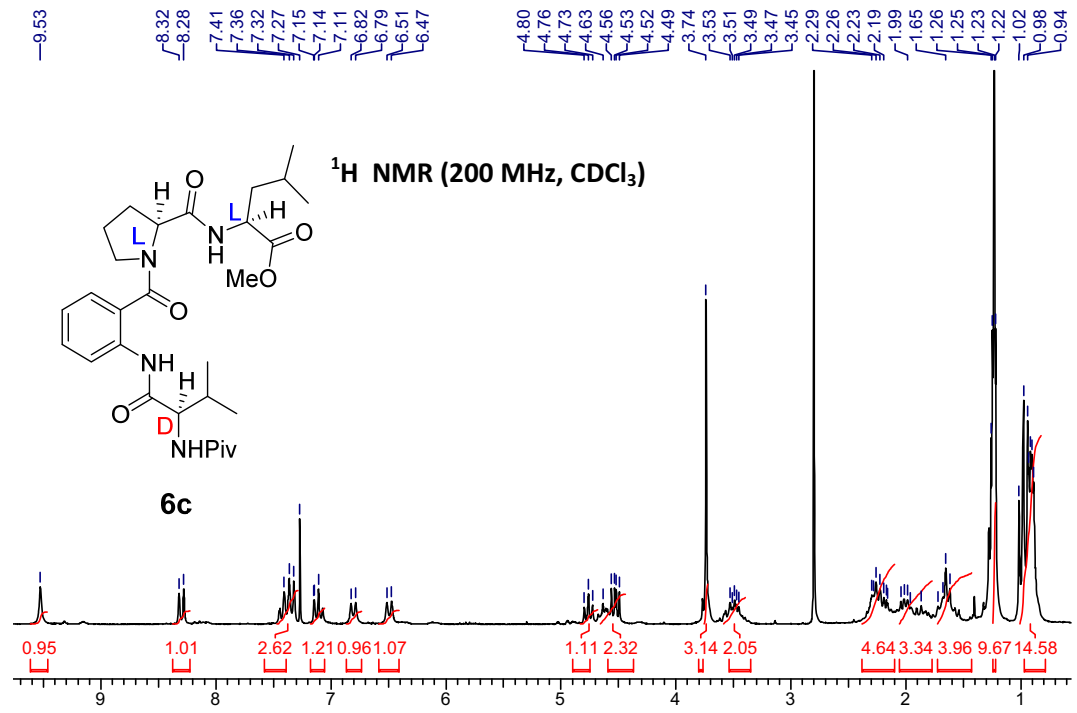
^{1}H NMR (200 MHz, CDCl$_3$)
6c
MeO
NHPiv

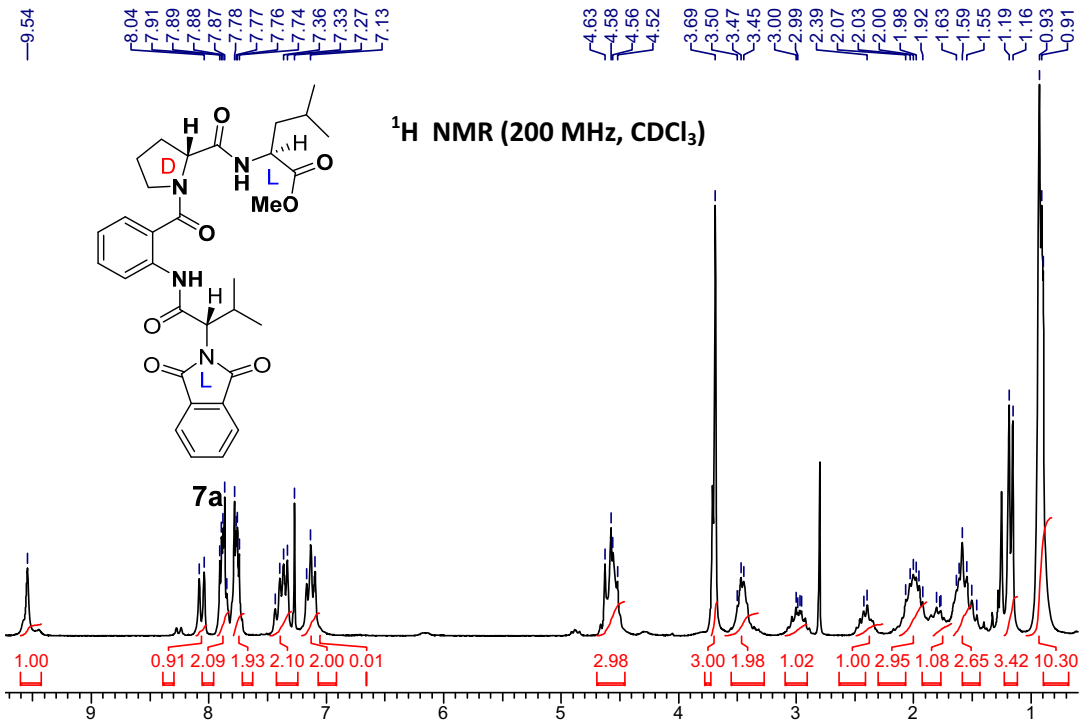
^{1}H NMR (200 MHz, CDCl$_3$)
7a
MeO

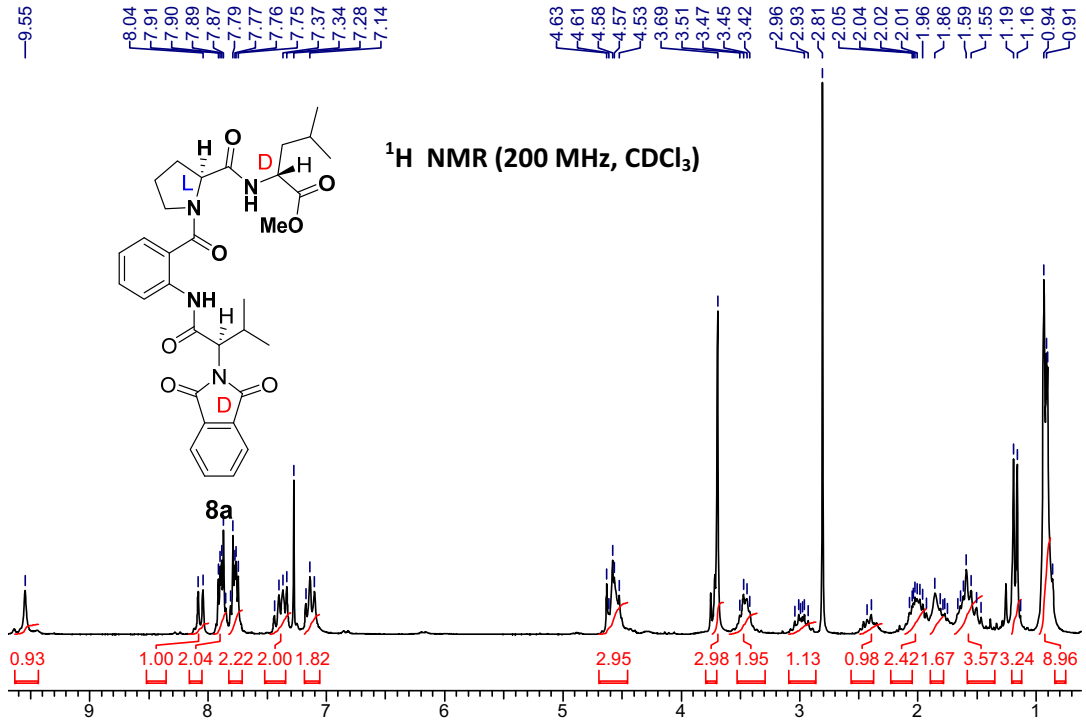
^{1}H NMR (200 MHz, CDCl$_3$)
8a
MeO
NH
D
L

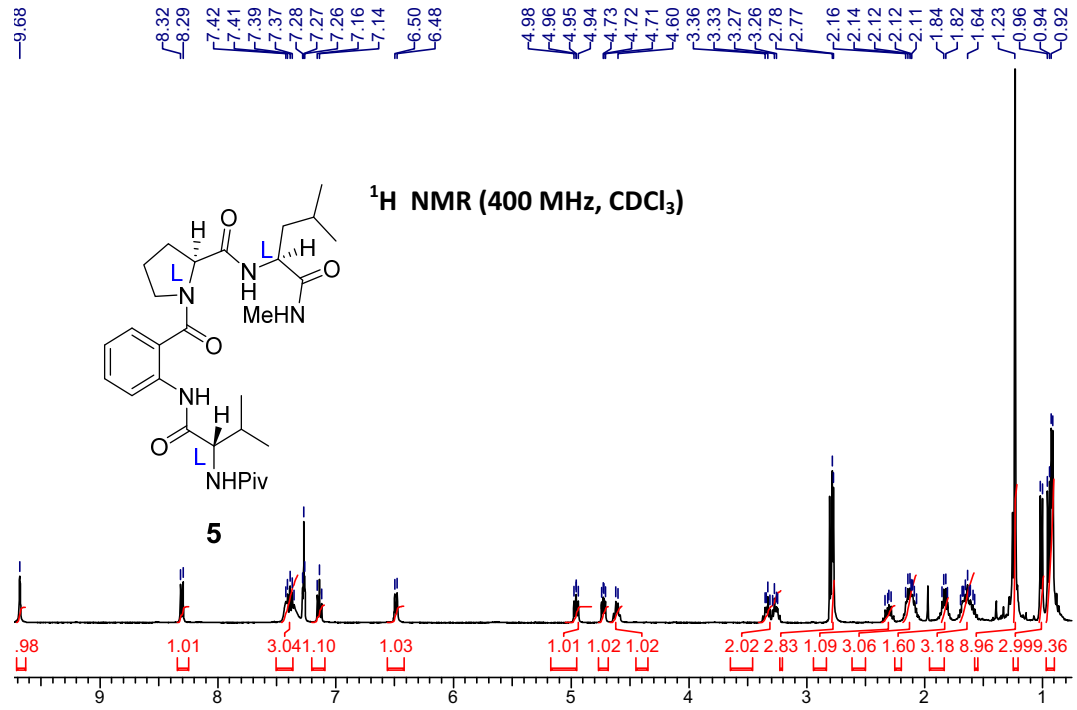
^{1}H NMR (400 MHz, CDCl$_3$)
5
MeHN
NHPiv
NH
L

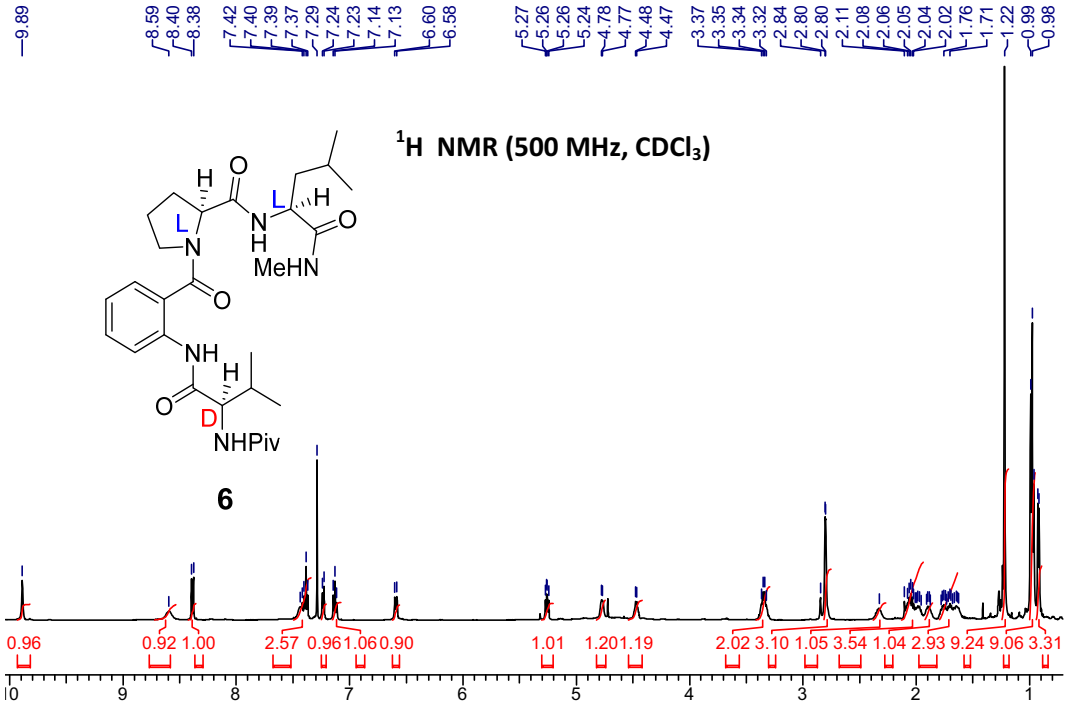
^{1}H NMR (500 MHz, CDCl$_3$)
MeHN
NHPiv
6

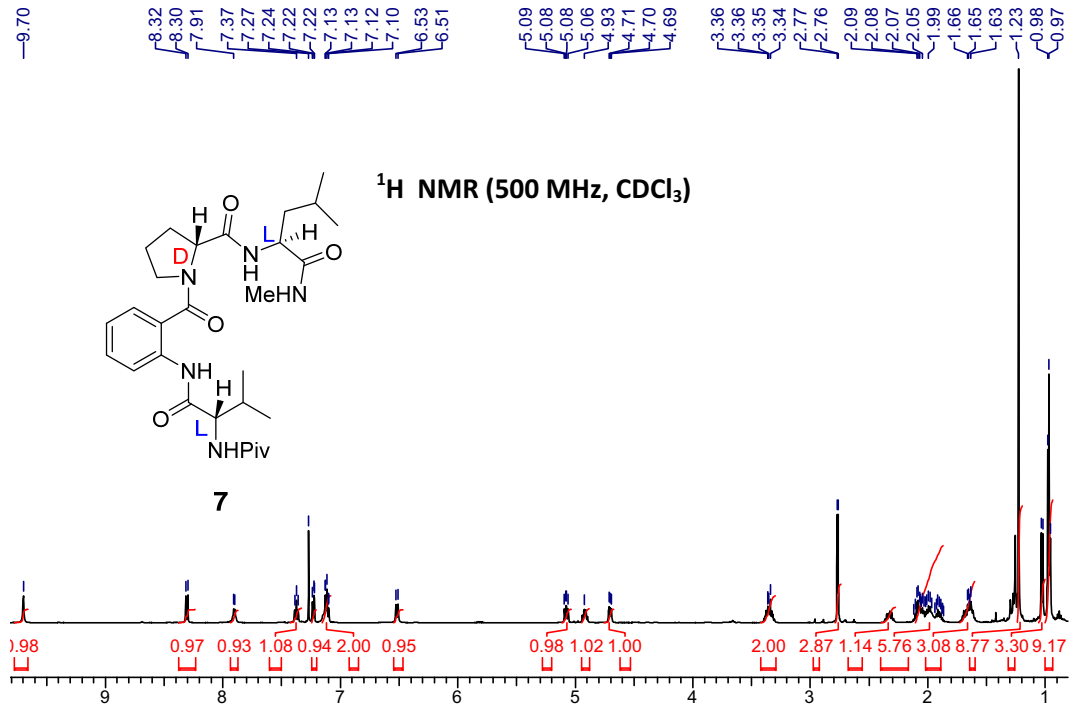
^{1}H NMR (500 MHz, CDCl$_3$)
MeHN
NHPiv
7

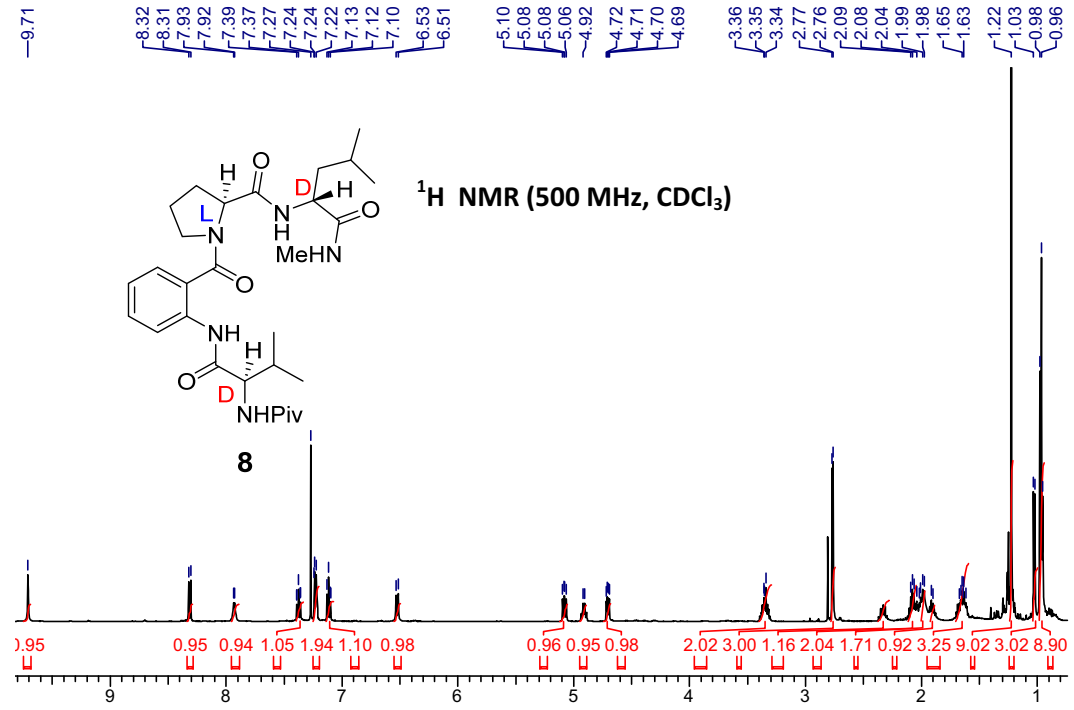

^{1}H NMR (500 MHz, $CDCl_3$)

8

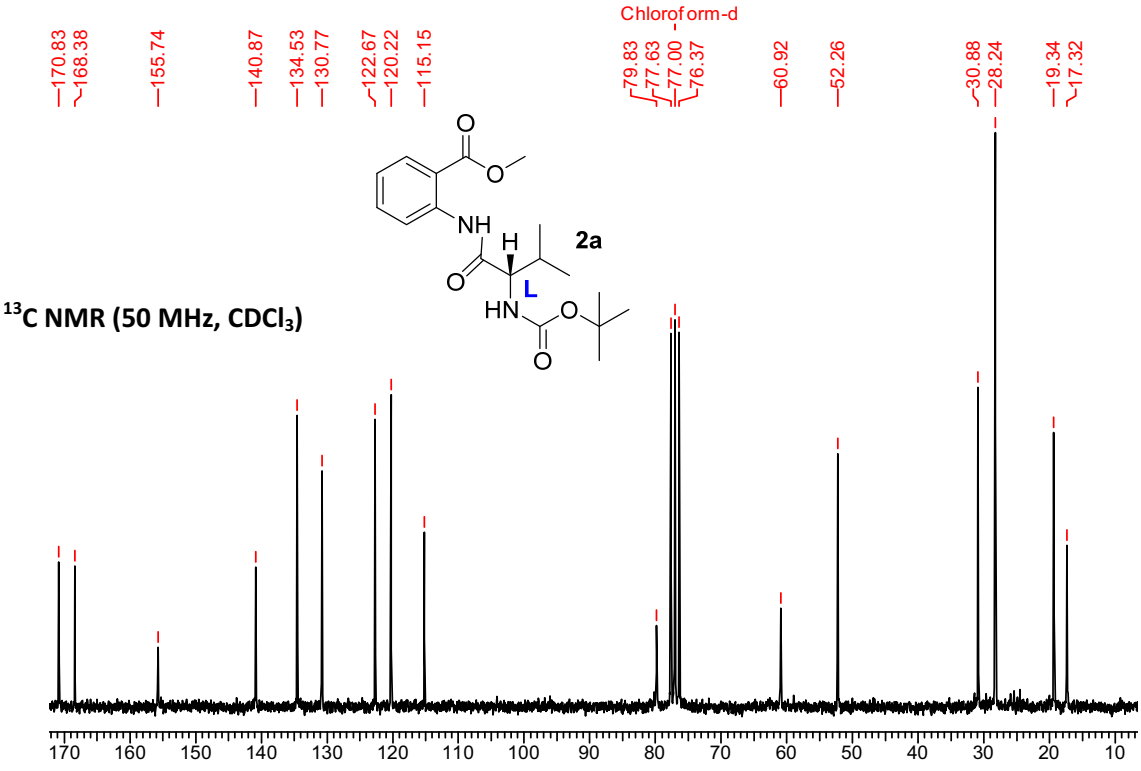

^{13}C NMR (50 MHz, $CDCl_3$)

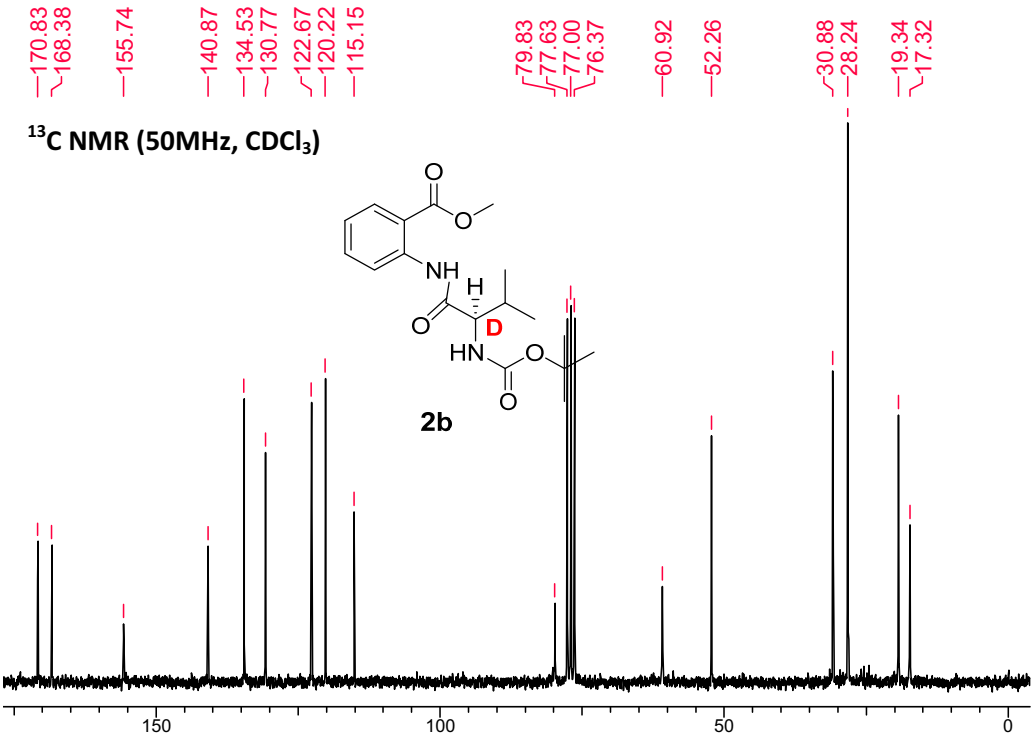
170.83
168.38
155.74
140.87
134.53
130.77
122.67
120.22
115.15
79.83
77.63
77.00
76.37
60.92
52.26
30.88
28.24
19.34
17.32
13C NMR (50MHz, CDCl3)
NH
H
O
D
HN
O
O
2b
150
100
50
0

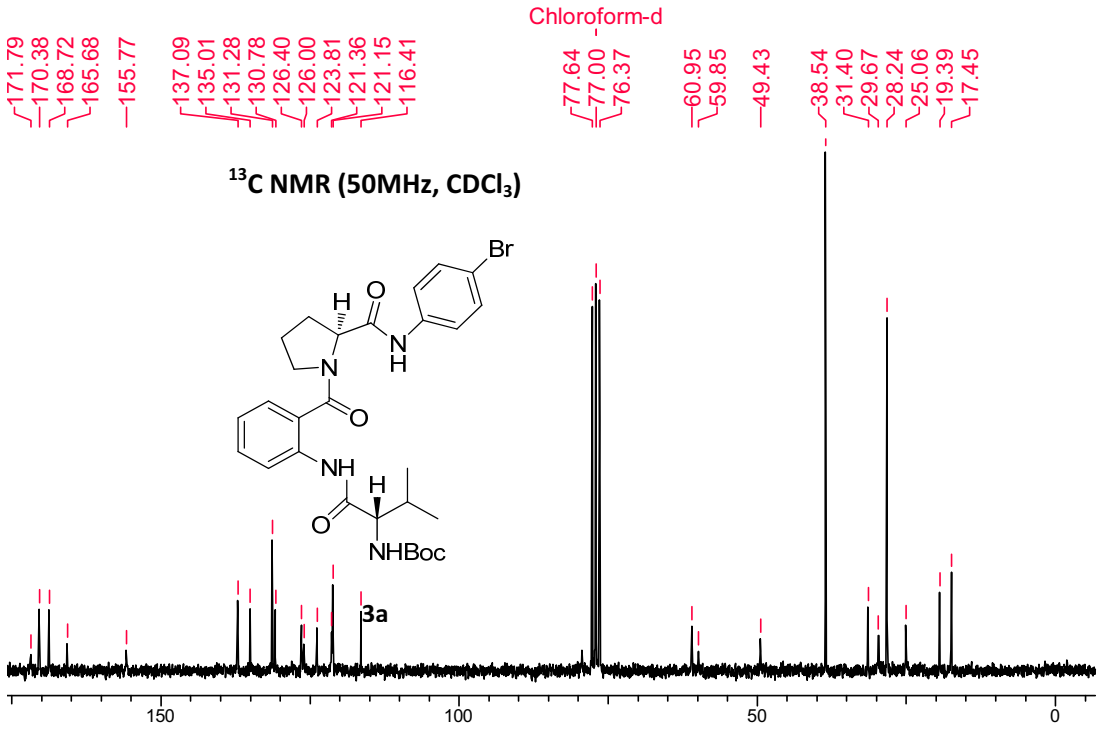
Chloroform-d
171.79
170.38
168.72
165.68
155.77
137.09
135.01
131.28
130.78
126.40
126.00
123.81
121.36
121.15
116.41
77.64
77.00
76.37
60.95
59.85
49.43
38.54
31.40
29.67
28.24
25.06
19.39
17.45
13C NMR (50MHz, CDCl3)
Br
H
O
N
H
N
O
NH
H
O
NHBoc
3a
150
100
50
0

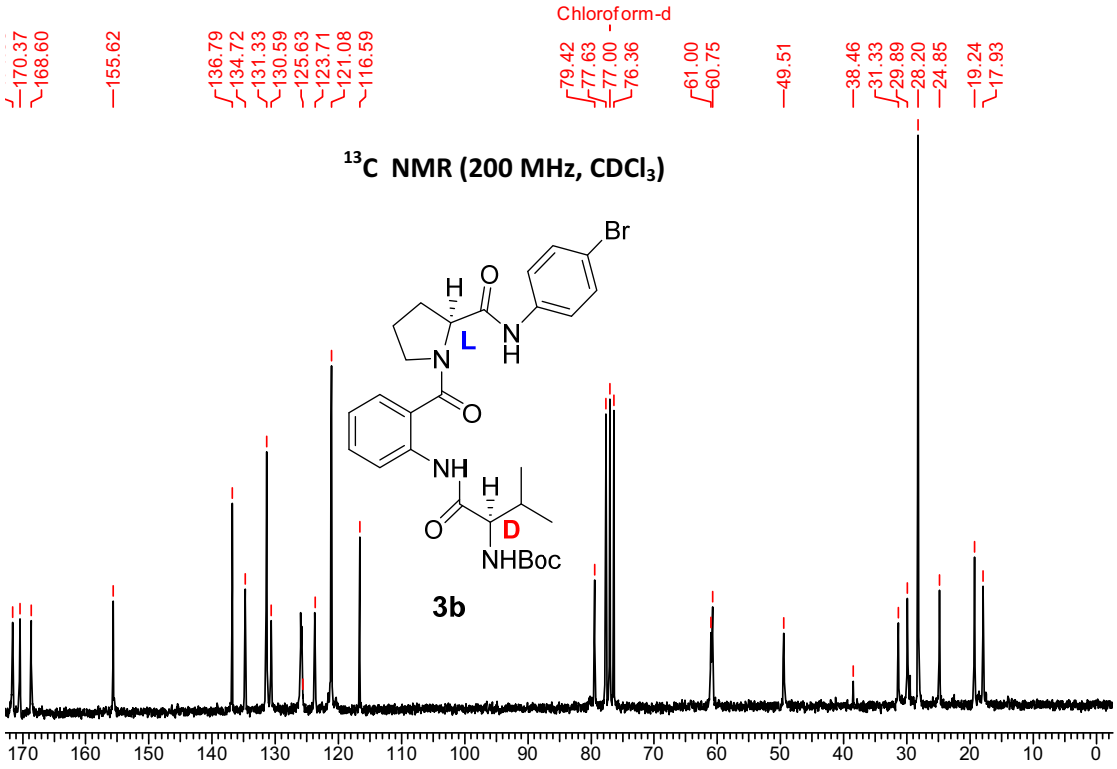
Chloroform-d
170.37
168.60
155.62
136.79
134.72
131.33
130.59
125.63
123.71
121.08
116.59
79.42
77.63
77.00
76.36
61.00
60.75
49.51
38.46
31.33
29.89
28.20
24.85
19.24
17.93
13C NMR (200 MHz, CDCl3)
Br
H
O
N
L
N
H
O
NH
H
O
D
NHBoc
3b
170
160
150
140
130
120
110
100
90
80
70
60
50
40
30
20
10
0

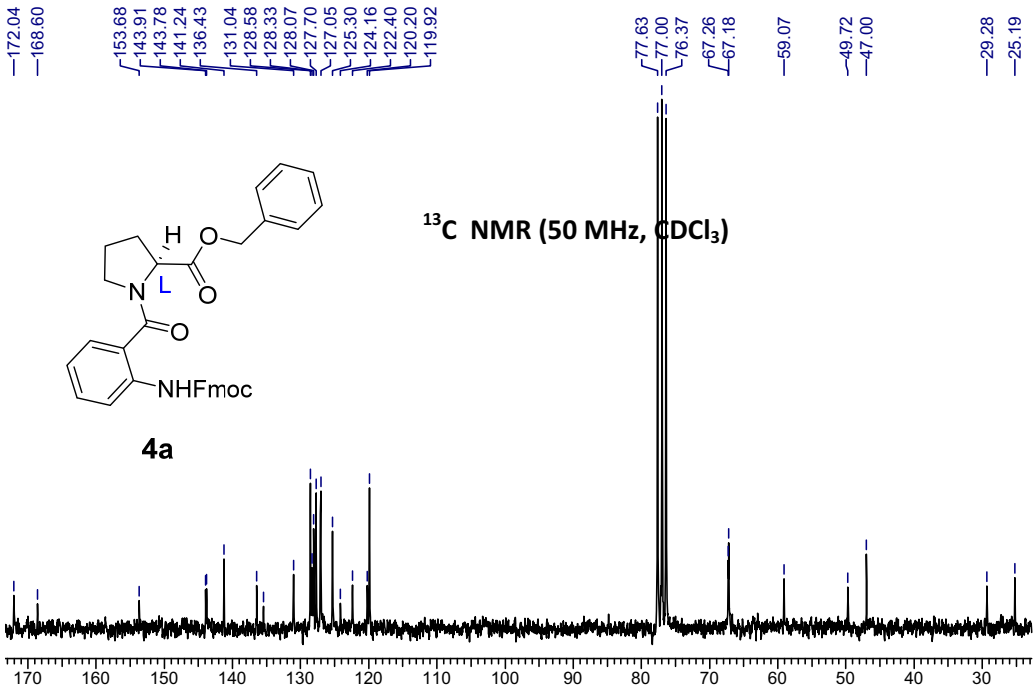
172.04
168.60
153.68
143.91
143.78
141.24
136.43
131.04
128.58
128.33
128.07
127.70
127.05
125.30
124.16
122.40
120.20
119.92
77.63
77.00
76.37
67.26
67.18
59.07
49.72
47.00
29.28
25.19
13C NMR (50 MHz, CDCl3)
H
O
N
L
O
O
NHFmoc
4a
170
160
150
140
130
120
110
100
90
80
70
60
50
40
30

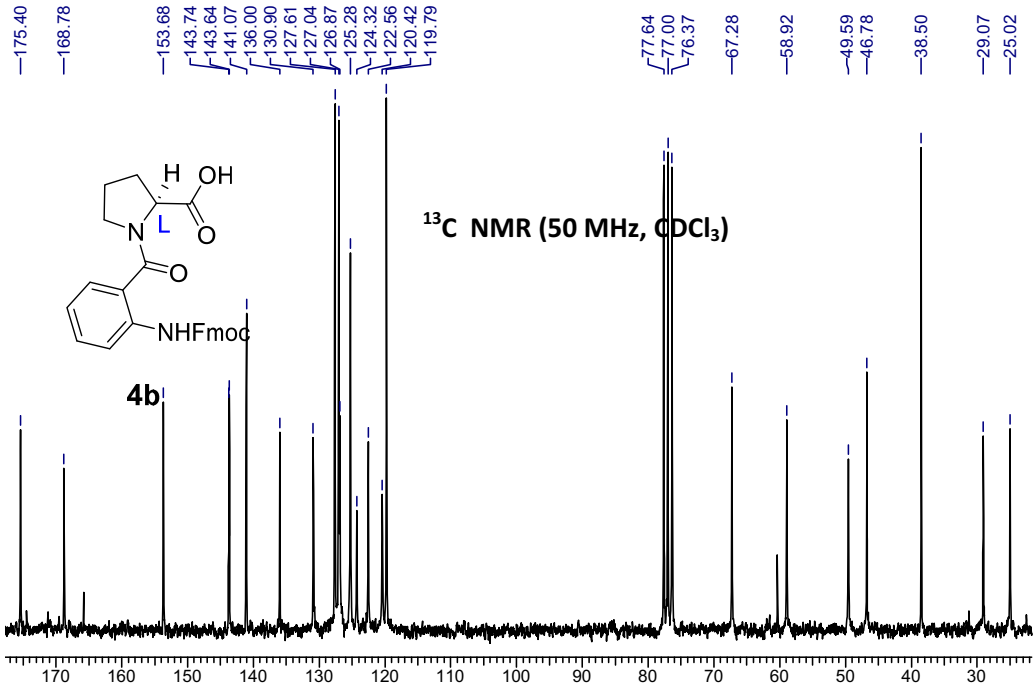
175.40
168.78
153.68
143.74
143.64
141.07
136.00
130.90
127.61
127.04
126.87
125.28
124.32
122.56
120.42
119.79
77.64
77.00
76.37
67.28
58.92
49.59
46.78
38.50
29.07
25.02
H
OH
L
N
O
O
NHFmoc
4b
13C NMR (50 MHz, CDCl3)
170
160
150
140
130
120
110
100
90
80
70
60
50
40
30

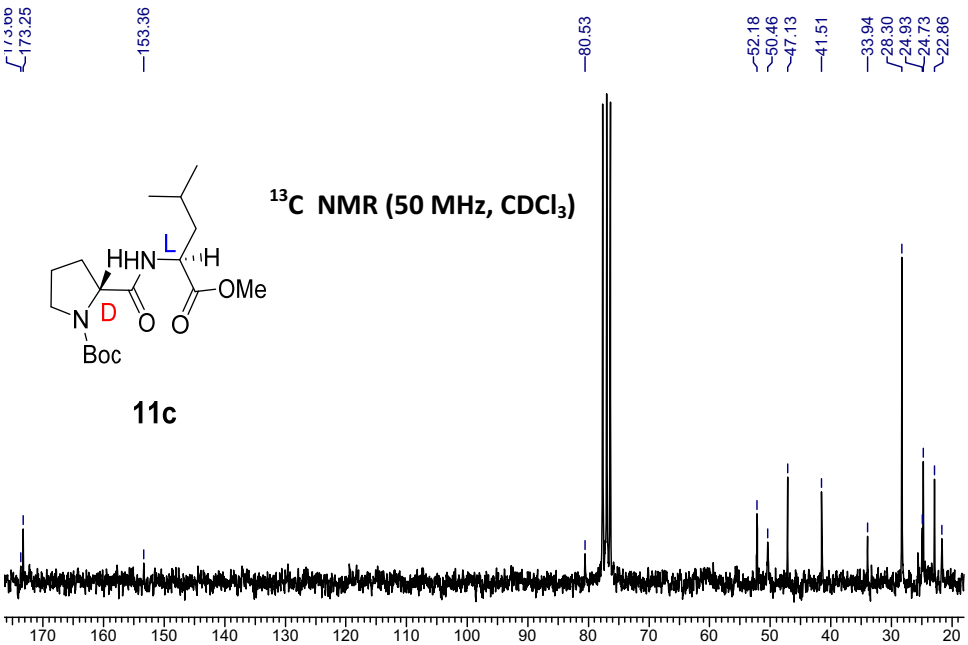
173.25
153.36
80.53
52.18
50.46
47.13
41.51
33.94
28.30
24.93
24.73
22.86
13C NMR (50 MHz, CDCl3)
L
HHN
H
OMe
N
D
O
O
Boc
11c
170
160
150
140
130
120
110
100
90
80
70
60
50
40
30
20

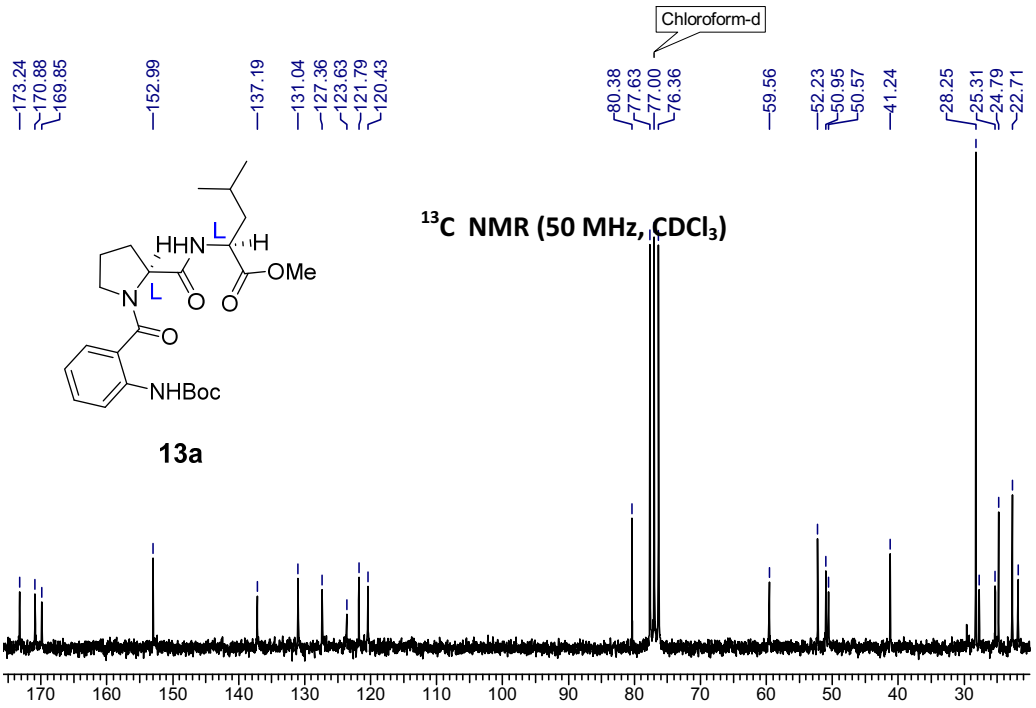
Chloroform-d
173.24
170.88
169.85
152.99
137.19
131.04
127.36
123.63
121.79
120.43
80.38
77.63
77.00
76.36
59.56
52.23
50.95
50.57
41.24
28.25
25.31
24.79
22.71
^{13}C NMR (50 MHz, CDCl$_3$)
HHN
L
H
OMe
N
L
O
O
O
NHBoc
13a
170
160
150
140
130
120
110
100
90
80
70
60
50
40
30

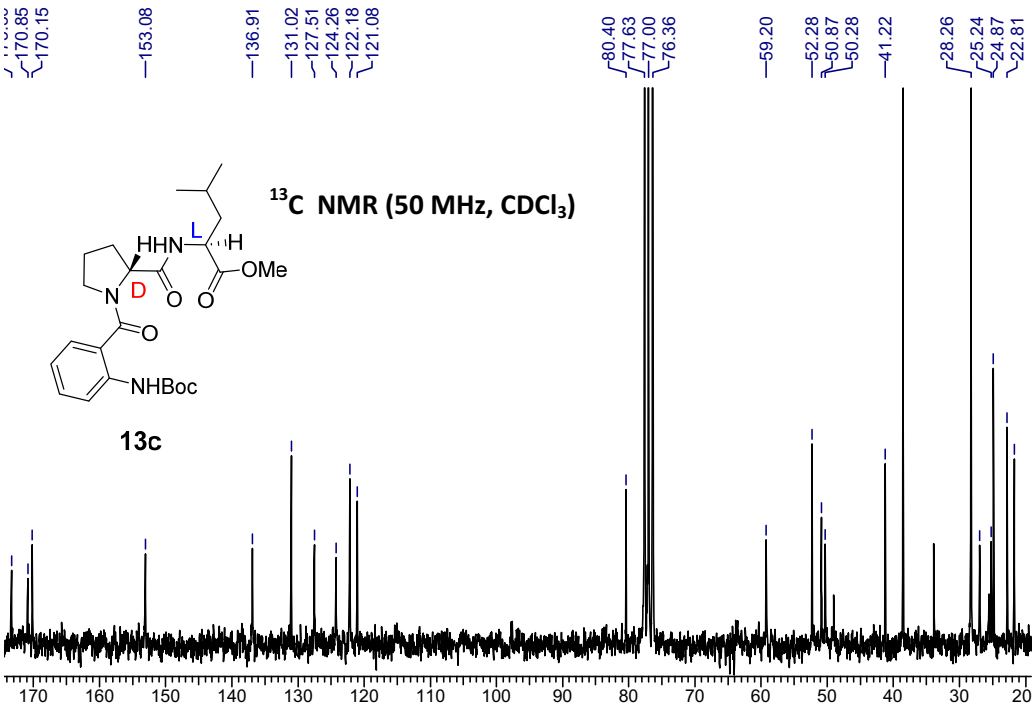
170.85
170.15
153.08
136.91
131.02
127.51
124.26
122.18
121.08
80.40
77.63
77.00
76.36
59.20
52.28
50.87
50.28
41.22
28.26
25.24
24.87
22.81
^{13}C NMR (50 MHz, CDCl$_3$)
HHN
L
H
OMe
N
D
O
O
O
NHBoc
13c
170
160
150
140
130
120
110
100
90
80
70
60
50
40
30
20

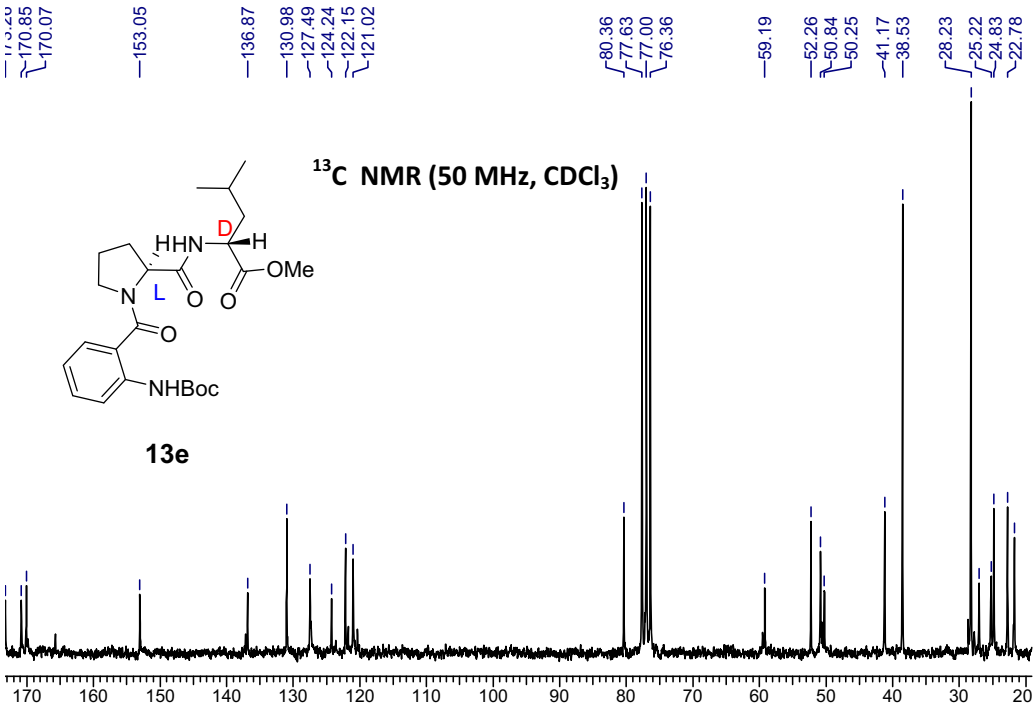
170.85
170.07
153.05
136.87
130.98
127.49
124.24
122.15
121.02
80.36
77.63
77.00
76.36
59.19
52.26
50.84
50.25
41.17
38.53
28.23
25.22
24.83
22.78
^{13}C NMR (50 MHz, CDCl$_3$)
HHN
D
H
OMe
N
L
O
O
O
NHBoc
13e
170
160
150
140
130
120
110
100
90
80
70
60
50
40
30
20

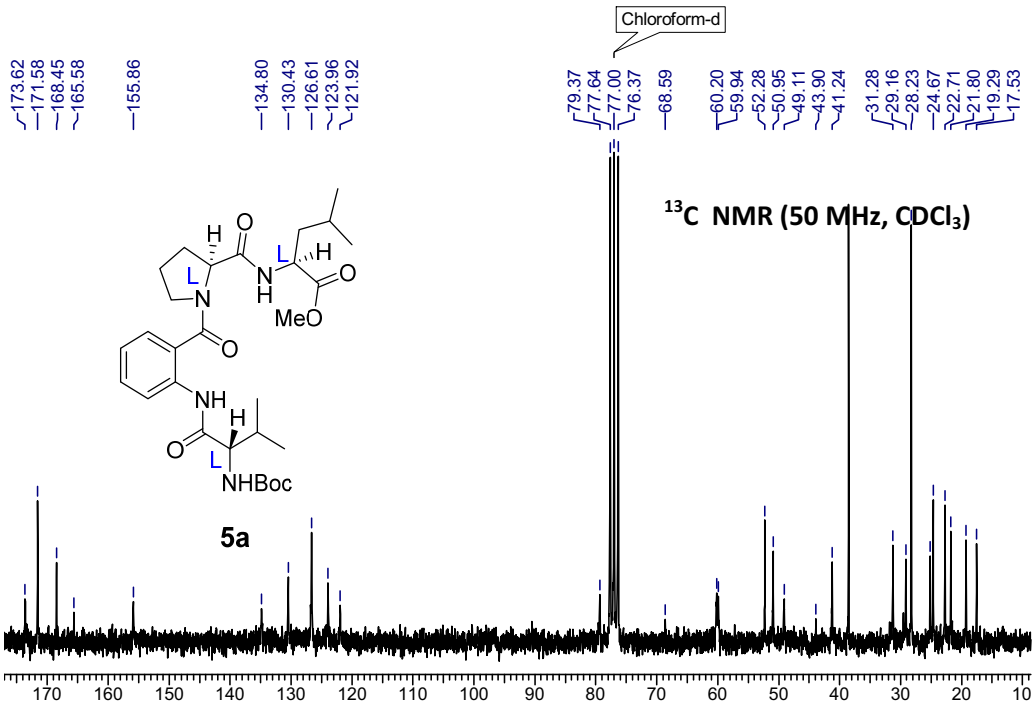
Chloroform-d
173.62
171.58
168.45
165.58
155.86
134.80
130.43
126.61
123.96
121.92
79.37
77.64
77.00
76.37
68.59
60.20
59.94
52.28
50.95
49.11
43.90
41.24
31.28
29.16
28.23
24.67
22.71
21.80
19.29
17.53
^{13}C NMR (50 MHz, CDCl$_3$)
H
O
L
H
N
L
N
H
O
MeO
O
NH
H
O
L
NHBoc
5a
170
160
150
140
130
120
110
100
90
80
70
60
50
40
30
20
10

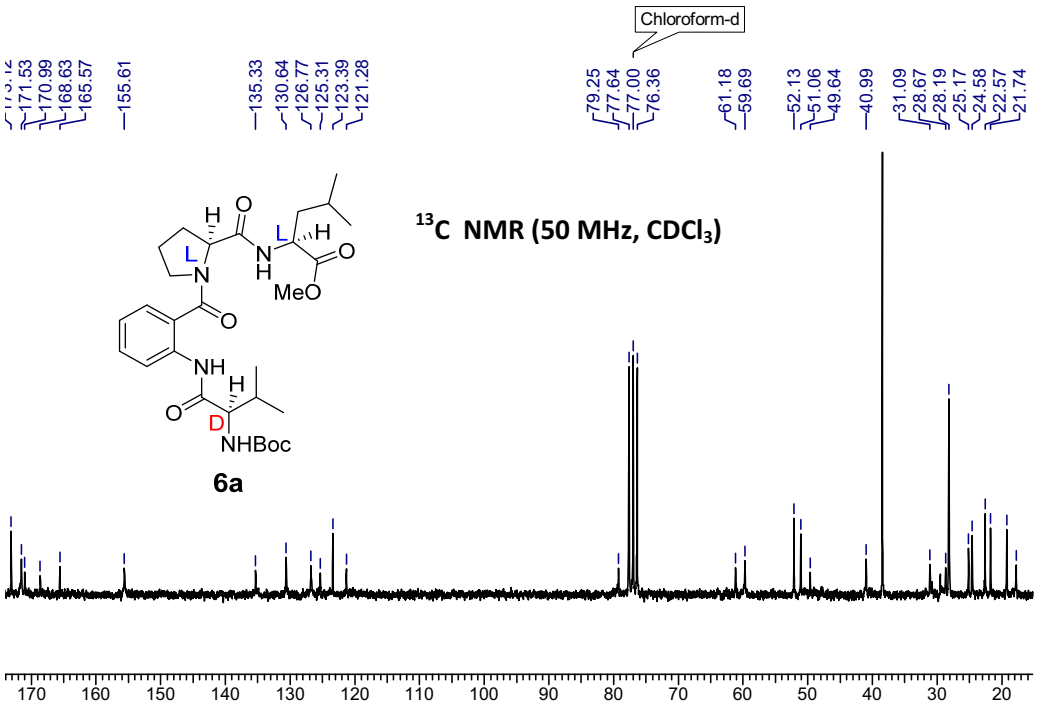

^{13}C NMR (50 MHz, $CDCl_3$)

6a

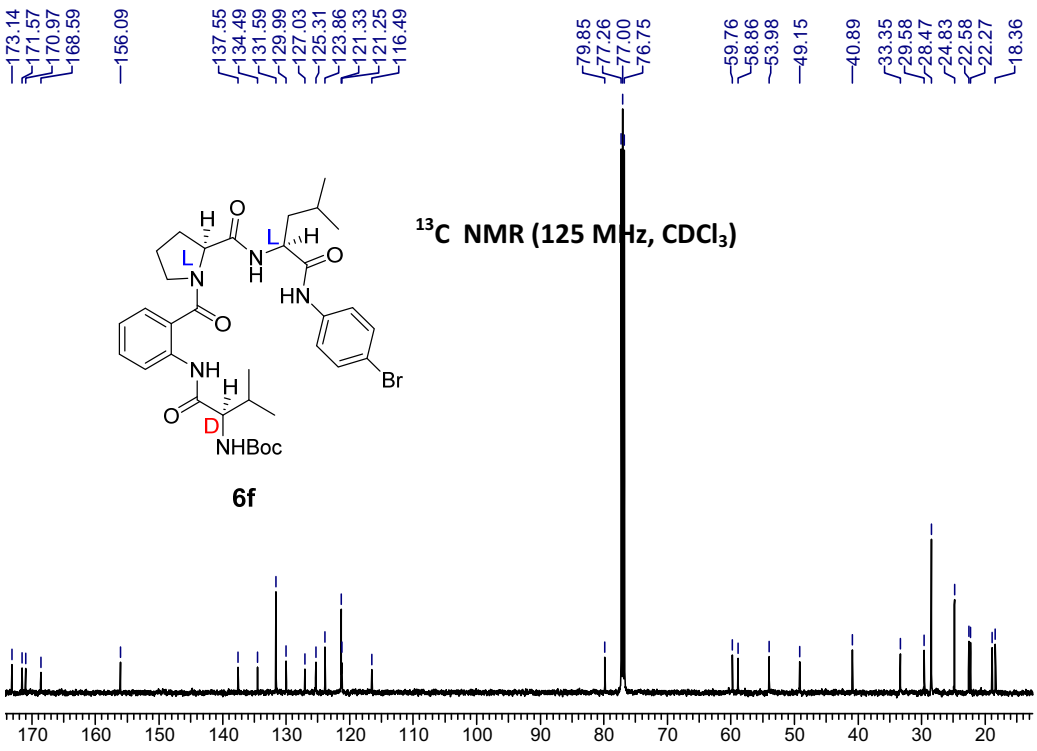

^{13}C NMR (125 MHz, $CDCl_3$)

6f

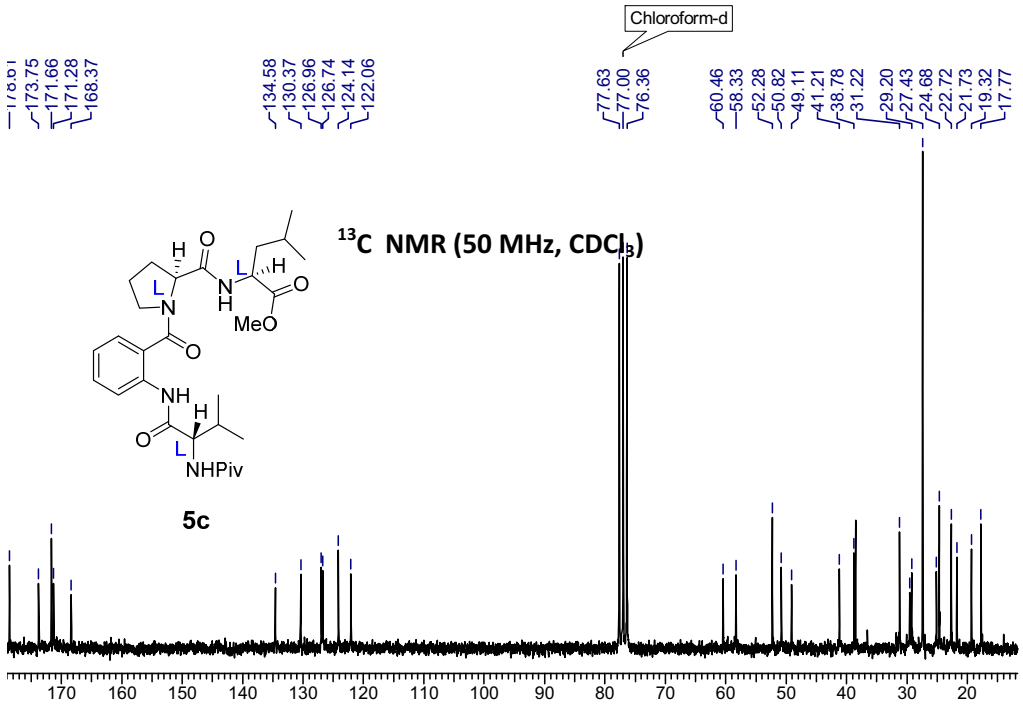
Chloroform-d
173.75
171.66
171.28
168.37
134.58
130.37
126.96
126.74
124.14
122.06
77.63
77.00
76.36
60.46
58.33
52.28
50.82
49.11
41.21
38.78
31.22
29.20
27.43
24.68
22.72
21.73
19.32
17.77
^{13}C NMR (50 MHz, CDCl$_3$)
MeO
NHPiv
5c
170 160 150 140 130 120 110 100 90 80 70 60 50 40 30 20

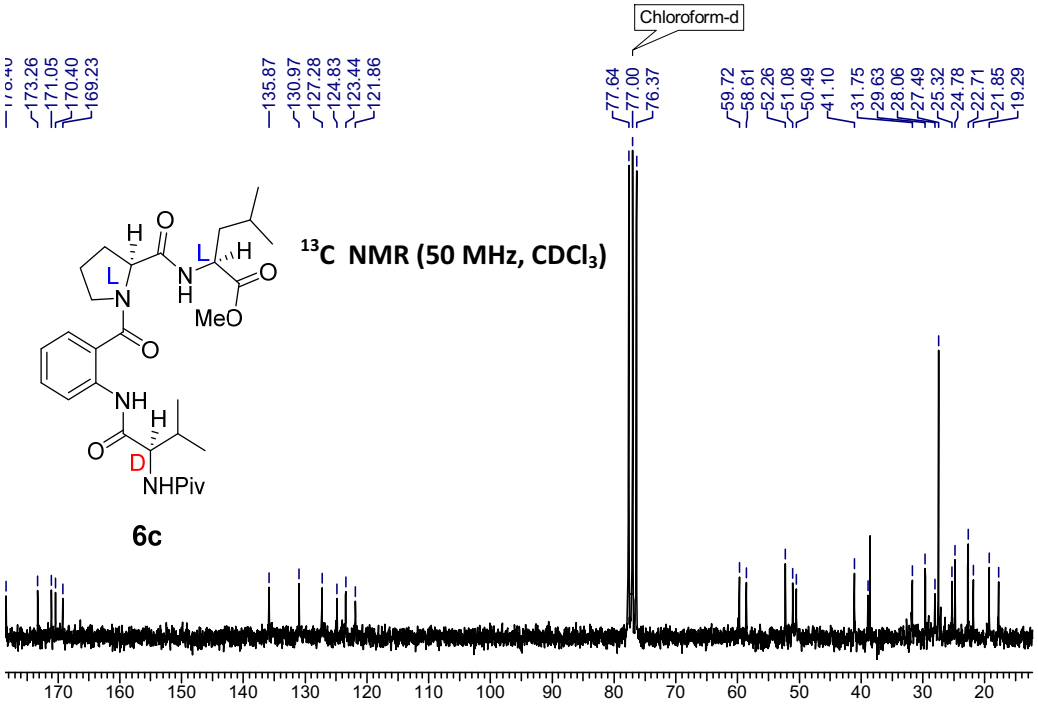
Chloroform-d
173.26
171.05
170.40
169.23
135.87
130.97
127.28
124.83
123.44
121.86
77.64
77.00
76.37
59.72
58.61
52.26
51.08
50.49
41.10
31.75
29.63
28.06
27.49
25.32
24.78
22.71
21.85
19.29
^{13}C NMR (50 MHz, CDCl$_3$)
MeO
NHPiv
6c
170 160 150 140 130 120 110 100 90 80 70 60 50 40 30 20

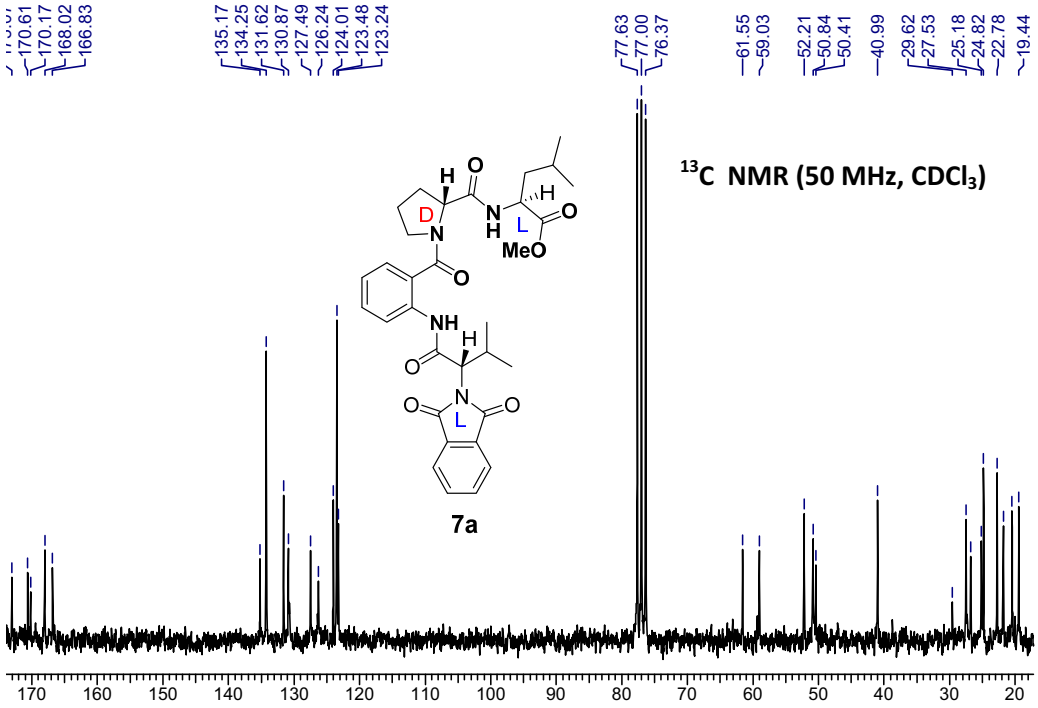
170.61
170.17
168.02
166.83
135.17
134.25
131.62
130.87
127.49
126.24
124.01
123.48
123.24
77.63
77.00
76.37
61.55
59.03
52.21
50.84
50.41
40.99
29.62
27.53
25.18
24.82
22.78
19.44
^{13}C NMR (50 MHz, CDCl$_3$)
7a

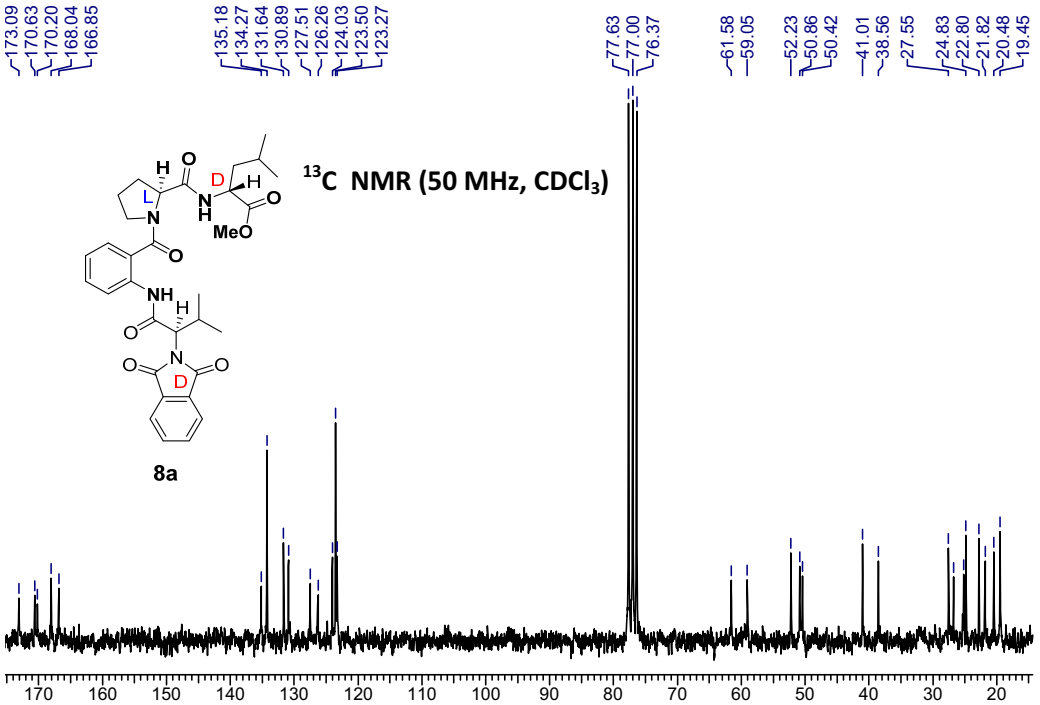
173.09
170.63
170.20
168.04
166.85
135.18
134.27
131.64
130.89
127.51
126.26
124.03
123.50
123.27
77.63
77.00
76.37
61.58
59.05
52.23
50.86
50.42
41.01
38.56
27.55
24.83
22.80
21.82
20.48
19.45
^{13}C NMR (50 MHz, CDCl$_3$)
8a

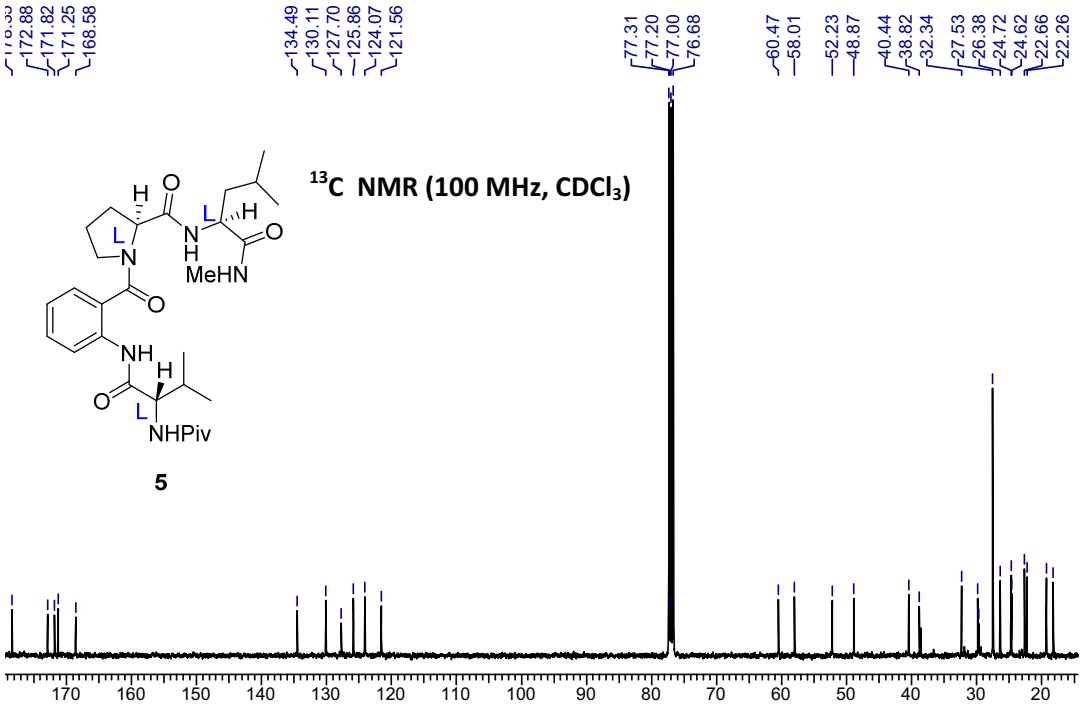
172.88
171.82
171.25
168.58
134.49
130.11
127.70
125.86
124.07
121.56
77.31
77.20
77.00
76.68
60.47
58.01
52.23
48.87
40.44
38.82
32.34
27.53
26.38
24.72
24.62
22.66
22.26
^{13}C NMR (100 MHz, CDCl$_3$)
MeHN
NHPiv
5

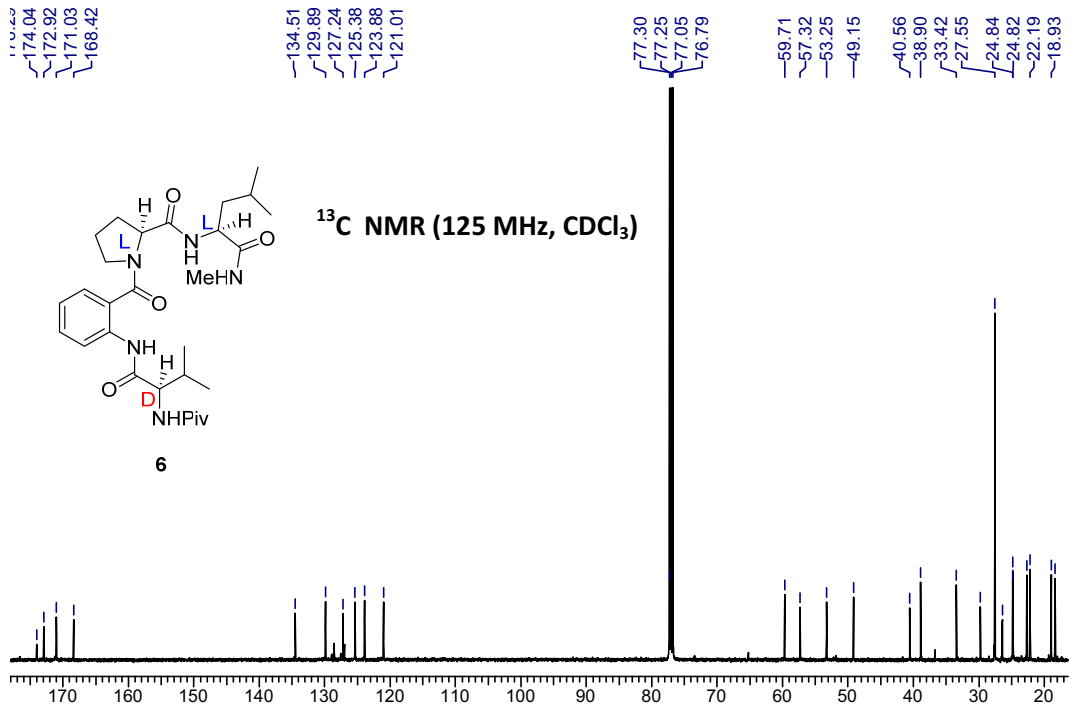
174.04
172.92
171.03
168.42
134.51
129.89
127.24
125.38
123.88
121.01
77.30
77.25
77.05
76.79
59.71
57.32
53.25
49.15
40.56
38.90
33.42
27.55
24.84
24.82
22.19
18.93
^{13}C NMR (125 MHz, CDCl$_3$)
MeHN
NHPiv
6

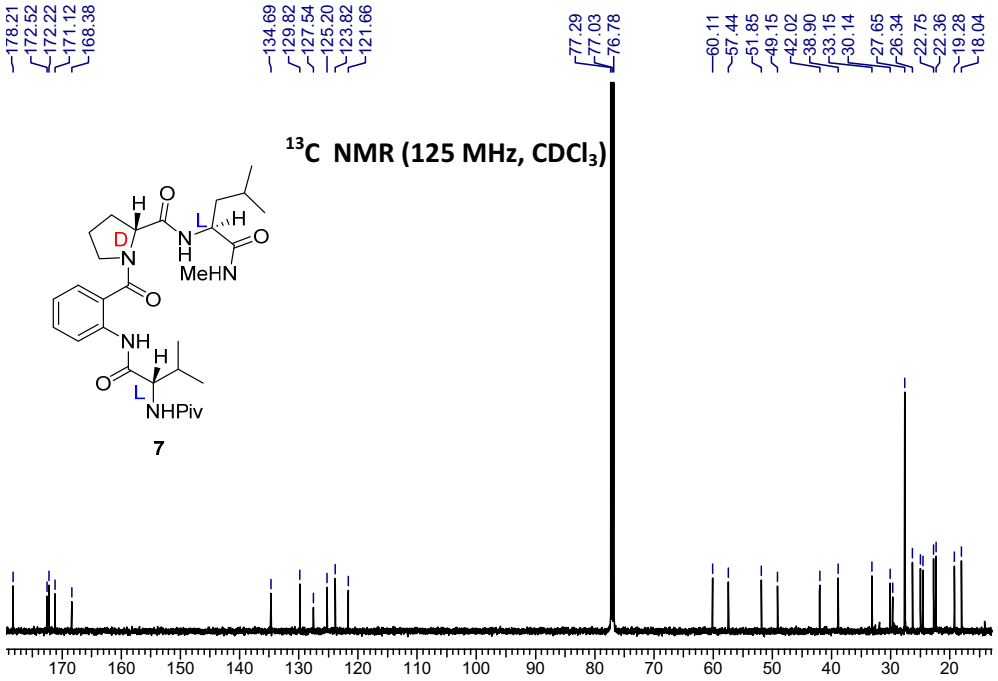
178.21
172.52
172.22
171.12
168.38
134.69
129.82
127.54
125.20
123.82
121.66
77.29
77.03
76.78
60.11
57.44
51.85
49.15
42.02
38.90
33.15
30.14
27.65
26.34
22.75
22.36
19.28
18.04
^{13}C NMR (125 MHz, CDCl$_3$)
MeHN
NHPiv
170 160 150 140 130 120 110 100 90 80 70 60 50 40 30 20

7

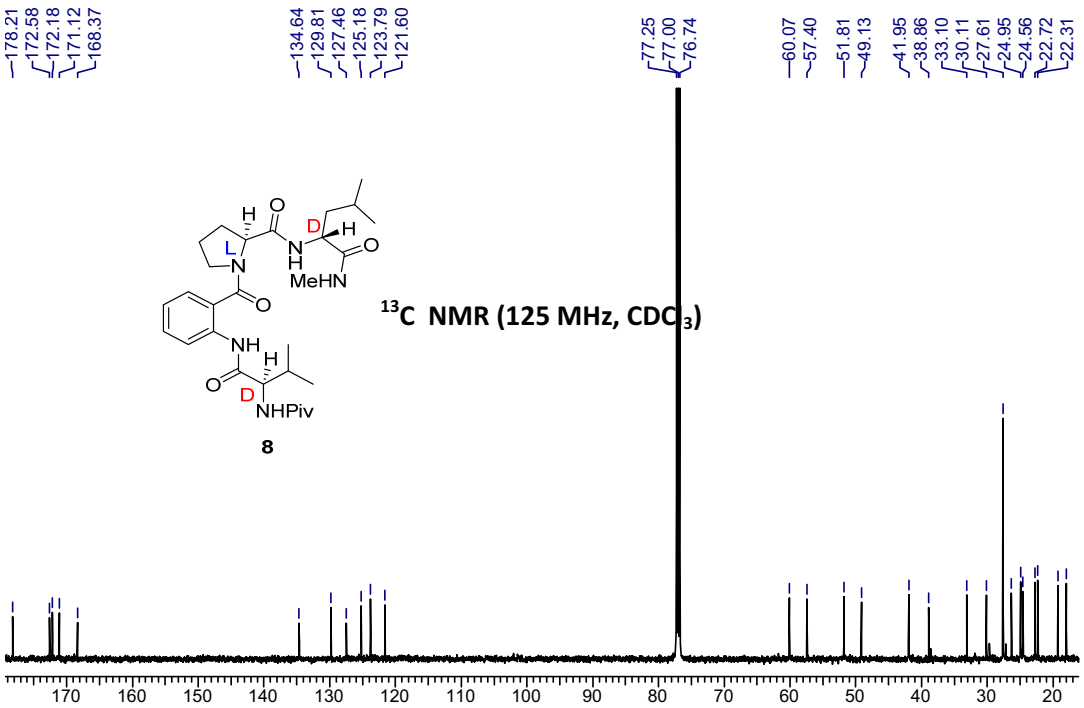
178.21
172.58
172.18
171.12
168.37
134.64
129.81
127.46
125.18
123.79
121.60
77.25
77.00
76.74
60.07
57.40
51.81
49.13
41.95
38.86
33.10
30.11
27.61
24.95
24.56
22.72
22.31
^{13}C NMR (125 MHz, CDCl$_3$)
MeHN
NHPiv
170 160 150 140 130 120 110 100 90 80 70 60 50 40 30 20

8

Table 2. Titration study of tetrapeptide 5 in $CDCl_3$ (2 mM) with DMSO-d_6 (volume of DMSO-d_6 used for each addition = 5 μl).

$V_{DMSO-d6}$ added (in μlit)	Chemical shift (in ppm)			
	δ_{NH2}	δ_{NH5}	δ_{NH4}	δ_{NH1}
0	9.5	7.16	6.65	6.45
5	9.56	7.19	6.86	6.45
10	9.57	7.2	7.03	6.43
15	9.59	7.22	7.18	6.42
20	9.6	7.22	7.27	6.41
25	9.61	7.23	7.37	6.41
30	9.61	7.23	7.42	6.4
35	9.6	7.23	7.51	6.4
40	9.6	7.22	7.54	6.39
45	9.59	7.21	7.57	6.38
50	9.59	7.21	7.61	6.37

Table 3. Titration study of tetrapeptide 6 in $CDCl_3$ (2 mM) with DMSO-d_6 (volume of DMSO-d_6 used for each addition = 5 μl).

$V_{DMSO-d6}$ added (in μlit)	Chemical shift (in ppm)			
	δ_{NH2}	δ_{NH5}	δ_{NH4}	δ_{NH1}
0	9.84	7.9	6.28	6.54
5	9.85	7.92	6.54	6.53
10	9.85	7.95	6.75	6.52
15	9.86	7.97	6.87	6.51
20	9.87	7.98	7.07	6.49
25	9.87	7.99	7.2	6.48
30	9.86	8.02	7.27	6.47
35	9.84	8.04	7.38	6.46
40	9.83	8.05	7.46	6.44
45	9.81	8.07	7.51	6.44
50	9.77	8.09	7.57	6.43

Table 4. Titration study of tetrapeptide 7 in $CDCl_3$ (2 mM) with DMSO-d_6 (volume of DMSO-d_6 used for each addition = 5 μl).

$V_{DMSO-d6}$ added (in μlit)	Chemical shift (in ppm)			
	δ_{NH2}	δ_{NH5}	δ_{NH4}	δ_{NH1}
0	9.55	7.86	6.52	6.51
5	9.6	7.83	7.12	6.51
10	9.63	7.82	7.26	6.52
15	9.64	7.81	7.36	6.52
20	9.65	7.78	7.53	6.52
25	9.64	7.76	7.67	6.52
30	9.63	7.74	7.73	6.52
35	9.62	7.72	7.82	6.52
40	9.61	7.71	7.86	6.52
45	9.6	7.7	7.89	6.52
50	9.58	7.68	7.94	6.52

Table 5. Titration study of tetrapeptide 8 in $CDCl_3$ (2 mM) with DMSO-d_6 (volume of DMSO-d_6 used for each addition = 5 μl).

$V_{DMSO-d6}$ added (in μlit)	Chemical shift (in ppm)			
	δ_{NH2}	δ_{NH5}	δ_{NH4}	δ_{NH1}
0	9.58	7.87	6.61	6.5
5	9.61	7.83	6.98	6.5
10	9.63	7.8	7.24	6.52
15	9.65	7.78	7.37	6.52
20	9.64	7.75	7.53	6.52
25	9.63	7.72	7.67	6.52
30	9.62	7.7	7.77	6.52
35	9.61	7.68	7.8	6.52
40	9.59	7.66	7.88	6.51
45	9.58	7.65	7.93	6.51
50	9.57	7.63	7.96	6.51

^{1}H NMR NH/D exchange study of tetramer 1 in Methanol-d_4

Deuterium exchange of the amide protons (NH/D) in the tetramer **1** was studied at 400 MHz by dissolving the compound in $CDCl_3$ (0.4 ml) and methanol-d_4 (0.1 ml). The experiment was started immediately after the dissolution of compound using the following parameters: number of scans = 16, relaxation delay = 1 sec, flip angle = 30°, spectral width = 8223. The ^{1}H NMR spectra were recorded then at different intervals at 296 K. A stacked plot at different time intervals is shown below.

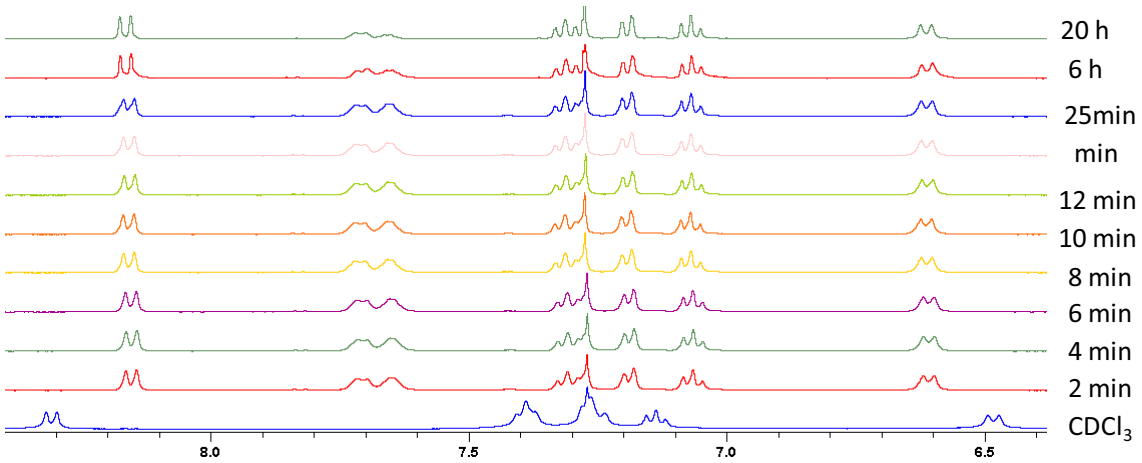

Figure 24: H/D Exchange of hexapeptide **1** (400MHz, $CDCl_3$ + methanol-d_4).

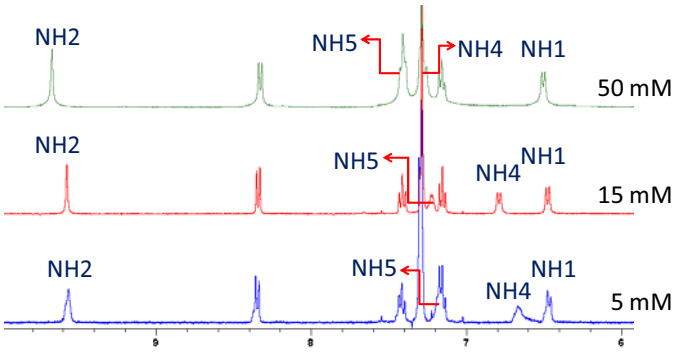

Figure 25. Concentration dependence study of tetrapeptide **5** (400 MHz, $CDCl_3$)

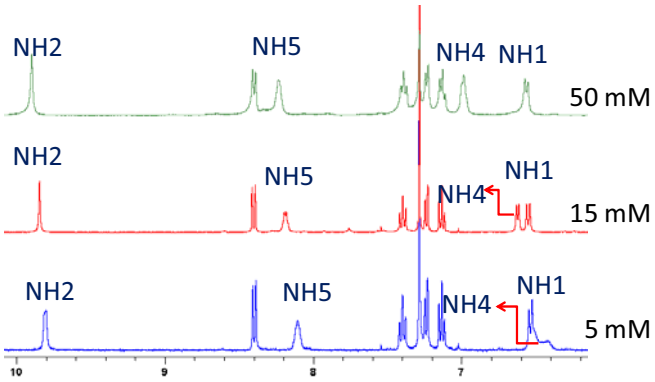

Figure 26. Concentration dependence study of tetrapeptide **6** (500 MHz, $CDCl_3$)

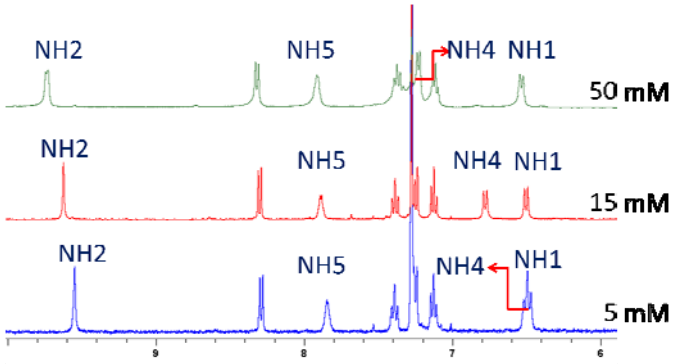

Figure 27. Concentration dependence study of tetrapeptide **7** (500 MHz, $CDCl_3$)

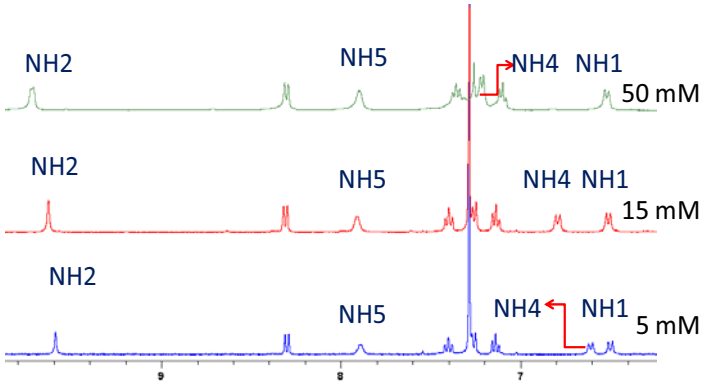

Figure 28. Concentration dependence study of tetrapeptide **8** (500 MHz, $CDCl_3$)

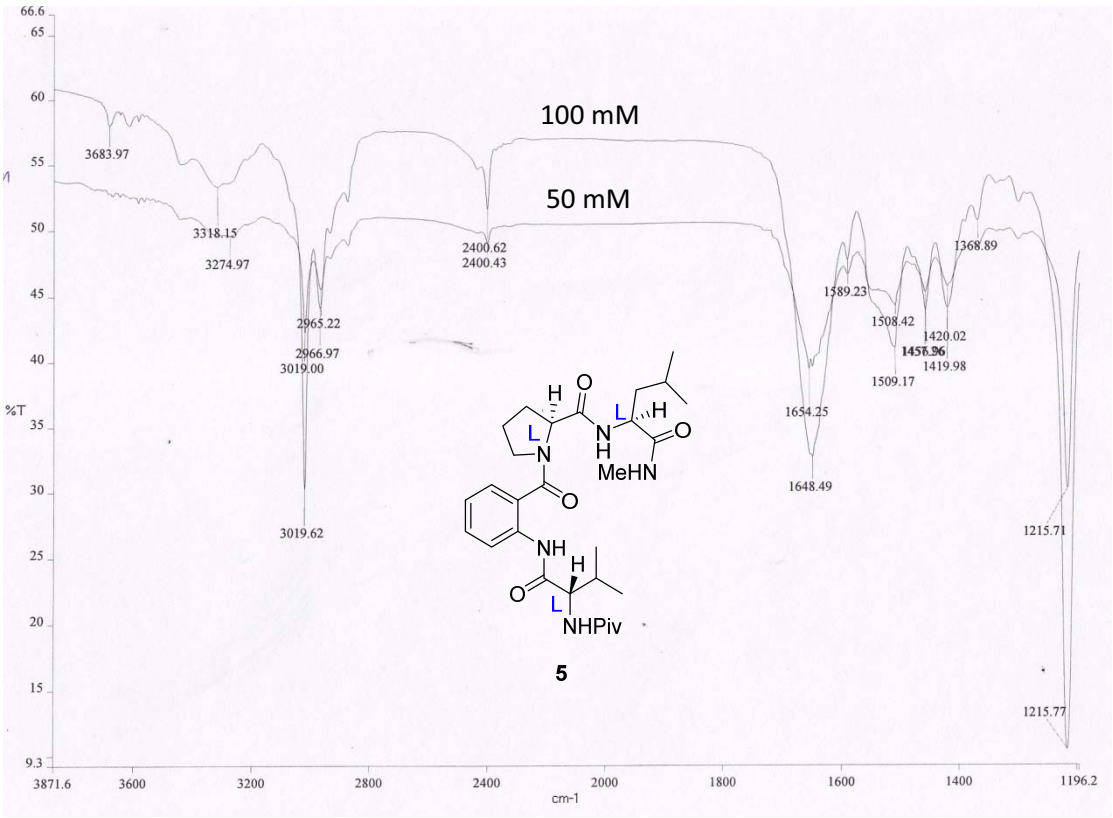
100 mM
50 mM
3683.97
3318.15
3274.97
2400.62
2400.43
2965.22
2966.97
3019.00
3019.62
1589.23
1508.42
1509.17
1420.02
1419.98
1368.89
1654.25
1648.49
1215.71
1215.77
%T
cm-1
MeHN
NHPiv

5

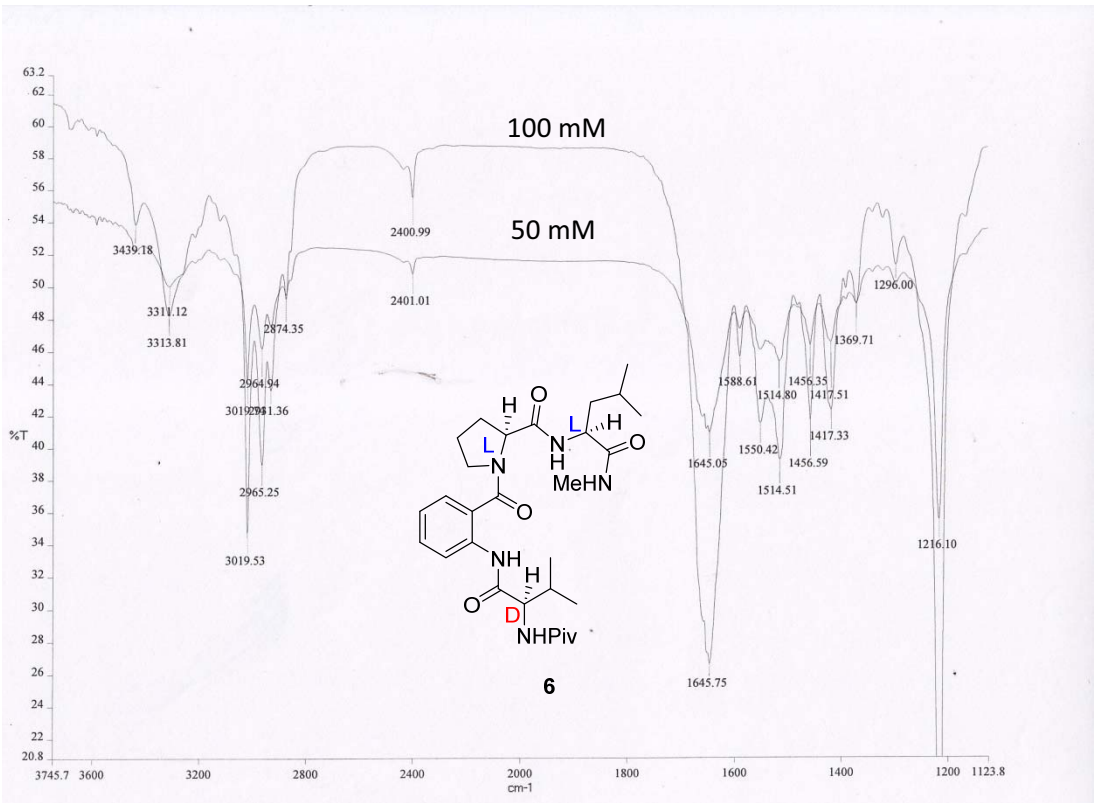
100 mM
50 mM
3439.18
3311.12
3313.81
2874.35
2400.99
2401.01
2964.94
2965.25
3019.53
1588.61
1514.80
1417.51
1369.71
1296.00
1550.42
1456.59
1417.33
1514.51
1645.05
1645.75
1216.10
%T
cm-1
MeHN
NHPiv

6

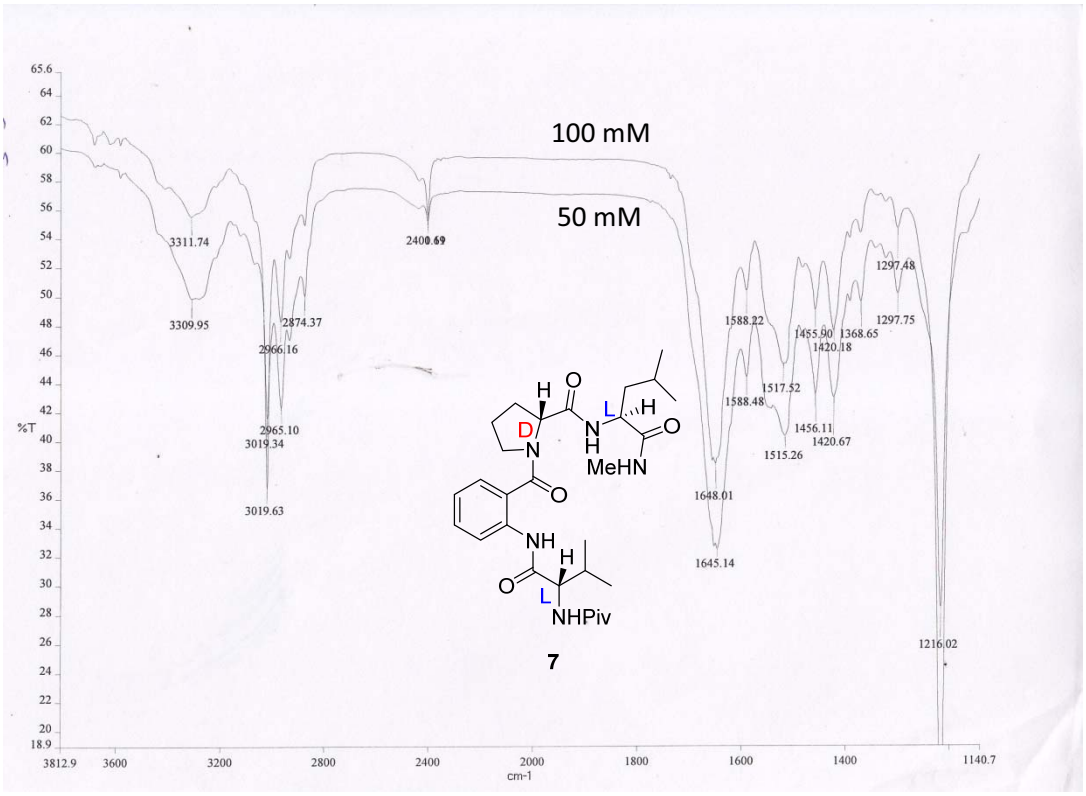
100 mM
50 mM
3311.74
3309.95
2874.37
2966.16
2965.10
3019.34
3019.63
2400.69
1588.22
1588.48
1517.52
1455.90
1420.18
1368.65
1297.48
1297.75
1456.11
1420.67
1515.26
1648.01
1645.14
1216.02
%T
cm-1
MeHN
NHPiv
7

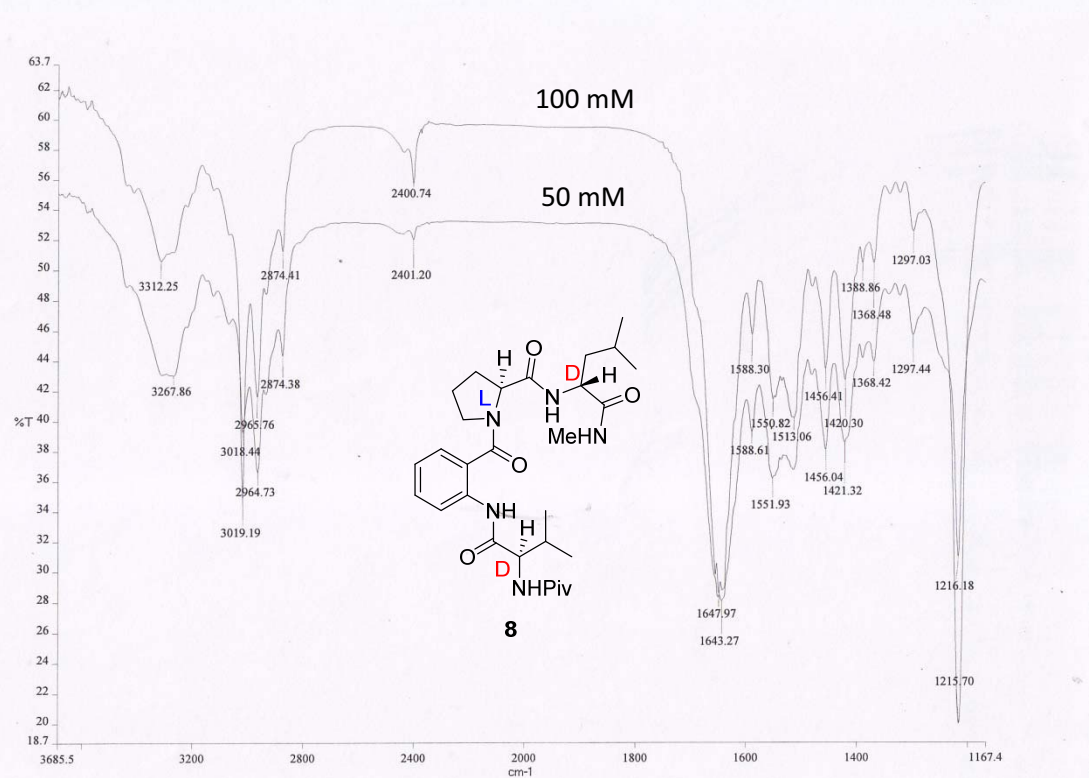
100 mM
50 mM
2400.74
2401.20
3312.25
3267.86
2874.41
2874.38
2965.76
3018.44
2964.73
3019.19
1588.30
1588.61
1550.82
1513.06
1456.41
1456.04
1421.32
1420.30
1388.86
1368.48
1368.42
1297.03
1297.44
1647.97
1643.27
1551.93
1216.18
1215.70
%T
cm-1
MeHN
NHPiv
8

Table 6: Temperature variation study of tetrapeptide **5** (2 mmol, 400 MHz, $CDCl_3$)

Temperature (in K)	Chemical shift (in ppm)			
	δ_{NH2}	δ_{NH5}	δ_{NH4}	δ_{NH1}
268	9.59	7.41	6.75	6.54
273	9.58	7.35	6.7	6.53
278	9.57	7.3	6.67	6.52
283	9.56	7.27	6.63	6.51
288	9.55	7.23	6.59	6.49
293	9.54	7.17	6.56	6.49
298	9.52	7.15	6.53	6.48
303	9.51	7.1	6.5	6.47
308	9.5	7.07	6.49	6.46
313	9.49	7.05	6.47	6.45
318	9.47	7.01	6.45	6.44
323	9.46	6.98	6.43	6.43

NH2 = -2.30 ppb/K
NH5 = -7.82 ppb/K
NH4 = -5.82 ppb/K
NH1 = -2.00 ppb/K

Table 7: Temperature variation study of tetrapeptide **6** (2 mmol, 400 MHz, $CDCl_3$)

Temperature (in K)	Chemical shift (in ppm)			
	δ_{NH2}	δ_{NH5}	δ_{NH4}	δ_{NH1}
268	9.84	8.38	6.57	6.42
273	9.83	8.33	6.57	6.38
278	9.82	8.28	6.56	6.36
283	9.81	8.24	6.56	6.33
288	9.8	8.19	6.55	6.31
293	9.79	8.16	6.55	6.29
298	9.77	8.1	6.54	6.27
303	9.76	8.03	6.53	6.26
308	9.74	7.98	6.53	6.25
313	9.73	7.93	6.52	6.24
318	9.72	7.88	6.52	6.23
323	9.7	7.82	6.51	6.22

NH2 = -2.54 ppb/K
NH5 = -10.18 ppb/K
NH4 = -10.90 ppb/K
NH1 = -3.64 ppb/K

Table 8: Temperature variation study of tetrapeptide **7** (2 mmol, 400 MHz, $CDCl_3$)

Temperature (in K)	Chemical shift (in ppm)			
	δ_{NH2}	δ_{NH5}	δ_{NH4}	δ_{NH1}
268	9.7	8	6.71	6.54
273	9.69	7.99	6.67	6.53
278	9.65	7.97	6.63	6.52
283	9.62	7.95	6.6	6.51
288	9.61	7.93	6.57	6.5
293	9.58	7.91	6.55	6.49
298	9.56	7.87	6.53	6.49
303	9.53	7.82	6.5	6.5
308	9.51	7.8	6.48	6.49
313	9.49	7.77	6.47	6.47
318	9.47	7.75	6.46	6.46
323	9.44	7.71	6.45	6.45

NH2 = -4.73 ppb/K
NH5 = -5.27 ppb/K
NH4 = -4.73 ppb/K
NH1 = -1.64 ppb/K

Table 9: Temperature variation study of tetrapeptide **8** (2 mmol, 400 MHz, $CDCl_3$)

Temperature (in K)	Chemical shift (in ppm)			
	δ_{NH2}	δ_{NH5}	δ_{NH4}	δ_{NH1}
268	9.74	8.03	6.85	6.54
273	9.71	8.02	6.79	6.53
278	9.68	8	6.75	6.52
283	9.65	7.97	6.7	6.52
288	9.63	7.94	6.69	6.515
293	9.62	7.93	6.66	6.51
298	9.6	7.89	6.63	6.505
303	9.59	7.85	6.58	6.5
308	9.55	7.81	6.55	6.495
313	9.5	7.78	6.53	6.48
318	9.48	7.75	6.51	6.47
323	9.45	7.73	6.49	6.46

NH2 = -5.27 ppb/K
NH5 = -5.45 ppb/K
NH4 = -6.45 ppb/K
NH1 = -1.45 ppb/K

Table 10: Temperature variation study of tetrapeptide **6f** (15 mmol, 400 MHz, $CDCl_3$)

Temperature (in K)	Chemical shift (in ppm)			
	δ_{NH2}	δ_{NH5}	δ_{NH4}	δ_{NH1}
268	9.59	9.59	6.81	5.58
273	9.58	9.73	6.79	5.57
278	9.57	9.69	6.74	5.56
283	9.55	9.67	6.70	5.55
288	9.54	9.64	6.66	5.55
293	9.52	9.61	6.63	5.54
298	9.51	9.58	6.60	5.54
303	9.50	9.55	6.57	5.53
308	9.48	9.52	6.54	5.53
313	9.46	9.49	6.52	5.52
318	9.45	9.45	6.51	5.51
323	9.42	9.42	6.49	5.50

NH2 = -3.24 ppb/K
NH5 = -5.93 ppb/K
NH4 = -6.11 ppb/K
NH1 = -0.41 ppb/K

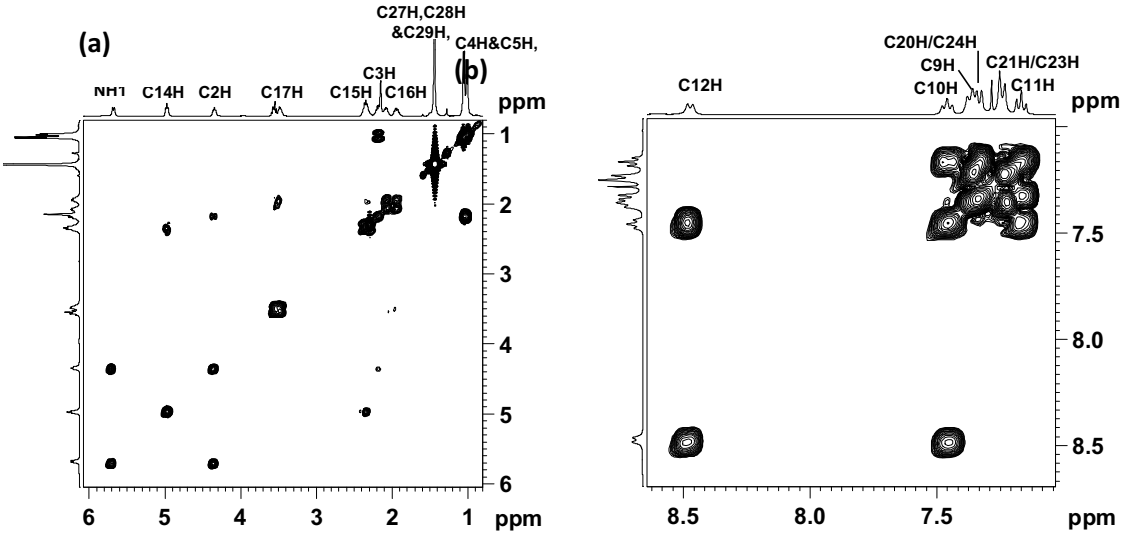

Figure 29: Partial COSY spectra of tripeptide **3b** (400MHz, $CDCl_3$): Aromatic **(a)** and Aliphatic regions **(b)**.

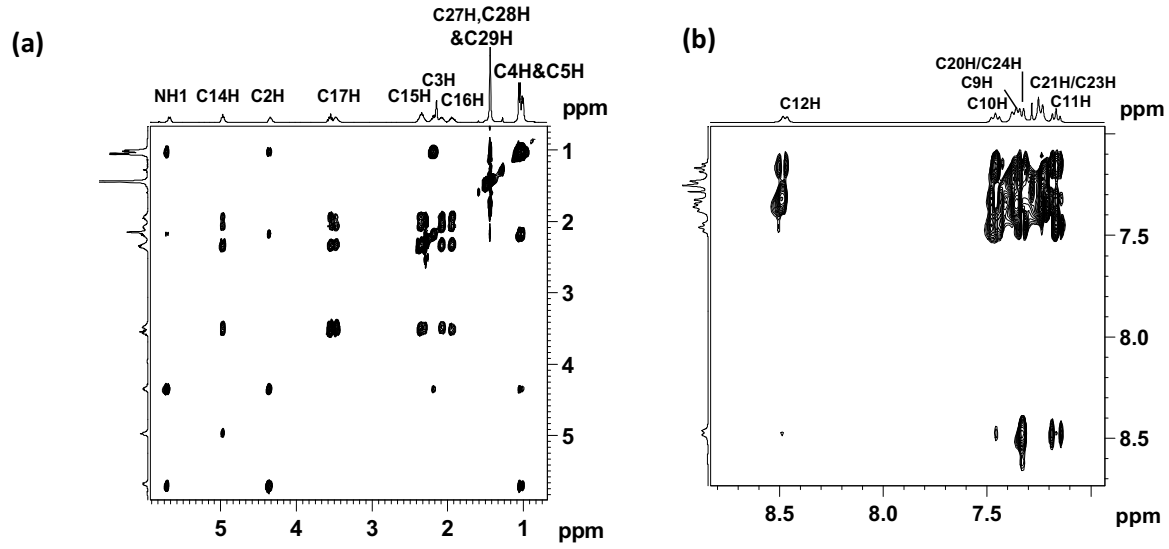

Figure 30: Partial TOCSY spectra of tripeptide **18** (400 MHz, $CDCl_3$): Aromatic **(a)** and Aliphatic regions **(b)**.

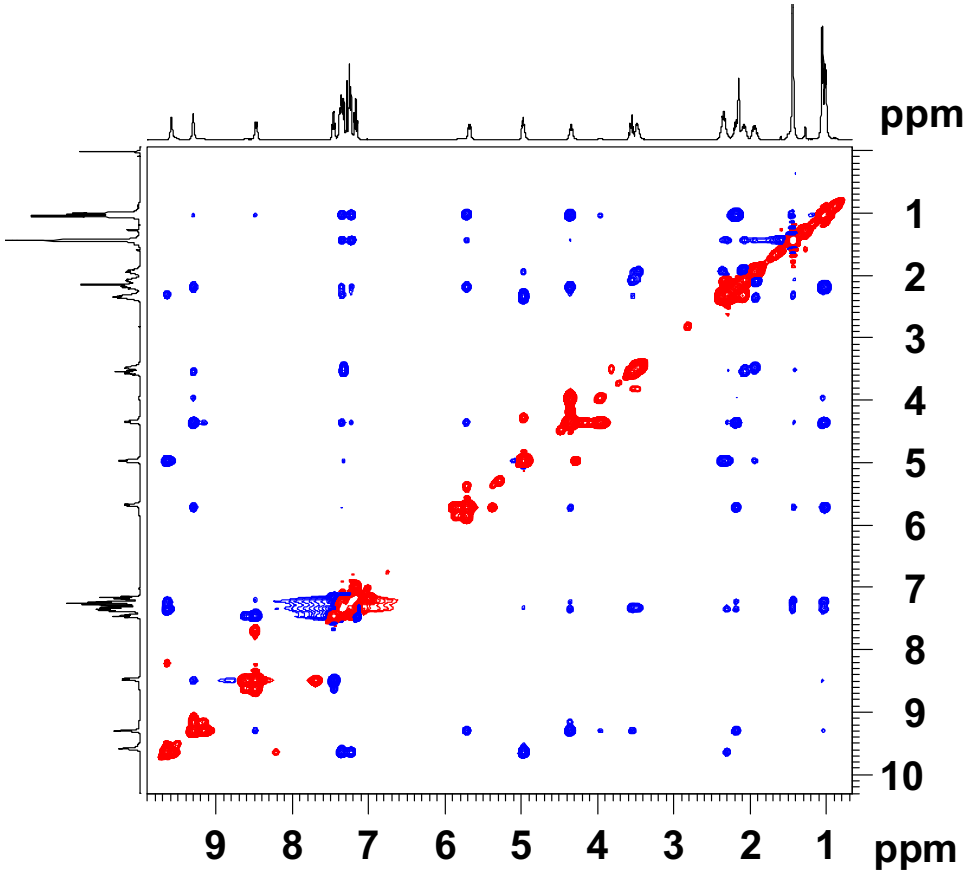

Figure 31: 2D NOESY spectrum of tripeptide **3b** (400 MHz, $CDCl_3$)

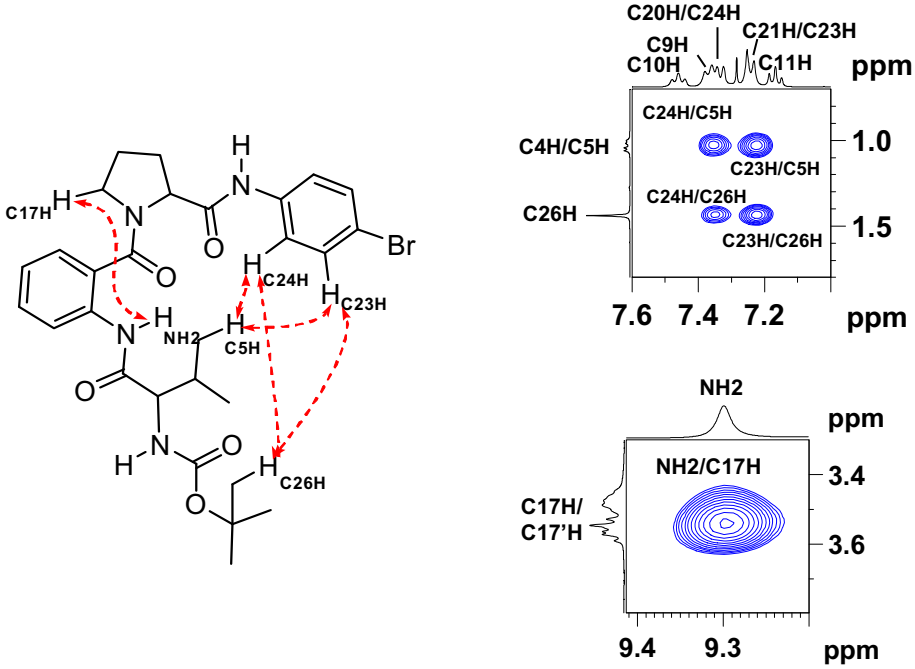

Figure 32: 2D NOESY excerpts of tripeptide **3b** (400 MHz, $CDCl_3$).

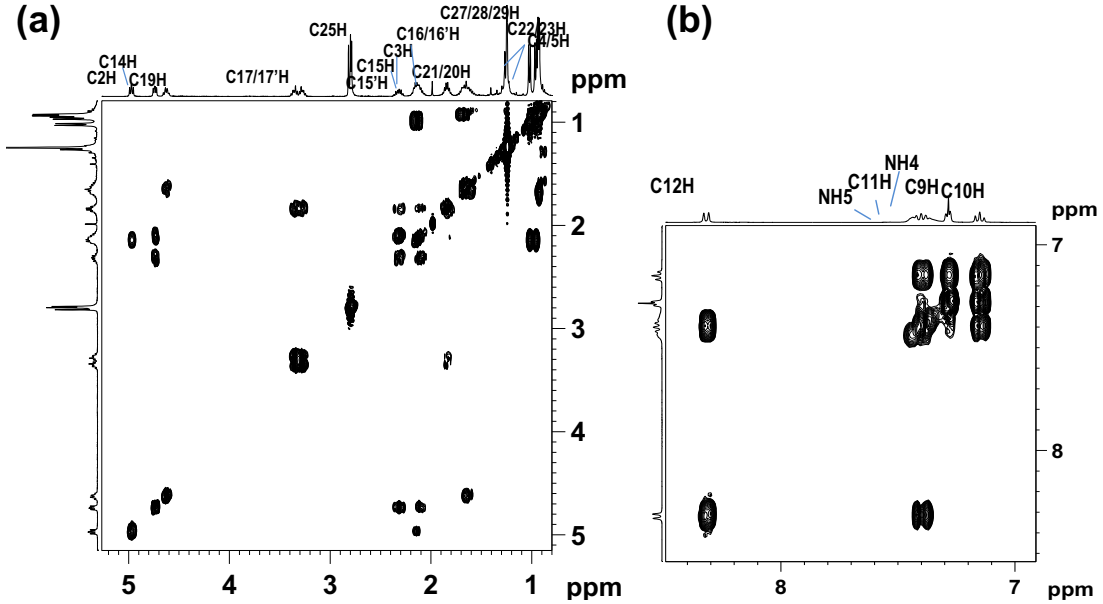

Figure 33. Partial COSY spectra of tetrapeptide **5** (500MHz, $CDCl_3$): Aliphatic **(a)** and aromatic region **(b)**.

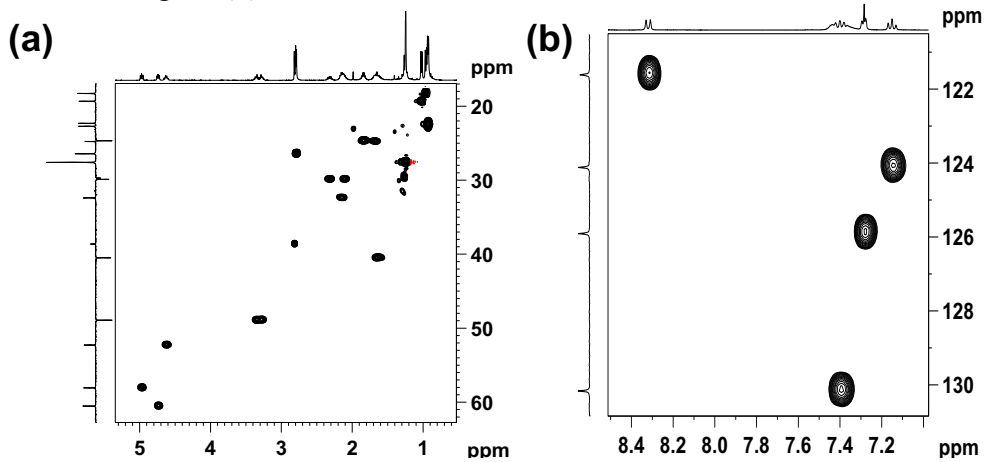

Figure 34. Partial HSQC spectra of tetrapeptide **5** (500MHz, $CDCl_3$): Aliphatic **(a)** and aromatic regions **(b)**.

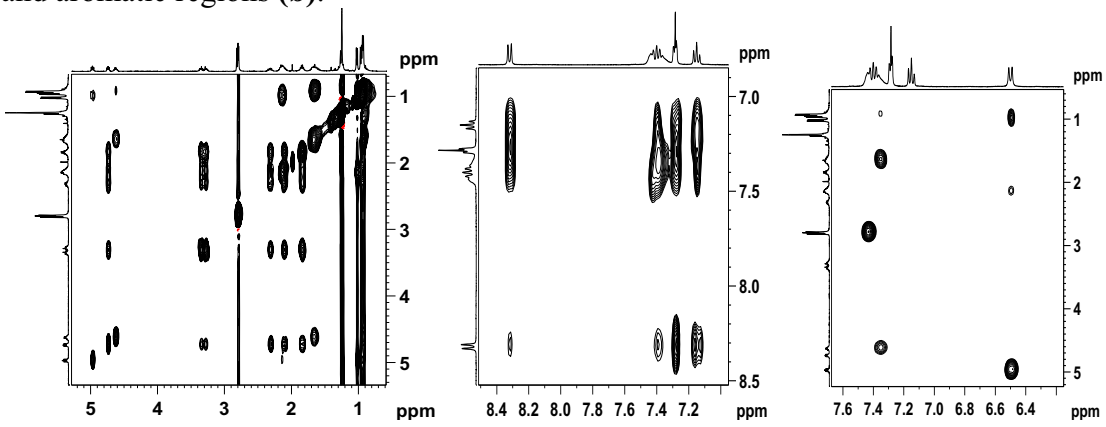

Figure 35. Partial TOCSY spectra of tetrapeptide **5** (500MHz, $CDCl_3$): Aliphatic **(a)** and aromatic regions **(b)**.

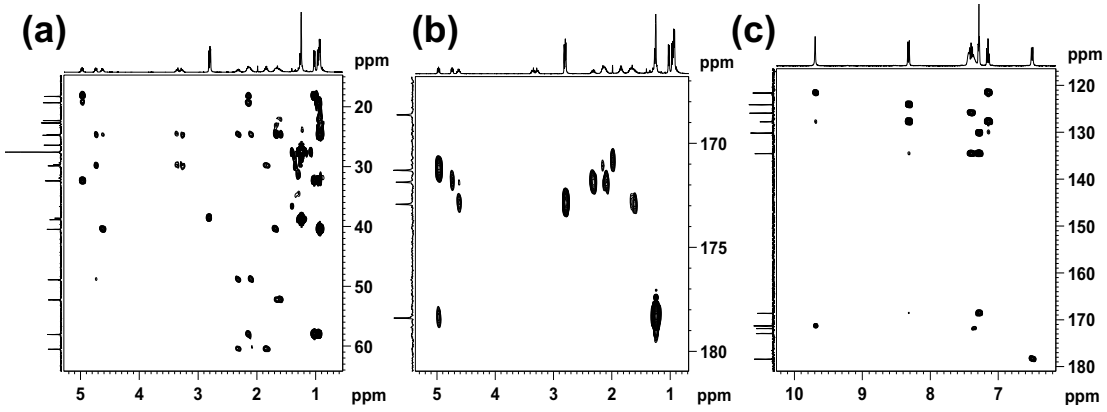

Figure 36. Partial HMBC spectra of tetrapeptide **5** (500MHz, $CDCl_3$): Aliphatic **(a**,**b)** and aromatic regions **(c)**.

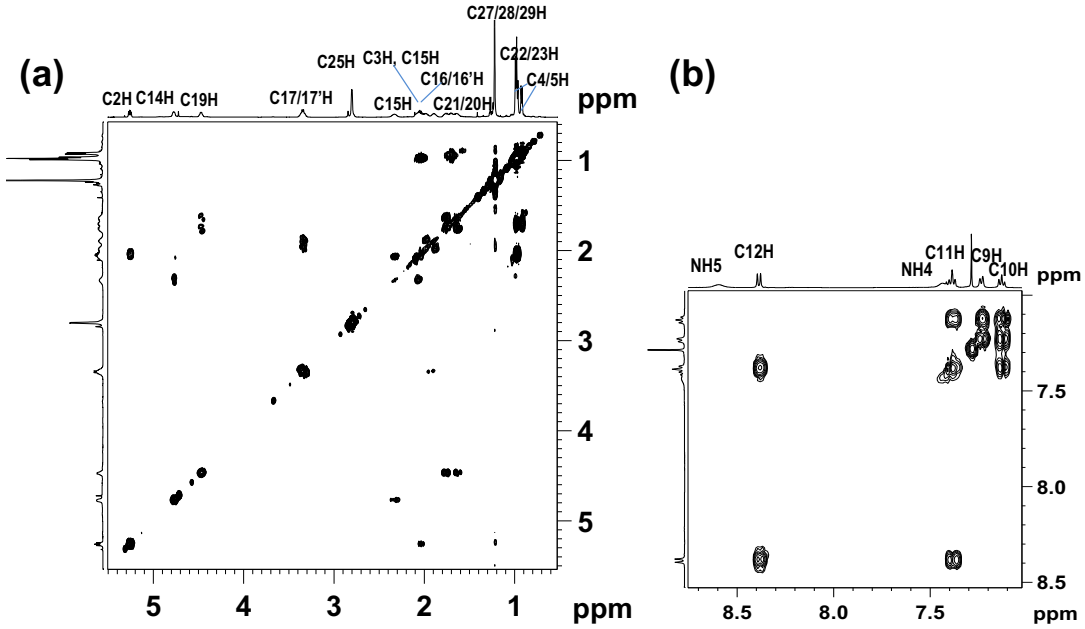

Figure 37. Partial COSY spectra of tetrapeptide **6** (500MHz, $CDCl_3$): Aliphatic **(a)** and aromatic region **(b)**.

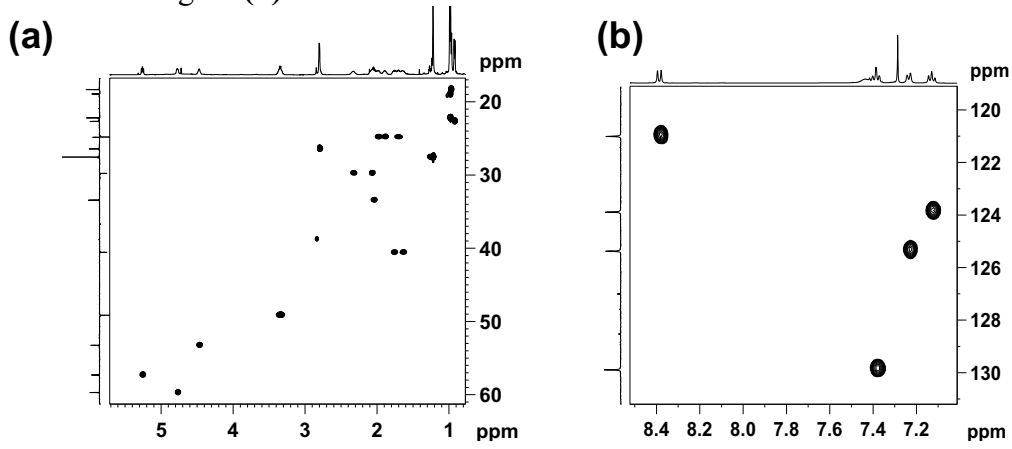

Figure 38. Partial HSQC spectra of tetrapeptide **6** (500MHz, $CDCl_3$): Aliphatic **(a)** and aromatic regions **(b)**.

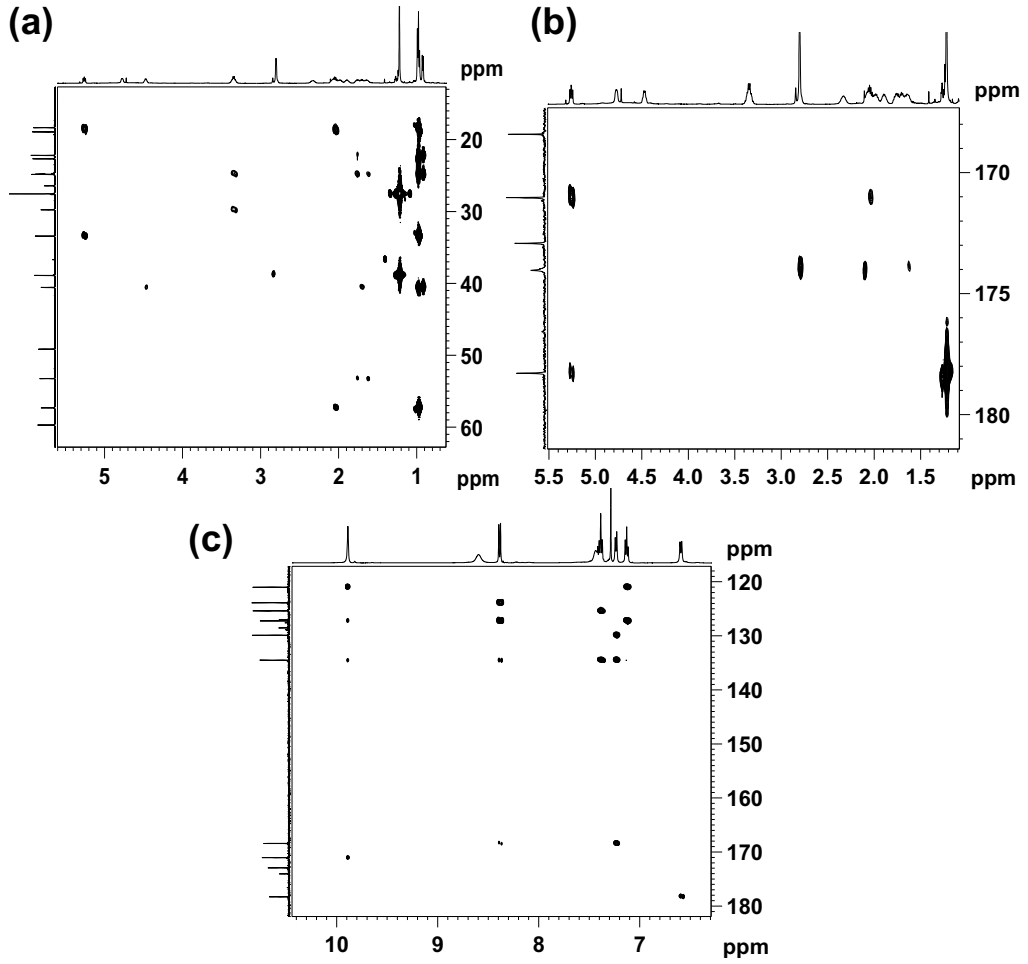

Figure 39. Partial HMBC spectra of tetrapeptide **6** (500MHz, $CDCl_3$): Aliphatic **(a**,**b)** and aromatic regions **(c)**.

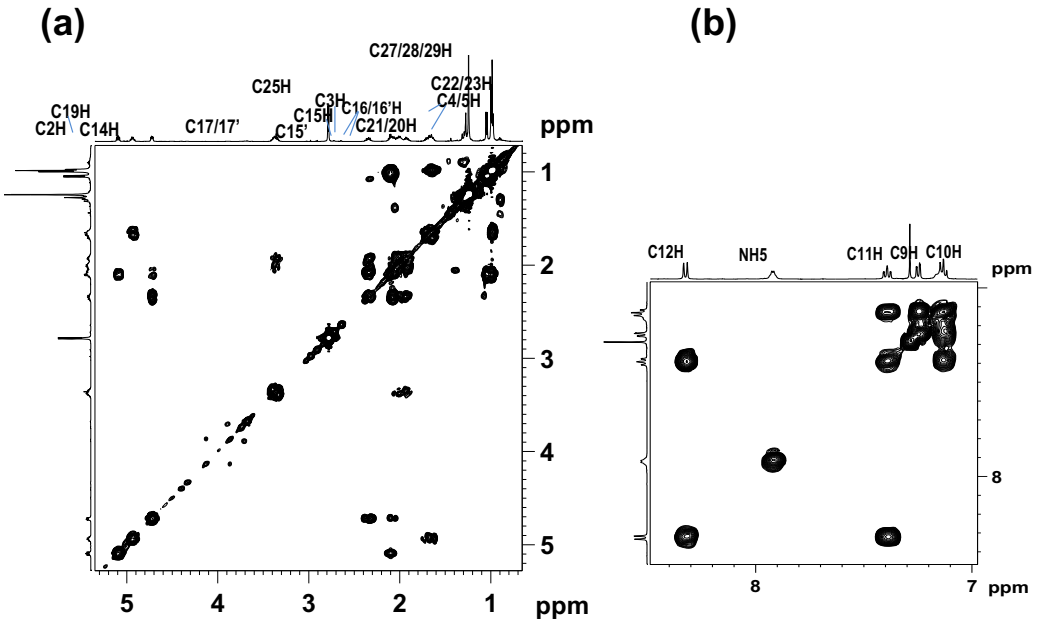

Figure 40. Partial COSY spectra of tetrapeptide **7** (500MHz, $CDCl_3$): Aliphatic **(a)** and aromatic region **(b)**.

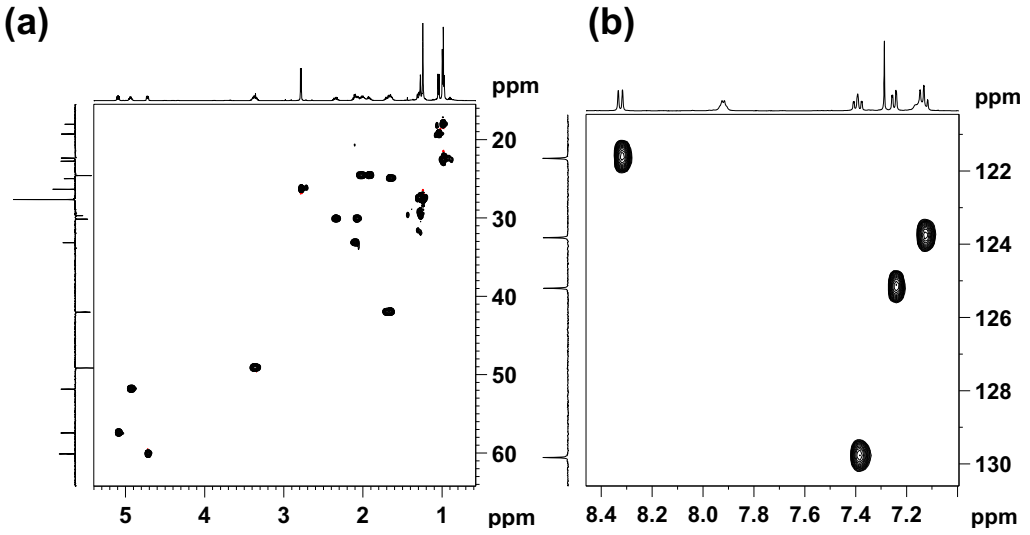

Figure 41. Partial HSQC spectra of tetrapeptide **7** (500MHz, $CDCl_3$): Aliphatic **(a)** and aromatic regions **(b)**.

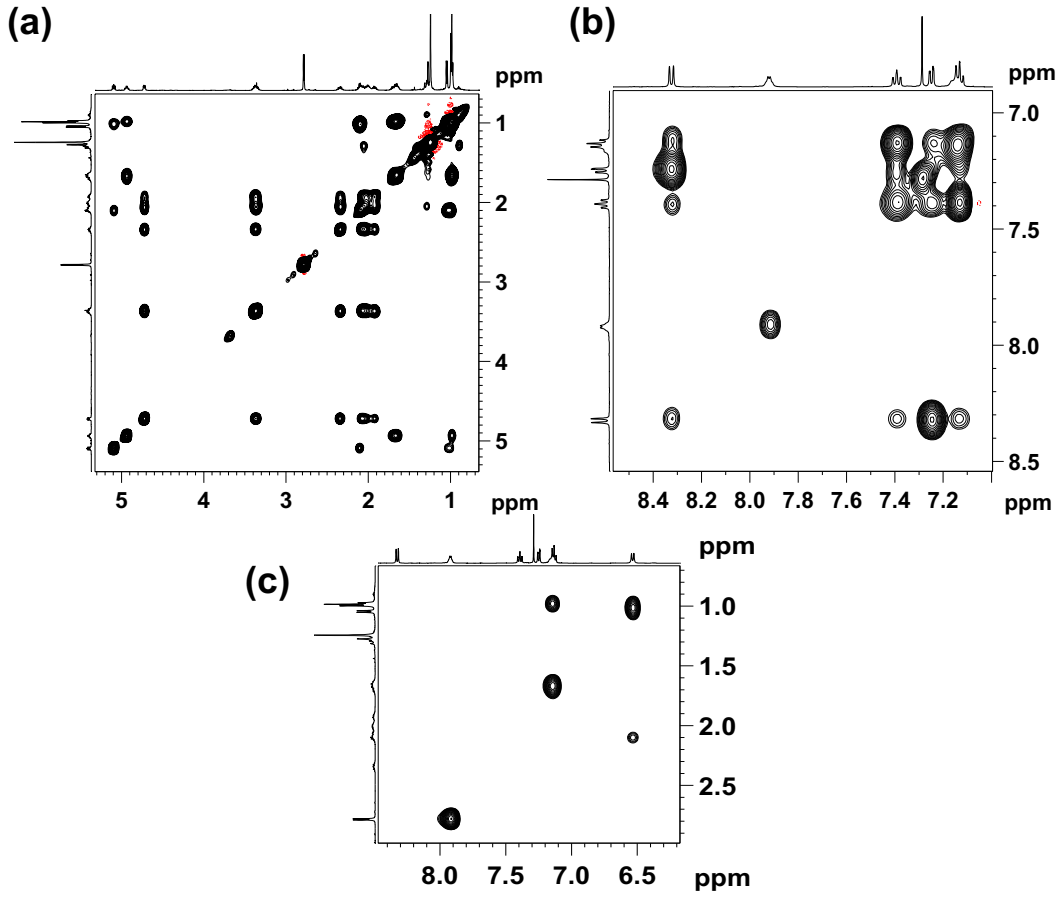

Figure 42. Partial TOCSY spectra of tetrapeptide **7** (500MHz, $CDCl_3$): Aliphatic **(a)** and aromatic regions **(b)**.

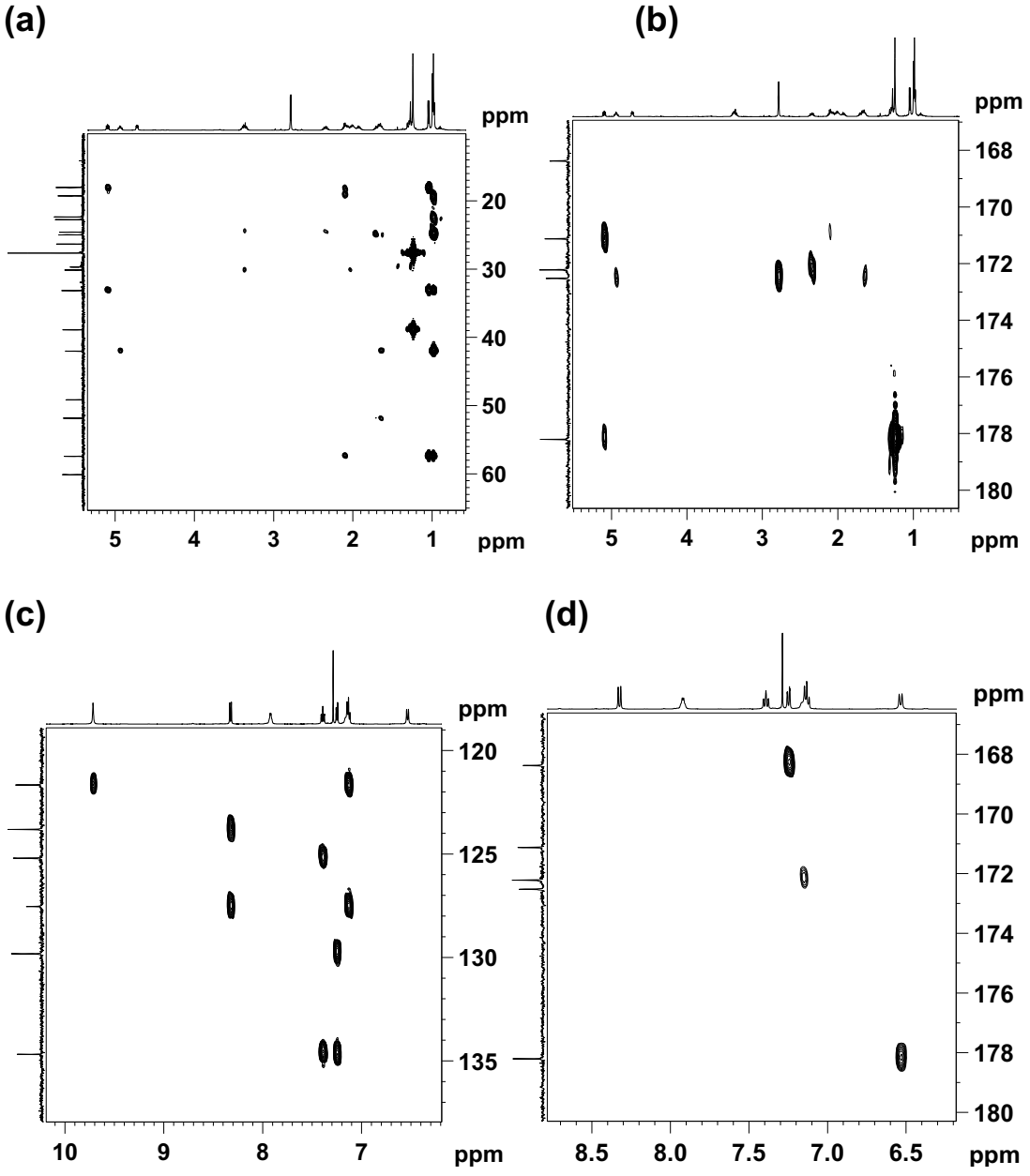

Figure 43. Partial HMBC spectra of tetrapeptide **7** (500MHz, $CDCl_3$): Aliphatic **(a**,**b)** and aromatic regions **(c,d)**.

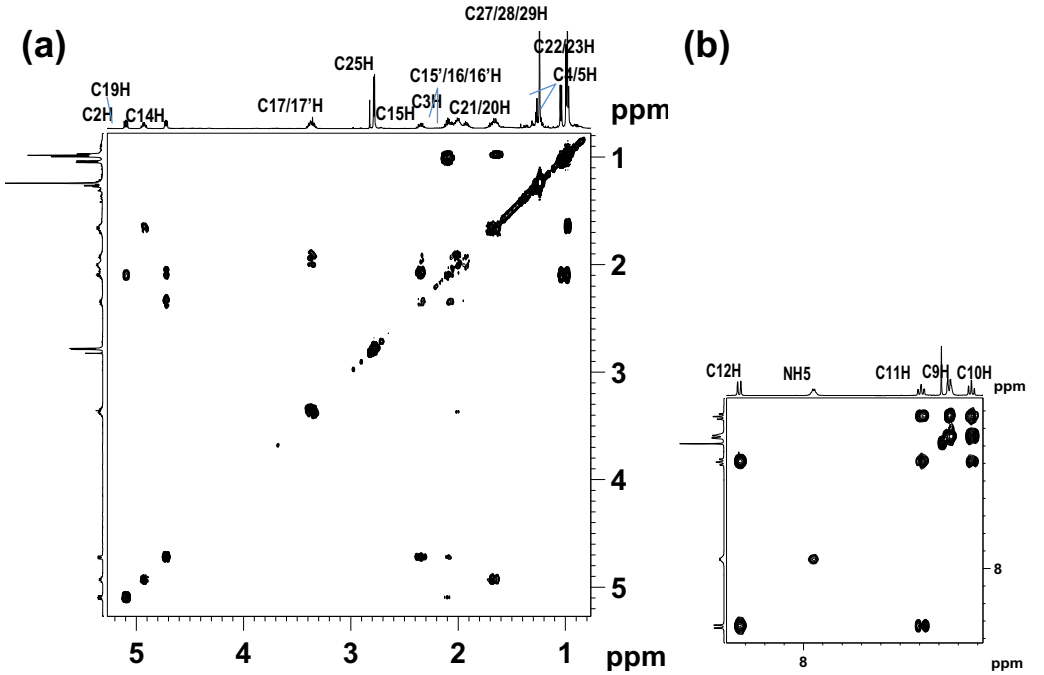

Figure 44. Partial COSY spectra of tetrapeptide **8** (500MHz, $CDCl_3$): Aliphatic **(a)** and aromatic regions **(b)**.

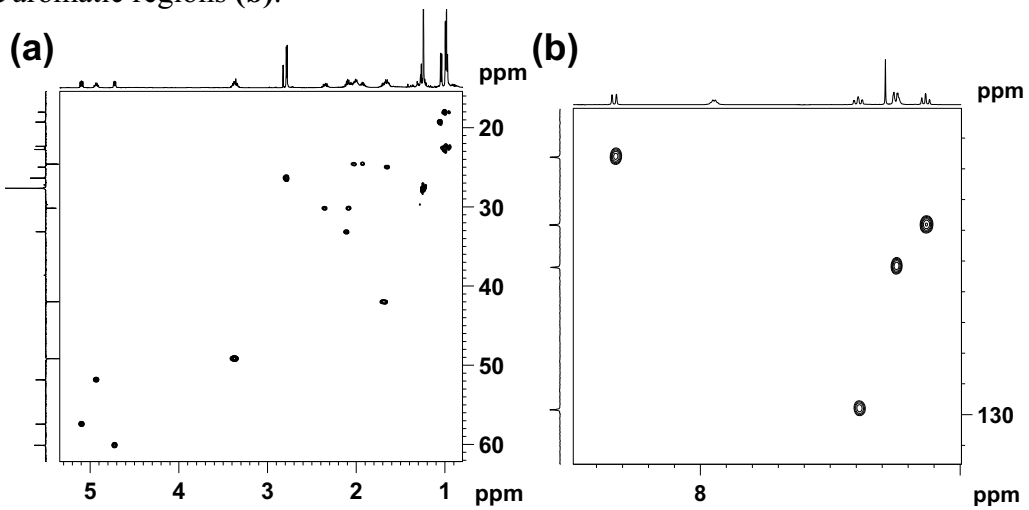

Figure 45. Partial HSQC spectra of tetrapeptide **8** (500MHz, $CDCl_3$): Aliphatic **(a)** and aromatic regions **(b)**.

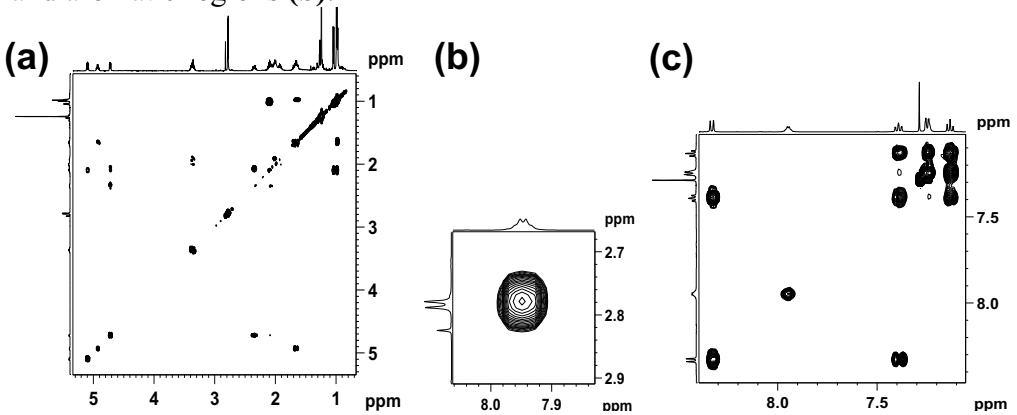

Figure 46. Partial TOCSY spectra of tetrapeptide **8** (500MHz, $CDCl_3$): Aliphatic **(a)** and aromatic regions **(b)**.

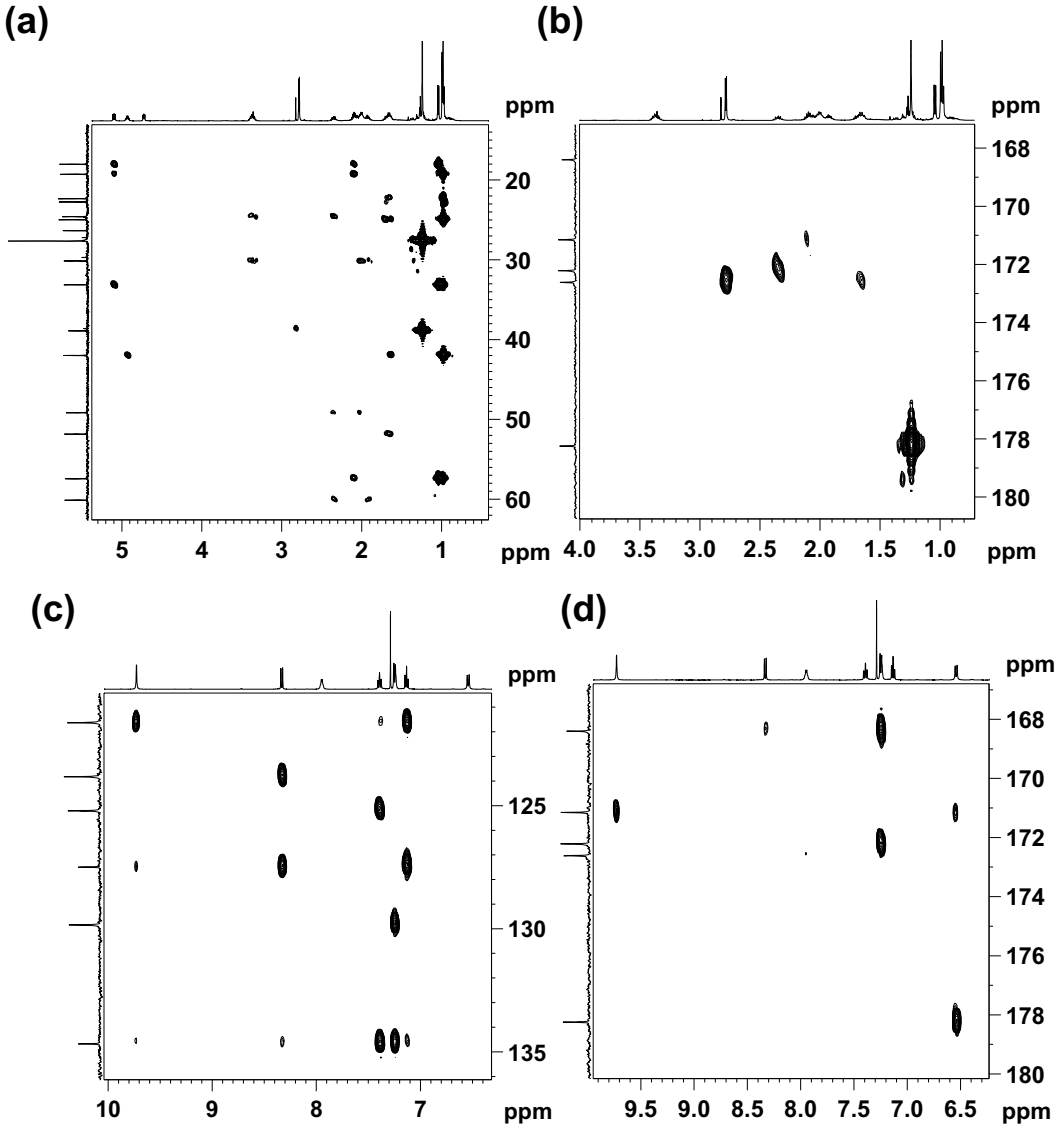

Figure 47. Partial HMBC spectra of tetrapeptide **8** (500MHz, $CDCl_3$): Aliphatic **(a**,**b)** and aromatic regions **(c,d)**.

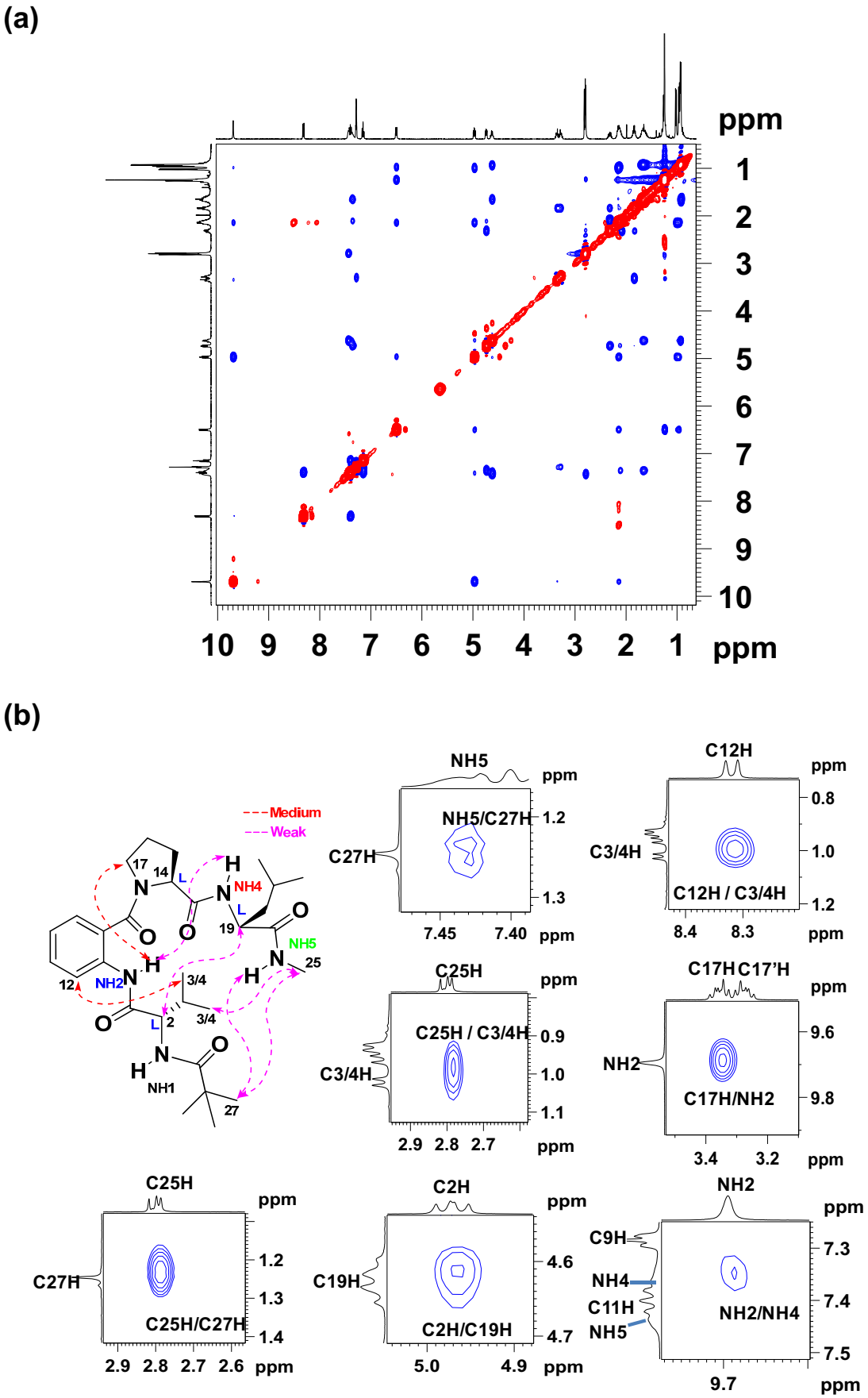

Figure 48. 2D NOESY spectrum (a), and excerpts (b) of **5** (400 MHz, $CDCl_3$).

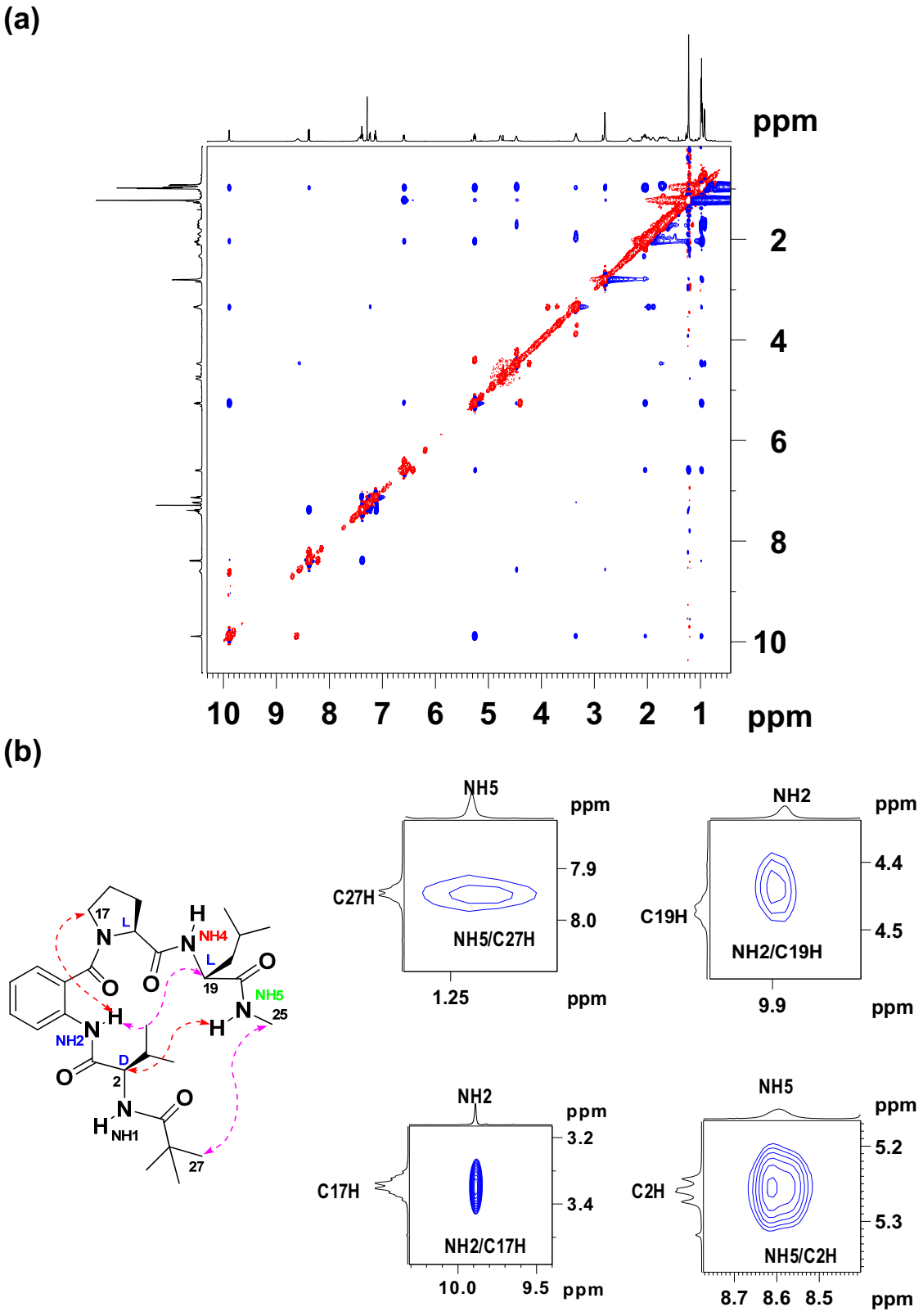

Figure 49. 2D NOESY spectrum (a), and excerpts (b) of **6** (500 MHz, $CDCl_3$).

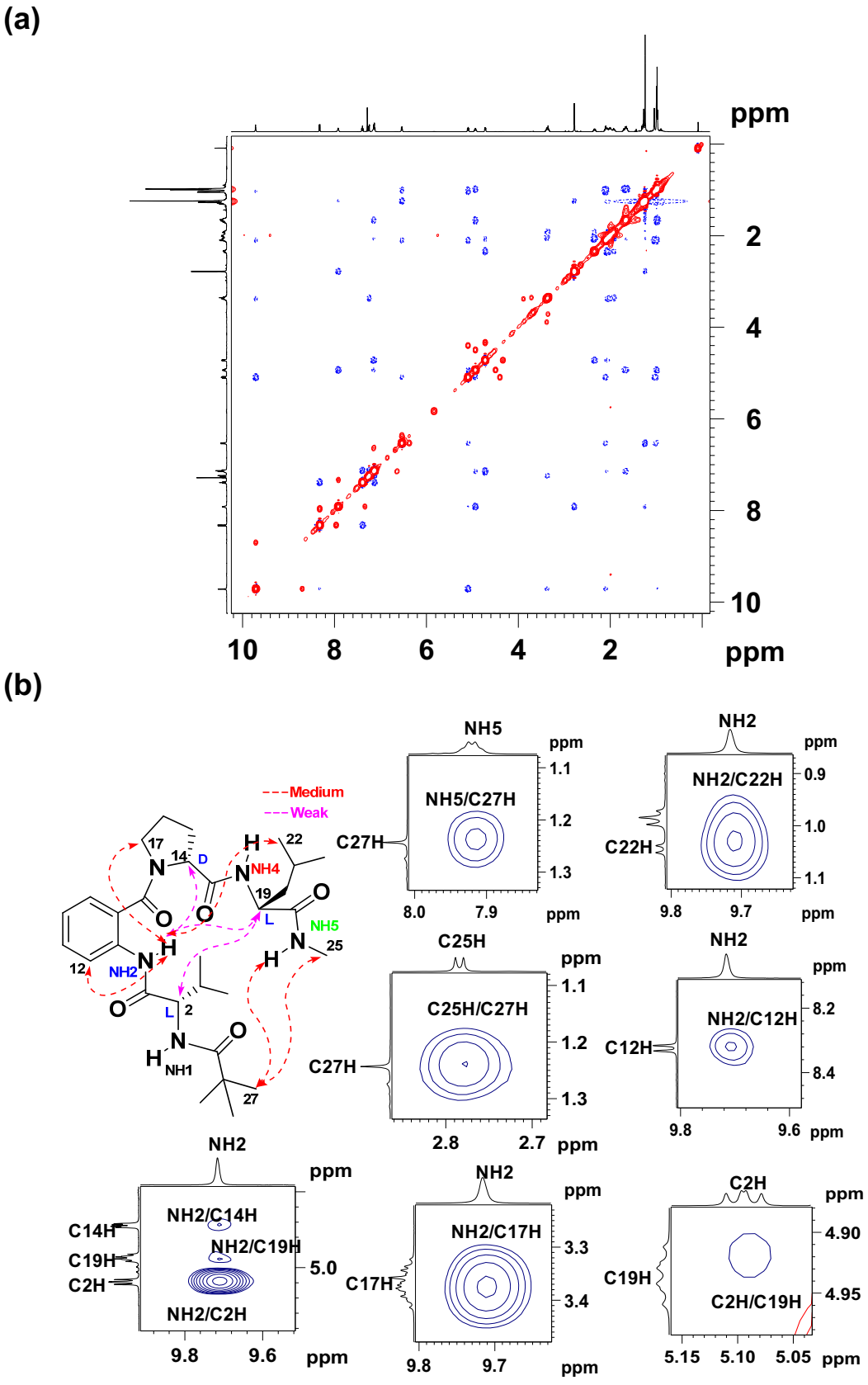

Figure 50. 2D NOESY spectrum (a), and excerpts (b) of **7** (500 MHz, $CDCl_3$).

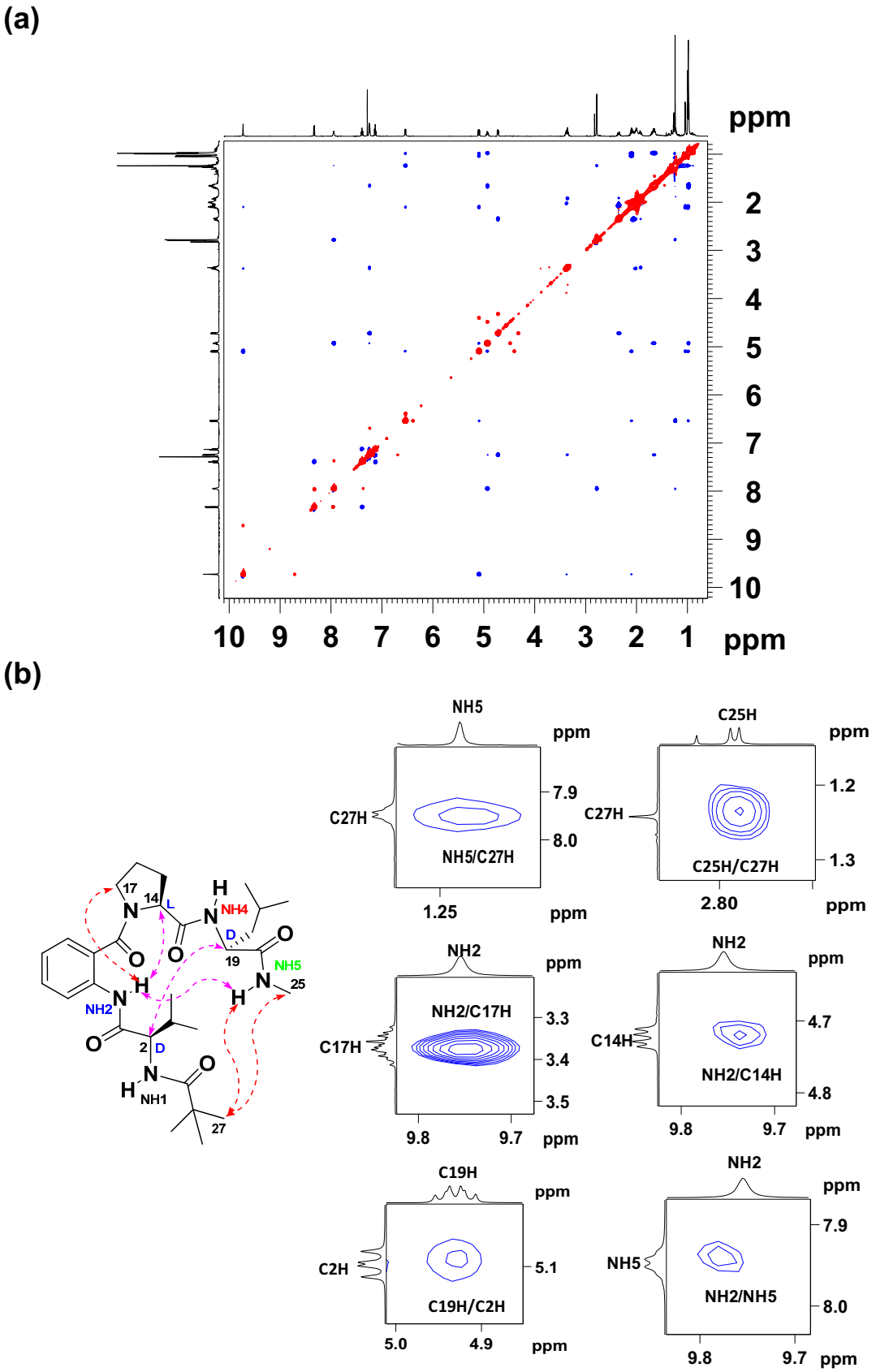

Figure 51. 2D NOESY spectrum (a), and excerpts (b) of **8** (500 MHz, $CDCl_3$).

1.21 References and Notes

(1) For reviews: (a) Hecht, S.; Huc, I. *Foldamers: Structure, Properties and Applications*; Eds.; Wiley-VCH: Weinheim, Germany, **2007**. (b) Martinek, T. A.; Fulop, F. *Chem. Soc. Rev.* **2012**, *41*, 687. (c) Roy, A.; Prabhakaran, P.; Baruah, P. K.; Sanjayan, G. J. *Chem. Comm.* **2011**, *47*, 11593. (d) Seebach, D.; Gardiner, J. *Acc. Chem. Res.* **2008**, *41*, 1366. (e) Hill, D. J.; Mio, M. J.; Prince, R. B.; Hughes, T. S.; Moore, J. S. *Chem. Rev.* 2001, *101*, 3893-4012. (f) Gellman, S. H. *Acc. Chem. Res.* **1998**, *31*, 173.

(2) (a) Horne, W. S.; Gellman, S. H. *Acc. Chem. Res.* **2008**, *41*, 1399. (b) Goodman, C. M.; Choi, S.; Shandler, S.; DeGrado, W. F. *Nat. Chem. Biol.* **2007**, *3*, 252.

(3) Marcelino, A. M. C.; Gierasch, L. M. *Biopolymers* **2008**, *89*, 380.

(4) Reverse turns play an important role in globular proteins: (a) Crawford, J. L.; Lipscomb, W. N.; Schellman, C. G. *Proc. Natl. Acad. Sci. U.S.A.* **1973**, *70*, 538.. (b) Fasman, G. D. *In Prediction of Protein Structure and the Principles of Protein Conformation* **1989**, 317. (c) Muller, G.; Hessler, G.; Decornez, H. Y. *Angew. Chem. Int. Ed.* **2000**, *39,* 894. (d) Prabakaran, P.; Gan, J.; Wu, Y. O.; Zhang, M. Y.; Dimitrov, D. S.; Ji, X. *J. Mol. Biol.* **2006**, *357*, 82.

(5) (a) Ruiz-Gómez, G.; Tyndall, J. D. A.; Pfeiffer, B.; Abbenante, G.; Fairlie, D. P. *Chem. Rev.* **2010**, *110*, PR1.. (b) Tyndall, J. D. A.; Pfeiffer, B.; Abbenante, G.; Fairlie, D. P. *Chem. Rev.* **2005**, *105*, 793.

(6) Toniolo C. *Crit. Rev. Biochem.* **1980**, *9*, 1.

(7) (a) Koch, O.; Klebe, G. *Proteins: Structure, Function, and Bioinformatics* **2009**, *74*, 353. (b) Lewis, P. N., Momany, F. A., Scheraga, H. A. *Biochim. Biophys. Acta* **1973**, *303*, 211. (c) Dasgupta, B.; Pal, L.; Basu, G.; Chakrabarti P. *Proteins* **2004**, *55*, 305.

(8) Freidinger, R.M.; Veber, D. F.; Perlow, D. S.; Brooks, J. R.; Saperstein, R. *Science* **1980**, *210*, 656..

(9) Che, Y.; Marshall, G. R., *J. Med. Chem.* **2005**, 49, (1), 111.

(10) (a) Kahn, M. *Tetrahedron*, **1993**, *49*, 3433. (b) Olson, G. L.; Voss, M. E.; Hill, D. E.; Kahn, M.; Madison, V. S.; Cook, C. M. *J. Am. Chem. Soc.* **1990**, *112*, 323.

(11) (a) Pinsker, A.; Einsiedel, J.; Harterich, S.; Waibel, R.; Gmeiner, P. *Org. Lett.*, **2011**, *13*, 3502. (b) Dietrich, S. A.; Banfi, L.; Basso, A.; Damonte, G.; Guanti, G.; Riva, R. *Org. Biomol. Chem* . **2005**, *3* , 97.

(12) (a) Hallberg et. al., *J. Med. Chem.* **1997,** *40,* 903. (b) Sukumaran, D. K.; Prorok, M.; Lawrence, D. S. *J. Am. Chem. Soc.* **1991**, *113*, 706. (c) Brady, S. F.; Paleveda, W. J., Jr.; Arison, B. H.; Saperstein, R.; Brady, E. J.; Raynor, K.; Reisine, T.; Veber, D. F.; Freidinger, R. M. *Tetrahedron* **1993**, *49*, 3449.

(13) Freidinger, R. M.; Perlow, D. S.; Veber, D. F. *J. Org. Chem.* **1982**, *47*, 104.

(14) (a) Hanessian, S.; McNaughtonSmith, G.; Lombart, H. G.; Lubell, W. D. *Tetrahedron* **1997**, *53*, 12789. (b) Cluzeau, J.; Lubell, W. D. *Biopolymers* **2005**, *80*, 98.

(15) (a) Sacchetti, A.; Silvani, A.; Lesma, G.; Pilati, T. *J. Org. Chem*. **2011**, *76*, 833. (b) Landoni, N.; Lesma, G.; Sacchetti, A.; Silvani, A. *J. Org. Chem.* **2007**, *72*, 9765. (c) Bittermann, H.; Gmeiner, P. *J. Org. Chem.* **2006**, *71*, 97. (d) Blomberg, D.; Hedenstrom, M.; Kreye, P.; Sethson, I.; Brickmann, K.; Kihlberg, J. *J. Org. Chem.* **2004**, *69*, 3500. (e) Genin, M. J.; Johnson, R. L. *J. Am. Chem. Soc.* **1992**, *114*, 8778. (f) Hinds, M. G.; Welsh, J. H.; Brennand, D. M.; Fisher, J.; Glennie, M. J.; Richards, N. G. J.; Turner, D. L.; Robinson, J. A. *J. Med. Chem.* **1991**, *34*, 1777. (g) Hinds, M. G.; Richards, N. G. J.; Robinson, J. *J. Chem. Soc., Chem. Commun.* **1988**, 1447.

(16) (a) Diaz, H.; Espina, J. R.; Kelly, J. W. A. *J. Am. Chem. Soc.* **1992**, *114*, 8316. (b) Diaz, H.; Tsang, K. Y.; Choo, D.; Kelly, J. W. *Tetrahedron* **1993**, *49*, 3533. (c) Tsang, K. Y.; Diaz, H.; Graciani, N.; Kelly, J. W. *J. Am. Chem. Soc.* **1994**, *116*, 3988.

(17) (a) Bach, A. C., II; Gierasch, L. M. *J. Am. Chem. Soc.* **1985**, *107*, 3349. (b) Bach, A. C., II; Gierasch, L. M. *Biopolymers* **1986**, *25*, 175. (c) Chauhan, V. S.; Sharma, A. K.; Uma, K.; Paul, P. K. C.; Balaram, P. *Int. J. Pept. Protein Res.* **1987**, *29*, 126. (25) Palmer, D. E.; Pattaroni, C.; Nunami, K.; Chadha, R. K.; Goodman, M.; Wakamiya, T.; Fukase, K.; Horimoto, S.; Kitazawa, M.; Fujita, H.; Kubo, A.; Shiba, T. *J. Am. Chem. Soc.* **1992**, *114*, 5634.

(18) (a) Ripka, W. C.; Delucca, G. V.; Bach, A. C.; Pottorf, R. S.; Blaney, J. M. *Tetrahedron* **1993**, *49*, 3593. (b) Hata, M.; Marshall, G. R. *J. Comput. Aided Mol. Des.* **2006**, 20, 321.

(19) (a) Golebiowski, A.; Klopfenstein, S. R.; Shao, X.; Chen, J. J.; Colson, A. O.; Grieb, A. L.; Russell, A. F. *Org. Lett.* **2000**, *2*, 2615. (b) Mieczkowski, A.; Kozminski, W.; Jurczak, J. *Synthesis* **2010**, 221.

(20) (a) Smith, A. B.; Sasho, S.; Barwis, B. A.; Sprengeler, P.; Barbosa, J.; Hirschmann, R.; Cooperman, B. S. *Bioorg. Med. Chem. Lett.* **1998**, *8*, 3133. (b) Hirschmann, R.; Nicolaou, K. C.; Pietranico, S.; Salvino, J.; Leahy, E. M.; Sprengeler, P. A.; Furst, G.; Smith, A. B.; Strader, C. D.; Cascieri, M. A.; Candelore, M. R.; Donaldson, C.; Vale, W.; Maechler, L. *J. Am. Chem. Soc.* **1992**, *114*, 9217.

(21) Rao, M. H. V. R.; Pinyol, E.; Lubell, W. D. *J. Org. Chem.* **2007**, *72*, 736.

(22) André, C.; Legrand, B.; Deng, C.; Didierjean, C.; Pickaert, G.; Martinez, J.; Averlant-Petit, M. C.; Amblard, M.; Calmes, M. *Org. Lett.* **2012**, *14*, 960.

(23) (a) Hickey, J. L.; Luyt L. G. *Tetrahedron Lett.* **2008**, *49*, 1293. (b) Tian, Z. Q.; Bartlett, P. A. *J. Am. Chem. Soc.* **1996**, *118*, 943.

(24) Che, Y.; Brooks, B. R.; Riley, D. P. Reaka, A. J. H.; Marshall, G. R. *Chem Biol Drug Des* **2007**, *69*, 99.

(25) Nagai, U.; Sato, K. *Tetrahedron Lett.* 1985, 26, 647.

(26) Peng, Y.; Sun, H.; Wang, S. *Tetrahedron Lett.* **2006**, *47*, 4769.

(27) (a) Baca, M.; Kent, S. B. H.; Alewood, P. F. *Protein Sci.* **1993**, *2*, 1085. (b) Viles, J. H.; Patel, S. U.; Mitchell, J. B.; Moody, C. M.; Justice, D. E.; Uppenbrink, J.; Doyle, P. M.; Harris, C. J.; Sadler, P. J.; Thornton, J. M. *J. Mol. Biol.* **1998**, *9*, 973. (c) Müller, G.; Hessler, G.; Decornez, H.Y. Angew. Chem.; Int. Ed. **2000**, *39*, 894.

(28) (a) Cluzeau, J.; Lubell, W. D. *Biopolymers* (*Pept. Sci.*) **2005**, *80*, 98. (b) Belvisi, L.; Bernardi, A.; Manzoni, L.; Potenza, D.; Scolastico, C. *Eur. J. Org. Chem.* **2000**, 2563.

(29) Toniolo, C.; Bonora, G. M.; Bavoso, A.; Benedetti, E.; Diblasio, B.; Pavone, V.; Pedone, C. *Biopolymers* **1983**, *22*, 205.

(30) Zerkout, S.; Dupont, V.; Aubry, A.; Vidal, J.; Collet, A.; Vicherat, A.; Marraud, M. *Int. J. Pept. Protein Res.* **1994**, *44*, 378.

(31) Pol, S. D.; Zorn, C.; Klein, C. D.; Zerbe, O.; Reiser, O. *Angew. Chem., Int. Ed*., **2004**, *43*, 511.

(32) S. H. Gellman, *Acc. Chem. Res*., **1998**, *31*, 173.

(33) (a) W. Seth Horne and S. H. Gellman, *Acc. Chem. Res.* **2008**, *41*, 1399. (b) I. M. Mandity, L. Fulop, E. Vass, G. K. Toth, T. A. Martinek and F. Fulop, *Org. Lett.*, **2010**, *12*, 5584.

(34) (a) Prabhakaran, P.; Kale, S. S.; Puranik, V. G.; Rajamohanan, P. R.; Chetina, O.; Howard, J. A. K.; Hofmann, H.-J. r.; Sanjayan, G. J. *J. Am. Chem. Soc.* **2008**, *130*, 17743. (b) Kale, S. S.; Kotmale, A. S.; Dutta, A. K.; Pal, S.; Rajamohanan, P. R.; Sanjayan, G. J. *Org. Biomol. Chem.* **2012**, *10*, 8426. (c) Ramesh, V. V. E.; Priya, G.; Kotmale, A. S.; Gonnade, R. G.; Rajamohanan, P. R.; Sanjayan, G. J. *Chem. Commun.* **2012**, *48*, 11205.

(35) (a) Huck, B. R.; Fisk, J. D.; Gellman, S. H. *Organic Letters* **2000**, *2*, 2607.(b) Chung, Y. J.; Christianson, L. A.; Stanger, H. E.; Powell, D. R.; Gellman, S. H. *J. Am. Chem. Soc.* **1998**, *120*, 10555.

(36) Vasudev, P. G.; Ananda, K.; Chatterjee, S.; Aravinda, S.; Shamala, N.; Balaram, P. *J. Am. Chem. Soc.* **2007**, *129*, 4039.

(37) (a) Vasudev, P. G.; Chatterjee, S.; Shamala, N.; Balaram, P. *Chem. Rev.* **2011**, *111*, 657. (b) Schramm, P.; Hofmann, H.-J. r. *J. Mol. Struct.: THEOCHEM* **2009**, *907*, 109. (c) Matthews, B. W. *Macromolecules* **1972**, *5*, 818.

(38) (a) Fleet, G. W. J.; Johnson, S. W.; Jones, J. H. J. *Pept. Sci.,* **2006**, *12*, 559. (b) Chakraborty, T. K.; Reddy, V. R.; Sudhakar, G.; Kumar, S. U.; Reddy, T. J.; Kuran, S. K.; Kunwar, A. C.; Mathur, A.; Sharma, R.; Gupta, N.; Prasad, S. *Tetrahedron*, **2004**, *60*, 8329. (c) Fuchs, E. -F.; Lehmann, J. *Chem. Ber.*, **1975***, 108,* 2254.

(39) Jones, C. R.; Qureshi, M. K. N.; Truscott, F. R.; Hsu, S.-T. D.; Morrison, A. J.; Smith, M. D. *Angew. Chem.* **2008**, *120*, 7207.

(40) Etter, M. C. *Acc. Chem. Res.* **1990,** *23*, 120.

(41) Prabhakaran, P.; Kale, S. S.; Puranik, V. G.; Rajamohanan, P. R.; Chetina, O.; Howard, J. A. K.; Hofmann, H.-J. r.; Sanjayan, G. J. *J. Am. Chem. Soc.* **2008**, *130*, 17743.

(42) Hamuro, Y.; Geib, S. J.; Hamilton, A. D. *J. Am. Chem. Soc.* **1997**, *119*, 10587.

(43) (a) Priya, G.; Kotmale, A. S.; Gawade, R. L.; Mishra, D.; Pal, S.; Puranik, V. G.; Rajamohanan, P. R.; Sanjayan, G. J. *Chem. Commun.* **2012**, *48*, 8922. (b) Vijayadas, K. N.; Davis, H. C.; Kotmale, A. S.; Gawade, R. L.; Puranik, V. G.; Rajamohanan, P. R.; Sanjayan, G. J. *Chem. Commun.* **2012**, *48*, 9747.

(44) Baruah, P. K.; Sreedevi, N. K.; Gonnade, R.; Ravindranathan, S.; Damodaran, K.; Hofmann, H.-J. r.; Sanjayan, G. J. *J. Org. Chem.* **2006**, *72*, 636.

(45) Gademann, K.; Ernst, M.; Hoyer, D.; Seebach, D. *Angew. Chem. Int. Ed.* **1999***, 38,* 1223.

(46) (a) Andreu, D.; Ruiz, S.; Carreno, C.; Alsina, J.; Albericio, F.; Jimenez, M. A.; Delafiguera, N.; Herranz, R.; Garcia-Lopez, M. T.; Gonzalez-Muniz, R. *J. Am. Chem. Soc.* **1997**, *119*, 10579. (b) Roy, S.; Lombart, H. G.; Lubell, W. D.; Hancock, R. E. W.; Farmer, S. W. *J. Peptide. Res.* **2002**, *60*, 198. (c) Ripka, W. C.; Delucca, G. V.; Bach, A. C.; Pottorf, R. S.; Blaney, J. M. *Tetrahedron* **1993**, *49*, 3609.

(47) (a) Qiu, W.; Gu, X.; Soloshonok, V. A.; Carducci, M. D.; Hruby, V. J. *Tetrahedron Lett.* **2001**, *42*, 145. (b) Xiong, C.; Zhang, J.; Davis, P.; Wang, W.; Ying, J.; Porreca, F.; Hruby, V. J. *Chem. Comm.* **2003**, *13*, 1598.

(48) Gosselin, F.; Lubell, W. D.; Tourwe´, D.; Ceusters, M.; Meert, T.; Heylen, L.; Jurzak, M. J Pept Res 2001, 57, 337.

(49) Grotenbreg, G. M.; Timmer, M. S. M.; Llamas-Saiz, A. L.; Verdoes, M.; van der Marel, G. A.; van Raaij, M. J.; Overkleeft, H. S.; Overhand, M. *J. Am. Chem. Soc.* **2004** , *126*, 3444.

(50) Berkessel, A.; Gasch, N.; Glaubitz, K.; Koch, C. *Org. Lett.* **2001**, *3*, 3839.

(51) (a) Davie, E. A. C.; Mennen, S. M.; Xu, Y.; Miller, S. J. Chem. Rev., **2007**, *107*, 5759. (b) Revell, J. D.; Wennemers, H. *Curr. Opin. Chem. Biol.,* **2007**, *11*, 269.

(52) Fiori, K. W.; Puchlopek , A. L. A.; Miller, S. J. *Nature Chemistry* 2009, **1**, 630.

(53) Lichtor, P. A.; Miller, S. J. *Nat. Chem*. **2009**, *1(8)*, 630.

(54) Sculimbrene, B. R.; Miller, S. J. *J. Am. Chem. Soc.* **2001**, *123*, 10125.

(55) Jarvo, E. R.; Copeland, G. T.; Papaioannou, N.; Bonitatebus, P. J.; Miller, S. J. *J. Am. Chem. Soc.* **1999,** *121,* 11638.

(56) Chen, P.; Qu, J. *J. Org. Chem.* **2011**, *76*, 2994.

(57) (a) Wiesner, M.; Revell, J. D.; Wennemers, H. *Angew. Chem.; Int. Ed*. **2008**, *47*, 1871. (b) Krattiger, P.; Kovhsy, R.; Revell, J. D.; Ivan, S.; Wennemers, H. *Org. Lett.* **2005**, *7*, 1101. (c) Revell, J. D.; Gantenbein, D.; Krattiger, P.; Wennemers, H. *Biopolymers* **2006**, *84*, 105.

(58) (a) P. K. Baruah, N. K. Sreedevi, R. Gonnade, S. Ravindranathan, K. Damodaran, H.-J. Hofmann, G. J. Sanjayan, *J. Org. Chem*. **2007**, *72***,** 636. (b) P.

K. Baruah, N. K. Sreedevi, B. Majumdar, R. Pasricha, P. Poddar, R. Gonnade, S. Ravindranathan, G. J. Sanjayan, *Chem. Commun.* **2008,** 712.

(59) (a) Woody, R. W. *Methods. Enzymol.* **1995,** *246,* 34. (b) Greenfield, N. J. *Encyclopedia of Spectroscopy and Spectrometry*, **2009**, *130*, 153. (c) E. L. Eliel, S. H. Wilen, "*Stereochemistry of Organic Compounds*" (Wiley, **1994**), 1000.

(60) Thorat, V. H.; Ingole, T. S.; Vijayadas, K. N.; Nair, R. V.; Kale, S. S.; Ramesh, V. V. E.; Davis, H. C.; Prabhakaran, P.; Gonnade, R. G.; Gawade, R. L.; Puranik, V. G.; Rajamohanan, P. R.; Sanjayan, G. J. *Eur. J. Org. Chem.* **2013**, *2013*, 3529.

(61) (a) Uceda, D. P-.; Santiveri, C. M.; Jimenez, M. A. *Methods Mol. Biol.* **2006**, *340*, 7. (b) Hughes R. M.; Waters, M. L. *Curr. Opin. Struct. Biol.*, **2006**, *16*, 514. (c) Arkin, M. R.; Wells, J. A. *Nat. Rev. Drug Discovery* **2004**, *3*, 301. (d) Manard, A. J.; Sharman, G. J.; Searle, M. S. *J. Am. Chem. Soc.* **1998**, *120*, 1996.

(62) Robinson, J. A. *Acc. Chem. Res.* **2008**, *41*, 1278.

(63) Chatterjee, B.; Saha, I.; Raghothama, S.; Aravinda, S.; Rai, R.; Shamala, N.; Balaram, P. *Chem. Eur. J.* 2008, **14**, 6192.

(64) Harini, V. V.; Aravinda, S.; Rai, R.; Shamala, N.; Balaram, P. *Chem. Eur. J.* 2005, 11, 3609.

(65) Kapoerchan, V. V.; Spalburg, E.; de Neeling, A. J.; Mars-Groenendijk, R. H.; Noort, D.; Otero, J. M.; Ferraces-Casais, P.; Llamas-Saiz, A. L.; van Raaij, M. J.; van Doorn, J.; van der Marel, G. A.; Overkleeft, H. S.; Overhand, M. *Chem. – Eur. J.* **2010**, *16*, 4259.

(66) (a) Aurora, R.; Creamer, T. P.; Srinivasan, R.; Rose, G. D. *J. Biol. Chem.* **1997**, *272*, 1413. (b) Nowick, J. S. *Acc. Chem. Res.* **1999**, *32*, 287. (c) Robinson, J. A. *Synlett.* **1999**, 429. (d) Venkatraman, J.; Shankaramma, S. C.; Balaram, P. *Chem. Rev.* **2001**, *101*, 3131.

(67) (a) Tsang, K. Y.; Diaz, H.; Graciani, N.; Kelly, J. W. *J. Am. Chem. Soc.* **1994**, *116*, 3988. (b) Nesloney, C. L.; Kelly, J. W. *J. Am. Chem. Soc.* **1996,** *118,* 5836.

(68) (a) Phillips, S.T.; Blasdel, L. K.; Bartlett, P. A. *J. Org. Chem.* **2005**, *70*, 1865. (b) Phillips, S.T.; Piersanti, G.; Bartlett, P. A. *Proc. Natl. Acad. Sci. USA* **2005**, *102*, 13737.

(69) Nowick, J. S. *Acc. Chem. Res.* **2008**, *41*, 1319.

(70) Fu, Y.; Bieschke, J.; Kelly, J.W. *J. Am. Chem. Soc.* **2005**, *127*, 15366.

(71) Chakraborty, K.; Shivakumar, P.; Raghothama, S.; Varadarajan, R. *Biochem. J.* **2005**, *390*, 573.

(72) Hughes, R. M.; Waters, M. L. *Curr. Opin. Str. Biol*. **2006**, *16*, 514.

(73) (a) Haque, T. S.; Little, J. C.; Gellman, S. H. *J. Am. Chem. Soc.* **1996**, *118,* 6975. (b) Langenhan, J. M.; Gellman, S. H. *Org. Lett.* **2004***, 6,* 937. (c) Royo, S.; Borggraeve, W. M. D.; Peggion, C.; Formaggio, F.; Crisma, M.; Jimenez, A. I.; Cativiela, C.; Toniolo, C. *J. Am. Chem. Soc.* **2005**, *127,* 2036.

(74) Flory, P. J. *Statistical Mechanics of Chain Molecules*; Interscience Publishers: New York, 1969.

(75) Demizu, Y.; Doi, M.; Sato, Y.; Tanaka, M.; Okudaa, H. Kuriharaa, M. *J. Pept. Sci.* **2011**, *17*, 420.

(76) Ramachandran, G. N.; Ramakrishnan, C.; Sasisekharan, V. *J. Mol. Biol.* **1963**, *7*, 95.

(77) (a) Chatterjee, B.; Saha, I.; Raghothama, S.; Aravinda, S.; Rai, R.; Shamala, N.; Balaram, P. *Chem. Eur. J.* **2008**, *14*, 6192. (b) Rao Raghothama, S.; Kumar Awasthi, S.; Balaram, P. *J. Chem. Soc., Perkin Trans. 2* **1998**, 137. (c) Stanger, H. E.; Gellman, S. H. *J. Am. Chem. Soc.* **1998**, *120*, 4236.

(78) (a) Haque, T. S.; Little, J. C.; Gellman, S. H. *J. Am. Chem. Soc.*, **1996**, *118*, 6975. (b) Mándity, I. M.; Wéber, E.; Martinek, T. A.; Olajos, G.; Tóth, G. K.; Vass, E.; Fülöp, F. *Angew. Chem.; Int. Ed.* **2009**, *48*, 2171; (c) Lengyel, G. A.; Horne, W. S. *J. Am. Chem. Soc.* **2012**, *134*, 15906. (d) Bomar, M. G.; Song, B.; Kibler, P.; Kodukula, K.; Galande, A. K. *Org.Lett.* **2011**, *13*, 5878. (e) Gibbs, A. C.; Bjorndahl, T. C.; Hodges, R. S.; Wishart, D. S. *J. Am. Chem. Soc.* **2002**, *124*, 1203. (f) de Alba, E.; Jiménez, M. A.; Rico, M. *J. Am. Chem. Soc.* **1997**, *119*, 175.

(79) (a) Andersen, N. H.; Neidigh, J. W.; Harris, S. M.; Lee, G. M.; Liu, Z.; Tong, H. *J. Am. Chem. Soc.* **1997**, *119*, 8547. (b) Llinás, M.; Klein, M. P. *J. Am. Chem. Soc.* **1997**, *97*, 4731.

(80) (a) Cierpicki, T.; Otlewski, J. *J. Biomol. NMR* **2001**, *21*, 249. (b) Baxter, N. J.; Williamson, M. P. *J. Biomol. NMR* **1997**, *9*, 359.

CHAPTER 2

Investigations of conformational pre-disposition of -α/β_n-oligomers (α = $^{L/D}$proline and β = anthranilic acid)

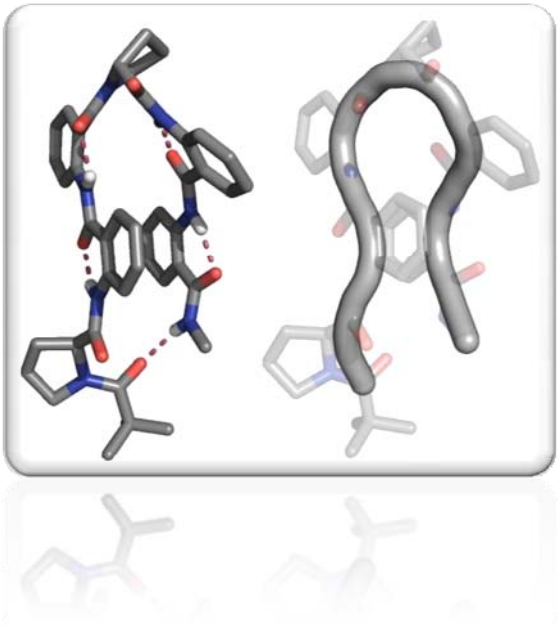

This chapter discusses conceptual background, design principles, and investigations about the effect of constitutional ratio variation of aliphatic-aromatic residue conjugates on the conformational disposition of oligomers.

It is the tension between creativity and skepticism that has produced the stunning and unexpected findings of science.

- Carl Sagan

2.0 Preamble

The three-dimensional architecture of molecules dictate the specific functions of different biopolymers. The structural features of such assemblies emanate from interplay of a set of non-covalent forces, which associate with the local constraints to render conformational ordering.[1] Nature exemplifies a range of structural and functional assemblies like DNA molecule, the genetic information stockpile, where non-covalent interactions co-operatively orchestrates the double helical assembly. Non-covalent interactions like directional H-bonding[2] and sequence-dependent aromatic stacking interactions[3] associate co-operatively with each other in order to assemble this unique architecture. The aromatic-stacking driven rigidified individual strands of DNA twist in double helical fashion by virtue of a series of complementary array of H-bonding interactions between the templates.[4] Another remarkable example is the most abundant fibrous protein 'collagen', commonly found in the connective tissues, which illustrates a luminous triple helical architecture formed by intertwining of individual helices with each other *via* an extensive intermolecular H-bonding network.[5] Structurally intriguing 'beta-barrel membrane proteins' exemplify the selective patterning of hydrophobic residues with brilliant complementary H-bonding arrangement, to create large beta-sheets containing closed structure. Its specific structural architecture directs its overt functions in ion- and lipid transportation in cells.[6]

With an intention of interpreting the mystery behind the complexity of such architectures and understanding its contribution towards its functions, investigations about their structural features have emerged as a discipline in biomolecular chemical sciences. The objective of recognizing the structure-and- function relationship marked beginning of the field called 'foldamers'. Considering the multitude of possibilities of achieving suitable templates for the design of biologically active molecules that can compete for a variety of protein-protein and protein membrane interactions, synthetic chemists constantly endeavour to create novel assemblies.[7] The consistent efforts in creating novel assemblies are often shown to successfully mimic few such complex assemblies. This part of work is an attempt to explore the forces involved in manifestation of some such intriguing structural architectures, chiefly originating from the varying constitutional combinations of natural and unnatural building blocks.

2.1 Magnitude of non-covalent forces: Their role in stabilising complex molecular architectures

Structure assembly process in proteins / ordered arrangements (conformations) of syntheric oligomers are governed by the interplay of multiple non-covalent forces like hydrogen bonding, hydrophobic, electrostatic and van der Waals forces either exclusively or in a co-operative manner. These interactions are widely responsible for various physiological events like signal transduction in cells, the transportation of ions/molecules in-and-out of membranes, enzymatic reactions *etc*. Due to participation of these forces in localized regions, polypeptide chains attain secondary structure which further associate into bonded aggregates (intramolecularly and intermolecularly) to direct tertiary structure and quaternary structure formation. A very coherent pictorial representation of co-operativity of non-covalent forces in protein folding process was provided by T. E. Creighton in *Current Biology* 1995 (Figure 1).[8] In a simple form as described by them, all interactions are apparently identical providing similar cooperativity, but in reality, some sets of interactions become more pronounced depending on the local constraints.

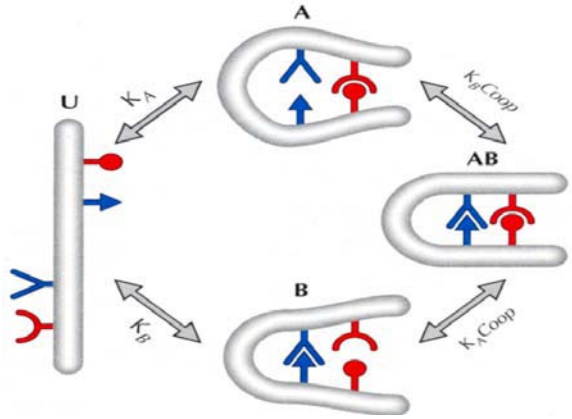

Figure 1: Schematic illustration of co-operativity between two interactions A and B, with respective equilibrium constants K_A and K_B in the unfolded polypeptide chain.

All these non-covalent interactions are equally critical in synthetic systems as well, often joined by solvophobic interactions[9] (detailed discussion follows in section 2.1b) to cause conformational modulations. Huc *et al* successfully designed double-helical assemblies in an attempt to emulate DNA assembly. In this inimitable system, the two strands are pulled together by aromatic stacking interactions and the template is organised and rigidified by *intra*-molecular bifurcated H-bonding interaction, unlike the natural duplex.[10] Such findings have allowed the applications of the field of

foldamers to expand its horizon from designing aptamers to molecular shuttles.[11] Following section discusses diverse synthetic molecular assemblies driven by non-covalent forces.

2.1.1 Role of hydrogen-bonding interactions

H-bonding interactions play a fundamental role in defining the secondary structure of proteins like α-helix, 3_{10}-helices, sheets, loops, linear strands, coils, turns, *etc*, when they participate *intra*-molecularly between the backbone amide groups. When the H-bonding sites are situated at the side chains, they often intermingle to form interesting architectures like the fibrous protein collagen.[5] The repeating Hyp-Pro-Gly tripeptide units adopt α-helical structure and by virtue of the hydroxyl groups present on each hydroxyproline (Hyp) residue, strong triple helix is shaped through extensive intermolecular H-bonding network (Figure 2A).

The polyamides featuring natural / unnatural amino acids and their analogues are heavily reflected in the foldamer units constructed by Gellman, Seebach, Balaram, Fulop, Guichard and others.[12] In this connection, a broad range of H-bonding-stabilised arylamide oligomers have been illustrated in various reviews by Li and group.[13] Also, a library of higher-order synthetic acrylamide oligomers featuring amide bonds on the side chains, instead of its backbone, presents an amazing display of hydrogen-bonded self-assembled extended sheet-like supramolecular network (Figure 2C).[14]

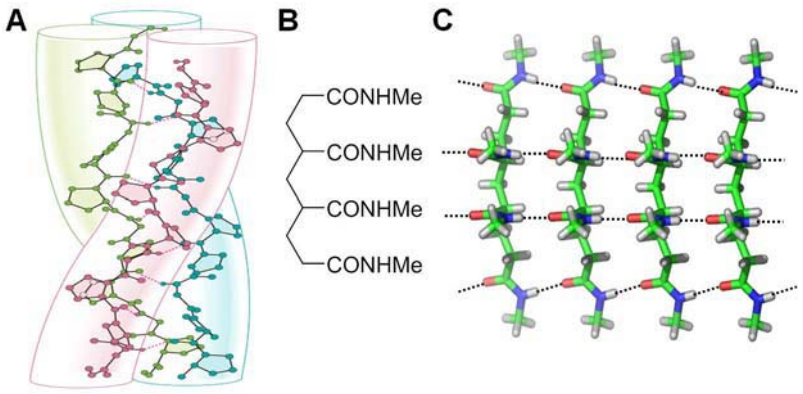

Figure 2: Structure of collagen (A), Molecular structure of acrylamide oligomer and PyMol-rendered top view of single crystal X-ray structure (B and C, respectively) of acrylamide oligomers showing arrangement of the individual strands in the H-bonded self-assembled extended parallel sheet-like supramolecular network

The area of *hetero*-foldamer design has been fast emerging, as it offers wide range of conformational diversity of the oligomers compared to the homogeneous oligomer counterparts.[15] Aliphatic-aromatic amino acid conjugates belong to this class of heterogeneous peptides wherein, the formation of the anticipated secondary structures are warded off to afford distinct 3D compact ensembles like knots,[16] tail biters,[17] pillars[18] and herringbone helices.[19] By virtue of an array of complementary *intra*-molecular H-bonding pattern, water-soluble 54-, 78-, and 102- membered giant macrolactams a.k.a. "cyclic modular *β*-sheets" have been generated by linking the two strands *via* a β-turn mimic δ-linked ornithine residue (Figure 3).[20] These structures developed by Nowick *et al.* used Hao (hydrazine, 5-amino-2-methoxybenzoic acid and oxalic acid mimic) units-based strands, which formed *β*-sheet mimics that are shown to exhibit very high association constants.[21] Using the knowledge of pre-organisation of templates through *intra*-molecular H-bonding, these strand mimics were found to inhibit peptide aggregation by binding to proteins through *β*-sheet interactions.[22]

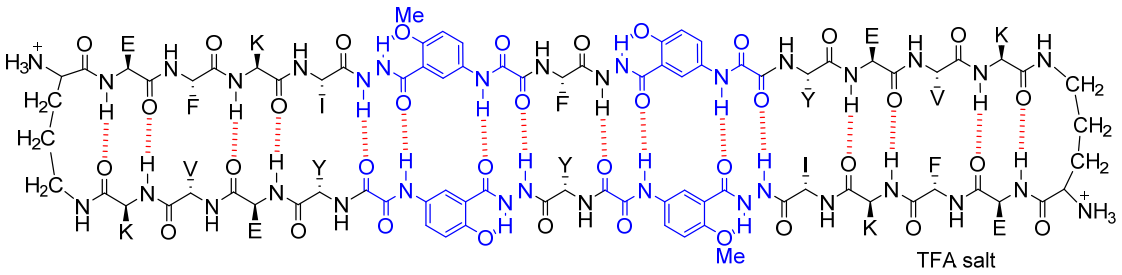

Figure 3. Nowick's 102-membered cyclic modular *β*-sheet (stabilised by an extensive array of complementary H-bonding interactions).

Inspired by DNA duplex assembly, Gong and co-workers developed molecules featuring amino methoxy benzoic acid (Amb) stabilised by S(6) H-bonding which offers directionality.[23] In combination with flexible aliphatic amino acid Gly the Gong group prepared molecular modules that delivered linear arrays of hydrogen bond donors (D) and acceptors (A), which were also stabilised by the van der Waals attraction between methylene protons.[24] Sequence-specific association of these motifs generated duplexes stable in polar media (association constant up to 10^9 M^{-1} in $CHCl_3$), formed by dynamic covalent cross-linking the templates at the termini.[25] Bulky side-chains in such systems have proven to be efficient gelators for aromatic solvents.[26] Such concepts have been very well utilised for the design of artificial duplexes for applications in host-guest assembly and self-assembling systems.[27]

2.1.2 Role of solvophobic forces

Peptide folding and quaternary structure stabilisation is largely influenced due to solubility contrast between the backbone and side chains (solvophobic/solvophilic sites). This modulates the folding↔defolding processes as the molecule tries folds to lock away the solvophobic portions. These forces also are of non-directional nature thus they do not make a good choice in the foldamer design strategy. Yet, it has been extensively explored in the case of oligomers with aromatic backbones.

Various synthetic systems such as oligo-*m*-PE oligomers assume compact helical conformation in polar solvents like acetonitrile, whereas it takes up a random coil conformation in non-polar solvents like chloroform (due to its polar side chains oriented towards the solvent).[28] Oligomers designed by Lehn *et al* comprising alternating naphthyridines and pyrimidines were shown to fold into one- and two-turn helices in chloroform and acetonitrile selectively (Figure 4). While on addition of Cs^+, it adopts 'molecular spring'-type structure (longer, hollow channel) in which further ions could also bind.[29]

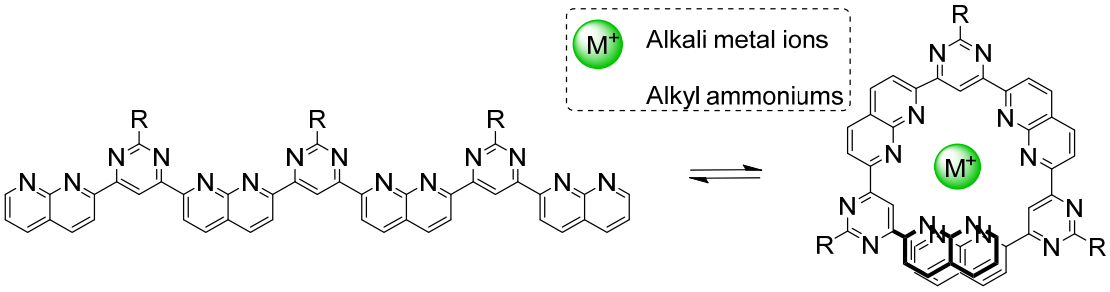

Figure 4: Representative example of consequence of solvophobic effects on folding: naphthyridine-pyrimidine metallofoldamer reported by Lehn.[29]

Another example is cholic acid-based aliphatic foldamer reported by Zhao *et al*., which was seen to favour helical conformation in non-polar solvent that underwent hydrophobically driven helix↔random coil transition.[30] Oligo(diaminopyridine-isophthalamide) designed by Lehn *et al* illustrated the supportive solvophobic and stacking effects. These factors forced amide NH to arrange inwards to stabilize a host-guest assembly (cyanuric acid), within its helical structure through H-bonding.[31]

2.1.3 Role of electrostatic interactions

These interactions mainly occur in charged molecules like in molecules bearing charged side chains. These include different types of interactions like charge-charge, charge-dipole and dipole-dipole *etc*. Cation-π interactions are one of the most important classes that belong to this category. [32]

2.1.4 Role of van der Waals (vdW) forces

Van der Waals forces are relatively weak compared to covalent bonds but occur in large peptide molecules and significantly contribute towards folding of proteins. These are less selective and directionally specific, which discourages their use to confer conformational uniqueness. These are of two types: attractive and repulsive which participate occasionally in protein folding.[24]

2.1.5 Role of aromatic stacking interactions

Aromatic stacking interactions are one of the major forces that render structural assembly to aromatic systems. They arise due to the charge transfer or polarization phenomena in the delocalised electron rich/deficient systems. Diederich *et al* have carried out extensive studies to establish the role played by the solvent on the π-π interaction in host-guest complexes in biological systems and concluded that the most stable complexes of apolar substrates are formed in water.[32]

Various interesting studies on synthetic oligomers comprising exclusively aromatic units were carried out by Iverson *et al*. These *hetero*-duplex self-assembled systems were termed as 'aedamers', which emanate from a stacked arrangement of electron-rich 1,5-dialkoxynaphthalene (DAN) and electon-deficient 1,4,5,8-naphthalenetetracarboxylic diimide (NDI) units to facilitate a columnar assembly (Figure 5) in aqueous environment.[33]

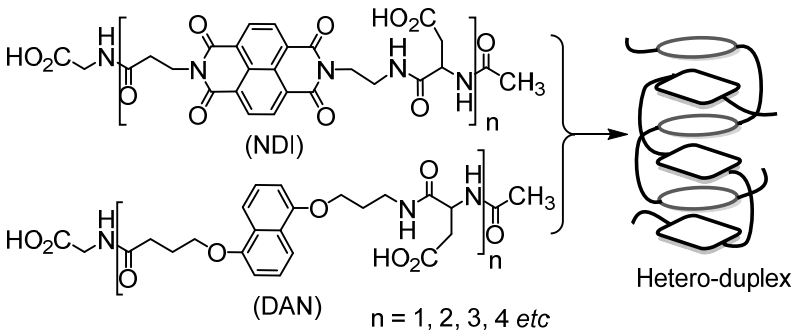

Figure 5. Aedamers designed by Iverson and group based on NDI and DAN units.[33]

Using a combination of crowded aromatic residues with aliphatic amines as linkers and synergy of H-bonding and intra-molecular pi-stacking effects, a foldamer with columnar arrangement was achieved by Nuckoll and co-workers.[34] The crowded mesogens are known for their property of forming discotic liquid crystals. Gong *et al* also designed and developed hybrid linear strands that self-assembled *via* H-bonding and folded due to pi-stacking effect (Figure 6). These self-assembled duplexes revealed good association constants, demonstrating an intelligent selection and sequencing of aliphatic and aromatic amino acids.[24]

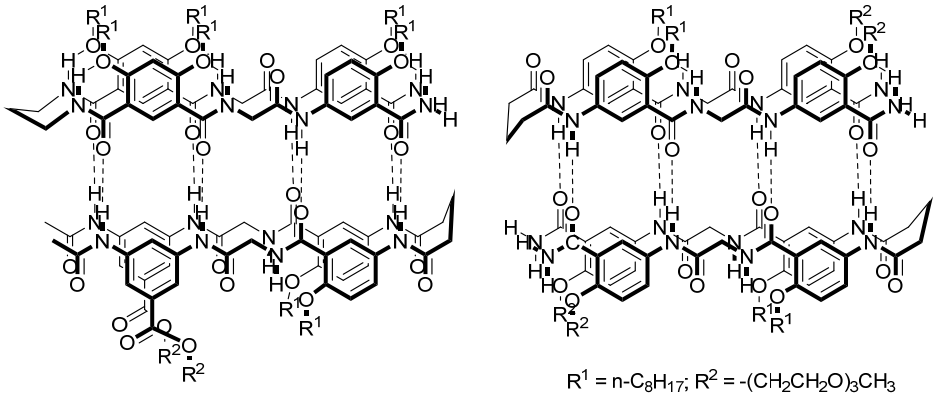

Figure 6. Highly stable, self-complementary hydrogen bonded molecular duplexes reported by Gong *et al.*[24]

2.2 Consequences of stoichiometric variation of residues: Outcome and factors affecting assembly

One of the much exploited practises in bottom-up approach in foldamer research is the development of oligomers with stoichiometric variation of amino acid residues, often result in striking H-bonding patterns.[35,36]

Gellman *et al* used varying constitutional ratios of α-amino acid-ACPC (β-amino acid) residues in distinct cases that afforded dissimilar helical assemblies (Figure 7). A 1:1 ratio of α/β residues furnished 11 or 14/15 helix, while 2:1 α/β residue ratio gave rise to 10/11/11 helices and 1:2 ratio resulted in a mixed 11/11/12-helix. These patterns bear high contrast when compared to the ACPC *homo*-oligomers, which usually adopt 12-helical conformation.[37] α:γ-amino acid unit repeats with varying constitutional ratio, recently reported by the same group, gave rise to a peculiar 12-helical network.[38]

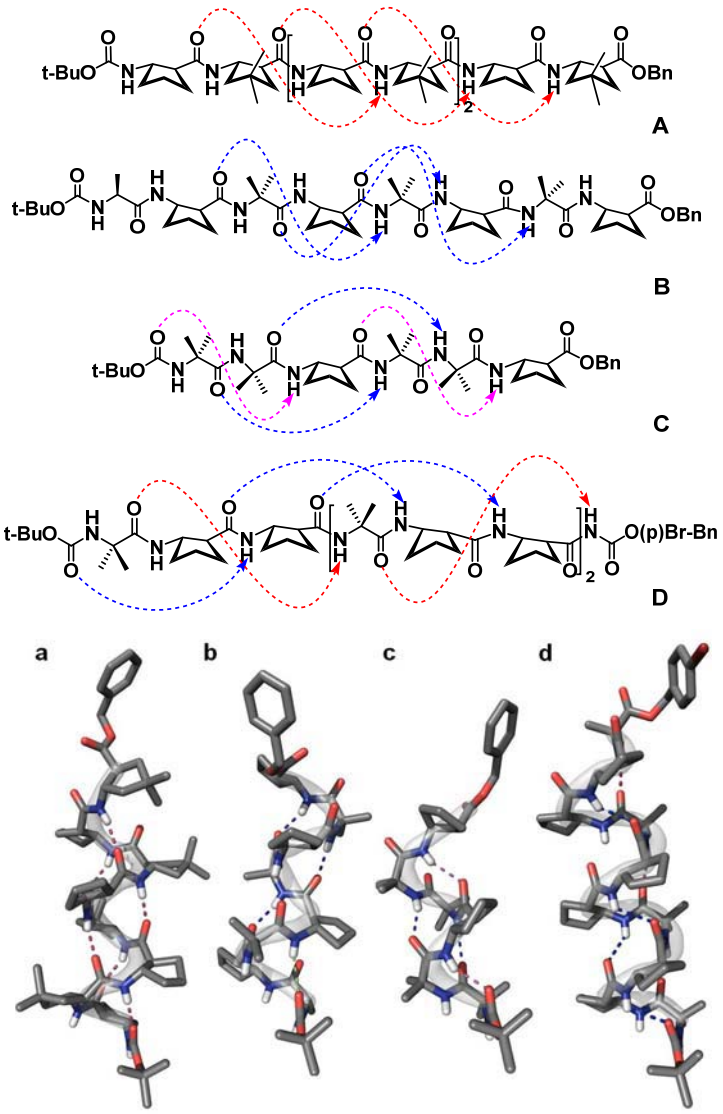

Figure 7. Comparison of H-bonding patterns observed in different helices formed by constitutional variation of α/β-peptide (α = Aib, β = ACPC) residue repeats. Crystal structure of : **A** (ACPC *homo*-oligomers) featuring 12-helix (a), 11-helix formed by **B** (1:1 α/β residue repeats) (b), **C** showing 10/11/11-helix formed by α/α/β repeats (c), **D** revealing11/11/12-helix formed by α/β/β repeats (d). (H-bonding patterns are highlighted in red, blue and pink for 12, 11 and 10-membered H-bonded rings, respectively).

The unprecedented folding and self-assembling patterns emanating from the stoichiometric disparity are often very intriguing. The progress of this field can be chiefly attributed to the development of unnatural amino-acids that has unfastened enormous opportunities for combinatorial structural effects on secondary structure.[39] Variation of the constitutional ratios afforded resultant structure as an outcome of the predominant non-covalent interaction. A very interesting example is that of the PQ sequential repeats developed by Huc *et al* (Q= 8-amino-2-quinoline carboxylic acid

and P=6-aminomethyl- 2-pyridinecarboxylic acid). 1:1 ratio of P and Q units exhibited rare herringbone helix architecture, which on varying the stoichiometric ratio of PQ_n to 1:4 revealed a rod like helical secondary structure.[40]

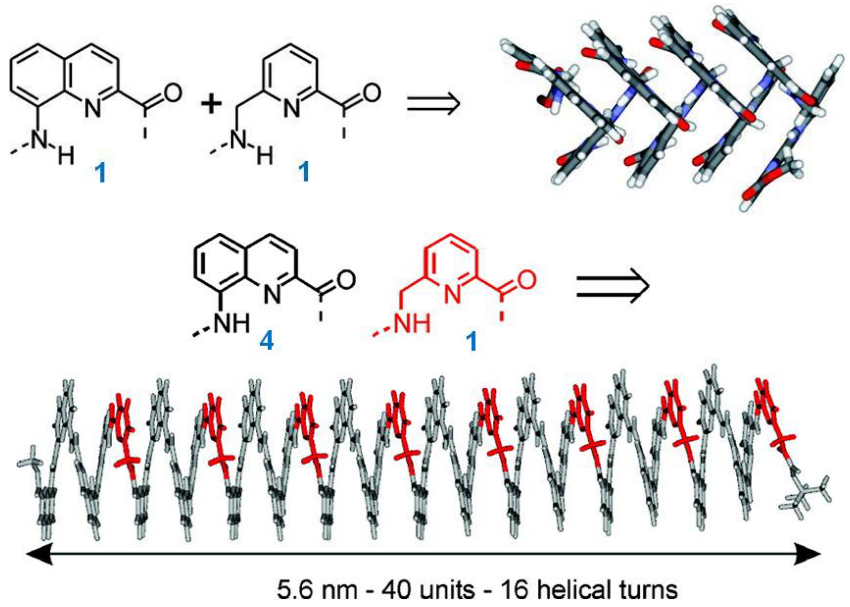

Figure 8: Consequence on the backbone conformation upon variation of stoichiometry of the residues. Molecular structure of repeating units (**Q** and **P**) and corresponding crystal structures of -$(PQ)_4$- repeats with 1:1 ratio of residues (above) and -$(PQ_4)_4$- repeats with 1:4 ratio of residues (below). (Isobutyl chains, solvents and hydrogens have been removed for clarity).

Constitutional ratio variation of residues, as seen in case of AcNH-Ant-Ant-Pro-NHMe trimer unit, have been shown to induce detrimental effect on the *pseudo-β*-turn assembly or the C(6) pattern observed generally in Ant_n repeats. Interestingly, the twin-fold observed in featuring a highly mutually dependent C10- and a C11-closed hydrogen-bonded network was formed by the tripeptide, when Ant preceded Pro residue (Figure 9). Alteration of any of these hydrogen-bonded networks, caused disruption of fully folded conformation of the peptide.[41]

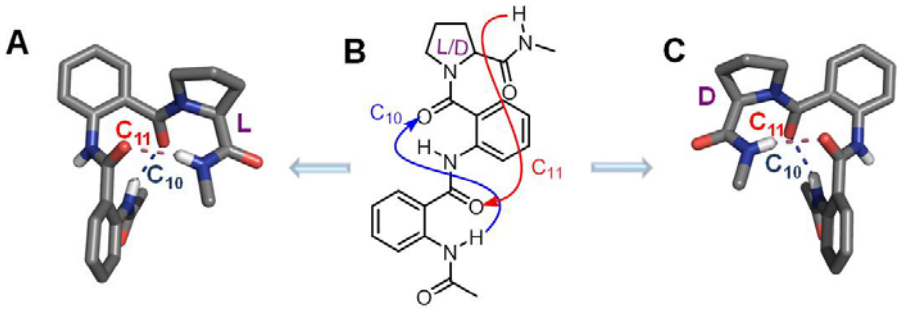

Figure 9. Molecular structure of AcNH-Ant-Ant-Pro-NHMe with H-bonding patterns (B), and crystal structures of its ^{L}Pro and ^{D}Pro analogues (B, C), respectively.

Section I
Synthesis and Conformational Evaluation of Homo-chiral -(^{L}Pro-Ant-Ant)$_n$- Oligomers

2.3 Objective of the work

As described in the preceding **section 2.2**, constitutional variation of distinct residues manifests intriguing assembling patterns. Hence, we sought out to develop and explore the conformational pre-disposition of oligomers featuring dissimilar stoichiometry and chiralities of Pro and Ant building blocks i.e. *homo*-chiral -(^{L}αβ$_n$^{L}αβ$_n$)- and *hetero*-chiral -(^{L}αβ$_n$^{D}αβ$_n$)- sequences with n = 2,3 *etc*. Also, in order to closely understand the 3D structural architecture of the oligomers and the crucial non-covalent interactions that contribute towards their conformational modulation, andstability, we undertook extensive solid- and solution-state structural studies.

2.4 Design strategy

Referring the information accrued from different studies regarding the conformational characteristics arising from distinct residue combinations and their individual preferences, we designed *homo*-chiral and *hetero*-chiral sequences with 1:2 Pro:Ant residues i.e. -*(^{L}Pro-Ant-Ant)$_n$*- and -*(^{L}Pro-Ant-Ant-^{D}Pro-Ant-Ant)$_n$*- repeats. We have already vindicated the robustness of the reverse-turn Ant-Pro motif in the previous chapter, which was found to be highly insensitive towards structural and chirality modulations in-and-around the turn segment. The Ant-Pro 1:1 sequentially repeating oligomers are known to adopt a compact, rigid right-handed helical secondary structure displaying 1→2 forward turns[42] and on the contrary, Ant$_n$ repeats have extended sheet forming propensity.[43]

Aliphatic amino acid "Pro" possesses constrained torsion angle and is highly prone towards *cis/trans* isomerization of the imidic peptidic bond. Pro is also known to affect the conformation of the amino acid preceding it in polypeptides and is a known sheet and helix breaker, even though it is found in triple helical assembly like collagen or poly(Pro)II helix.[44] On the other hand, β aromatic amino acid "Ant" has highly constrained dihedral angles ϕ and ψ ≈ 180°, with an additional dihedral angle θ = 0°. Also, the aromatic amino acids act as fine candidates for construction of *shape persistent* molecular structures owing to their intrinsic hybridisation-induced planarity and locked dihedral angles.

We anticipated that with the blending of α/β aliphatic:aromatic amino acids of such contrasting nature and alteration in their ratios, structural predilection will compete with each other and would deliver unprecedented and interesting structural arrangements.

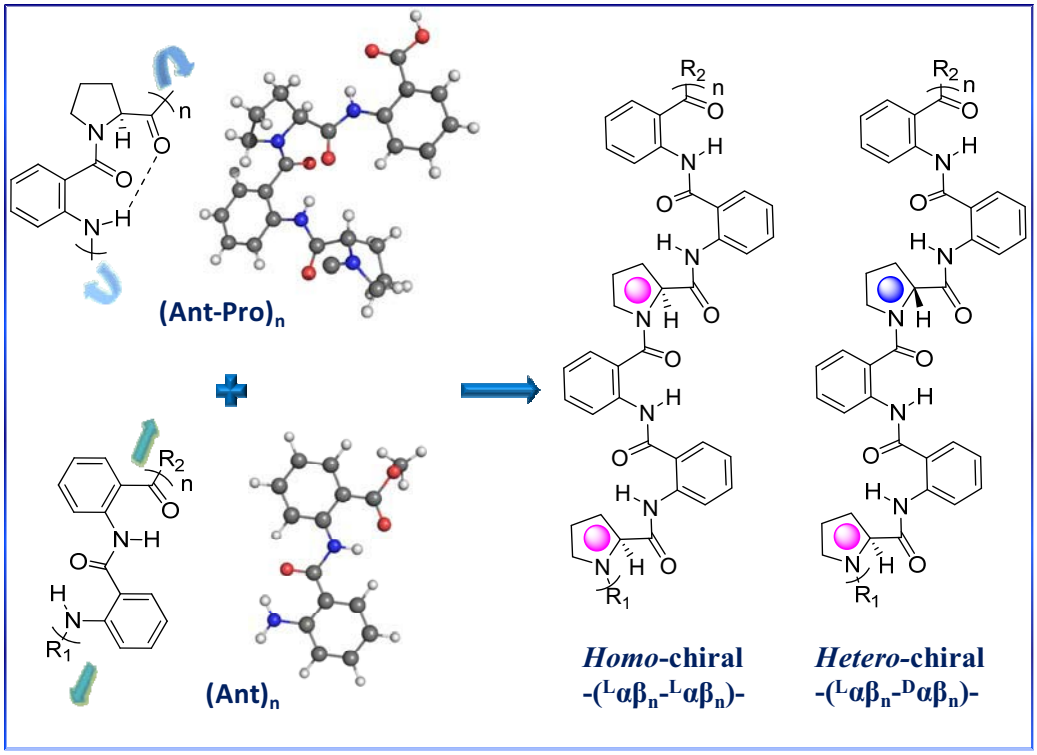

Figure 10: Design principle of the hybrid –(Pro-Ant-Ant)- repeats.

2.5 Synthesis

For the preparation of the oligomers of –(Pro-Ant-Ant)- series, monomers units (trimer segments -$^{L/D}$Pro-Ant-Ant- segment) with altered chiralities were prepared. Owing to reduced reactivity of aromatic amine, we initially attempted acid chloride-mediated coupling of amine H_2N-Ant-Ant-OMe **2b** with Cbz-^{L}Pro-OH, which afforded excellent yields of tripeptide monomer unit **3a**. But, difficulties with Cbz- deprotection during oligomerisation forced us to modify the protecting group. Thus for simplification, trimer synthesis standardisation employing mixed anhydride coupling method was carried out wih Boc-$^{L/D}$Pro-OH and **2b**. With the monomer units **3c** and **3h** (^{D}Pro for *hetero*-chiral oligomer preparation) in hand, corresponding acid and amine counterparts were generated by ester cleavage, under basic condition with $LiOH{\cdot}2H_2O$ and TFA-mediated deprotection of ^{t}Boc- group, respectively.

All these oligomers experienced peak broadening and / or multiplication of signals in NMR spectrum, due to rotameric effect at the N-terminus.[45] This led to

serious hassles in NMR studies. Thus, the N-^{t}Boc substituted tripeptide **3c** (known to undergo *cis-trans* isomerizations and hamper NMR studies [46]) was converted into its corresponding pivaloyl derivative **3f** from **3e** using pivaloyl chloride in presence of TEA in DCM. The efforts to segment double the monomer units were unrewarding, even with a range of coupling agents, due to the formation of benzoxazinone.[47] Thus, as a modified strategy, all the corresponding oxazinones i.e. **3j-l** were isolated by activating their corresponding acids with simple coupling agent like EDC·HCl in good yields.

Scheme 2.1: Synthesis of monomer units **3a-l**

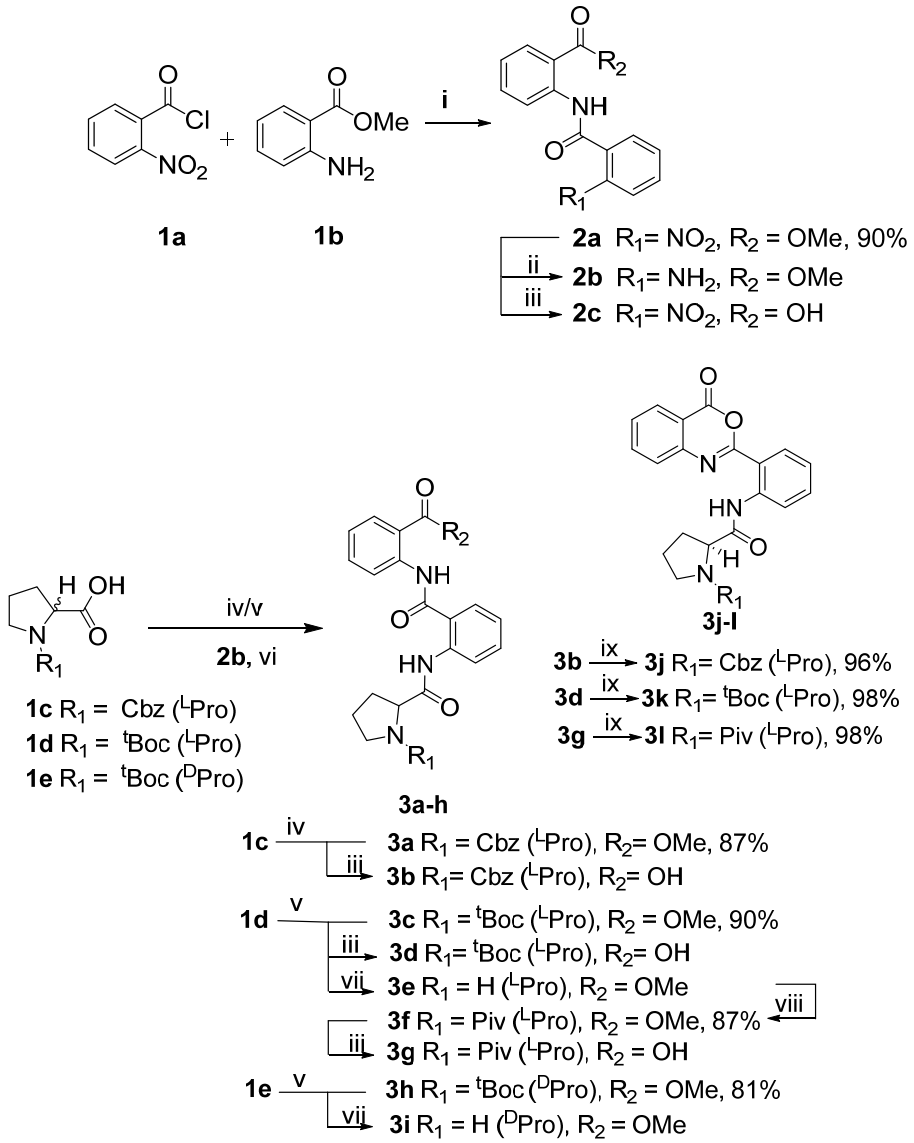

Reagents and conditions: (i) TEA, DCM; (ii) $Pd(OH)_2$, MeOH, 4h; (iii) $LiOH.2H_2O$, MeOH, rt, 4 h; (iv) $(COCl)_2$, cat. DMF, DCM, 0 ^oC, 30 min., (v) ClCOOEt, Et_3N, THF, 0 ^oC - rt, 2h; (vi) THF, reflux, 6h; (vii) TFA:DCM (1:1), rt, 2 h; (viii) Piv-Cl, TEA, DCM, 1h; (viii) EDC.HCl, DCM, 0^oC-rt, 4h.

The purified stable oxazinone derivatives isolated were then subjected to DBU-mediated opening, a strategy explored and established in our group.[48] Resultant hexamers **4a** and **4c** with amine **3e** and oxazinones **3j** and **3k**, respectively, were obtained in good yields.

Scheme 2.2: Synthesis of *homo*-chiral hexapeptides **4a-j**

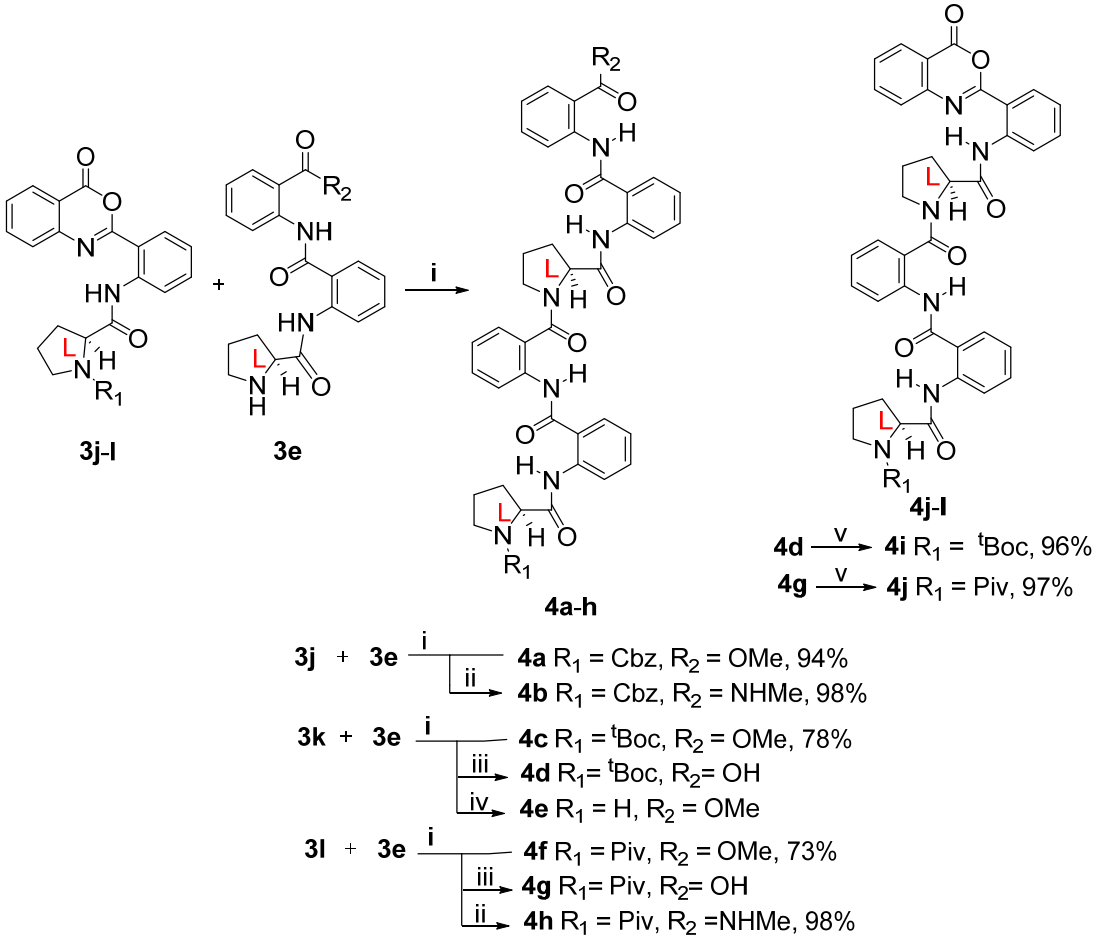

Reagents and conditions: (i) DBU, DMF, 4Å molecular sieves, rt, 2 h; (ii) methanolic methylamine, rt,1h; (iii) aq. LiOH, MeOH, rt, 4 h; (vi) TFA:DCM (1:1), rt, 2 h; (v) EDC.HCl, DCM, 0^{o}C-rt, 4h.

Following the same strategy, higher oligomers *i.e.* dodecamers **5a** and **5d** were prepared by reacting oxazinones **4i** and **4j** with amine **4e**, to afford corresponding ^{t}Boc- and Piv- protected oligomers, respectively. Similarly, octadecapeptides **6a** and **6b** were obtained from the oxazinones **4i** and **4j**, by reacting amine **5b**. The C-terminal methyl amides **4b** and **4h** (hexamers), **5e** (dodecamer) and **6c** (octadecamer) were accessed readily by direct amidation of the corresponding esters **4a**, **4f**, **5c** and **6b**, respectively, using saturated methanolic methylamine.

Scheme 2.3: Synthesis of *homo*-chiral dodecapeptides **5a-e** and octadecapeptides **6a-c**

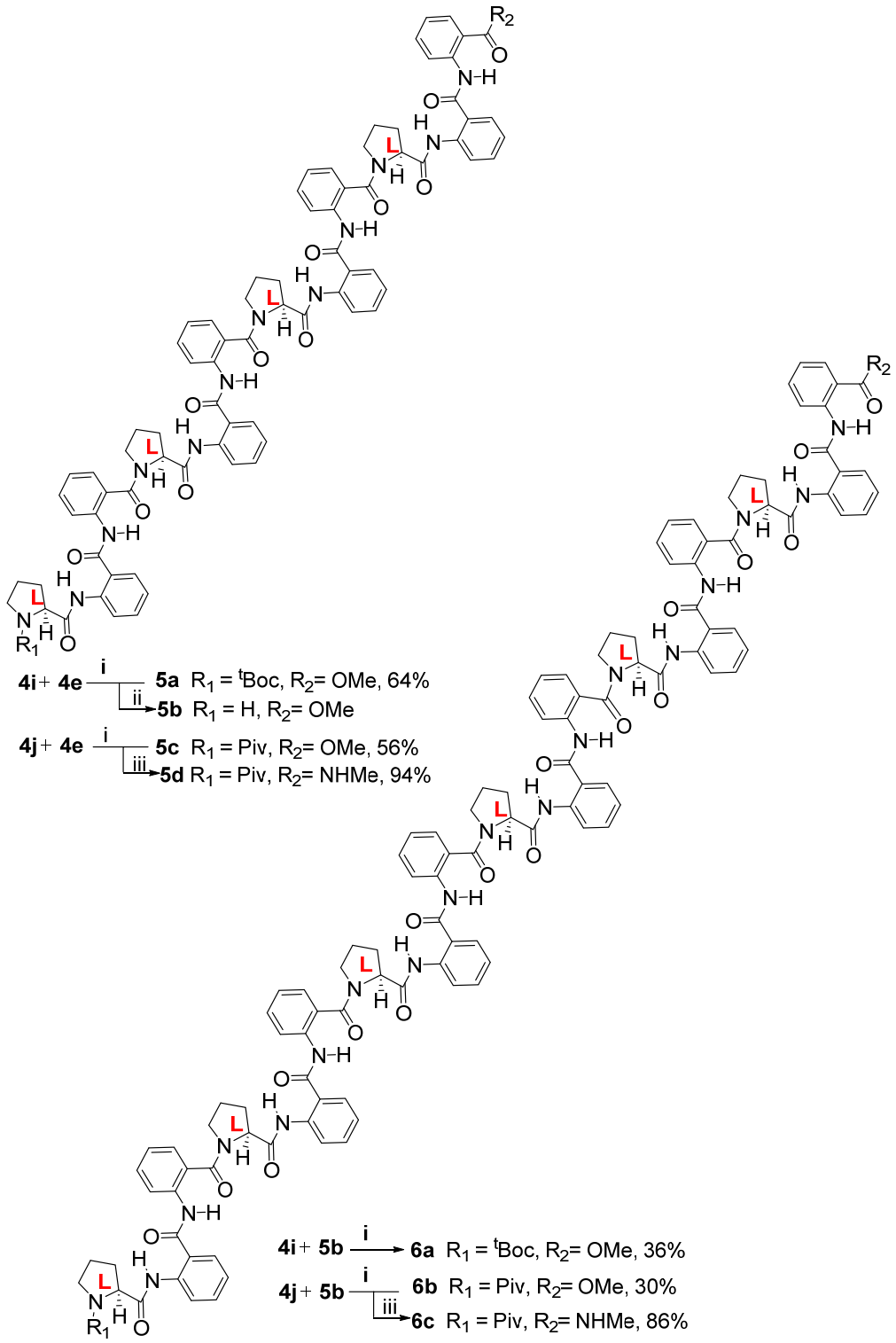

Reagents and conditions: (i) DBU, DMF, 4Å molecular sieves, rt, 2h; (ii) TFA:DCM (1:1), rt, 2h; (iii) methanolic methylamine, rt,1h.

2.6 Conformational analyses

Secondary structural analyses were carried out *via* extensive 2D NMR, X-ray diffraction and CD studies.

2.6.1 Single crystal X-ray diffraction studies

Intense crystallisation efforts afforded needle shaped fine colourless crystals of **4b** and **4h** from MeOH and mixture of DCM:EtOH, respectively (Figure 11b,d). Interestingly, both the crystal structures shared striking similarity, where the structures featured clear absence of C9- turn in both the oligomers and the involvement of all amide NHs of the Ant residues in strong *intra*-residual 6-membered-ring H-bonding, except the terminal methylamide NH7. Crystal structures of both *homo*-oligomers **4b** and **4h** revealed that Ant2-Ant3 units almost adopted orthogonality with respect to each other and Pro4 unit induced another turn. Substantial strain was observed by Ant3 residue of **4h**, where its φ = - 46.93° and θ = -16.04°, which is notably higher. The Ant5-Ant6 units also deviated from planarity introducing further twist in the structure, resulting in a nearly helical disposition.

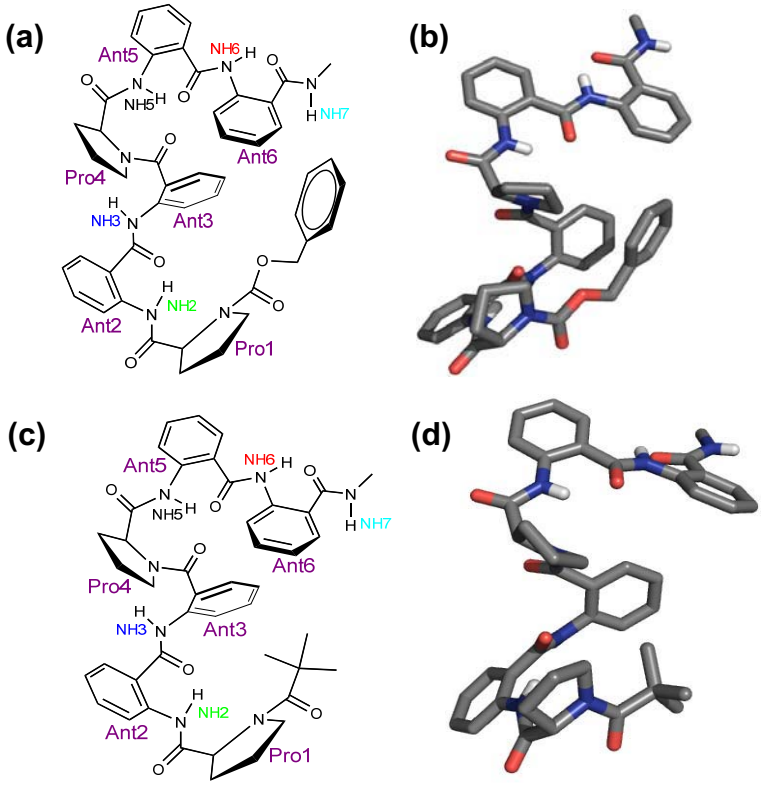

Figure 11: Single crystal X-ray structures of **4b** and **4h** in capped stick representation (b and d, respectively) revealing a nearly helical disposition, with their molecular structures (a and c, respectively). Hydrogens, other than at the hydrogen bonding sites, have been deleted for clarity.

2.6.2 NMR studies

The signals assignments were done using a combination of 2D- COSY, HSQC, HMBC, TOCSY and NOESY experiments ($CDCl_3$, 500 MHz). Details of the peak assignments are provided in the experimental section of this chapter, pages 246-247.

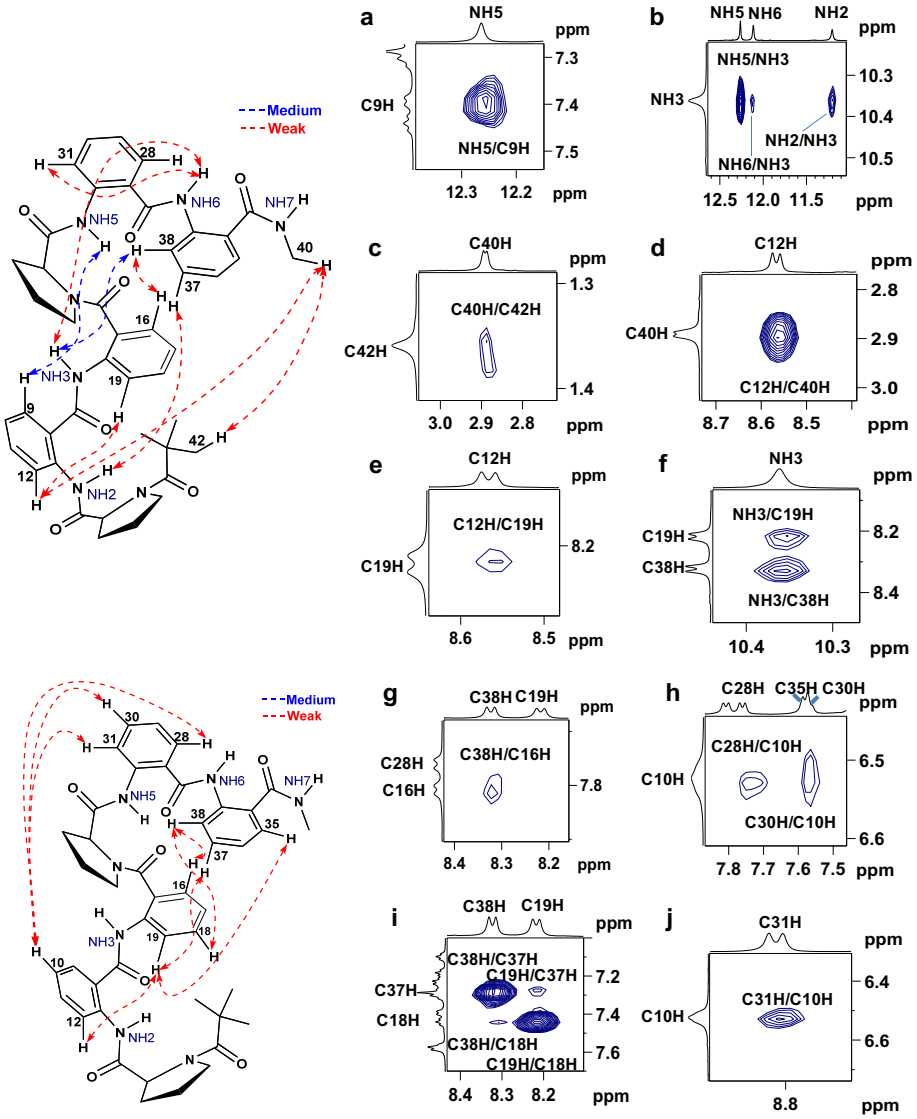

Figure 12: Selected NOE extracts from the 2D NOESY data of **4h** ($CDCl_3$, 500 MHz)**,** (a) Ar-H region *vs* NH region, (b) NH *vs* NH region, (c) Piv *vs* NH-$\underline{CH_3}$, (d) Ar-H region *vs* NH-$\underline{CH_3}$, (e) Ar-H *vs* Ar-H region, (f) Ar-H *vs* NH region, (g), (h), (i) and (j) Ar-H *vs* Ar-H region.

As an outcome of the twists, pi-stacking interactions are observed by the proton C10H (Ant2) causing it to appear considerably upfield at 6.5 ppm. It can be evidenced from the nOe crosspeaks C10H/C31H, C30H and C28H (Figure 12h,j). Also, another dipolar coupling is observed between C16H/C38H (Figure 12g), strongly suggesting the presence of another turn promoted by Pro4 residue. Also the

presence of free terminal methylamide –NH7 of **4h** was confirmed by titration studies with DMSO-*d*$_6$ (5 μL on each addition) in $CDCl_3$ (Figure 13), revealing a chemical shift variation [Δδ (NH) > 0.6 ppm].

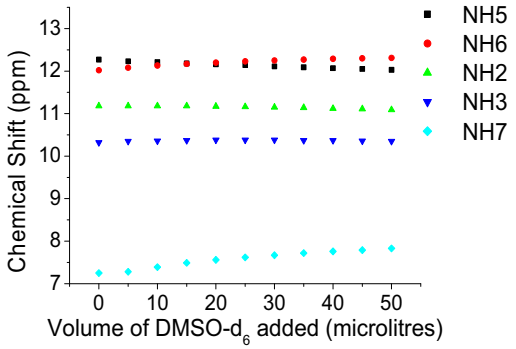

Figure 13: ^{1}H NMR DMSO-d$_6$ titration study (5 mM) of the hexamer **4h.**

2.6.3 CD studies

Strikingly, CD spectra of both the ester and methylamide counterparts of *homo*-chiral oligomers displayed exactly similar pattern, revealing analogous folding features (Figure 14). All the compounds displayed maxima ≈ 214 nm, zero crossing at ca. 222 nm and a strong minima at about 230 nm in case of each oligomer (Figure 14). A strong Cotton effect was also observed (second minima) around 320 nm owing to the backbone aromatic groups/aromatic electronic transitions in the oligomers.[49] Higher order oligomers *i.e.* dodecamer and octadecamer revealed defined CD signatures, when compared with hexapeptides, revealing further ordering in their structure.

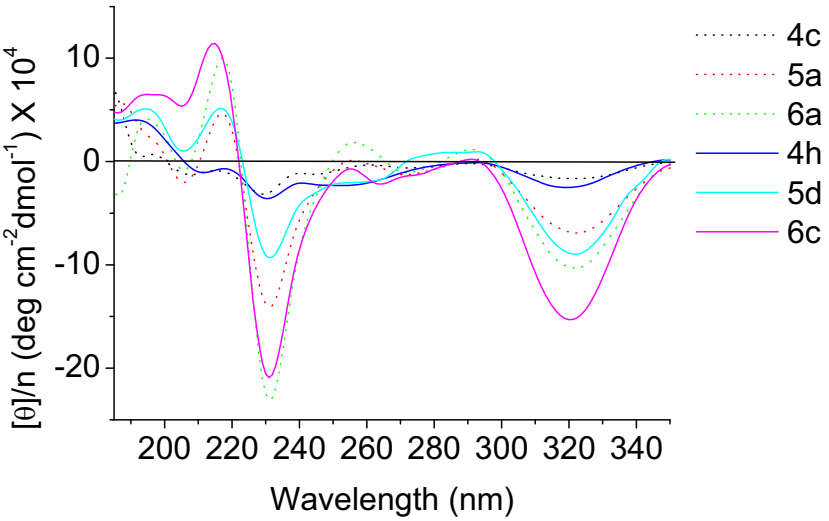

Figure 14: Representative CD spectra of *homo*-chiral Pro-Ant-Ant oligomers: ester derivatives (dotted lines) and methylamide derivatives (solid lines) in trifluroethanol. All spectra were recorded at 293 K with a concentration of 0.05 mM.

Synthesis and Conformational Evaluation of Hetero-chiral -(^{L}Pro-Ant-Ant-^{D}Pro-Ant-Ant)$_n$- Oligomers

2.7 Synthesis

Synthesis of *hetero*-chiral -Pro-Ant-Ant- repeats initiated from DBU-mediated opening of oxazinones **3k** and **3l** with amine **3i** (described in Scheme 2.1), that afforded hexamers **7a** and **7d**, respectively. Oxazinones **7h** and **7i** with N-terminal ^{t}Boc- and Piv-, respectively were generated for further oligomerisation.

Scheme 2.4: Synthesis of *hetero*-chiral hexapeptides **7a-i**

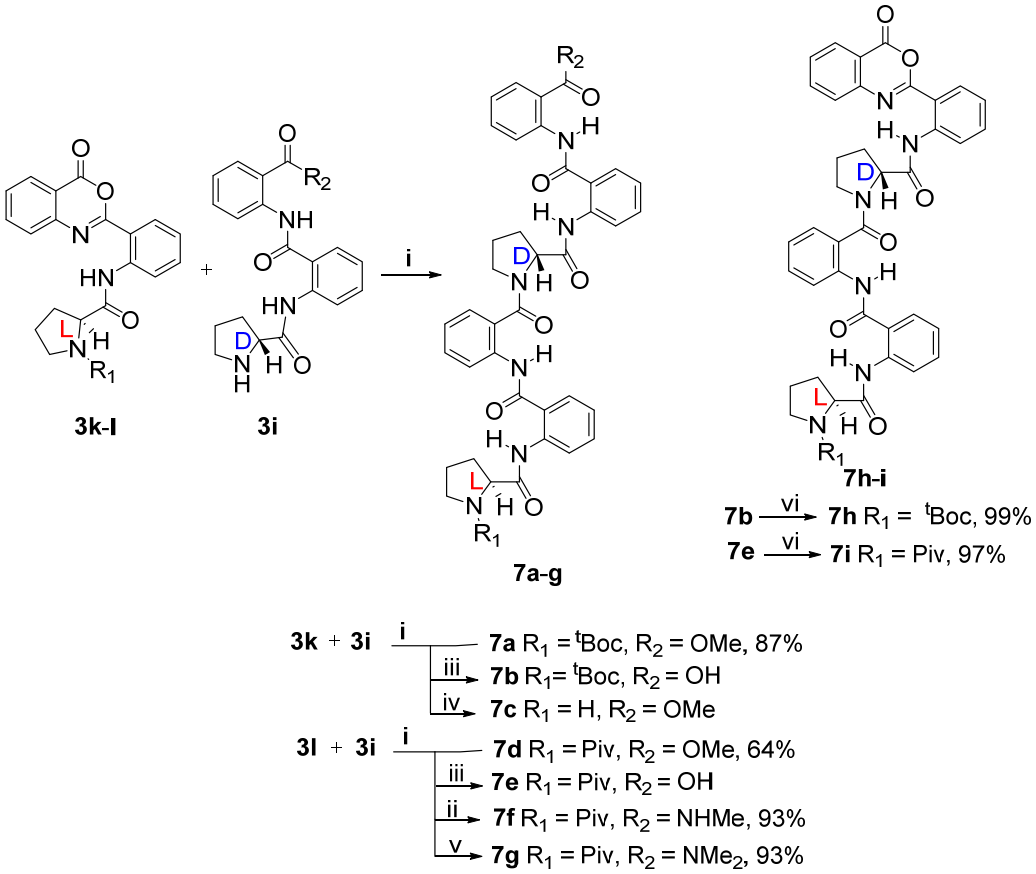

Reagents and conditions: (i) DBU, DMF, 4Å molecular sieves, rt, 2 h; (ii) methanolic methylamine, rt,1h; (iii) aq. LiOH, MeOH, rt, 4 h; (iv) TFA:DCM (1:1), rt, 2 h; (v) methanolic dimethylamine, rt, 2h; (vi) EDC.HCl, DCM, 0^{o}C-rt, 4h.

Following the same strategy described earlier for *homo*-chiral analogues, higher oligomers i.e. dodecamers **8a** and **8c**, and octadecamers **9a** and **9c** were synthesized from their corresponding oxazinones and amines. The C-terminal amidation afforded analogous *hetero*-chiral derivatives **8d** (dodecamer) and **9c** (octadecamer).

Scheme 2.5: Synthesis of *hetero*-chiral dodecapeptides **8a-d** and octadecapeptides **9a-c**

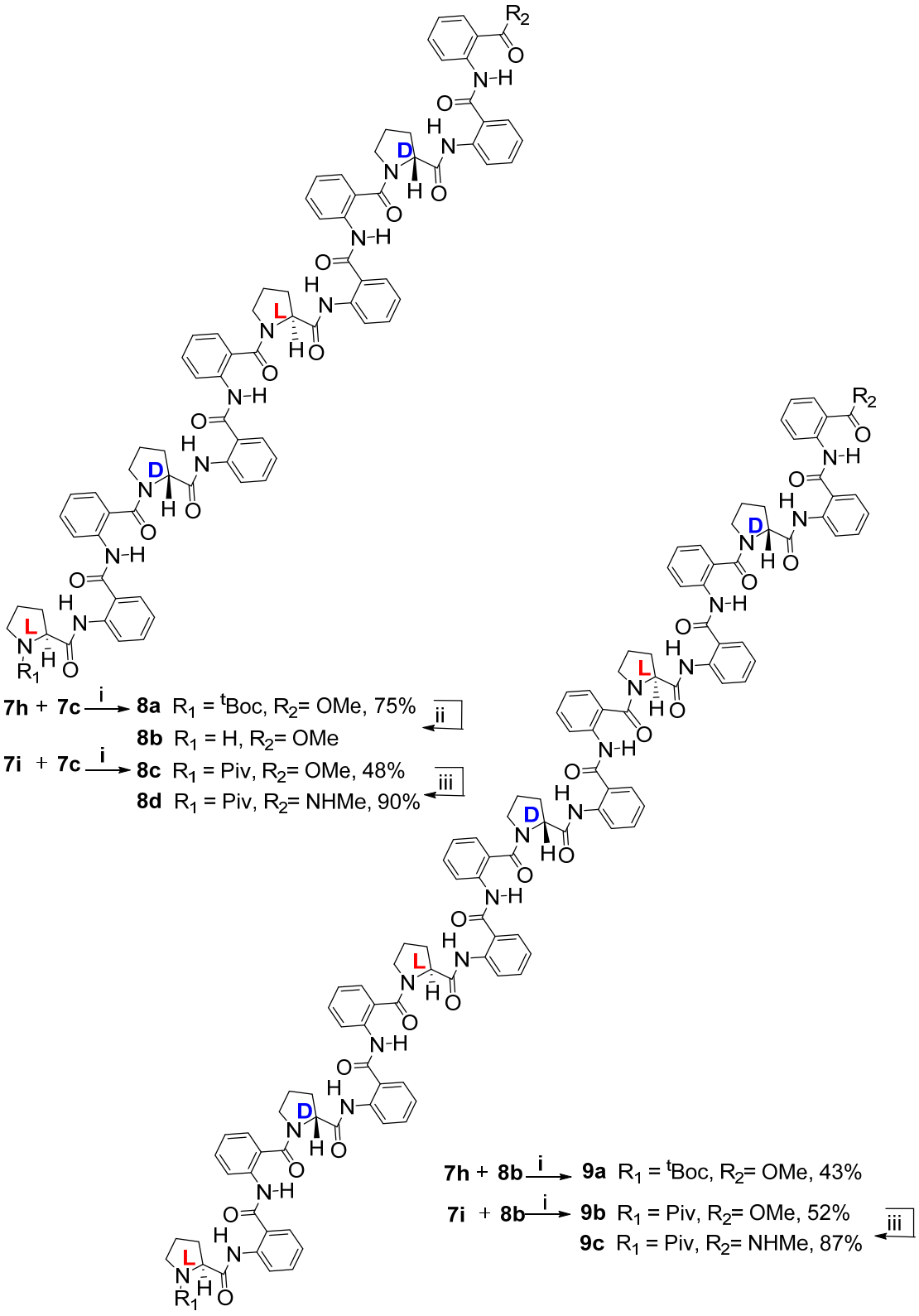

Reagents and conditions: (i) DBU, DMF, 4Å molecular sieves, rt, 2 h; (ii) TFA:DCM (1:1), rt, 2 h; (iii) methanolic methylamine, rt,1h.

2.8 Conformational analyses

Secondary structural analyses were accomplished by extensive 2D NMR, X-ray diffraction and CD studies.

2.8.1 Single crystal X-ray diffraction studies

Extensive efforts to crystallize the oligomers resulted in crystals of **7f** from PEG. Remarkably, the crystal structure featured a unique folded conformation having the oligomer arms zipped together *via* an unusually long-range intramolecular hydrogen bond at the termini encompassing 26 atoms in the H-bonded ring.

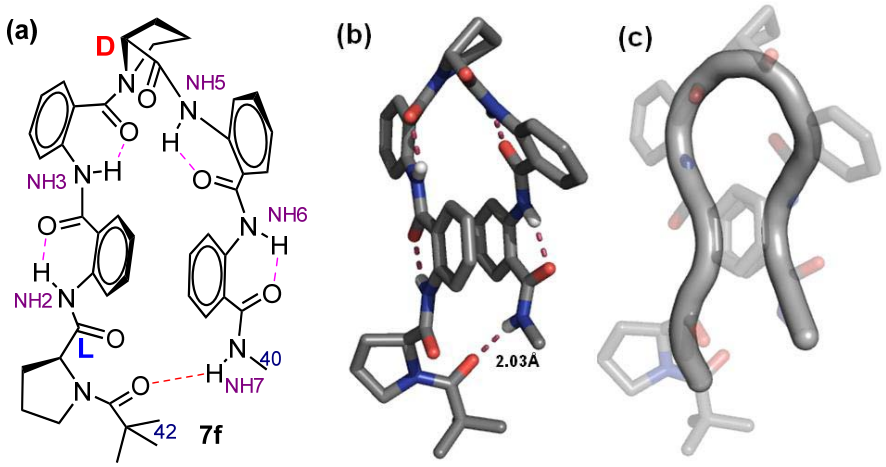

Figure 15. Molecular structure of peptide **7f** (a), and crystal structure of **7f** represented in sticks and cartoon, (b and c, respectively). (Hydrogens, other than the polar amide hydrogens have been removed for clarity).

These non-covalent interactions were found to be apparently stronger, characterized by the H-bonding parameters *d*(H···O) = 2.03 Å, *d*(N···O) = 2.848(3) Å, (N-H···O) = 153° and the torsion angle (NH···O=C) = 8°. Apart from the unusually long-range *intra*-molecular hydrogen bond observed at the termini, all the four anthranilic acid residues of **7f** displayed their characteristic 6- membered H-bonding interactions usually observed in oligoanthranilamides.[43] All the other anthranilic acid residues retained perfect geometries as displayed by *N*-acylated anthranilamides[50] i.e. S(6)-type *intra*-molecular H-bonding interaction [H-bond geometric parameters: bond distance d(N···O) = 2.6 Å, d(H···O) = 1.9 Å, bond angle (N–H···O) = 138°, and the planarity of the hydrogen bond torsion angle (N–H···O=C) = 5°]. The terminal H-bond also influenced the planarity of Ant5-Ant6 units, contributing substantially to direct acceptor-donor sites into proximity. This could be clearly visualised from the crystal structure, where the strained dihedral angle θ = -9.66° and ψ = -150.23° was observed

by Ant5. Aromatic stacking interactions were also clearly evident from the crystal structure and aromatic proton – aromatic ring centroid distance featuring edge-to-face stacking[51] effect [*d*(C10 Ar-H – Cg(5) = 3.11 Å (Cg = centroid of Ant5)].

2.8.2 NMR studies

The peptide **7f** exhibited excellent solubility in non-polar organic solvents (>>100 mM in $CDCl_3$), despite having several amide groups, suggesting the fact that the polar hydrogen-bonding groups are not solvent exposed and not prone towards aggregation.[52] The negligible ^{1}H NMR chemical shifts (Δ NH: <0.15 ppm) observed for all the amide protons of **7f** up on DMSO-d_6 titration studies (up to 10% of DMSO-d6 in $CDCl_3$) (Figure 16, left), strongly supported the *intra*-molecular nature of the hydrogen bonds in the solution-state. Further strong confirmation for the *intra*-molecular nature of H-bonding was obtained from MeOD exchange studies where the amide protons could not be completely exchanged even after prolonged time (>22 h) (see experimental section, page 245, Figure 28). Also, NH7 revealed temperature gradients more positive than -4.3 ppb/K (Figure 16, right) that reassured the strength of the inter-residual H-bonding (see experimental section, page 244, Tables 7 and 8).

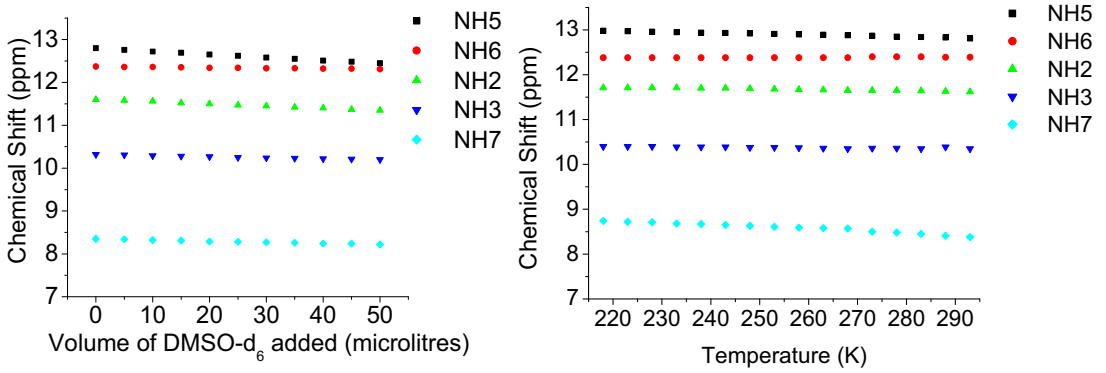

Figure 16: ^{1}H NMR DMSO-d_6 titration study (5 mM) (left), and variable temperature (20 mM) (right), respectively of the hexamer **7f**.

To elucidate the solution-state NMR based structure, the signals were assigned using a combination of 2D- COSY, HSQC, HMBC, TOCSY and NOESY experiments ($CDCl_3$, 400 MHz). Details of the peak assignments with tables and spectra are provided in the experimental section of this chapter, pages 250-251. The distinctive long-range inter-residual nOes observed between the groups positioned at the termini (C42H/C40H and C42H/NH7; Figure 17a,b) were some of the diagnostic dipolar coupling interactions that explicitly indicated the fact that the solid-state fully

folded conformation clearly prevailed in the solution-state as well. Other characteristic nOes in support of the folded conformations were the dipolar interactions between amide NH3/NH5 (Figure 17c), P$_{1\alpha}$H/C35H (Figure 17e), C10H/C40H (Figure 17f), C10H/NH5 and C10H/NH6 (Figure 17g).

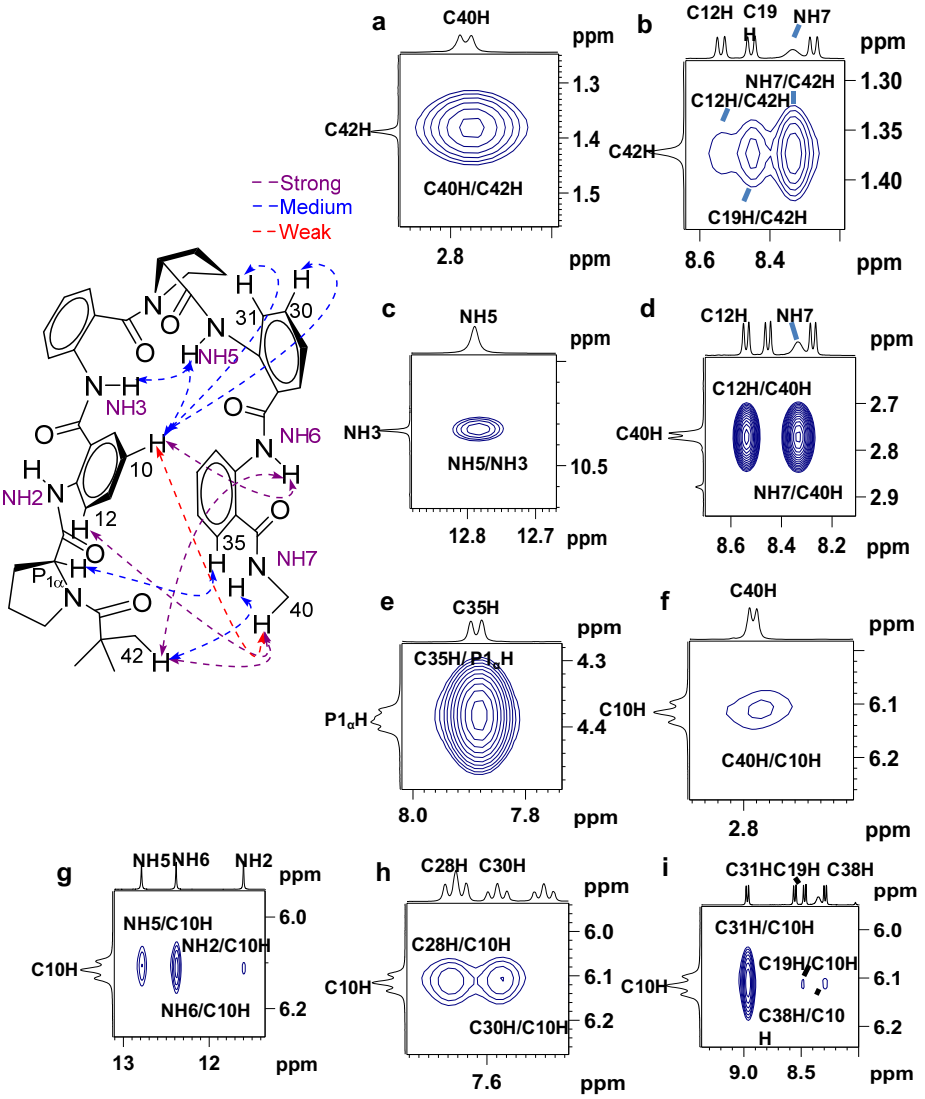

Figure 17: Selected NOE extracts from the 2D NOESY data of **7f** ($CDCl_3$, 400 MHz)**,** (a) Piv *vs* NH-$\underline{CH_3}$, (b) Piv *vs* $\underline{NH}$-CH_3, (c) NH *vs* NH, (d) $\underline{NH}$-CH_3 *vs* Ar-H, (e) P$_{1\alpha}$H *vs* Ar-H region, (f) Ar-H region *vs* NH-$\underline{CH_3}$, (g) Ar-H region *vs* NH region, (h) and (i) Ar-H *vs* Ar-H region.

Solution-state NMR studies also supported an *edge-to-face* stacking interaction faced by C10H (Ant2) causing the proton to appear relatively upfield at 6.1δ. Distinctive nOes that validate the stacking interactions are between C10H/C30H and C31H (Figure 17h,i).

2.8.3 CD Studies

The CD signatures of all oligomers recorded in TFE (trifluoroethanol; 0.05 mM concentrations) revealed comparable features, particularly in the region 185-250 nm. CD spectra of *hetero*-chiral (*Pro-Ant*-Ant) oligomers displayed a defined minima around 215 nm, zero crossing at ca. 222 nm and a strong minima at about 232 nm in case of each oligomer (Figure 18). Unlike the *homo*-chiral oligomers, where all C-terminal ester and amide derivatives revealed good conformational ordering, *hetero*-chiral analogues showed slight disparity in CD signatures.

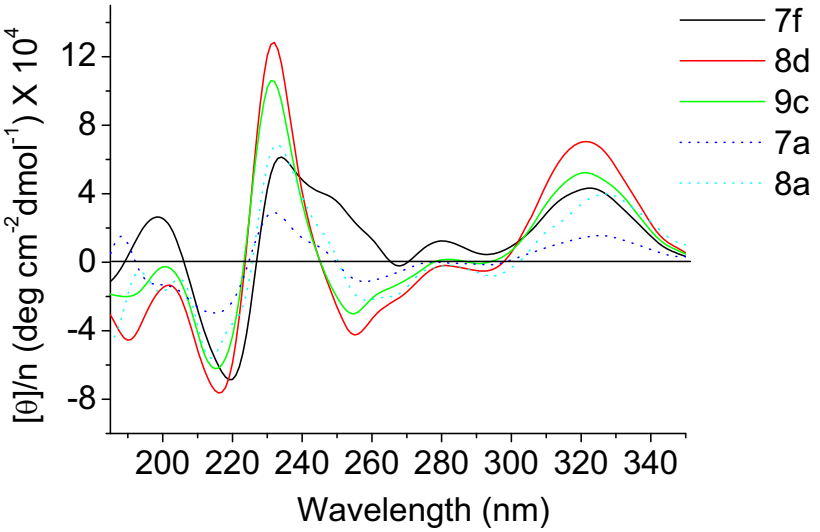

Figure 18: Representative CD spectra of *hetero*-chiral oligomers: ester derivatives (dotted lines) and methylamide derivatives (solid lines) in trifluroethanol. All spectra were recorded at 293 K with a concentration of 0.05 mM.

2.9 Role of Non-Covalent Forces in Manifestation of the Synthetic Peptide Zipper (consequence and impact of non-covalent forces)

The crystal structure of *hetero*-chiral hexapeptide **7f** evoked further questions about the forces that participate to orchestrate the zipper architecture. Three plausible aspects come into picture like: (1) the possible dihedral constraints introduced by the pentacyclic proline unit, (2) the aromatic stacking interactions arising due to anthranilic acid residues, and/or (3) the strong and directional non-covalent H- bond interaction between the termini. Amongst which, the constrained dihedrals of Pro at the center facilitate the turn formation; which is the first step towards the zipper architecture formation, but cannot possibly coerce the termini into proximity. Thus, the competition remains between the two major non-covalent forces overtly i.e. aromatic stacking and H-bonding interactions. Various solution-state studies were

undertaken in order to expound the role of each interaction towards the conformational ordering.

2.9.1 Role of Remote Hydrogen-Bonding

From the outset, the formation of the terminal long range inter-residual hydrogen bonding observed in **7f** was intriguing, considering its size encompassing 26 atoms in the hydrogen bonded network. Therefore, we were curious to see the outcome, when this H-bonding is disengaged. Therefore, we prepared and analysed structural features of derivatives of **7f**, lacking a H-bonding amide donor at the C-terminal and lacking the amide carbonyl acceptor (-C=O) attached to Pro1 at the N-terminal, both of which are essential for H-bonding.

2.9.1a Effect in absence of H-bond donor

In order to evaluate the role of the H-bond donor site at the N-terminus using solid state structural studies, we prepared some ester derivatives by substituting different alcohols like isobutyl, neopentyl *etc*.

2.9.1b Synthesis

Ester derivatives **7j-m** were obtained using simple DBU-mediated opening of the hexapeptide benzoxazinone derivatives **7h** and **7i** at 0 °C in 1h (Table *vide infra*).

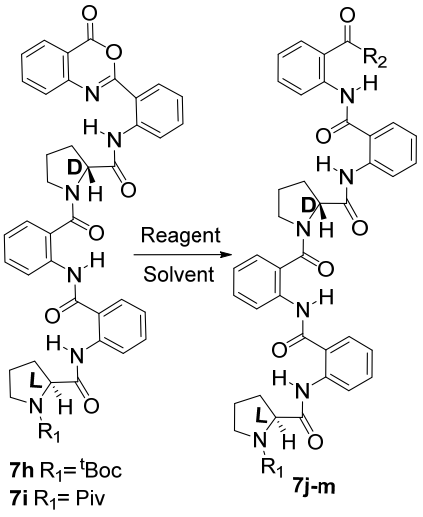

Table 1

Comp.	Reactant	Reagent	Solvent	Yield
7j	**7i**	DBU	^{i}BuOH	87%
7k	**7i**	DBU, n-PenOH	DMF	89%
7l	**7h**	DBU	^{i}BuOH	82%
7m	**7h**	DBU, n-PenOH	DMF	95%

2.9.1c Conformational analysis

Intense derivatisation and crystallisation trials of ester analogues weren't fruitful, thus we were forced to undertake solution-state structural investigations of the methyl ester analogue **7d** and dimethylamide derivative **7g** (scheme 2.4), both devoid of H-bonding donor sites at the C-terminal, which is essential for H-bonding, as seen in **7f**.

Notably, the diagnostic terminal nOe interactions which were present in **7f** were clearly absent in both **7d** and **7g**, which confirmed fraying of the termini (Figure 19, 20). In both the hexapeptides **7d** and **7g**, pivaloyl group attached to Pro1 experienced fraying, well evident from the strong dipolar coupling it experiences with C19H (Ant3). Folding induction at Ant-Pro segment remained intact similar to hexapeptide **7f**, leading to similar diagnostic nOe between NH3/NH5 (Figure 19c).

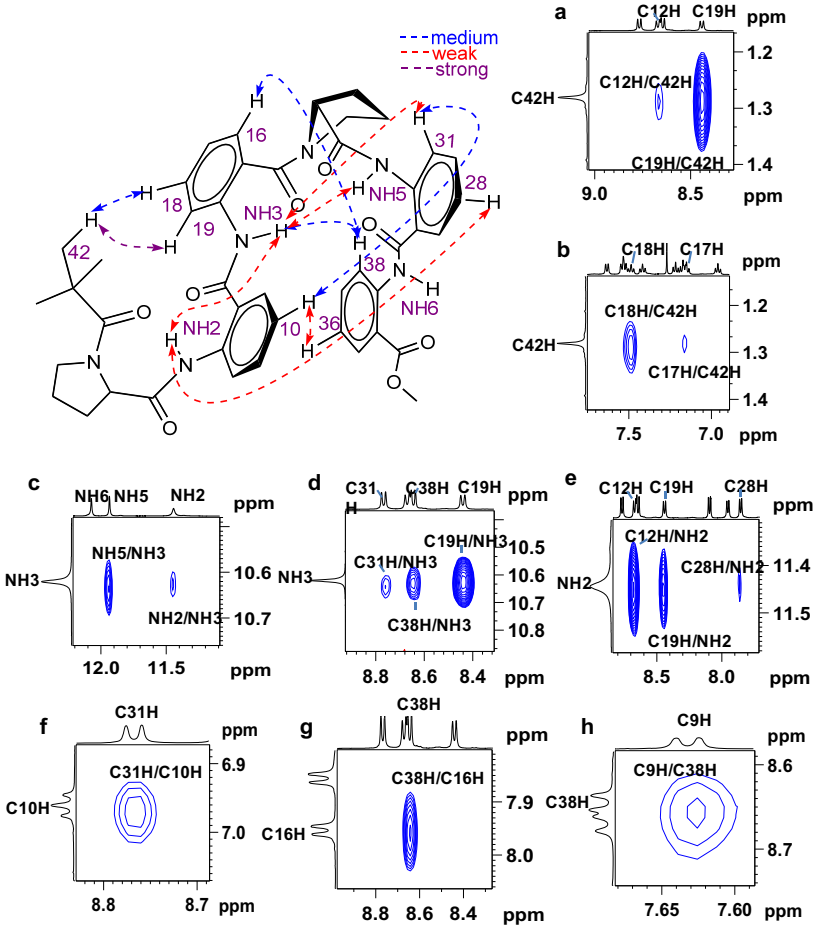

Figure 19: Selected NOE extracts from the 2D NOESY data of **7d** ($CDCl_3$, 400 MHz)**,** (a) and (b) Piv *vs* Ar-H region, (c) NH *vs* NH, (d) and (e) Ar-H region *vs* NH region, (f), (g) and (h) Ar-H *vs* Ar-H region.

Another strange dipolar coupling that supported the staggered conformation of the structures (facilitating free movement C-terminus) is C16H/C38H (Figure 19g). Surprisingly, the effect of aromatic interactions remains discernible in **7d**, as dipolar couplings were observed between C10H/C31H (Figure 19f), whereas in **7g**, stacking effect was very scarcely observed (Figure 20g). This effect demonstrated that the weak existence of *edge-to-face* aromatic interactions too failed to bring remote H-bonding sites into proximity, consequently evading the zipper architecture.

All the amide NHs of both analogues **7d** and **7g** displayed strong *intra*-molecular S(6)-type H-bonding interactions, substantiated by the negligible chemical shift differences with DMSO-d_6 addition, reflecting the H-bond stability of anthranilamides. MeOD exchange studies of **7d** also supported the fact, as amide protons did not undergo complete exchange even after 5 days. This observation implied that the planarity of the Ant-Ant units remained conserved in this case (spectra and stacked plots are provided in Experimental section page 245, figure 27). These results clearly suggested that the long-range inter-residual hydrogen bonding has substantial role to play in maintaining the zipper conformation of the peptide.

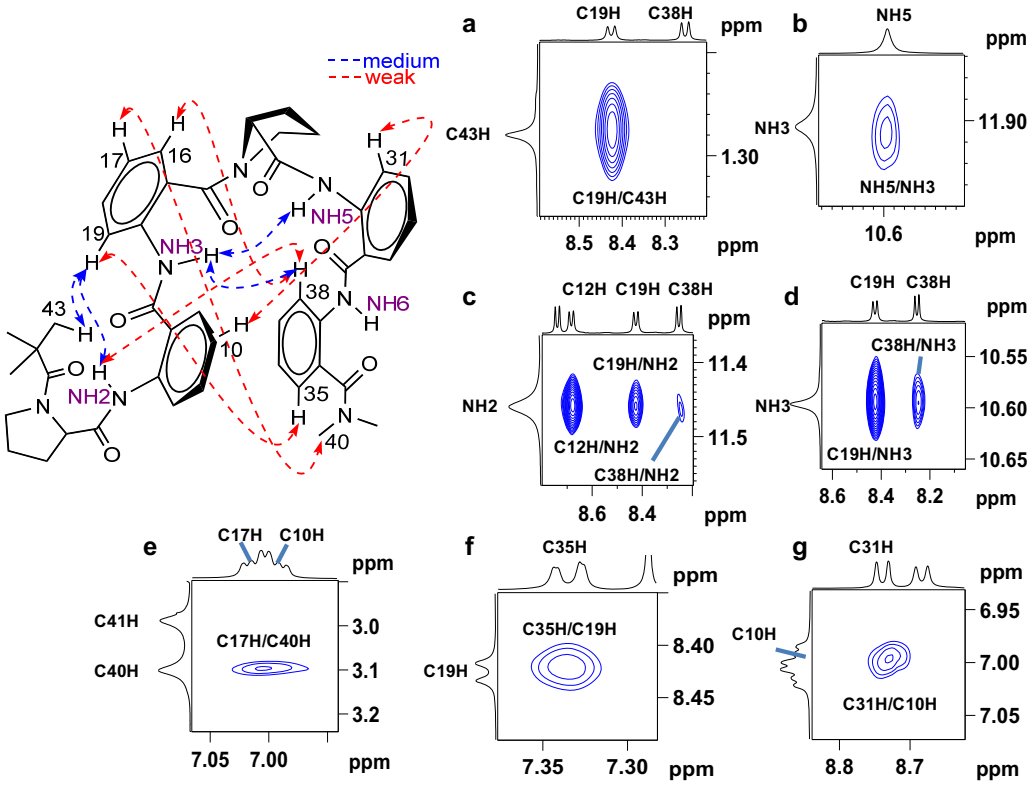

Figure 20: Selected NOE extracts from the 2D NOESY data of **7g** ($CDCl_3$, 400 MHz)**,** (a) Piv *vs* Ar-H region, (b) NH *vs* NH, (c) and (d) NH *vs* Ar-H region, (e), (f) and (g) Ar-H region *vs* NH region.

2.9.1d Effect in absence of H-bond acceptor

To attain a clear picture of the structural architecture, the pentapeptide derivatives devoid of acceptor site were prepared and analysed. After a great deal of efforts, thin needle-shaped crystals of bromo-isobutyryl-substituted pentapeptide analogue **10d** was obtained, from which the conformational investigations were performed.

2.9.1e Synthesis

Preparation of **10d** was achieved in simple steps by reacting corresponding pentapeptide amine **10c** with bromo-isobutyryl-bromide using TEA as base in DCM with 65% yield. The pentapeptide amine **10c** was obtained by reducing corresponding pentapeptide **10b**, which was obtained by DBU-mediated opening of benzoxazinone **2d** with amine **9f**.

Scheme 2.7: Synthesis of pentapeptide derivatives **10d** and hexapeptide **10g**

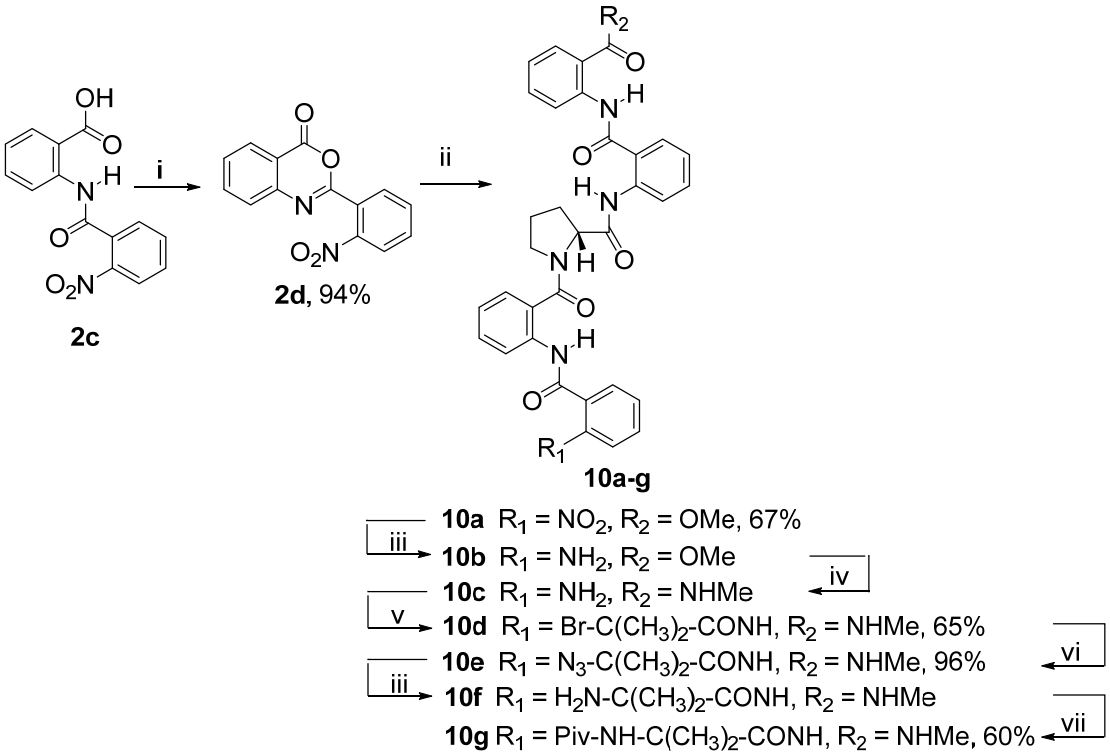

Reagents and Conditions: (i) $(COCl)_2$, cat. DMF, DCM, 0^{o}C-rt, 1h; (ii) **3i**, DBU, DMF, 4Å molecular sieves, rt, 2 h; (iii) $Pd(OH)_2$, MeOH, 4h; (iv) methanolic methylamine, rt, 1h; (v) α-bromoisobutyryl bromide, TEA, DCM, 1h, 0 °C; (vi) NaN_3, cat. LiCl, DMF, rt, 12h; (vii) Piv-Cl, TEA, DCM, 1h.

2.9.1f Conformational analyses

Crystal structure of **10d** clearly revealed absence of folded conformation, featuring an unexpected deviation from planarity observed at Ant1-Ant2 link, which can be ascribed to the packing effects of the crystal (Figure 21).

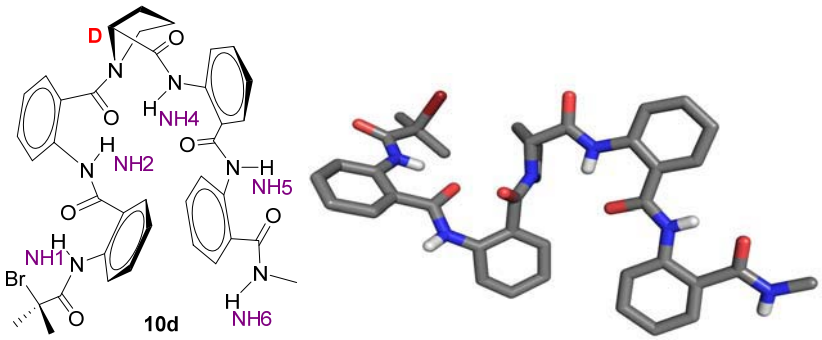

Figure 21. Molecular structure (left) and crystal structure (right) of pentamer **10d** (other hydrogens except for the amide hydrogen are not displayed for clarity).

Surprisingly, solution-state NMR studies disclosed fair amount of terminal interaction, epitomizing the importance of the aromatic interactions (Figure 22). The terminal interactions were apparent from the dipolar coupling interactions observed between C37H/C31H, C37H/ NH6 (Figure 22f) and C37H/ C35H (Figure 22c). Also, a weak aromatic stacking effect was evident from interactions between C5H/C23H and C26H (Figure 22). The investigation of the structural feature of the pentapetide **10d** also supported the significance of collective co-operative effect of H-bonding and aromatic-aromatic interactions to render the zipper structural ensemble.

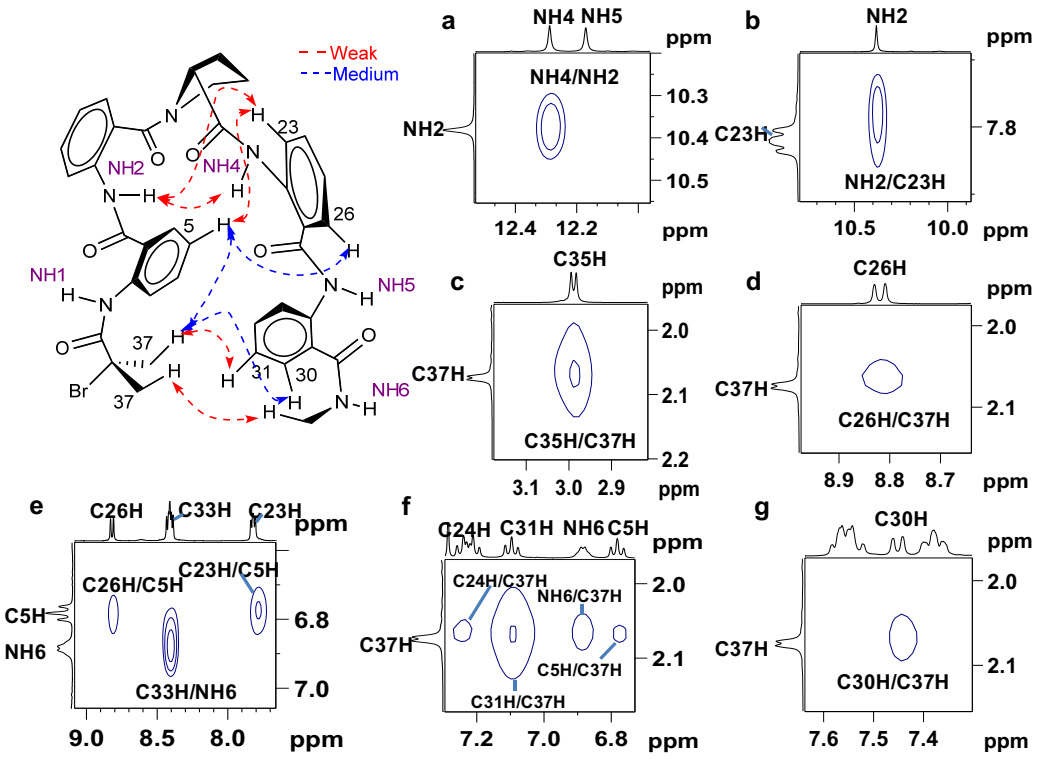

Figure 22: Selected NOE extracts from the 2D NOESY data of **10d** ($CDCl_3$, 400 MHz)**,** (a) NH *vs* NH, (b) Ar-H region *vs* NH region, (c), (d) and (e) Ar-H *vs* Ar-H region, (f) Aib *vs* Ar-H region; Aib *vs* NH-CH_3, (g) Aib *vs* Ar-H region.

2.9.2 Evidence for aromatic stacking interactions

Crystal structure of **7f** clearly indicated the presence of an *edge-to-face* aromatic stacking interaction featuring aromatic proton – aromatic ring centroid distance [*d*(C10 Ar-H – Cg(5) = 3.11 Å (Cg = centroid of Ant5)]. Solution-state NMR studies also supported the *edge-to-face* stacking interaction faced by C10H (Ar-H Ant2), causing the proton to appear relatively upfield at 6.1δ compared to ester derivative **7d**. In the solution-state 2D NOESY spectrum, distinctive nOes that validated the stacking interactions were between C10H/C30H and C31H, with the observed distances *d*(C10 Ar-H - C30 Ar-H) = 3.8 Å and *d*(C10 Ar-H - C31 Ar-H) = 3.6 Å from the crystal structure.

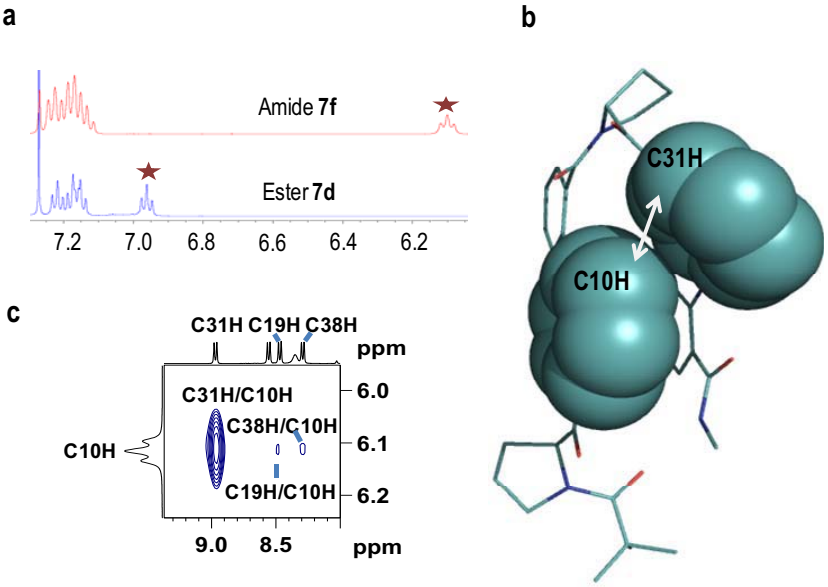

Figure 23: Comparison of the diagnostic ^{1}H NMR shielding effects observed by ester **7d** and amides **7f** (a), wireframe representation of crystal structure of amide **7f** (b) and 2D-NOESY excerpt displaying diagnostic dipolar coupling between C10H *vs* C31H (c). *Note*: Aromatic rings bearing upfield protons that observe shielding effects due to aromatic stacking interactions are represented as spheres.

2.9.3 Effect of chirality in folding

Inspection of the crystal structure of both *homo*-oligomers **4b** (Cbz-^{L}Pro-Ant-Ant-^{L}Pro-Ant-Ant-NHMe) and **4h** (Piv-^{L}Pro-Ant-Ant-^{L}Pro-Ant-Ant-NHMe) and the solution-state NMR studies undertaken for **4h** confirmed a nearly helical disposition for the oligomers (discussed in Section **2.6**), asserting the role of chirality in zipper architecture formation. Further, we became keen on evaluating the effect on zipper architecture on substitution of an achiral constrained residue like α-amino butyric acid (Aib) in place of Pro1. Therefore, Piv-Aib-Ant-Ant-^{D}Pro-Ant-Ant-NHMe **10g** was

synthesized from **10d** following few simple steps *via* conversion of bromo- to azido-substitution, followed by reduction and pivoloyl protection. However, in case **10g** terminal interactions between Piv- and methylamide -CH_3 were not observed, due to probable orientation of terminus exerted by the constrained germinal α-disubstitution. Similar to compound **7f**, aromatic stacking effect in **10g** was clearly evidenced from C9H proton of Ant2 as it appeared at 6.4 ppm in the ^{1}H-spectrum, which showed diagnostic dipolar coupling between C9H/C30H (Figure 24d). An unequivocal proof for folding feature was obtained from the strong nOe among C11H/C39H (Figure 24e). Also, the presence of H-bonding interaction was evidenced from the DMSO-d_6 titration experiment that revealed chemical shift variation of ≈ 0.43 ppm for NH7 and the slow H/D exchange rate in MeOD (see experimental section, page 245, Figure 29).

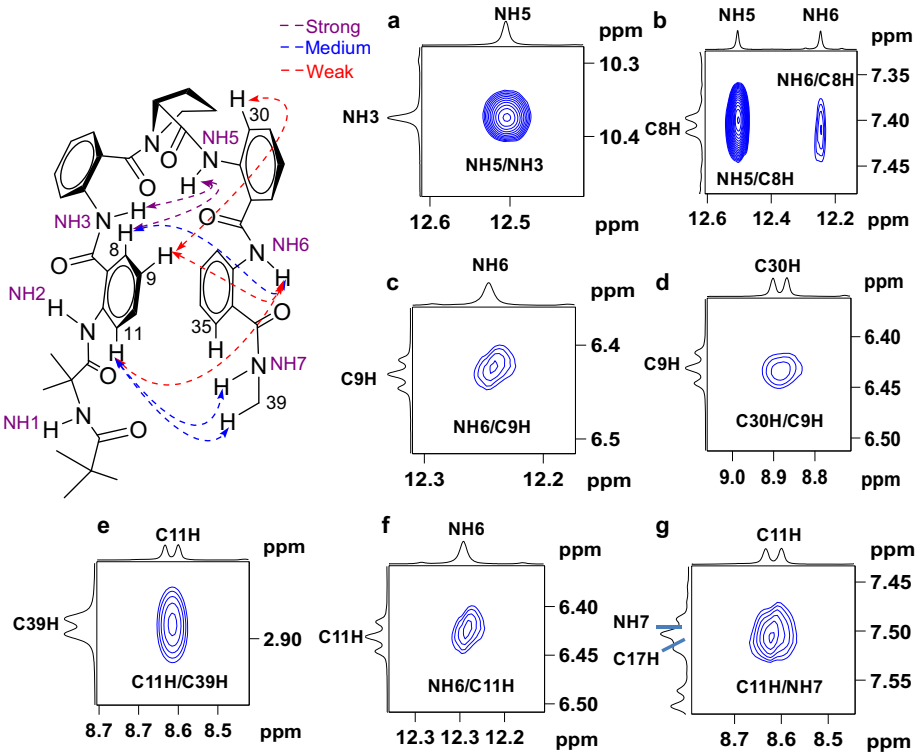

Figure 24: Selected NOE extracts from the 2D NOESY data of **10g** ($CDCl_3$, 400 MHz)**,** (a) NH *vs* NH, (b), (c) and (f) Ar-H region *vs* NH region, (d) and (e) Ar-H *vs* Ar-H region, (g) Ar-H region *vs* NH-CH_3.

2.9.4 CD studies

Conformational ordering of oligomers **7d**, **7g** and **10g** were also assessed using circular dichroism studies. Ester and dimethylamide derivatives **7d** and **7g** revealed comparable patterns with a minima ≈ 218 nm and a broad, undefined

positive absorption around 233 nm. On the other hand, **10g** featured a sharp minima ca. 212 nm, zero crossing at 222 nm with a positive absorption peak about 230 nm, akin to hexapeptide **7f**, validating folded pattern.

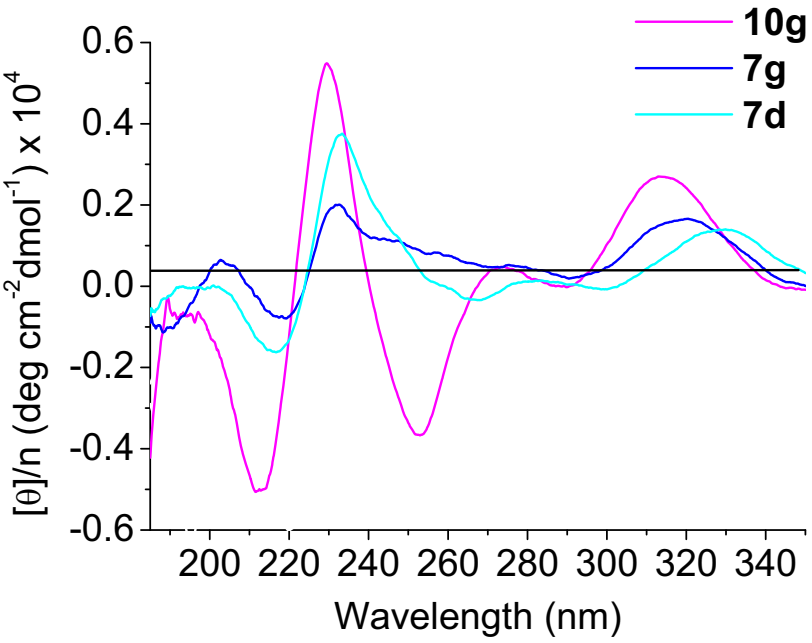

Figure 25: Representative CD spectra of hexapeptide **7d**, **7g** and **10g**. All spectra were recorded at 293 K in TFE with a concentration of 0.05 mM.

2.10 Conclusions

In conclusion, this part of chapter discloses unique structural assemblies of peptides derived from a blend of α/β- aliphatic:aromatic heterogeneous backbone with 1:2 stoichiometric combination of amino acid residues. The *hetero*-chiral hexapeptide Piv-^{L}Pro-Ant-Ant-^{D}Pro-Ant-Ant-NHMe **7f** was seen to assume a firm folded "zipper" architecture featuring an atypically large remote inter-residual H-bonding interaction encompassing 26 atoms. Structural studies carried out both in solid- and solution-state vindicated the stability of the synthetic zipper peptide is *via* a co-operative interplay of hydrogen bonding, aromatic stacking and backbone chirality. Influence of stereochemistry of building blocks on the structural assembly phenomenon was found to play significant role on the conformational bias, where *homo*-chiral hexapeptides **4d** and **4h** displayed nearly helical disposition.

The results highlight the utility of non-covalent forces in engineering complex synthetic molecules with intriguing structural architectures. Such studies are anticipated to increase our understanding of biomolecular folding and function.

SECTION II
Synthesis and Conformational Evaluation of Hetero-chiral Pro-Ant-Ant-Ant Repeats

2.11 Objective of the work

Having explored the unique zipper architecture adopted by the *hetero*-chiral sequence -^{L}αβ$_2$^{D}αβ$_2$- comprising Pro(α):Ant(β) building blocks that featured an unusually long range intra-residual contact, our objective was to evaluate the conformational propensity of -^{L}αβ$_3$^{D}αβ$_3$- hybrid oligomer.

2.12 Synthesis

Oligomers were synthesized using similar conditions (as described in section I of the chapter) utilizing DBU-mediated opening of oxazinones.

Scheme 2.8: Synthesis of tetramers **11a-i**.

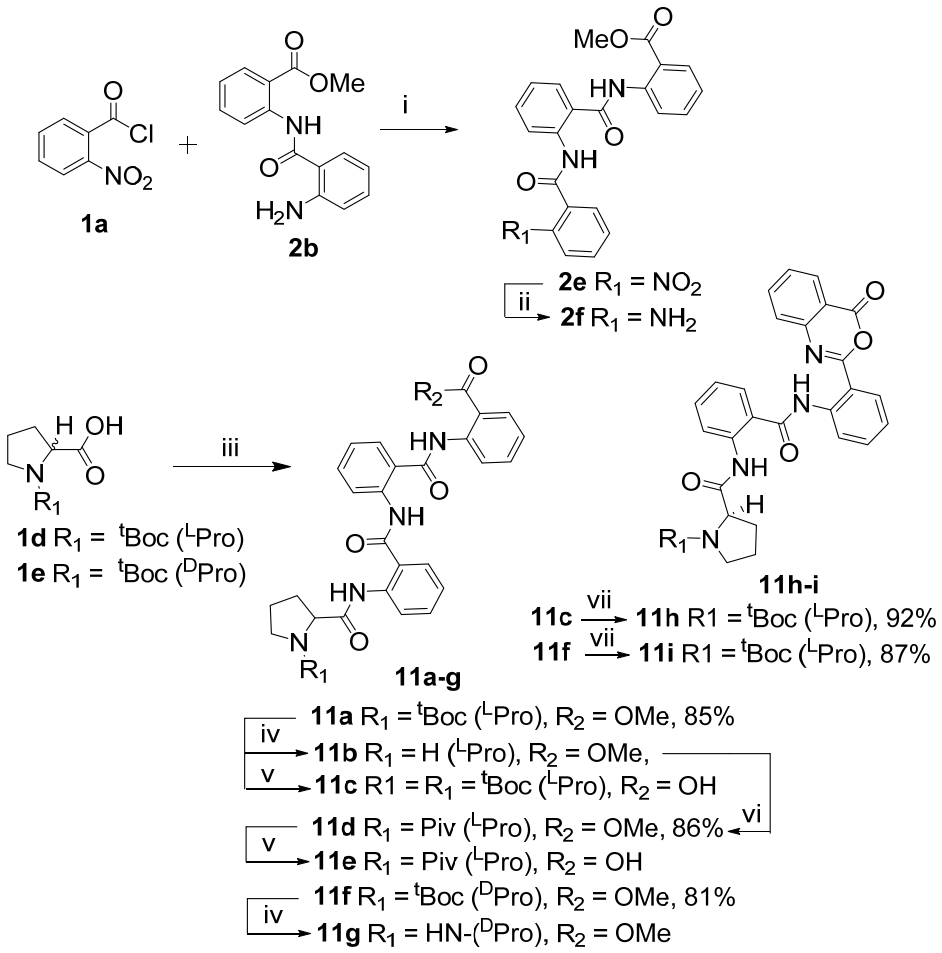

Reagents and conditions: (i) Et_3N, DCM, 1h, 0 ^{o}C- rt; (ii) H_2, Pd/C, DMF, 4h; (iii) (a) ClCOOEt, Et_3N, THF, 0 ^{o}C- rt, (b) **2f**, reflux, 6h; (iv) TFA:DCM, 1:1, 2h; (v) LiOH, MeOH,2h; (vi) Piv-Cl, Et_3N, DCM, 2h; (vii) EDC.HCl, DCM, 1h.

Monomer units with alternating chirality for -Pro-Ant-Ant-Ant- oligomers were prepared by coupling using ethyl chloroformate-mediated mixed anhydride activation of acids Boc-^{L}Pro-OH and Boc-^{D}Pro-OH with amine H_2N-Ant-Ant-Ant-OMe **4**, in THF to furnish tetramers **11a** and **11f**, respectively. Piv- protected tetramer **11d** was synthesized from amine generated from **11a**. Corresponding benzoxazinones **11h** and **11i** were prepared by activation of acids **11c** and **11e**, respectively. Boc- and Piv- protected octapeptides **12a** and **12d** were generated by reacting **11h** and **11i**, respectively, with amine **11g** (HN-^{D}Pro-Ant-Ant-Ant-OMe), further which were treated with methanolic methylamine to afford their methylamide derivatives meant for structural studies.

Scheme 2.9: Synthesis of octamers **12a-e**

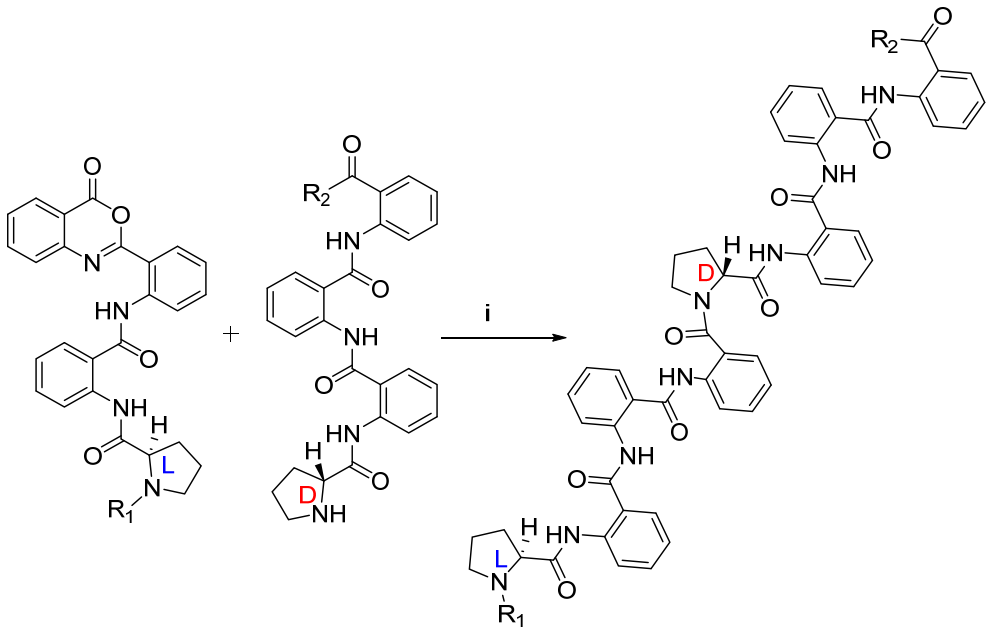

Reagents and conditions: (i) DBU, DMF, 4Å MS; (ii) TFA:DCM, 1:1, 2h; (iii) $MeNH_2$, MeOH, 4h.

2.13 Conformational analyses

Solution-state investigations revealed that the terminal interactions between methylamide NH and CH_3 groups prevailed in nOe spectra, in spite of the absence of

terminal H-bond (evident from DMSO-d$_6$ titration studies, where methylamide NH9 observed drastic chemical shift variation; see experimental section page 243, table 6). Also weak cross-peaks observed between the residues of the two arms authenticated this conclusion. However surprisingly, a weak but significant dipolar coupling was witnessed between C56H/NH9 (Figure 26a), C56H/C54H (Figure 26b), and C56H/C50H and C49H (Figure 26g,h), confirming a folded architecture for the octapeptide **12e**. Also, further evidence came from the dipolar coupling between P$_{1\alpha}$H/CC54H (Figure 26c). A slight effect of *edge-to-face* aromatic stacking effect was also evident, but of weaker intensity (Figure 26e).

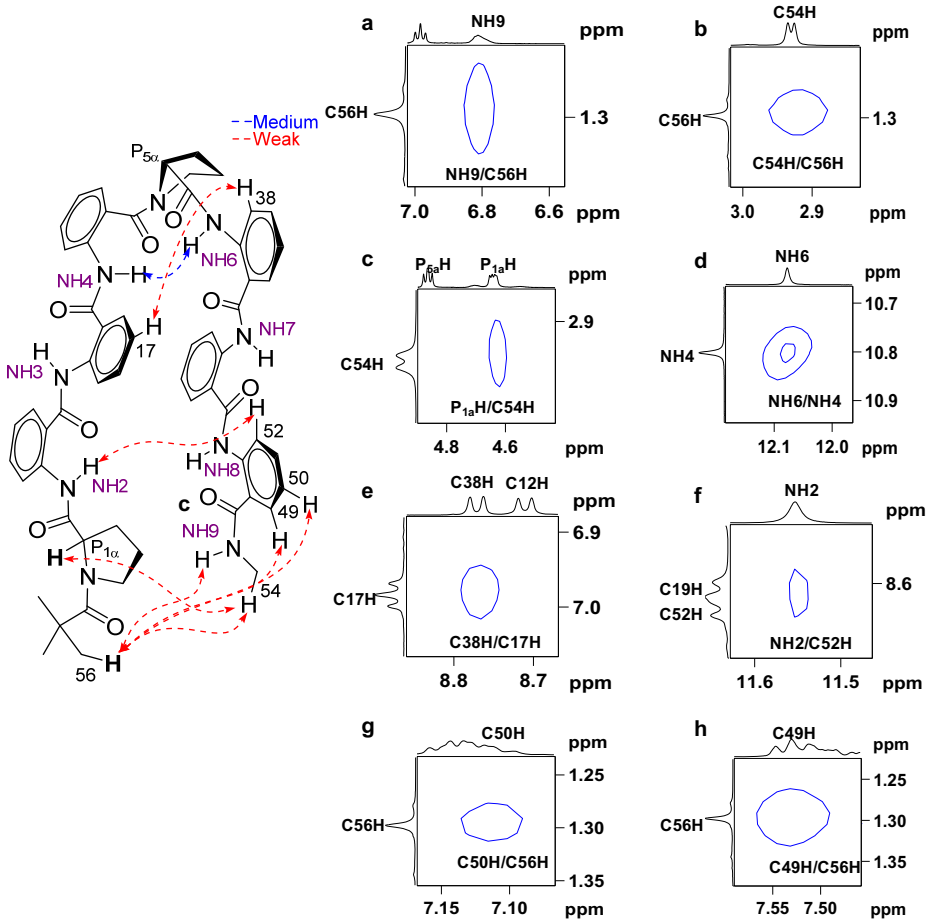

Figure 26: Selected NOE extracts from the 2D NOESY data of **12e** ($CDCl_3$, 400 MHz), (a) Piv *vs* NH-CH_3, (a) Piv *vs* NH-CH_3, (c) P$_{1\alpha}$H *vs* NH-CH_3, (d) NH *vs* NH, (e), (g) and (h) Ar-H *vs* Ar-H region, (f) Ar-H region *vs* NH region.

2.14 Conclusions

Hetero-chiral octamer derived from Pro-Ant-Ant-Ant [α/β/β/β] unit also indicated a folded conformation even in the absence of remote H-bond, validating prominence of aromatic interactions in increment of aliphatic:aromatic amino acid ratio.

2.15 Experimental section

Compounds *2-(2-Nitro-benzoylamino)-benzoic acid methyl ester* **2a**, *2-(2-Amino-benzoylamino)-benzoic acid methyl ester* **2b,** *2-(2-nitrophenyl)-4H-benzo[d][1,3] oxazin-4-one* **2d** and *methyl 2-(2-(2-nitrobenzamido)benzamido)benzoate* **2e** were synthesized as per the reported procedure.[43b]

benzyl 2-((2-((2-(methoxycarbonyl)phenyl)carbamoyl)phenyl)carbamoyl) pyrrolidine-1-carboxylate 3a: ***CAS Registry Number:*** 1129527-29-2

References: (1) Tseng, M.-C.; Yang, H.-Y.; Chu, Y.-H. *Org. Biomol. Chem.* **2010**, *8*, 419-427.

(2) Tseng, M.-C.; Lai, C.-Y.; Chu, Y.-W.; Chu, Y.-H. *Chem. Commun.* **2009**, 445-447.

***tert*-butyl (*S*)-2-((2-((2-(methoxycarbonyl)phenyl)carbamoyl)phenyl)carbamoyl) pyrrolidine-1-carboxylate 3c:**

To a solution of Boc-^{L}Pro-OH (6g, 27.9 mmol, 1.02 equiv.) and Et_3N (3.807 mL, 1.02 equiv.) in THF (60mL) at 0 °C, ethyl chloroformate (3.028 mL, 1.02 equiv.) was added drop wise and the reaction mixture was stirred for 1 h at 0 °C. A solution of the amine **2b** (7.38 g, 27.3 mmol, 1 equiv.) in THF (40 mL) was added slowly to the mixed anhydride solution, prepared above. The reaction mixture was stirred at 0 °C for an hour, then at room temperature for 2 h, followed by reflux at 70 °C for 6 h. After completion of reaction, THF was removed under reduced pressure and then the compound was taken into DCM. The combined organic layers were washed sequentially with solutions of $KHSO_4$, $NaHCO_3$ and brine. Organic layer was then dried over Na_2SO_4 and was evaporated *in vacuo.* The crude product was purified by column chromatography (eluent: 30% AcOEt/pet. Ether, R_f: 0.3) to furnish **3c** (10.3 g, 90%) as a fluffy white solid. mp: 71-73 °C; $[\alpha]^{24.87}_{D}$: -119.448° (*c* 1, $CHCl_3$); IR ($CHCl_3$) *v* (cm^{-1}): 3448, 2976, 1693, 1655, 1607, 1584, 1524, 1435, 1388, 1318, 1271, 1164, 1097; ^{1}H NMR (200 MHz, $CDCl_3$) δ: $12.09_{rotamer}$ (s, 0.6H, amide), $12.05_{rotamer}$ (s, 0.4H, amide), $11.82_{rotamer}$ (s, 0.4H, amide), $11.76_{rotamer}$ (s, 0.6H, amide), 8.9-8.71(m, 2H), 8.11-8.07 (dd, *J* = 1.52 Hz, *J* = 7.96 Hz, 1H), 7.92-7.85 (m, 1H), 7.88-7.49 (m, 2H), 7.29-7.12 (m, 2H), 4.5-4.27 (m, 1H), 3.96 (s, 3H), 3.85-3.74 (m, 2H), 2.37-2.11 (m, 2H), 2.04- 1.87 (m, 2H), $1.45_{rotamer}$ (s, 3H), $1.33_{rotamer}$ (s, 6H); ^{13}C NMR (50 MHz, $CDCl_3$) δ: 172.2, 171.7, 168.9, 168.8, 167.4, 167.3, 154.8, 154.0, 141.2, 141.0, 139.8, 134.9, 134.3, 132.9, 130.8, 127.0, 123.2, 122.9, 121.1, 120.5,

115.4, 115.2, 80.0, 79.8, 62.5, 61.9, 52.47, 49.9, 47.7, 36.5, 31.4, 30.4, 29.5, 28.3, 28.2, 28.1, 24.5, 24.1, 23.8, 23.6, 23.3; MALDI-TOF/TOF: 490.310 $(M+Na)^+$, 506.3015 $(M+K)^+$; Elemental analysis calculated for $C_{25}H_{29}N_3O_6$: C, 64.23; H, 6.25; N, 8.99. Found: C, 64.21; H, 6.33; N, 9.02.

General procedure for methyl ester cleavage:

Compounds **3b**, **3g**, **4d**, **4g**, **7b**, **7e**, **11c**, **11e** *etc.,* were prepared following this procedure.

(*S*)-2-(2-(1-(*tert*-butoxycarbonyl)pyrrolidine-2-carboxamido)benzamido)benzoic acid 3d:

To a solution of **3c** (7 g, 0.019 mmol, 1 equiv.) in THF:H_2O (2:1 v/v), $LiOH.2H_2O$ (1.98 g, 0.033 mmol, 2 equiv.) was added and the reaction mixture was stirred for 12 h. After completion of the reaction, THF was removed *in vacuo* and the solution was neutralized using $KHSO_4$ solution. The crude product was extracted into ethyl acetate and was washed with brine solution. The organic layer was dried over Na_2SO_4 and evaporated *in vacuo* to afford **3d**. The crude product obtained was used for the next step without further purification.

General procedure for Boc deprotection:

Compounds **3e**, **3i**, **4e**, **5b**, **7c**, **8b**, **11b**, **11g**, **12b**, **12d** *etc.,* were prepared following the same procedure.

methyl (*S*)-2-(2-(pyrrolidine-2-carboxamido)benzamido)benzoate 3e:

To a 1:1 mixture of TFA and DCM (50 mL), **3c** (7.5g) was added at room temperature. After stirring for 30 min., the reaction mixture was stripped off the volatiles under reduced pressure. The waxy residue obtained was dissolved in EtOAc (50 mL) and was washed with saturated $NaHCO_3$ solution, followed by brine. Later, the organic layer was dried over Na_2SO_4 and concentrated under reduced pressure to afford crude **3e**, which was used for the next step without further purification.

(*R*)-methyl 2-(2-(1-pivaloylpyrrolidine-2-carboxamido)benzamido)benzoate 3f:

To a solution of **3e** (7g, 19.1 mmol, 1 equiv.) in dry DCM (70 mL), Et_3N (3.86 mL, 28.5 mmol, 1.5 equiv.) and Piv-Cl (2.57 mL, 20.9 mmol, 1.1 equiv.) were added at 0 $^{\circ}$C. After completion of reaction, DCM (30 mL) was added to the reaction mixture and the combined DCM layer was washed sequentially with saturated $NaHCO_3$ solution, water and brine solution. DCM layer was then dried over Na_2SO_4, filtered and the solvent was stripped off under reduced pressure. The product was purified by

column chromatography (30% AcOEt/pet. Ether, R_f: 0.3) furnishing **3f** (7.5 g, 87%) as a white fluffy solid. mp: 128-130 °C; $[\alpha]^{28.6}_D$: -52.0° (*c* 1, $CHCl_3$); IR ($CHCl_3$) *v* (cm^{-1}): 3460, 3020, 1634, 1625, 1524, 1403; ^{1}H NMR (200 MHz, $CDCl_3$) δ: 12.04 (s, 1H, amide), 11.44 (s, 1H, amide), 8.81-8.72 (dt, *J* = 0.88 Hz, 8.59Hz, 2H), 8.11-8.06 (dd, *J* = 1.52 Hz, *J* = 7.96Hz, 1H), 7.92-7.85 (dd, *J* = 1.39 Hz, *J* = 7.96 Hz, 1H), 7.63-7.46 (m, 2H), 7.23-7.11 (m, 2H), 4.67-4.61 (m, 1H), 4.03-3.81(m, 2H), 3.95 (s, 3H), 2.19-1.93 (m, 4H), 1.33 (s, 9H); ^{13}C NMR (50 MHz, $CDCl_3$) δ: 177.5, 171.5, 168.8, 167.5, 141.1, 140.2, 134.5, 132.9, 131.0, 126.9, 123.0, 121.5, 120.5, 120.4, 115.5, 64.16, 52.6, 48.5, 39.1, 27.4; MALDI-TOF/TOF: 474.255 $(M+Na)^+$, 490.2446 $(M+K)^+$; Elemental analysis calculated for $C_{25}H_{29}N_3O_5$: C, 66.50; H, 6.47; N, 9.31. Found: C, 66.34; H, 4.45; N, 9.36.

***tert*-butyl (*R*)-2-((2-((2-(methoxycarbonyl)phenyl)carbamoyl)phenyl)carbamoyl) pyrrolidine-1-carboxylate 3h:**

Compound **3h** was synthesized, following the procedure for **3c,** using Boc-^{D}Pro-OH and **2b**. Purification by column chromatography (eluent: 30% AcOEt/ pet. Ether, R_f: 0.3) afforded **3h** (81%) as a fluffy white solid. mp:101-103 °C; $[\alpha]^{25.36}$: 103.78° (*c* 1, $CHCl_3$); IR ($CHCl_3$) *v* (cm^{-1}): 3448, 3020, 2401, 1689, 1608, 1585, 1525, 1435, 1390, 1271, 1166, 1097, 929; ^{1}H NMR (200 MHz, $CDCl_3$) δ: $12.08_{rotamer}$ (s, 0.6H, amide), $12.04_{rotamer}$ (s, 0.4H, amide), $11.79_{rotamer}$ (s, 0.4H, amide), $11.73_{rotamer}$ (s, 0.6H, amide), 8.9-8.71 (m, 2H), 8.12-8.07 (dd, *J* = 1.52 Hz, *J* = 7.96 Hz, 1H), 7.91-7.85 (m, 1H), 7.68-7.51 (m, 2H), 7.23-7.12 (m, 2H), 4.49-4.24 (m, 0.4H), 4.34-4.26 (m, 0.6H), 3.96 (s, 3H), 3.84-3.73 (m, 1H), 3.65-3.41 (m, 1H), 2.36-2.15 (m, 2H), 1.98-1.86 (m, 2H), $1.44_{rotamer}$ (s, 3H), $1.32_{rotamer}$ (s, 6H); ^{13}C NMR (50 MHz, $CDCl_3$) δ: 172.15, 171.7, 168.9, 167.3, 154.8, 154, 141.1, 139.9, 134.8, 134.4, 132.9, 130.9, 126.9, 123.2, 123.0, 121.1, 120.5, 115.3, 79.9, 62.9, 62.5, 61.9, 52.5, 46.9, 46.7, 31.4, 30.4, 28.1, 24.2, 23.7; MALDI-TOF/TOF: 490.1408 $(M+Na)^+$, 506.0963 $(M+K)^+$; Elemental analysis calculated for $C_{25}H_{29}N_3O_6$: C, 64.23; H, 6.25; N, 8.99. Found: C, 64.18; H, 6.28; N, 8.92.

***General procedure for oxazinone preparation*:**

Compounds **3j**, **3k**, **4i**, **4j**, **7h**, **7i**, **11h**, **11i** *etc.,* were prepared following the mentioned procedure.

(*S*)-*N*-(2-(4-oxo-4H-benzo[d][1,3]oxazin-2-yl)phenyl)-1-pivaloylpyrrolidine-2-carboxamide 3l:

To a solution of **3g** (1.8g, 4.12 mmol, 1equiv.) in dry DCM (20 mL), EDC.HCl (0.94 g, 4.94 mmol, 1.2 equiv.) was added. After completion of the reaction, the reaction mixture was diluted with DCM and was sequentially washed with $NaHCO_3$, water and brine solution. The organic layer was dried over Na_2SO_4 and evaporated *in vacuo*. The residue obtained was purified by column chromatography (eluent: 30% AcOEt/pet. Ether, R_f: 0.4) to afford **3l** (1.69 g, 98%) as a fluffy white solid. mp: 78-80 °C; $[\alpha]^{25.84}_D$: -2.18° (*c* 1, $CHCl_3$); IR ($CHCl_3$) *v* (cm^{-1}): 3448, 2968, 2927, 1769, 1700, 1611, 1585, 1538, 1476, 1467, 1447, 1363, 1288, 1234, 1164, 1034, 1007; ^{1}H NMR (200 MHz, $CDCl_3$) δ: 12.48 (s, 1H, amide), 8.75-8.70 (d, *J*= 8.08 Hz, 1H), 8.24-8.20 (m, 2H), 7.87-7.80 (m, 1H), 7.70-7.66 (m, 1H), 7.56-7.44 (m, 2H), 7.17-7.10 (m, 1H), 4.74-4.72 (m, 1H), 3.85 (s, 3H), 2.23-2.01 (m, 4H), 1.30 (s, 9H); ^{13}C NMR (50 MHz, $CDCl_3$) δ: 177, 171.6, 158.2, 157.2, 145.3, 140.6, 136.8, 133.9, 129.3, 128.7, 126.7, 122.8, 120.8, 116.6, 114.8, 64.7, 48.6, 38.8, 28.6, 27.3, 25.9; MALDI-TOF/TOF: 420.1408 $(M+H)^+$, 442.0936 $(M+Na)^+$, 458.0855 $(M+K)^+$; Elemental analysis calculated for $C_{24}H_{25}N_3O_4$: C, 68.72; H, 6.01; N, 10.02. Found: C, 68.79; H, 5.98; N, 9.96.

benzyl (*S*)-2-((2-(4-oxo-4H-benzo[d][1,3]oxazin-2-yl)phenyl)carbamoyl) pyrrolidine-1-carboxylate 3j:

Compound **3j** was synthesized from **3b**, following the procedure for **3l**. Purification by column chromatography (eluent: 30% AcOEt/ pet. Ether, R_f: 0.3) afforded **3j** (96%) as a fluffy white solid. mp:134-135 °C; $[\alpha]^{27.2}$: 0.488° (*c* 1, $CHCl_3$); IR ($CHCl_3$) *v* (cm^{-1}): 3459, 3020, 1775, 1622, 1541, 1402, 1216; ^{1}H NMR (200 MHz, $CDCl_3$) δ: $12.25_{rotamer}$ (s, 0.3H, amide), $12.06_{rotamer}$ (s, 0.7H, amide), 8.84-8.80 (d, *J* = 8.34 Hz, 1H), 8.23-8.18 (m, 2H), 7.85-7.85 (m, 1H), 7.74-7.70 (m, 1H), 7.59-7.51 (m, 2H), 7.33 (b, 1H), 7.24-7.16 (m, 1H), 7.03-6.95 (m, 2H), 6.86-6.82 (m, 1H), 5.22-5.16 (m, 1H), 5.08-5.02 $_{rotamer}$ (m, 0.3H), $4.88\text{-}4.82_{rotamer}$ (m, 0.7H), 4.57-4.47 (m, 1H), 3.87-3.68 (m, 2H), 2.46-2.13 (m, 2H), 2.03-1.88 (m, 2H); ^{13}C NMR (50 MHz, $CDCl_3$) δ: 171.8, 158.2, 156.6, 155.3, 145.2, 139.6, 136.7, 135.7, 133.7, 129.4, 128.6, 128.4, 127.9, 127.8, 126.9, 126.5, 123.1, 120.9, 116.4, 115.6, 67.3, 62.5, 48.0, 31.8, 24.0; MALDI-TOF/TOF: 470.8876 $(M+H)^+$, 493.0232 $(M+Na)^+$, 509.0346 $(M+K)^+$; Elemental analysis calculated for $C_{27}H_{23}N_3O_5$: C, 69.07; H, 4.94; N, 8.95. Found: C, 69.15; H, 4.78; N, 8.69.

(*S*)-*tert*-butyl 2-((2-(4-oxo-4H-benzo[d][1,3]oxazin-2-yl)phenyl)carbamoyl) pyrrolidine-1-carboxylate 3k:

Compound **3k** was synthesized from **3d**, following the procedure for **3l**. The crude product was purified by column chromatography (eluent: 30% AcOEt/pet. Ether, R_f: 0.3) to furnish **3k** (4.5 g, 98%) as a fluffy white solid. mp: 95-97°C; $[\alpha]^{25.58}$: -18.316° (*c* 1, $CHCl_3$); IR ($CHCl_3$) *v* (cm^{-1}): 3448, 2977, 1770, 1694, 1606, 1584, 1520, 1477, 1446, 1388, 1293, 1251, 1163, 1119, 1036, 1009; ^{1}H NMR (200 MHz, $CDCl_3$) δ: $12.05_{rotamer}$ (0.8H, amide), 11.79-$11.72_{rotamer}$ (0.2H, amide), 8.9-8.68 (m, 1H), 8.23-8.19 (m, 1H), 8.06-8.02 (m, 1H), 7.94-7.85 (m, 1H), 7.58-7.50 (m, 2H), 7.22-7.12 (m, 1H), 4.44-4.23 (m, 1H), 3.76-3.39 (m, 2H), 2.43-2.28 (m, 1H), 2.24-2.05 (m, 1H), 1.96-1.86 (m, 2H), 1.43-$1.36_{rotamer}$ (m, 3H), $1.31_{rotamer}$ (s, 6H); ^{13}C NMR (50 MHz, $CDCl_3$) δ 172.2, 167.2, 158.1, 156.9, 154.9, 145.3, 141.0, 139.8, 137.0, 133.7, 132.8, 130.7, 129.5, 128.7, 128.4, 127.1, 126.8, 123.0, 120.9, 120.6, 120.5, 116.4, 115.7, 95.9, 80.5, 79.9, 62.8, 62.4, 61.5, 52.4, 47.4, 46.6, 31.7, 28.0, 27.2, 24.0; MALDI-TOF: 458.1276 ($M+Na^+$); 474.0995 ($M+K^+$);. Anal. calcd for $C_{15}H_{12}N_2O_5$: C, 66.19; H, 5.79; N, 9.65. Found: C, 66.39; H, 5.89; N, 9.55.

***General procedure for oligomer preparation via bezoxazinone opening with DBU*:**

Compounds **4a**, **4c**, **5a**, **5c**, **6a**, **6b**, **7a**, **7d**, **7j-m**, **8a**, **8c**, **9a**, **9b**, **10a**, **12a**, **12e** *etc.,* were prepared following the same procedure.

Methyl 2-(2-((*S*)-1-(2-(2-((*S*)-1-pivaloylpyrrolidine-2-carboxamido)benzamido) benzoyl)pyrrolidine-2-carboxamido) benzamido)benzoate 4f:

To a solution containing **3l** (0.23 g, 0.88 mmol, 1 equiv.), amine **3e** (0.37 g, 0.88 mmol, 1 equiv.) and 4Å MS in dry DMF (3 mL), DBU (0.134 mL, 3.01 mmol, 1 equiv.) was added at 0 °C. After completion of the reaction, molecular sieves were filtered off and DCM (50 mL) was added to the reaction mixture and the combined organic layer was washed with $KHSO_4$ solution followed by water and brine repeatedly to ensure complete removal of DMF. DCM layer was dried over Na_2SO_4 and was concentrated under reduced pressure. Column chromatographic purification (eluent: 50% AcOEt/pet. Ether, R_f: 0.3) of the residue yielded **4f** (0.5 g, 73%) as a white fluffy solid. mp: 107-109 °C; $[\alpha]^{26.3}_D$: -93.844° (*c* 1, $CHCl_3$); IR ($CHCl_3$) *v* (cm^{-1}): 3293, 3268, 3019, 2882, 2436, 2400, 2317, 1694, 1607, 1586, 1526, 1447, 1271, 1216; ^{1}H NMR (200 MHz, $CDCl_3$) δ: 12.09 (s, 1H, amide), 11.94 (s, 1H, amide), 11.33 (s, 1H, amide), 10.62 (s, 1H, amide), 8.80-8.76 (d, *J* = 7.83 Hz, 1H), 8.68-8.64 (d, *J* = 7.96 Hz, 1H), 8.62-8.58 (d, *J* = 8.34 Hz, 1H), 8.36-8.32 (d, *J* = 8.21 Hz, 1H), 8.11-8.07 (dd, *J* = 1.52 Hz, *J* = 7.96 Hz, 1H), 8.0-7.96 (dd, *J* = 1.14 Hz, *J* = 7.71

Hz, 1H), 7.89-7.85 (dd, *J* = 1.01 Hz, *J* = 7.96 Hz, 1H), 7.67-7.63 (dd, *J* = 1.14 Hz, *J* = 7.96 Hz, 1H), 7.58-7.38 (m, 4H), 7.26-7.11 (m, 3H), 7.02-6.94 (m, 1H), 4.90-4.82 (m, 1H), 4.60-4.55 (m, 1H), 3.95 (s, 3H), 3.90-3.75 (m, 4H), 2.58-2.41 (m, 1H), 2.28-1.86 (m, 7H), 1.29 (s, 9H); ^{13}C NMR (50 MHz, $CDCl_3$) δ 177.2, 171.5, 170.5, 170.4, 168.9, 168.8, 167.2, 140.9, 140.3, 139.7, 137.2, 134.4, 133.3, 132.7, 131.14, 131.1, 128.9, 127.3, 127.0, 124.3, 123.4, 123.2, 123.0, 122.3, 121.5, 121.4, 120.7, 120.6, 120.1, 115.8, 64.0, 62.6, 52.6, 51.2, 48.5, 39.0, 30.0, 28.9, 27.4, 25.5; MALDI-TOF/TOF: 809.6099 $(M+Na)^+$, 825.5373 $(M+K)^+$; Anal. calcd. for $C_{44}H_{46}N_6O_8$: C, 67.16; H, 5.89; N, 10.68. Found: C, 67.09; H, 5.80; N, 10.45.

benzyl (*S*)-2-((2-((2-((*S*)-2-((2-((2-(methoxycarbonyl)phenyl)carbamoyl)phenyl) carbamoyl)pyrrolidine-1-carbonyl)phenyl)carbamoyl)phenyl)carbamoyl) pyrrolidine-1-carboxylate 4a:

Compound **4a** was synthesized, following the procedure for **4f**, employing oxazinone **3j** and amine **3e**. Column chromatographic purification (eluent: 40% AcOEt/pet. Ether, R_f: 0.3) of the residue afforded **3** as a white fluffy solid (94%). mp: 89-91 °C; $[\alpha]^{26.1}_D$: -108.07° (*c* 1, $CHCl_3$); IR ($CHCl_3$) *ν* (cm^{-1}): 3445, 3020, 2401, 2341, 1695, 1627, 1585, 1521, 1435, 1297, 929; ^{1}H NMR (200 MHz, $CDCl_3$) δ: 12.09 (s, 1H, amide), $11.99_{rotamer}$ (s, 0.5H, amide), $11.94_{rotamer}$ (s, 0.5H, amide), $11.86_{rotamer}$ (s, 0.5H, amide), $11.77_{rotamer}$ (s, 0.5H, amide), 10.64 (s, 1H, amide), 8.82-8.75 (m, 1H), 8.67-8.63 (m, 2H), 8.43-8.35 (m, 1H), 8.10-8.06 (dd, *J* = 1.14 Hz, *J* = 7.96 Hz, 1H), 8.0-7.85 (m, 2H), 7.69-7.33 (m, 6H), 7.23-7.13 (m, 4H), 7.03-6.96 (m, 3H), 5.35-4.96 (m, 2H), 4.92-4.83 (m, 1H), 4.52-4.37 (m, 1H), 3.94 (s, 3H), 3.90-3.52 (m, 4H), 2.57-2.43 (m, 1H), 2.35-1.88 (m, 7H); ^{13}C NMR (50 MHz, $CDCl_3$) δ: 171.6, 170.3, 168.9, 167.8, 140.9, 140.3, 137.2, 134.5, 133.3, 132.8, 131.1, 128.9, 128.4, 128.1, 127.7, 127.1, 123.4, 123.2, 123.0, 122.1, 121.4, 120.5, 120.3, 120.1, 115.8, 77.2, 67.1, 67.0, 62.7, 62.3, 52.8, 51.3, 47.3, 46.9, 36.6, 31.5, 30.5, 30.0, 25.5, 23.6; MALDI-TOF/TOF: 859.4677 $(M+Na)^+$, 876.5307 $(M+K)^+$; Anal. calcd for $C_{47}H_{44}N_6O_9$: C, 67.45; H, 5.30; N, 10.04; Found: C, 67.71; H, 5.21; N, 10.24.

***tert*-butyl (*S*)-2-((2-((2-((*S*)-2-((2-((2-(methoxycarbonyl)phenyl)carbamoyl) phenyl)carbamoyl)pyrrolidine-1-carbonyl)phenyl)carbamoyl)phenyl)carbamoyl) pyrrolidine-1-carboxylate 4c**:

Compound **4c** was synthesized, following the procedure for **4f**, employing oxazinone **3k** and amine **3e**. Column chromatographic purification (eluent: 45% AcOEt/pet. Ether, R_f: 0.3) of the residue afforded **4c** as a white fluffy solid (78%). mp: 111-113

°C; $[\alpha]^{26.2}_D$: -161.548° (*c* 1, $CHCl_3$); IR ($CHCl_3$) *v* (cm^{-1}): 3448, 3030, 2401, 2346, 1670, 1655, 1585, 1524, 1475, 1449, 1392, 1297, 1271, 1166, 1030; ^{1}H NMR (200 MHz, $CDCl_3$) δ: 12.09 (s, 1H, amide), $11.97_{rotamer}$ (s, 0.6H, amide), $11.93_{rotamer}$ (s, 0.4H, amide), $11.81_{rotamer}$ (s, 0.6H, amide), $11.65_{rotamer}$ (s, 0.4H, amide), $10.76_{rotamer}$ (s, 0.6H, amide), $10.59_{rotamer}$ (s, 0.6H, amide), 8.80-8.76 (d, *J* = 8.34 Hz, 1H), 8.71-8.63 (m, 2H), 8.57-8.47 (m, 1H), 8.11-8.07 (dd, *J* = 1.52 Hz, *J* = 7.96 Hz, 1H), 7.99-7.95 (m, 1H), 7.89-7.86 (m, 1H), 7.72-7.43 (m, 5H), 7.23-7.13 (m, 3H), 7.06-6.98 (m, 1H), 4.93-4.86 (m, 1H), $4.45\text{-}4.39_{rotamer}$ (m, 0.4H), $4.30\text{-}4.24_{rotamer}$ (m, 0.6H), 3.95 (s, 3H), 3.81-3.70 (m, 2H), 3.59-3.38 (m, 2H), 2.54-2.40 (m, 1H), 2.3-1.85 (m, 7H), $1.48_{rotamer}$ (s, 3H), $1.32_{rotamer}$ (s, 6H); ^{13}C NMR (50 MHz, $CDCl_3$) δ: 172.2, 170.5, 170.3, 168.8, 167.7, 166.9, 154.1, 140.9, 140.3, 139.9, 137.3, 134.4, 133.3, 132.3, 132.9, 131.7, 131.1, 128.9, 127.3, 127.1, 123.4, 123.2, 123.0, 122.1, 121.3, 120.8, 120.5, 120.4, 120.1, 119.9, 115.8, 80.0, 62.6, 61.9, 52.6, 51.4, 47.0, 46.7, 31.4, 30.4, 30.0, 29.6, 28.2, 25.5, 24.2, 23.7; MALDI-TOF/TOF: 825.3741 $(M+Na)^+$, 841.0604 $(M+K)^+$; Anal. calcd for $C_{44}H_{46}N_6O_9$: C, 65.82; H, 5.78; N, 10.47; Found: C, 65.36; H, 5.56; N, 10.41.

***General procedure for methylamide derivative preparation*:**

Compounds **4b**, **5d**, **6c**, **7f**, **8d**, **9c**, **10c**, **12c**, **12f** *etc.,* were prepared following the same procedure.

(*S*)-*N*-(2-((2-(methylcarbamoyl)phenyl)carbamoyl)phenyl)-1-(2-(2-((*S*)-1-pivaloyl pyrrolidine-2-carboxamido)benzamido)benzoyl)pyrrolidine-2-carboxamide 4h:

The ester **4f** (0.2g, 0.25 mmol) was taken in saturated methanolic methylamine solution (2 mL) and stirred at room temperature for 2 h. The solvent was removed under reduced pressure, and the residue was purified by column chromatography (eluent: 60% AcOEt/pet. Ether, R_f: 0.2) to afford **4h** (0.19 g, 98%) as a white solid. mp: 147-149 °C; $[\alpha]^{26.38}_D$: -15.148° (*c* 1, $CHCl_3$); IR ($CHCl_3$) *v* (cm^{-1}): 3300, 3268, 3019, 2400, 1694, 1659, 1626, 1586, 1520, 1447, 1435, 1271; ^{1}H NMR (200 MHz, $CDCl_3$) δ: 12.25 (s, 1H, amide), 12.16 (s, 1H, amide), 11.21 (s, 1H, amide), 10.38 (s, 1H, amide), 8.80-8.77 (d, *J* = 7.96 Hz, 1H), 8.57-8.53 (d, *J* = 8.08 Hz, 1H), 8.33-8.29 (d, *J* = 8.08 Hz, 1H), 8.23-8.19 (d, *J* = 8.21 Hz, 1H), 8.45-8.43 (d, *J* = 8.55 Hz, 1H), 7.82-7.78 (d, *J* = 7.83 Hz, 1H), 7.76-7.72 (d, *J* = 7.58 Hz, 1H), 7.58-7.54 (d, *J* = 7.83 Hz, 1H), 7.51-7.01 (m, 6H), 6.57-6.49 (m, 1H), 4.93-4.86 (dd, *J* = 7.96 Hz, *J* = 5.31 Hz, 1H), 4.62-4.56 (m, 1H), 3.96-3.67 (m, 4H), 2.86-2.84 (d, *J* = 4.67

Hz, 3H), 2.46-2.25 (m, 2H), 2.16-1.89 (m, 8H), 2.12-2.04 (m, 2H), 1.33 (s, 9H); ^{13}C NMR (50 MHz, $CDCl_3$) δ: 177.8, 171.4, 170.3, 170.2, 169.5, 167.6, 167.6, 166.7, 140.1, 139.5, 138.4, 136.7, 133.1, 132.5, 131.6, 130.9, 128.5, 127.4, 127.2, 127.15, 124.6, 123.6, 123.4, 123.3, 123.0, 122.1, 121.2, 121.1, 120.0, 64.1, 62.8, 50.7, 48.5, 39.0, 29.6, 28.8, 27.5, 26.8, 25.5, 25.2; MALDI-TOF/TOF: 808.6611 $(M+Na)^+$, 824.6780 $(M+K)^+$; Elemental analysis calculated for $C_{44}H_{47}N_7O_7$: C, 67.25; H, 6.03; N, 12.48. Found: C, 67.09; H, 6.04; N, 12.37.

benzyl (*S*)-2-((2-((2-((*S*)-2-((2-((2-(methylcarbamoyl)phenyl)carbamoyl)phenyl) carbamoyl)pyrrolidine-1-carbonyl)phenyl)carbamoyl)phenyl)carbamoyl) pyrrolidine-1-carboxylate 4b:

Compound **4b** was synthesized from **4a**, following the procedure for **4h**. Column chromatographic purification (eluent: 75% AcOEt/pet. Ether, R_f: 0.3) of the residue afforded **4b** as a white solid (98%). mp: 126-128 °C; $[\alpha]^{25.1}_D$: -179.49° (*c* 1, $CHCl_3$); IR ($CHCl_3$) *v* (cm^{-1}): 3445, 2874, 1695, 1627, 1585, 1521, 1435, 1297, 1270, 1215, 1029; ^{1}H NMR (200 MHz, $CDCl_3$) δ: 12.40 (s, 0.7H, amide), $12.28_{rotamer}$ (s, 0.3H, amide), $12.17_{rotamer}$ (s, 0.3H, amide), $11.97_{rotamer}$ (s, 0.7H, amide), $11.78_{rotamer}$ (s, 0.7H, amide), $11.71_{rotamer}$ (s, 0.3H, amide), $10.57_{rotamer}$ (s, 0.6H, amide), $10.48_{rotamer}$ (s, 0.6H, amide), 8.90-8.86 (d, *J* = 8.21 Hz, 0.6H), 8.81-8.77 (d, *J* = 8.34 Hz, 0.4H),), 8.65-8.61 (d, *J* = 8.34 Hz, 0.6H), 8.50-8.46 (d, *J* = 8.21 Hz, 0.4H), 8.38-8.34 (d, *J* = 8.08 Hz, 0.4H), 8.24-8.16 (m, 1.6H), 7.94-7.43 (m, 8H), 7.31-6.81 (m, 8H), 6.31-6.23 (m, 1H), 5.34-5.04 (m, 2H), 4.98-4.78 (m, 1H), 4.54-$4.49_{rotamer}$ (m, 0.7H), 4.43-$4.37_{rotamer}$ (m, 0.3H), 4.13-3.84 (m, 2H), 3.73-3.51 (m, 2H), 2.95-$2.92_{rotamer}$ (d, *J* = 4.43 Hz, 1H), 2.81-$2.79_{rotamer}$ (d, *J* = 4.43 Hz, 2H), 2.46-1.86 (m, 8H); ^{13}C NMR (50 MHz, $CDCl_3$) δ: 170.8, 170.5, 169.8, 169.7, 167.6, 166.6, 155.9, 140.1, 139.3, 138.3, 137.5, 136.3, 133.2, 132.6, 131.6, 131.2, 128.6, 128.0, 127.6, 127.4, 127.2, 123.6, 123.3, 123.1, 123.0, 122.7, 122.3, 121.7, 121.4, 120.9, 120.5, 119.8, 77.2, 67.6, 67.0, 63.4, 62.3, 50.8, 46.9, 30.3, 29.9, 29.6, 26.7, 25.1, 24.0; MALDI-TOF/TOF: 858.5309 $(M+Na)^+$, 874.5634 $(M+K)^+$; Anal. calcd for $C_{47}H_{45}N_7O_8$: C, 67.53; H, 5.43; N, 11.73; Found: C, 67.42; H, 5.13; N, 11.89.

***tert*-butyl (*S*)-2-((2-((2-((*S*)-2-((2-(4-oxo-4H-benzo[d][1,3]oxazin-2-yl)phenyl) carbamoyl)pyrrolidine-1-carbonyl)phenyl)carbamoyl)phenyl)carbamoyl) pyrrolidine-1-carboxylate 4i:**

Compound **4i** was synthesized from **4d**, following the procedure for **3l**. Column chromatographic purification (eluent: 60% AcOEt/pet. Ether, R_f: 0.3) of the residue

afforded **4i** as a fluffy white solid (96%). mp: 99-101 °C; $[\alpha]^{26.0}_D$: -5.776° (*c* 1, $CHCl_3$); IR ($CHCl_3$) *v* (cm^{-1}): 3448, 1770, 1690, 1606, 1585, 1518, 1476, 1449, 1412, 1296, 1249, 1220, 1165, 1125, 1034; ^{1}H NMR (200 MHz, $CDCl_3$) δ: 12.74 (s, 1H, amide), $11.65_{rotamer}$ (s, 0.55H, amide), $11.55_{rotamer}$ (s, 0.45H, amide), $10.34_{rotamer}$ (s, 0.55H, amide), $10.27_{rotamer}$ (s, 0.45H, amide), 8.68-8.64 (m, 2H), 8.58-8.47 (m, 1H), 8.54-8.50 (d, *J* = 8.21 Hz, 1H), 8.11-8.07 (d, *J* = 7.96 Hz, 1H), 7.99-7.82 (m, 2H), 8.28-8.18 (m, 2H), 7.76-7.30 (m, 7H), 7.23-7.16 (m, 2H), 6.84-6.76 (m, 1H), 4.98-4.92 (m, 1H), 4.46-$4.40_{rotamer}$ (m, 0.45H), 4.32-$4.26_{rotamer}$ (m, 0.55H), 3.78-3.43 (m, 4H), 2.53-2.44 (m, 1H), 2.36-1.86 (m, 7H), $1.46_{rotamer}$ (s, 4H), $1.34_{rotamer}$ (s, 5H); ^{13}C NMR (50 MHz, $CDCl_3$) δ: 172.0, 171.5, 169.8, 169.0, 167.2, 167.0, 157.8, 157.1, 154.7, 154.0, 144.9, 140.1, 139.5, 136.8, 136.5, 133.9, 132.5, 131.2, 130.8, 129.3, 128.8, 128.7, 127.5, 127.2, 126.0, 124.8, 124.2, 123.3, 123.0, 122.9, 121.9, 120.8, 120.5, 116.4, 114.6, 95.9, 79.9, 79.7, 62.4, 61.9, 61.7, 50.4, 46.9, 46.6, 31.3, 30.3, 29.6, 28.2, 28.1, 25.1, 24.1, 23.6; MALDI-TOF/TOF: 793.2239 $(M+Na)^+$, 809.1860 $(M+K)^+$; Anal. calcd for $C_{43}H_{42}N_6O_8$: C, 67.00; H, 5.49; N, 10.90; Found: C, 67.24; H, 5.56; N, 10.79.

(*S*)-*N*-(2-(4-oxo-4H-benzo[d][1,3]oxazin-2-yl)phenyl)-1-(2-(2-((*S*)-1-pivaloyl pyrrolidine-2-carboxamido)benzamido)benzoyl)pyrrolidine-2-carboxamide 4j:

Compound **4j** was synthesized from **4g**, following the procedure for **3l**. Column chromatographic purification (eluent: 60% AcOEt/pet. Ether, R_f: 0.3) of the residue afforded **4j** as a fluffy white solid (97%). mp: 134-136 °C; $[\alpha]^{27.3}_D$: -78.556° (*c* 1, $CHCl_3$); IR ($CHCl_3$) *v* (cm^{-1}): 3420, 3310, 3020, 2401, 1771, 1662, 1610, 1583, 1521, 1442, 1406, 1293, 1216, 1006; ^{1}H NMR (200 MHz, $CDCl_3$) δ: 12.78 (s, 1H, amide), 11.20 (s, 1H, amide), 10.34 (s, 1H, amide), 8.70-8.65 (d, *J* = 8.46 Hz, 1H), 8.58-8.54 (d, *J* = 8.21 Hz, 1H), 8.33-8.19 (m, 3H), 7.73-7.32 (m, 8H), 7.22-7.15 (m, 2H), 6.83-6.76 (m, 1H), 4.96-4.89 (m, 1H), 4.59-4.53 (m, 1H), 3.97-3.65 (m, 4H), 2.54-2.40 (m, 1H), 2.33-1.84 (m, 7H), 1.29 (s, 9H); ^{13}C NMR (50 MHz, $CDCl_3$) δ: 177.2, 171.4, 170.0, 168.9, 167.3, 157.9, 157.1, 144.9, 140.2, 139.4, 140.0, 136.4, 133.9, 132.3, 130.9, 129.2, 128.8, 128.6, 127.6, 127.4, 126.1, 124.9, 123.4, 123.0, 122.9, 122.3, 121.2, 121.0, 120.5, 116.3, 114.6, 63.9, 62.0, 50.6, 48.4, 38.8, 29.6, 28.7, 27.2, 25.6, 25.3; MALDI-TOF/TOF: 777.3426 $(M+Na)^+$, 793.3498 $(M+K)^+$; Anal. calcd for $C_{43}H_{42}N_6O_7$: 68.42; H, 5.61; N, 11.13; Found: 68.32; H, 5.48; N, 11.01.

***Homo*-chiral Boc dodecamer 5a**:

Compound **5a** was synthesized, following the procedure for **4f**, employing oxazinone **4i** and amine **4e**. Column chromatographic purification (eluent: 70% AcOEt/pet. Ether, R_f: 0.2) of the residue afforded **5a** as a white fluffy solid (64%). mp: 165-167 °C; $[\alpha]^{26.6}_D$: -126.74° (*c* 1, $CHCl_3$); IR ($CHCl_3$) *v* (cm^{-1}): 3458, 3021, 1710, 1656, 1589, 1452, 1398, 1297, 1212, 930; ^{1}H NMR (500 MHz, $CDCl_3$) δ: 12.05 (s, 1H, amide), 11.96$_{rotamer}$ (s, 0.7H, amide), 11.92 (s, 1H, amide), 11.89 (s, 1.3H, amide), 11.81$_{rotamer}$ (s, 0.6H, amide), 11.69$_{rotamer}$ (s, 0.4H, amide), 10.78-10.61$_{rotamer}$ (s, 3H, amide), 8.72-8.55 (m, 6H), 8.26-8.23 (m, 2H), 8.03-8.01 (d, *J* = 7.70 Hz, 1H), 7.95-7.90 (m, 2H), 7.84-7.82 (d, *J* = 7.70 Hz, 1H), 7.70-7.65 (m, 3H), 7.55-7.40 (m, 8H), 7.21-7.07 (m, 5H), 7.00-6.95 (m, 3H), 4.84-4.78 (m, 3H), 4.43-4.41$_{rotamer}$ (m, 0.5H), 4.28-4.25$_{rotamer}$ (m, 0.5H), 3.97-3.76 (m, 4H), 3.90 (s, 3H), 3.70-3.41 (m, 4H), 2.43-2.37 (m, 3H), 2.32-2.25 (m, 1H), 2.17-2.10 (m, 4H), 2.04-1.94 (m, 4H), 1.90-1.82 (m, 4H), 1.42 (s, 3H), 1.32 (s, 6H); ^{13}C NMR (125 MHz, $CDCl_3$) δ: 172.1, 171.6, 170.2, 170.1, 170.0, 169.8, 168.7, 167.6, 167.3, 167.2, 166.9, 154.7, 150.0, 140.7, 140.1, 139.8, 137.2, 136.9, 136.7, 134.3, 133.2, 132.9, 132.8, 130.8, 131.6, 130.9, 128.8, 128.7, 128.7, 127.4, 127.3, 127.0, 124.3, 124.2, 123.3, 123.2, 123.1, 122.9, 122.2, 122.0, 121.1, 120.9, 120.7, 120.3, 120.2, 119.9, 119.5, 115.6, 96.0, 79.9, 79.9, 79.7, 2.6, 62.5, 62.4, 61.8, 52.5, 51.2, 50.9, 50.9, 46.9, 46.6, 31.4, 30.4, 29.9, 29.5, 29.5, 28.3, 28.1, 25.4, 25.3, 24.2, 23.7; MALDI-TOF/TOF: 1486.3385 $(M+Na)^+$, 1512.5137 $(M+K)^+$; Anal. calcd for $C_{82}H_{80}N_{12}O_{15}$: C, 66.84; H, 5.47; N, 11.41; Found: C, 66.66; H, 5.21; N, 11.71.

***Homo*-chiral Piv dodecamer 5c**:

Compound **5c** was synthesized, following the procedure for **4f**, employing oxazinone **4j** and amine **4e**. Column chromatographic purification (eluent: 80% AcOEt/pet. Ether, R_f: 0.2) of the residue afforded **5c** as a white fluffy solid (56%). mp: 140-142 °C; $[\alpha]^{26.3}_D$: -99.546° (*c* 1, $CHCl_3$); IR ($CHCl_3$) *v* (cm^{-1}): 3458, 3018, 1693, 1631, 1520, 1406, 1218, 1006; ^{1}H NMR (200 MHz, $CDCl_3$) δ: 12.06 (s, 1H, amide), 11.93 (s, 2H, amide), 11.88 (s, 1H, amide), 11.36 (s, 1H, amide), 10.70 (s, 1H, amide), 10.68 (s, 1H, amide), 10.65 (s, 1H, amide), 8.73-8.55 (m, 5H), 8.39-8.34 (d, *J* = 8.34 Hz, 1H), 8.29-8.22 (m, 2H), 8.06-7.82 (m, 5H), 7.71-7.64 (m, 3H), 7.55-7.39 (m, 9H), 7.25-7.07 (m, 6H), 7.04-6.93 (m, 3H), 4.83-4.78 (m, 3H), 4.60-4.55 (m, 1H), 3.95-3.57 (m, 8H), 3.91 (s, 3H), 2.50-2.35 (m, 3H), 2.26-1.81 (m, 13H), 1.29 (s, 9H); ^{13}C NMR (50 MHz, $CDCl_3$) δ: 177.2, 171.5, 170.2, 170.1, 170.0, 169.9, 168.8, 167.7,

167.4, 167.3, 167.2, 140.7, 140.1, 139.9, 139.8, 139.7, 137.1, 136.9, 136.7, 134.3, 133.2, 133.0, 132.6, 140.0, 128.9, 128.7, 127.3, 127.0, 124.4, 124.2, 123.4, 123.3, 123.2, 122.2, 131.4, 121.2, 121.0, 120.6, 120.4, 120.0, 119.8, 119.6, 115.7, 77.2, 63.9, 62.6, 62.4, 52.6, 51.1, 50.9, 48.5, 38.9, 29.9, 29.6, 27.4, 25.5, 25.4; MALDI-TOF/TOF: 1480.3448 $(M+Na)^+$, 1497.3956 $(M+K)^+$; Anal. calcd for $C_{82}H_{80}N_{12}O_{14}$: C, 67.57; H, 5.53; N, 11.53; Found: C, 67.81; H, 5.32; N, 11.59.

***Homo*-chiral Piv dodecamer 5d**:

Compound **5d** was synthesized from **5c**, following the procedure for **4h**. Column chromatographic purification (eluent: 85% AcOEt/pet. Ether, R_f: 0.3) of the residue afforded **5d** as a fluffy white solid (94%). mp: 175-176 °C; $[\alpha]^{26.8}_D$: 108.448° (*c* 1, $CHCl_3$); IR ($CHCl_3$) *v* (cm^{-1}): 3458, 1682, 1636, 1520, 1404, 1299, 1010; ^1H NMR (200 MHz, $CDCl_3$) δ: 12.42 (s, 1H, amide), 12.12 (s, 1H, amide), 11.91 (s, 2H, amide), 11.34 (s, 1H, amide), 10.79 (s, 1H, amide), 10.62 (s, 1H, amide), 10.59 (s, 1H, amide), 8.86-8.83 (d, *J* = 7.83 Hz, 1H), 8.72-8.68 (d, *J* = 8.21 Hz, 1H), 8.65-8.57 (m, 2H), 8.41-8.37 (d, *J* = 8.46 Hz, 1H), 8.35-8.31 (d, *J* = 7.83 Hz, 1H), 8.15-8.11 (d, *J* = 7.96 Hz, 1H), 8.13-8.09 (d, *J* = 7.96 Hz, 1H), 8.0-7.90 (m, 2H), 7.77-6.91 (m, 20H), 6.42-6.31 (m, 2H), 4.86-4.77 (m, 3H), 4.61-4.55 (m, 1H), 4.02-3.68 (m, 8H), 2.88-2.84 (d, *J* = 4.55 Hz, 3H), 2.53-2.30 (m, 4H), 2.21-1.85 (m, 12H), 1.31 (s, 9H); ^{13}C NMR (50 MHz, $CDCl_3$) δ: 171.5, 170.8, 170.4, 170.2, 170.0, 169.6, 169.4, 167.6, 167.3, 167.2, 166.7, 140.1, 140.0, 139.6, 138.3, 137.2, 137.1, 137.0, 133.2, 132.9, 132.7, 131.6, 131.4, 131.2, 130.9, 129.7, 129.0, 127.5, 127.2, 127.0, 124.2, 123.9, 123.6, 123.6, 123.2, 123.0, 122.3, 121.6, 121.4, 120.7, 120.6, 119.8, 119.6, 118.9, 77.2, 64.0, 63.4, 62.9, 62.6, 48.5, 41.7, 39.0, 31.9, 30.1, 29.6, 27.4, 26.8, 25.4, 25.1; MALDI-TOF/TOF: 1479.5386 $(M+Na)^+$, 1495.4143 $(M+K)^+$; Anal. calcd for $C_{82}H_{81}N_{13}O_{13}$: C, 67.62; H, 5.61; N, 12.50; Found: C, 67.48; H, 5.52; N, 12.23.

***Homo*-chiral Boc octadecamer 6a**:

Compound **6a** was synthesized, following the procedure for **4f**, employing oxazinone **4i** and amine **5b**. Column chromatographic purification (eluent: 80% AcOEt/pet. Ether, R_f: 0.3) of the residue afforded **6a** as a waxy solid (36%). $[\alpha]^{26.7}_D$: -119.48° (*c* 0.5, $CHCl_3$); IR ($CHCl_3$) *v* (cm^{-1}): 3460, 3020, 1683, 1586, 1448, 1395, 1299, 1217, 930; ^1H NMR (400 MHz, $CDCl_3$) δ: $12.17_{rotamer}$ (s, 0.1H, amide), 12.07 (s, 1H, amide), $11.98_{rotamer}$ (s, 0.9H, amide), 11.93 (s, 1H, amide), 11.89 (broad, 3H, amide),

11.84$_{rotamer}$ (s, 0.7H, amide), 11.69$_{rotamer}$ (s, 0.3H, amide), 10.78-10.62 (m, 5H, amide), 8.76-8.57 (m, 8H), 8.29-8.22 (m, 3H), 8.06-8.04 (d, *J* = 7.78 Hz, 1H), 7.97-7.84 (m, 6H), 7.72-7.66 (m, 5H), 7.56-7.42 (m, 12H), 7.24-7.08 (m, 8H), 7.04-6.97 (m, 5H), 4.87-4.78 (m, 5H), 4.44-4.42$_{rotamer}$ (m, 0.5H), 4.29-4.26$_{rotamer}$ (m, 0.5H), 3.96-3.35 (m, 12H), 3.92 (s, 3H), 2.48-2.43 (m, 4H), 2.31-2.14 (m, 8H), 2.00-1.82 (m, 12H), 1.33$_{rotamer}$ (s, 5H), 1.25$_{rotamer}$ (s, 4H); ^{13}C NMR (100 MHz, $CDCl_3$) δ: 172.3, 171.2, 170.4, 170.1, 169.9, 169.8, 167.5, 167.3, 167.0, 154.1, 140.8, 140.2, 140.0, 137.3, 136.9, 136.8, 134.4, 133.3, 133.1, 131.7, 131.1, 128.9, 128.8, 127.5, 127.4, 127.1, 124.4, 124.3, 123.4, 123.4, 123.2, 123.0, 121.2, 121.1, 120.5, 120.0, 119.7, 119.6, 115.8, 80.1, 77.2, 62.7, 62.5, 60.4, 52.7, 51.0, 46.7, 31.9, 31.5, 31.4, 30.0, 29.9, 29.7, 29.3, 28.4, 28.2, 25.4, 24.3, 23.8, 22.7, 21.1; MALDI-TOF/TOF: 2167.4343 $(M+Na)^+$, 2183.2896 $(M+K)^+$; Anal. calcd for $C_{120}H_{114}N_{18}O_{21}$: C, 67.22; H, 5.36; N, 11.76; Found: C, 67.02; H, 5.12; N, 11.71.

***Homo*-chiral Piv octadecamer 6b**:

Compound **6b** was synthesized, following the procedure for **4f**, employing oxazinone **4j** and amine **5b**. Column chromatographic purification (eluent: 85% AcOEt/pet. Ether, R_f: 0.2) of the residue afforded **6b** as a white fluffy solid (30%). mp: 193-195 °C; $[\alpha]^{27.1}_D$: -96.368° (*c* 1, $CHCl_3$); IR ($CHCl_3$) *v* (cm^{-1}): 3460, 3019, 1626, 1526, 1404, 1216, 1009; ^{1}H NMR (400 MHz, $CDCl_3$) δ: 12.05 (s, 1H, amide), 11.91 (broad, 2H, amide), 11.88 (broad, 3H, amide), 11.35 (s, 1H, amide), 10.69 (broad, 3H, amide), 10.67 (s, 1H, amide), 10.62 (s, 1H, amide), 8.73-8.68 (m, 2H), 8.64-8.57 (m, 4H), 8.39-8.35 (m, 1H), 8.30-8.22 (m, 3H), 8.06-8.04 (d, *J* = 7.78 Hz, 1H), 7.97-7.95 (d, *J* = 7.53 Hz, 1H), 7.91-7.84 (m, 5H), 7.71-7.66 (m, 5H), 7.54-7.42 (m, 12H), 7.23-7.09 (m, 8H), 7.02-6.95 (m, 5H), 4.86-4.79 (m, 5H), 4.60-4.56 (m, 1H), 3.90-3.57 (m, 12H), 3.92 (s, 3H), 2.49-2.41 (m, 4H), 2.19-2.13 (m, 7H), 2.00-1.86 (m, 13H), 1.30 (s, 9H); ^{13}C NMR (100 MHz, $CDCl_3$) δ: 177.2, 171.5, 170.3, 170.1, 169.9, 168.8, 167.8, 167.5, 167.3, 167.2, 140.8, 140.2, 140.0, 139.9, 139.2, 137.1, 136.8, 136.8, 134.4, 133.3, 132.7, 131.1, 128.8, 127.5, 127.4, 127.3, 127.1, 124.5, 124.3, 123.4, 123.2, 123.1, 122.4, 122.3, 121.5, 121.3, 121.1, 120.6, 120.5, 120.0, 119.8, 119.6, 115.8, 114.0, 96.1, 77.2, 64.0, 62.6, 62.6, 62.5, 52.6, 51.2, 51.0, 48.5, 39.0, 36.6, 33.8, 31.9, 30.0, 29.7, 29.5, 29.3, 29.1, 28.9, 28.3, 27.4, 25.4, 24.8, 24.6, 22.6; MALDI-TOF/TOF: 2151.6296 $(M+Na)^+$, 2168.3511 $(M+K)^+$; Anal. calcd for $C_{120}H_{114}N_{18}O_{20}$: C, 67.72; H, 5.40; N, 11.85; Found: C, 67.46; H, 5.36; N, 11.69.

***Homo*-chiral Piv octadecamer 6c**:

Compound **6c** was synthesized from **6b**, following the procedure for **4h**. Column chromatographic purification (eluent: 90% AcOEt/pet. Ether, R_f: 0.2) of the residue afforded **6c** as a white fluffy solid (86%). mp: 186-188 °C; $[\alpha]^{27.1}_D$: -152.648° (*c* 1, $CHCl_3$); IR ($CHCl_3$) *v* (cm^{-1}): 3461, 3020, 1627, 1526, 1450, 1409, 1298, 1216, 929; ^{1}H NMR (500 MHz, $CDCl_3$) δ: 12.38 (s, 1H, amide), 12.17 (s, 1H, amide), 11.92 (broad, 2H, amide), 11.88 (s, 1H, amide), 11.87 (s, 1H, amide), 11.36 (s, 1H, amide), 10.78 (s, 1H, amide), 10.72 (s, 1H, amide), 10.69 (s, 1H, amide), 10.64 (s, 1H, amide), 10.59 (s, 1H, amide), 8.83-8.82 (d, *J* = 8.53 Hz, 1H), 8.69-8.6 (d, *J* = 8.25 Hz, 1H), 8.65-8.59 (m, 4H), 8.38-8.37 (d, *J* = 7.98 Hz, 1H), 8.29-8.25 (m, 3H), 8.18-8.16 (d, *J* = 7.98 Hz, 1H), 8.10-8.09 (d, *J* = 8.25 Hz, 1H), 7.97-7.96 (d, *J* = 7.43 Hz, 1H), 7.92-7.91 (m, 3H), 7.71-7.65 (m, 5H), 7.56-7.28 (m, 15H), 7.23-7.15 (m, 7H), 7.07-6.95 (m, 5H), 6.46-6.43 (t, *J* = 7.43 Hz, 1H), 6.39-6.36 (t, *J* = 7.43 Hz, 1H), 4.84-4.79 (m, 5H), 4.57 (m, 1H), 3.96-3.59 (m, 12H), 2.85-2.84 (d, *J* = 4.13 Hz, 1H), 2.50-2.38 (m, 4H), 2.30-2.27 (m, 1H), 2.17-1.84 (m, 19H), 1.30 (s, 9H); ^{13}C NMR (125 MHz, $CDCl_3$) δ: 177.3, 171.6, 170.8, 170.4, 170.3, 170.1, 170.0, 169.7, 169.4, 167.6, 167.5, 167.4, 167.3, 166.8, 140.2, 140.0, 139.84, 139.8, 139.7, 138.4, 137.2, 137.2, 137.0, 136.8, 133.2, 133.1, 133.0, 132.7, 131.7, 131.4, 131.1, 130.9, 129.6, 129.0, 128.9, 128.3, 127.5, 127.3, 127.3, 127.1, 124.5, 124.4, 124.0, 123.7, 123.6, 123.4, 123.3, 123.2, 123.17, 123.0, 122.4, 122.3, 121.8, 121.4, 120.8, 120.7, 120.6, 119.8, 119.6, 119.0, 114.1, 96.1, 64.1, 63.3, 62.9, 62.6, 62.55, 51.5, 51.3, 51.1, 50.9, 48.6, 39.0, 33.8, 31.9, 31.6, 30.1, 30.0, 29.7, 29.6, 29.5, 29.3, 29.1, 27.4, 26.8, 26.4, 25.5, 25.2, 23.1, 22.7; MALDI-TOF/TOF: 2149.2512 $(M+Na)^+$; Anal. calcd for $C_{120}H_{115}N_{19}O_{19}$: C, 67.75; H, 5.45; N, 12.51; Found: C, 67.52; H, 5.26; N, 12.29.

***tert*-butyl (*S*)-2-((2-((2-((*R*)-2-((2-((2-(methoxycarbonyl)phenyl)carbamoyl) phenyl)carbamoyl)pyrrolidine-1-carbonyl)phenyl)carbamoyl)phenyl)carbamoyl) pyrrolidine-1-carboxylate 7a:**

Compound **7a** was synthesized, following the procedure for **4f**, employing oxazinone **3k** and amine **3i**. Column chromatographic purification (eluent: 45% AcOEt/pet. Ether, R_f: 0.3) of the residue afforded **3** as a white fluffy solid (64%). mp: 111-113 °C; $[\alpha]^{27.3}_D$: 49.556° (*c* 1, $CHCl_3$); IR ($CHCl_3$) *v* (cm^{-1}): 3460, 3020, 1634, 1625, 1524, 1403; ^{1}H NMR (200 MHz, $CDCl_3$) δ: 12.08 (s, 1H, amide), $11.99_{rotamer}$ (s, 0.6H, amide), $11.96_{rotamer}$ (s, 0.4H, amide), $11.79_{rotamer}$ (s, 0.4H, amide), $11.74_{rotamer}$ (s, 0.6H,

amide), 10.66$_{rotamer}$ (s, 0.6H, amide), 10.64$_{rotamer}$ (s, 0.6H, amide), 8.81-8.77 (d, *J* = 8.46 Hz, 1H), 8.73-8.60 (m, 2H), 8.54-8.50 (d, *J* = 8.21 Hz, 1H), 8.11-8.07 (d, *J* = 7.96 Hz, 1H), 7.99-7.82 (m, 2H), 7.67-7.39 (m, 5H), 7.26-7.13 (m, 3H), 7.01-6.88 (m, 1H), 4.90-4.83 (m, 1H), 4.46-4.40$_{rotamer}$ (m, 0.5H), 4.28-4.22$_{rotamer}$ (m, 0.5H), 3.97-3.43 (m, 4H), 3.95 (s, 3H), 2.53-2.43 (m, 1H), 2.3-1.85 (m, 7H), 1.39 (s, 4H), 1.29 (s, 5H); ^{13}C NMR (50 MHz, $CDCl_3$) δ: 172.2, 171.6, 170.3, 168.8, 167.7, 166.8, 154.0, 140.9, 140.3, 139.8, 137.5, 137.3, 134.4, 133.3, 132.8, 131.5, 131.0, 128.9, 128.6, 127.4, 127.0, 123.4, 123.2, 122.9, 122.1, 121.2, 120.5, 120.0, 115.7, 80.0, 62.7, 61.9, 52.6, 51.2, 47.0, 46.6, 31.4, 30.0, 29.6, 28.1, 25.4, 24.2, 23.7; MALDI-TOF/TOF: 825.2853 $(M+Na)^+$, 841.8370 $(M+K)^+$; Anal. calcd for $C_{44}H_{46}N_6O_9$: C, 65.82; H, 5.77; N, 10.47; Found: C, 65.99; H, 5.57; N, 10.40.

2-[2-({1-[2-(2-{[1-(2,2-Dimethyl-propionyl)-pyrrolidine-2-carbonyl]-amino}-benzoylamino)-benzoyl]-pyrrolidine-2-carbonyl}-amino)-benzoylamino]-benzoic acid methyl ester 7d:

Compound **7d** was synthesized, following the procedure for **4f,** employing oxazinone **3l** and amine **3i**. Column chromatographic purification (eluent: 50% AcOEt/pet. Ether, R_f: 0.3) of the residue afforded **3** as a white fluffy solid (64%). mp: 100-102 °C; $[\alpha]^{25.6}_D$: 47.512° (*c* 1, $CHCl_3$); IR ($CHCl_3$) *ν* (cm^{-1}): 3444, 3020, 2400, 1673, 1606, 1585, 1523, 1477, 1439, 1297, 1097, 929; ^{1}H NMR (500 MHz, $CDCl_3$) δ: 12.07 (s, 1H, amide), 11.93 (s, 1H, amide), 11.44 (s, 1H, amide), 10.62 (s, 1H, amide), 8.78-8.76 (d, *J* = 8.24 Hz, 1H), 8.68-8.66 (d, *J* = 8.54 Hz, 1H), 8.65-8.64 (d, *J* = 8.54 Hz, 1H), 8.45-8.43 (d, *J* = 8.55 Hz, 1H), 8.10-8.08 (dd, *J* = 1.53 Hz, *J* = 7.93 Hz, 1H), 7.96-7.95 (d, *J* = 7.02 Hz, 1H), 7.86-7.85 (d, *J* = 7.32 Hz, 1H), 7.64-7.63 (d, *J* = 7.32 Hz, 1H), 7.55-7.52 (m, 2H), 7.50-7.47 (t, *J* = 7.32 Hz, 1H), 7.43-7.40 (t, *J* = 7.32 Hz, 1H), 7.23-7.20 (t, *J* = 7.32 Hz, 1H), 7.19-7.14 (m, 2H), 6.98-6.95 (t, *J* = 7.32 Hz, 1H), 4.89-4.86 (m, 1H), 4.63-4.61 (m, 1H), 3.96 (s, 3H), 3.93-3.91 (m, 2H), 3.82-3.78 (m, 1H), 3.75-3.70 (m, 1H), 2.52-2.45 (m, 1H), 2.24-2.15 (m, 2H), 2.12-2.04 (m, 2H), 1.98-1.90 (m, 2H), 1.78-1.71 (m, 1H), 1.28 (s, 9H); ^{13}C NMR (125 MHz, $CDCl_3$) δ: 177.5, 171.5, 170.4, 170.3, 168.9, 168.8, 167.1, 141.0, 140.3, 140.0, 137.4, 134.4, 133.3, 132.8, 131.2, 131.1, 128.9, 127.1, 123.8, 123.4, 123.2, 123.1, 122.9, 122.2, 121.4, 121.3, 120.6, 120.1, 115.9, 64.2, 62.6, 52.6, 51.3, 48.5, 39.1, 36.6, 30.0, 29.0, 27.5, 25.5, 24.7; MALDI-TOF/TOF: 809.4837 $(M+Na)^+$, 825.4543

$(M+K)^+$; Elemental analysis calculated for $C_{44}H_{46}N_6O_8$: C, 67.16; H, 5.89; N, 10.68. Found: C, 67.24; H, 5.76; N, 10.46.

2-[2-({1-[2-(2-{[1-(2,2-Dimethyl-propionyl)-pyrrolidine-2-carbonyl]-amino}-benzoylamino)-benzoyl]-pyrrolidine-2-carbonyl}-amino)-benzoylamino]-benzoic acid methyl amide 7f:

Compound **7f** was synthesized from ester **7d**, following the procedure for **4h**. Column chromatographic purification (eluent: 60% AcOEt/pet. Ether, R_f: 0.2) of the residue afforded **1** as white solid (93%). mp: 225-227 °C; $[\alpha]^{25.84}_D$: 156.356° (*c* 1, $CHCl_3$); IR ($CHCl_3$) *v* (cm^{-1}): 3260, 3020, 2401, 1681, 1651, 1623, 1583, 1520, 1428, 1297. ^1H NMR (400 MHz, $CDCl_3$) δ: 12.78 (s, 1H, amide), 12.37 (s, 1H, amide), 11.59 (s, 1H, amide), 10.32 (s, 1H, amide), 8.98-8.96 (d, *J* = 8.28 Hz, 1H), 8.56-8.54 (d, *J* = 8.28 Hz, 1H), 8.48-8.46 (d, *J* = 8.53 Hz, 1H), 8.33 (s, 1H, amide), 8.29-8.27 (d, *J* = 8.53 Hz, 1H), 7.89-7.88 (d, *J* = 7.78 Hz, 1H), 7.68-7.65 (d, *J* = 9.54 Hz, 1H), 7.65-7.63 (d, *J* = 8.78 Hz, 1H), 7.59-7.55 (m, 1H), 7.5-7.46 (m, 1H), 7.25-7.12 (m, 6H), 6.12-6.08 (m, 1H), 4.8-4.77 (dd, *J* = 2.76Hz, *J* = 7.78Hz, 1H), 4.5-4.27 (m, 1H), 4.4-4.37 (m, 1H), 4.13-4.08 (m, 1H), 4.03-3.97 (m, 1H), 3.9-3.77 (m, 2H), 2.78-2.77 (d, 4.52Hz, 2H), 2.42- 2.4 (m, 2H), 2.14- 2.11 (m, 4H), 1.94- 1.91 (m, 2H), 1.39 (s, 9H); ^{13}C NMR (100 MHz, $CDCl_3$) δ: 177.5, 171.0, 170.6, 169.6, 169.2, 167.7, 165.9, 140.7, 140.4, 138.4, 138.7, 137.8, 133.1, 132.7, 131.9, 131.3, 128.0, 127.7, 127.3, 127.0, 123.4, 123.1, 123.0, 122.5, 121.4, 120.5, 120.1, 119.1, 117.5, 64.0, 63.7, 50.7, 48.6, 38.9, 30.4, 28.5, 27.4, 26.8, 25.9, 25.0; MALDI-TOF/TOF: 809.8082 $(M+Na)^+$, 825.7921 $(M+K)^+$; Elemental analysis calculated for $C_{44}H_{47}N_7O_7$: C, 67.25; H, 6.03; N, 12.48. Found: C, 67.09; H, 6.04; N, 12.47.

(*R*)-*N*-(2-((2-(dimethylcarbamoyl)phenyl)carbamoyl)phenyl)-1-(2-(2-((*S*)-1-pivaloyl pyrrolidine-2-carboxamido)benzamido)benzoyl)pyrrolidine-2-carboxamide 7g:

The ester **4d** (0.1g) was taken in saturated methanolic dimethylamine solution (2 mL) and stirred at room temperature for 2 h. The solvent was removed under reduced pressure, and the residue was purified by column chromatography (eluent: 80% AcOEt/pet. Ether, R_f: 0.3) to afford **7g** (0.093 g, 93%) as a white solid. mp: 87-89 °C; $[\alpha]^{24.05}_D$: 41.952° (*c* 0.5, $CHCl_3$); IR ($CHCl_3$) *v* (cm^{-1}): 3340, 3020, 2401, 1600, 1522 1425, 1045, 929; ^1H NMR (500 MHz, $CDCl_3$) δ: 11.89 (s, 1H, amide), 11.44 (s, 1H, amide), 10.58 (s, 1H, amide), 10.27 (s, 1H, amide), 8.73-8.71 (d, *J* = 8.24 Hz, 1H), 8.67-8.66 (d, *J* = 8.24 Hz, 1H), 8.42-8.40 (d, *J* = 8.24 Hz, 1H), 8.24-8.23 (d, *J* =

8.24 Hz, 1H), 7.91-7.89 (d, *J* = 7.02 Hz, 1H), 7.70-7.68 (d, *J* = 7.02 Hz, 1H), 7.65-7.63 (d, *J* = 7.32 Hz, 1H), 7.52-7.49 (t, *J* = 8.24 Hz, 1H), 7.46-7.41 (m, 3H), 7.33-7.31 (d, *J* = 7.63 Hz, 1H), 7.20-7.15 (m, 2H), 7.00-6.97 (m, 2H), 4.84-4.81 (m, 1H), 4.62-4.60 (m, 1H), 3.96-3.90 (m, 2H), 3.82-3.79 (m, 1H), 3.69-3.66 (m, 1H), 3.08 (s, 3H), 2.97 (s, 3H), 2.52-2.46 (m, 1H), 2.20-2.14 (m, 2H), 2.10-2.02 (m, 2H), 1.97-1.87 (m, 3H), 1.27 (s, 9H); ^{13}C NMR (125 MHz, $CDCl_3$) δ: 177.5, 171.5, 170.3, 170.2, 167.2, 167.1, 140.0, 139.97, 137.1, 136.6, 133.2, 132.8, 131.1, 130.6, 128.9, 128.1, 127.1, 136.9, 124.7, 123.8, 123.5, 123.46, 123.1, 122.9, 122.0, 121.3, 121.2, 120.1, 119.8, 64.2, 62.6, 51.2, 48.5, 40.1, 35.7, 30.0, 29.0, 28.4, 27.4, 25.5, 24.6; MALDI-TOF/TOF: 800.8156 $(M+H)^+$, 823.1161 $(M+Na)^+$, 839.2504 $(M+K)^+$; Elemental analysis calculated for $C_{45}H_{49}N_7O_7$: C, C, 67.57; H, 6.17; N, 12.26. Found: C, 67.69; H, 6.02; N, 12.06.

(*S*)-*tert*-butyl 2-((2-((2-((*R*)-2-((2-(4-oxo-4H-benzo[d][1,3]oxazin-2-yl)phenyl)carbamoyl) pyrrolidine-1-carbonyl)phenyl)carbamoyl)phenyl) carbamoyl)pyrrolidine-1-carboxylate 7h:

Compound **7h** was synthesized from acid **7b**, following the procedure for **3g**. Column chromatographic purification (eluent: 60% AcOEt/pet. Ether, R_f: 0.3) of the residue afforded **1** as white solid (99%). mp: 115-117 °C; $[\alpha]^{27.7}_D$: -43.704° (*c* 1, $CHCl_3$); IR ($CHCl_3$) *v* (cm^{-1}): 2459, 3020, 1780, 1665, 1622, 1524, 1449, 1400; ^{1}H NMR (200 MHz, $CDCl_3$) δ: $12.85_{rotamer}$ (s, 0.5H, amide), $12.77_{rotamer}$ (s, 0.5H, amide), 12.09-$11.66_{rotamer}$ (s, 1H, amide), 10.67-$10.64_{rotamer}$ (d, 0.3H, amide), 10.40-$10.32_{rotamer}$ (d, 0.7H, amide), 8.81-8.43 (m, 3H), 8.34-8.26 (t, *J* = 8.59 Hz, 2H), 8.11-7.68 (m, 2H), 7.60-7.34 (m, 5H), 7.27-7.15 (m, 3H), 7.02-6.72 (m, 1H), 5.05-$5.02_{rotamer}$ (m, 0.1H), 4.95-4.83 (m, 0.9H), 4.46-$4.41_{rotamer}$ (m, 0.5H), 4.31-$4.23_{rotamer}$ (m, 0.5H), 3.84-3.40 (m, 4H), 2.51-1.9 (m, 8H), 1.43-$1.36_{rotamer}$ (m, 4H), $1.32_{rotamer}$ (s, 5H); ^{13}C NMR (50 MHz, $CDCl_3$) δ: 172.3, 171.8, 170.3, 170.0, 169.2, 167.1, 166.9, 158.1, 157.5, 154.5, 155.0, 154.1, 145.2, 140.4, 137.2, 136.9, 134.2, 133.3, 132.9, 132.7, 131.5, 131.1, 129.6, 128.9, 127.9, 127.5, 127.2, 126.1, 124.3, 123.3, 123.1, 122.3, 120.7, 116.6, 114.9, 114.1, 80.1, 79.9, 62.6, 62.1, 52.7, 51.3, 50.9, 50.7, 47.1, 46.8, 33.8, 31.9, 31.5, 30.6, 29.7, 29.5, 29.3, 29.1, 28.9, 28.2, 25.5, 25.2, 24.3, 23.8, 22.7, 14.1; MALDI-TOF/TOF: 793.7233 $(M+Na^+)$, 809.7417 $(M+K^+)$; Anal. calcd for $C_{43}H_{42}N_6O_7$: C, 67.44; H, 6.13; N, 10.22; Found: C, 67.58; H, 6.08; N, 10.10.

(R)-*N*-(2-(4-oxo-4H-benzo[d][1,3]oxazin-2-yl)phenyl)-1-(2-(2-((*S*)-1-pivaloylpyrrolidine-2-carboxamido)benzamido)benzoyl)pyrrolidine-2-carboxamide 7i:

Compound **7i** was synthesized from acid **7e**, following the procedure for **3g**. Column chromatographic purification (eluent: 60% AcOEt/pet. Ether, R_f: 0.3) of the residue afforded **1** as white solid (97%). mp: 115-117 °C; $[\alpha]^{27.7}_D$: -43.704° (*c* 1, $CHCl_3$); IR ($CHCl_3$) *v* (cm^{-1}): 3460, 3020, 1781, 1634, 1625, 1524, 1403; ^{1}H NMR (200 MHz, $CDCl_3$) δ: 12.79 (s, 1H, amide), 11.25 (s, 1H, amide), 10.34 (s, 1H, amide), 8.81-8.64 (m, 2H), 8.48-8.37 (m, 1H), 8.30-8.22 (m, 2H), 8.02-7.91 (m, 1H), 7.77-7.70 (m, 1H), 7.66-7.35 (m, 6H), 7.25-7.15 (m, 2H), 6.83-6.75 (m, 1H), 4.96-4.90 (m, 1H), 4.75-4.58 (m, 1H), 4.07-3.58 (s, 4H), 2.48-1.96 (m, 8H), 1.26 (s, 9H); ^{13}C NMR (50 MHz, $CDCl_3$) δ: 177.6, 171.4, 169.9, 168.9, 167.2, 162.9, 162.4, 161.3, 158.0, 157.2, 145.0, 140.2, 139.5, 137.1, 136.6, 134.0, 132.4, 130.9, 129.3, 128.8, 128.7, 127.7, 127.2, 126.1, 124.4, 123.3, 123.1, 122.9, 122.2, 121.1, 120.7, 120.6, 116.4, 114.7, 64.3, 61.9, 59.2, 50.7, 48.5, 46.9, 39.0, 36.4, 31.3, 29.6, 28.9, 27.3, 25.6, 25.3, 24.2; MALDI-TOF/TOF: 777.6476 $(M+Na)^+$, 794.7167 $(M+K)^+$; Anal. calcd for $C_{43}H_{42}N_6O_7$: C, 67.44; H, 6.13; N, 10.22; Found: C, 67.58; H, 6.08; N, 10.10.

(*S*)-*tert*-butyl 2-((2-((2-((*R*)-2-((2-((2-(isobutoxycarbonyl)phenyl)carbamoyl) phenyl)carbamoyl) pyrrolidine-1-carbonyl)phenyl)carbamoyl)phenyl) carbamoyl)pyrrolidine-1-carboxylate 7j:

Compound **7j** was synthesized by reacting benzoxazinone **7h** with isobutanol, following the procedure for **4f** using isobutanol as solvent. Column chromatographic purification (eluent: 60% AcOEt/pet. Ether, R_f: 0.3) of the residue afforded **7j** as white solid (87%). mp: 83-85 °C completes at 96 °C; $[\alpha]^{25.8}_D$: 30.856° (*c* 1, $CHCl_3$); IR ($CHCl_3$) *v* (cm^{-1}): 3444, 3019, 2400, 1680, 1654, 1523, 1449, 929; ^{1}H NMR (200 MHz, $CDCl_3$) δ: 12.20 (s, 1H, amide), $12.01_{rotamer}$ (s, 0.6H, amide), $11.98_{rotamer}$ (s, 0.4H, amide), $11.79_{rotamer}$ (s, 0.4H, amide), $11.74_{rotamer}$ (s, 0.6H, amide), 10.66 (bs, 1H, amide), 8.80-8.76 (d, *J* = 8.34 Hz, 1H), 8.73-8.61 (m, 2H), 8.54-8.50 (d, *J* = 8.34 Hz, 1H), 8.12-8.08 (d, *J* = 7.71 Hz, 1H), 8.00-7.83 (m, 2H), 7.68-7.64 (d, *J* = 7.71 Hz, 1H), 7.57-7.39 (m, 4H), 7.25-7.12 (m, 4H), 7.02-6.89 (m, 1H), 5.17-5.08 (m, 1H), 4.90-4.83 (m, 1H), $4.49\text{-}4.40_{rotamer}$ (m, 0.5H), $4.28\text{-}4.22_{rotamer}$ (m, 0.5H), 3.97-3.42 (m, 4H), 2.51-1.68 (m, 9H), 1.39-1.30 (m, 12H), 1.01-0.9 (m, 3H); ^{13}C NMR (50 MHz, $CDCl_3$) δ: 172.2, 171.7, 170.3, 168.0, 167.7, 166.9, 154.1, 140.9, 140.3, 139.8, 137.5, 137.3, 134.2, 133.2, 132.8, 131.5, 131.1, 130.9, 129.0, 128.6, 127.1, 123.4, 123.1,

122.1, 121.2, 120.6, 120.0, 116.4, 80.0, 73.9, 62.6, 61.9, 51.2, 47.0, 46.7, 36.6, 31.5, 30.5, 30.0, 28.7, 28.2, 25.4, 23.7, 19.4; MALDI-TOF/TOF: 867.7450 $(M+Na)^+$, 883.7388 $(M+K)^+$; Anal. calcd for $C_{47}H_{52}N_6O_9$: C, 66.81; H, 6.20; N, 9.95; Found: C, 66.61; H, 6.09; N, 9.88.

(*S*)-*tert*-butyl 2-((2-((2-((*R*)-2-((2-((2-((pentyloxy)carbonyl)phenyl)carbamoyl) phenyl)carbamoyl)pyrrolidine-1-carbonyl)phenyl)carbamoyl)phenyl) carbamoyl)pyrrolidine-1-carboxylate 7k:

Compound **7k** was by reacting benzoxazinone **7h** with isobutanol, following the procedure for **4f** in DMF as solvent. Column chromatographic purification (eluent: 60% AcOEt/pet. Ether, R_f: 0.3) of the residue afforded **7k** as white solid (87%). mp: 81-83 °C completes at 98 °C; $[\alpha]^{25.2}_D$: 30.892° (*c* 1, $CHCl_3$); IR ($CHCl_3$) *v* (cm^{-1}): 3445, 2926, 1691, 1655, 1585, 1522, 1448, 1391, 1296, 1260, 1164; ^{1}H NMR (200 MHz, $CDCl_3$) δ: 12.16 (s, 1H, amide), $12.00_{rotamer}$ (s, 0.6H, amide), $11.97_{rotamer}$ (s, 0.4H, amide), $11.79_{rotamer}$ (s, 0.4H, amide), $11.74_{rotamer}$ (s, 0.6H, amide), 10.66 (bs, 1H, amide), 8.80-8.76 (d, *J* = 8.34 Hz, 1H), 8.67-8.63 (m, 2H), 8.54-8.50 (d, *J* = 8.34 Hz, 1H), 8.13-8.09 (d, *J* = 7.83 Hz, 1H), 8.01-7.82 (m, 2H), 7.68-7.64 (d, *J* = 7.96 Hz, 1H), 7.57-7.39 (m, 4H), 7.24-7.12 (m, 3H), 6.97-6.89 (m, 1H), 4.90-4.83 (m, 1H), $4.45\text{-}4.40_{rotamer}$ (m, 0.5H), $4.28\text{-}4.22_{rotamer}$ (m, 0.5H), 4.04 (s, 2H), 3.97-3.42 (m, 4H), 2.51-1.85 (m, 8H), $1.39\text{-}1.38_{rotamer}$ (m, 4H), $1.30_{rotamer}$ (m, 5H), 1.05 (s, 9H); ^{13}C NMR (50 MHz, $CDCl_3$) δ: 172.2, 171.7, 170.3, 168.4, 167.7, 166.9, 154.8, 154.1, 141.0, 140.3, 139.8, 137.5, 137.3, 134.4, 133.3, 132.8, 131.6, 131.1, 130.7, 128.9, 128.6, 127.0, 123.4, 123.2, 122.9, 121.2, 120.8, 120.6, 120.0, 116.0, 80.01, 79.8, 74.9, 62.5, 61.9, 51.2, 47.0, 46.7, 36.6, 31.5, 30.5, 30.0, 28.2, 26.5, 25.4, 24.6, 23.7; MALDI-TOF/TOF: 881.8750 $(M+Na)^+$, 898.4380 $(M+K)^+$; Anal. calcd for $C_{48}H_{54}N_6O_9$: C, 67.12; H, 6.34; N, 9.78; Found: C, 67.00; H, 6.58; N, 9.79.

isobutyl 2-(2-((*R*)-1-(2-(2-((*S*)-1-pivaloylpyrrolidine-2-carboxamido)benzamido) benzoyl)pyrrolidine-2-carboxamido)benzamido)benzoate 7l:

Compound **7l** was synthesized by reacting benzoxazinone **7i** with isobutanol, following the procedure for **4f**, using isobutanol as solvent. Column chromatographic purification (eluent: 60% AcOEt/pet. Ether, R_f: 0.3) of the residue afforded **7l** as white solid (82%). mp: 102-104 °C; $[\alpha]^{25.7}_D$: 47.104° (*c* 1, $CHCl_3$); IR ($CHCl_3$) *v* (cm^{-1}): 3448, 3020, 2401, 1655, 1625, 1606, 1585, 1522, 1477, 1439, 1297, 1026, 929; ^{1}H

NMR (200 MHz, $CDCl_3$) δ: 12.13 (s, 1H, amide), 11.90 (s, 1H, amide), 11.37 (s, 1H, amide), 10.55 (s, 1H, amide), 8.70-8.66 (d, 8.34 Hz, 1H), 8.61-8.55 (dd, *J* = 3.66 Hz, *J* = 8.21 Hz, 2H), 8.37-8.33 (d, *J* = 8.21 Hz, 1H), 8.04-8.00 (d, *J* = 7.96 Hz, 1H), 7.91-7.88 (d, *J* = 7.45 Hz, 1H), 7.80-7.76 (d, *J* = 7.71 Hz, 1H), 7.58-7.54 (d, *J* = 7.83 Hz, 1H), 7.48-7.30 (m, 4H), 7.16-7.05 (m, 3H), 6.93-6.86 (t, *J* = 7.58 Hz, 1H), 5.09-5.00 (m, 1H), 4.82-4.75 (m, 1H), 4.56-4.50 (m, 1H), 3.87-3.58 (m, 4H), 2.49-2.36 (m, 1H), 2.12-1.59 (m, 9H), 1.29-1.26 (d, *J* = 5.94 Hz, 1H), 1.19 (s, 9H), 1.13-1.12 (d, *J* = 3.54 Hz, 1H); ^{13}C NMR (50 MHz, $CDCl_3$) δ: 177.5, 171.6, 170.4, 168.1, 167.8, 167.1, 141.0, 140.3, 140.0, 137.3, 134.2, 133.3, 132.8, 131.2, 131.0, 129.0, 127.1, 123.8, 123.4, 123.2, 123.0, 122.2, 120.6, 120.2, 116.5, 74.0, 64.3, 62.7, 60.4, 51.3, 48.6, 39.1, 30.1, 28.8, 27.5, 27.1, 25.5, 21.0, 19.4, 14.2, 9.7; MALDI-TOF/TOF: 851.7893 $(M+Na)^+$, 867.7849 $(M+K)^+$; Anal. calcd for $C_{47}H_{52}N_6O_8$: C, 68.10; H, 6.32; N, 10.14; Found: C, 68.17; H, 6.21; N, 10.00.

pentyl 2-(2-((*R*)-1-(2-(2-((*S*)-1-pivaloylpyrrolidine-2-carboxamido)benzamido) benzoyl)pyrrolidine-2-carboxamido)benzamido)benzoate 7m:

Compound **7m** was synthesized by reacting benzoxazinone **7i** with n-pentanol, following the procedure for **4f** using DMF as solvent. Column chromatographic purification (eluent: 60% AcOEt/pet. Ether, R_f: 0.3) of the residue afforded **7m** as white solid (95%). mp: 85-87 °C; $[\alpha]^{25.8}_D$: 51.316° (*c* 1, $CHCl_3$); IR ($CHCl_3$) *v* (cm^{-1}): 3445, 3020, 2400, 1673, 1606, 1585, 1523, 1477, 1439, 1297, 1096, 1030, 928; ^{1}H NMR (200 MHz, $CDCl_3$) δ: 12.12 (s, 1H, amide), 11.89 (s, 1H, amide), 11.38 (s, 1H, amide), 10.55 (s, 1H, amide), 8.70-8.67 (d, *J* = 7.83 Hz, 1H), 8.61-8.55 (dd, *J* = 4.29 Hz, *J* = 8.21 Hz, 2H), 8.38-8.34 (d, *J* = 8.21 Hz, 1H), 8.04-8.00 (d, *J* = 1.52 Hz, *J* = 7.96 Hz, 1H), 7.93-7.88 (m, 2H), 7.80-7.76 (d, *J* = 7.96 Hz, 1H), 7.58-7.55 (d, *J* = 7.96 Hz, 1H), 7.48-7.31 (m, 4H), 7.18-7.05 (m, 3H), 6.93-6.86 (m, 1H), 5.27-5.15 (m, 1H), 4.83-4.75 (m, 1H), 4.56-4.50 (m, 1H), 3.93-3.58 (m, 4H), 2.50-2.37 (m, 1H), 2.17-1.82 (m, 9H), 1.30-1.30 (d, *J* = 6.16 Hz, 1H), 1.20 (s, 9H); ^{13}C NMR (50 MHz, $CDCl_3$) δ: 177.6, 171.6, 170.4, 168.0, 167.8, 167.2, 141.0, 140.3, 140.0, 137.3, 134.2, 133.3, 132.8, 131.3, 131.1, 129.0, 127.2, 123.8, 123.5, 123.2, 123.0, 122.2, 121.4, 120.6, 120.2, 116.5, 69.5, 64.3, 62.7, 51.4, 48.6, 39.2, 36.5, 31.5, 30.1, 29.1, 27.5, 25.6, 21.9; MALDI-TOF/TOF: 865.7764 $(M+Na)^+$, 881.8735 $(M+K)^+$; Anal. calcd for $C_{48}H_{54}N_6O_8$: C, 68.39; H, 6.46; N, 9.97; Found: C, 68.48; H, 6.40; N, 9.69.

Boc *hetero*-chiral dodecamer OMe 8a:

Compound **8a** was synthesized from benzoxazinone **7h** and amine **7c**, following the procedure for **4f**. Column chromatographic purification (eluent: 70% AcOEt/pet. Ether, R_f: 0.3) of the residue afforded **8a** as fluffy white solid (75%). mp: 132-134 °C; $[\alpha]^{27.9}_D$: 18.78° (*c* 1, $CHCl_3$); IR ($CHCl_3$) *v* (cm^{-1}): 3458, 3020, 1653, 1585, 1521, 1449, 1396, 1298, 1216, 929; ^{1}H NMR (500 MHz, $CDCl_3$) δ: 12.08 (s, 1H, amide), 11.95 (s, 2H, amide), 11.92 (s, 1H, amide), $11.77_{rotamer}$ (s, 0.5H, amide), $11.71_{rotamer}$ (s, 0.5H, amide), $10.71\text{-}10.62_{rotamer}$ (s, 3H, amide), 8.77-8.60 (m, 5H), 8.49-8.45 (d, *J* = 8.34 Hz, 1H), 8.37-8.33 (m, 2H), 8.11-8.07 (dd, *J* = 1.14 Hz, *J* = 7.83 Hz, 1H), 7.93-7.81 (m, 4H), 7.69-7.60 (m, 3H), 7.56-7.37 (m, 8H), 7.23-7.13 (m, 3H), 7.07-7.89 (m, 5H), 4.84-4.72 (m, 3H), $4.45\text{-}4.40_{rotamer}$ (m, 0.5H), $4.29\text{-}4.23_{rotamer}$ (m, 0.5H), 3.95-3.44 (m, 8H), 3.94 (s, 3H), 2.55-2.35 (m, 3H), 2.21-1.78 (m, 13H), $1.38_{rotamer}$ (s, 3H), $1.31_{rotamer}$ (s, 6H); ^{13}C NMR (125 MHz, $CDCl_3$) δ: 172.2, 171.7, 170.3, 170.2, 170.1, 170.0, 169.8, 168.7, 167.3, 167.2, 166.9, 140.9, 140.2, 140.0, 139.8, 137.3, 137.1, 134.4, 133.3, 133.1, 131.4, 131.0 129.1, 128.7, 127.2, 124.0, 123.4, 123.3, 123.2, 123.0, 122.2, 121.9, 121.2, 120.9, 120.5, 120.2, 120.1, 119.9, 119.6, 119.5, 115.8, 80.0, 79.8, 62.7, 52.6, 51.3, 51.1, 31.5, 29.9, 28.2, 25.5, 25.4, 24.2, 23.7; MALDI-TOF/TOF: 1497.3073 $(M+Na)^+$, 1513.5162 $(M+K)^+$; Anal. calcd for $C_{82}H_{80}N_{12}O_{15}$: C, 66.84; H, 5.47; N, 11.41; Found: C, 66.91; H, 5.36; N, 11.29.

Piv *hetero*-chiral dodecamer OMe 8c:

Compound **8c** was synthesized from benzoxazinone **7i** and amine **7c**, following the procedure for **4f**. Column chromatographic purification (eluent: 75% AcOEt/pet. Ether, R_f: 0.2) of the residue afforded **8c** as a fluffy white solid (48%). mp: 171-172 °C; $[\alpha]^{27.8}_D$: 15.852° (*c* 1, $CHCl_3$); IR ($CHCl_3$) *v* (cm^{-1}): 3455, 3020, 1635, 1522, 1402, 1216; ^{1}H NMR (200 MHz, $CDCl_3$) δ: 12.07 (s, 1H, amide), 11.95 (s, 1H, amide), 11.91 (broad, 2H, amide), 11.45 (s, 1H, amide), 10.70 (broad, 2H, amide), 10.62 (s, 1H, amide), 8.78-8.60 (m, 5H), 8.41-8.32 (m, 1H), 8.12-8.07 (dd, *J* = 1.53 Hz, *J* = 7.96 Hz, 1H), 7.95-7.81 (m, 4H), 7.67-7.37 (m, 11H), 7.26-7.14 (m, 3H), 7.07-6.89 (m, 5H), 4.85-4.71 (m, 3H), 4.63-4.58 (m, 1H), 3.95-3.51 (m, 8H), 3.95 (s, 3H), 2.53-2.37 (m, 3H), 2.26-1.89 (m, 13H), 1.27 (s, 9H); ^{13}C NMR (50 MHz, $CDCl_3$) δ: 177.5, 174.9, 172.4, 171.5, 170.2, 170.3, 170.2, 170.1, 168.8, 167.8, 167.4, 167.3, 167.1, 166.2, 140.9, 140.3, 140.0, 137.7, 137.2, 137.0, 135.7, 134.4, 133.3, 132.8, 131.1, 129.1, 128.8, 127.2, 127.0, 124.1, 124.0, 123.8, 123.4, 123.2, 123.1, 122.8, 122.7,

122.2, 122.1, 122.0, 121.3, 121.2, 121.0, 120.9, 120.6, 120.1, 119.9, 119.7, 119.5, 115.8, 64.2, 62.7, 52.7, 51.2, 48.5, 39.1, 30.0, 29.6, 27.4, 25.5, 25.4; MALDI-TOF/TOF: 1481.0557 $(M+Na)^+$, 1496.2532 $(M+K)^+$; Anal. calcd for $C_{82}H_{80}N_{12}O_{14}$: C, 67.57; H, 5.53; N, 11.53; Found: C, 67.69; H, 5.41; N, 11.33.

Piv *hetero*-chiral dodecamer NHMe 8d:

Compound **8d** was synthesized from **8b**, following the procedure for **4h**. Column chromatographic purification (eluent: 80% AcOEt/pet. Ether, R_f: 0.3) of the residue afforded **8d** as a fluffy white solid (90%). mp: 162-164 °C; $[\alpha]^{28.0}_D$: 54.088° (*c* 1, $CHCl_3$); IR ($CHCl_3$) *v* (cm^{-1}): 3456, 1635, 1521, 1404, 1298; ^1H NMR (200 MHz, $CDCl_3$) δ: 12.40 (s, 1H, amide), 12.30 (s, 1H, amide), 11.69 (s, 1H, amide), 11.69 (s, 1H, amide), 11.38 (s, 1H, amide), 10.54 (s, 1H, amide), 10.42 (s, 1H, amide), 10.37 (s, 1H, amide), 8.79-8.75 (d, *J* = 8.34 Hz, 1H), 8.64-8.56 (m, 2H), 8.39-8.21 (m, 5H), 7.87-7.83 (d, *J* = 7.58 Hz, 1H), 7.71-7.54 (m, 7H), 7.49-7.31 (m, 1H), 7.21-7.07 (m, 1H), 6.45-6.35 (t, *J* = 7.58 Hz, 1H), 4.76-4.70 (m, 2H), 4.60-4.49 (m, 2H), 3.88-3.55 (m, 7H), 3.38-3.25 (m, 1H), 2.74-2.72 (d, *J* = 4.42 Hz, 3H), 2.45-2.23 (m, 3H), 2.05-1.91 (m, 13H), 1.19 (s, 9H); ^{13}C NMR (50 MHz, $CDCl_3$) δ: 177.5, 171.5, 170.4, 170.3, 169.7, 169.2, 167.5, 167.5, 167.1, 166.4, 140.3, 139.9, 139.8, 138.9, 137.1, 137.0, 136.3, 133.1, 132.8, 132.0, 131.0, 130.9, 129.0, 128.5, 128.2, 127.2, 127.1, 126.9, 124.9, 124.1, 123.7, 123.6, 123.5, 123.1, 122.9, 122.6, 122.0, 121.3, 121.0, 120.7, 120.6, 120.3, 120.0, 119.2, 118.8, 64.2, 63.2, 62.7, 62.1, 60.3, 54.0, 53.4, 53.1, 51.3, 50.8, 50.7, 48.5, 39.0, 30.1, 30.0, 29.8, 29.6, 27.4, 26.8, 26.3, 25.6, 25.3, 25.1; MALDI-TOF/TOF: 1478.1663 $(M+Na)^+$, 1498.2644 $(M+K)^+$; Anal. calcd for $C_{82}H_{81}N_{13}O_{13}$: C, 67.62; H, 5.61; N, 12.50; Found: C, 67.89; H, 5.49; N, 12.69.

Piv *hetero*-chiral octadecamer OMe 9a:

Compound **9b** was synthesized from benzoxazinone **7i** and amine **8b**, following the procedure for **4f**. Column chromatographic purification (eluent: 85% AcOEt/pet. Ether, R_f: 0.2) of the residue afforded **9a** as a fluffy white solid (52%). mp: 173-175 °C; $[\alpha]^{28.2}_D$: 22.312° (*c* 1, $CHCl_3$); IR ($CHCl_3$) *v* (cm^{-1}): 3461, 3020, 1626, 1524, 1403, 1216; ^1H NMR (400 MHz, $CDCl_3$) δ: 12.07 (s, 1H, amide), 11.93 (s, 1H, amide), 11.90 (broad, 4H, amide), 11.44 (s, 1H, amide), 10.70 (broad, 4H, amide), 10.60 (s, 1H, amide), 8.77-8.75 (d, *J* = 8.28 Hz, 1H), 8.72-8.67 (m, 4H), 8.64-8.62 (d, *J* = 8.28 Hz, 1H), 8.41-8.34 (m, 5H), 8.11-8.09 (d, *J* = 7.78 Hz, 1H), 7.94-7.90 (m, 5H), 7.85-

7.83 (d, *J* = 7.78 Hz, 1H), 7.68-7.62 (m, 5H), 7.55-7.50 (m, 3H), 7.47-7.42 (m, 9H), 7.23-7.16 (m, 4H), 7.08-7.01 (m, 9H), 6.99-6.92 (m, 2H), 4.84-4.76 (m, 5H), 4.64-4.61 (m, 1H), 3.95 (s, 3H), 3.94-3.80 (m, 7H), 3.67-3.62 (m, 2H), 3.54-3.49 (m, 3H), 2.50-2.39 (m, 4H), 2.21-1.92 (m, 8H), 1.91-1.80 (m, 4H), 1.28 (s, 9H); ^{13}C NMR (100 MHz, $CDCl_3$) δ: 177.5, 171.5, 170.4, 170.23, 170.2, 170.1, 167.8, 167.4, 167.3, 140.3, 140.0, 137.2, 137.1, 134.4, 133.4, 133.2, 132.9, 131.1, 131.0, 129.1, 128.8, 127.2, 127.1, 124.1, 123.5, 123.2, 123.1, 122.8, 122.2, 122.1, 121.3, 121.0, 120.6, 119.6, 77.2, 64.2, 62.7, 52.7, 51.3, 51.2, 48.6, 39.1, 31.6, 30.0, 29.7, 29.3, 27.5, 25.6, 25.5; MALDI-TOF/TOF: 2149.7144 $(M+Na)^+$, 2165.8052 $(M+K)^+$; Anal. calcd for $C_{120}H_{114}N_{18}O_{20}$: C, 67.72; H, 5.40; N, 11.85; Found: C, 67.56; H, 5.52; N, 12.02.

Piv *hetero*-chiral octadecamer NHMe 9b:

Compound **9b** was synthesized from **9a**, following the procedure for **4h**. Column chromatographic purification (eluent: 90% AcOEt/pet. Ether, R_f: 0.2) of the residue afforded **9c** as a fluffy white solid (87%). mp: 163-165 °C; $[\alpha]^{28.2}_D$: 39.624° (*c* 1, $CHCl_3$); IR ($CHCl_3$) *v* (cm^{-1}): 3461, 3020, 1627, 1525, 1450, 1410, 1298, 1216, 929; ^{1}H NMR (500 MHz, $CDCl_3$) δ: 12.49 (s, 1H, amide), 12.33 (s, 1H, amide), 11.89 (s, 1H, amide), 11.88 (s, 1H, amide), 11.75 (s, 1H, amide), 11.74 (s, 1H, amide), 11.45 (s, 1H, amide), 10.68 (s, 1H, amide), 10.66 (s, 1H, amide), 10.60 (s, 1H, amide), 10.50 (s, 1H, amide), 10.43 (s, 1H, amide), 8.89-8.87 (d, *J* = 8.24 Hz, 1H), 8.72-8.67 (m, 4H), 8.43-8.33 (m, 7H), 7.94-7.90 (m, 3H), 7.77-7.62 (m, 8H), 7.57-7.51 (m, 3H), 7.48-7.39 (m, 9H), 7.24-7.18 (m, 4H), 7.06-6.93 (m, 8H), 6.47-6.44 (t, *J* = 7.63 Hz, 1H), 4.84-4.76 (m, 4H), 4.66-4.61 (m, 2H), 3.95-3.79 (m, 8H), 3.70-3.65 (m, 2H), 3.55-3.53 (m, 1H), 3.46-3.42 (m, 1H), 2.82-2.81 (d, *J* = 4.88 Hz, 3H), 2.51-2.31 (m, 6H), 2.21-1.78 (m, 18H), 1.28 (s, 9H); ^{13}C NMR (125 MHz, $CDCl_3$) δ: 170.4, 170.3, 169.7, 169.6, 169.2, 167.7, 167.4, 140.5, 140.0, 139.9, 139.0, 137.2, 137.1, 137.0, 133.3, 133.2, 132.9, 132.8, 132.2, 131.1, 131.0, 129.1, 127.3, 127.1, 127.0, 124.1, 124.0, 123.8, 123.5, 123.1, 123.0, 122.8, 122.7, 122.1, 120.8, 120.6, 119.8, 63.3, 62.7, 62.0, 51.2, 50.7, 48.6, 39.1, 34.7, 30.2, 30.1, 30.0, 29.8, 29.7, 27.5, 26.9, 25.6, 25.4, 25.1; MALDI-TOF/TOF: 2149.7996 $(M+Na)^+$, 2166.7605 $(M+K)^+$; Anal. calcd for $C_{120}H_{115}N_{19}O_{19}$: C, 67.75; H, 5.45; N, 12.51; Found: C, 67.56; H, 5.36; N, 12.36.

(*R*)-methyl 2-(2-(1-(2-(2-nitrobenzamido)benzoyl)pyrrolidine-2 carboxamido) benzamido)benzoate 10a:

Compound **10a** was synthesized, following the procedure for **4f,** using oxazinone **2d** and amine **3i**. Purification by column chromatography (eluent: 60% AcOEt/pet. Ether, R_f: 0.3) afforded **10a** as a waxy solid (67%). $[\alpha]^{26.35}_D$: 36.9° (*c* 1, $CHCl_3$); IR ($CHCl_3$) *v* (cm^{-1}): 3461, 3020, 2401, 1673, 1587, 1532, 1475, 1435, 1314, 1271, 929; ^1H NMR (500 MHz, $CDCl_3$) δ: 12.08 (s, 1H, amide), 11.76 (s, 1H, amide), 9.92 (s, 1H, amide), 8.70-8.68 (d, *J* = 8.24 Hz, 1H), 8.51-8.49 (d, *J* = 8.24 Hz, 1H), 8.34-8.32 (d, *J* = 8.54 Hz, 1H), 8.11-8.09 (d, *J* = 7.93 Hz, 1H), 8.07-8.06 (d, *J* = 8.24 Hz, 1H), 7.86-7.85 (d, *J* = 7.93 Hz, 1H), 7.72-7.71 (d, *J* = 7.63 Hz, 1H), 7.86-7.57 (m, 4H), 7.52-7.49 (t, *J* = 7.93 Hz, 1H), 7.46-7.43 (t, *J* = 8.24 Hz, 1H), 7.23-7.17 (m, 3H), 4.81-4.78 (m, 1H), 3.96 (s, 3H), 3.82-3.77 (m, 1H), 3.60-3.56 (m, 1H), 2.50-2.42 (m, 1H), 2.18-1.94 (m, 3H); ^{13}C NMR (125 MHz, $CDCl_3$) δ: 170.4, 169.4, 168.9, 167.7, 165.0, 146.3, 140.9, 140.1, 135.9, 134.6, 133.7, 133.1, 133.0, 131.1, 131.0, 130.2, 129.1, 127.4, 127.1, 125.8, 124.4, 123.9, 123.4, 123.3, 122.2, 121.3, 120.6, 120.2, 115.8, 62.0, 52.6, 50.3, 30.1, 29.7, 25.2; MALDI-TOF/TOF: 658.5194 $(M+Na)^+$, 674.6186 $(M+K)^+$; Anal. calcd. for $C_{34}H_{29}N_5O_8$: C, 64.25; H, 4.60; N, 11.02. Found: C, 64.36; H, 4.52; N, 11.12.

(*R*)-methyl 2-(2-(1-(2-(2-aminobenzamido)benzoyl)pyrrolidine-2-carboxamido) benzamido)benzoate 10b:

Compound **10b** was synthesized from **10a**, following the procedure for **2b**. **10b** was directly used for the next reaction without further purification.

(*R*)-1-(2-(2-aminobenzamido)benzoyl)-*N*-(2-((2-(methylcarbamoyl)phenyl) carbamoyl)phenyl)pyrrolidine-2-carboxamide 10c:

10c was synthesized from **4b,** following the procedure for **4h**. Compound **10c** was isolated as a fluffy white solid and was used for the next reaction without further purification.

(*R*)-1-(2-(2-((2-bromopropan-2-yl)amino)benzamido)benzoyl)-*N*-(2-((2-(methylcarbamoyl)phenyl)carbamoyl)phenyl) pyrrolidine-2-carboxamide 10d:

To a solution of **10c** (0.1 g, 0.1574 mmol, 1 equiv.) and triethylamine (0.03 mL, 0.2204 mmol, 1.4 equiv.) in DCM (1 mL), α-bromoisobutyryl bromide (0.023 mL, 0.1888 mmol, 1.2 equiv.) was added drop wise at 0 °C. After completion of the reaction, the reaction mixture was diluted with DCM and was washed with $NaHCO_3$ solution followed by water and then $KHSO_4$ solution. DCM layer was dried over Na_2SO_4 and was concentrated *in vacuo*. The compound **10d** (0.08 g, 65%) was

obtained by column purification (eluent: 60% AcOEt/pet. Ether, R_f: 0.3) as a white solid. mp: 144-146°C; $[\alpha]^{24.06}_D$: 110.06° (*c* 1, $CHCl_3$); IR ($CHCl_3$) *v* (cm^{-1}): 3421, 3310, 3020, 2401, 1676, 1647, 1604, 1584, 1525, 1474, 1436, 1301, 1037; ^{1}H NMR (400 MHz, $CDCl_3$) δ: 12.27 (s, 1H, amide), 12.16 (s, 1H, amide), 11.83 (s, 1H, amide), 10.37 (s, 1H, amide), 8.82-8.79 (d, *J* = 8.28 Hz, 1H), 8.42-8.37 (m, 3H), 7.82-7.79 (m, 2H), 7.57-7.51 (m, 3H), 7.45-7.43 (d, *J* = 7.28 Hz, 1H), 7.39-7.35 (m, 2H), 7.24-7.18 (m, 2H), 7.1-7.06 (t, *J* = 7.53 Hz, 3H), 6.87 (m,1H), 6.79-6.75 (t, *J* = 7.53 Hz, 1H), 4.93-4.89 (dd, *J* = 5.27 Hz, *J* = 8.28 Hz, 1H), 3.87-3.83 (m, 1H), 3.78-3.74 (m, 1H), 2.98-2.97 (d, *J* = 4.52 Hz, 3H), 2.48-2.39 (m, 2H), 2.35- 2.37 (m, 2H), 2.06 (s, 6H); ^{13}C NMR (100 MHz, $CDCl_3$) δ: 170.8, 170.3, 170.1, 169.6, 167.8, 166.7, 140.4, 139.1, 138.5, 136.5, 133.4, 132.2, 131.9, 1287.7, 127.3, 127.9, 125.0, 123.7, 123.65, 123.6, 123.55, 122.6, 121.6, 121.3, 121.25, 121.1, 119.4, 77.2, 62.8, 60.1, 50.7, 31.8, 31.7, 29.9, 26.8, 25.2; MALDI-TOF/TOF: 777.4641 $(M+Na)^+$, 793.4367 $(M+K)^+$; Elemental analysis calculated for $C_{38}H_{37}BrN_6O_6$: C, 60.56; H, 4.95; Br, 10.60; N, 11.15. Found: C, 60.66; H, 4.98; Br, 10.62; N, 11.15.

(*R*)-1-(2-(2-(2-azido-2-methylpropanamido)benzamido)benzoyl)-*N*-(2-((2-(methyl carbamoyl)phenyl)carbamoyl)phenyl)pyrrolidine-2-carboxamide 10e:

To a solution of **10d** (0.11 g, 0.146 mmol, 1 equiv) in dry DMF (1 mL) was added sodium azide (0.028 g, 0.439 mmol, 3 equiv) and catalytic amount of LiCl. The reaction mixture was stirred at room temperature for 24h. The reaction mixture was then added to water and the water layer was extracted with DCM. The combined organic layer was given water and brine wash. The organic layer was dried over Na_2SO_4, filtered and solvent was stripped off under reduced pressure. The compound **10e** (0.1 g, 96%) was obtained by column purification (eluent: 55% AcOEt/pet. Ether, R_f: 0.3) as a white solid. mp: 120-122 °C; $[\alpha]^{24.5}_D$: 80.176° (*c* 1, $CHCl_3$); IR ($CHCl_3$) *v* (cm^{-1}): 3295, 2926, 2114, 1655, 1584, 1513, 1433, 1407, 1299, 1163, 1048; ^{1}H NMR (200 MHz, $CDCl_3$) δ: 12.25 (s, 1H, amide), 12.14 (s, 1H, amide), 11.71 (s, 1H, amide), 10.36 (s, 1H, amide), 8.82-8.78 (d, *J* = 8.21 Hz, 1H), 8.47-8.39 (m, 3H), 7.84-7.79 (m, 2H), 7.58-7.50 (m, 3H), 7.45-7.33 (m, 3H), 7.23-7.05 (m, 3H), 6.84-6.77 (m, 2H), 4.95-4.88 (m, 1H), 3.93-3.69 (m, 2H), 3.0-2.98 (d, *J* = 4.80 Hz, 3H), 2.50-2.25 (m, 2H), 2.11- 1.85 (m, 2H), 1.63 (s, 3H), 1.60 (s, 3H); ^{13}C NMR (125 MHz, $CDCl_3$) δ: 171.7, 170.3, 170.2, 169.7, 167.8, 166.7, 140.4, 138.8, 136.6, 133.4, 132.2, 132.0, 131.3, 128.7, 127.3, 127.26, 126.9, 124.8, 123.8, 123.6, 123.5, 122.7,

121.6, 121.56, 121.4, 121.3, 119.4, 64..7, 62.8, 50.8, 29.9, 29.6, 26.8, 25.3, 24.7, 24.6; MALDI-TOF/TOF: 738.9874 $(M+Na)^+$, 755.0415 $(M+K)^+$; Elemental analysis calculated for $C_{38}H_{37}N_9O_6$: C, 63.77; H, 5.21; N, 17.61. Found: C, 63.69; H, 5.03; N, 17.69.

(*R*)-1-(2-(2-(2-amino-2-methylpropanamido)benzamido)benzoyl)-*N*-(2-((2-(methylcarbamoyl)phenyl)carbamoyl)phenyl)pyrrolidine-2-carboxamide 10f:

Compound **10f** was synthesized from **10e**, following the procedure for **2b**. **10f** was directly used for the next reaction without further purification.

(*R*)-1-(2-(2-(2-methyl-2-pivalamidopropanamido)benzamido)benzoyl)-*N*-(2-((2-(methylcarbamoyl)phenyl)carbamoyl)phenyl)pyrrolidine-2-carboxamide 10g:

Compound **10g** was synthesized, following the procedure for **3f,** from **10f**. Purification by column chromatography (eluent: 60% AcOEt/ pet. Ether, R_f: 0.3) afforded **10g** (60%) as a fluffy white solid. mp:119-121 °C; $[\alpha]^{25.36}_D$: 111.160° (*c* 0.5, $CHCl_3$); IR ($CHCl_3$) *v* (cm^{-1}): 3339, 3020, 2927, 2856, 1655, 1585, 1518, 1436, 1408, 1299, 1162; ^1H NMR (500 MHz, $CDCl_3$) δ: 12.49 (s, 1H, amide), 12.23 (s, 1H, amide), 11.74 (s, 1H, amide), 10.36 (s, 1H, amide), 8.88-8.87 (d, *J* = 8.24 Hz, 1H), 8.60-8.58 (d, *J* = 8.24 Hz, 1H), 8.42-8.40 (d, *J* = 8.24 Hz, 1H), 8.34-8.32 (d, *J* = 8.24 Hz, 1H), 7.75-7.73 (d, *J* = 7.93 Hz, 2H), 7.68-7.66 (d, *J* = 7.63 Hz, 1H), 7.58-7.54 (d, *J* = 7.93 Hz, 1H),7.58-7.54 (d, *J* = 7.93 Hz, 1H), 7.50-7.47 (m, 2H), 7.40-7.38 (d, *J* = 7.63 Hz, 1H), 7.30-7.27 (m, 2H), 7.23-7.19 (d, *J* = 7.93 Hz, 1H), 7.19-7.16 (d, *J* = 7.32 Hz, 1H), 7.10-7.07 (d, *J* = 7.32 Hz, 1H), 6.43-6.40 (d, *J* = 7.32 Hz, 1H), 8.30 (s, 1H, amide), 4.86-4.83 (d, *J* = 3.66 Hz, *J* = 8.54 Hz, 1H), 4.01-3.98 (m, 1H), 3.88-3.85 (m, 1H), 2.88-2.87 (d, *J* = 4.58, 3H), 2.45-2.39 (m, 1H), 2.36-2.32 (m, 1H), 2.15-2.09 (m, 1H), 2.04-2.01 (m, 1H), 1.66 (s, 3H), 1.57 (s, 1H), 1.27 (s, 9H); ^{13}C NMR (125 MHz, $CDCl_3$) δ: 178.5, 173.2, 170.5, 169.9, 169.4, 167.7, 166.5, 140.4, 138.6, 137.3, 133.2, 132.7, 131.9, 131.2, 128.3, 127.5, 127.3, 127.1, 123.8, 123.5, 123.3, 123.0, 122.9, 121.8, 121.0, 120.9, 120.5, 119.5, 118.9, 63.3, 57.6, 50.8, 38.9, 30.1, 27.5, 26.9, 26.0, 25.2, 24.5; MALDI-TOF/TOF: 797.1769 $(M+Na)^+$, 813.2659 $(M+K)^+$; Elemental analysis calculated for $C_{43}H_{47}N_7O_7$: C, 66.74; H, 6.12; N, 12.67. Found: C, 66.61; H, 6.20; N, 12.87.

(*S*)-*tert*-butyl 2-((2-((2-((2-(methoxycarbonyl)phenyl)carbamoyl)phenyl) carbamoyl) phenyl)carbamoyl)pyrrolidine-1-carboxylate 11a:

mp: 105-107 °C; $[\alpha]^{26.7}_D$: -93.472° (*c* 1, $CHCl_3$); IR ($CHCl_3$) *v* (cm^{-1}): 3303, 3020, 1659, 1521, 1428, 1296, 1272, 1019; ^{1}H NMR (200 MHz, $CDCl_3$) δ: $12.32_{rotamer}$ (s, 0.6H, amide), $12.25_{rotamer}$ (s, 0.4H, amide), 12.17 (s, 1H, amide), $11.87_{rotamer}$ (s, 0.4H, amide), $11.80_{rotamer}$ (s, 0.6H, amide), 8.85-8.71 (m, 3H), 8.12-8.08 (d, *J* = 8.08 Hz, 1H), 7.97-7.88 (m, 2H), 7.67-7.51 (m, 3H), 7.33-7.03 (m, 3H), 4.49-$4.44_{rotamer}$ (m, 0.4H), 4.32-$4.26_{rotamer}$ (m, 0.6H), 3.97-3.96 (bs, 3H), 3.81-3.73 (m, 1H), 3.65-3.41 (m, 1H), 2.36-2.14 (m, 2H), 2.05-1.73 (m, 2H), 1.49-$1.45_{rotamer}$ (m, 4H), $1.33_{rotamer}$ (s, 5H); ^{13}C NMR (50 MHz, $CDCl_3$) δ: 172.3, 171.8, 169.0, 167.9, 167.3, 154.2, 140.9, 140.1, 139.9, 134.8, 133.4, 132.9, 131.1, 127.2, 123.8, 123.3, 121.9, 121.1, 120.7, 115.7, 80.1, 63.6, 63.4, 62.6, 62.0, 52.6, 47.0, 46.8, 31.5, 30.5, 28.3, 28.2, 24.3, 23.8; MALDI-TOF/TOF: 610.1946 $(M+Na)^+$, 626.2477 $(M+K)^+$; Anal. calcd for $C_{32}H_{34}N_4O_7$: C, 65.52; H, 5.84; N, 9.55; Found: C, 65.48; H, 5.98; N, 9.56.

(*S*)-methyl 2-(2-(2-(1-pivaloylpyrrolidine-2-carboxamido)benzamido)benzamido) benzoate 11d:

mp: 86-88 °C, fuses; $[\alpha]^{27.2}_D$: -53.064° (*c* 1, $CHCl_3$); IR ($CHCl_3$) *v* (cm^{-1}): 3301, 3019, 2400, 1609, 1625, 1584, 1514, 1428, 1296, 1271, 1047, 929; ^{1}H NMR (400 MHz, $CDCl_3$) δ: 12.24 (s, 1H, amide), 12.15 (s, 1H, amide), 11.53 (s, 1H, amide), 8.83-8.79 (dd, *J* = 0.63 Hz, *J* = 8.46 Hz, 1H), 8.76-8.72 (broad, 2H), 8.12-8.07 (dd, *J* = 1.52 Hz, *J* = 8.08 Hz, 1H), 7.97-7.86 (m, 2H), 7.67-7.47 (m, 3H), 7.32-7.13 (m, 3H), 4.68-4.62 (m, 1H), 4.03-3.93 (m, 1H), 3.96 (s, 3H), 3.87-3.79 (m, 1H), 2.18-1.93 (m, 4H), 1.32 (s, 9H); ^{13}C NMR (100 MHz, $CDCl_3$) δ: 177.5, 171.6, 169.0, 167.8, 167.5, 140.9, 140.3, 140.1, 134.8, 132.9, 132.8, 131.1, 127.3, 127.1, 123.7, 123.4, 123.1, 121.9, 121.5, 121.2, 120.8, 120.6, 115.7, 77.2, 64.2, 52.6, 48.6, 39.1, 29.7, 29.0, 27.5, 25.9, 25.5; MALDI-TOF/TOF: 594.2542 $(M+Na)^+$, 610.2675 $(M+K)^+$; Anal. calcd for $C_{32}H_{34}N_4O_6$: C, 65.52; H, 5.84; N, 9.55; Found: C, 65.56; H, 5.63; N, 9.59.

(*R*)-*tert*-butyl 2-((2-((2-((2-(methoxycarbonyl)phenyl)carbamoyl)phenyl) carbamoyl)phenyl)carbamoyl)pyrrolidine-1-carboxylate 11f:

mp: 92-94 °C; $[\alpha]^{27.0}_D$: 98.324° (*c* 1, $CHCl_3$); IR ($CHCl_3$) *v* (cm^{-1}): 3377, 3020, 2400, 1653, 1513, 1428, 1321, 1019; ^{1}H NMR (400 MHz, $CDCl_3$) δ: $12.31_{rotamer}$ (s, 0.6H, amide), $12.24_{rotamer}$ (s, 0.4H, amide), 12.17 (s, 1H, amide), $11.85_{rotamer}$ (s, 0.4H, amide), $11.78_{rotamer}$ (s, 0.6H, amide), 8.85-8.71 (m, 3H), 8.13-8.09 (d, *J* = 7.58 Hz, 1H), 7.97-7.91 (m, 2H), 7.68-7.51 (m, 3H), 7.33-7.14 (m, 3H), 4.49-$4.44_{rotamer}$ (m, 0.4H), 4.32-$4.25_{rotamer}$ (m, 0.6H), 3.97 (s, 3H), 3.81-3.73 (m, 1H), 3.64-3.41 (m, 1H), 2.36-2.07 (m, 2H), 2.05-1.72 (m, 2H), $1.45_{rotamer}$ (m, 4H), $1.33_{rotamer}$ (s, 5H); ^{13}C NMR

(100 MHz, $CDCl_3$) δ: 172.3, 169.0, 167.9, 167.3, 154.2, 141.0, 140.2, 140.0, 134.8, 133.4, 132.9, 131.1, 127.2, 123.8, 124.0, 123.4, 121.9, 121.1, 120.7, 115.7, 80.1, 62.6, 62.1, 52.6, 47.1, 46.8, 31.5, 30.5, 28.2, 24.3, 23.8; MALDI-TOF/TOF: 610.1331 $(M+Na)^+$, 626.2562 $(M+K)^+$; Anal. calcd for $C_{32}H_{34}N_4O_7$: C, 65.52; H, 5.84; N, 9.55; Found: C, 65.45; H, 5.89; N, 9.59.

(*S*)-*tert*-butyl 2-((2-((2-(1-oxo-1H-isochromen-3-yl)phenyl)carbamoyl)phenyl) carbamoyl)pyrrolidine-1-carboxylate 11h:

mp: 167-169 °C, fuses; $[\alpha]^{25.1}_D$: -99.744° (*c* 1, $CHCl_3$); IR ($CHCl_3$) *v* (cm^{-1}): 3445, 3309, 3257, 3019, 1772, 1677, 1607, 1582, 1542, 1523, 1474, 1442, 1388, 1292.1260, 1167, 1126, 1036, 928; ^1H NMR (400 MHz, $CDCl_3$) δ: 13.17 (s, 1H, amide), $11.55_{rotamer}$ (s, 0.4H, amide), $11.50_{rotamer}$ (s, 0.6H, amide), 8.97-8.93 (d, *J* = 8.59 Hz, 1H), 8.82-8.71 (m, 1H), 8.33-8.21 (m, 1H), 8.02-7.94 (m, 1H), 7.87-7.80 (m, 1H), 7.63-7.49 (m, 4H), 7.32-7.20 (m, 2H), $4.48\text{-}4.43_{rotamer}$ (m, 0.5H), $4.34\text{-}4.28_{rotamer}$ (m, 0.5H), 3.83-3.69 (m, 1H), 3.65-3.09 (m, 1H), 3.65-3.41 (m, 1H), 2.36-2.17 (m, 2H), 2.06-1.84 (m, 2H), $1.43_{rotamer}$ (m, 4H), $1.33_{rotamer}$ (s, 5H); ^{13}C NMR (100 MHz, $CDCl_3$) δ: 172.3, 171.9, 167.6, 157.9, 157.5, 154.9, 153.1, 145.0, 140.4, 139.8, 137.0, 134.5, 134.0, 133.1, 129.6, 129.0, 128.9, 127.4, 125.8, 123.4, 122.8, 121.9, 121.5, 120.7, 116.6, 115.0, 80.1, 62.5, 62.0, 47.1, 46.8, 42.9, 31.5, 30.5, 28.2, 24.3, 23.7; MALDI-TOF/TOF: 578.1309 $(M+Na)^+$, 594.1654 $(M+K)^+$; Anal. calcd for $C_{32}H_{31}N_3O_6$: C, 69.43; H, 5.64; N, 7.59; Found: C, 69.42; H, 5.69; N, 7.45.

(*S*)-*N*-(2-((2-(1-oxo-1H-isochromen-3-yl)phenyl)carbamoyl)phenyl)-1-pivaloylpyrrolidine-2-carboxamide 11i:

mp: 209-211 °C, fuses; $[\alpha]^{25.8}_D$: -57.432° (*c* 1, $CHCl_3$); IR ($CHCl_3$) *v* (cm^{-1}): 3422, 3310, 3261, 3020, 2882, 2715, 2401, 1771, 1663, 1607, 1582, 1521, 1478, 1469, 1442, 1405, 1365, 1293, 1247, 1168, 1128, 1036, 1006, 929; ^1H NMR (200 MHz, $CDCl_3$) δ: 12.48 (1H, amide), 8.75-8.70 (m, 1H), 8.25-8.20 (m, 2H), 7.87-7.80 (m, 1H), 7.70-7.66 (m, 1H), 7.58-7.44 (m, 2H), 7.17-7.10 (m, 1H), 4.74-4.72 (m, 1H), 3.85 (m, 2H), 2.26-2.01 (m, 4H), 1.30 (s, 9H); ^{13}C NMR (50 MHz, $CDCl_3$) δ: 177.6, 171.6, 167.8, 157.3, 145.0, 140.4, 140.0, 137.0, 134.0, 133.1, 129.6, 129.0, 128.9, 127.3, 125.8, 123.4, 122.6, 121.9, 121.8, 120.6, 116.5, 115.1, 64.2, 48.6, 39.1, 28.9, 27.4, 25.7; MALDI-TOF/TOF: 562.2572 $(M+Na)^+$, 578.3078 $(M+K)^+$; Anal. calcd for C32H31N3O5: C, 71.49; H, 5.81; N, 7.82; Found: C, 71.38; H, 5.68; N, 7.96.

(*S*)-*tert*-butyl 2-((2-((2-((2-((*R*)-2-((2-((2-((2-(methoxycarbonyl)phenyl) carbamoyl)phenyl)carbamoyl)phenyl)carbamoyl)pyrrolidine-1-carbonyl) phenyl)carbamoyl) phenyl)carbamoyl)phenyl)carbamoyl)pyrrolidine-1-carboxylate 12a:

mp: 227-229 °C; $[\alpha]^{26.9}_D$: 33.100° (*c* 1, $CHCl_3$); IR ($CHCl_3$) *v* (cm^{-1}): 3421, 3309, 3258, 3021, 2401, 1677, 1583, 1542, 1524, 1473, 1452, 1432, 1297, 1270, 1005, 929; ^{1}H NMR (400 MHz, $CDCl_3$) δ: 12.40-12.33$_{rotamer}$ (m, 2H, amide), 12.14-12.07$_{rotamer}$ (m, 2H, amide), 11.91$_{rotamer}$ (s, 0.4H, amide), 11.81$_{rotamer}$ (s, 0.6H, amide), 10.63 (s, 1H, amide), 8.79-8.70 (m, 4H), 8.59-8.55 (m, 1H), 8.48-8.45 (m, 1H), 8.10-8.08 (m, 1H), 7.97-7.80 (m, 4H), 7.74-7.72 (m, 1H), 7.65-7.61 (m, 1H), 7.55-7.46 (m, 5H), 7.32-7.28 (m, 1H), 7.25-7.14 (m, 4H), 7.05-7.02 (m, 1H), 4.88-4.85 (m, 1H), 4.46-4.45$_{rotamer}$ (m, 0.4H), 4.29-4.26$_{rotamer}$ (m, 0.6H), 3.98-3.95 (m, 1H), 3.95 (s, 3H), 3.79-3.75 (m, 2H), 3.60-3.43 (m, 1H), 2.49-2.44 (m, 1H), 2.3-1.85 (m, 7H), 1.39$_{rotamer}$ (s, 3H), 1.29$_{rotamer}$ (s, 6H); ^{13}C NMR (100 MHz, $CDCl_3$) δ: 172.3, 171.8, 170.2, 169.0, 167.7, 167.6, 167.4, 167.3, 167.2, 154.9, 154.1, 140.8, 140.3, 140.2, 140.0, 139.8, 137.1, 134.8, 133.2, 132.9, 132.8, 131.5, 131.1, 128.9, 127.3, 127.27, 127.1, 123.9, 123.8, 123.76, 123.6, 123.4, 123.2, 123.0, 122.2, 121.9, 121.9, 121.6, 121.5, 121.3, 121.1, 121.0, 120.7, 120.5, 120.2, 119.9, 115.6, 80.1, 79.9, 77.2, 62.8, 62.6, 62.0, 52.6, 51.3, 47.1, 46.8, 31.5, 30.5, 30.0, 28.4, 28.2, 25.5, 24.2, 23.8; MALDI-TOF: 1064.5446 $(M+Na)^+$, 1081.1713 $(M+K)^+$; Anal. calcd for $C_{58}H_{56}N_8O_{11}$: C, 66.91; H, 5.42; N, 10.76; Found: C, 66.95; H, 5.32; N, 10.50.

(*S*)-*tert*-butyl 2-((2-((2-((2-((*R*)-2-((2-((2-((2-(methylcarbamoyl)phenyl) carbamoyl)phenyl)carbamoyl)phenyl)carbamoyl)pyrrolidine-1-carbonyl) phenyl)carbamoyl) phenyl)carbamoyl)phenyl)carbamoyl)pyrrolidine-1-carboxylate 12c:

mp: 122-124 °C completes at 165 °C; $[\alpha]^{24.6}_D$: 44.324° (*c* 1, $CHCl_3$); IR ($CHCl_3$) *v* (cm^{-1}): 3461, 3020, 2401, 1649, 1605, 1583, 1512, 1449, 1428, 1326, 1297, 1122, 929, 909; ^{1}H NMR (200 MHz, $CDCl_3$) δ: 12.48 (s, 2H, amide), 12.37$_{rotamer}$ (s, 0.6H, amide), 12.34$_{rotamer}$ (s, 0.4H, amide), 12.11 (s, 1H, amide), 11.91$_{rotamer}$ (s, 0.6H, amide), 11.80$_{rotamer}$ (s, 0.4H, amide), 10.81 (s, 1H, amide), 8.75-8.43 (m, 6H), 7.99-7.68 (m, 1H), 7.31-6.97 (m, 7H), 4.87-4.80 (m, 1H), 4.45-4.4$_{rotamer}$ (m, 0.5H), 4.29-4.23$_{rotamer}$ (m, 0.5H), 3.97-3.93 (m, 1H), 3.77-3.73 (m, 2H), 3.58-3.39 (m, 1H), 2.86 (s, 3H), 2.51-2.41 (m, 1H), 2.27-1.87 (m, 6H), 1.43$_{rotamer}$ (s, 4H), 1.31$_{rotamer}$ (s, 4H); ^{13}C NMR (200 MHz, $CDCl_3$) δ: 170.2, 169.6, 167.4, 162.5, 140.2, 139.9, 139.7, 138.9, 137.0, 133.0, 132.7, 132.6, 132.4, 131.5, 128.9, 127.5, 127.3, 126.8, 124.0,

123.7, 123.5, 123.3, 122.2, 121.7, 121.2, 120.9, 120.7, 120.2, 120.0, 80.1, 62.8, 62.5, 51.2, 36.4, 31.4, 30.0, 28.3, 28.2, 26.8, 25.4; MALDI-TOF: 1063.3723 $(M+Na)^+$, 1079.4132 $(M+K)^+$; Anal. calcd for $C_{58}H_{57}N_9O_{10}$: C, 66.97; H, 5.52; N, 12.12; Found: C, 66.69; H, 5.25; N, 12.06.

methyl 2-(2-(2-((*R*)-1-(2-(2-(2-((*S*)-1-pivaloylpyrrolidine-2-carboxamido) benzamido)benzamido)benzoyl)pyrrolidine-2-carboxamido)benzamido) benzamido)benzoate 12e:

mp: 94-96 °C, completes at 126 °C; $[\alpha]^{26.8}_D$: 50.996° (*c* 1, $CHCl_3$); IR ($CHCl_3$) *v* (cm^{-1}): 3309, 3259, 3020, 2401, 1675, 1624, 1607, 1583, 1523, 1450, 1430, 1271, 1168, 1093, 1048, 928; ^1H NMR (200 MHz, $CDCl_3$) δ: 12.33 (s, 1H, amide), 12.13 (s, 1H, amide), 12.09 (s, 1H, amide), 11.57 (s, 1H, amide), 10.80 (s, 1H, amide), 8.78-8.62 (m, 4H), 8.57-8.53 (d, *J* = 8.21 Hz, 1H), 8.45-8.41 (d, *J* = 8.21 Hz, 1H), 8.09-7.42 (m, 12H), 7.33-7.25 (m, 1H), 7.20-6.97 (m, 5H), 4.88-4.81 (m, 1H), 4.66-4.60 (m, 1H), 3.98-3.90 (m, 2H), 3.94 (s, 3H), 3.82-3.78 (m, 2H), 2.54-2.36 (m, 1H), 2.24-1.90 (m, 3H), 1.31 (s, 9H); ^{13}C NMR (50 MHz, $CDCl_3$) δ: 177.5, 171.6, 170.3, 168.9, 167.6, 167.5, 167.3, 162.6, 140.7, 140.2, 139.9. 139.7, 137.0, 134.7, 133.1, 132.8, 132.7, 131.4, 131.0, 128.8, 127.4, 127.2, 127.1, 123.9, 123.8, 123.6, 123.4, 123.2, 123.0, 122.2, 121.8, 121.3, 121.1, 121.0, 120.6, 120.4, 120.3, 119.9, 115.5, 64.2, 62.8, 52.6, 51.2, 48.5, 39.1, 36.5, 31.4, 30.0, 29.0, 27.4, 25.4; MALDI-TOF: 1050.2642 $(M+Na)^+$, 1066.8655 $(M+K)^+$; Anal. calcd for $C_{58}H_{56}N_8O_{10}$: C, 67.96; H, 5.51; N, 10.93; Found: C, 67.90; H, 5.41; N, 10.75.

(*R*)-*N*-(2-((2-((2-(methylcarbamoyl)phenyl)carbamoyl)phenyl)carbamoyl) phenyl)-1-(2-(2-(2-((*S*)-1-pivaloylpyrrolidine-2-carboxamido)benzamido) benzamido)benzoyl) pyrrolidine-2-carboxamide 12f:

mp: 176-178 °C; $[\alpha]^{26.5}_D$: 59.448° (*c* 1, $CHCl_3$); IR ($CHCl_3$) *v* (cm^{-1}): 3260, 3020, 2401, 1682, 1652, 1624, 1605, 1583, 1520, 1450, 1428, 1410, 1327, 1297, 1170, 1049, 952, 909; ^1H NMR (500 MHz, $CDCl_3$) δ: 12.41 (s, 1H, amide), 12.34 (s, 1H, amide), 12.31 (s, 1H, amide), 12.08 (s, 1H, amide), 11.55 (s, 1H, amide), 10.80 (s, 1H, amide), 8.78-8.76 (d, *J* = 8.54 Hz, 1H), 8.72-8.70 (d, *J* = 8.24 Hz, 1H), 8.63-8.60 (m, 2H), 8.54-8.53 (d, *J* = 8.24 Hz , 1H), 8.46-8.44 (d, *J* = 8.24 Hz, 1H), 7.95-7.93 (d, *J* = 7.93 Hz, 1H), 7.93-7.91 (d, *J* = 8.24 Hz, 1H), 7.87-7.85 (d, *J* = 7.93 Hz, 1H), 7.80-7.78 (d, *J* = 7.63 Hz, 1H), 7.69-7.68 (d, *J* = 7.63 Hz, 1H), 7.55-7.43 (m, 8H), 7.31-7.29 (m, 1H), 7.23-7.20 (t, *J* = 7.63 Hz, 1H), 7.16-7.10 (m, 1H), 7.00-6.97 (t, *J* = 7.63 Hz, 1H), 6.81 (bs, 1H, amide), 4.88-4.85 (m, 1H), 4.65-4.63 (m, 1H), 4.01-3.94 (m,

2H), 3.84-3.76 (m, 2H), 2.93 (d, *J* = 4.58 Hz, 3H), 2.52-2.45 (m, 1H), 2.27-2.16 (m, 2H), 2.13-2.06 (m, 3H), 1.99-1.91 (m, 2H), 1.30 (s, 9H); ^{13}C NMR (125 MHz, $CDCl_3$) δ: 177.7, 171.6, 170.4, 170.3, 169.7, 167.7, 167.5, 167.4, 167.3, 140.2, 139.9, 139.8, 139.0, 137.2, 133.1, 132.7, 132.7, 132.5, 131.6, 128.9, 127.5, 127.4, 127.2, 126.9, 124.0, 123.7, 123.6, 123.5, 123.3, 123.1, 122.2, 121.9, 121.7, 121.5, 121.4, 121.1, 120.9, 120.6, 120.5, 120.3, 64.3, 63.0, 51.3, 48.6, 39.2, 30.1, 29.7, 27.5, 26.8, 25.5; MALDI-TOF: 1047.9636 $(M+Na)^+$, 1064.1530 $(M+K)^+$; Anal. calcd for C58H57N9O9: C, 68.02; H, 5.61; N, 12.31; Found: C, 68.30; H, 5.65; N, 12.32.

X-ray Crystal Structure Analysis For 7f, 10d and 4h

X-ray intensity data measurements of compounds **7f** and **10d** were carried out on a Bruker SMART APEX II CCD diffractometer with graphite-monochromatized (MoK_α= 0.71073Å) radiation at 100 (2) K. The X-ray generator was operated at 50 kV and 30 mA. Data were collected with ω scan width of 0.5° at different settings of φ and 2θ with a frame time of 10 sec keeping the sample-to-detector distance fixed at 50 mm. The X-ray data collection was monitored by APEX2 program (Bruker, 2006).[1] The data was corrected for Lorentzian, polarization and absorption effects using SAINT and SADABS programs integrated in APEX2 program package (Bruker, 2006). SHELX-97 was used for structure solution and full matrix least-squares refinement on F^2.[2] H-atoms located in the difference Fourier map of **1** were refined isotropically whereas H-atoms which could not be located in the difference Fourier properly were placed in geometrically idealized positions and constrained to ride on their parent atoms. All the H-atoms in **10d** were placed in geometrically idealized positions and constrained to ride on their parent atoms. placed in geometrically idealized position and constrained to ride on their parent atoms. The X-ray diffraction results for **10d** were analyzed using PWT-PLATON (v1.16) to estimate the solvent accessible void space. The analysis revealed ~ 353.4 Å^3 as total area volume void space for the potential solvents which counts to 9.3% of the total unit cell volume 3795.2 Å^3. Due to highly orientational disorder exhibited by the included solvent molecule (ethyl acetate and water) in the void space, the PLATON SQUEEZE program was utilized for solving the crystal structure.

Crystal data of **7f.** $C_{44}H_{47}N_7O_7$, M = 785.89, colorless plate, 0.31 x 0.14 x 0.06 mm^3, orthorhombic, space group $P2_12_12_1$, a = 9.3778(9), b = 13.4883(12), c = 31.293(3) Å, V = 3958.3(6)Å^3, Z = 2, T = 100(2) K, $2\theta_{max}$ = 50.00°, D_{calc} (g cm^{-3}) = 1.319, $F(000)$ =1664, μ (mm^{-1}) = 0.091, 20191 reflections collected, 6958 unique reflections (R_{int}=0.0467), 6392 observed ($I > 2\sigma(I)$) reflections, multi-scan absorption correction, T_{min} = 0.973, T_{max} = 0.995, 667refined parameters, S = 1.165, $R1$=0.0497, $wR2$=0.0948 (all data R = 0.0563, $wR2$ = 0.975), maximum and minimum residual electron densities; $\Delta\rho_{max}$ = 0.19, $\Delta\rho_{min}$= -0.18 (eÅ^{-3}).

Crystal data of **10d.** $C_{38}H_{37}Br_1N_6O_8$, 0.5($C_4H_8O_2$), 0.25(CH_3OH), 1.75(H_2O), M = 837.24, colorless needle, 0.28 x 0.11 x 0.03 mm^3, triclinic, space group $P1$, a = 12.6540(18), b = 16.041(2), c = 20.114(3) Å, α = 90.701(8)°, β = 105.291(8)°, γ = 104.722(8)°, V = 3795.1(9) Å^3, Z = 4, T = 10(2) K, $2\theta_{max}$=57.04°, D_{calc} (g cm^{-3}) = 1.465, $F(000)$ = 1744, μ (mm^{-1}) = 1.149, 118413 reflections collected, 37772 unique reflections (R_{int}=0.0671), 27315 observed ($I > 2\sigma(I)$) reflections, multi-scan absorption correction, T_{min} = 0.739, T_{max} = 0.966, 1903 refined parameters, 262 restrains applied, S = 1.514, $R1$=0.1384, $wR2$=0.3860 (all data R = 0.1636, $wR2$ = 0.3983), maximum and minimum residual electron densities; $\Delta\rho_{max}$ = 1.74, $\Delta\rho_{min}$= -2.33 (eÅ^{-3}).

Data for compound **4h** was collected on SMART APEX CCD Single Crystal X-ray diffractometer using Mo-Kα radiation (λ = 0.7107 Å) to a maximum θ range of 25.00°. Crystal to detector distance 6.05 cm, 512 x 512 pixels / frame, Oscillation / frame -0.3º, maximum detector swing angle = –30.0º, beam center = (260.2, 252.5), in plane spot width = 1.24, SAINT integration with different exposure time per frame and SADABS correction applied. The structures were solved by direct methods using SHELXTL. All the data were corrected for Lorentzian, polarisation and absorption effects. SHELX-97 (ShelxTL)[ref] was used for structure solution and full matrix least squares refinement on F^2. Hydrogen atoms were included in the refinement as per the riding model. The refinements were carried out using SHELXL-97.

Crystal data of **4h:** Single crystals of the complex were grown by slow evaporation of the solution of DCM and MeOH. Colourless plate like crystal of approximate size 0.45 x 0.19 x 0.09 mm^3, was used for data collection. Hemisphere data acquisition. Total scans = 3, total frames = 1271, exposure / frame = 10.0 sec / frame, θ range =

1.90 to 25.00º, completeness to θ of 25.00 º is 100 %. C_{44} H_{51} N_7 O_9, M = 821.92. Crystals belong to orthorhombic, space group $P2_12_12_1$, a = 10.2506(5) b = 19.2039(9) c = 21.485(1) Å, V = 4229.4(3) Å^3, Z = 4, D_c = 1.291 g /cc, μ (Mo–Kα) = 0.092 mm^{-1}, 1744, reflections measured, 21448 unique [I>2σ(I)], R value 0.0857, wR2 = 0.1797. Largest diff. peak and hole 0.308 and -0.208 e. Å $^{-3}$.

References

(1) Bruker (2006). *APEX2*, *SAINT* and *SADABS*. Bruker AXS Inc., Madison, Wisconsin, USA.

(2) G. M. Sheldrick, *Acta Crystallogr*., **2008**, *64*, 112.

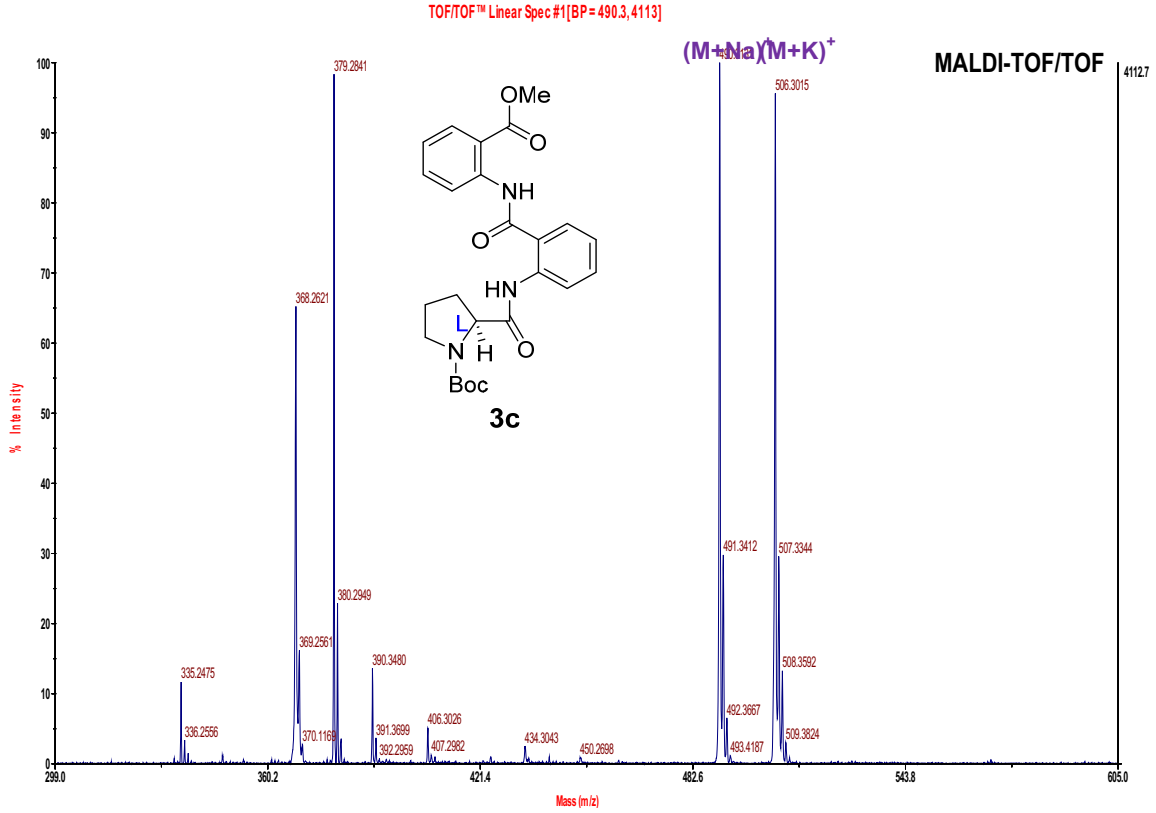
TOF/TOF™ Linear Spec #1[BP = 490.3, 4113]
MALDI-TOF/TOF
(M+Na)+
(M+K)+
OMe
O
NH
O
HN
L
N H
O
Boc
3c
% Intensity
Mass (m/z)
379.2841
506.3015
368.2621
491.3412
507.3344
380.2949
369.2561
390.3480
508.3592
335.2475
492.3667
406.3026
391.3699
509.3824
336.2556
370.1161
392.2959
407.2982
434.3043
450.2698
493.4187
299.0
360.2
421.4
482.6
543.8
605.0
4112.7

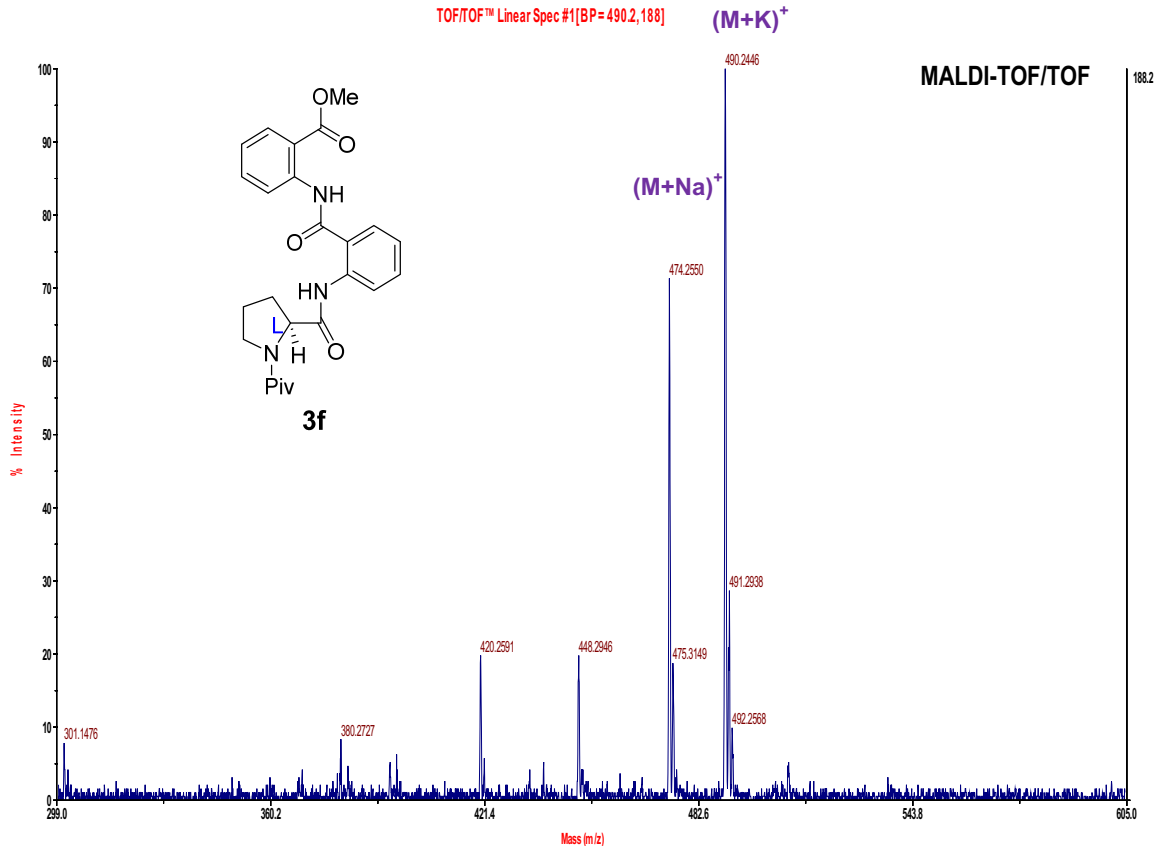
TOF/TOF™ Linear Spec #1[BP = 490.2, 188]
(M+K)+
MALDI-TOF/TOF
OMe
O
NH
O
HN
L
N H
O
Piv
3f
(M+Na)+
% Intensity
Mass (m/z)
490.2446
474.2550
491.2938
420.2591
448.2946
475.3149
301.1476
380.2727
492.2568
299.0
360.2
421.4
482.6
543.8
605.0
188.2

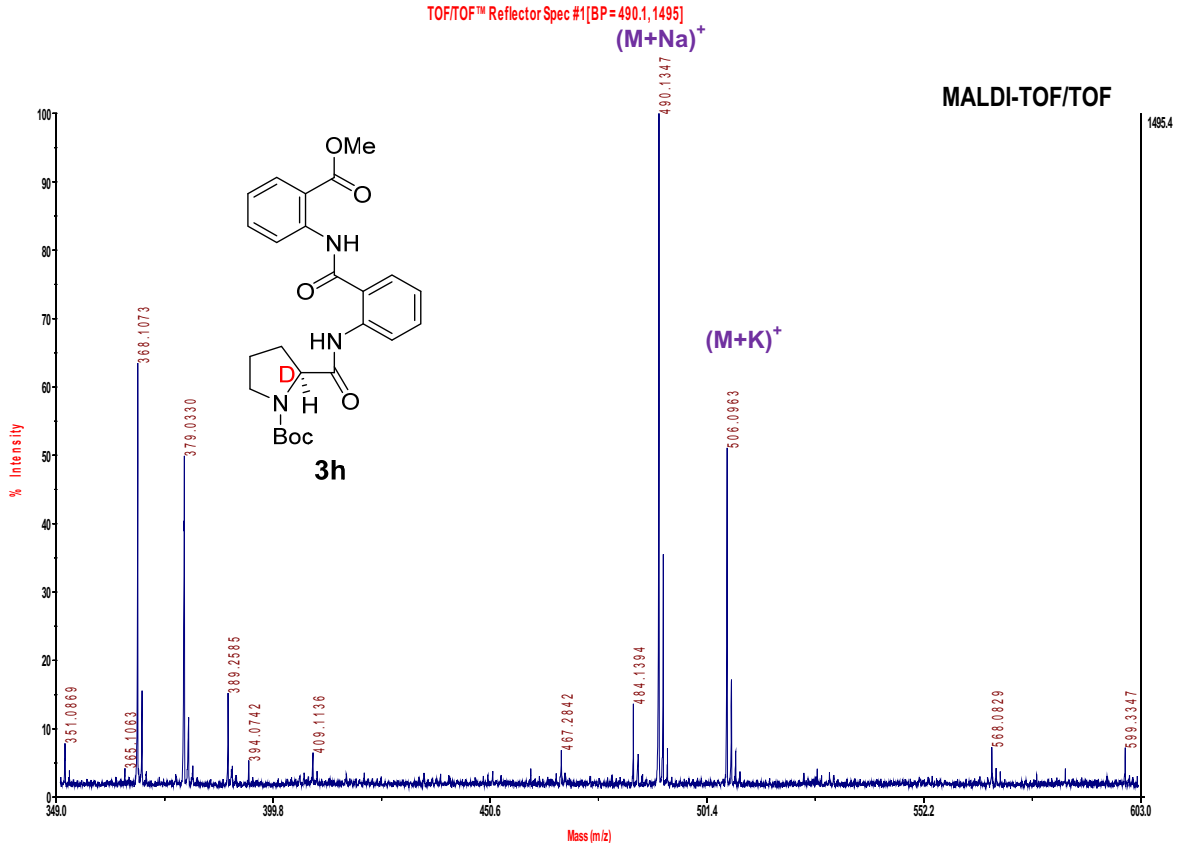
TOF/TOF™ Reflector Spec #1[BP = 490.1, 1495]
(M+Na)+
MALDI-TOF/TOF
OMe
O
NH
O
HN
D
N H
O
Boc
3h
(M+K)+
490.1347
506.0963
368.1073
379.0330
389.2585
351.0869
365.1063
394.0742
409.1136
467.2842
484.1394
568.0829
599.3347
1495.4
% Intensity
Mass (m/z)

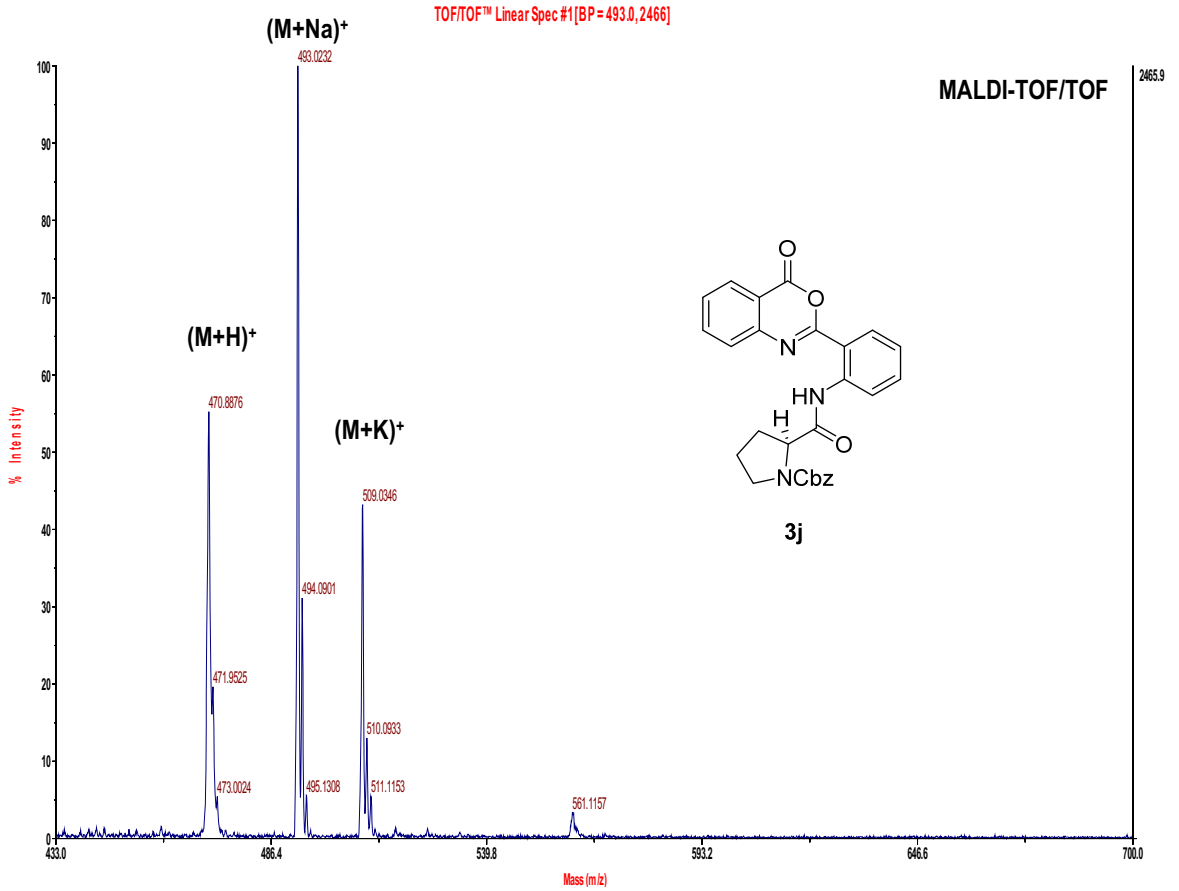
TOF/TOF™ Linear Spec #1[BP = 493.0, 2466]
(M+Na)+
493.0232
MALDI-TOF/TOF
2465.9
(M+H)+
470.8876
(M+K)+
509.0346
494.0901
471.9525
510.0933
473.0024
495.1308
511.1153
561.1157
O
O
N
HN
H
O
NCbz
3j
% Intensity
Mass (m/z)

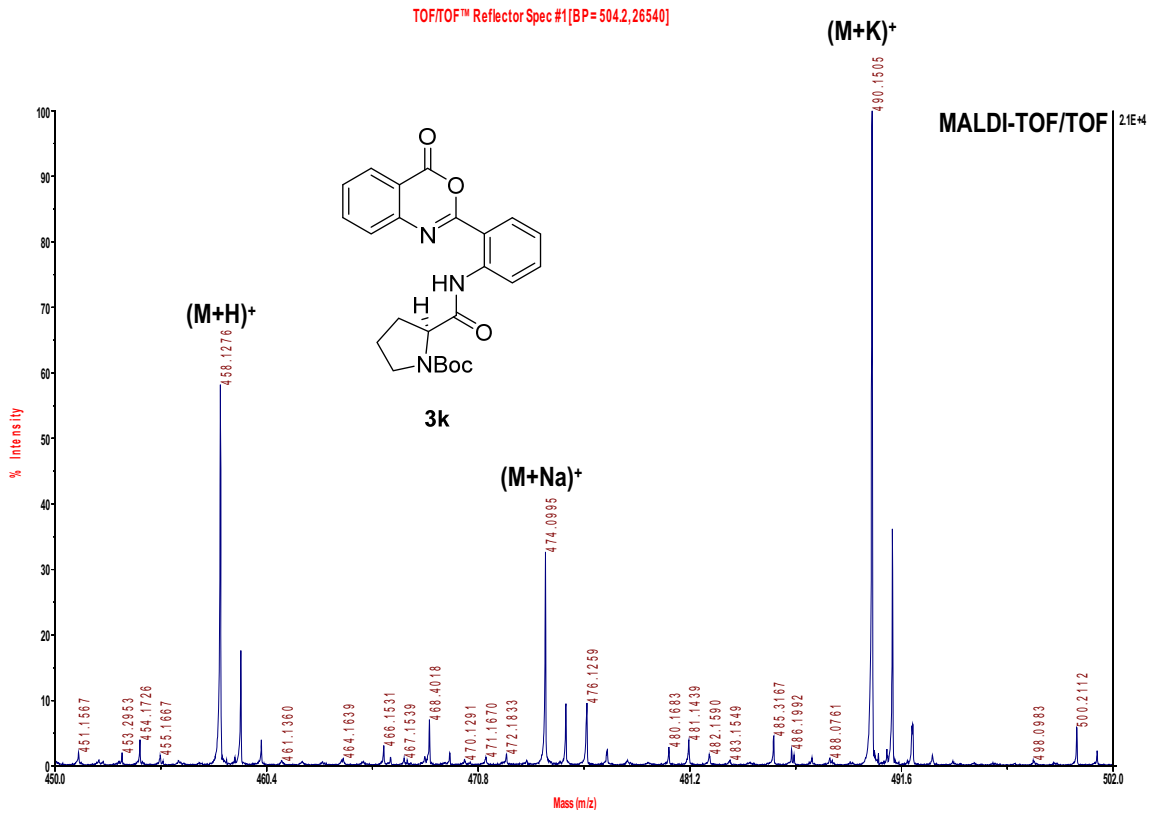
TOF/TOF™ Reflector Spec #1[BP = 504.2, 26540]
(M+K)+
490.1505
MALDI-TOF/TOF
2.1E+4
(M+H)+
458.1276
(M+Na)+
474.0995
3k
% Intensity
Mass (m/z)

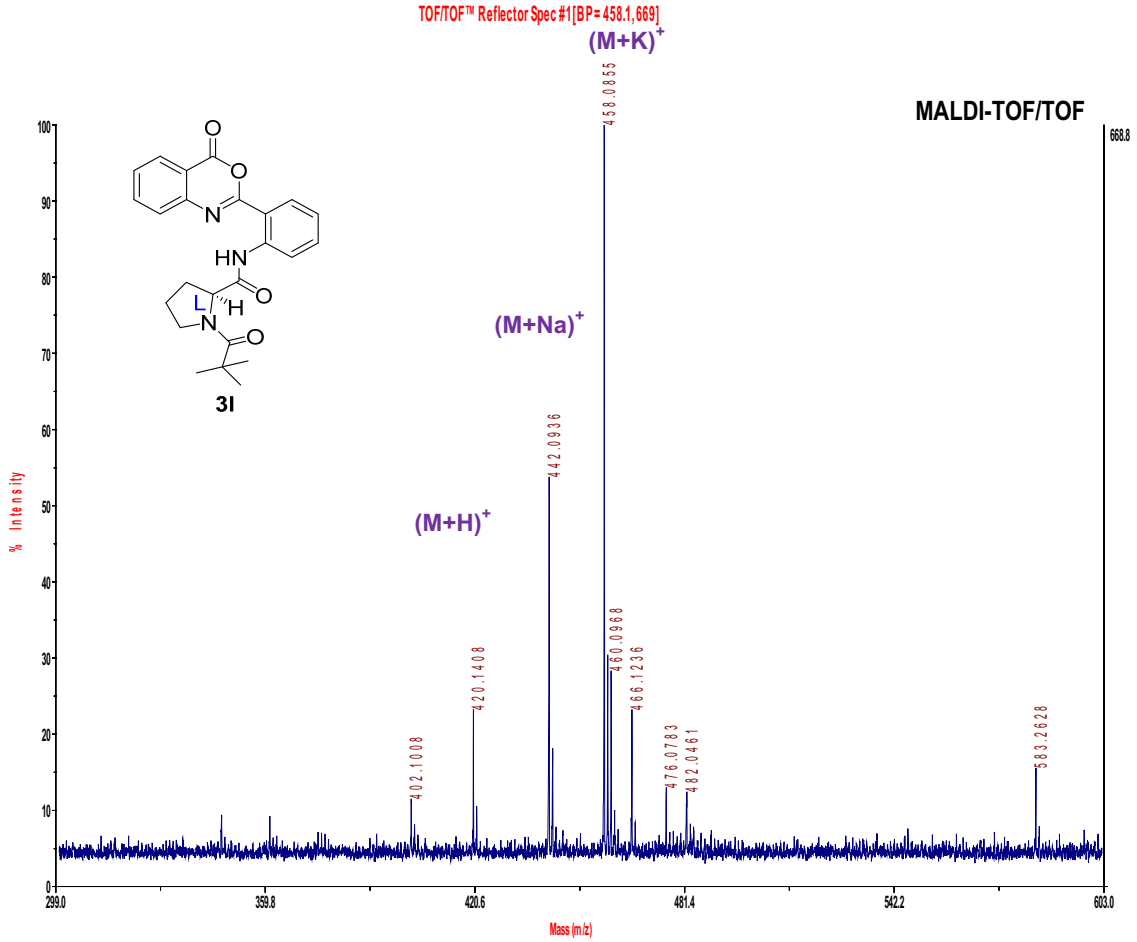
TOF/TOF™ Reflector Spec #1[BP = 458.1, 669]
(M+K)+
458.0855
MALDI-TOF/TOF
668.8
(M+Na)+
442.0936
(M+H)+
402.1008
420.1408
460.0968
466.1236
476.0783
482.0461
583.2628
3l
% Intensity
Mass (m/z)

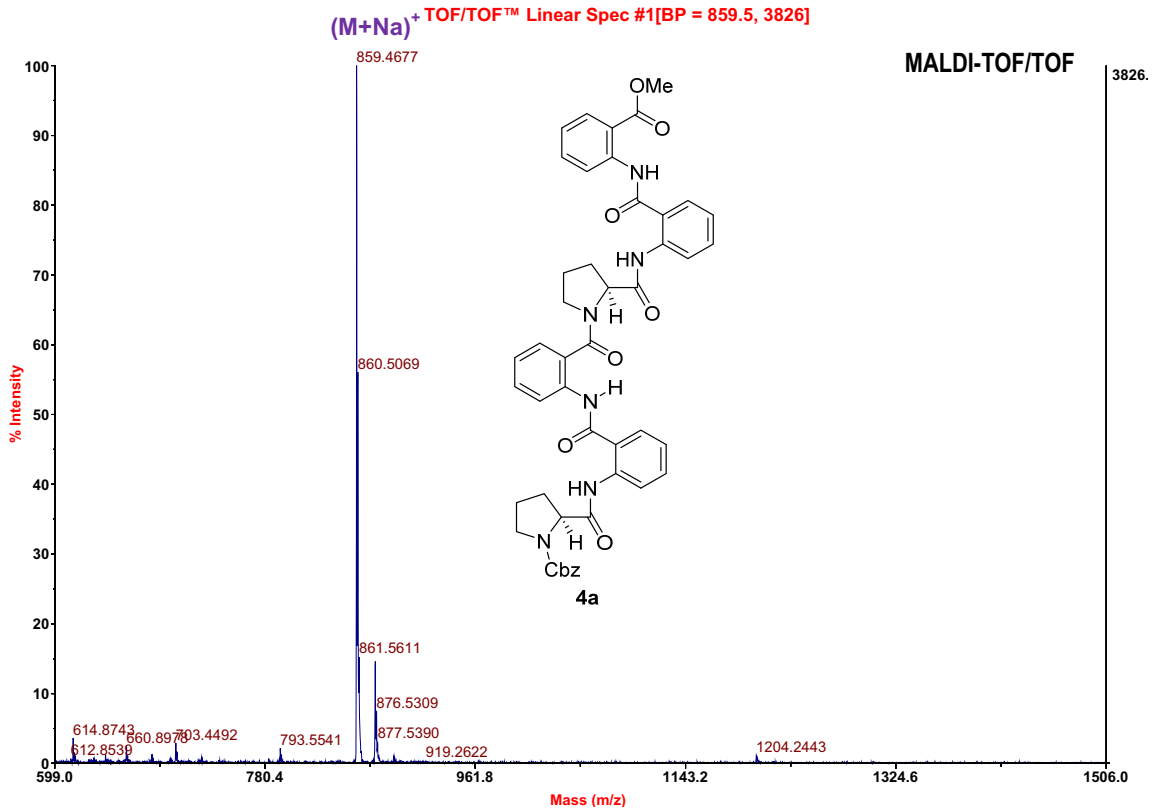
(M+Na)+ TOF/TOF™ Linear Spec #1[BP = 859.5, 3826]
MALDI-TOF/TOF
3826.
859.4677
860.5069
861.5611
876.5309
877.5390
919.2622
1204.2443
614.8743
612.8539
660.8978
703.4492
793.5541
% Intensity
Mass (m/z)
OMe
NH
HN
Cbz
4a

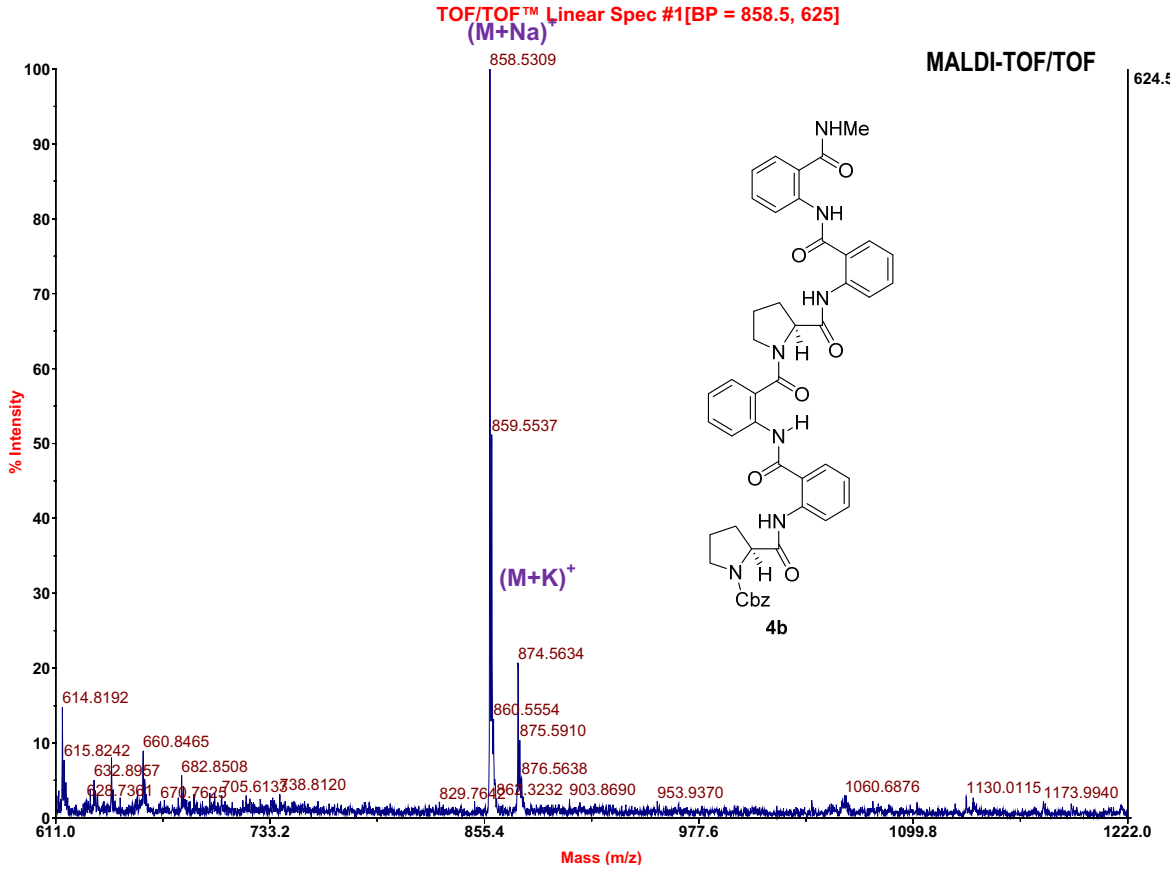
TOF/TOF™ Linear Spec #1[BP = 858.5, 625]
(M+Na)+
MALDI-TOF/TOF
624.5
858.5309
859.5537
(M+K)+
874.5634
860.5554
875.5910
876.5638
614.8192
615.8242
660.8465
632.8957
682.8508
705.6137
738.8120
829.7645
903.8690
953.9370
1060.6876
1130.0115
1173.9940
% Intensity
Mass (m/z)
NHMe
NH
HN
Cbz
4b

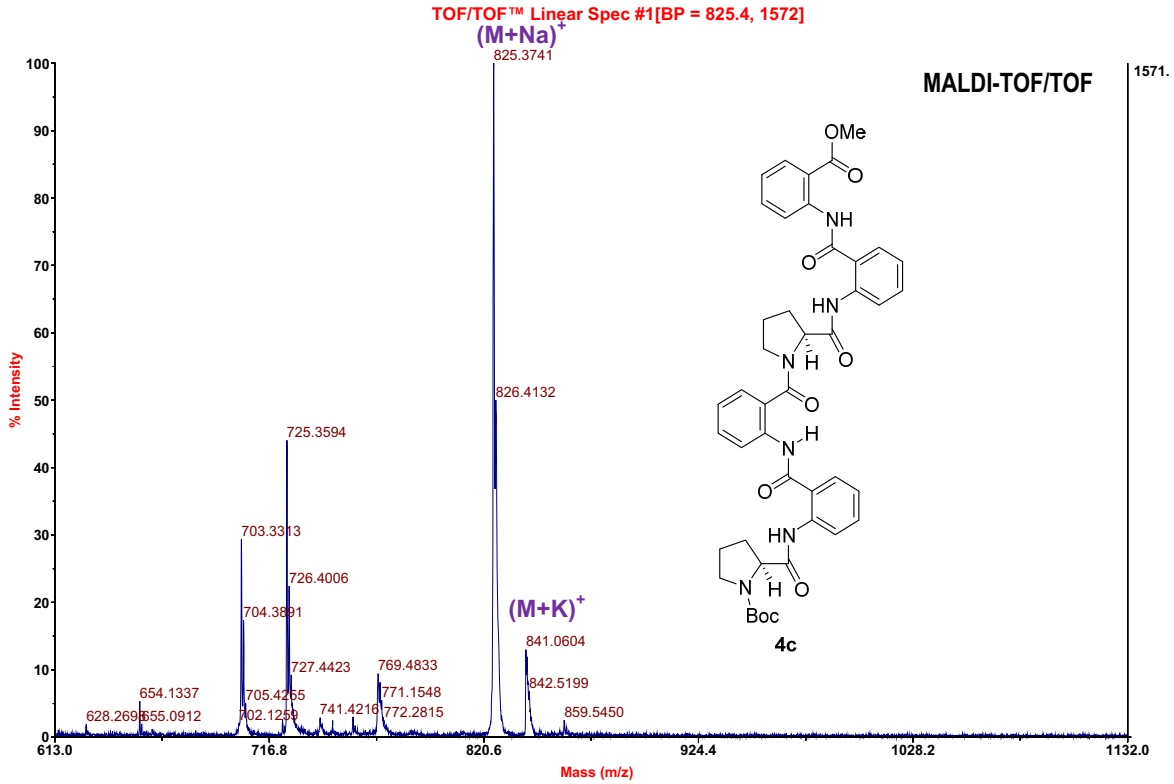
TOF/TOF™ Linear Spec #1[BP = 825.4, 1572]
(M+Na)+
825.3741
MALDI-TOF/TOF
1571.
% Intensity
826.4132
725.3594
703.3313
726.4006
704.3891
(M+K)+
841.0604
727.4423
769.4833
654.1337
705.4255
771.1548
842.5199
628.2696
655.0912
702.1259
741.4216
772.2815
859.5450
OMe
NH
HN
Boc
4c
613.0
716.8
820.6
924.4
1028.2
1132.0
Mass (m/z)

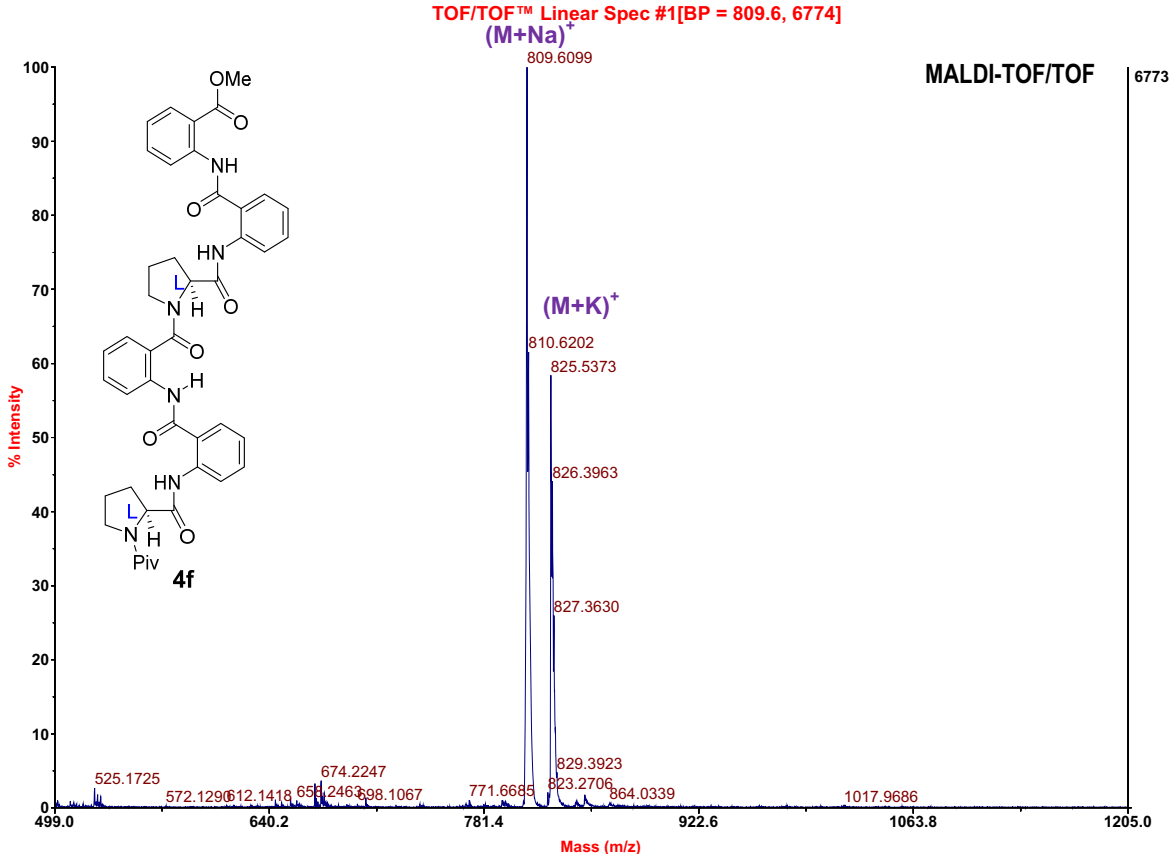
TOF/TOF™ Linear Spec #1[BP = 809.6, 6774]
(M+Na)+
809.6099
MALDI-TOF/TOF
6773
% Intensity
(M+K)+
810.6202
825.5373
826.3963
827.3630
674.2247
525.1725
829.3923
572.1296
612.1418
658.2463
698.1067
771.6685
823.2706
864.0339
1017.9686
OMe
NH
HN
Piv
4f
499.0
640.2
781.4
922.6
1063.8
1205.0
Mass (m/z)

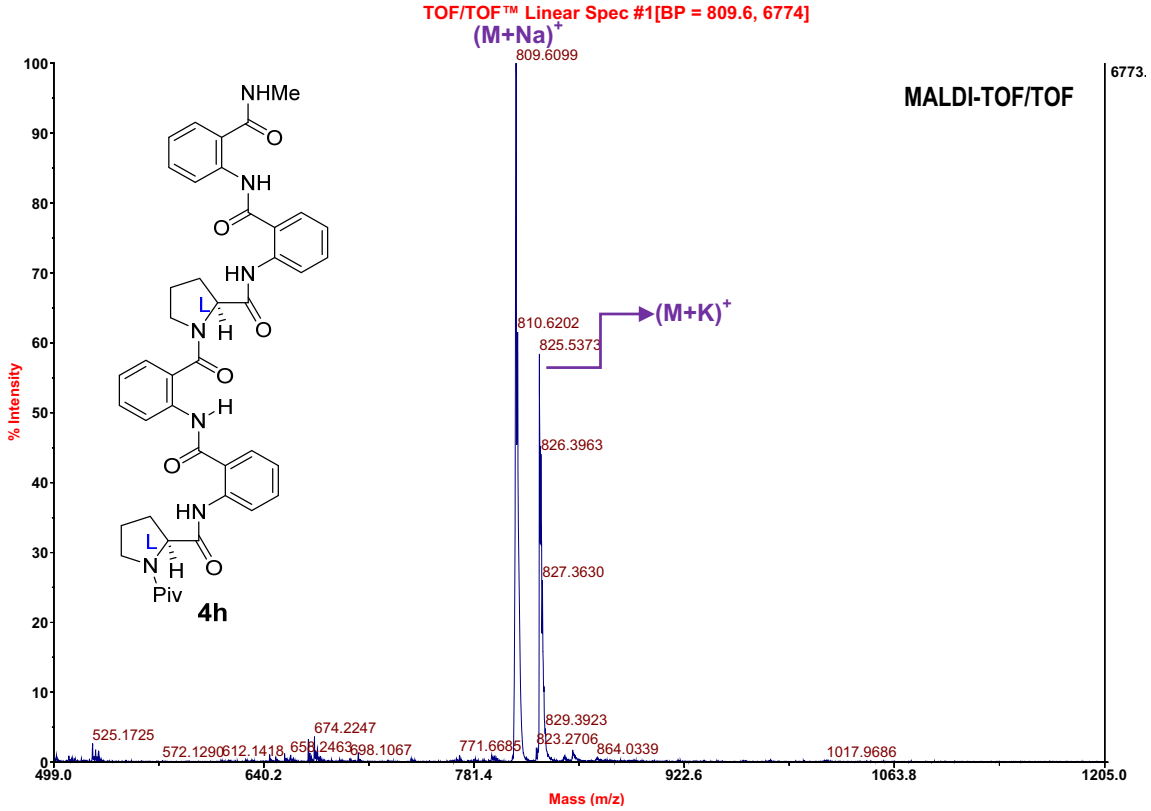
TOF/TOF™ Linear Spec #1[BP = 809.6, 6774]
(M+Na)+
809.6099
MALDI-TOF/TOF
6773.
NHMe
O
NH
O
HN
L
N H
O
O
N H
O
HN
L
N H O
Piv
4h
(M+K)+
810.6202
825.5373
826.3963
827.3630
% Intensity
100
90
80
70
60
50
40
30
20
10
0
525.1725
572.1290
612.1418
674.2247
698.1067
771.6685
823.2706
829.3923
864.0339
1017.9686
499.0
640.2
781.4
922.6
1063.8
1205.0
Mass (m/z)

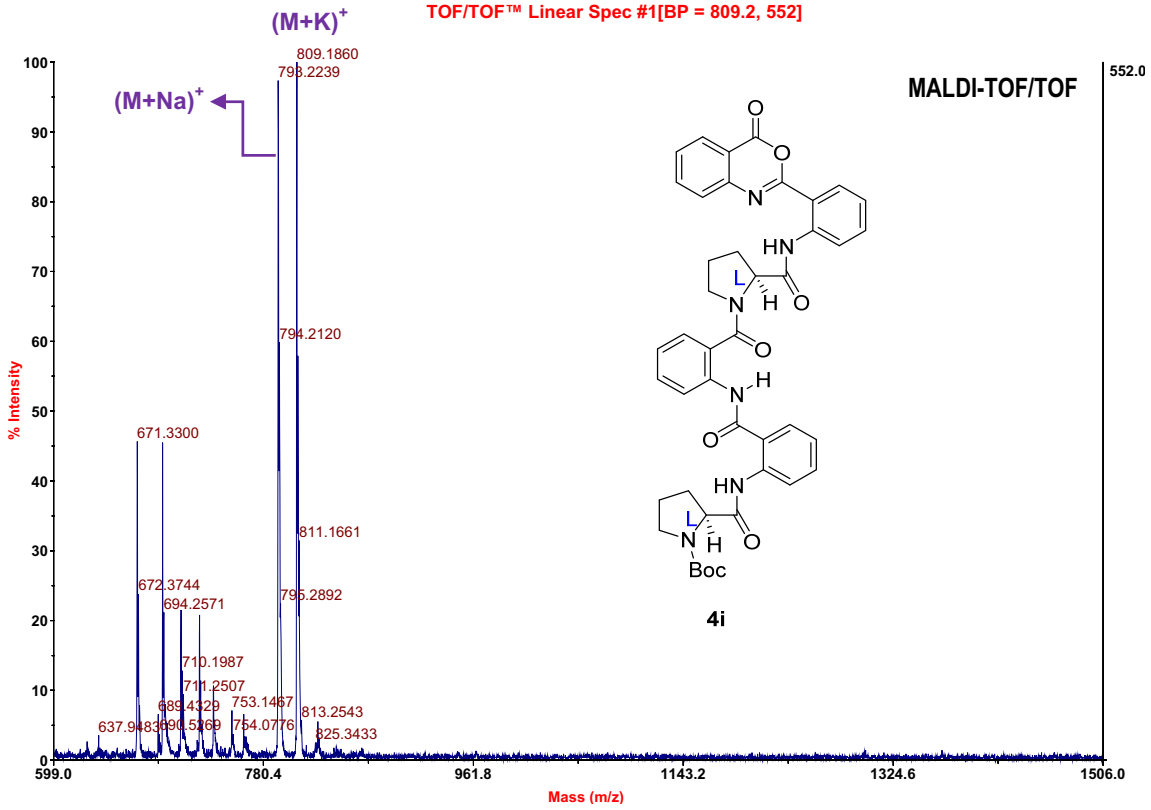
TOF/TOF™ Linear Spec #1[BP = 809.2, 552]
(M+K)+
809.1860
798.2239
(M+Na)+
MALDI-TOF/TOF
552.0
O
O
N
HN
L
N H O
O
N H
O
HN
L
N H O
Boc
4i
794.2120
671.3300
811.1661
672.3744
694.2571
795.2892
710.1987
711.2507
689.4329
753.1467
637.9483
690.5269
754.0776
813.2543
825.3433
% Intensity
100
90
80
70
60
50
40
30
20
10
0
599.0
780.4
961.8
1143.2
1324.6
1506.0
Mass (m/z)

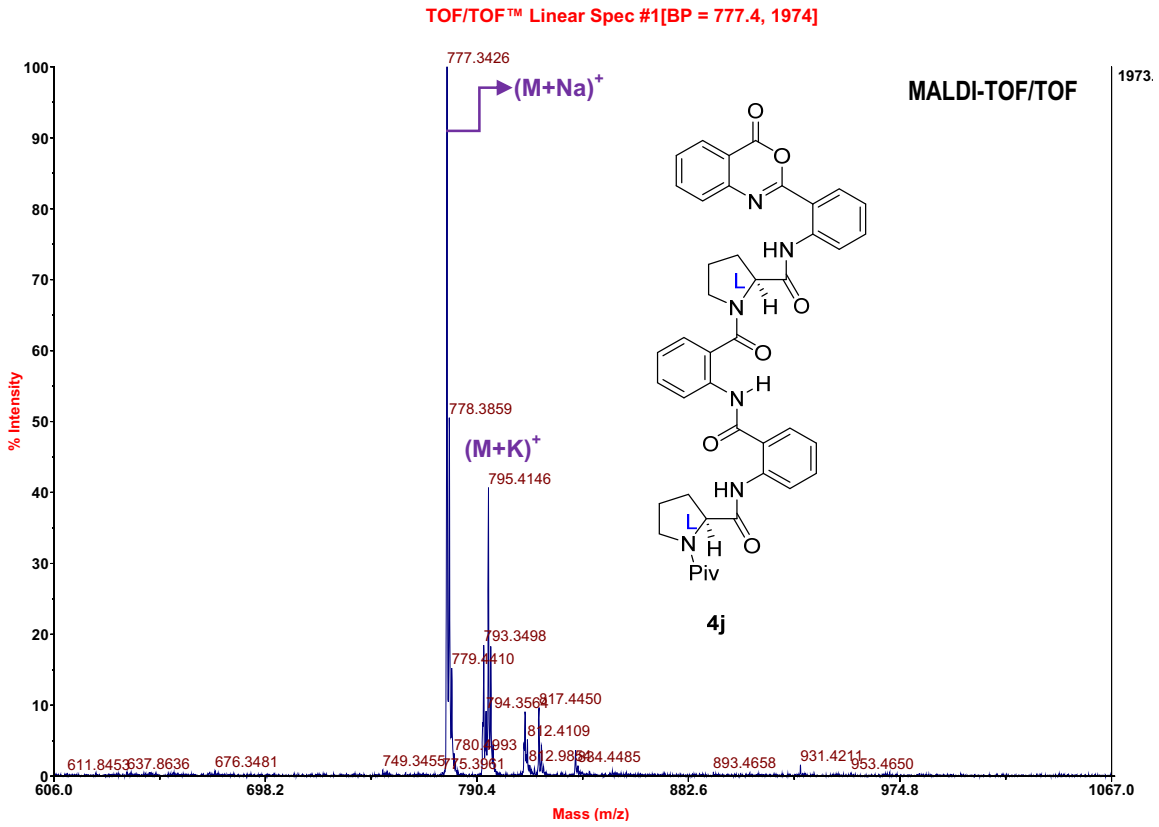
TOF/TOF™ Linear Spec #1[BP = 777.4, 1974]
MALDI-TOF/TOF
777.3426
(M+Na)+
778.3859
(M+K)+
795.4146
793.3498
779.4410
794.3564
817.4450
812.4109
611.8453
637.8636
676.3481
749.3455
893.4658
931.4211
953.4650
% Intensity
Mass (m/z)
606.0
698.2
790.4
882.6
974.8
1067.0
Piv
4j

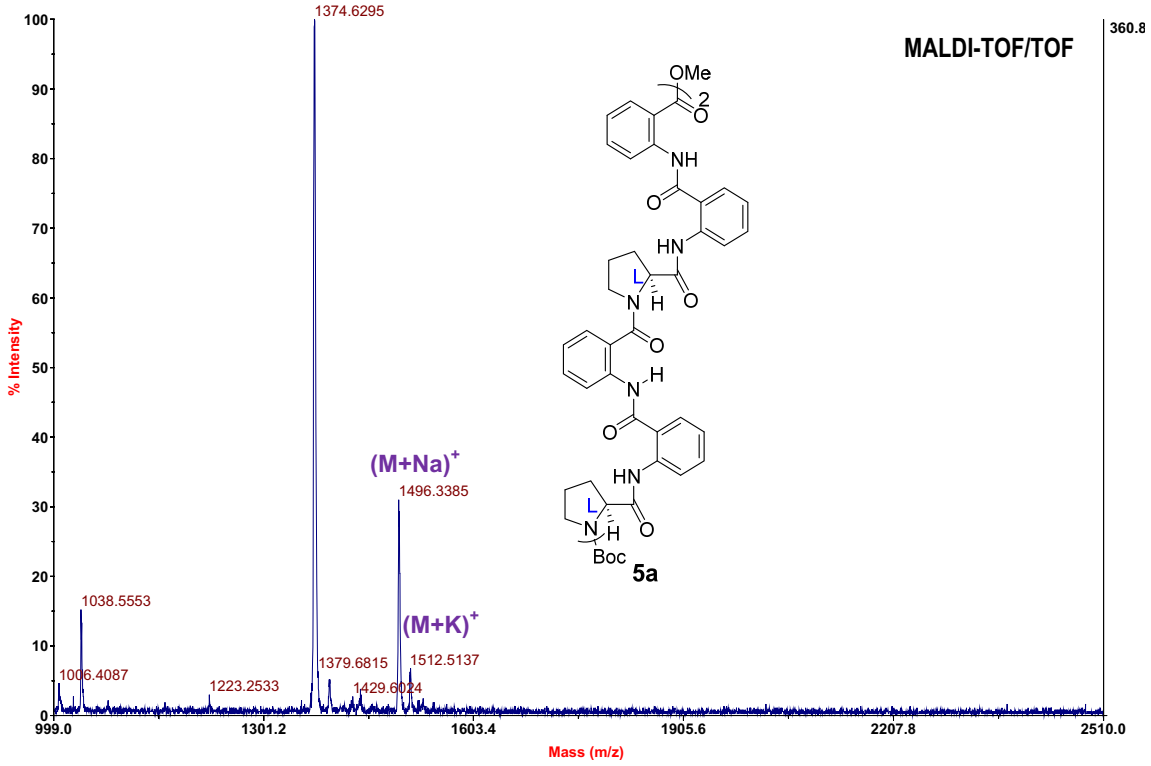
TOF/TOF™ Linear Spec #1[BP = 1374.5, 361]
MALDI-TOF/TOF
1374.6295
(M+Na)+
1496.3385
(M+K)+
1512.5137
1038.5553
1006.4087
1223.2533
1379.6815
1429.6024
% Intensity
Mass (m/z)
999.0
1301.2
1603.4
1905.6
2207.8
2510.0
OMe
Boc
5a

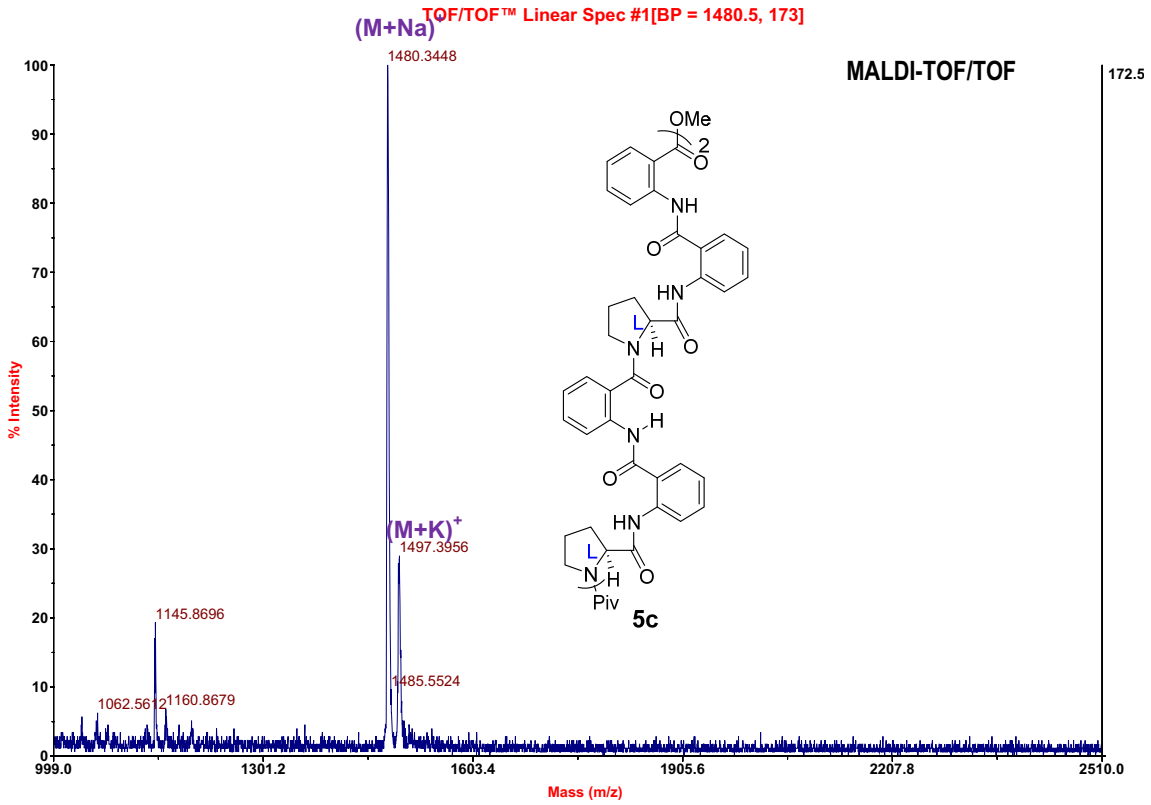
TOF/TOF™ Linear Spec #1[BP = 1480.5, 173]
(M+Na)+
1480.3448
MALDI-TOF/TOF
(M+K)+
1497.3956
1145.8696
1485.5524
1062.5612
1160.8679
% Intensity
Mass (m/z)
999.0
1301.2
1603.4
1905.6
2207.8
2510.0
OMe
NH
HN
Piv
5c

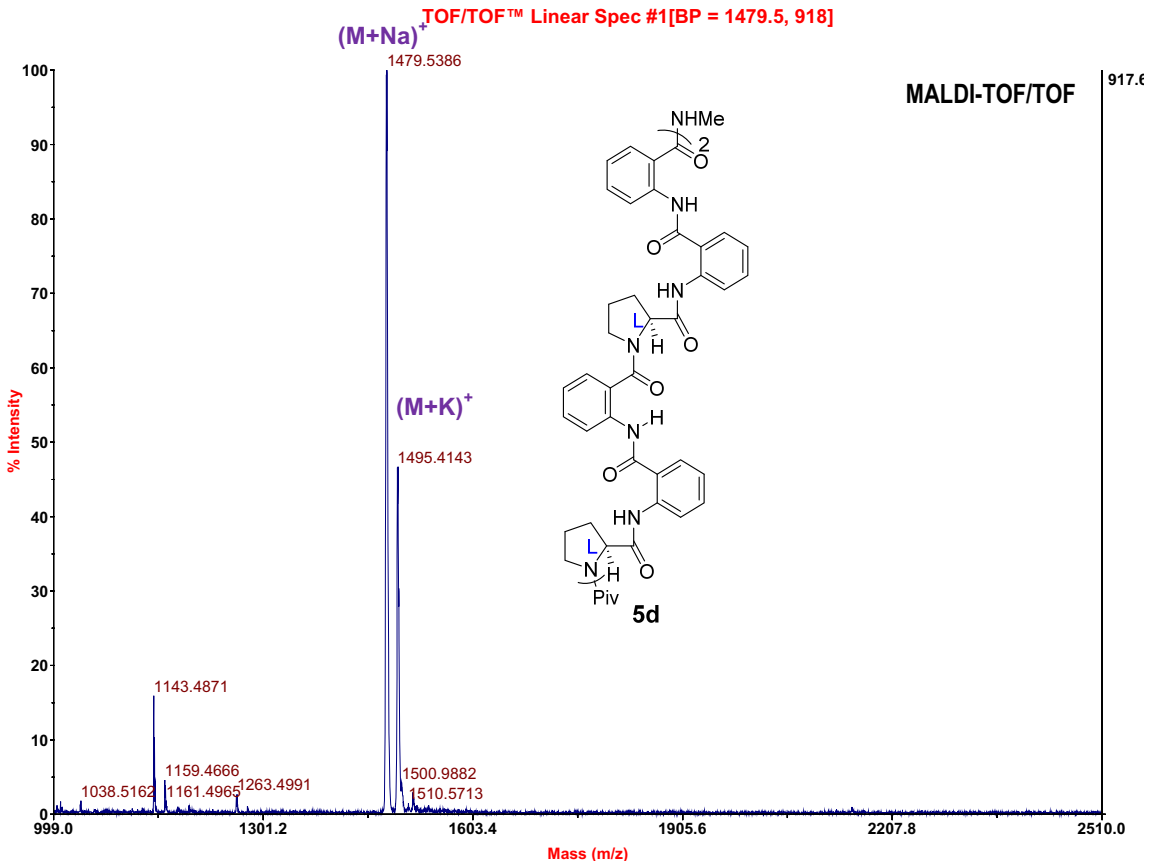
TOF/TOF™ Linear Spec #1[BP = 1479.5, 918]
(M+Na)+
1479.5386
MALDI-TOF/TOF
(M+K)+
1495.4143
1143.4871
1159.4666
1038.5162
1161.4965
1263.4991
1500.9882
1510.5713
% Intensity
Mass (m/z)
999.0
1301.2
1603.4
1905.6
2207.8
2510.0
NHMe
NH
HN
Piv
5d

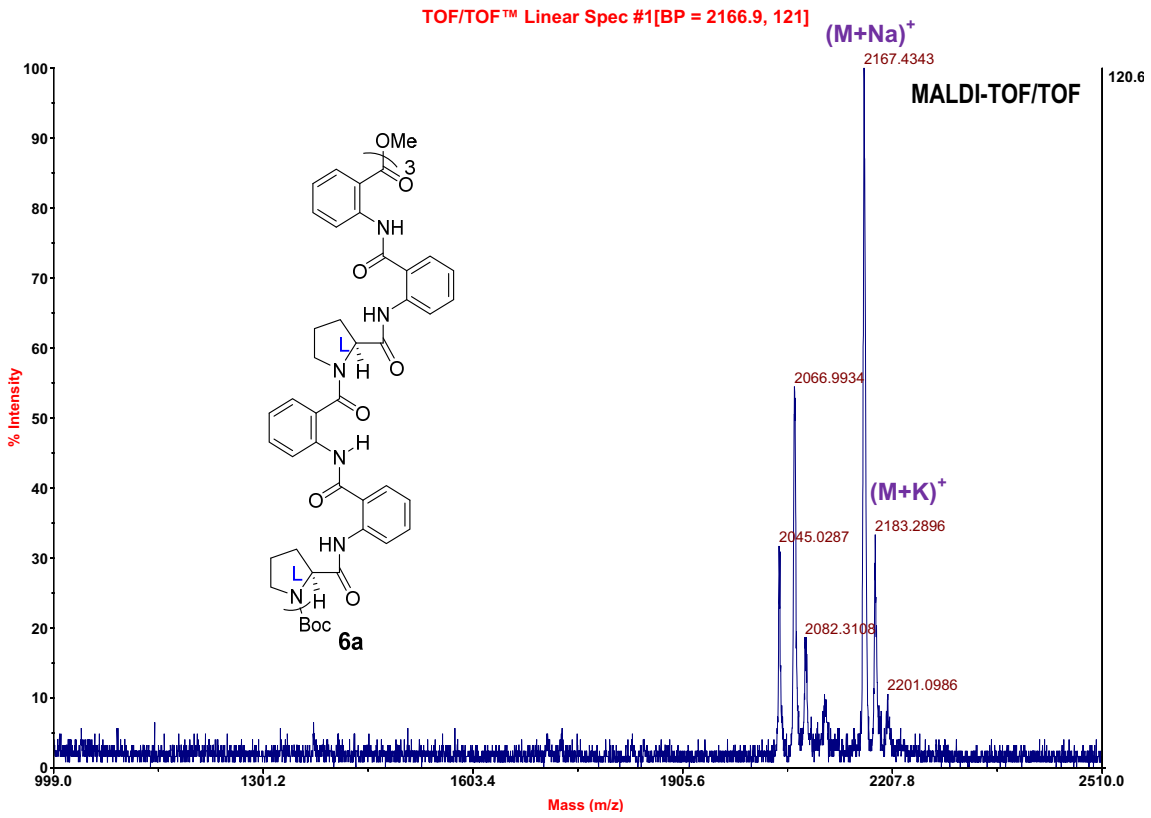
TOF/TOF™ Linear Spec #1[BP = 2166.9, 121]
(M+Na)+
2167.4343
MALDI-TOF/TOF
2066.9934
(M+K)+
2045.0287
2183.2896
2082.3108
2201.0986
% Intensity
Mass (m/z)
6a

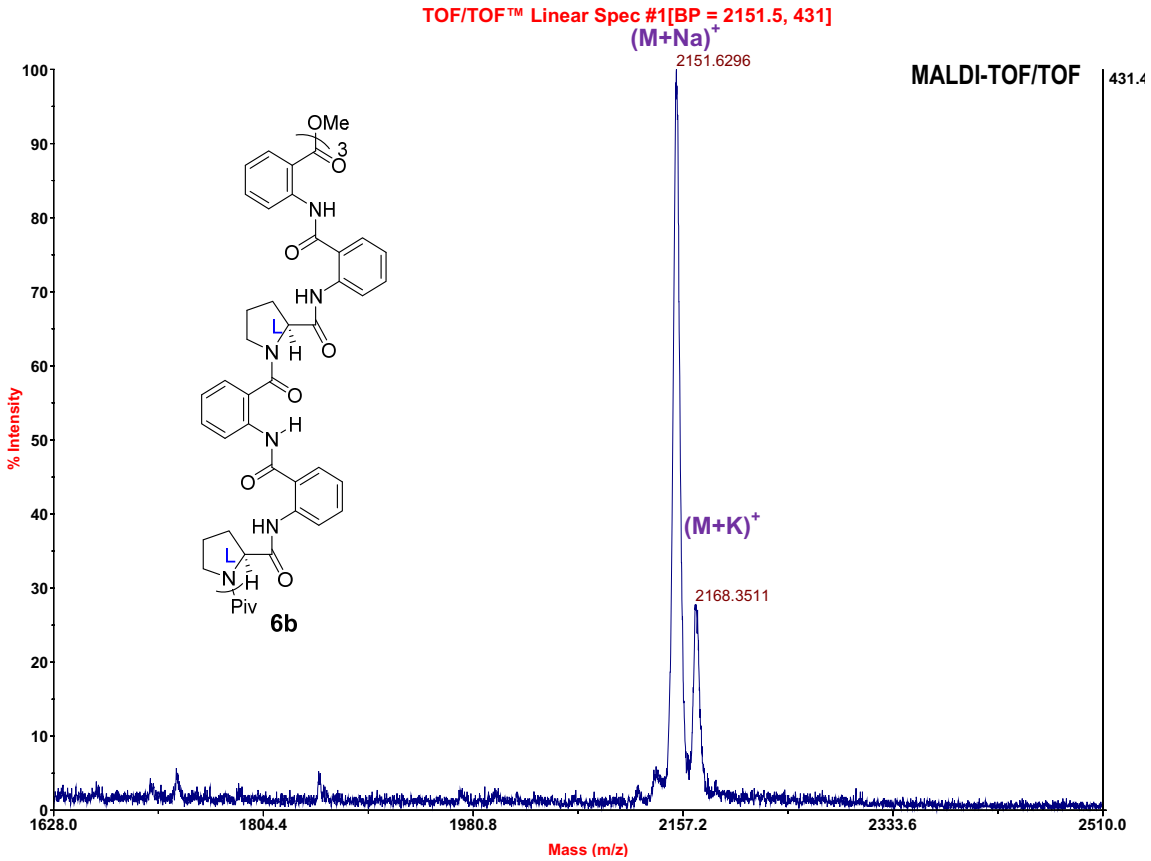
TOF/TOF™ Linear Spec #1[BP = 2151.5, 431]
(M+Na)+
2151.6296
MALDI-TOF/TOF
(M+K)+
2168.3511
% Intensity
Mass (m/z)
6b

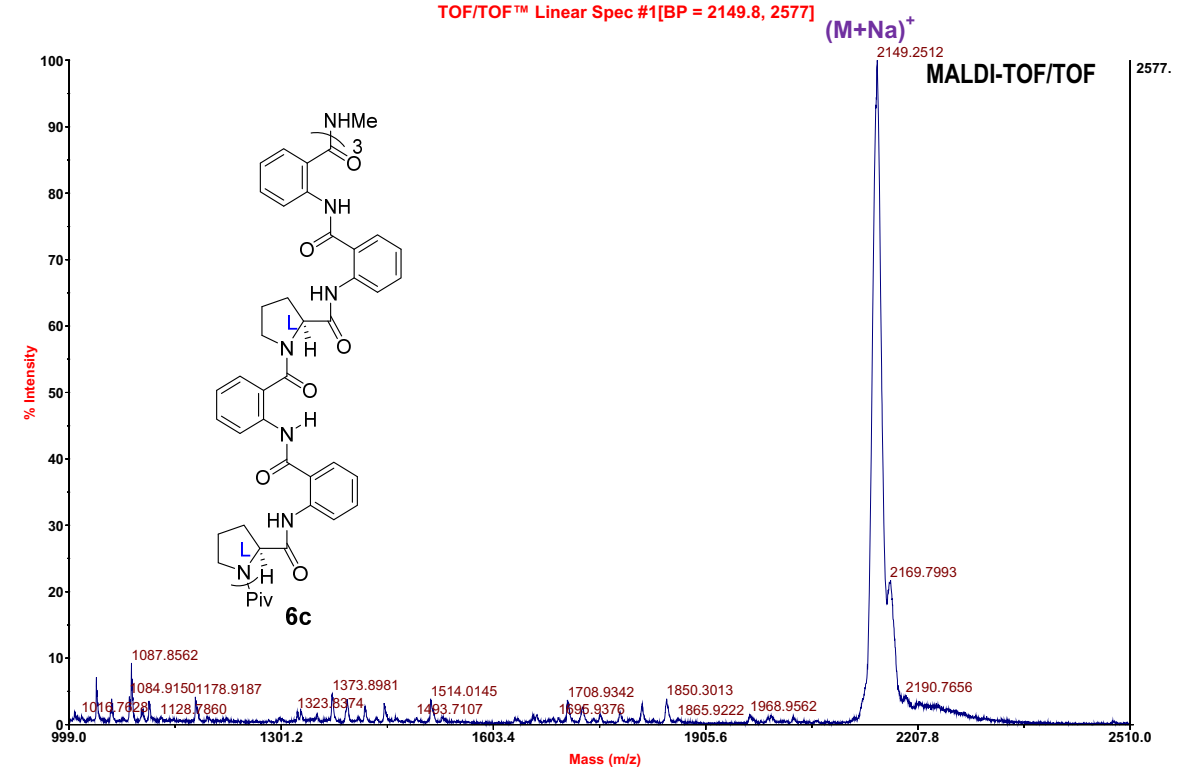
TOF/TOF™ Linear Spec #1[BP = 2149.8, 2577]
(M+Na)+
2149.2512
MALDI-TOF/TOF
2577.
NHMe
3
O
NH
O
HN
L
N H
O
O
N H
O
HN
L
N H
O
Piv
6c
% Intensity
100
90
80
70
60
50
40
30
20
10
0
1087.8562
1084.9150
1178.9187
1373.8981
1514.0145
1708.9342
1850.3013
2169.7993
2190.7656
1016.7628
1128.7860
1323.8374
1493.7107
1696.9376
1865.9222
1968.9562
999.0
1301.2
1603.4
1905.6
2207.8
2510.0
Mass (m/z)

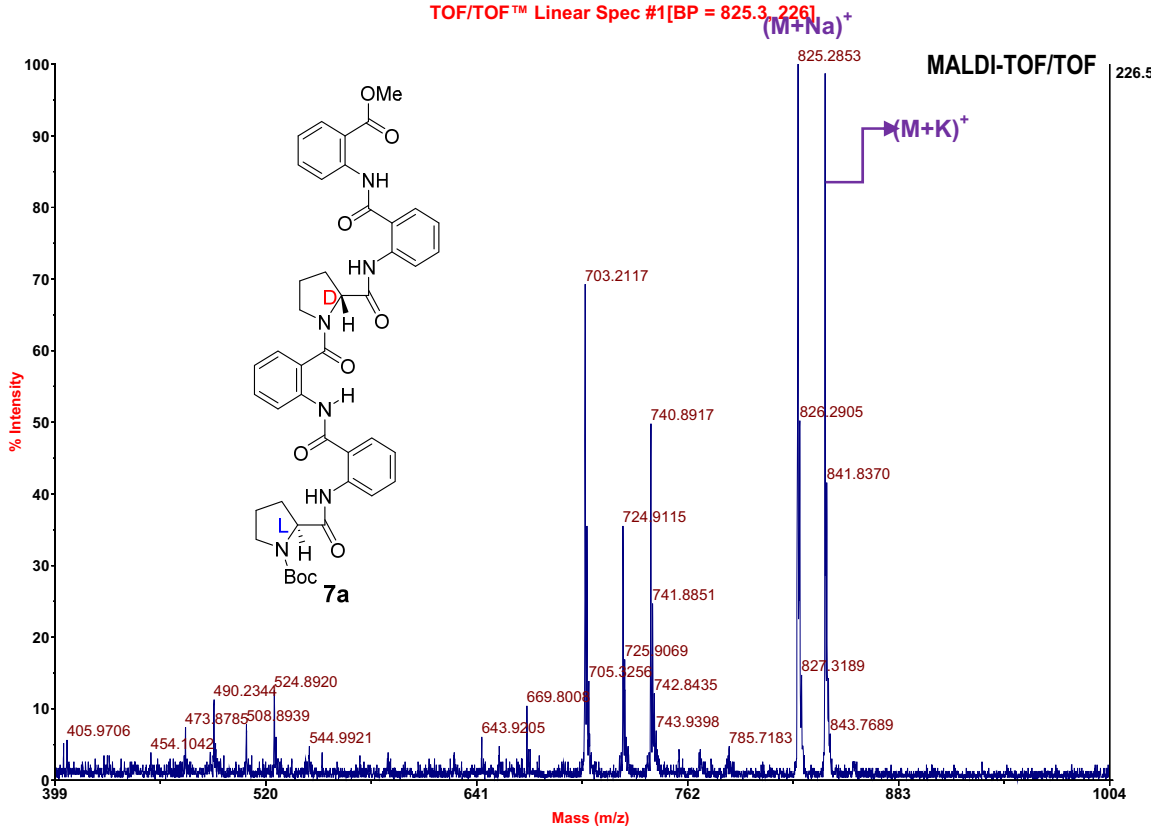
TOF/TOF™ Linear Spec #1[BP = 825.3, 226]
(M+Na)+
825.2853
MALDI-TOF/TOF
226.5
(M+K)+
OMe
O
NH
O
HN
D
N H
O
O
N H
O
HN
L
N H
O
Boc
7a
% Intensity
100
90
80
70
60
50
40
30
20
10
0
703.2117
740.8917
826.2905
841.8370
724.9115
741.8851
725.9069
705.3256
742.8435
827.3189
490.2344
524.8920
669.8008
473.8785
508.8939
743.9398
843.7689
405.9706
454.1042
544.9921
643.9205
785.7183
399
520
641
762
883
1004
Mass (m/z)

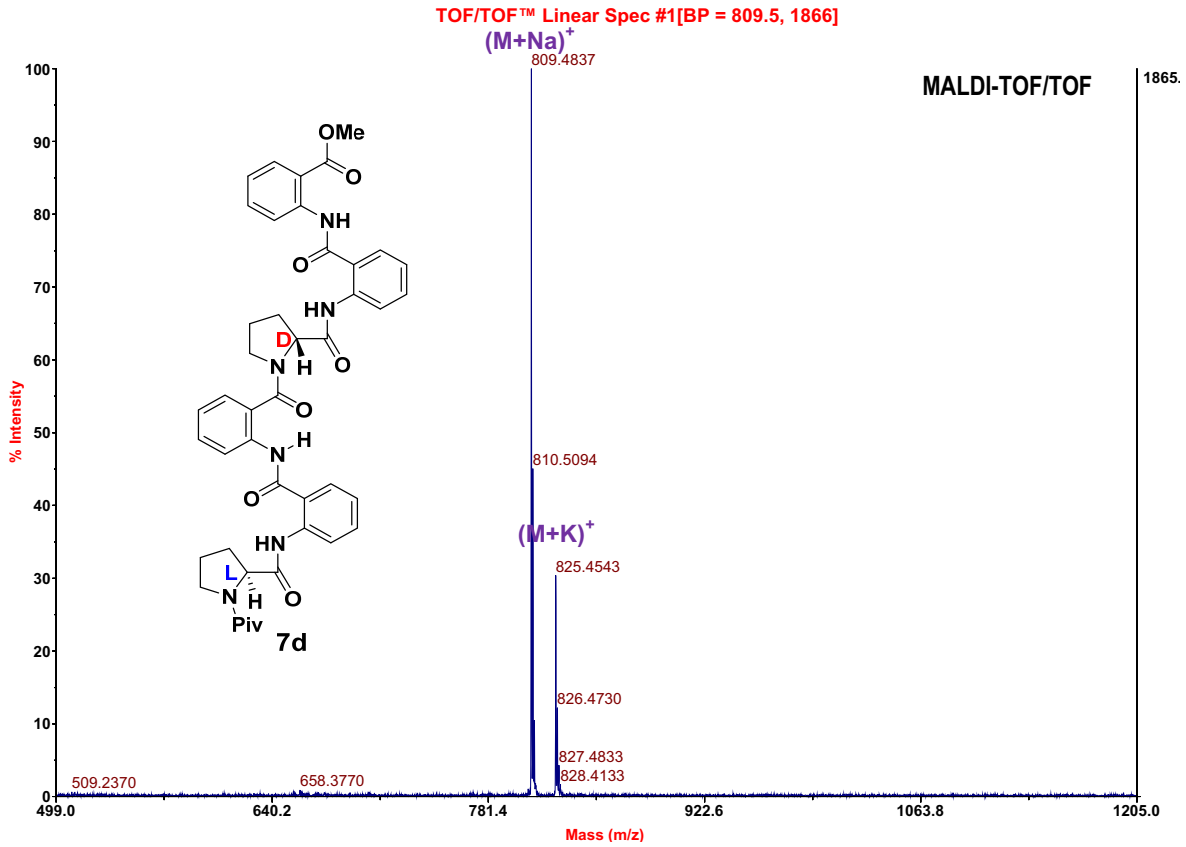
TOF/TOF™ Linear Spec #1[BP = 809.5, 1866]
(M+Na)+
809.4837
MALDI-TOF/TOF
1865.
OMe
NH
HN
D
N H
Piv
7d
% Intensity
810.5094
(M+K)+
825.4543
826.4730
827.4833
828.4133
509.2370
658.3770
499.0
640.2
781.4
922.6
1063.8
1205.0
Mass (m/z)

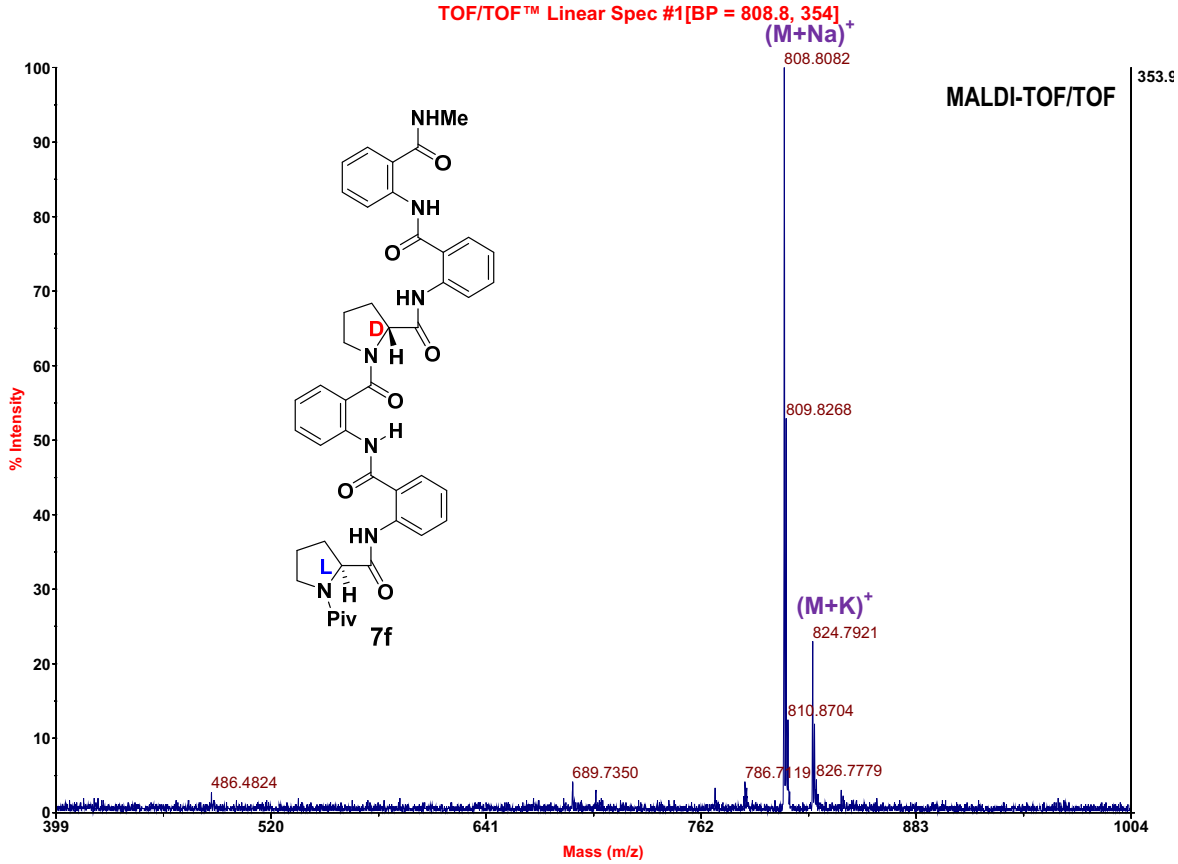
TOF/TOF™ Linear Spec #1[BP = 808.8, 354]
(M+Na)+
808.8082
MALDI-TOF/TOF
353.9
NHMe
NH
HN
D
N H
L
Piv
7f
% Intensity
809.8268
(M+K)+
824.7921
810.8704
826.7779
486.4824
689.7350
786.7119
399
520
641
762
883
1004
Mass (m/z)

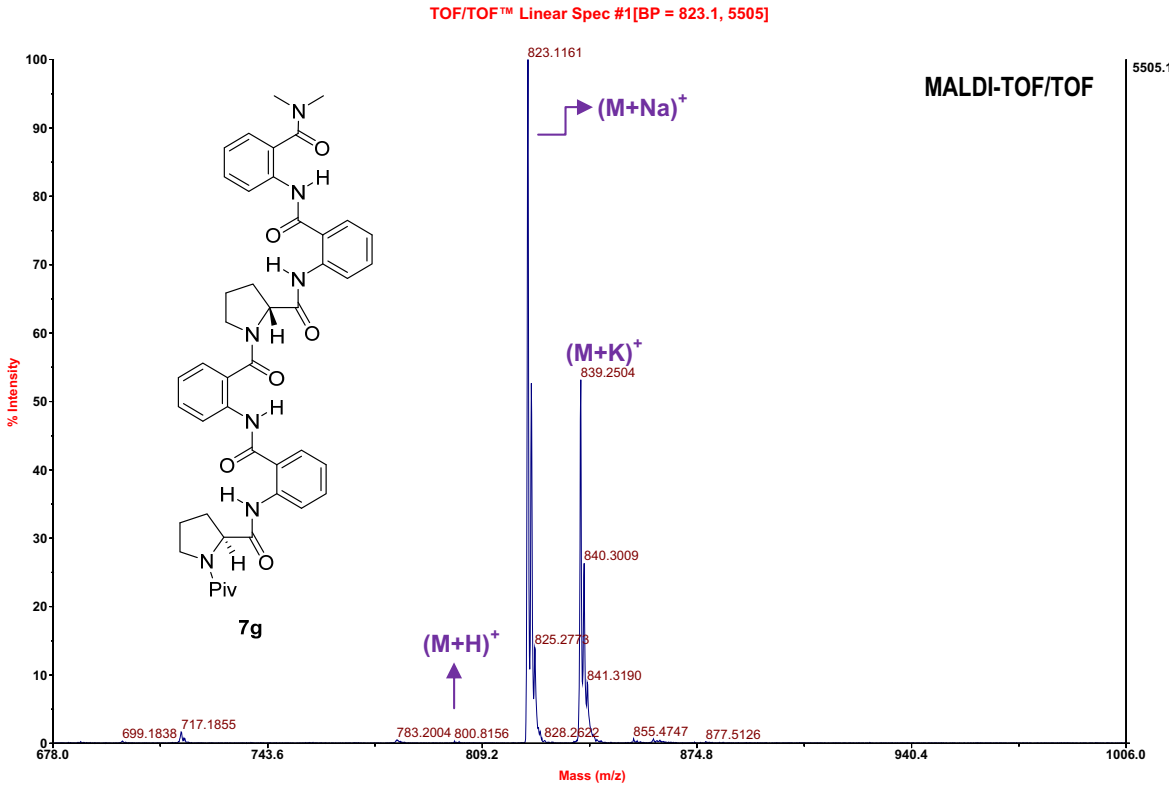
TOF/TOF™ Linear Spec #1[BP = 823.1, 5505]
MALDI-TOF/TOF
5505.1
823.1161
(M+Na)+
(M+K)+
839.2504
840.3009
825.2773
841.3190
(M+H)+
699.1838
717.1855
783.2004
800.8156
828.2622
855.4747
877.5126
Piv
7g
% Intensity
Mass (m/z)
678.0
743.6
809.2
874.8
940.4
1006.0

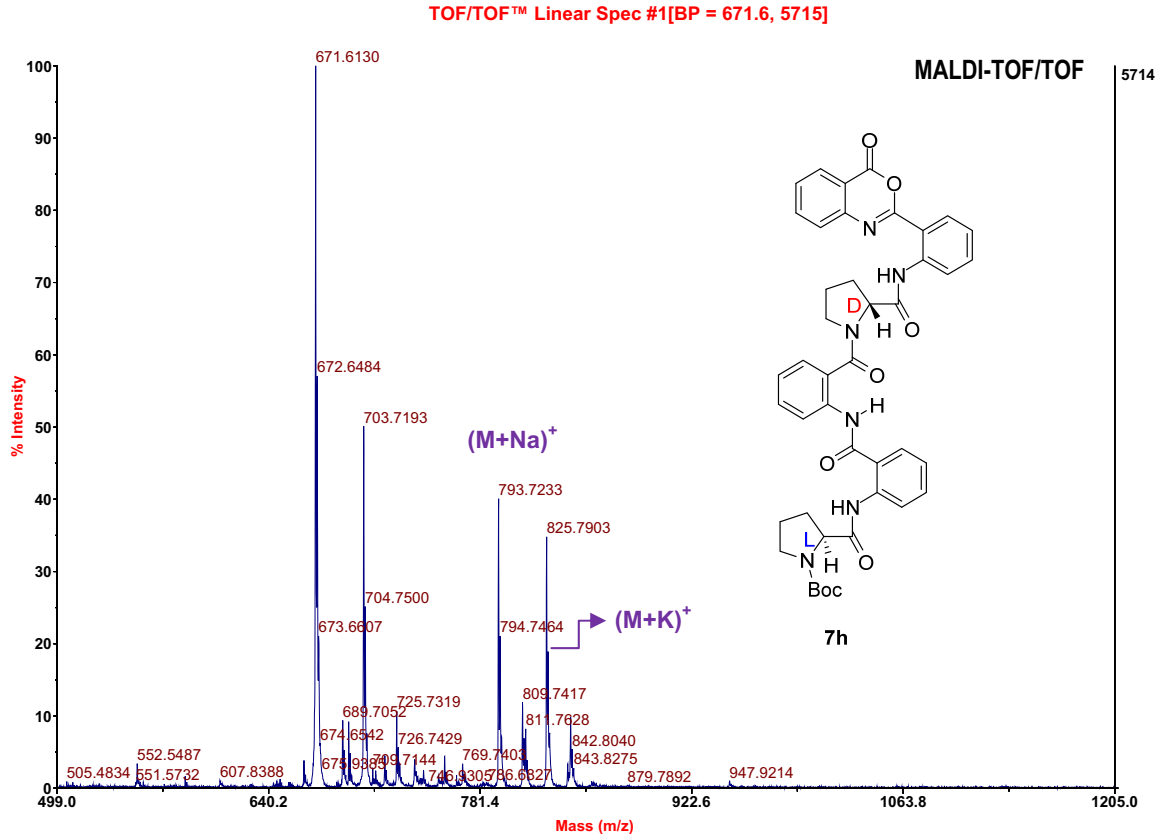
TOF/TOF™ Linear Spec #1[BP = 671.6, 5715]
MALDI-TOF/TOF
5714
671.6130
672.6484
703.7193
(M+Na)+
793.7233
825.7903
704.7500
673.6607
794.7464
(M+K)+
809.7417
725.7319
689.7052
811.7628
674.6542
726.7429
842.8040
769.7403
843.8275
552.5487
505.4834
551.5732
607.8388
879.7892
947.9214
Boc
7h
% Intensity
Mass (m/z)
499.0
640.2
781.4
922.6
1063.8
1205.0

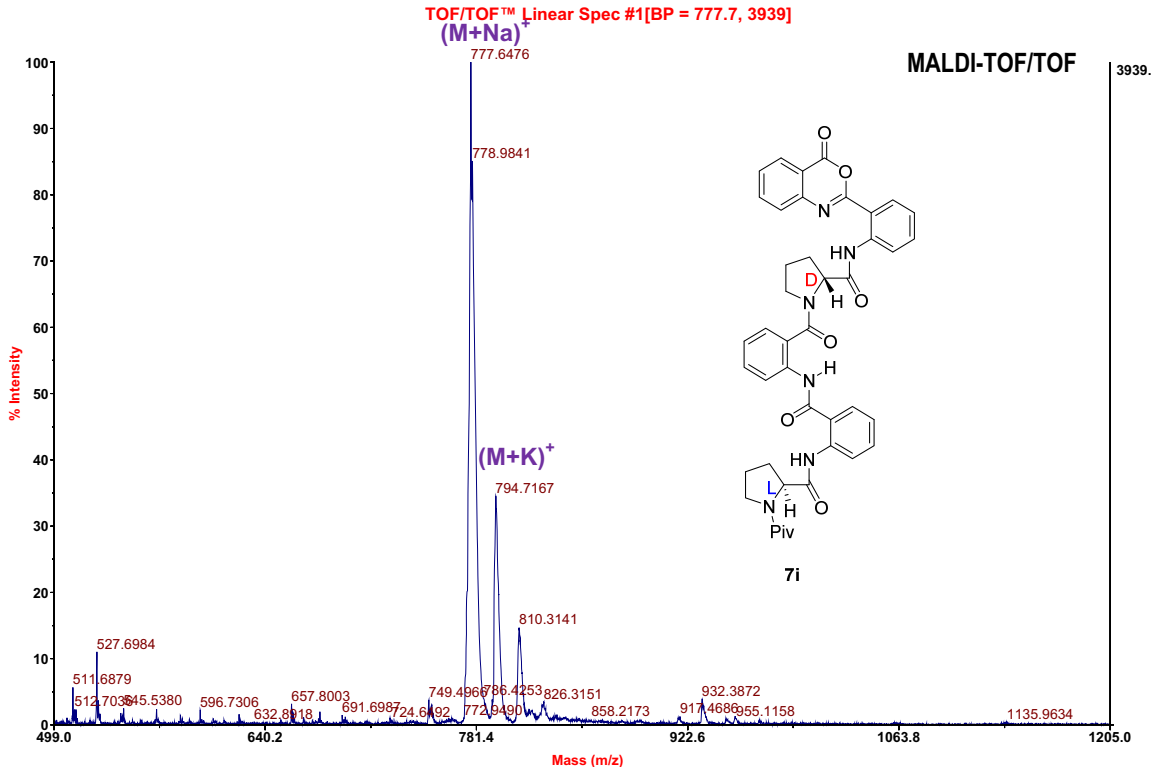
TOF/TOF™ Linear Spec #1[BP = 777.7, 3939]
MALDI-TOF/TOF
3939.
(M+Na)+
777.6476
778.9841
(M+K)+
794.7167
810.3141
527.6984
511.6879
512.7038
545.5380
596.7306
632.8018
657.8003
691.6987
724.6492
749.4966
772.9490
786.4253
826.3151
858.2173
917.4686
932.3872
955.1158
1135.9634
% Intensity
Mass (m/z)
7i

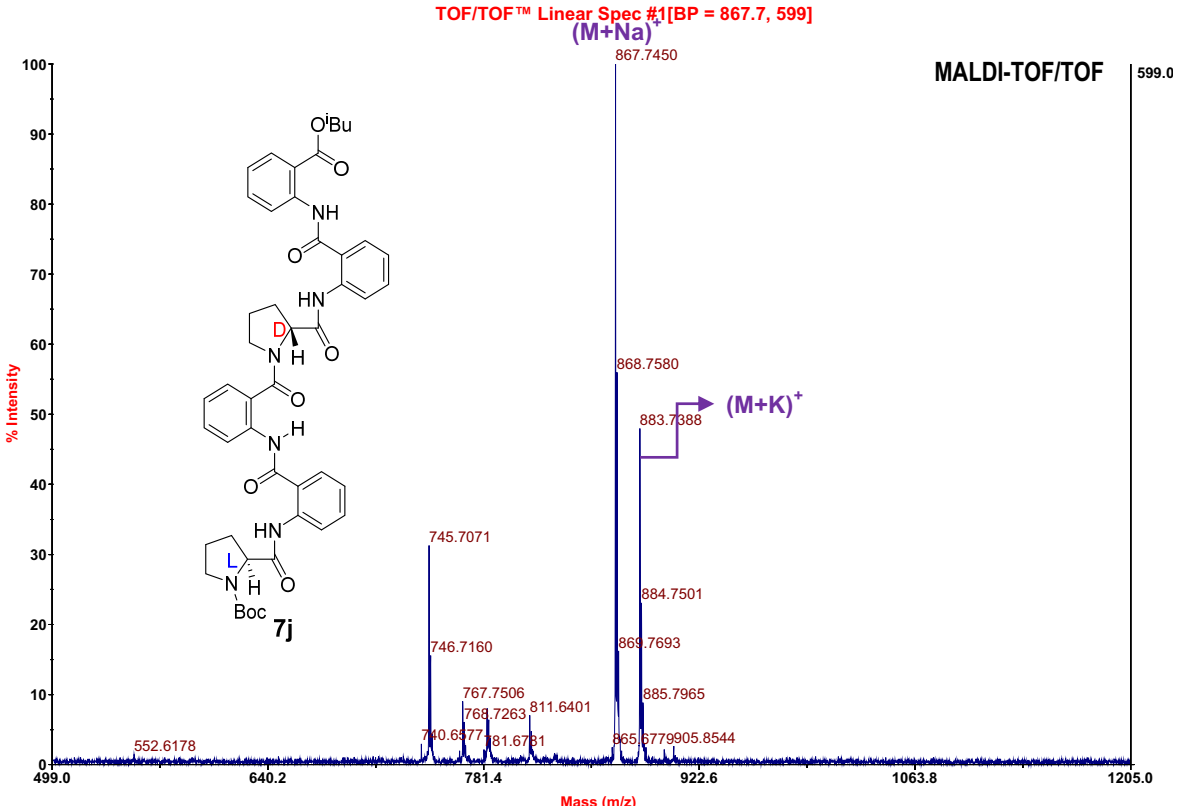
TOF/TOF™ Linear Spec #1[BP = 867.7, 599]
MALDI-TOF/TOF
599.0
(M+Na)+
867.7450
868.7580
(M+K)+
883.7388
884.7501
885.7965
745.7071
746.7160
767.7506
768.7263
811.6401
552.6178
740.6877
781.6781
865.6779
905.8544
% Intensity
Mass (m/z)
7j

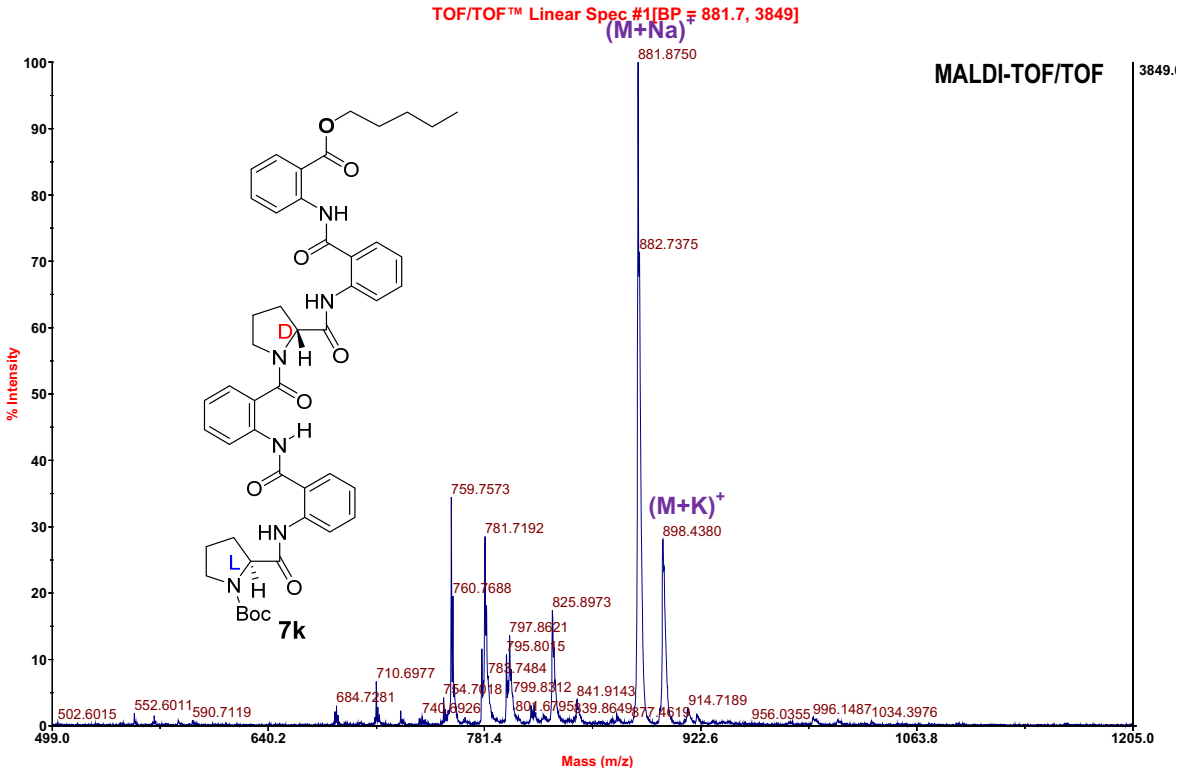
TOF/TOF™ Linear Spec #1[BP = 881.7, 3849]
(M+Na)+
881.8750
MALDI-TOF/TOF
3849.
882.7375
759.7573
781.7192
(M+K)+
898.4380
760.7688
825.8973
797.8621
795.8015
710.6977
684.7281
754.7018
799.8312
841.9143
914.7189
502.6015
552.6011
590.7119
740.6926
839.8649
956.0355
996.1487
1034.3976
% Intensity
Mass (m/z)
499.0
640.2
781.4
922.6
1063.8
1205.0
Boc
7k

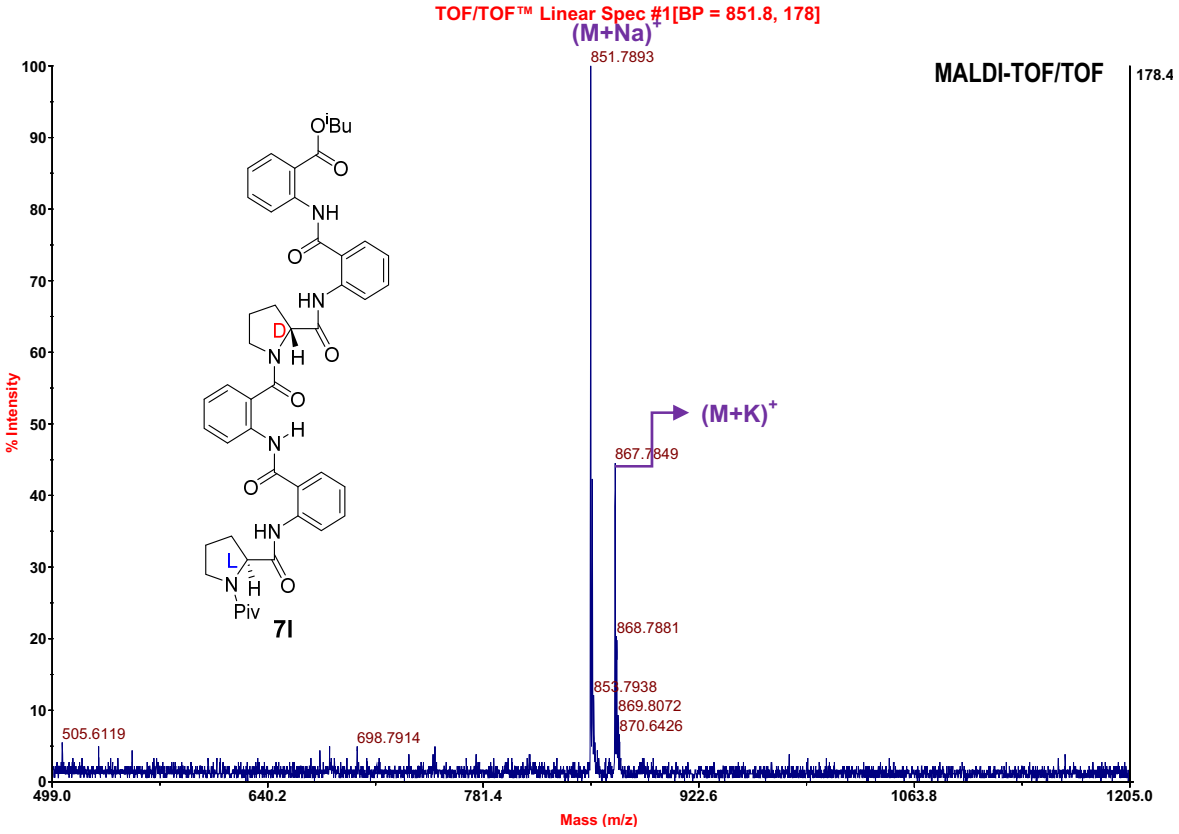
TOF/TOF™ Linear Spec #1[BP = 851.8, 178]
(M+Na)+
851.7893
MALDI-TOF/TOF
178.4
(M+K)+
867.7849
868.7881
851.7938
869.8072
870.6426
505.6119
698.7914
% Intensity
Mass (m/z)
499.0
640.2
781.4
922.6
1063.8
1205.0
Piv
7l

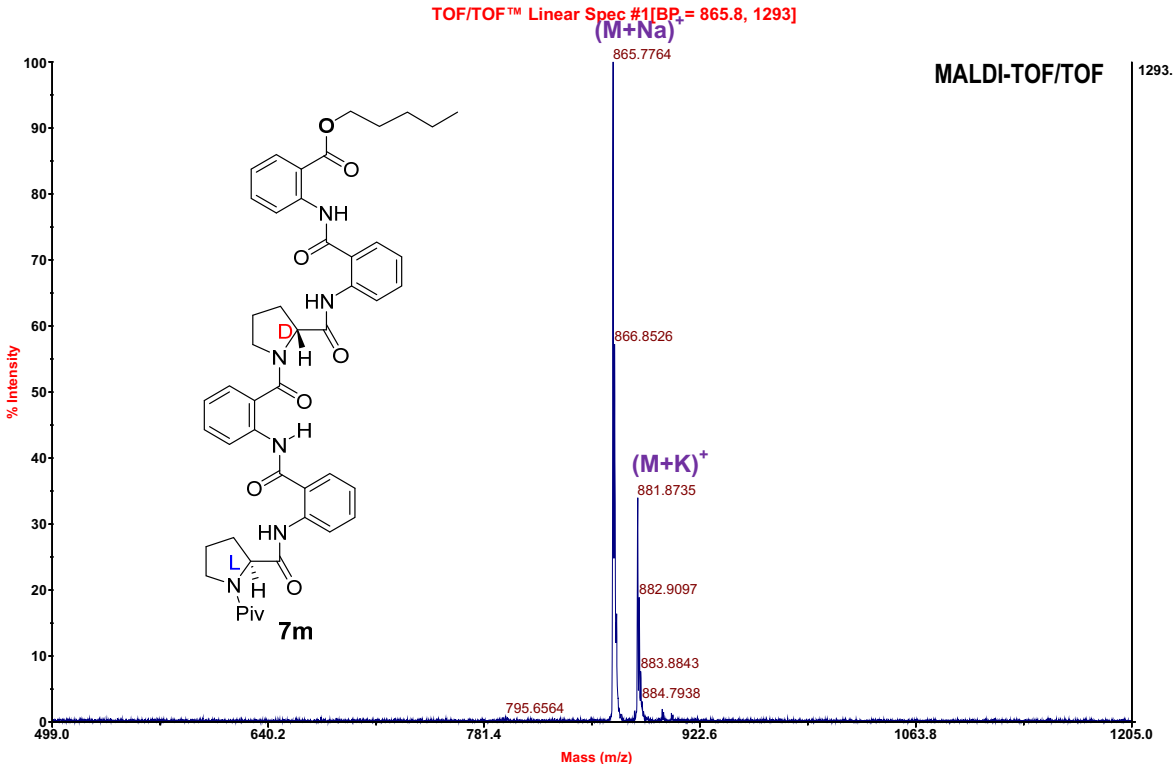
TOF/TOF™ Linear Spec #1[BP = 865.8, 1293]
MALDI-TOF/TOF
1293.
(M+Na)+
865.7764
866.8526
(M+K)+
881.8735
882.9097
883.8843
884.7938
795.6564
% Intensity
Mass (m/z)
499.0
640.2
781.4
922.6
1063.8
1205.0
7m

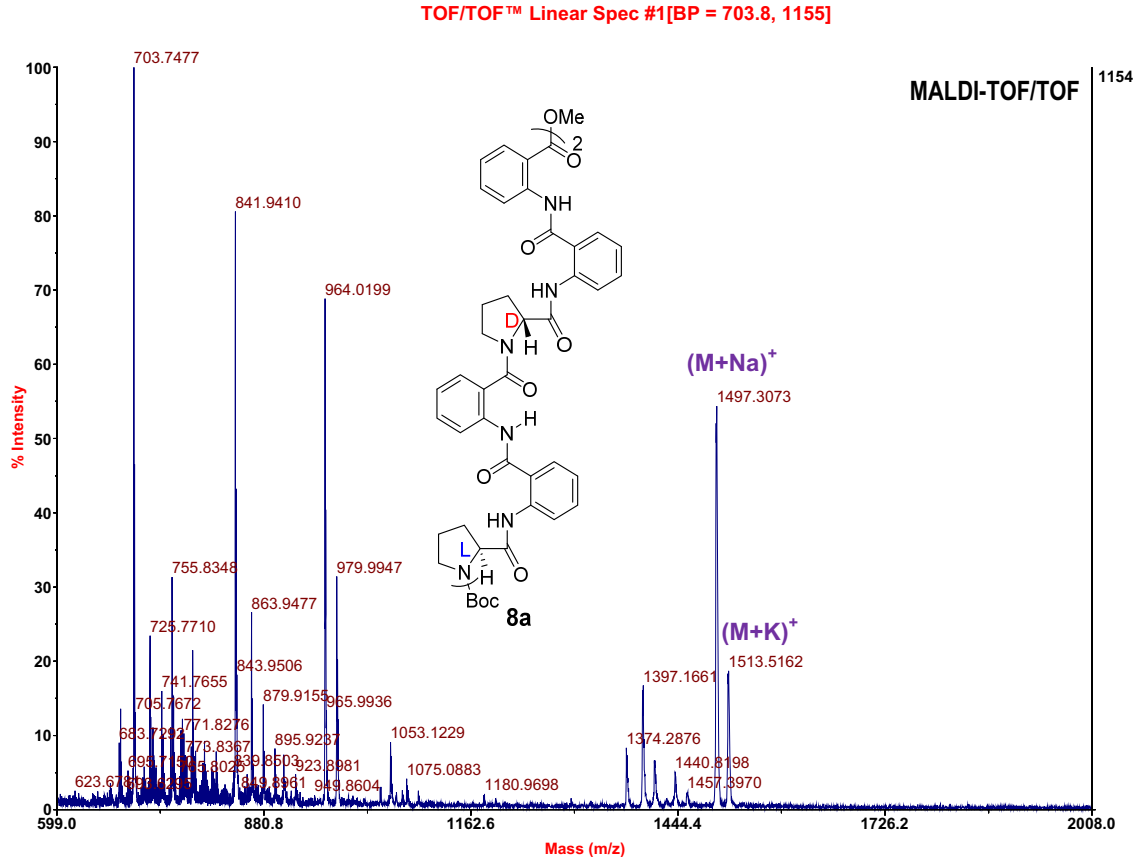
TOF/TOF™ Linear Spec #1[BP = 703.8, 1155]
MALDI-TOF/TOF
1154
703.7477
841.9410
964.0199
(M+Na)+
1497.3073
(M+K)+
1513.5162
755.8348
979.9947
863.9477
725.7710
843.9506
741.7655
879.9155
965.9936
705.7672
771.8276
683.7295
895.9237
1053.1229
1374.2876
1397.1661
1440.8198
1457.3970
1075.0883
1180.9698
% Intensity
Mass (m/z)
599.0
880.8
1162.6
1444.4
1726.2
2008.0
8a

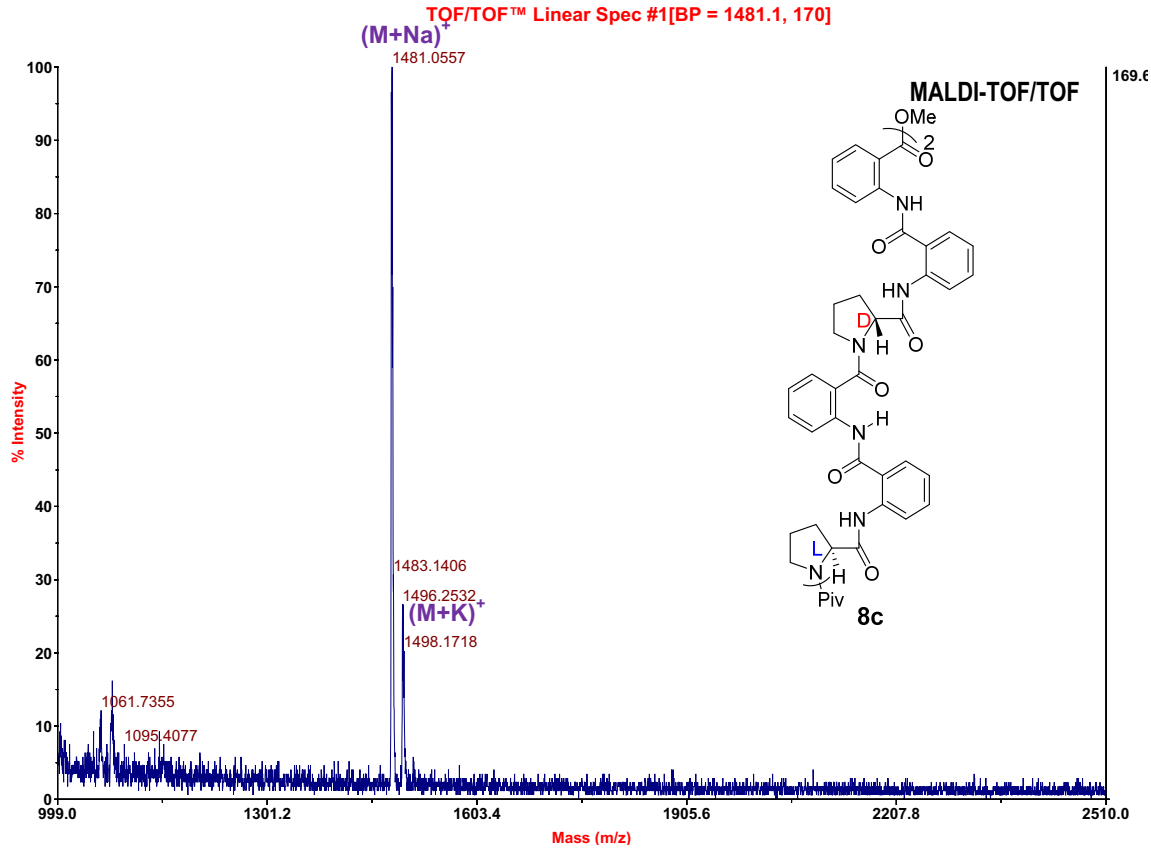
TOF/TOF™ Linear Spec #1[BP = 1481.1, 170]
(M+Na)+
1481.0557
MALDI-TOF/TOF
OMe
2
O
NH
O
HN
D
N H
O
O
N H
O
HN
L
N H
O
Piv
8c
1483.1406
1496.2532
(M+K)+
1498.1718
1061.7355
1095.4077
% Intensity
Mass (m/z)
999.0
1301.2
1603.4
1905.6
2207.8
2510.0

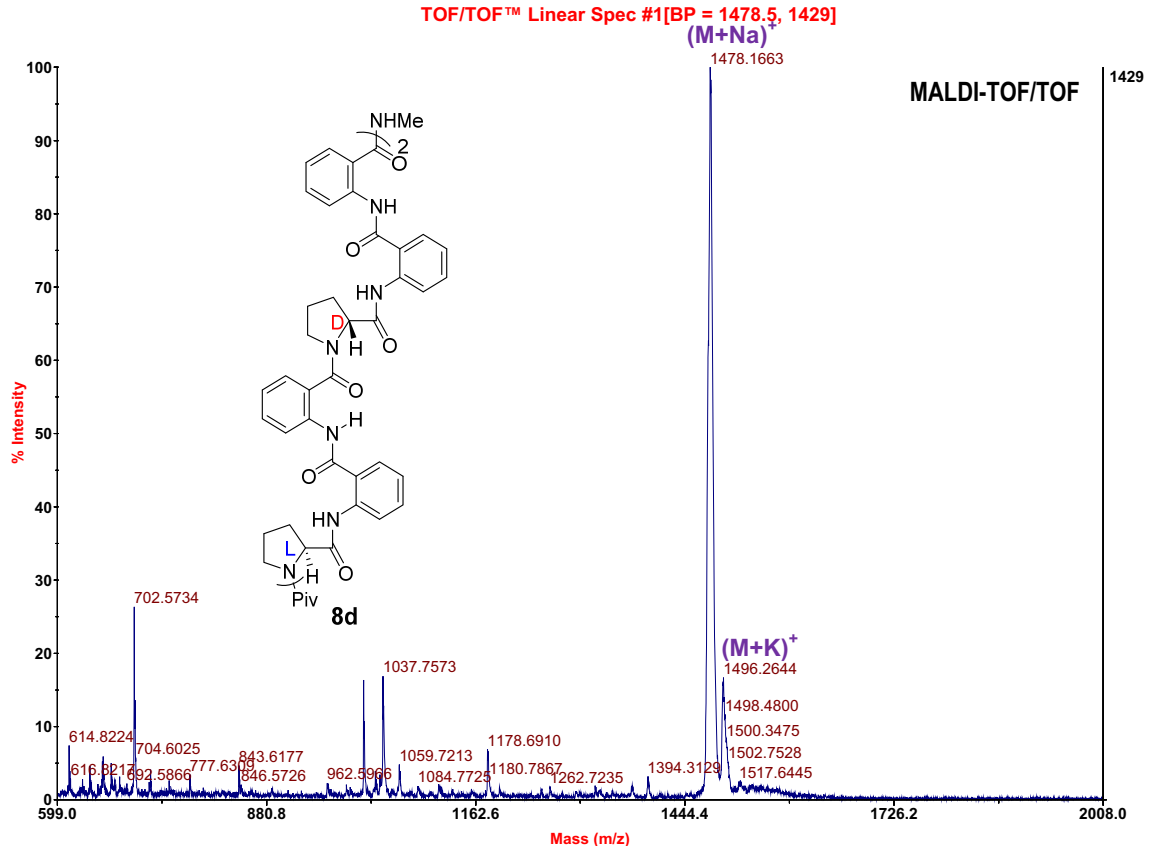
TOF/TOF™ Linear Spec #1[BP = 1478.5, 1429]
(M+Na)+
1478.1663
MALDI-TOF/TOF
NHMe
2
O
NH
O
HN
D
N H
O
O
N H
O
HN
L
N H
O
Piv
8d
702.5734
1037.7573
(M+K)+
1496.2644
1498.4800
1500.3475
1502.7528
1517.6445
614.8224
704.6025
843.6177
1059.7213
1178.6910
1180.7867
1394.3129
962.5966
1084.7725
1262.7235
% Intensity
Mass (m/z)
599.0
880.8
1162.6
1444.4
1726.2
2008.0

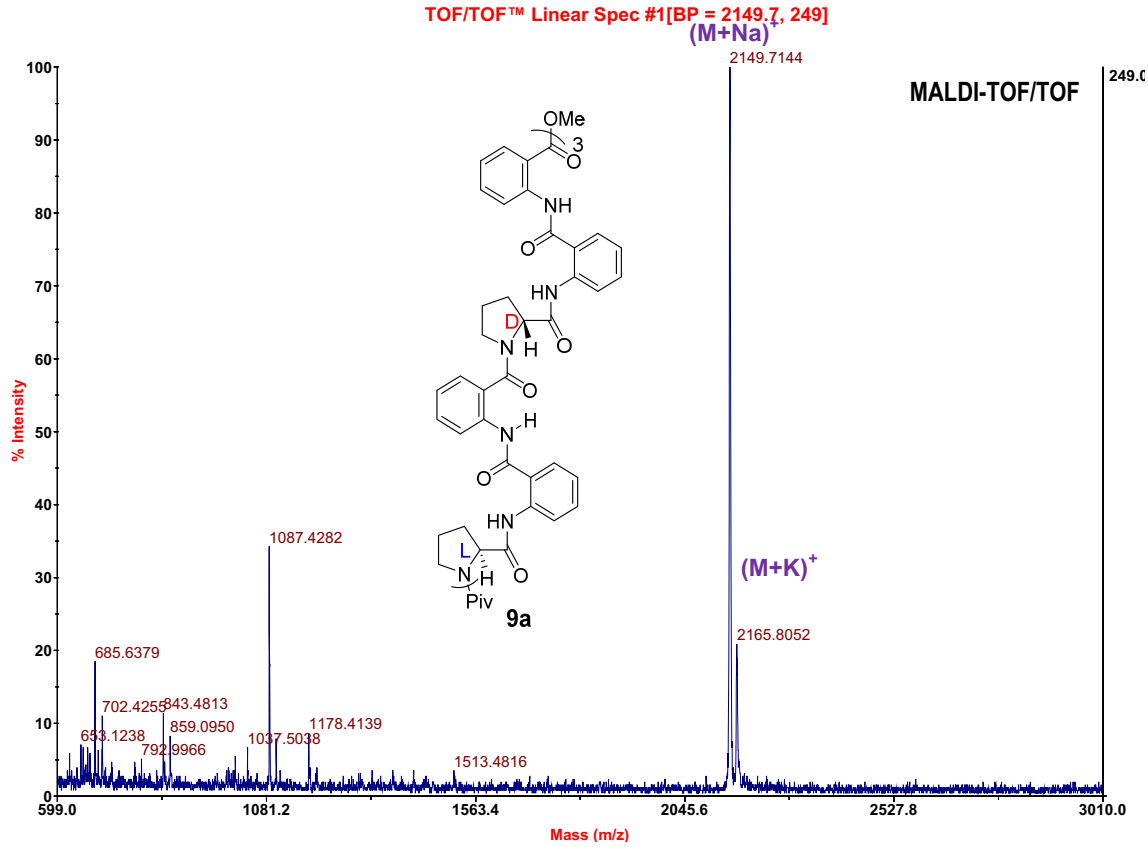
TOF/TOF™ Linear Spec #1[BP = 2149.7, 249]
(M+Na)+
2149.7144
MALDI-TOF/TOF
OMe
NH
HN
D
N H
N H
HN
L
N H
Piv
9a
(M+K)+
2165.8052
1087.4282
685.6379
702.4255
843.4813
859.0950
653.1238
792.9966
1037.5038
1178.4139
1513.4816
% Intensity
Mass (m/z)
599.0
1081.2
1563.4
2045.6
2527.8
3010.0

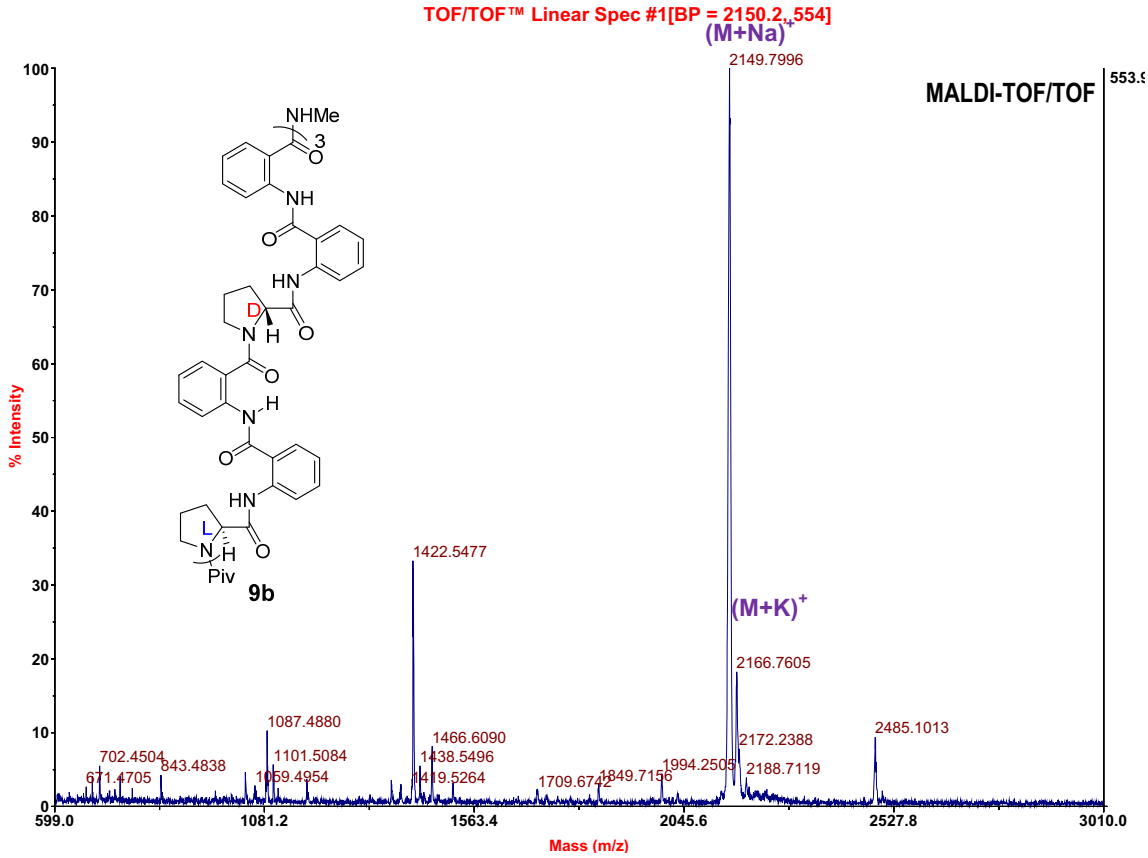
TOF/TOF™ Linear Spec #1[BP = 2150.2, 554]
(M+Na)+
2149.7996
MALDI-TOF/TOF
NHMe
NH
HN
D
N H
N H
HN
L
N H
Piv
9b
1422.5477
(M+K)+
2166.7605
1087.4880
1466.6090
2172.2388
2485.1013
1101.5084
1438.5496
2188.7119
702.4504
843.4838
671.4705
1059.4954
1419.5264
1709.6742
1849.7156
1994.2505
% Intensity
Mass (m/z)
599.0
1081.2
1563.4
2045.6
2527.8
3010.0

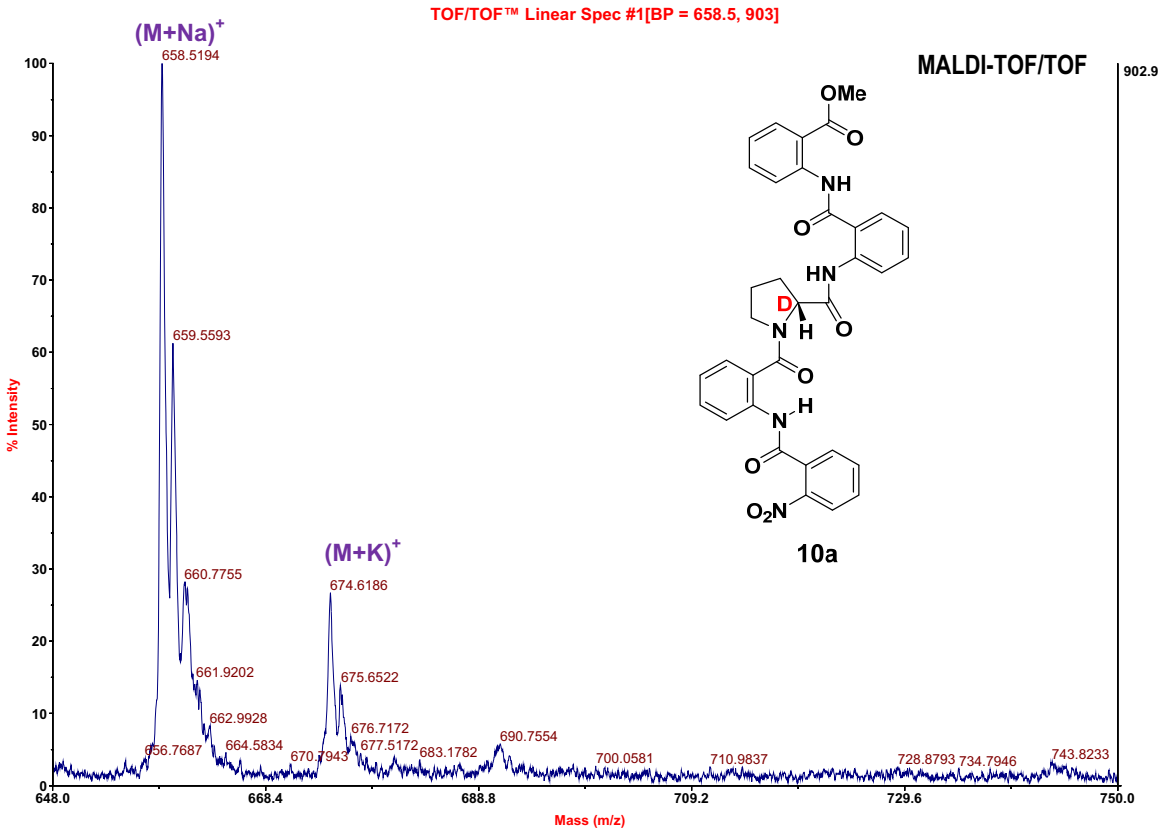
TOF/TOF™ Linear Spec #1[BP = 658.5, 903]
MALDI-TOF/TOF
902.9
(M+Na)+
658.5194
659.5593
660.7755
661.9202
662.9928
656.7687
664.5834
(M+K)+
674.6186
675.6522
676.7172
677.5172
670.7943
683.1782
690.7554
700.0581
710.9837
728.8793
734.7946
743.8233
OMe
O
NH
HN
D
N H
10a
% Intensity
Mass (m/z)
648.0
668.4
688.8
709.2
729.6
750.0

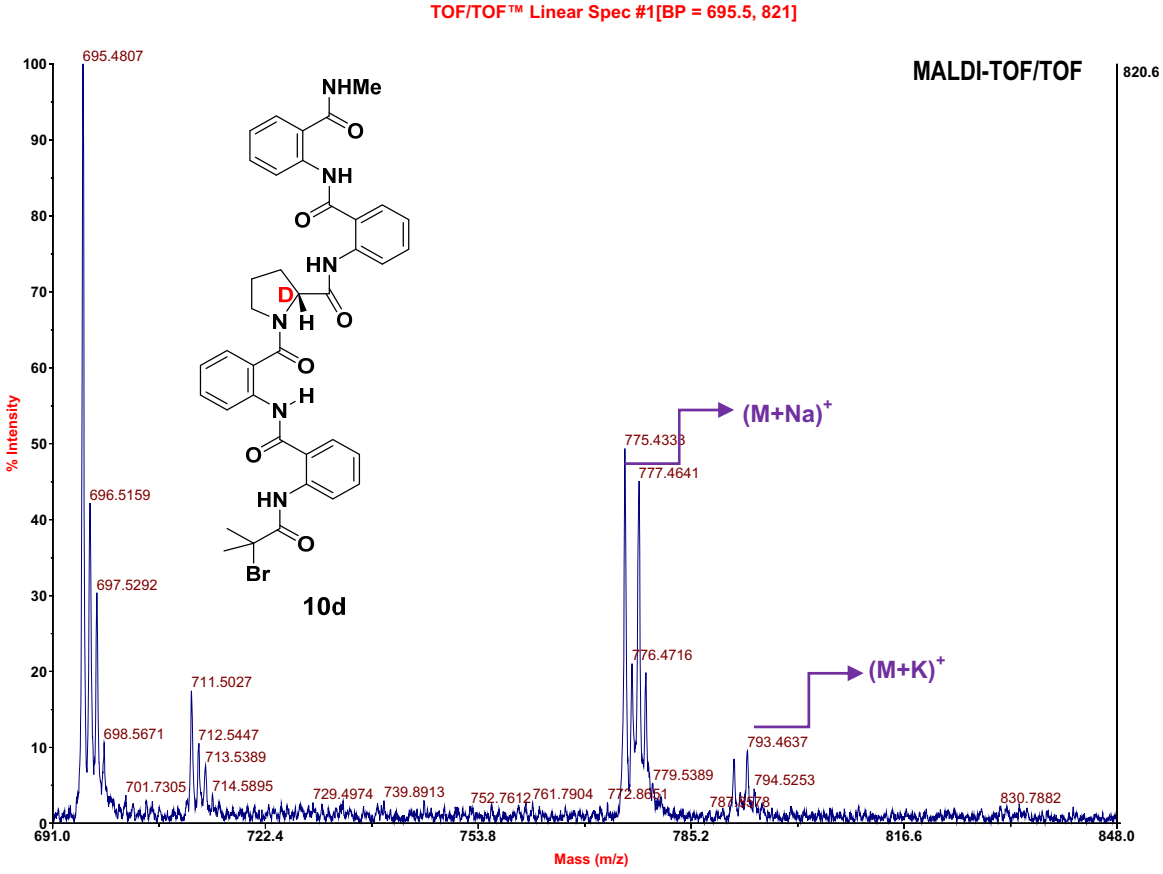
TOF/TOF™ Linear Spec #1[BP = 695.5, 821]
MALDI-TOF/TOF
820.6
695.4807
696.5159
697.5292
698.5671
701.7305
711.5027
712.5447
713.5389
714.5895
729.4974
739.8913
752.7612
761.7904
772.8651
NHMe
O
NH
HN
D
N H
Br
10d
(M+Na)+
775.4333
777.4641
776.4716
(M+K)+
793.4637
794.5253
779.5389
830.7882
% Intensity
Mass (m/z)
691.0
722.4
753.8
785.2
816.6
848.0

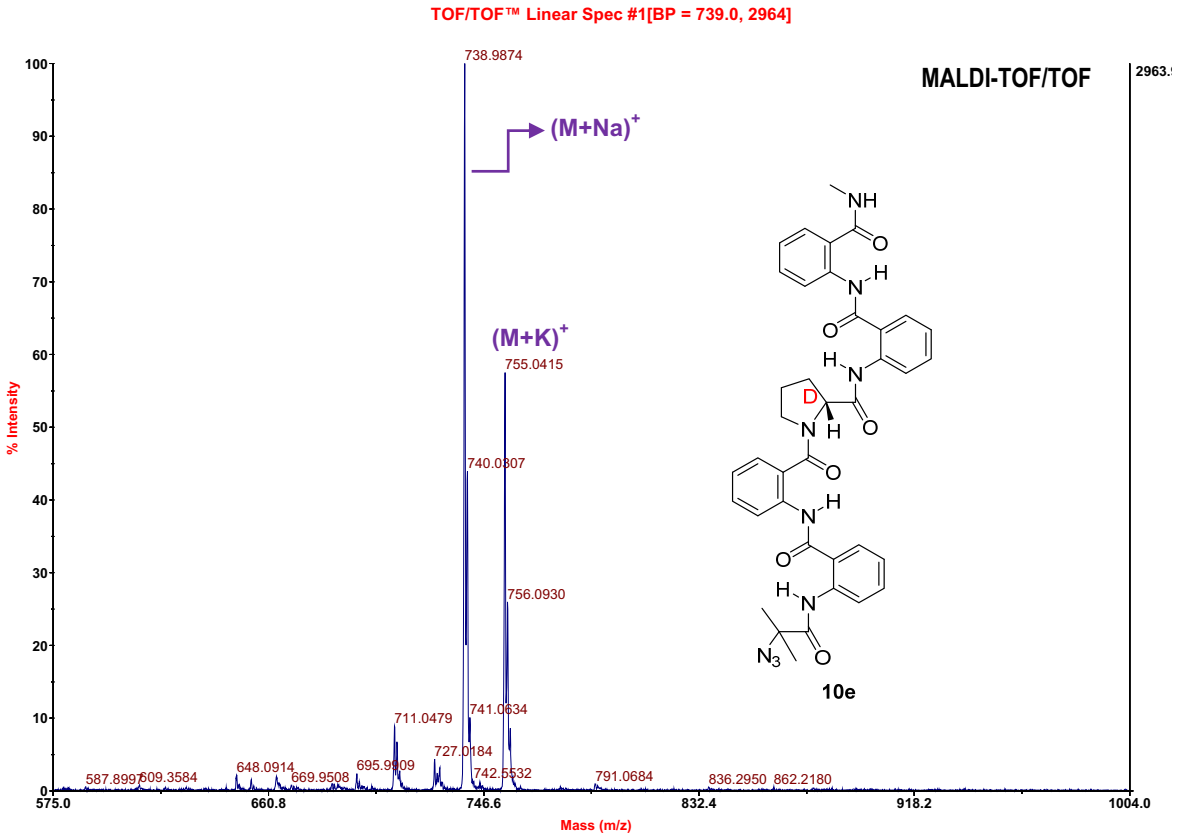
TOF/TOF™ Linear Spec #1[BP = 739.0, 2964]
MALDI-TOF/TOF
738.9874
(M+Na)+
(M+K)+
755.0415
740.0307
756.0930
711.0479
741.0634
727.0184
742.5532
587.8997
609.3584
648.0914
669.9508
695.9909
791.0684
836.2950
862.2180
10e
% Intensity
Mass (m/z)
575.0
660.8
746.6
832.4
918.2
1004.0

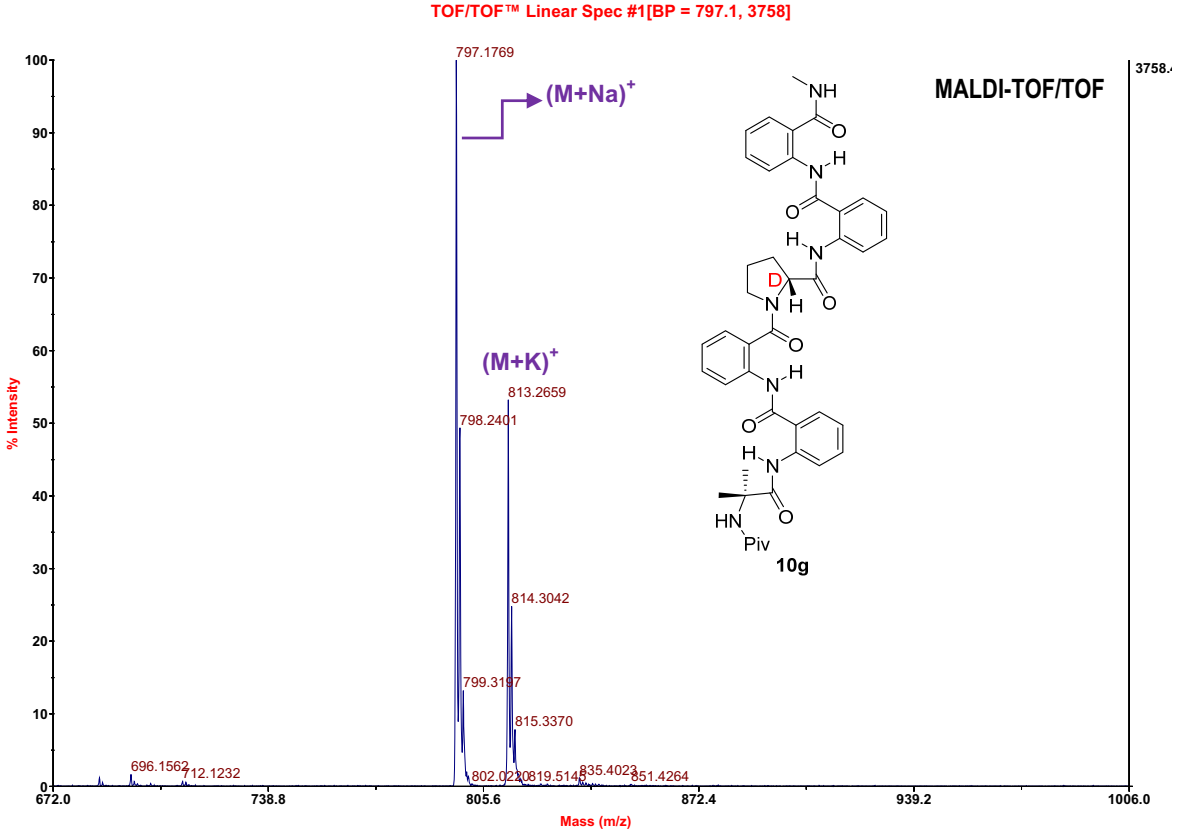
TOF/TOF™ Linear Spec #1[BP = 797.1, 3758]
MALDI-TOF/TOF
797.1769
(M+Na)+
(M+K)+
813.2659
798.2401
814.3042
799.3187
815.3370
696.1562
712.1232
802.0220
819.5145
835.4023
851.4264
10g
% Intensity
Mass (m/z)
672.0
738.8
805.6
872.4
939.2
1006.0

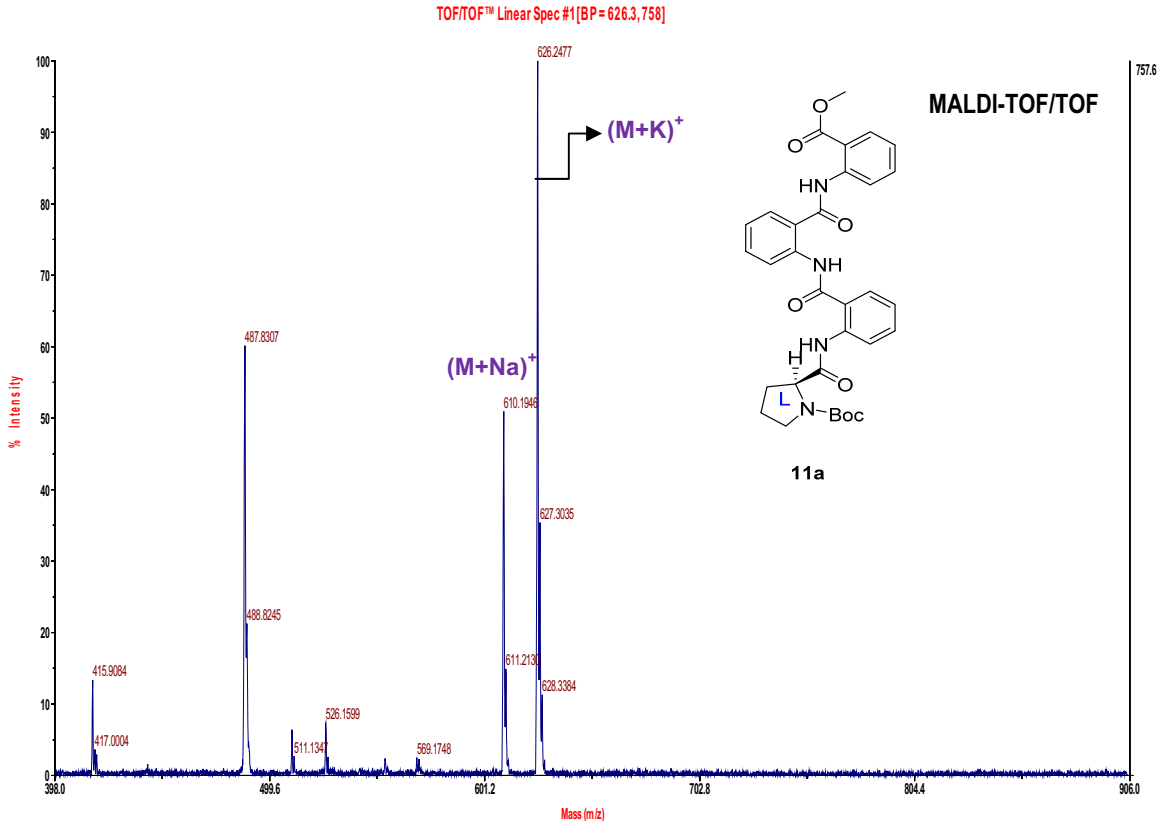
TOF/TOF™ Linear Spec #1[BP = 626.3, 758]
626.2477
(M+K)+
(M+Na)+
487.8307
610.1946
627.3035
488.8245
611.2136
628.3384
415.9084
526.1599
417.0004
511.1347
569.1748
% Intensity
Mass (m/z)
MALDI-TOF/TOF
11a

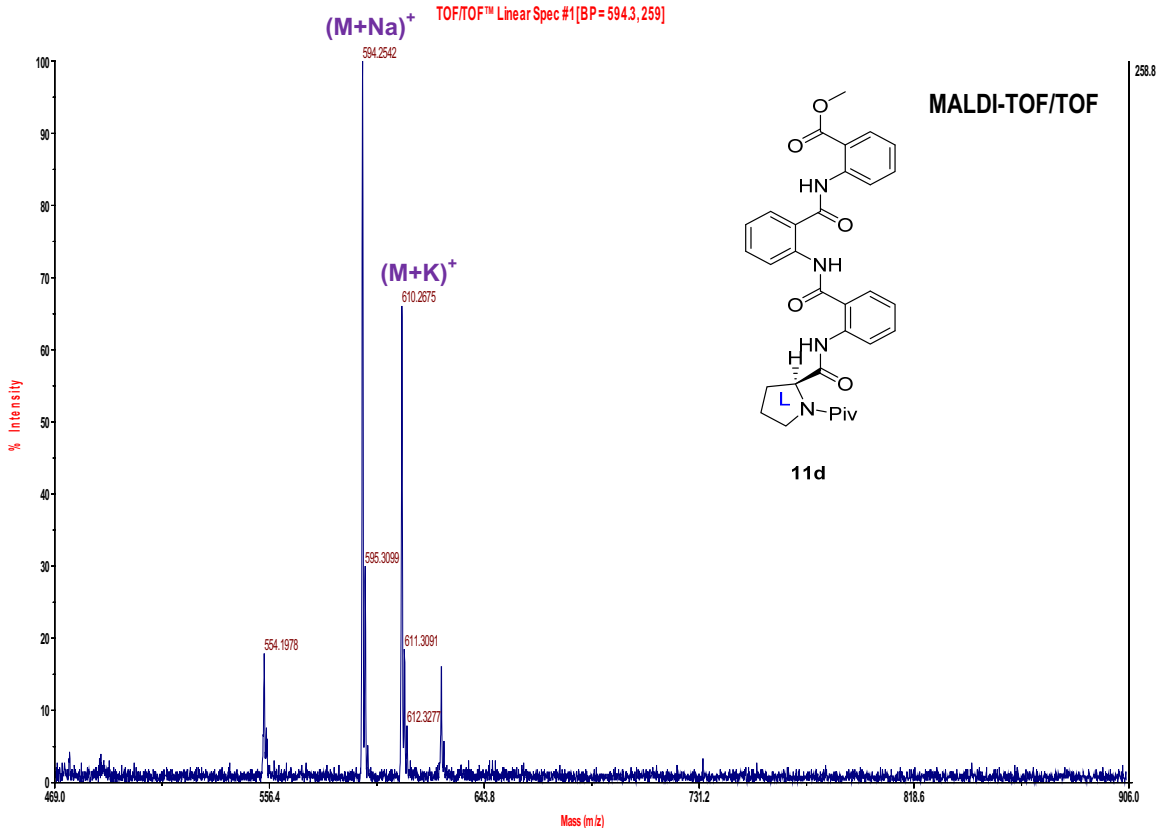
(M+Na)+
TOF/TOF™ Linear Spec #1[BP = 594.3, 259]
594.2542
(M+K)+
610.2675
595.3099
554.1978
611.3091
612.3277
% Intensity
Mass (m/z)
MALDI-TOF/TOF
11d

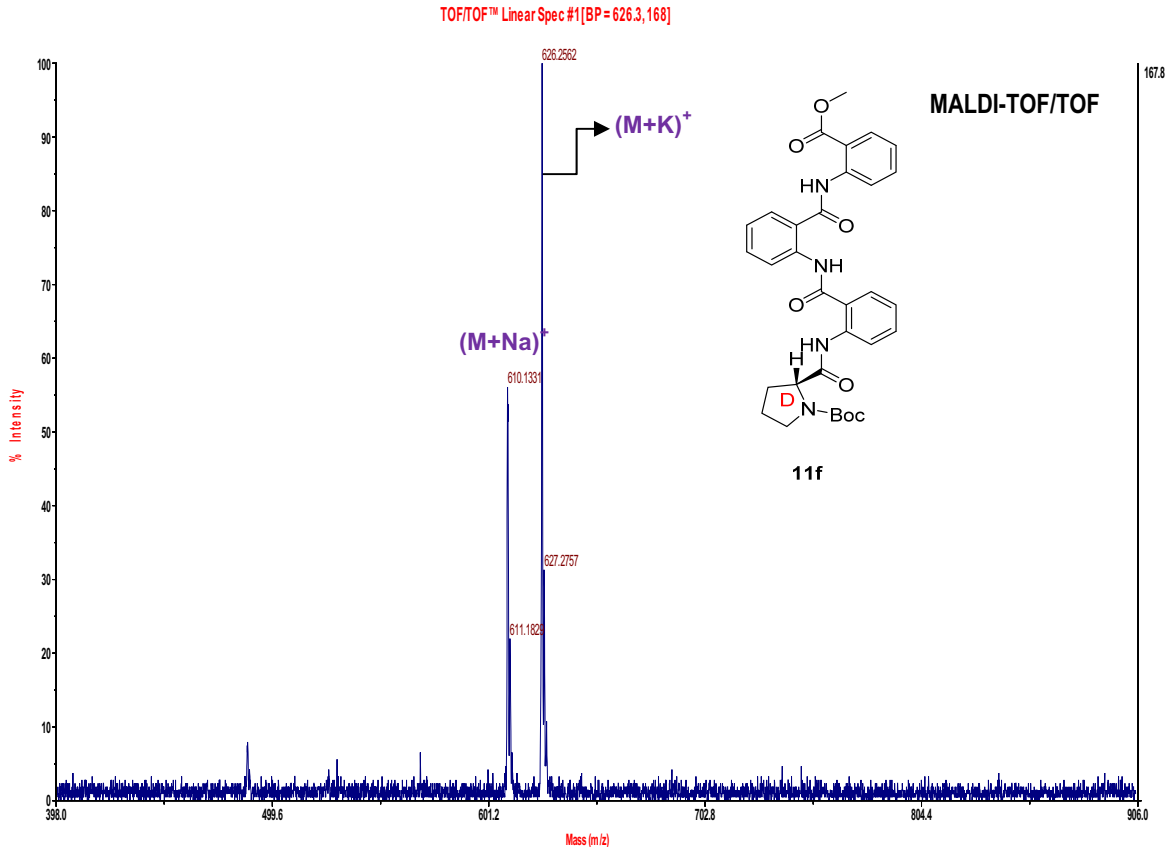
TOF/TOF™ Linear Spec #1[BP = 626.3, 168]
626.2562
(M+K)+
(M+Na)+
610.1331
627.2757
611.1829
MALDI-TOF/TOF
11f
% Intensity
Mass (m/z)
398.0
499.6
601.2
702.8
804.4
906.0
167.8

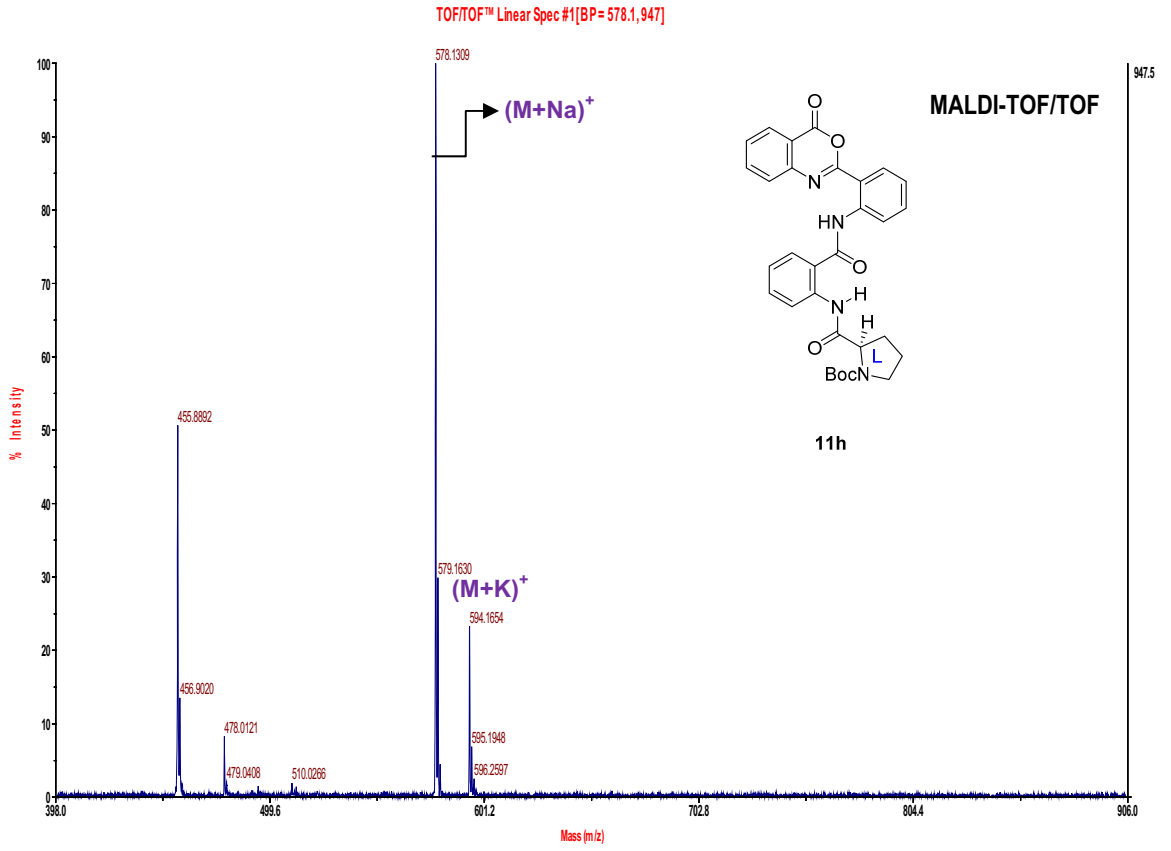
TOF/TOF™ Linear Spec #1[BP = 578.1, 947]
578.1309
(M+Na)+
MALDI-TOF/TOF
11h
455.8892
579.1630
(M+K)+
594.1654
456.9020
478.0121
595.1948
479.0408
510.0266
596.2597
% Intensity
Mass (m/z)
398.0
499.6
601.2
702.8
804.4
906.0
947.5

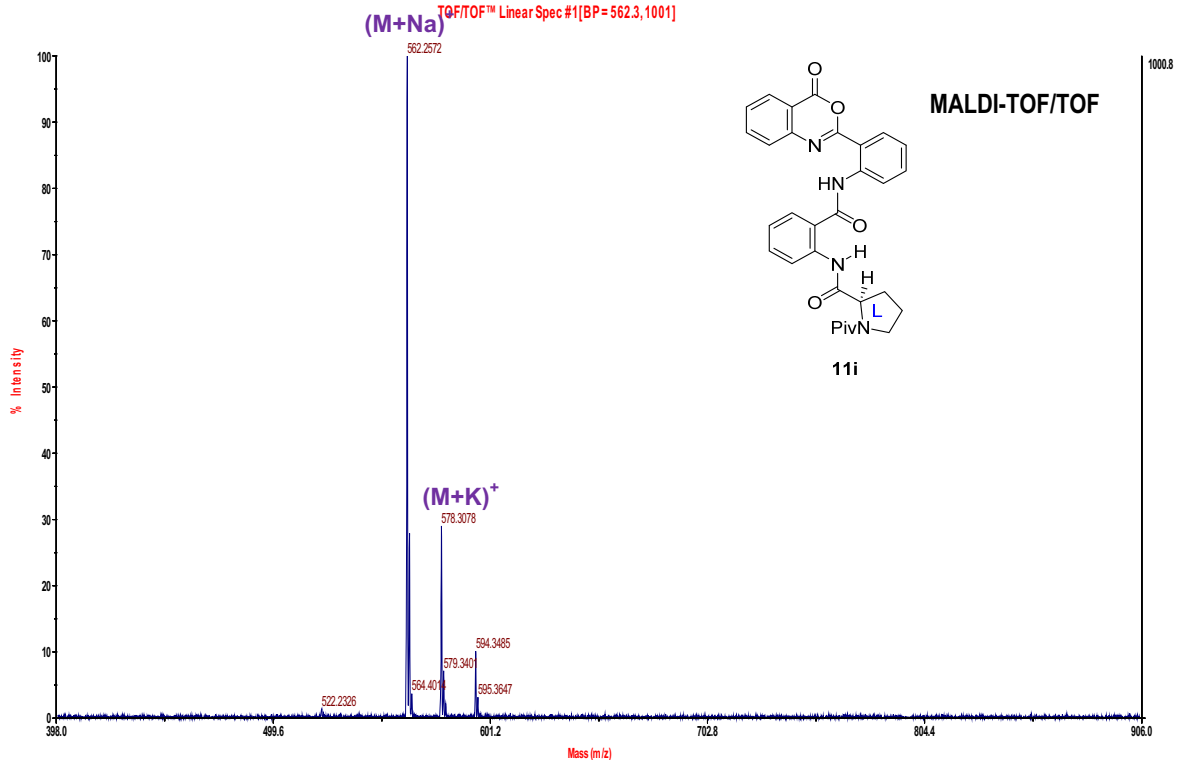
TOF/TOF™ Linear Spec #1[BP = 562.3, 1001]
(M+Na)+
562.2572
(M+K)+
578.3078
594.3485
579.340
564.4014
595.3647
522.2326
MALDI-TOF/TOF
PivN
11i
% Intensity
Mass (m/z)

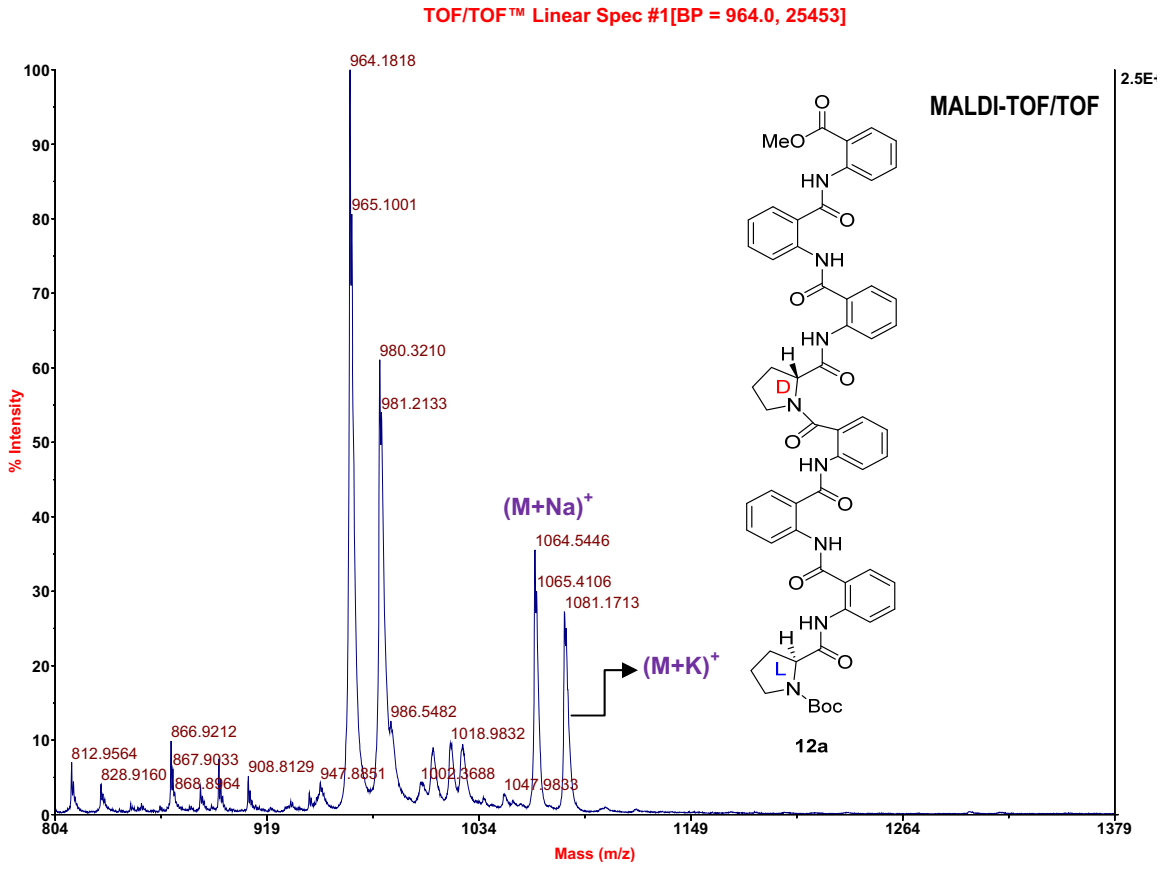
TOF/TOF™ Linear Spec #1[BP = 964.0, 25453]
964.1818
965.1001
980.3210
981.2133
(M+Na)+
1064.5446
1065.4106
1081.1713
(M+K)+
986.5482
1018.9832
866.9212
812.9564
867.9033
828.9160
868.8964
908.8129
947.8851
1002.3688
1047.9833
MALDI-TOF/TOF
MeO
D
L
Boc
12a
% Intensity
Mass (m/z)

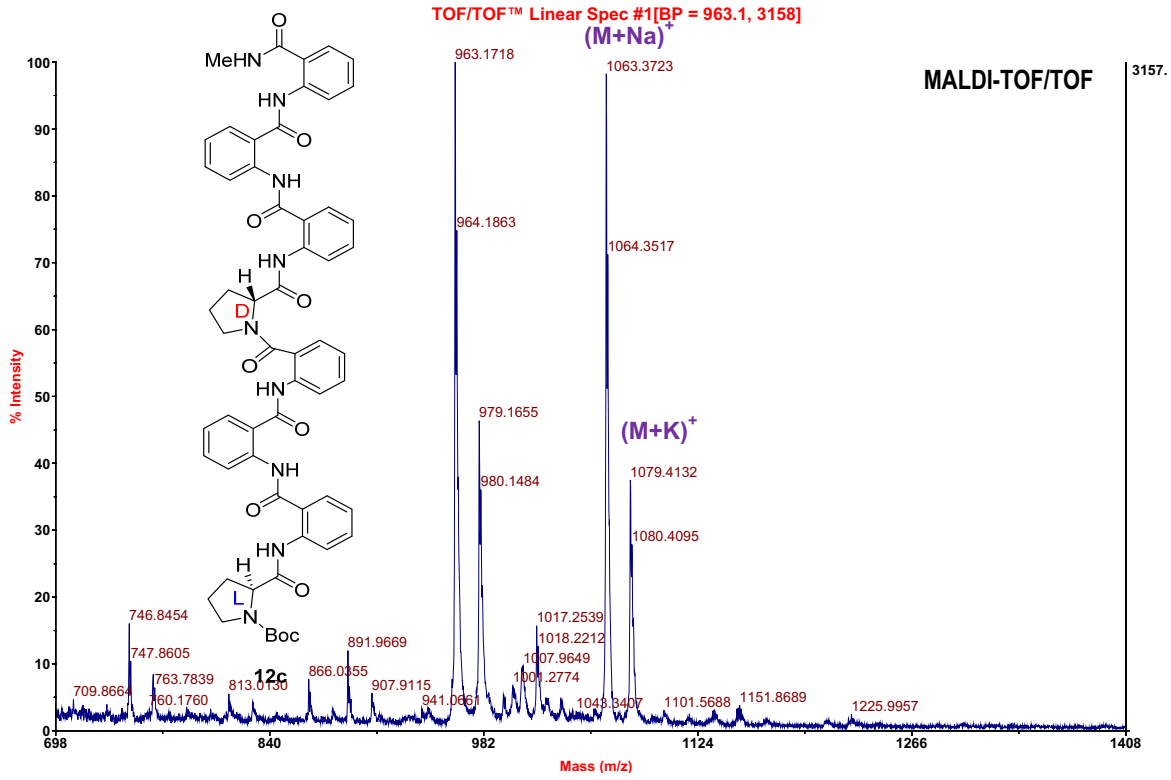
TOF/TOF™ Linear Spec #1[BP = 963.1, 3158]
(M+Na)+
MALDI-TOF/TOF
3157.
963.1718
1063.3723
964.1863
1064.3517
979.1655
(M+K)+
980.1484
1079.4132
1080.4095
746.8454
747.8605
763.7839
760.1760
709.8664
813.0130
866.0355
891.9669
907.9115
941.0661
1017.2539
1018.2212
1007.9649
1001.2774
1043.3407
1101.5688
1151.8689
1225.9957
MeHN
HN
NH
HN
H
D
N
HN
NH
HN
H
L
N
Boc
12c
% Intensity
Mass (m/z)
698
840
982
1124
1266
1408

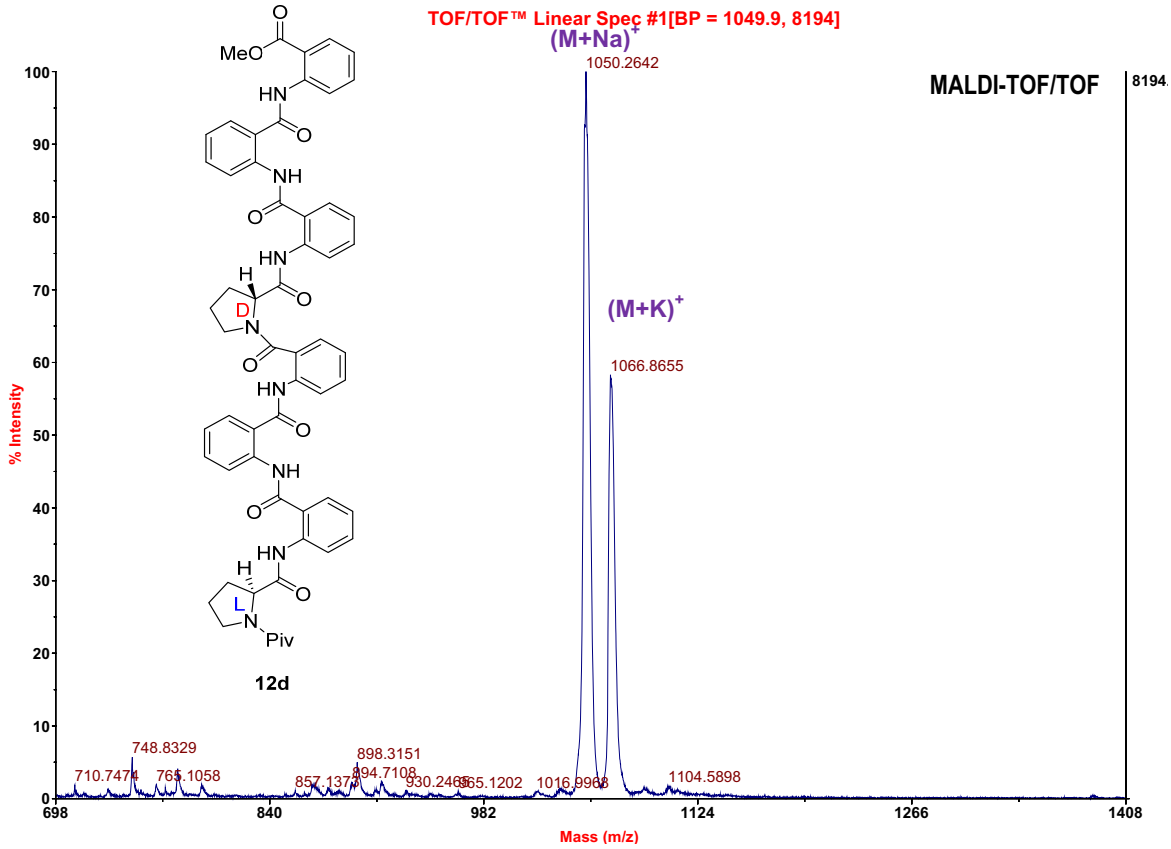
TOF/TOF™ Linear Spec #1[BP = 1049.9, 8194]
(M+Na)+
MALDI-TOF/TOF
8194.
1050.2642
(M+K)+
1066.8655
748.8329
710.7474
765.1058
898.3151
894.7108
857.1374
930.2466
965.1202
1016.9968
1104.5898
MeO
HN
NH
HN
H
D
N
HN
NH
HN
H
L
N
Piv
12d
% Intensity
Mass (m/z)
698
840
982
1124
1266
1408

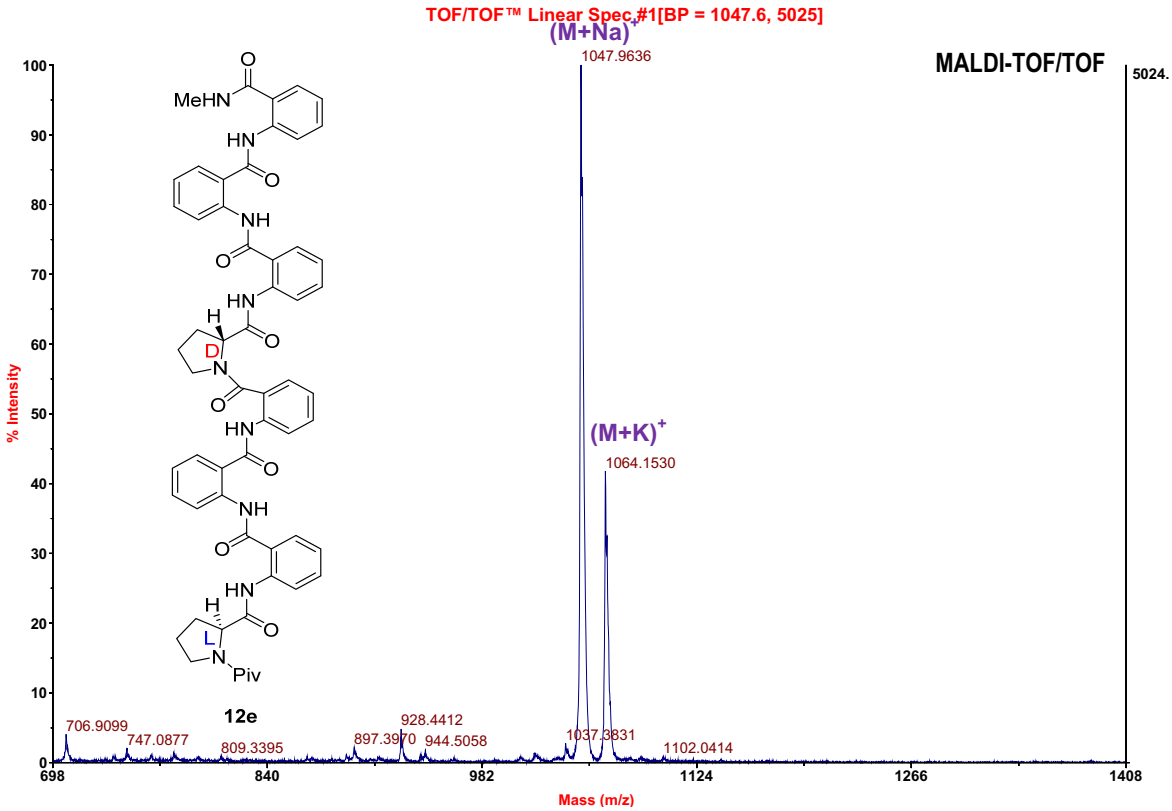

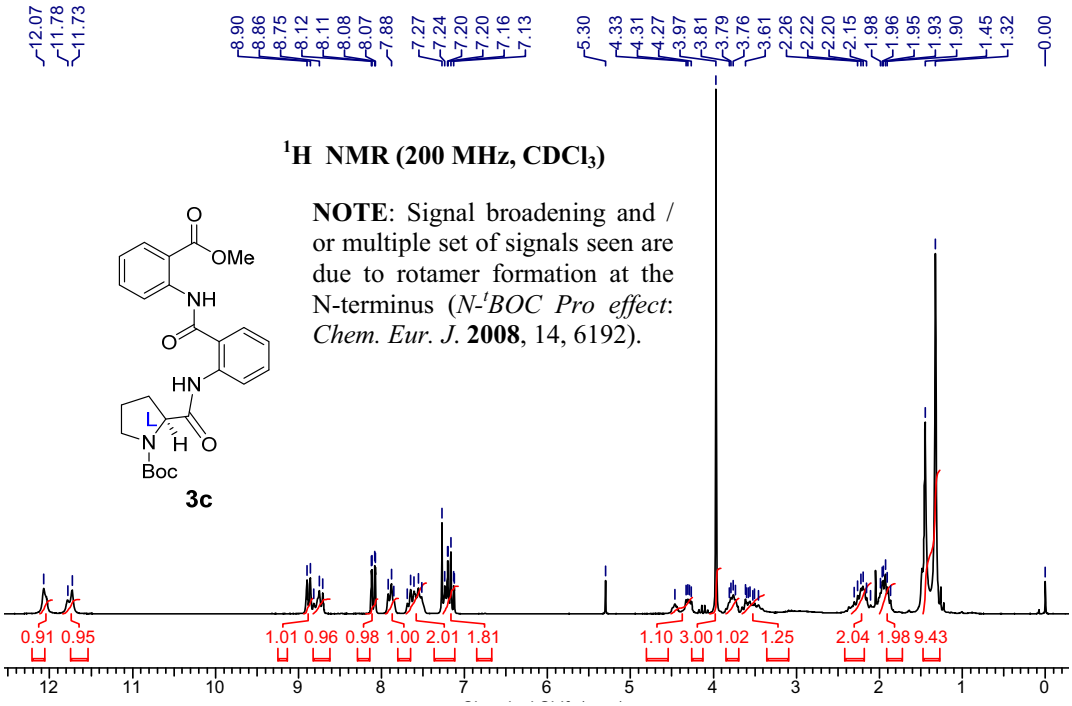

NOTE: Signal broadening and / or multiple set of signals seen are due to rotamer formation at the N-terminus (*N-^{t}BOC Pro effect*: *Chem. Eur. J.* **2008**, 14, 6192).

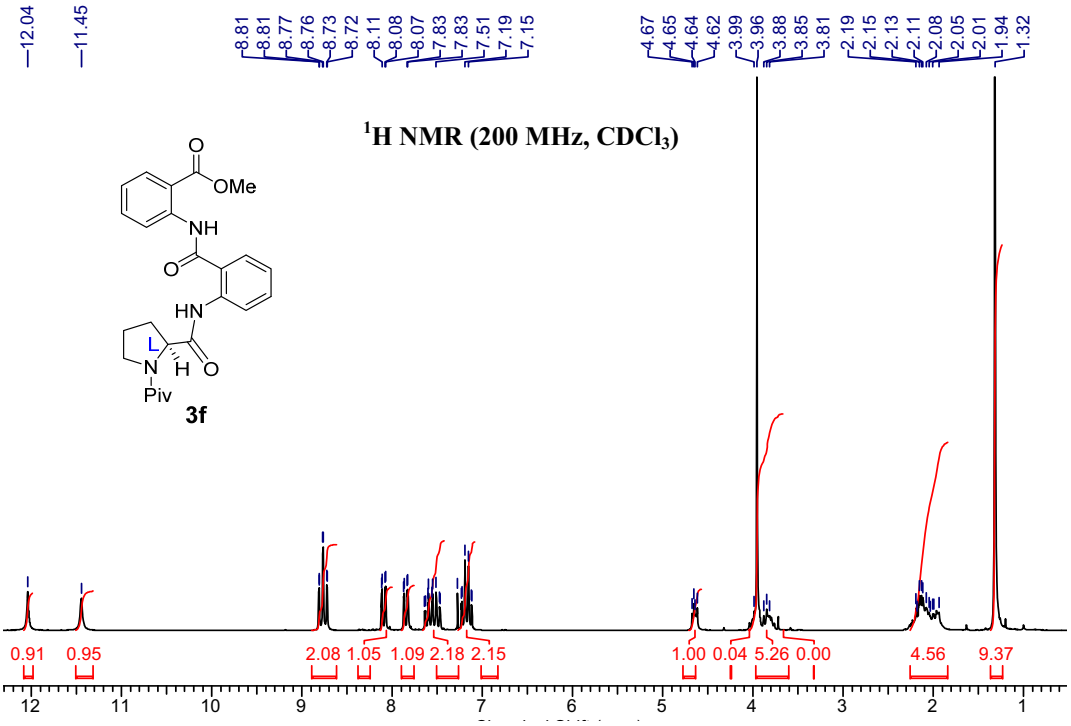
12.04
11.45
8.81
8.81
8.77
8.76
8.73
8.72
8.11
8.08
8.07
7.83
7.83
7.51
7.19
7.15
4.67
4.65
4.64
4.62
3.99
3.96
3.88
3.85
3.81
2.19
2.15
2.13
2.11
2.08
2.05
2.01
1.94
1.32
^{1}H NMR (200 MHz, CDCl$_3$)
OMe
NH
HN
Piv
3f
0.91 0.95 2.08 1.05 1.09 2.18 2.15 1.00 0.04 5.26 0.00 4.56 9.37
12 11 10 9 8 7 6 5 4 3 2 1

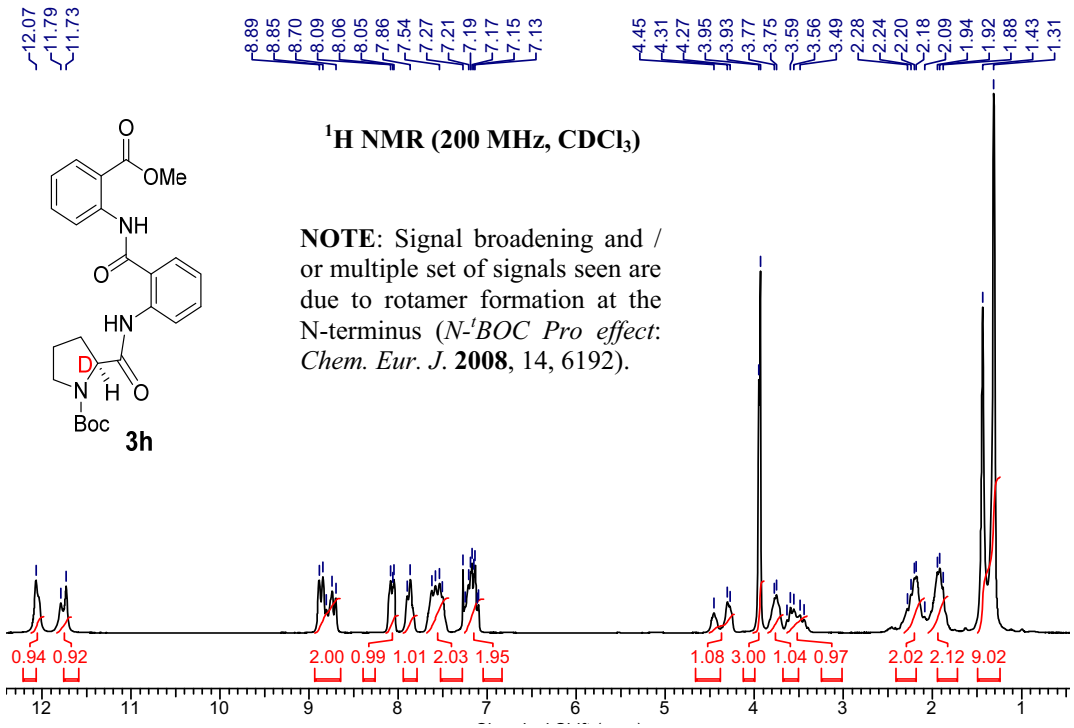
12.07
11.79
11.73
8.89
8.85
8.70
8.09
8.06
8.05
7.86
7.54
7.27
7.21
7.19
7.17
7.15
7.13
4.45
4.31
4.27
3.95
3.93
3.77
3.75
3.59
3.56
3.49
2.28
2.24
2.20
2.18
2.09
1.94
1.92
1.88
1.43
1.31
^{1}H NMR (200 MHz, CDCl$_3$)
OMe
NH
HN
Boc
3h
NOTE: Signal broadening and / or multiple set of signals seen are due to rotamer formation at the N-terminus (*N-^{t}BOC Pro effect*: *Chem. Eur. J.* **2008**, 14, 6192).
0.94 0.92 2.00 0.99 1.01 2.03 1.95 1.08 3.00 1.04 0.97 2.02 2.12 9.02
12 11 10 9 8 7 6 5 4 3 2 1

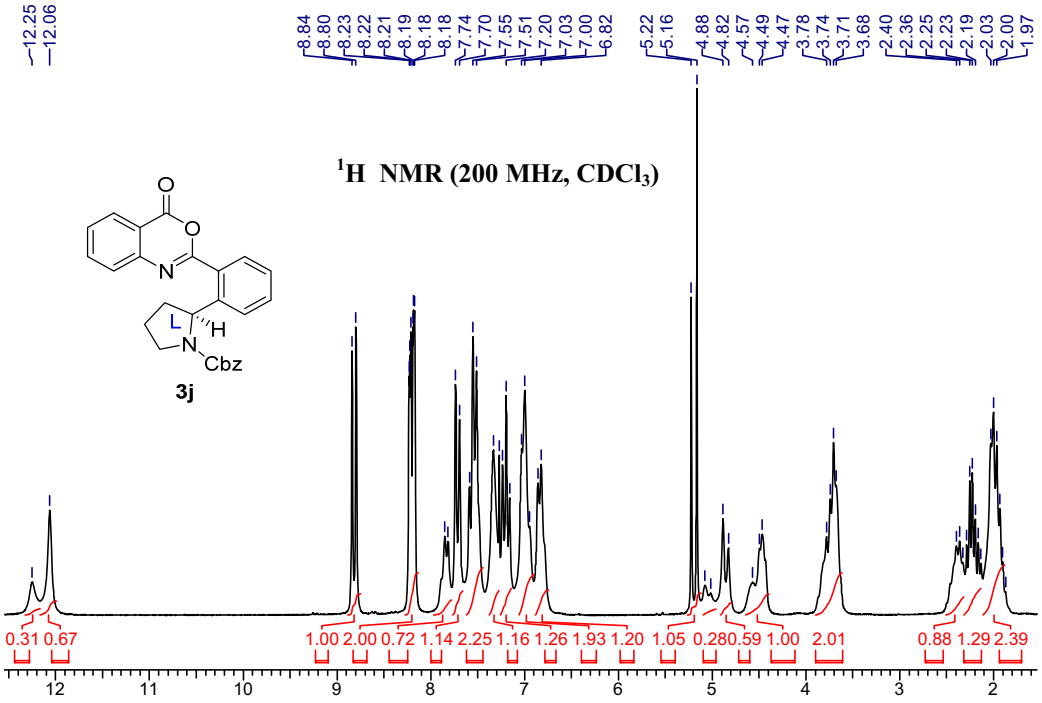

NOTE: Signal broadening and / or multiple set of signals seen are due to rotamer formation at the N-terminus (*N-^{t}BOC Pro effect*: *Chem. Eur. J*. **2008**, 14, 6192).

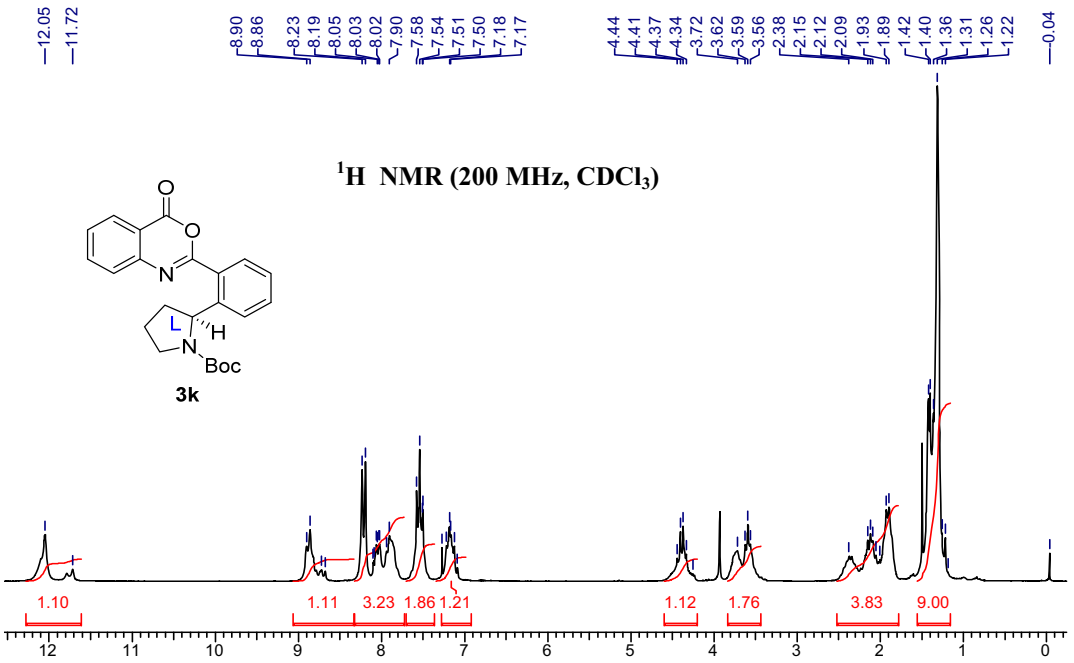

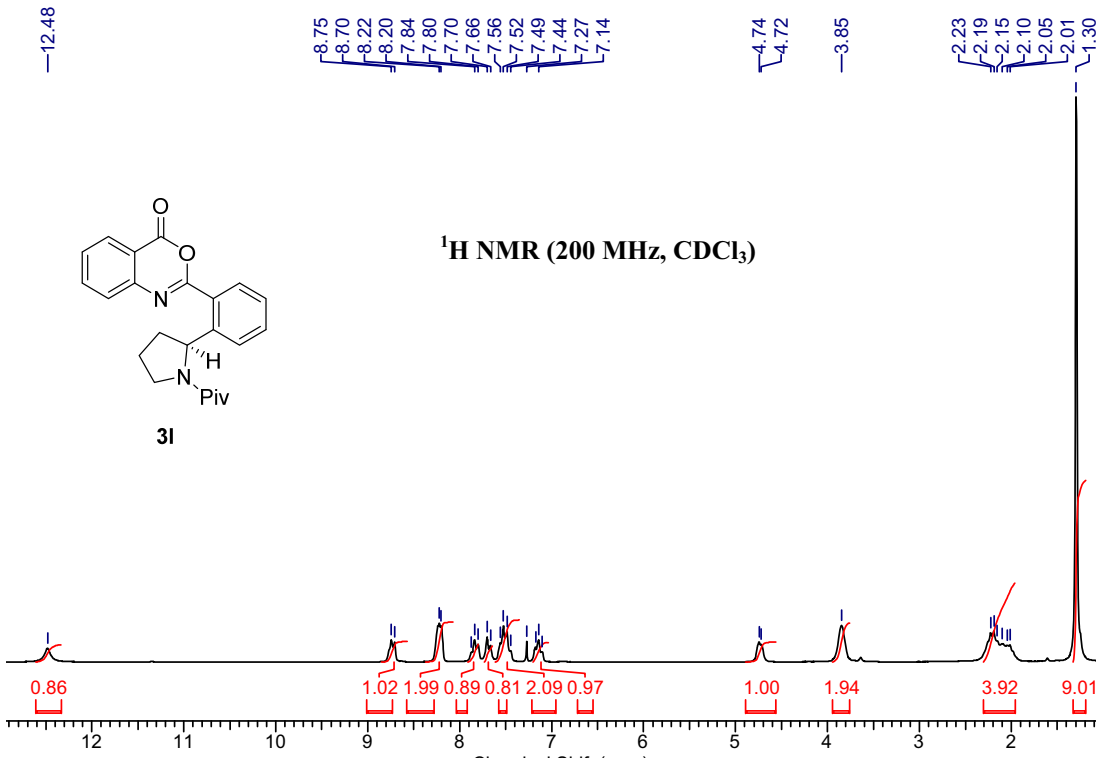

3l

^{1}H NMR (200 MHz, $CDCl_3$)

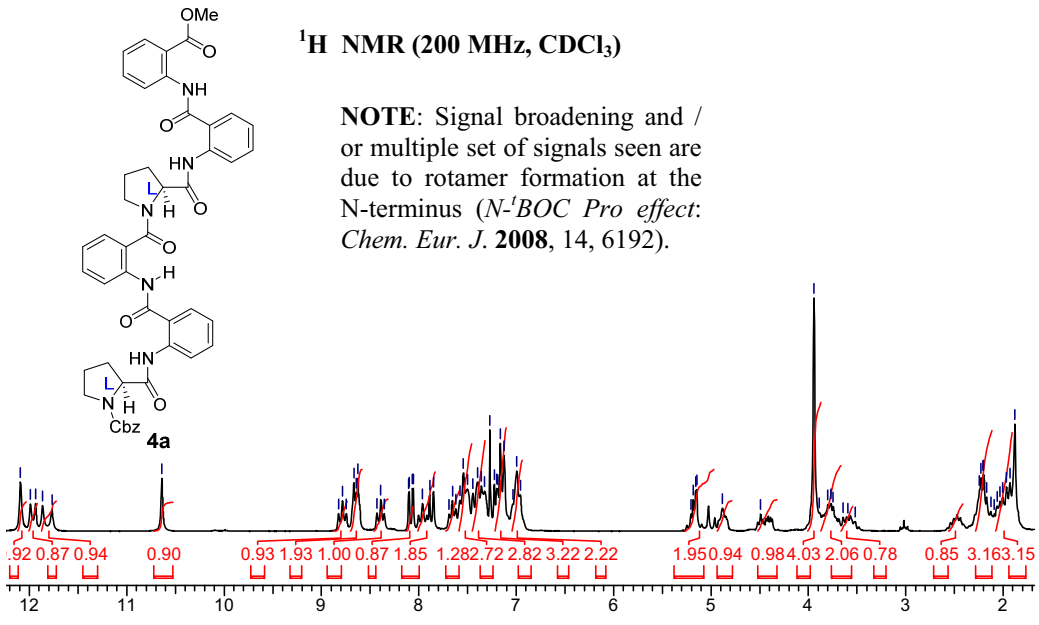

4a

^{1}H NMR (200 MHz, $CDCl_3$)

NOTE: Signal broadening and / or multiple set of signals seen are due to rotamer formation at the N-terminus (*N-^{t}BOC Pro effect*: *Chem. Eur. J.* **2008**, 14, 6192).

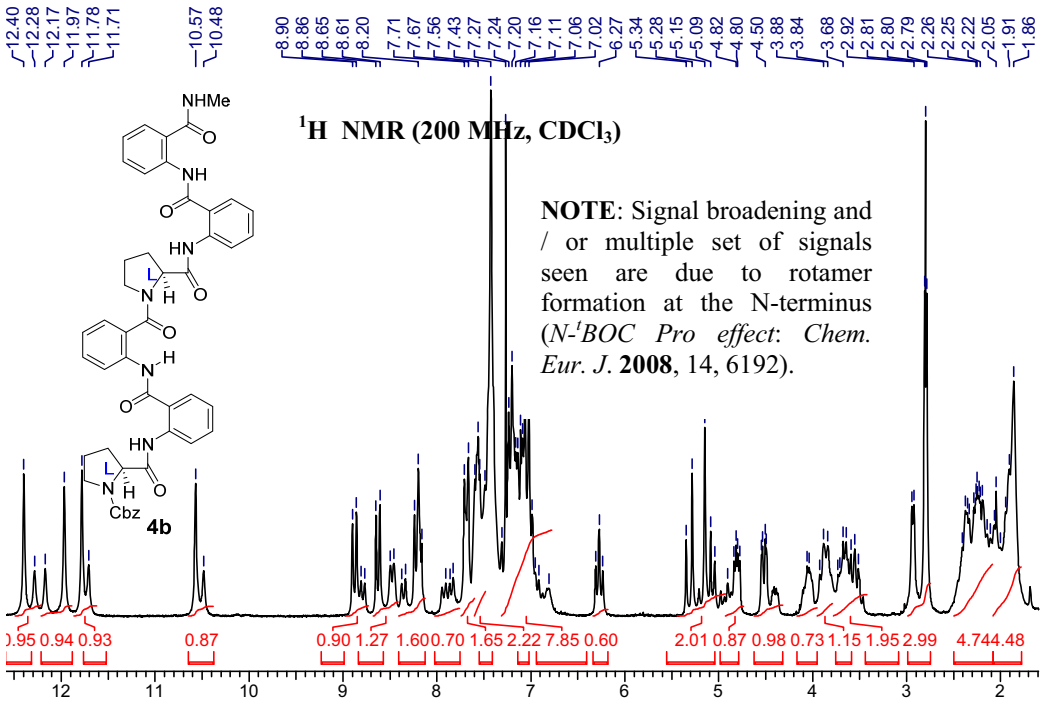
12.40 12.28 12.17 11.97 11.78 11.71 10.57 10.48
8.90 8.86 8.65 8.61 8.20 7.71 7.67 7.56 7.43 7.27 7.24 7.20 7.16 7.11 7.06 7.02 6.27 5.34 5.28 5.15 5.09 4.82 4.80 4.50 3.88 3.84 3.68 2.92 2.81 2.80 2.79 2.26 2.25 2.22 2.05 1.91 1.86
NHMe
NH
HN
HN
Cbz
4b
^{1}H NMR (200 MHz, CDCl$_3$)
NOTE: Signal broadening and / or multiple set of signals seen are due to rotamer formation at the N-terminus (*N-^{t}BOC Pro effect*: *Chem. Eur. J.* **2008**, 14, 6192).
0.95 0.94 0.93 0.87 0.90 1.27 1.60 0.70 1.65 2.22 7.85 0.60 2.01 0.87 0.98 0.73 1.15 1.95 2.99 4.74 4.48
12 11 10 9 8 7 6 5 4 3 2

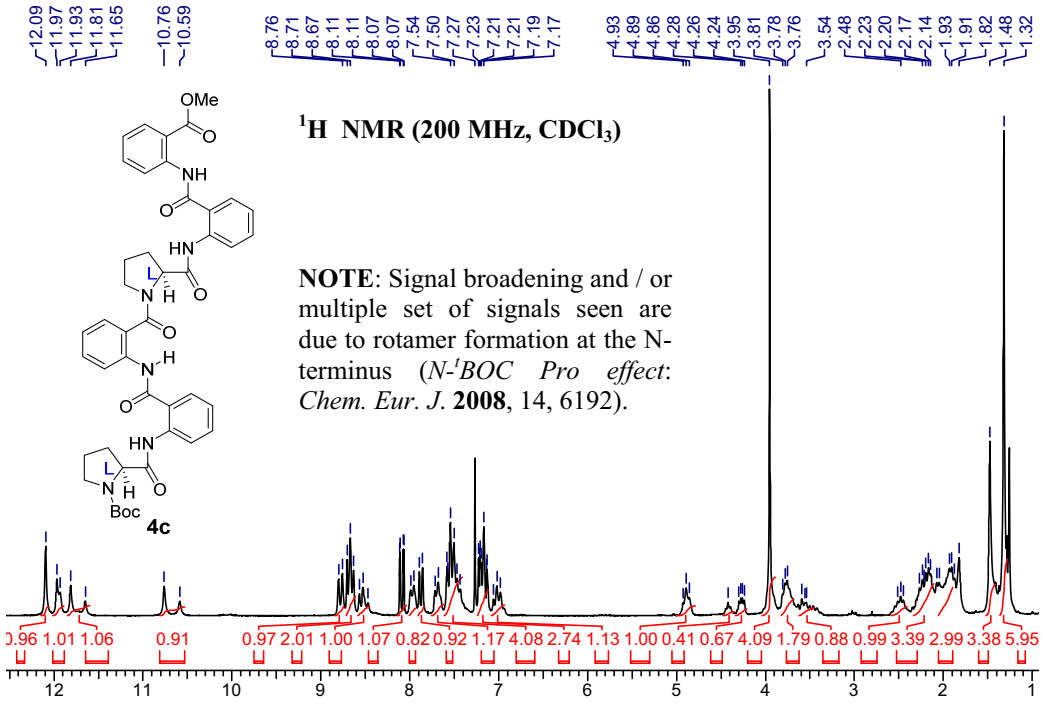
12.09 11.97 11.93 11.81 11.65 10.76 10.59
8.76 8.71 8.67 8.11 8.11 8.07 8.07 7.54 7.50 7.27 7.23 7.21 7.21 7.19 7.17
4.93 4.89 4.86 4.28 4.26 4.24 3.95 3.81 3.78 3.76 3.54 2.48 2.23 2.20 2.17 2.14 1.93 1.91 1.82 1.48 1.32
OMe
NH
HN
HN
Boc
4c
^{1}H NMR (200 MHz, CDCl$_3$)
NOTE: Signal broadening and / or multiple set of signals seen are due to rotamer formation at the N-terminus (*N-^{t}BOC Pro effect*: *Chem. Eur. J.* **2008**, 14, 6192).
0.96 1.01 1.06 0.91 0.97 2.01 1.00 1.07 0.82 0.92 1.17 4.08 2.74 1.13 1.00 0.41 0.67 4.09 1.79 0.88 0.99 3.39 2.99 3.38 5.95
12 11 10 9 8 7 6 5 4 3 2 1

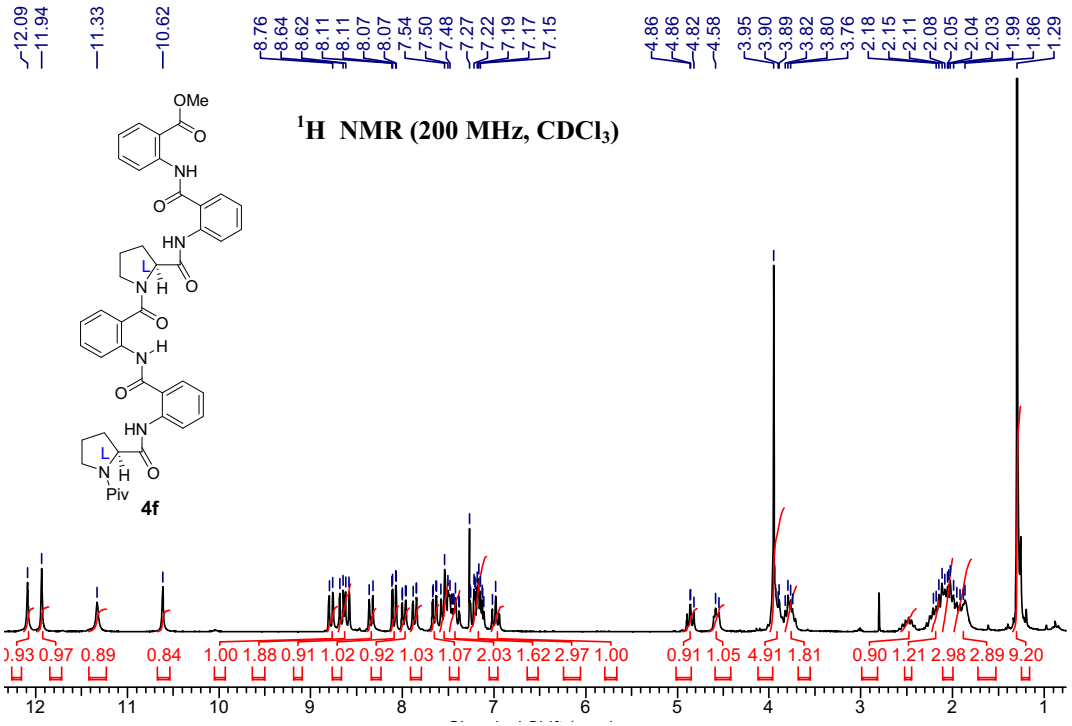
12.09
11.94
11.33
10.62
8.76
8.64
8.62
8.11
8.11
8.07
8.07
7.54
7.50
7.48
7.27
7.22
7.19
7.17
7.15
4.86
4.86
4.82
4.58
3.95
3.90
3.89
3.82
3.80
3.76
2.18
2.15
2.11
2.08
2.05
2.04
2.03
1.99
1.86
1.29
OMe
NH
HN
Piv
4f
^{1}H NMR (200 MHz, CDCl$_3$)
0.93 0.97 0.89 0.84 1.00 1.88 0.91 1.02 0.92 1.03 1.07 2.03 1.62 2.97 1.00 0.91 1.05 4.91 1.81 0.90 1.21 2.98 2.89 9.20
12 11 10 9 8 7 6 5 4 3 2 1

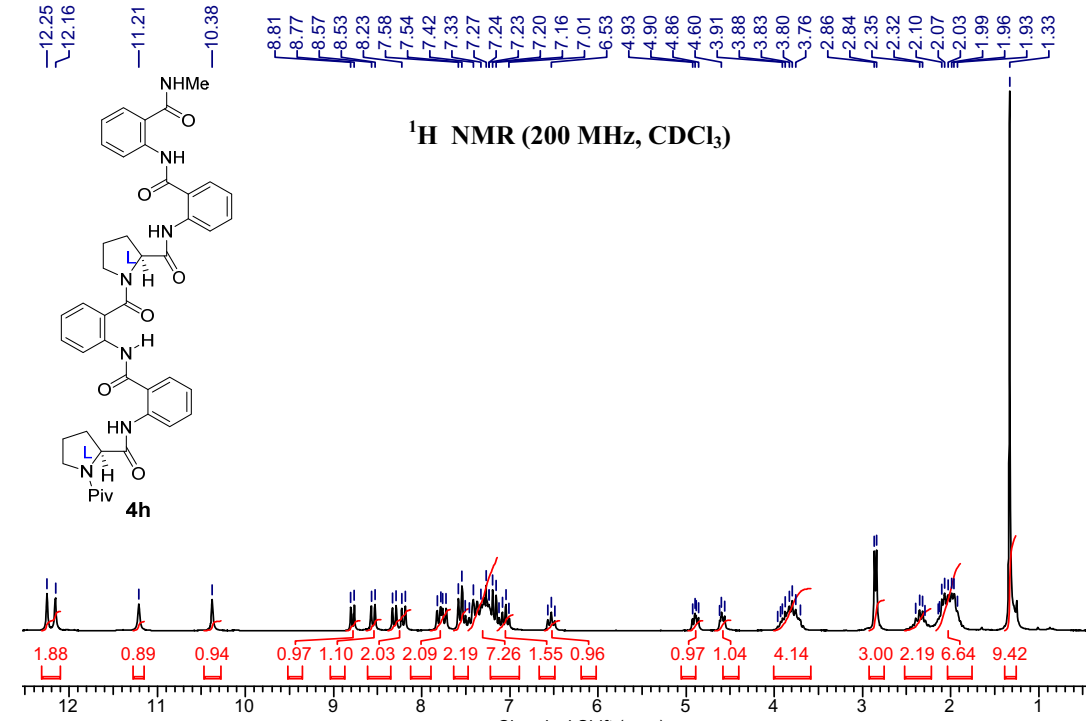
12.25
12.16
11.21
10.38
8.81
8.77
8.57
8.53
8.23
7.58
7.54
7.42
7.33
7.27
7.24
7.23
7.20
7.16
7.01
6.53
4.93
4.90
4.86
4.60
3.91
3.88
3.83
3.80
3.76
2.86
2.84
2.35
2.32
2.10
2.07
2.03
1.99
1.96
1.93
1.33
NHMe
NH
HN
Piv
4h
^{1}H NMR (200 MHz, CDCl$_3$)
1.88 0.89 0.94 0.97 1.10 2.03 2.09 2.19 7.26 1.55 0.96 0.97 1.04 4.14 3.00 2.19 6.64 9.42
12 11 10 9 8 7 6 5 4 3 2 1

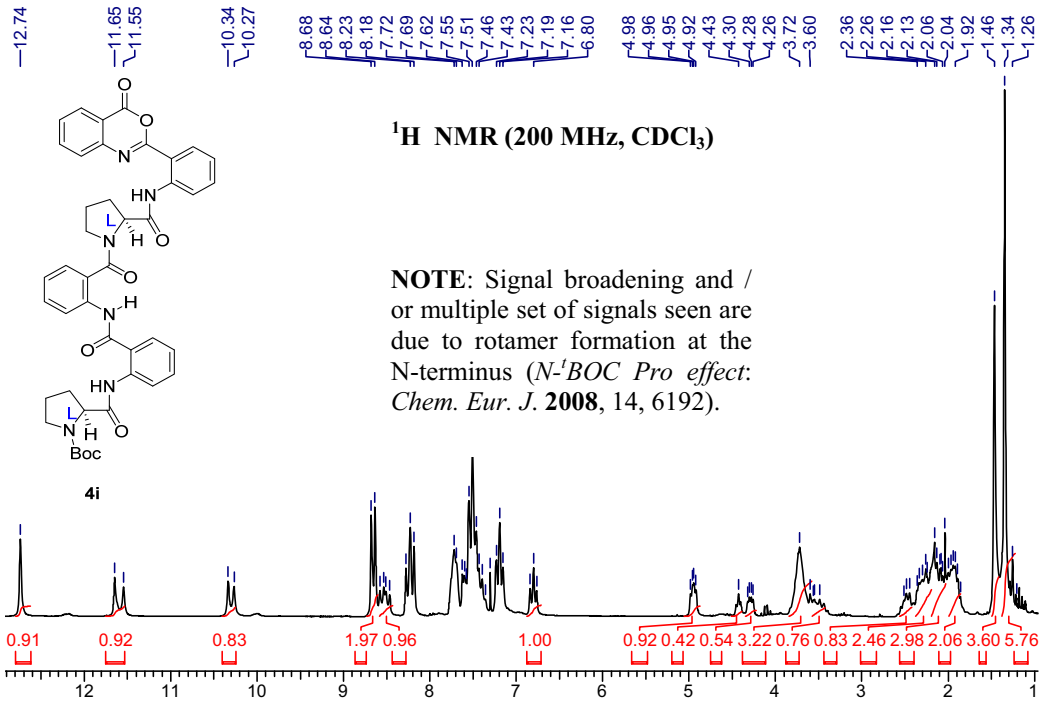

^{1}H NMR (200 MHz, $CDCl_3$)

NOTE: Signal broadening and / or multiple set of signals seen are due to rotamer formation at the N-terminus (*N-^{t}BOC Pro effect*: *Chem. Eur. J.* **2008**, 14, 6192).

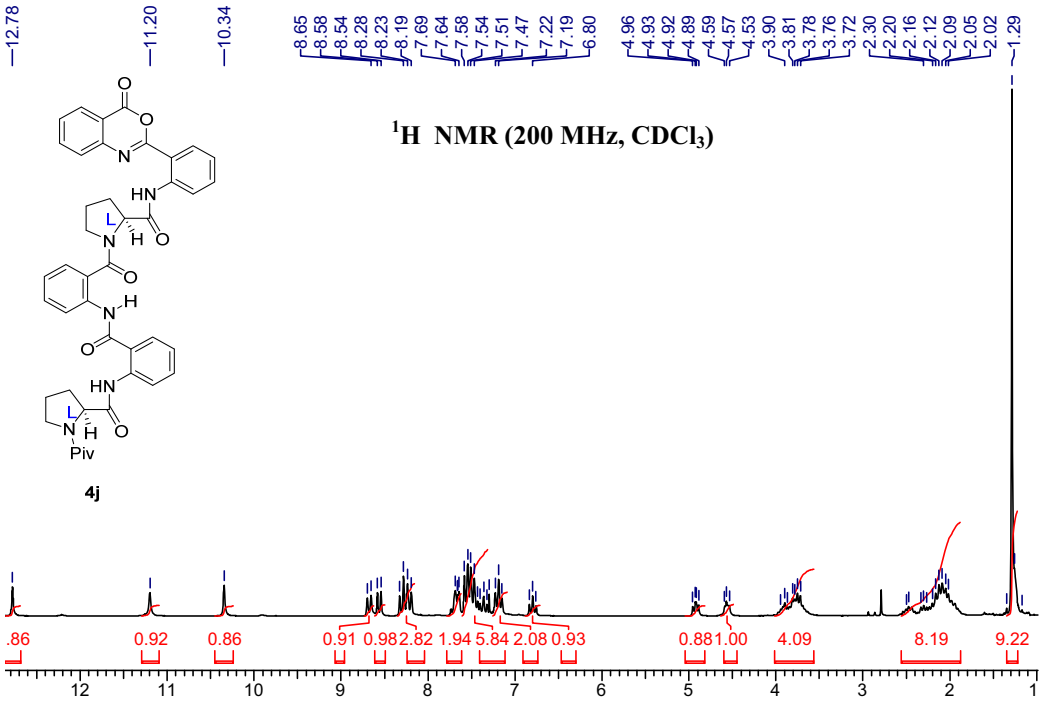

^{1}H NMR (200 MHz, $CDCl_3$)

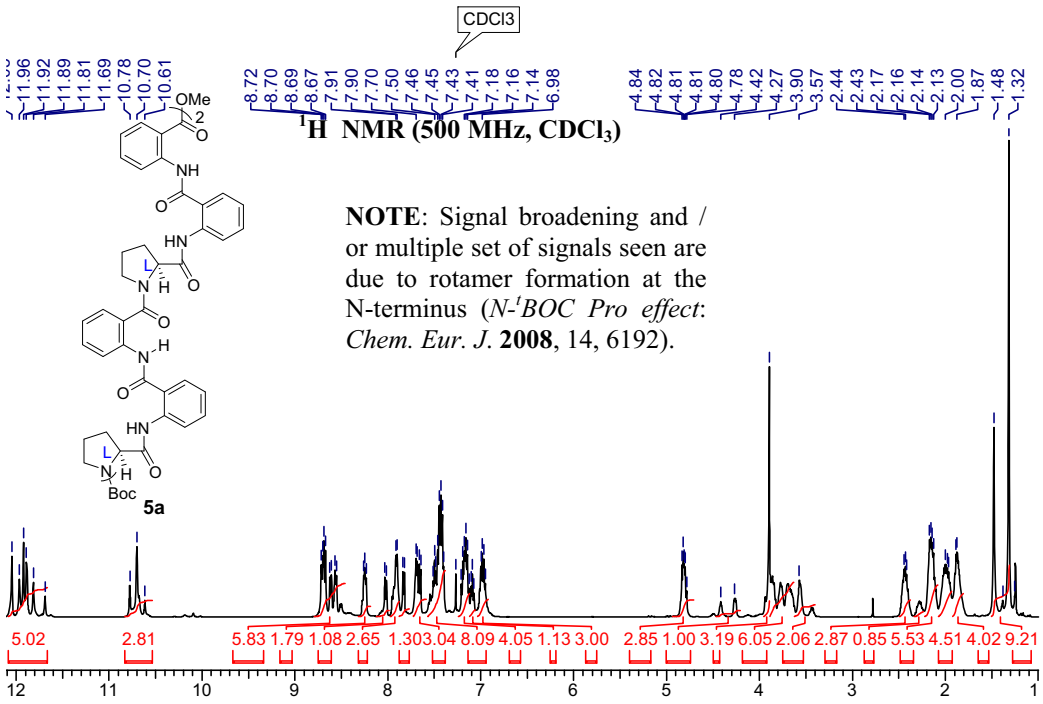

^{1}H NMR (500 MHz, CDCl$_3$)

NOTE: Signal broadening and / or multiple set of signals seen are due to rotamer formation at the N-terminus (*N-^{t}BOC Pro effect*: *Chem. Eur. J.* **2008**, 14, 6192).

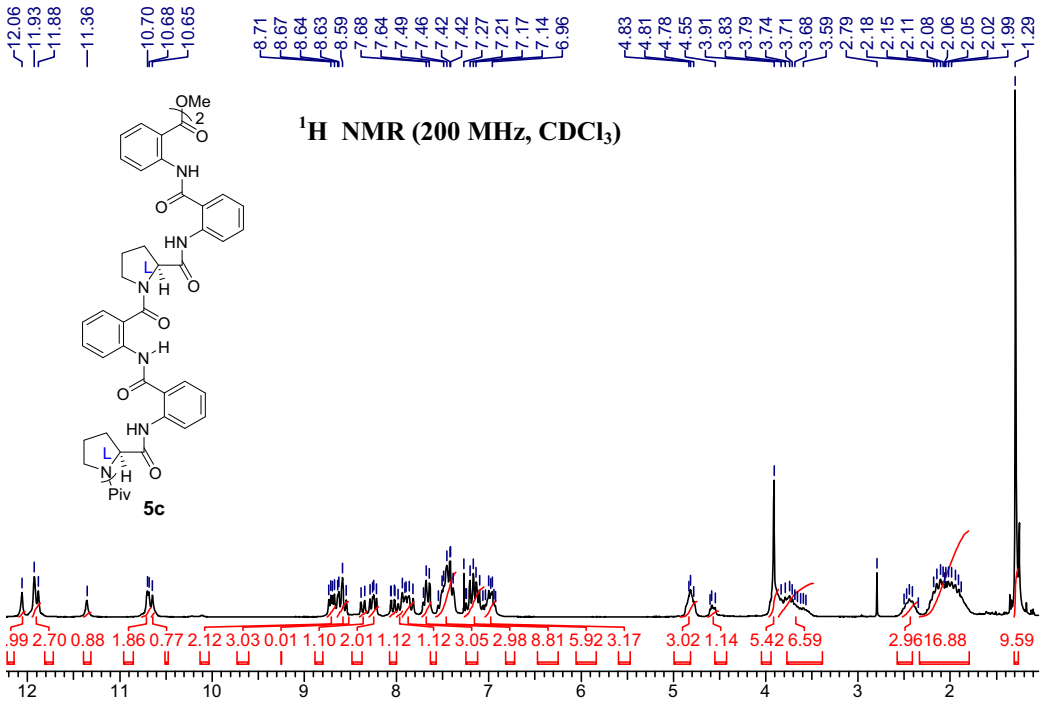

^{1}H NMR (200 MHz, CDCl$_3$)

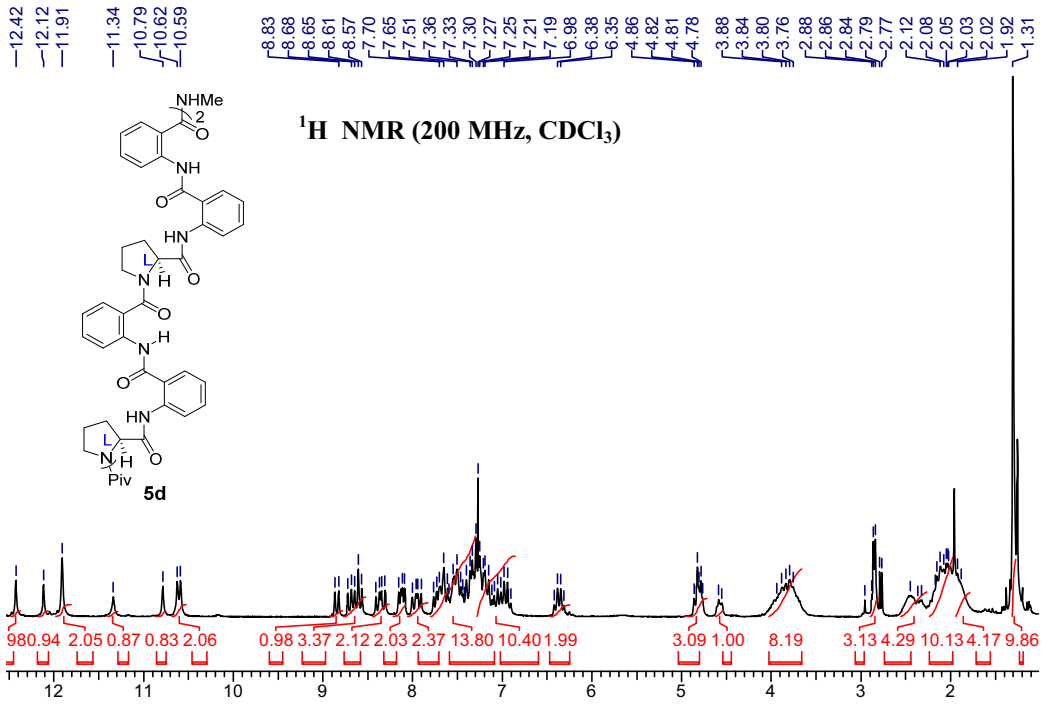

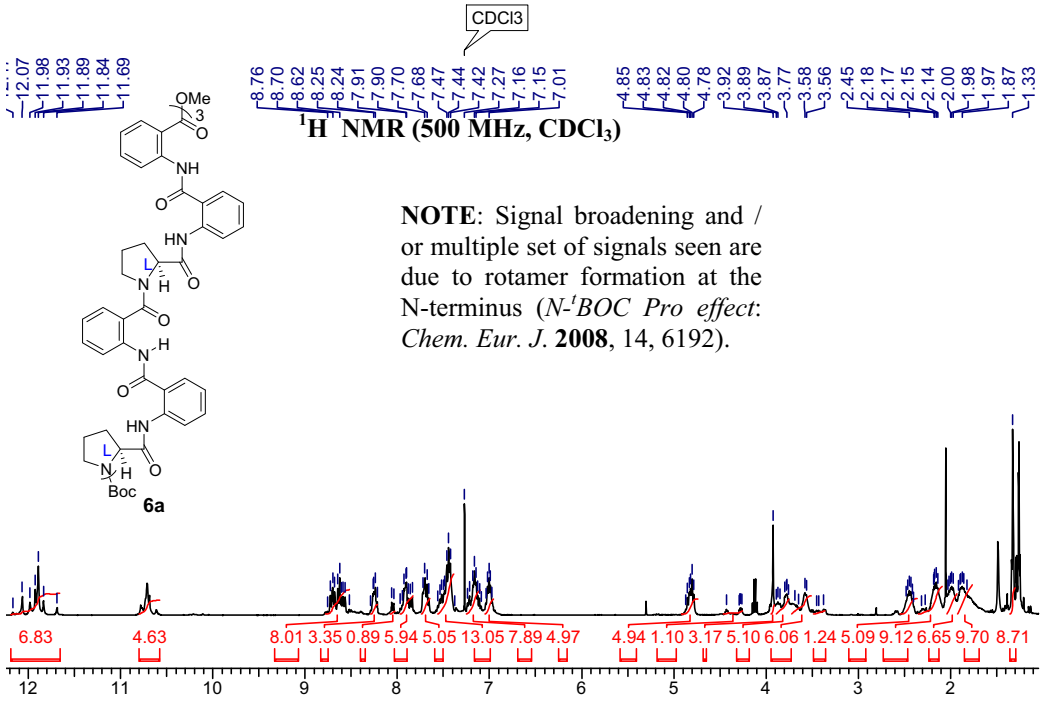

NOTE: Signal broadening and / or multiple set of signals seen are due to rotamer formation at the N-terminus (*N-^{t}BOC Pro effect*: *Chem. Eur. J.* **2008**, 14, 6192).

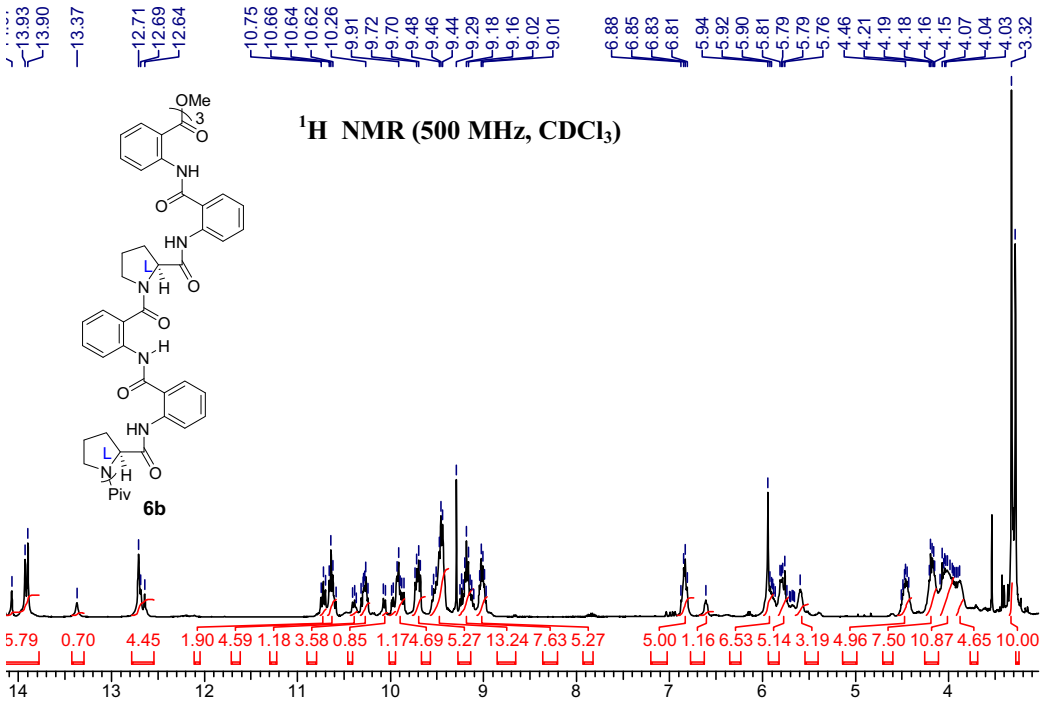
^{1}H NMR (500 MHz, CDCl$_3$)
6b

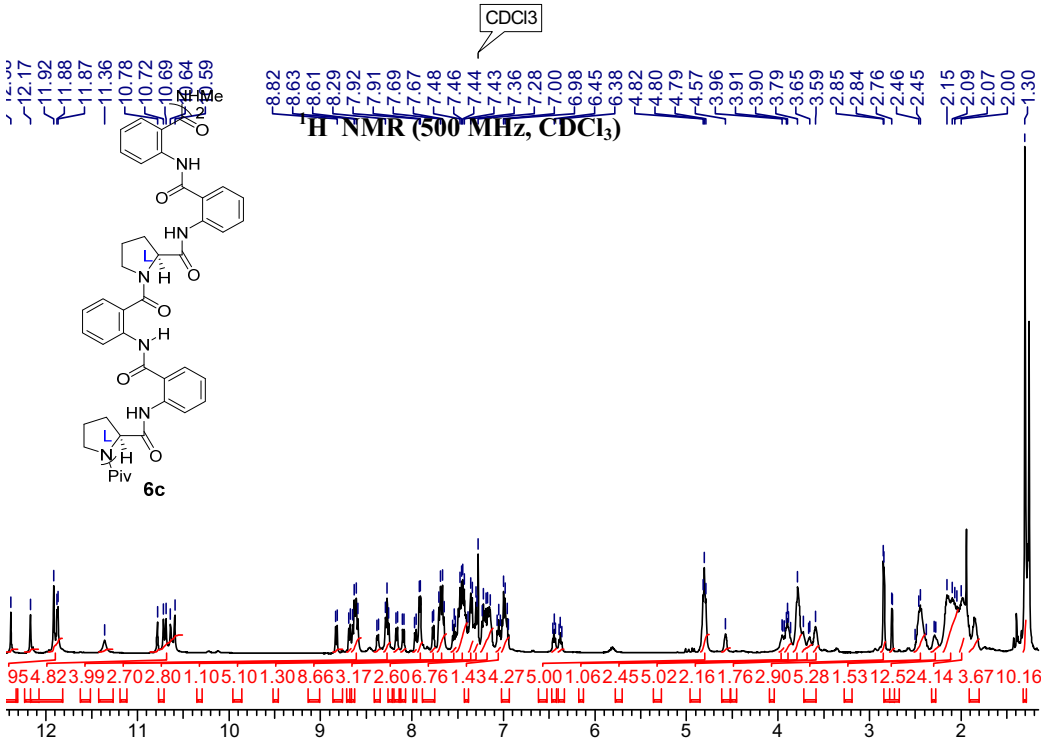
CDCl3
^{1}H NMR (500 MHz, CDCl$_3$)
6c

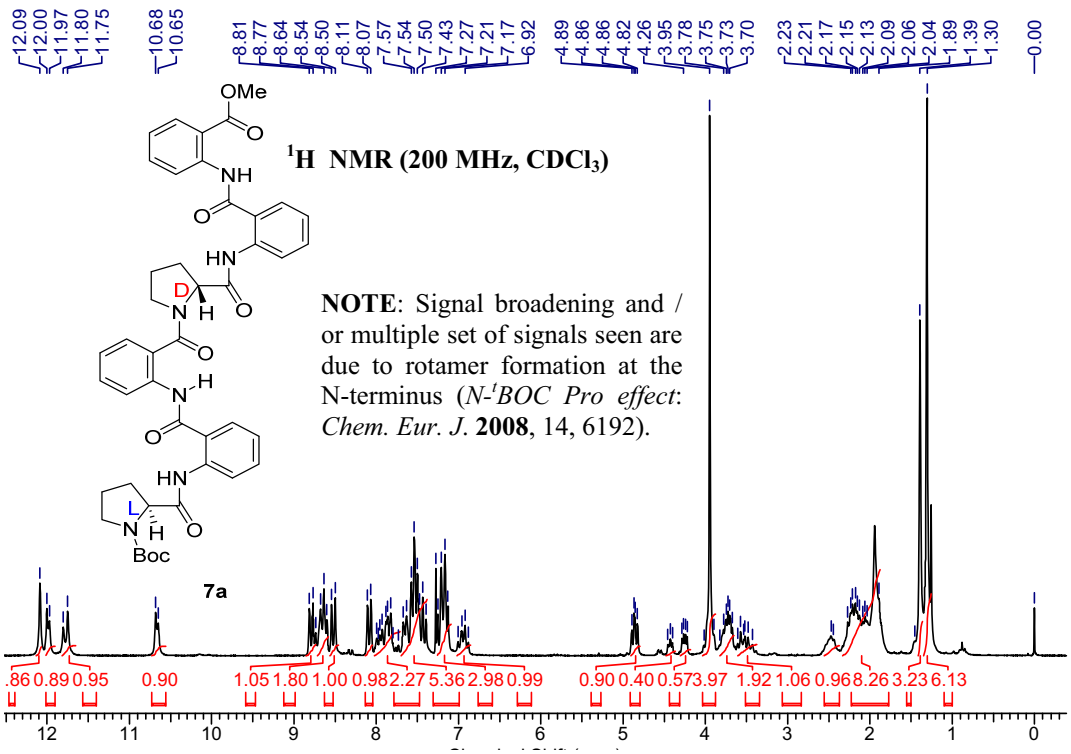
^{1}H NMR (200 MHz, CDCl$_3$)
NOTE: Signal broadening and / or multiple set of signals seen are due to rotamer formation at the N-terminus (*N-^{t}BOC Pro effect*: *Chem. Eur. J.* **2008**, 14, 6192).
7a

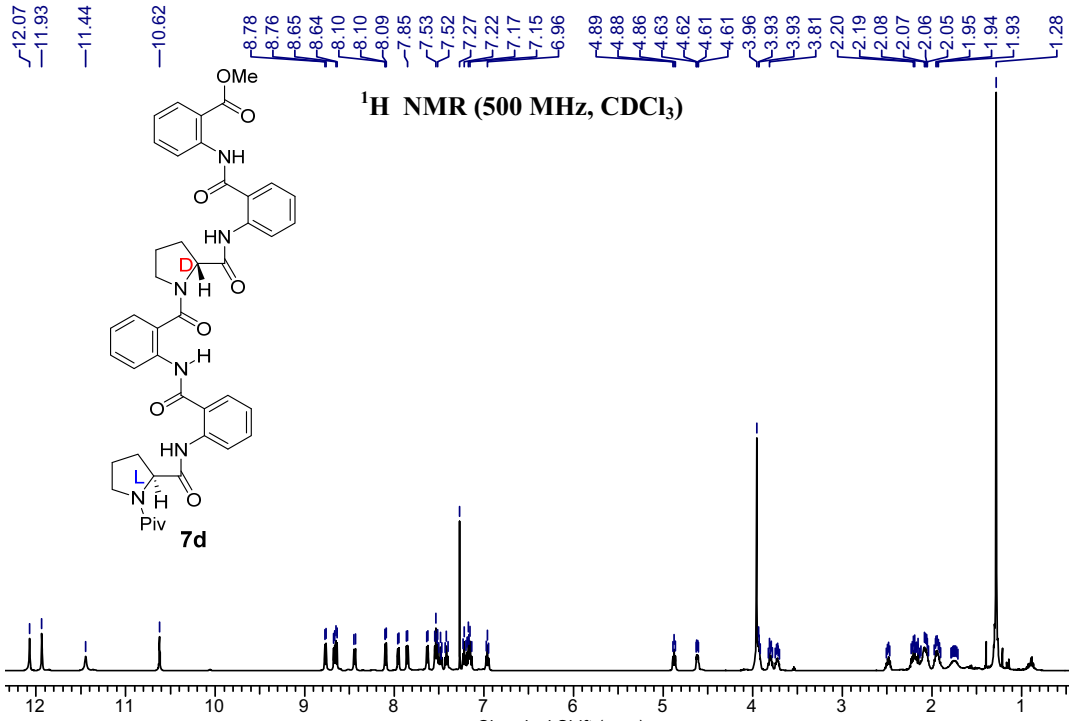
^{1}H NMR (500 MHz, CDCl$_3$)
7d

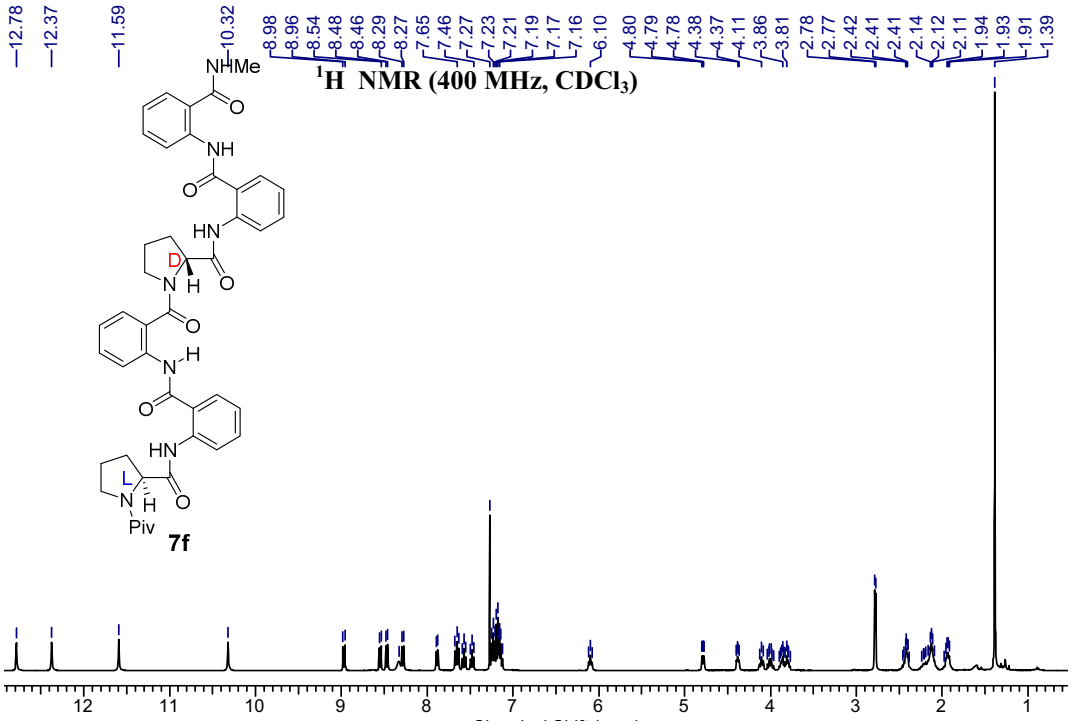
12.78
12.37
11.59
10.32
8.98
8.96
8.54
8.48
8.46
8.29
8.27
7.65
7.46
7.27
7.23
7.21
7.19
7.17
7.16
6.10
4.80
4.79
4.78
4.38
4.37
4.11
3.86
3.81
2.78
2.77
2.42
2.41
2.41
2.14
2.12
2.11
1.94
1.93
1.91
1.39
^{1}H NMR (400 MHz, CDCl$_3$)
NHMe
NH
HN
Piv
7f

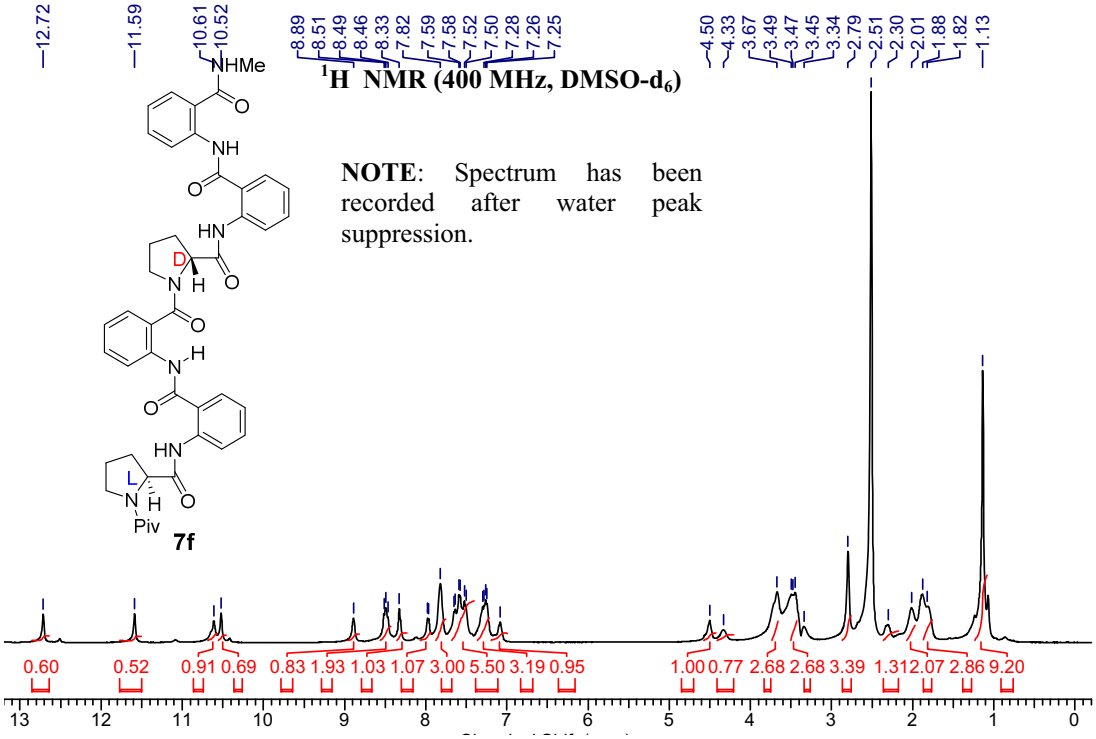
12.72
11.59
10.61
10.52
8.89
8.51
8.49
8.46
8.33
7.82
7.59
7.58
7.52
7.50
7.28
7.26
7.25
4.50
4.33
3.67
3.49
3.47
3.45
3.34
2.79
2.51
2.30
2.01
1.88
1.82
1.13
^{1}H NMR (400 MHz, DMSO-d$_6$)
NOTE: Spectrum has been recorded after water peak suppression.
NHMe
NH
HN
Piv
7f
0.60
0.52
0.91
0.69
0.83
1.93
1.03
1.07
3.00
5.50
3.19
0.95
1.00
0.77
2.68
2.68
3.39
1.31
2.07
2.86
9.20

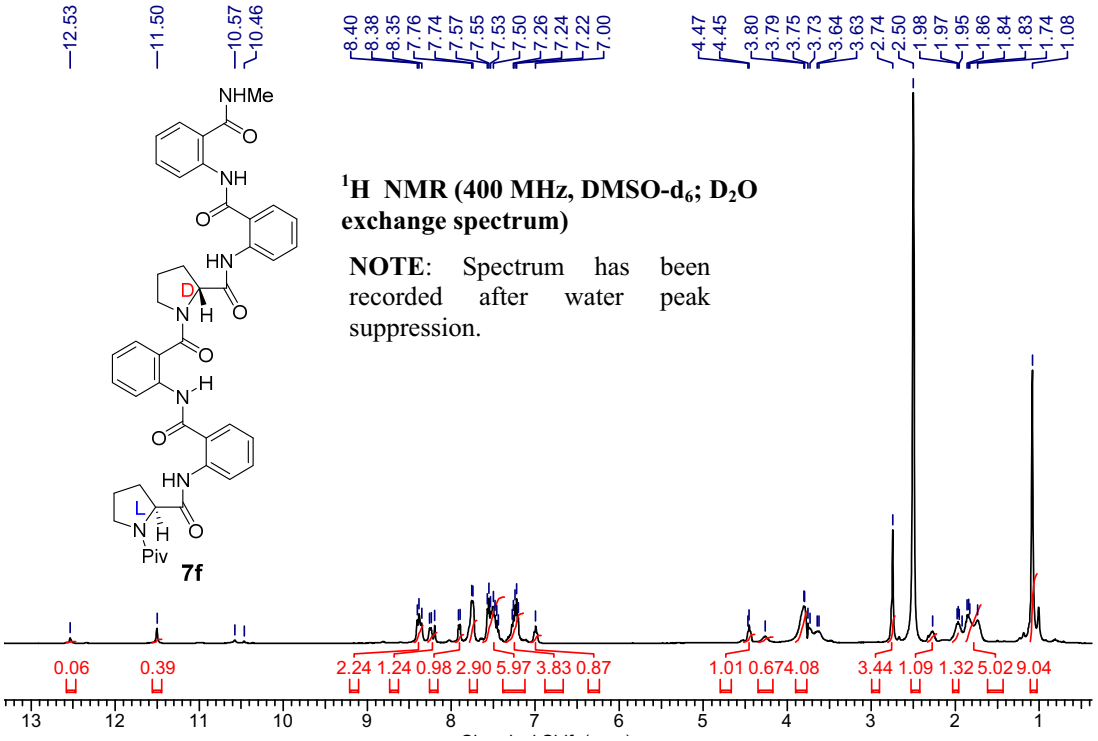

^{1}H NMR (400 MHz, DMSO-d$_6$; D$_2$O exchange spectrum)

NOTE: Spectrum has been recorded after water peak suppression.

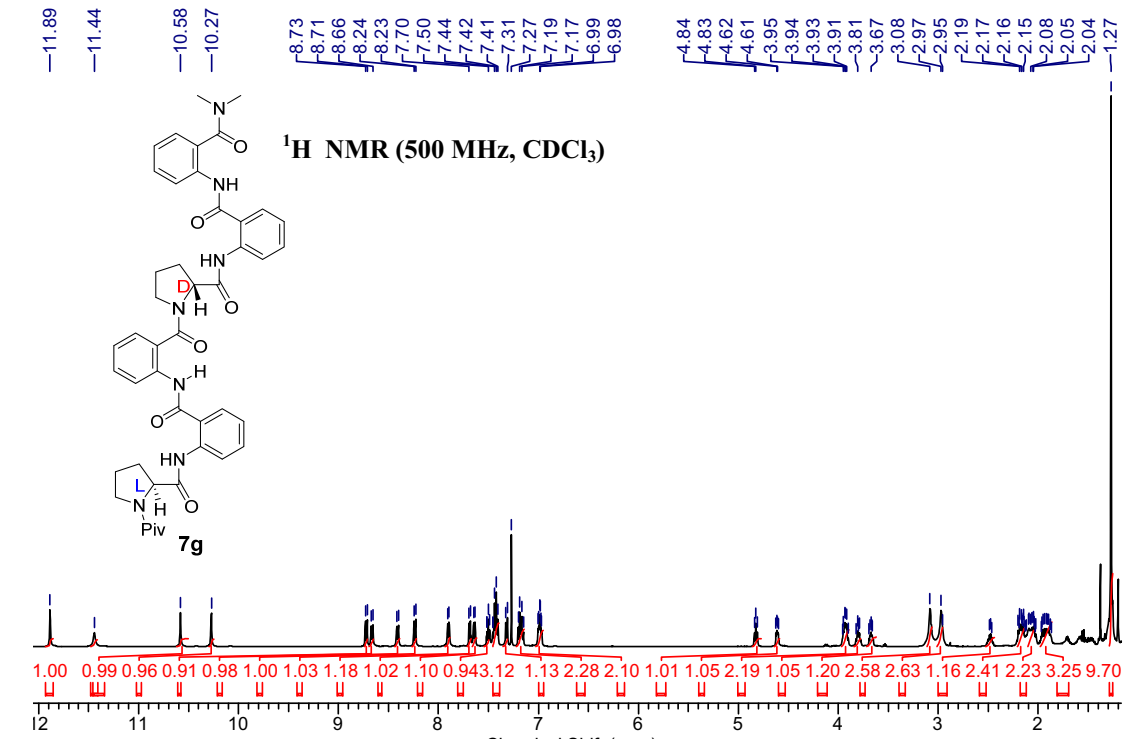

^{1}H NMR (500 MHz, CDCl$_3$)

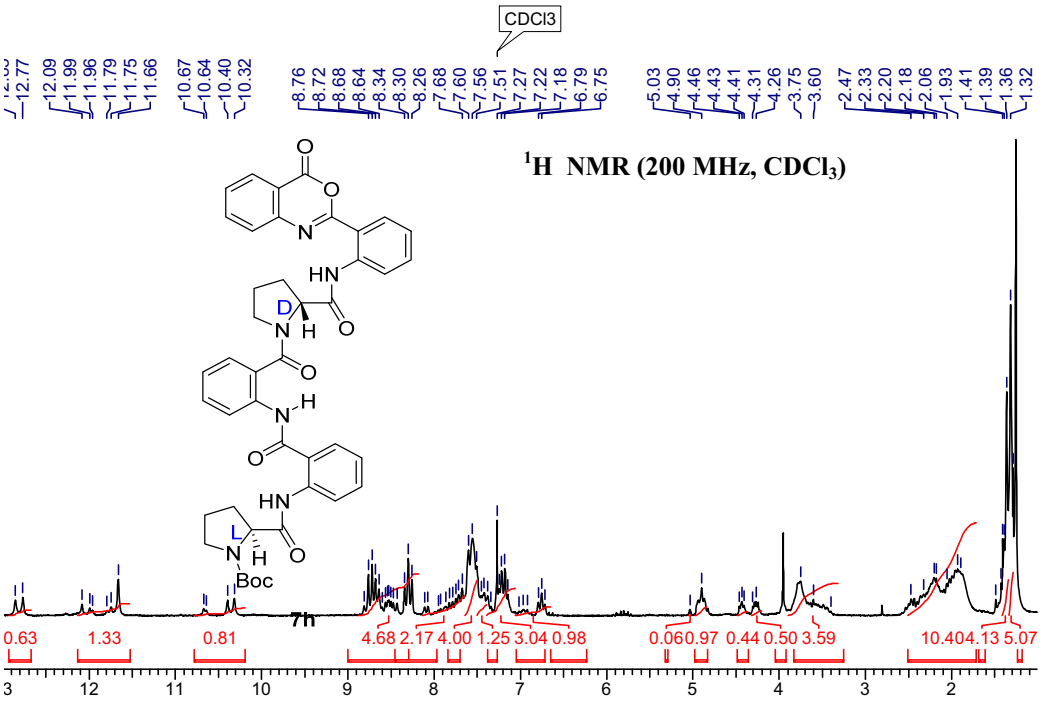
CDCl3
^{1}H NMR (200 MHz, CDCl$_3$)
7h
Boc
0.63 1.33 0.81 4.68 2.17 4.00 1.25 3.04 0.98 0.06 0.97 0.44 0.50 3.59 10.40 4.13 5.07

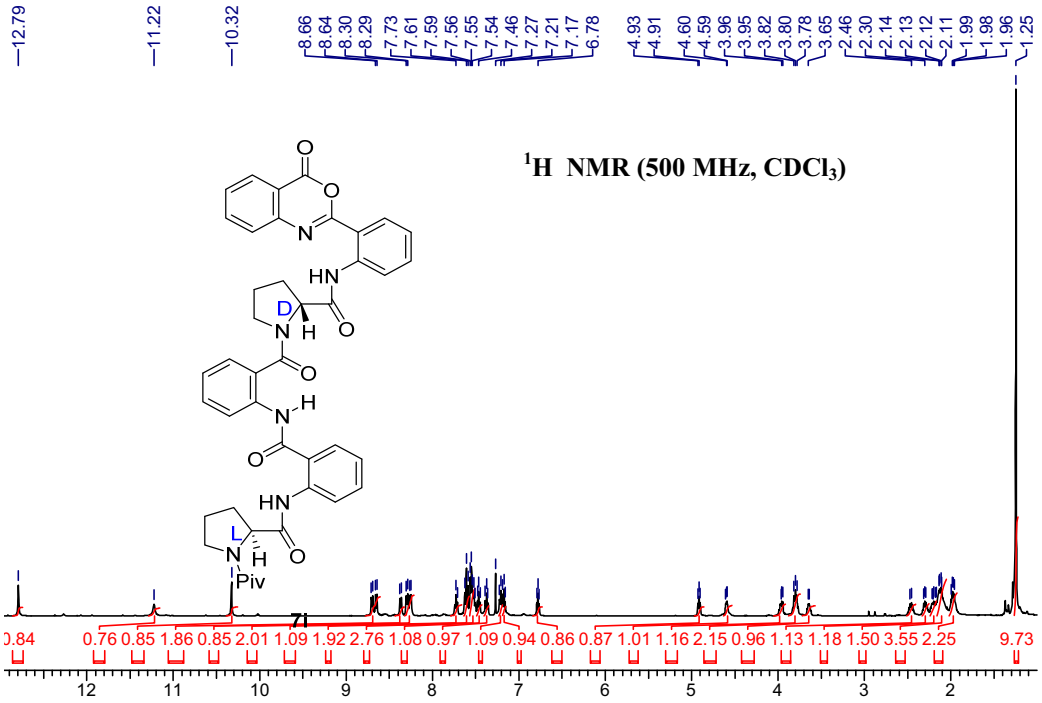
^{1}H NMR (500 MHz, CDCl$_3$)
7l
Piv
0.84 0.76 0.85 1.86 0.85 2.01 1.09 1.92 2.76 1.08 0.97 1.09 0.94 0.86 0.87 1.01 1.16 2.15 0.96 1.13 1.18 1.50 3.55 2.25 9.73

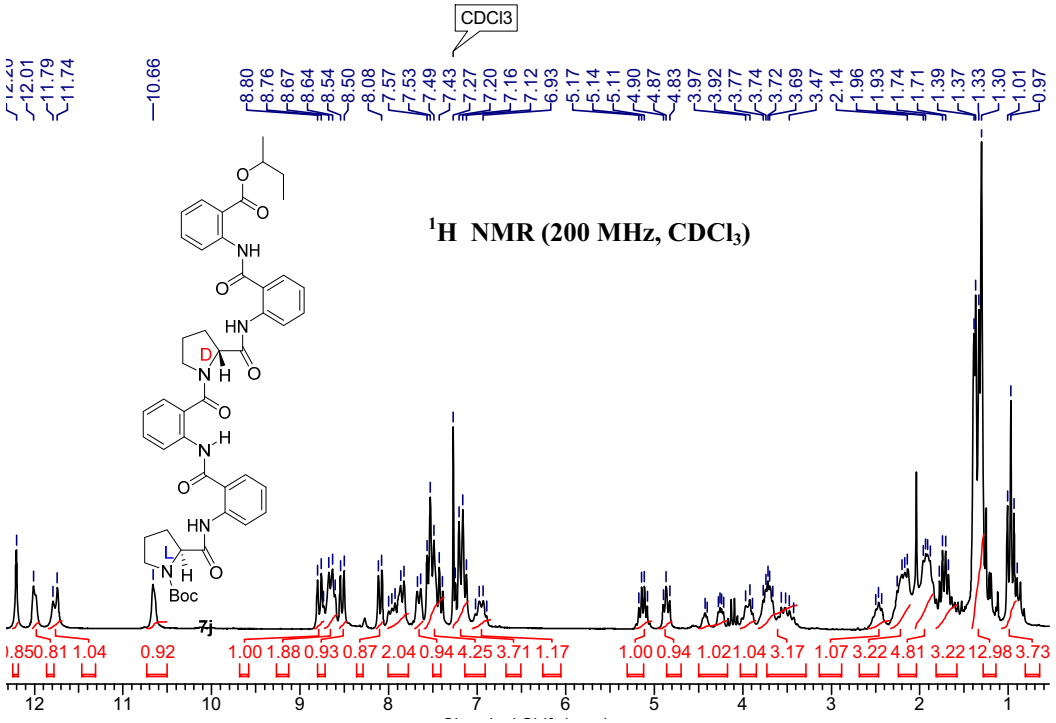
CDCl3
^{1}H NMR (200 MHz, CDCl$_3$)
7j

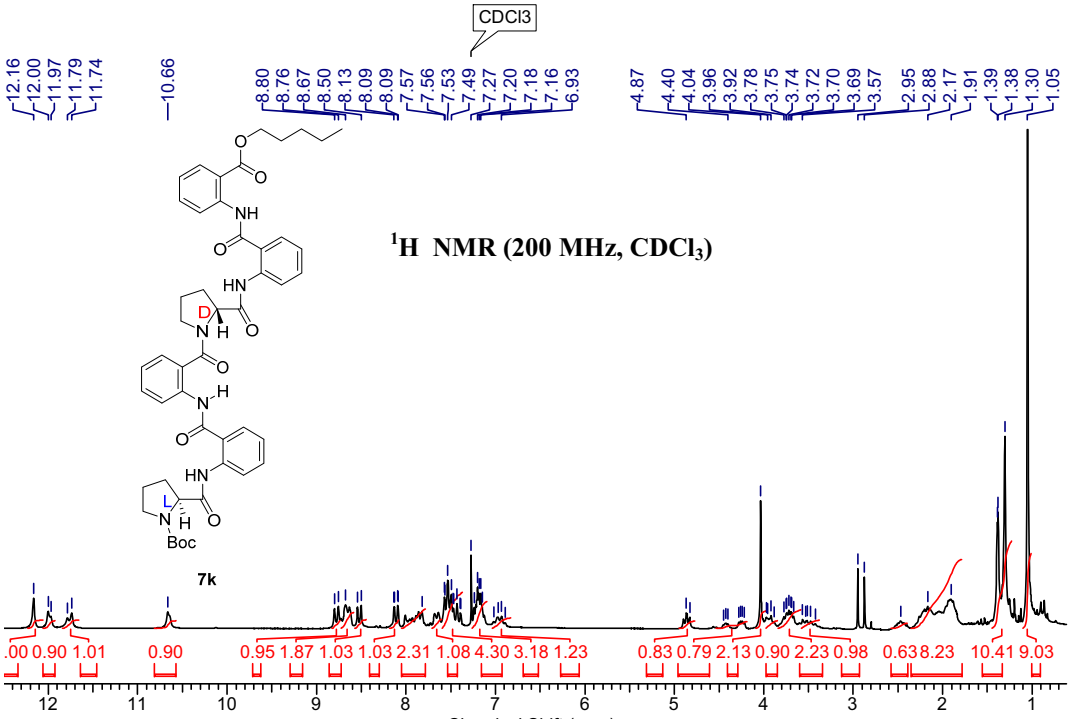
CDCl3
^{1}H NMR (200 MHz, CDCl$_3$)
7k

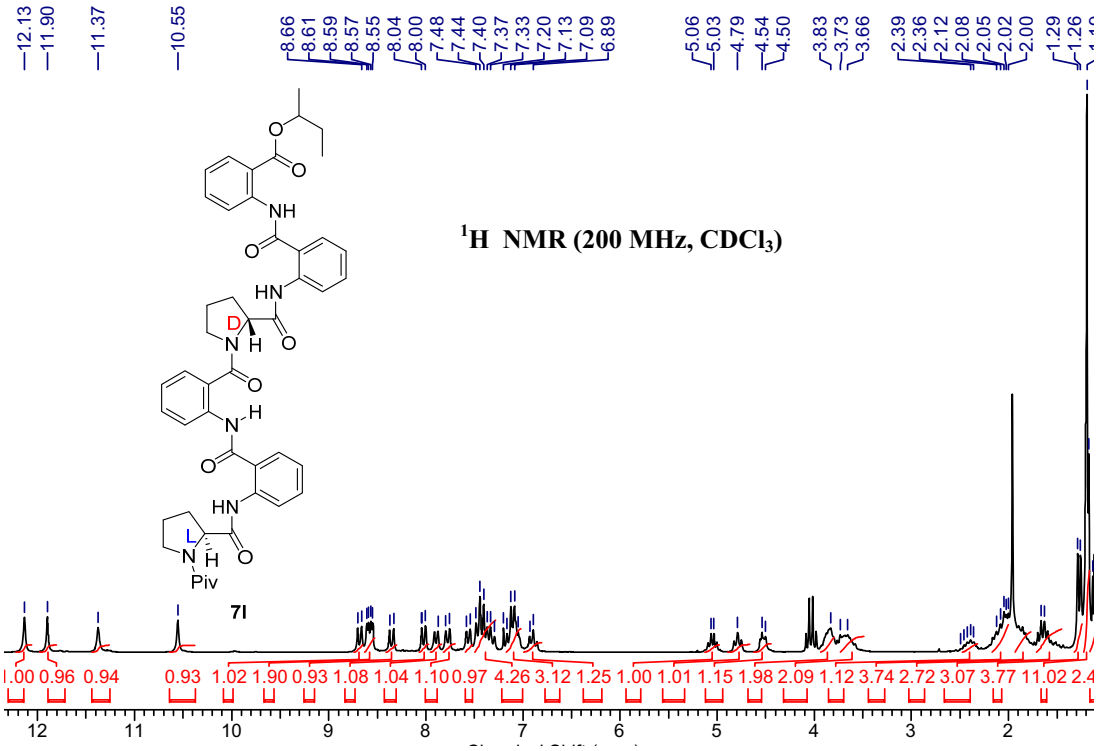

^{1}H NMR (200 MHz, $CDCl_3$)

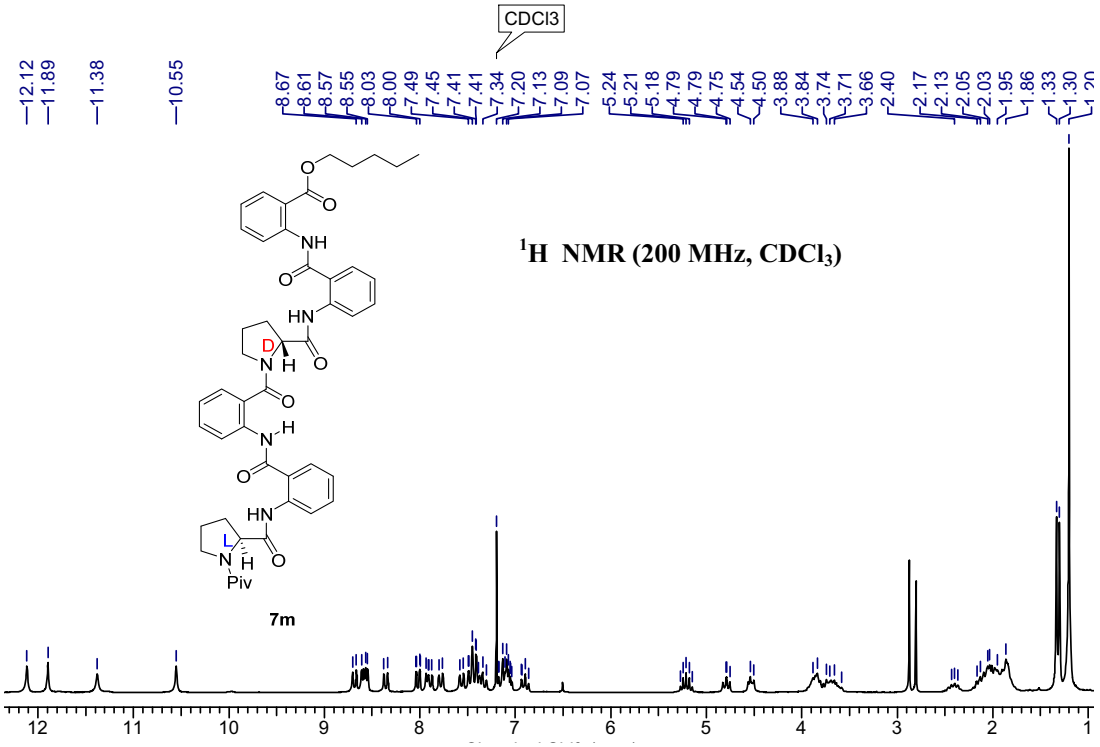

^{1}H NMR (200 MHz, $CDCl_3$)

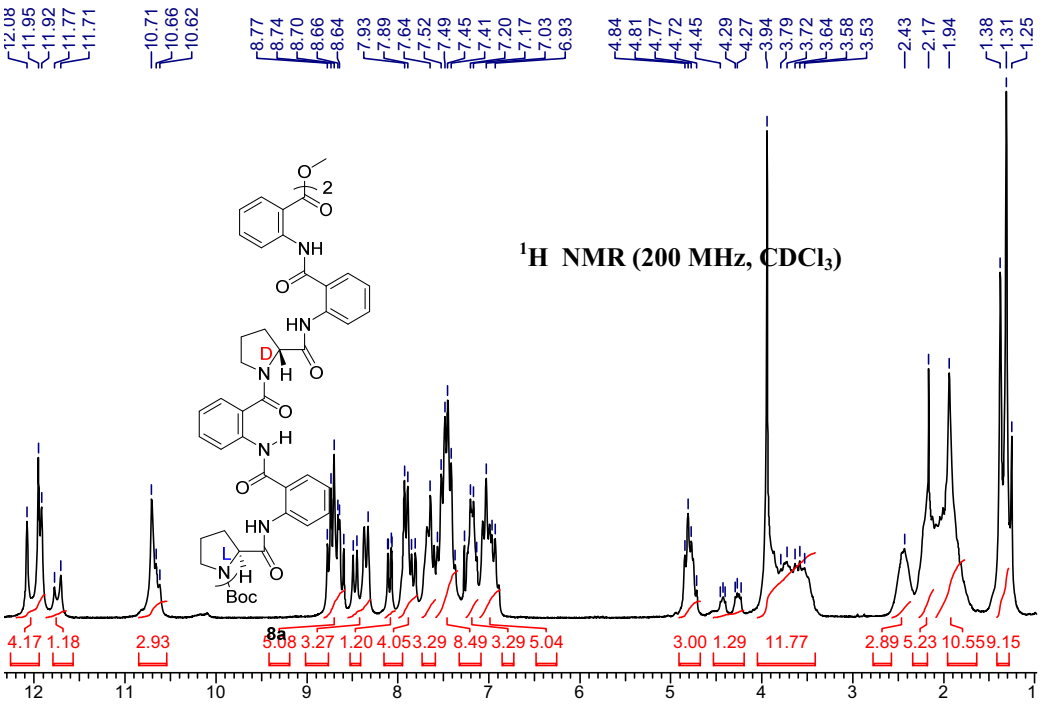
12.08
11.95
11.92
11.77
11.71
10.71
10.66
10.62
8.77
8.74
8.70
8.66
8.64
7.93
7.89
7.64
7.52
7.49
7.45
7.41
7.20
7.17
7.03
6.93
4.84
4.81
4.77
4.72
4.45
4.29
4.27
3.94
3.79
3.72
3.64
3.58
3.53
2.43
2.17
1.94
1.38
1.31
1.25
^{1}H NMR (200 MHz, CDCl$_3$)
Boc
8a
4.17 1.18 2.93 3.08 3.27 1.20 4.05 3.29 8.49 3.29 5.04 3.00 1.29 11.77 2.89 5.23 10.55 9.15

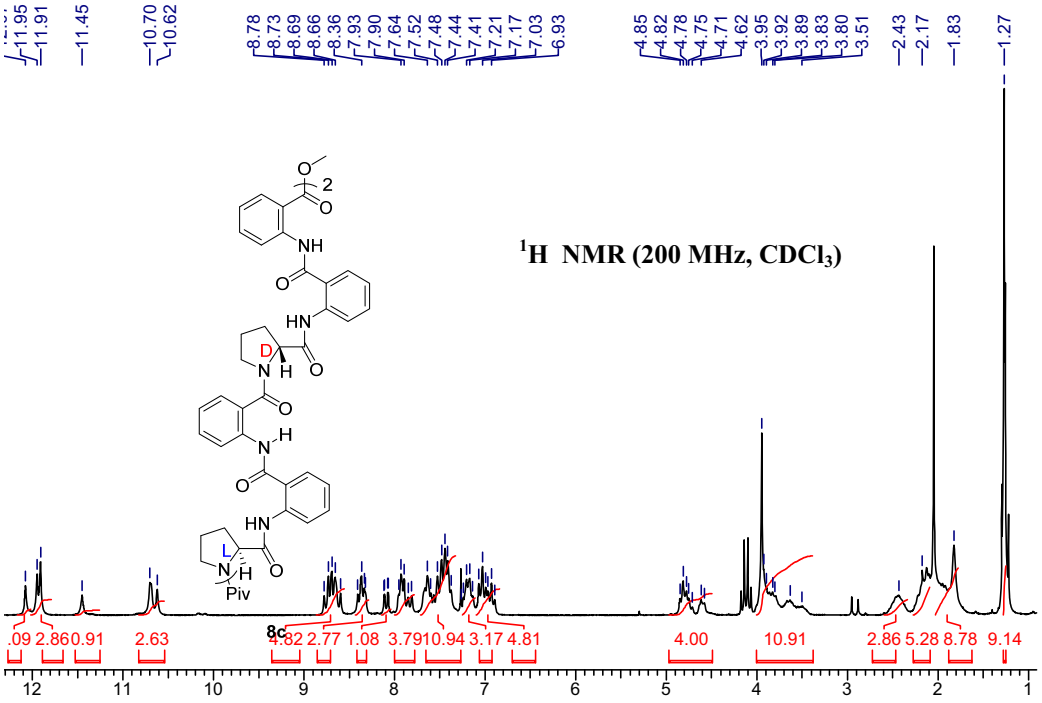
11.95
11.91
11.45
10.70
10.62
8.78
8.73
8.69
8.66
8.36
7.93
7.90
7.64
7.52
7.48
7.44
7.41
7.21
7.17
7.03
6.93
4.85
4.82
4.78
4.75
4.71
4.62
3.95
3.92
3.89
3.83
3.80
3.51
2.43
2.17
1.83
1.27
^{1}H NMR (200 MHz, CDCl$_3$)
Piv
8c
.09 2.86 0.91 2.63 4.82 2.77 1.08 3.79 10.94 3.17 4.81 4.00 10.91 2.86 5.28 8.78 9.14

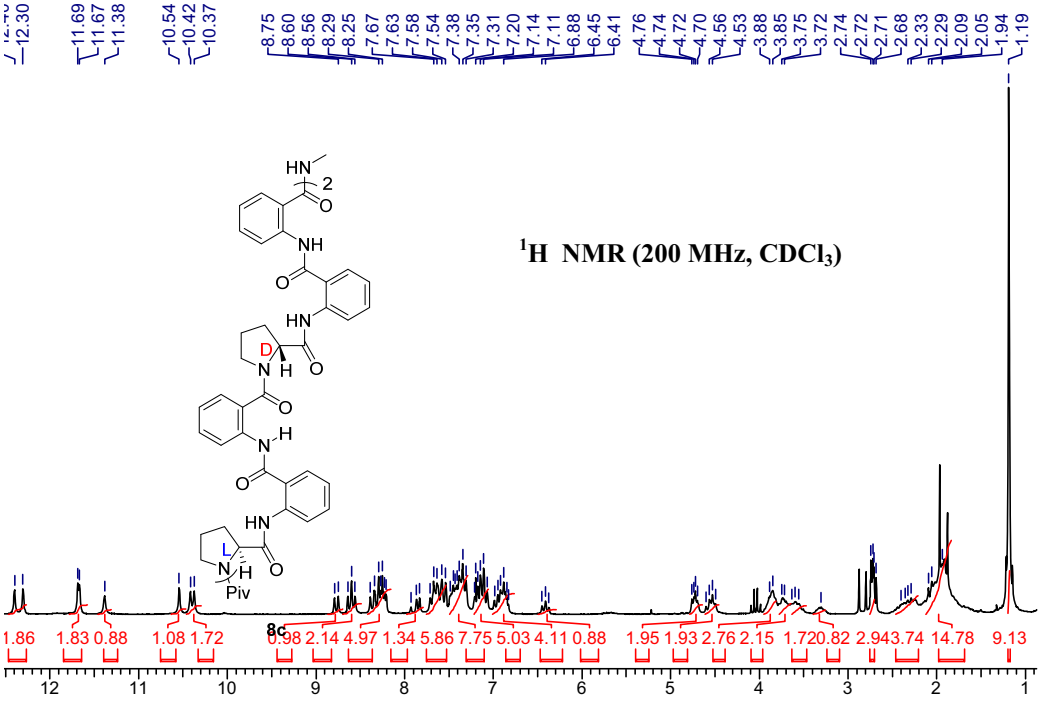
12.30
11.69
11.67
11.38
10.54
10.42
10.37
8.75
8.60
8.56
8.29
8.25
7.67
7.63
7.58
7.54
7.38
7.35
7.31
7.20
7.14
7.11
6.88
6.45
6.41
4.76
4.74
4.72
4.70
4.56
4.53
3.88
3.85
3.75
3.72
2.74
2.72
2.71
2.68
2.33
2.29
2.09
2.05
1.94
1.19
HN
2
O
NH
O
HN
D
N H
O
O
N H
O
HN
L
N H
O
Piv
^{1}H NMR (200 MHz, CDCl$_3$)
8c
1.86 1.83 0.88 1.08 1.72 0.98 2.14 4.97 1.34 5.86 7.75 5.03 4.11 0.88 1.95 1.93 2.76 2.15 1.72 0.82 2.94 3.74 14.78 9.13
12 11 10 9 8 7 6 5 4 3 2 1

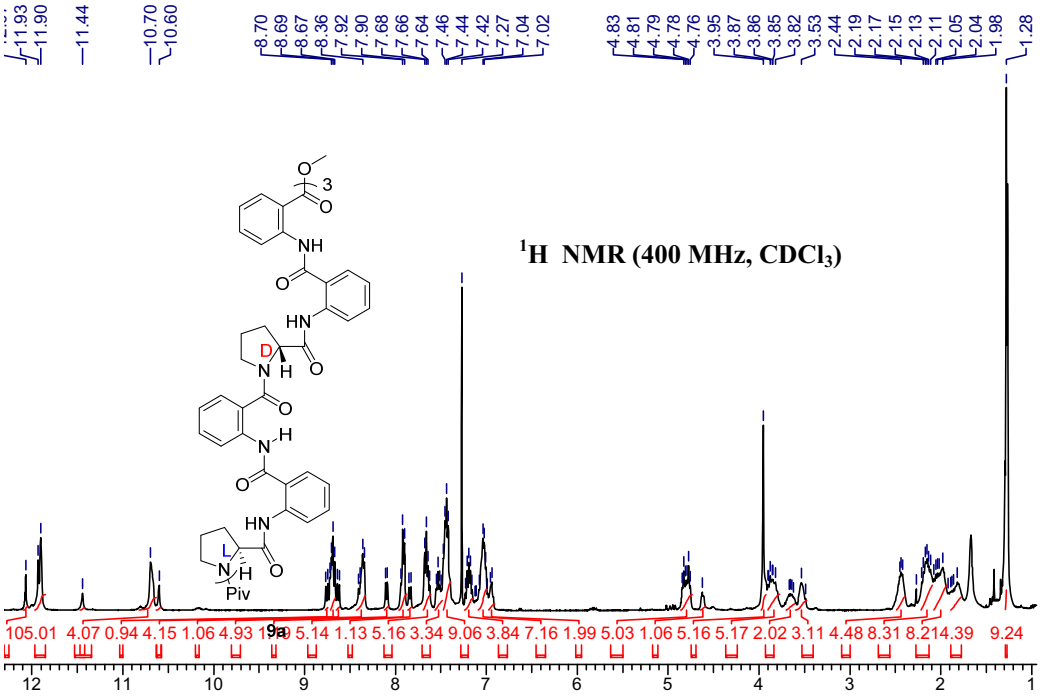
11.93
11.90
11.44
10.70
10.60
8.70
8.69
8.67
8.36
7.92
7.90
7.68
7.66
7.64
7.46
7.44
7.42
7.27
7.04
7.02
4.83
4.81
4.79
4.78
4.76
3.95
3.87
3.86
3.85
3.82
3.53
2.44
2.19
2.17
2.15
2.13
2.11
2.05
2.04
1.98
1.28
O
3
O
NH
O
HN
D
N H
O
O
N H
O
HN
L
N H
O
Piv
^{1}H NMR (400 MHz, CDCl$_3$)
9a
105.01 4.07 0.94 4.15 1.06 4.93 1.13 5.16 3.34 9.06 3.84 7.16 1.99 5.03 1.06 5.16 5.17 2.02 3.11 4.48 8.31 8.21 4.39 9.24
12 11 10 9 8 7 6 5 4 3 2 1

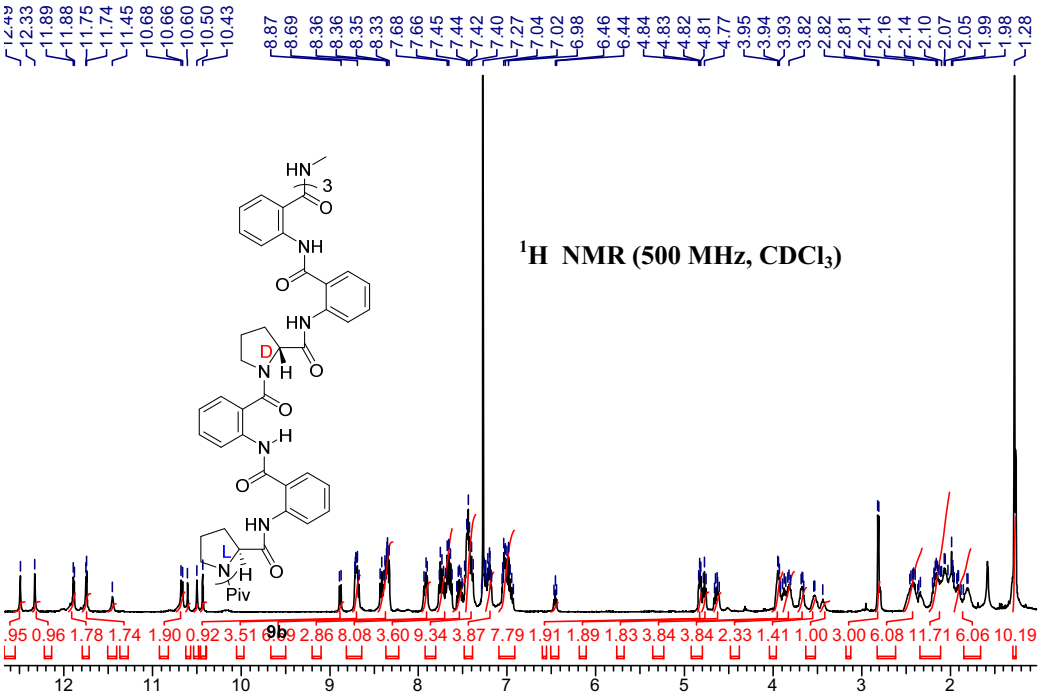
1H NMR (500 MHz, CDCl3)
9b

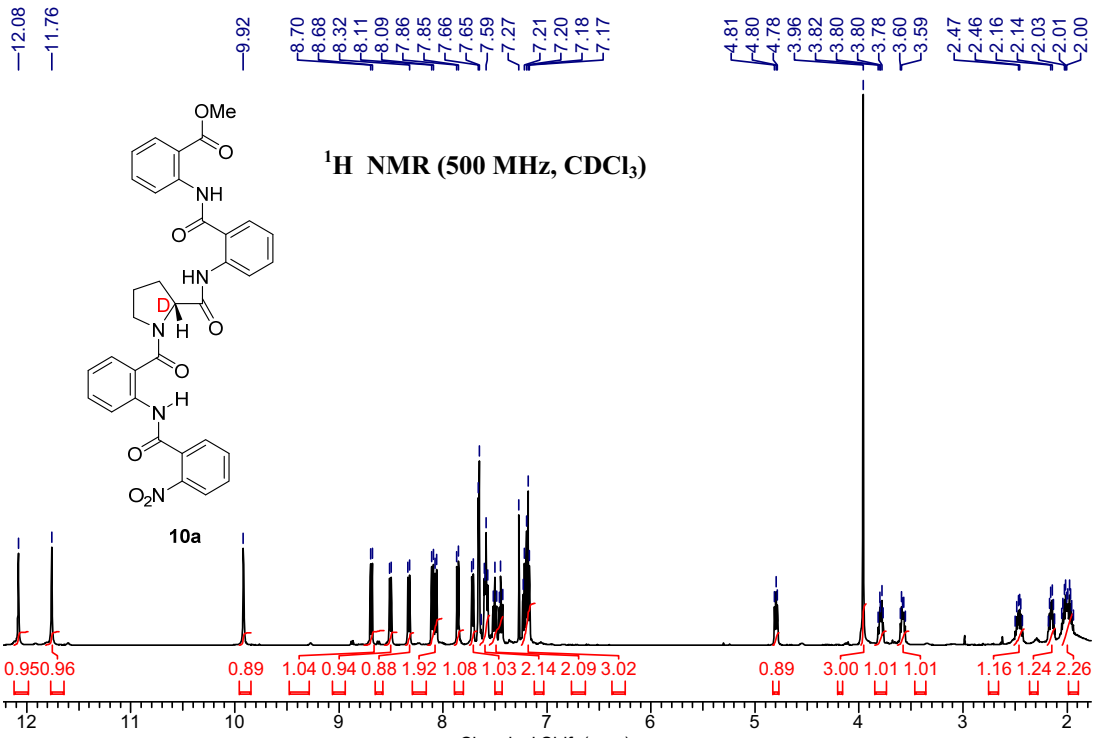
1H NMR (500 MHz, CDCl3)
10a

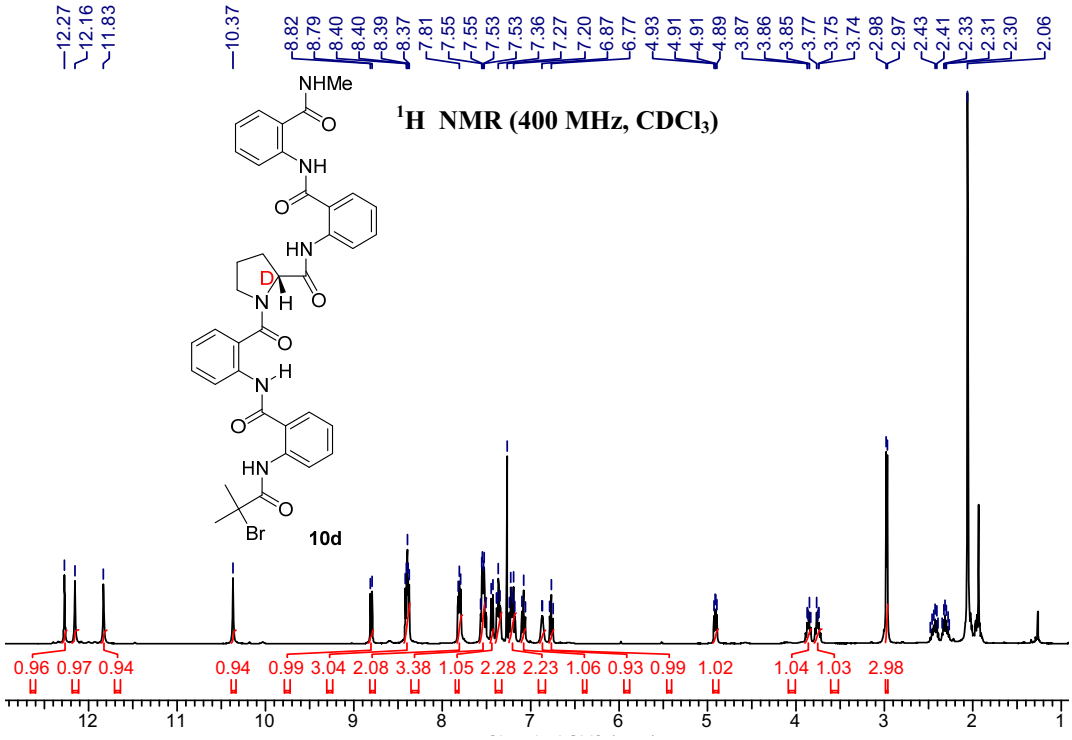
12.27
12.16
11.83
10.37
8.82
8.79
8.40
8.40
8.39
8.37
7.81
7.55
7.55
7.53
7.53
7.36
7.27
7.20
6.87
6.77
4.93
4.91
4.91
4.89
3.87
3.86
3.85
3.77
3.75
3.74
2.98
2.97
2.43
2.41
2.33
2.31
2.30
2.06
^{1}H NMR (400 MHz, CDCl$_3$)
NHMe
NH
HN
D
N H
N H
HN
Br
10d
0.96 0.97 0.94
0.94
0.99 3.04 2.08 3.38 1.05 2.28 2.23 1.06 0.93 0.99 1.02
1.04 1.03 2.98
12 11 10 9 8 7 6 5 4 3 2 1

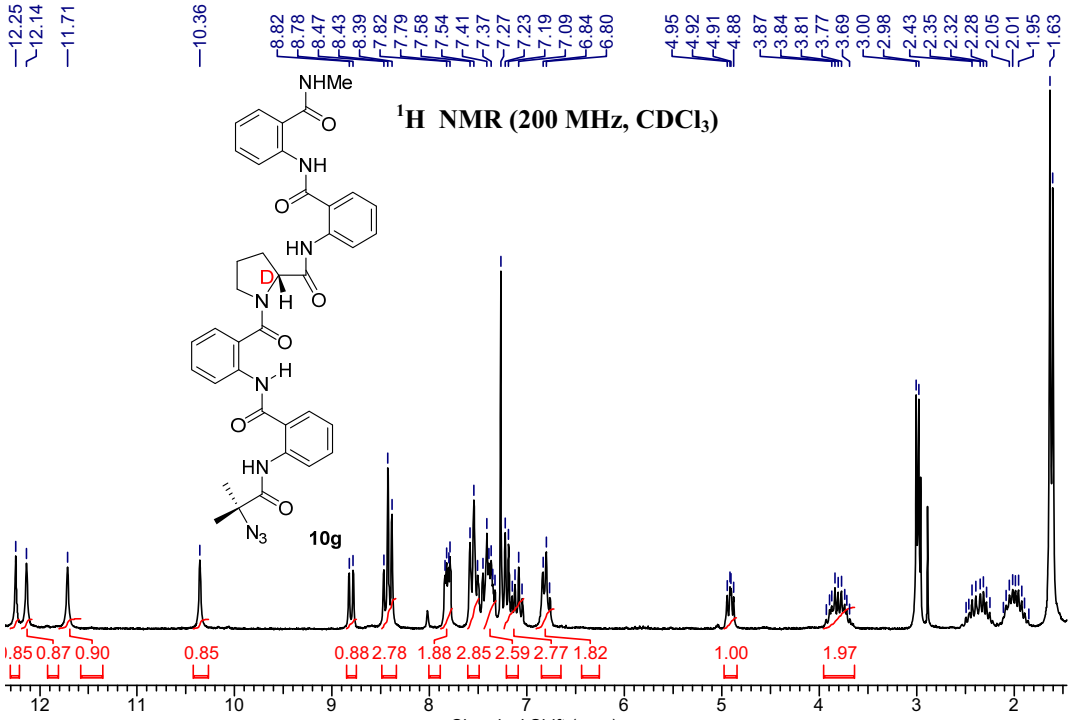
12.25
12.14
11.71
10.36
8.82
8.78
8.47
8.43
8.39
7.82
7.79
7.58
7.54
7.41
7.37
7.27
7.23
7.19
7.09
6.84
6.80
4.95
4.92
4.91
4.88
3.87
3.84
3.81
3.77
3.69
3.00
2.98
2.43
2.35
2.32
2.28
2.05
2.01
1.95
1.63
^{1}H NMR (200 MHz, CDCl$_3$)
NHMe
NH
HN
D
N H
N H
HN
N$_3$
10g
.85 0.87 0.90
0.85
0.88 2.78 1.88 2.85 2.59 2.77 1.82
1.00
1.97
12 11 10 9 8 7 6 5 4 3 2

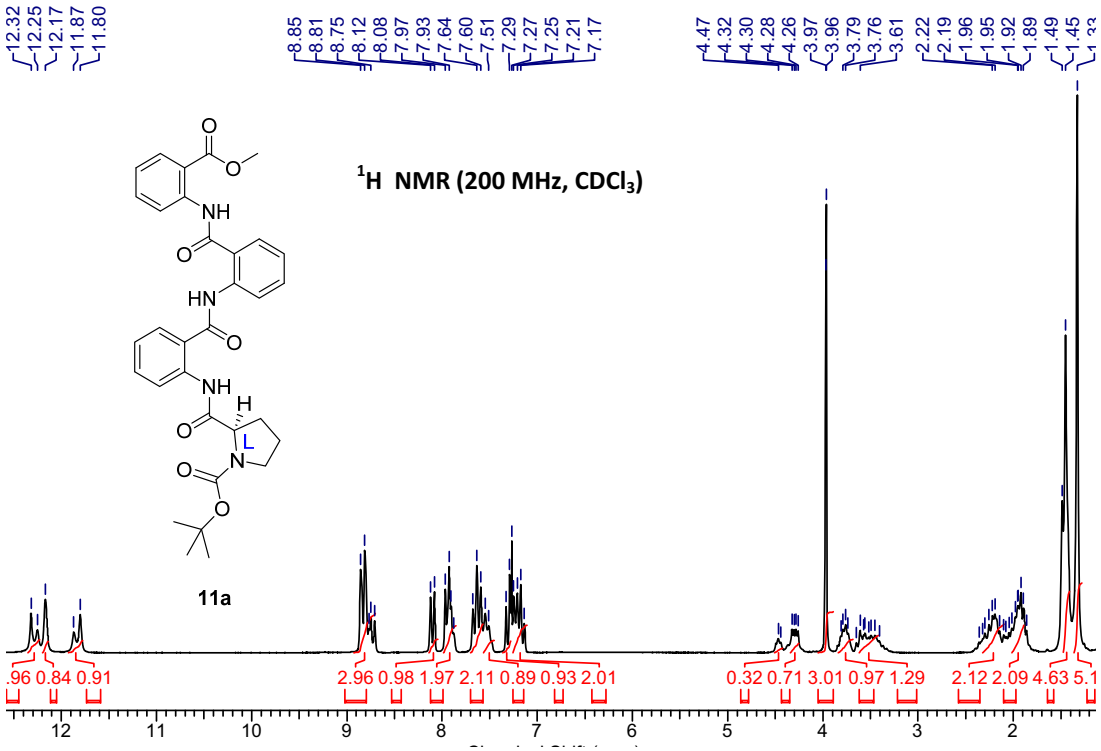
^{1}H NMR (200 MHz, CDCl$_3$)
11a

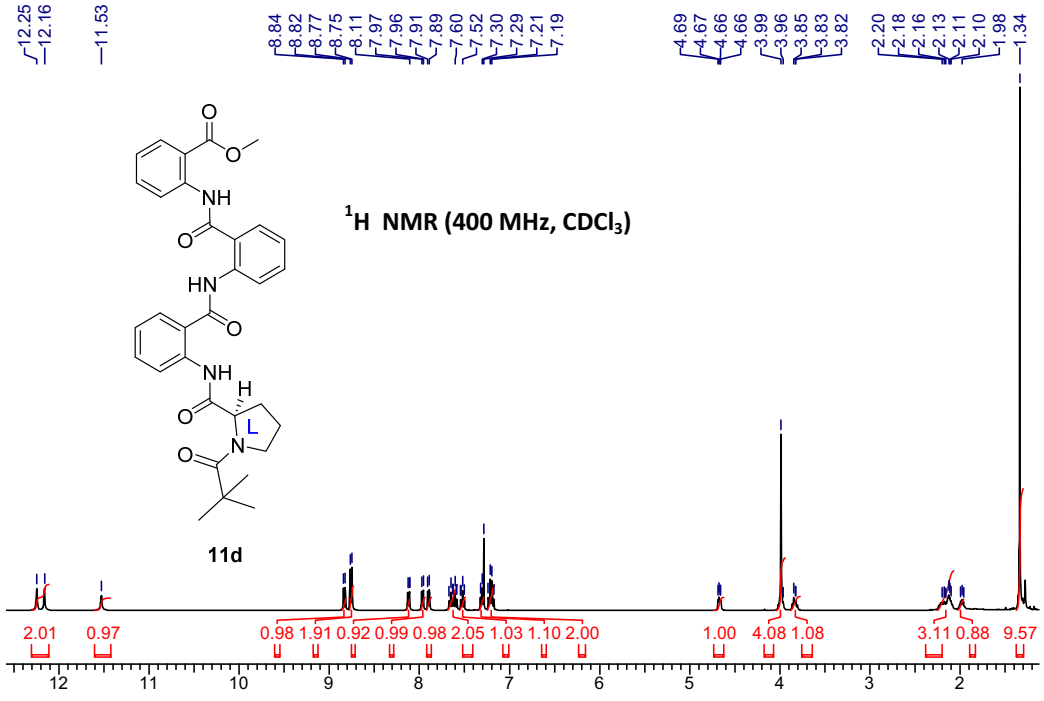
^{1}H NMR (400 MHz, CDCl$_3$)
11d

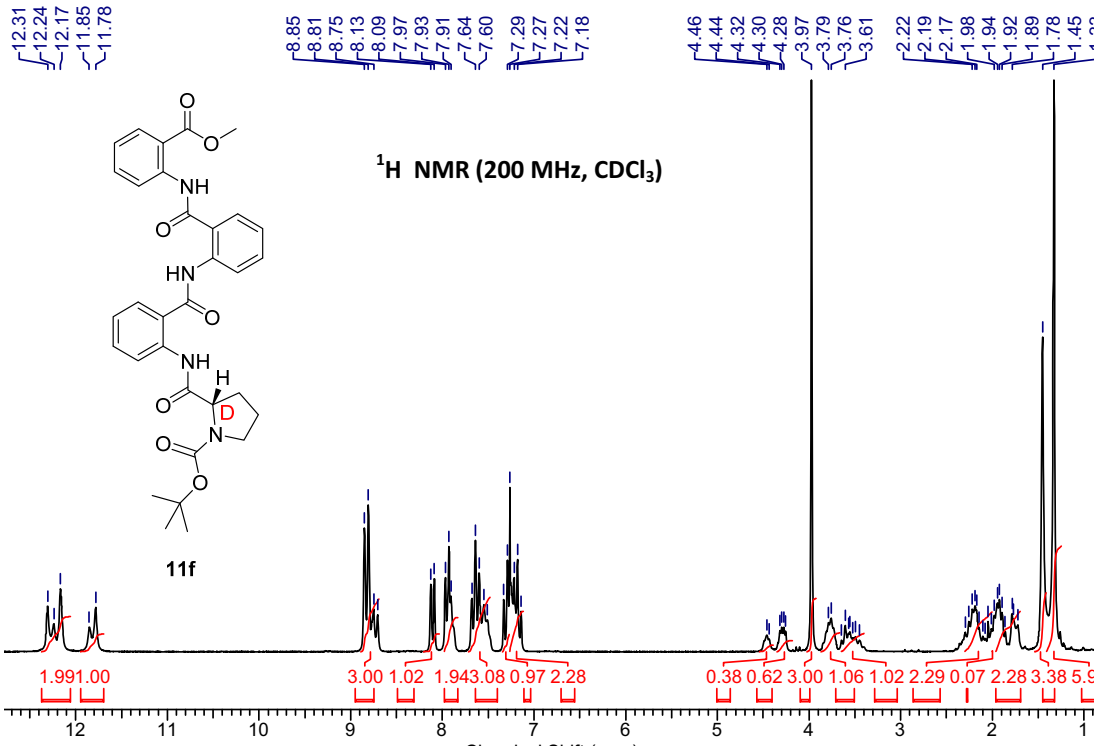
^{1}H NMR (200 MHz, CDCl$_3$)
11f

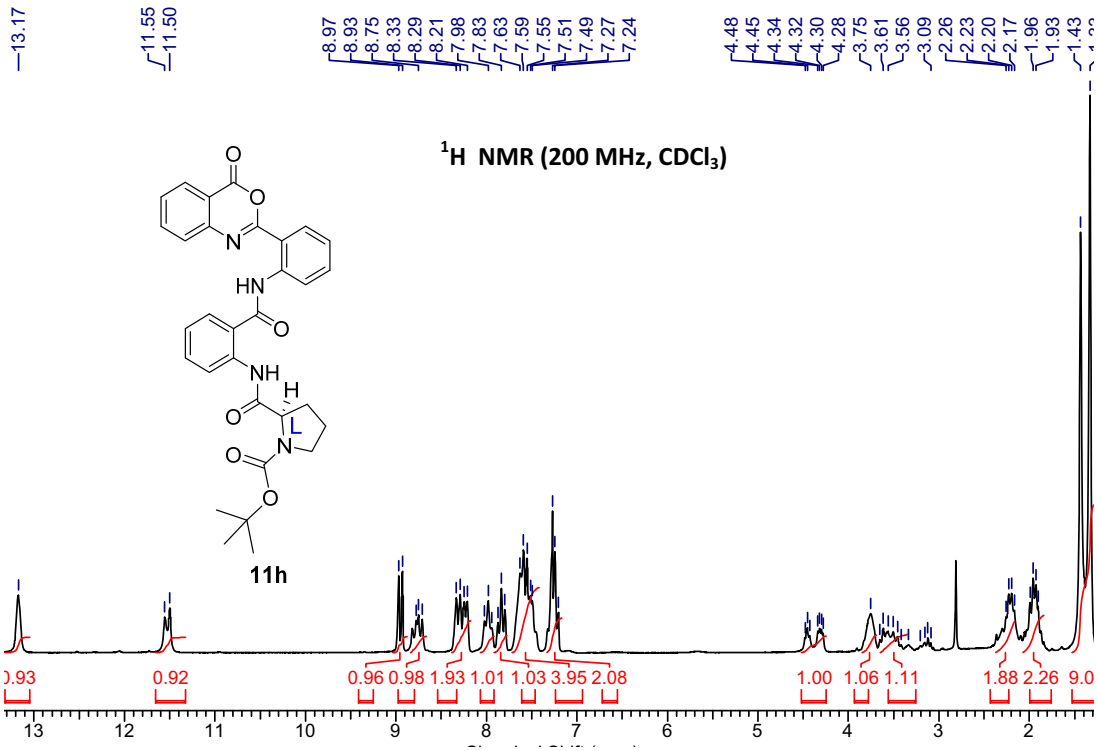
^{1}H NMR (200 MHz, CDCl$_3$)
11h

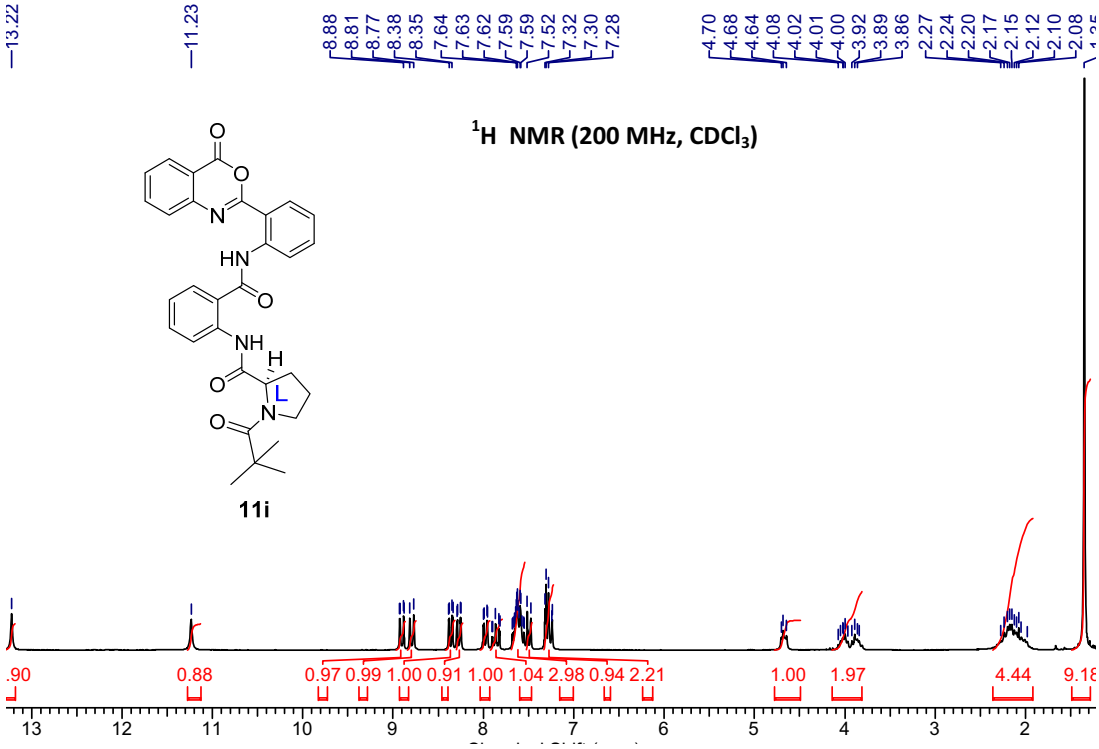
^{1}H NMR (200 MHz, CDCl$_3$)
11i
13.22
11.23
8.88 8.81 8.77 8.38 8.35 7.64 7.63 7.62 7.59 7.59 7.52 7.32 7.30 7.28
4.70 4.68 4.64 4.08 4.02 4.01 4.00 3.92 3.89 3.86
2.27 2.24 2.20 2.17 2.15 2.12 2.10 2.08
.90 0.88 0.97 0.99 1.00 0.91 1.00 1.04 2.98 0.94 2.21 1.00 1.97 4.44 9.18
13 12 11 10 9 8 7 6 5 4 3 2

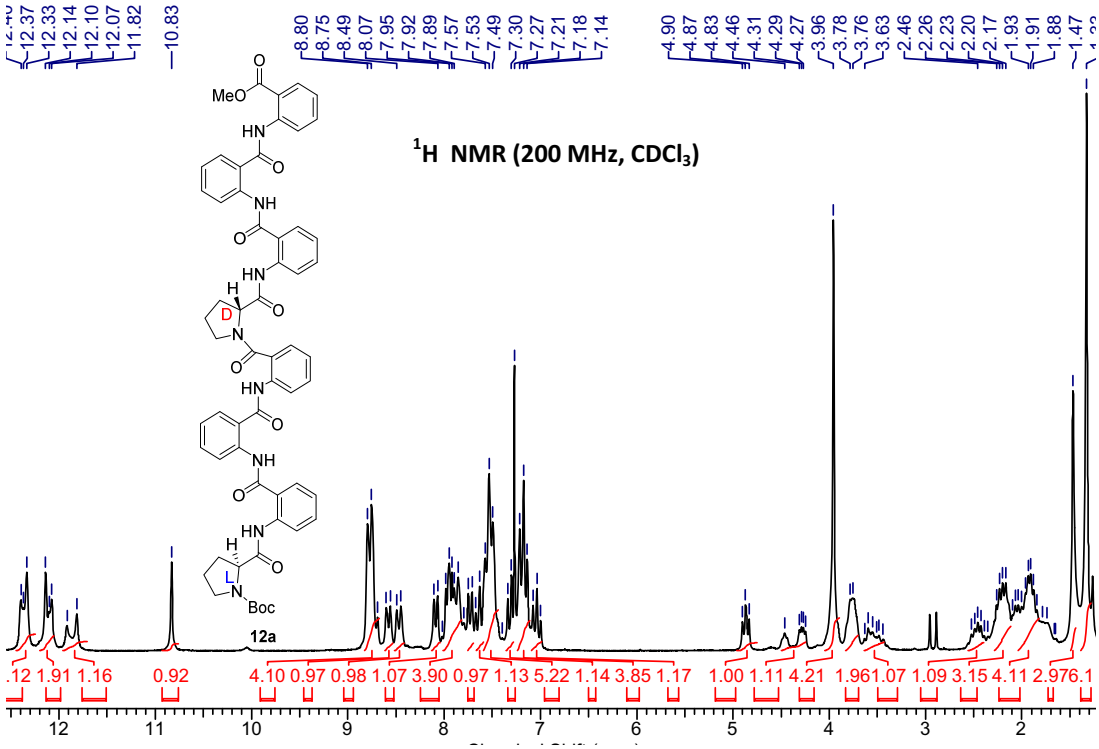
^{1}H NMR (200 MHz, CDCl$_3$)
12a
12.37 12.33 12.14 12.10 12.07 11.82
10.83
8.80 8.75 8.49 8.07 7.95 7.92 7.89 7.57 7.53 7.49 7.30 7.27 7.21 7.18 7.14
4.90 4.87 4.83 4.46 4.31 4.29 4.27
3.96 3.78 3.76 3.63
2.46 2.26 2.23 2.20 2.17 1.93 1.91 1.88 1.47
.12 1.91 1.16 0.92 4.10 0.97 0.98 1.07 3.90 0.97 1.13 5.22 1.14 3.85 1.17 1.00 1.11 4.21 1.96 1.07 1.09 3.15 4.11 2.97 6.1
12 11 10 9 8 7 6 5 4 3 2

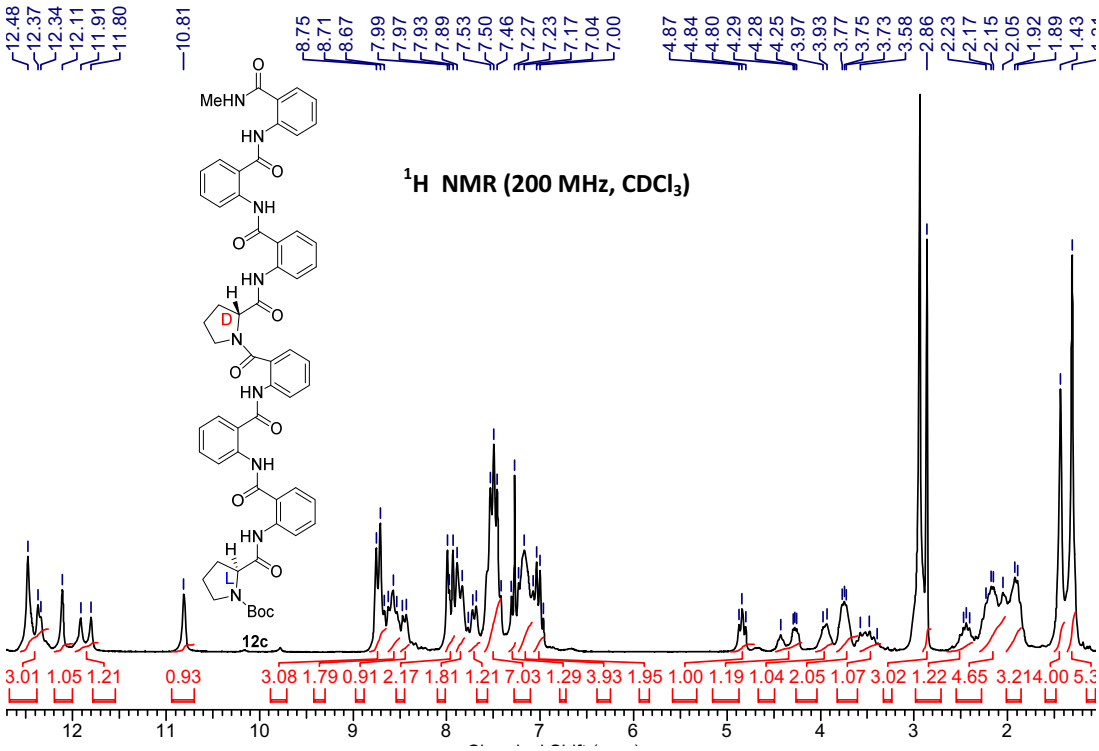
12.48
12.37
12.34
12.11
11.91
11.80
10.81
8.75
8.71
8.67
7.99
7.97
7.93
7.89
7.53
7.50
7.46
7.27
7.23
7.17
7.04
7.00
4.87
4.84
4.80
4.29
4.28
4.25
3.97
3.93
3.77
3.75
3.73
3.58
2.86
2.23
2.17
2.15
2.05
1.92
1.89
1.43
MeHN
HN
NH
Boc
12c
^{1}H NMR (200 MHz, CDCl$_3$)
3.01 1.05 1.21 0.93 3.08 1.79 0.91 2.17 1.81 1.21 7.03 1.29 3.93 1.95 1.00 1.19 1.04 2.05 1.07 3.02 1.22 4.65 3.21 4.00 5.3
12 11 10 9 8 7 6 5 4 3 2

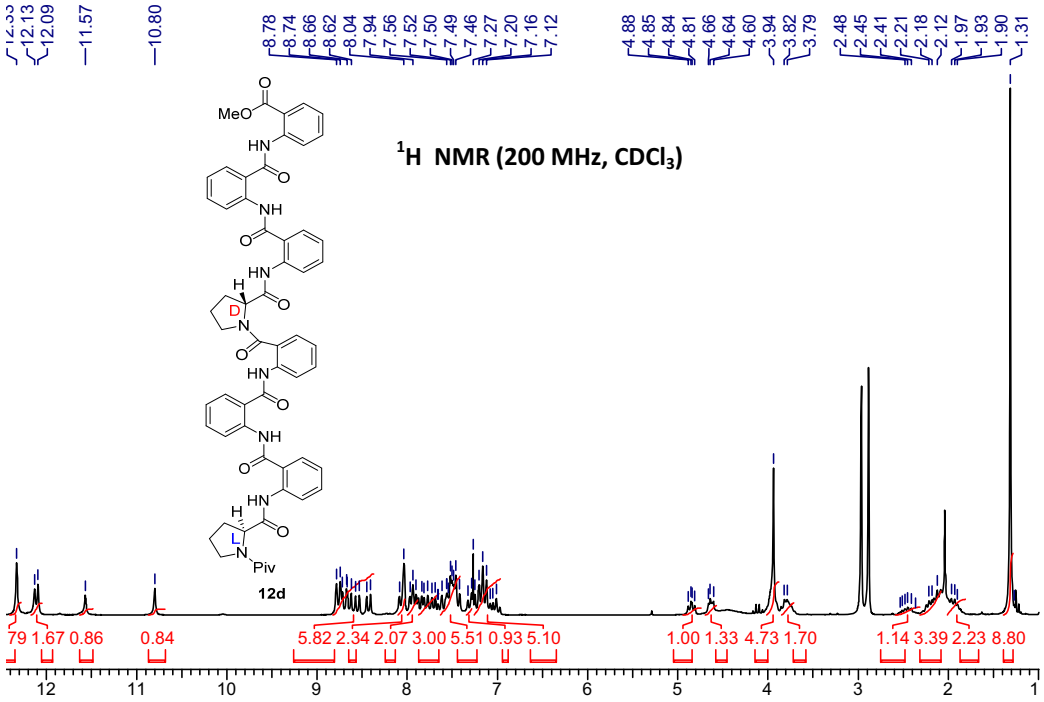
12.13
12.09
11.57
10.80
8.78
8.74
8.66
8.62
8.04
7.94
7.56
7.52
7.50
7.49
7.46
7.27
7.20
7.16
7.12
4.88
4.85
4.84
4.81
4.66
4.64
4.60
3.94
3.82
3.79
2.48
2.45
2.41
2.21
2.18
2.12
1.97
1.93
1.90
1.31
MeO
HN
NH
Piv
12d
^{1}H NMR (200 MHz, CDCl$_3$)
79 1.67 0.86 0.84 5.82 2.34 2.07 3.00 5.51 0.93 5.10 1.00 1.33 4.73 1.70 1.14 3.39 2.23 8.80
12 11 10 9 8 7 6 5 4 3 2 1

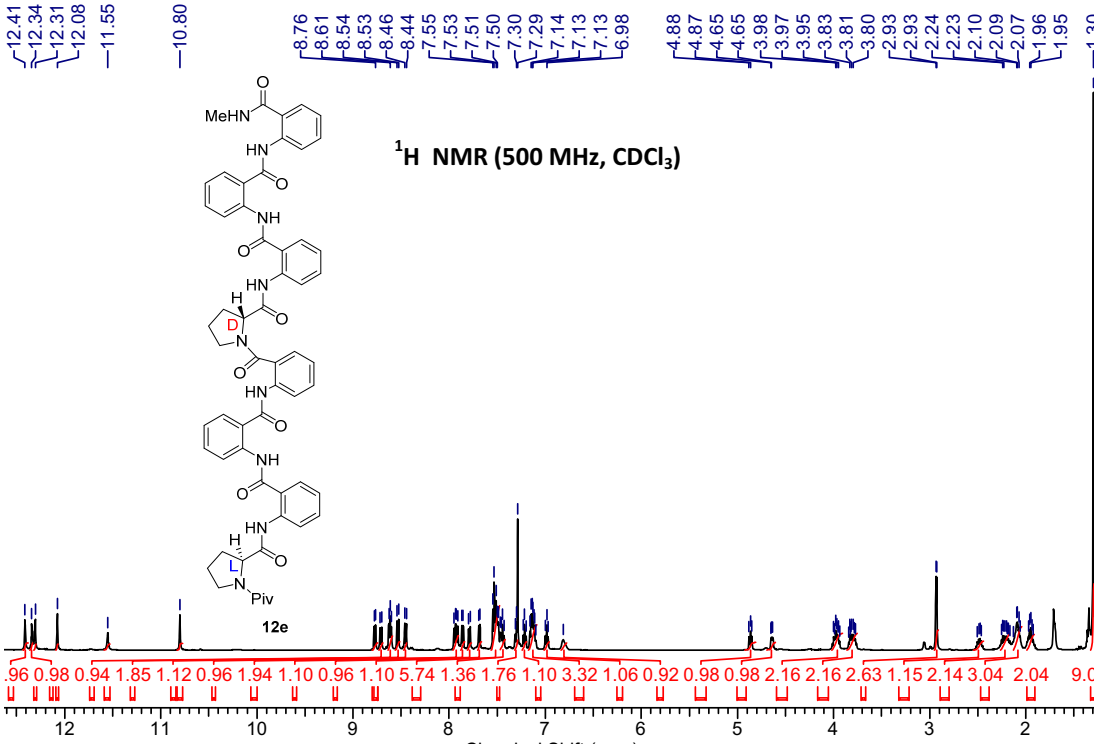

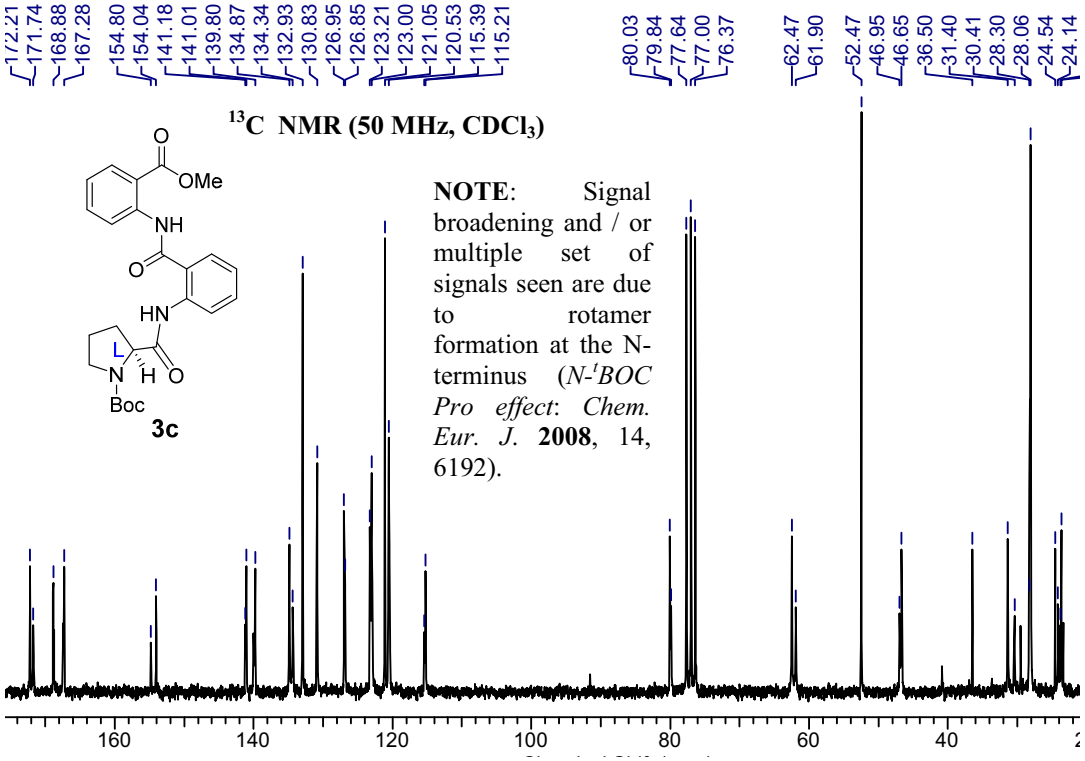

NOTE: Signal broadening and / or multiple set of signals seen are due to rotamer formation at the N-terminus (*N-^{t}BOC Pro effect*: *Chem. Eur. J.* **2008**, 14, 6192).

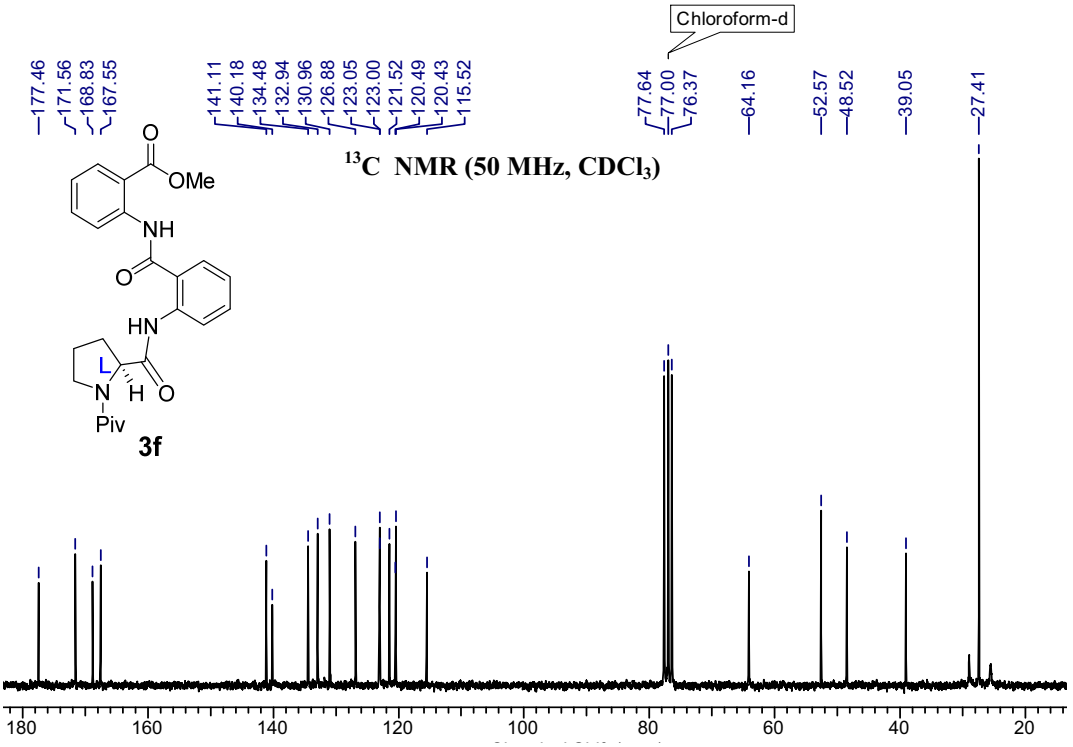
Chloroform-d
177.46
171.56
168.83
167.55
141.11
140.18
134.48
132.94
130.96
126.88
123.05
123.00
121.52
120.49
120.43
115.52
77.64
77.00
76.37
64.16
52.57
48.52
39.05
27.41
^{13}C NMR (50 MHz, CDCl$_3$)
OMe
NH
HN
L
N H O
Piv
3f
180
160
140
120
100
80
60
40
20

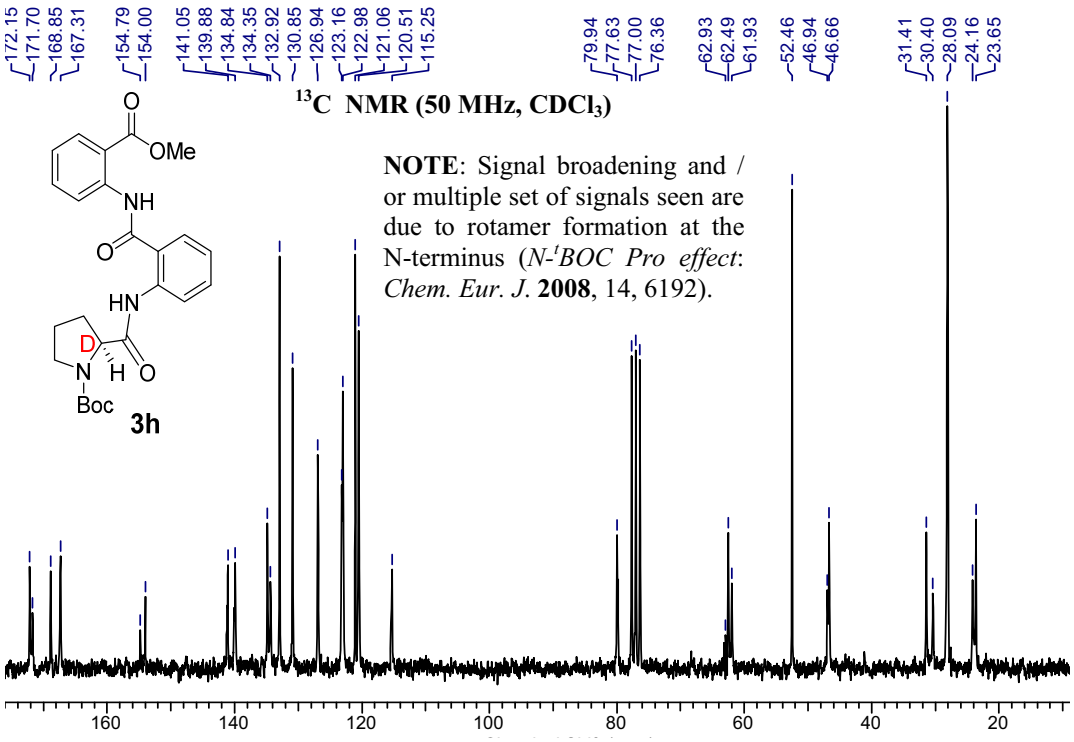
172.15
171.70
168.85
167.31
154.79
154.00
141.05
139.88
134.84
134.35
132.92
130.85
126.94
123.16
122.98
121.06
120.51
115.25
79.94
77.63
77.00
76.36
62.93
62.49
61.93
52.46
46.94
46.66
31.41
30.40
28.09
24.16
23.65
^{13}C NMR (50 MHz, CDCl$_3$)
OMe
NH
HN
D
N H O
Boc
3h
NOTE: Signal broadening and / or multiple set of signals seen are due to rotamer formation at the N-terminus (*N-^{t}BOC Pro effect*: *Chem. Eur. J.* **2008**, 14, 6192).
160
140
120
100
80
60
40
20

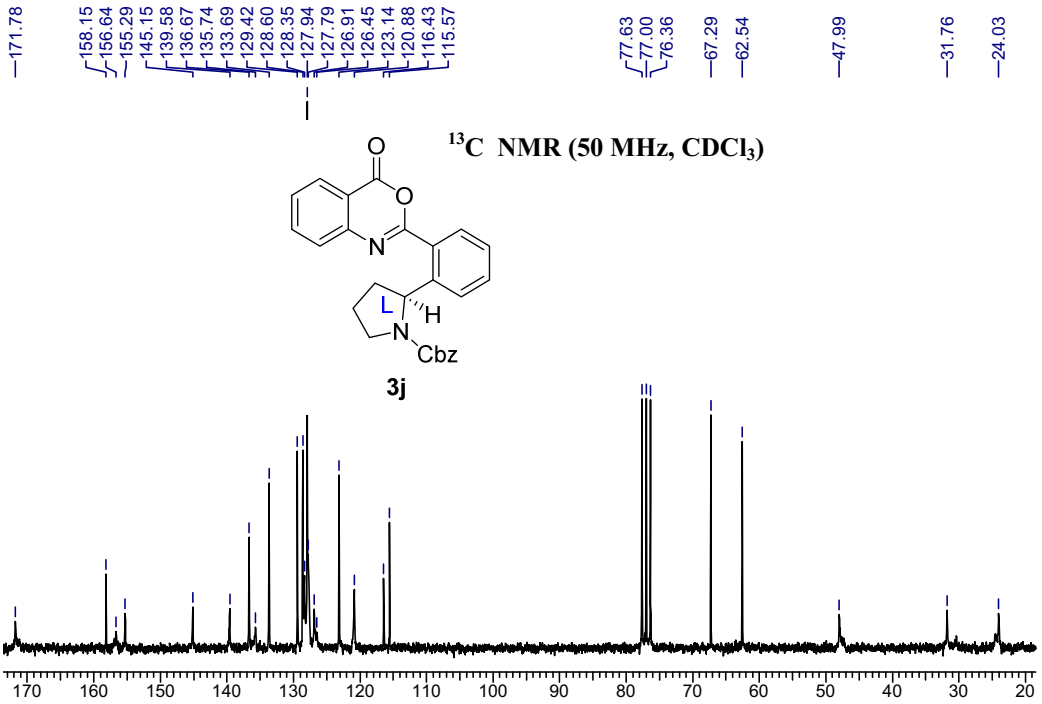

^{13}C NMR (50 MHz, CDCl$_3$)

3j

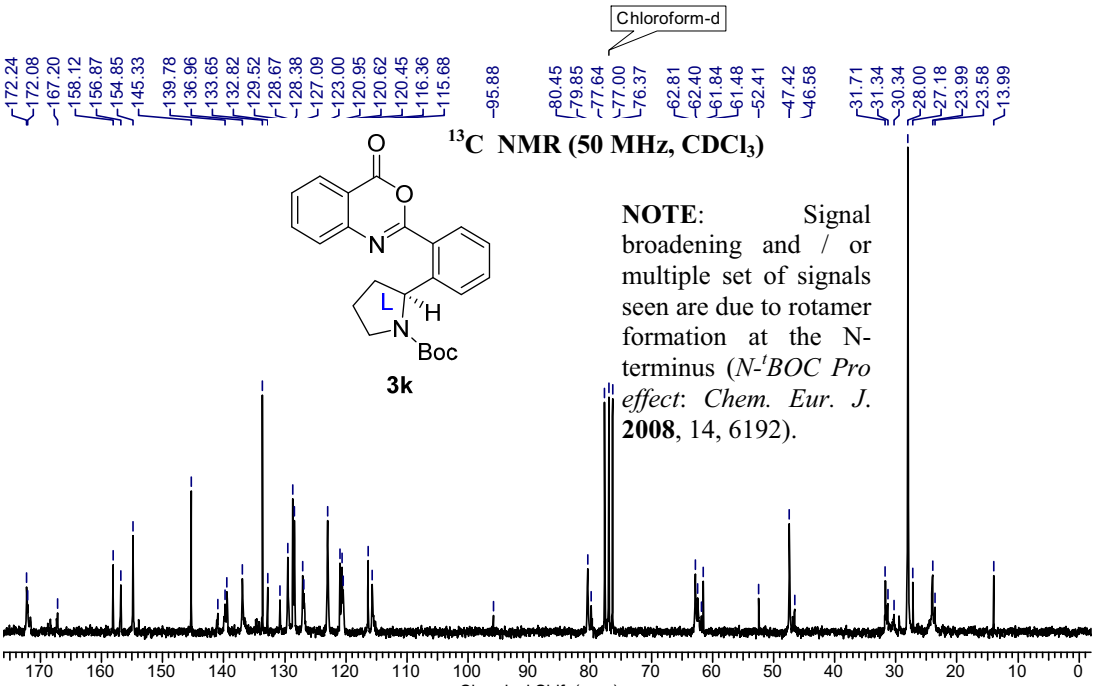

^{13}C NMR (50 MHz, CDCl$_3$)

3k

NOTE: Signal broadening and / or multiple set of signals seen are due to rotamer formation at the N-terminus (*N-^{t}BOC Pro effect*: *Chem. Eur. J.* **2008**, 14, 6192).

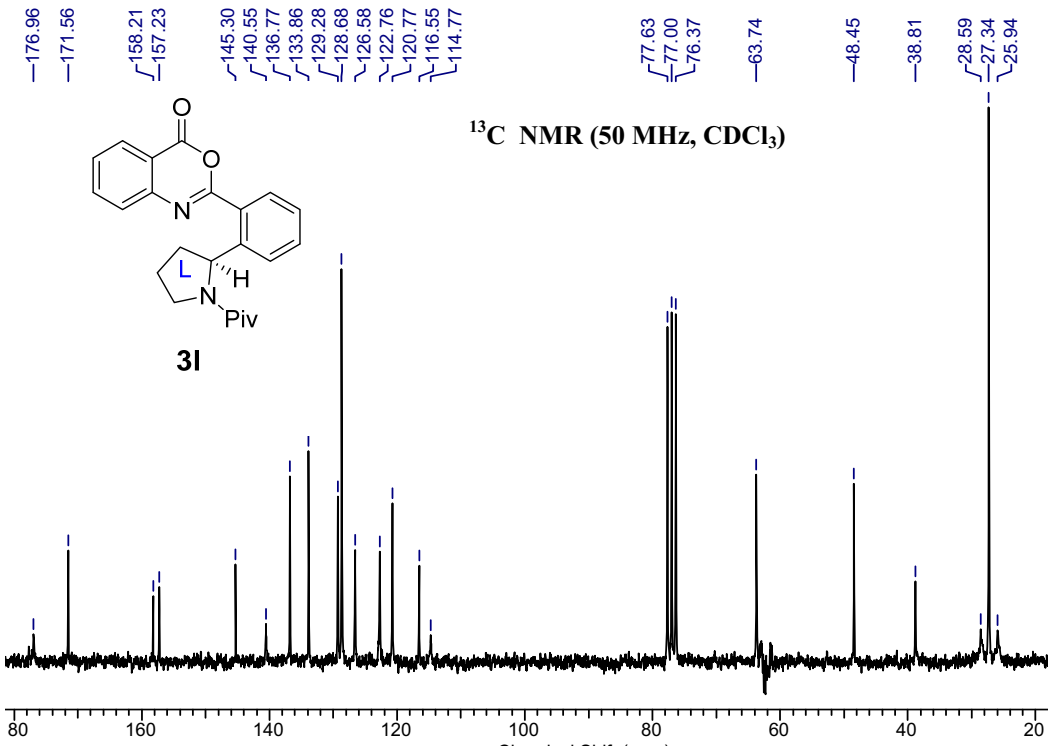

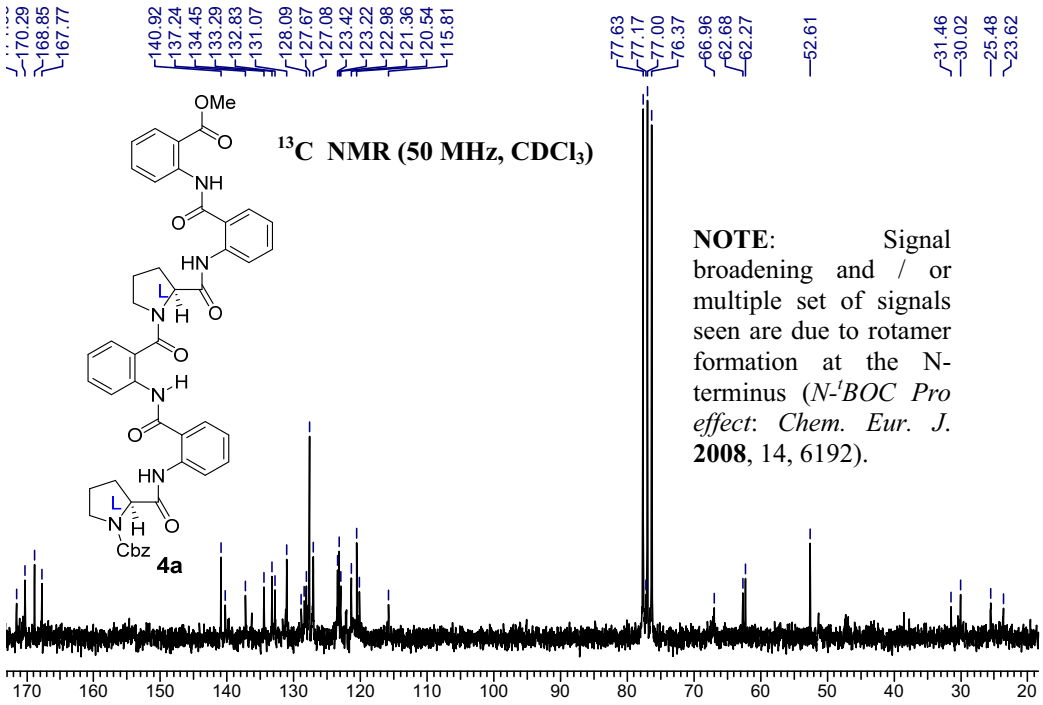

NOTE: Signal broadening and / or multiple set of signals seen are due to rotamer formation at the N-terminus (*N-^{t}BOC Pro effect*: *Chem. Eur. J.* **2008**, 14, 6192).

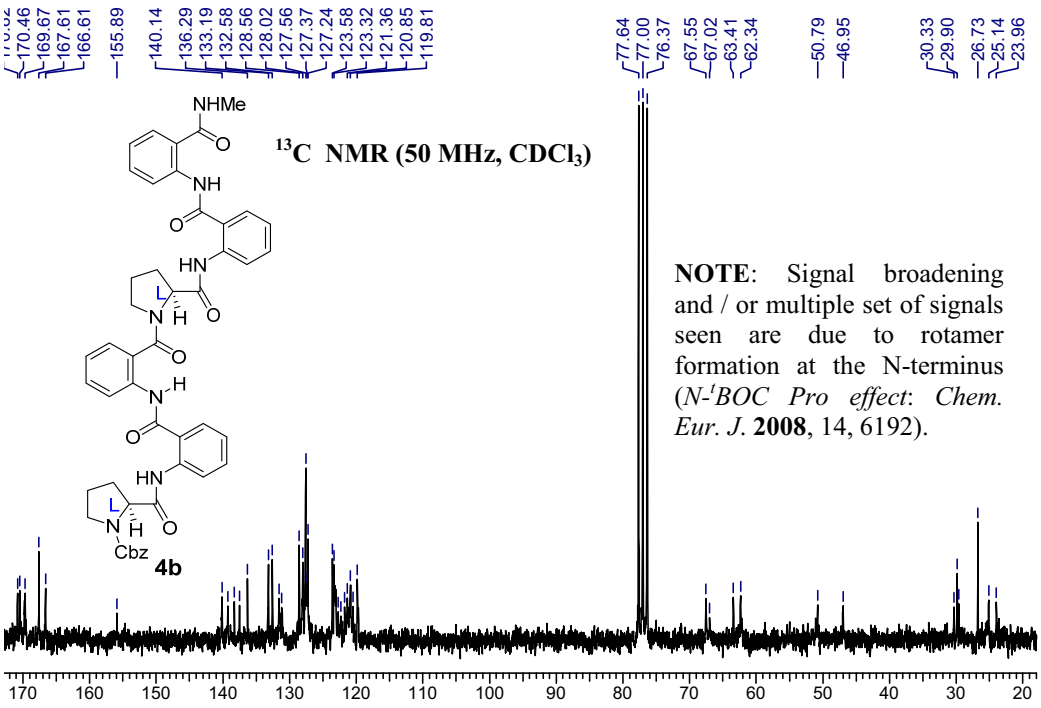

NOTE: Signal broadening and / or multiple set of signals seen are due to rotamer formation at the N-terminus (*N-^{t}BOC Pro effect*: *Chem. Eur. J.* **2008**, 14, 6192).

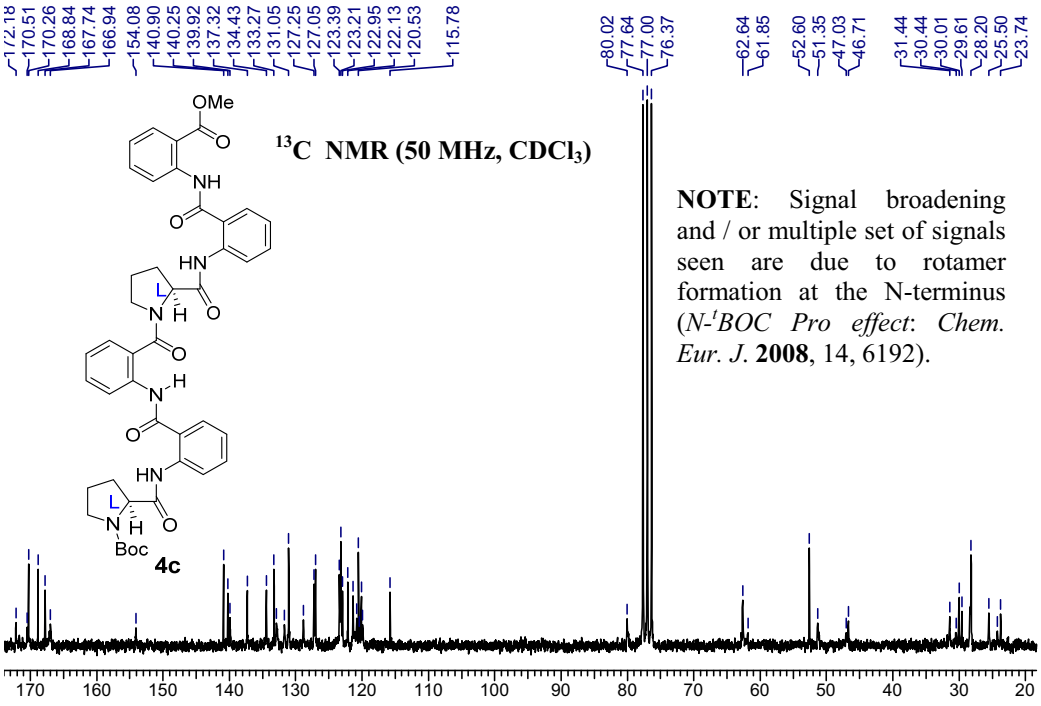

NOTE: Signal broadening and / or multiple set of signals seen are due to rotamer formation at the N-terminus (*N-^{t}BOC Pro effect*: *Chem. Eur. J.* **2008**, 14, 6192).

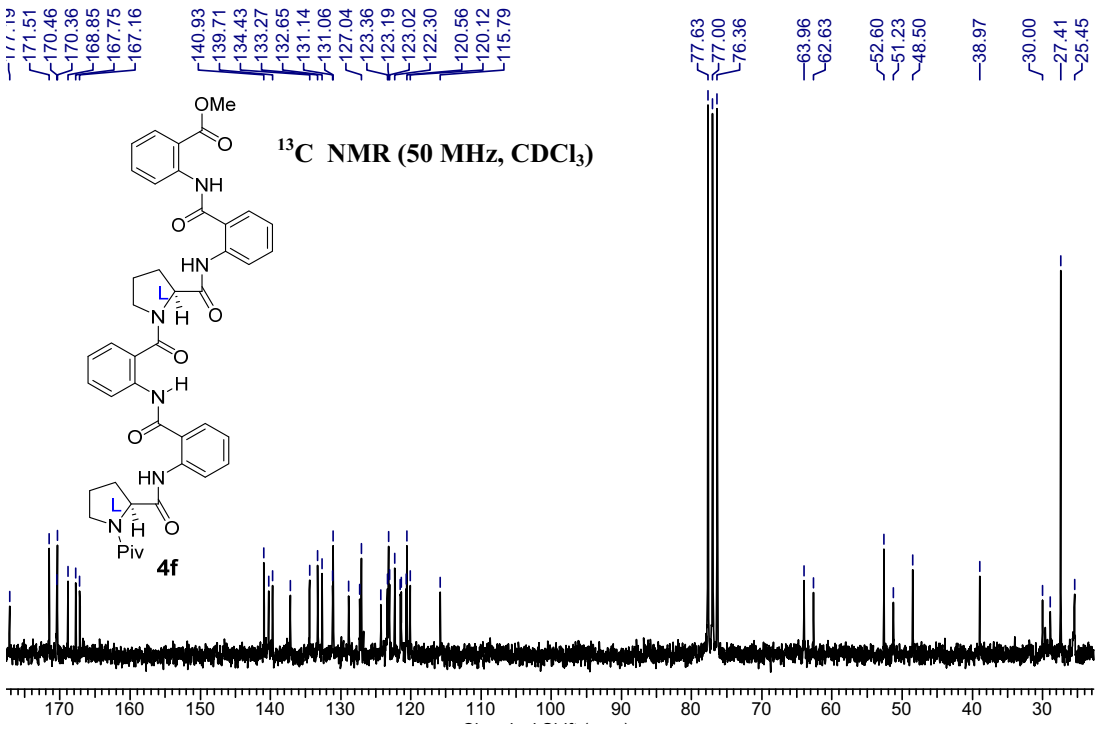
171.51
170.46
170.36
168.85
167.75
167.16
140.93
139.71
134.43
133.27
132.65
131.14
131.06
127.04
123.36
123.19
123.02
122.30
120.56
120.12
115.79
77.63
77.00
76.36
63.96
62.63
52.60
51.23
48.50
38.97
30.00
27.41
25.45
OMe
NH
HN
Piv
4f
^{13}C NMR (50 MHz, CDCl$_3$)
170
160
150
140
130
120
110
100
90
80
70
60
50
40
30

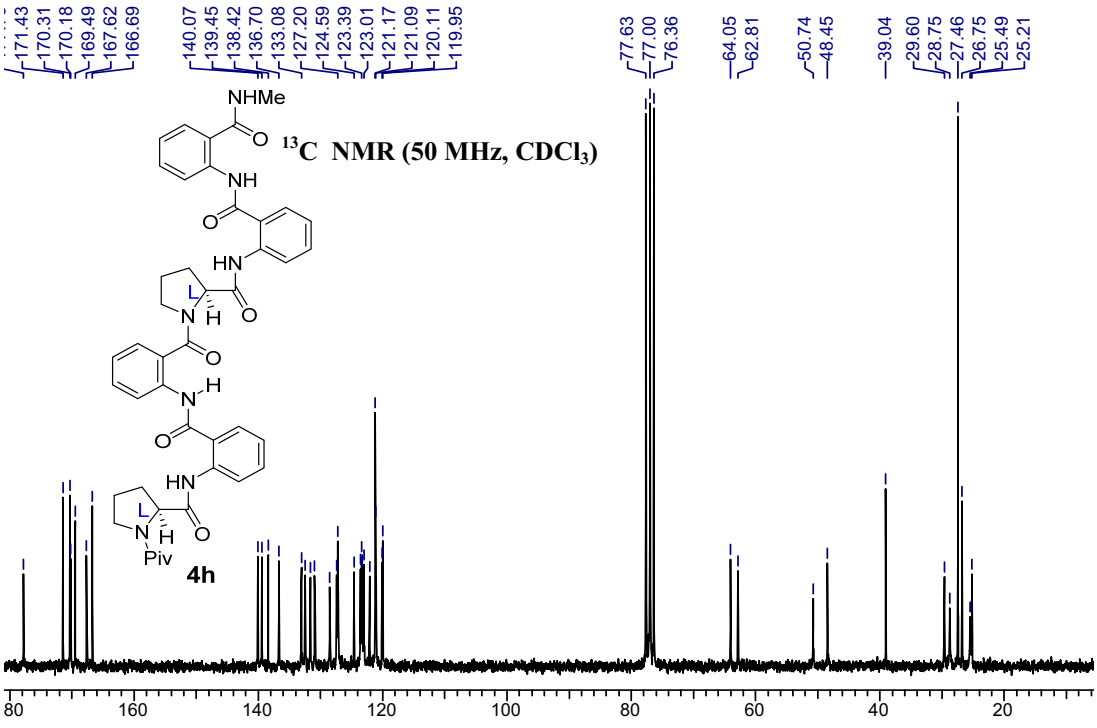
171.43
170.31
170.18
169.49
167.62
166.69
140.07
139.45
138.42
136.70
133.08
127.20
124.59
123.39
123.01
121.17
121.09
120.11
119.95
77.63
77.00
76.36
64.05
62.81
50.74
48.45
39.04
29.60
28.75
27.46
26.75
25.49
25.21
NHMe
NH
HN
Piv
4h
^{13}C NMR (50 MHz, CDCl$_3$)
80
160
140
120
100
80
60
40
20

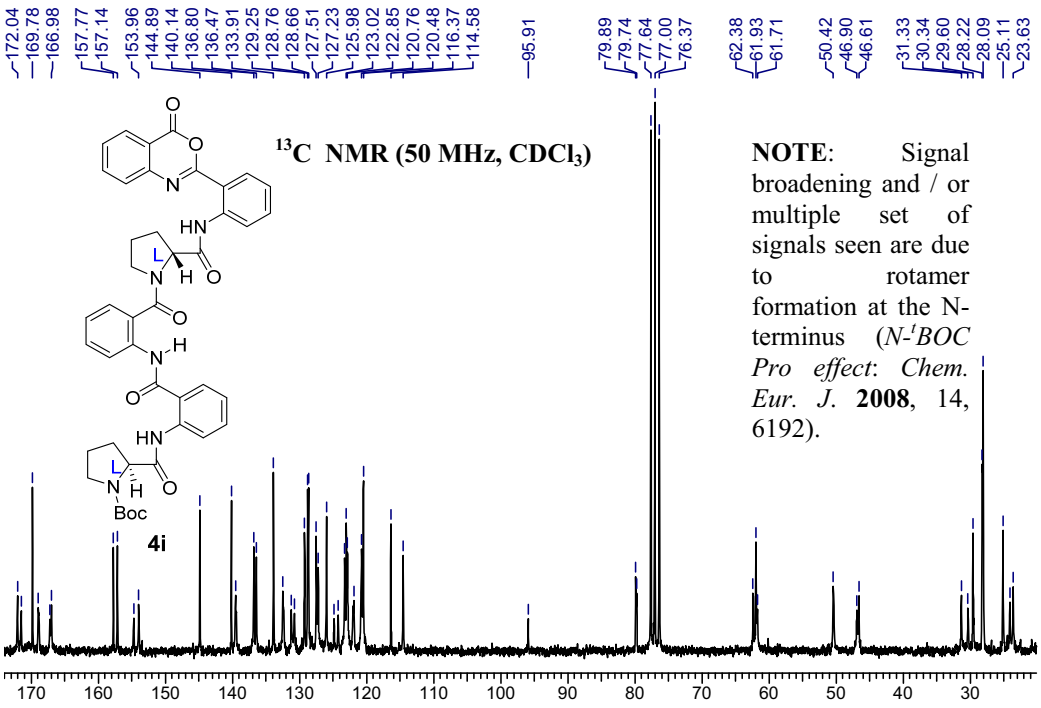

NOTE: Signal broadening and / or multiple set of signals seen are due to rotamer formation at the N-terminus (*N-^{t}BOC Pro effect*: *Chem. Eur. J.* **2008**, 14, 6192).

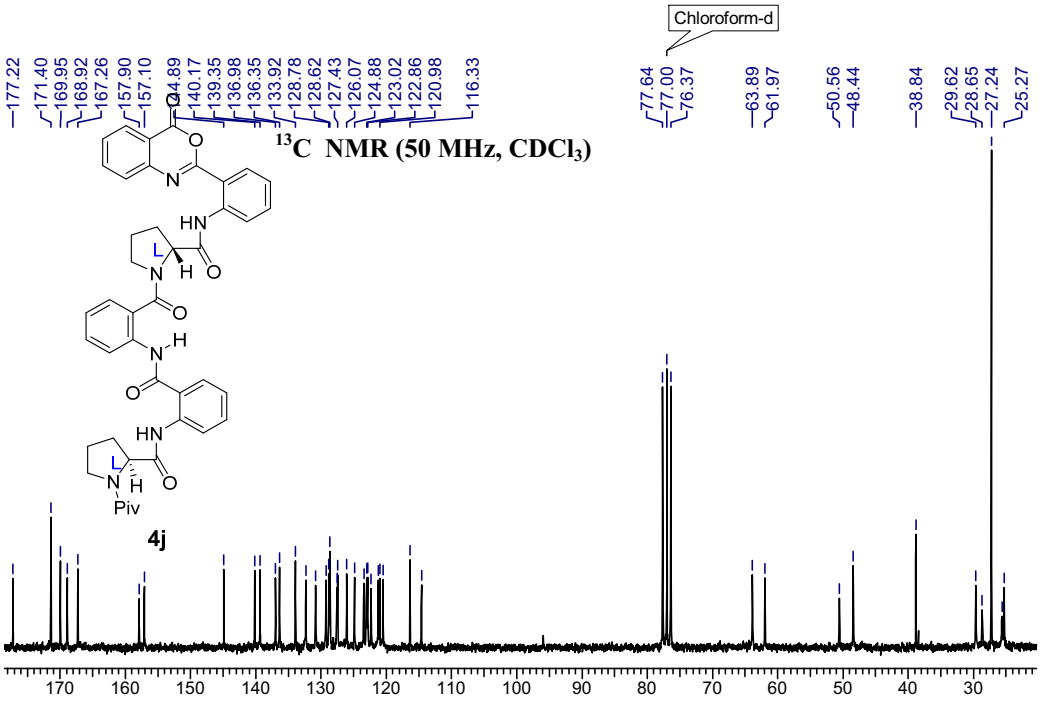

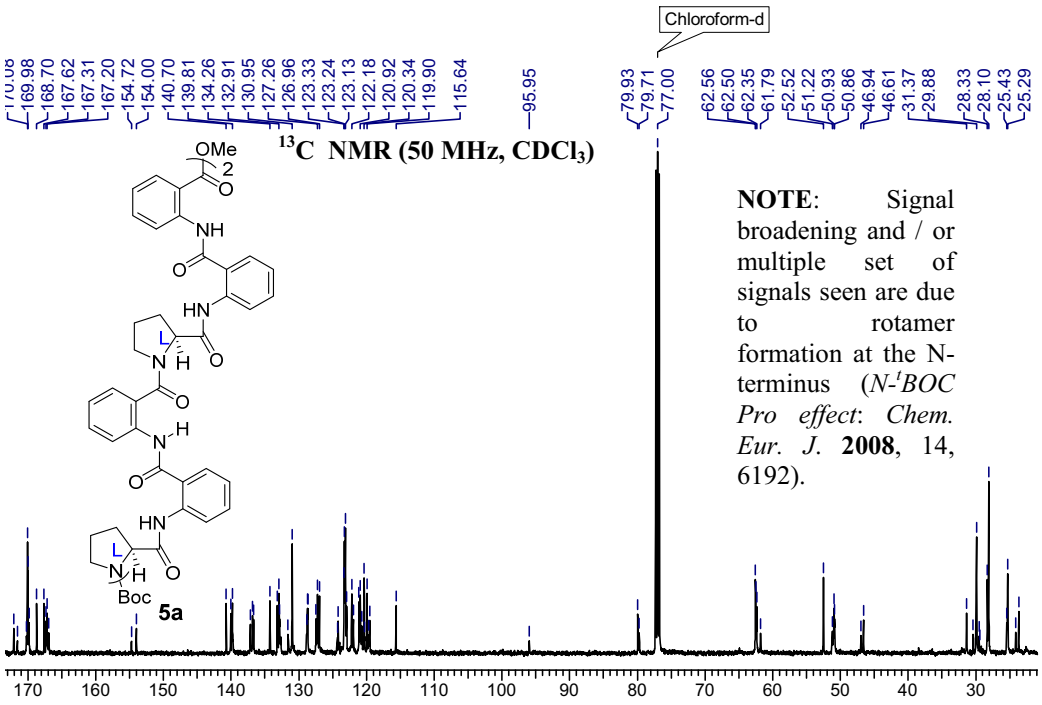

NOTE: Signal broadening and / or multiple set of signals seen are due to rotamer formation at the N-terminus (*N-^{t}BOC Pro effect*: *Chem. Eur. J.* **2008**, 14, 6192).

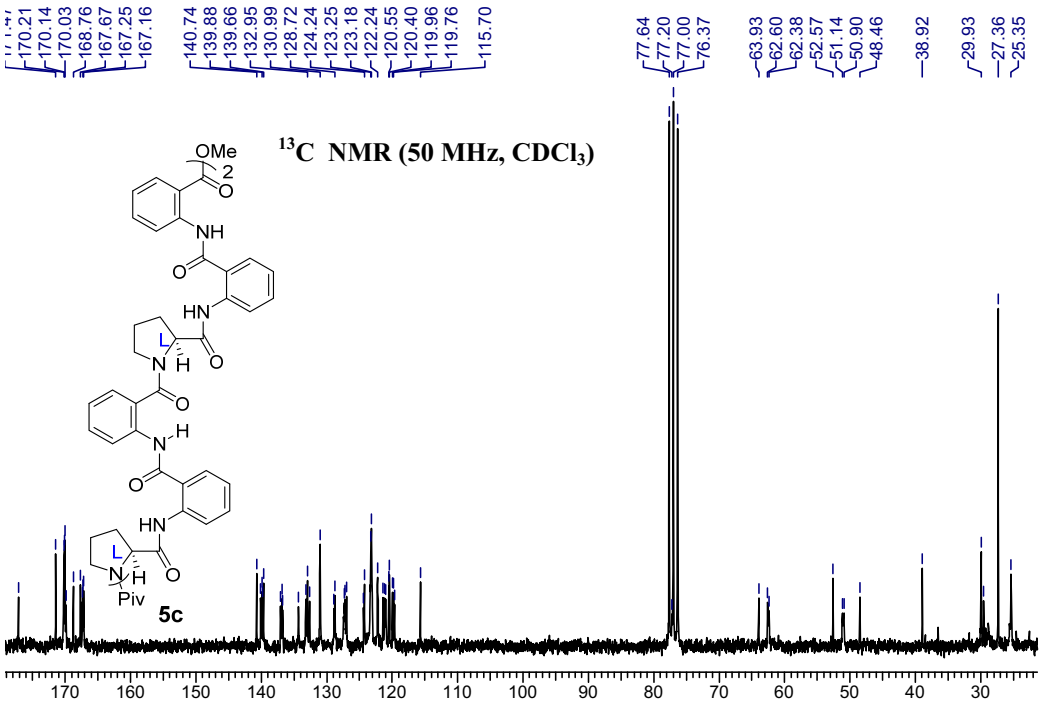

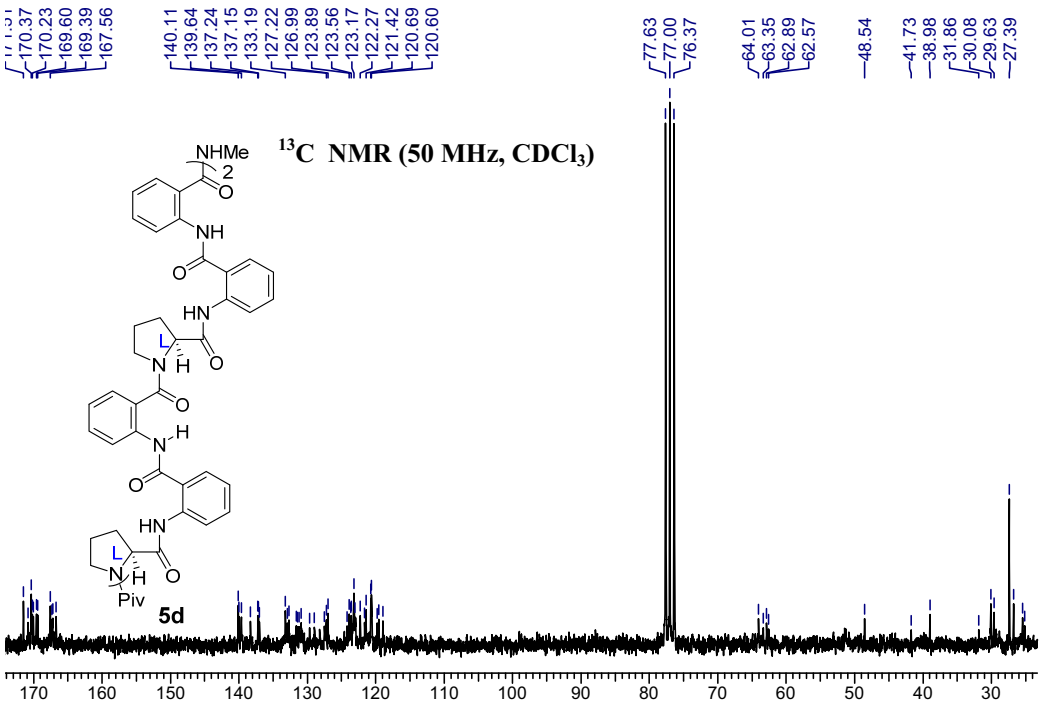

^{13}C NMR (50 MHz, $CDCl_3$)

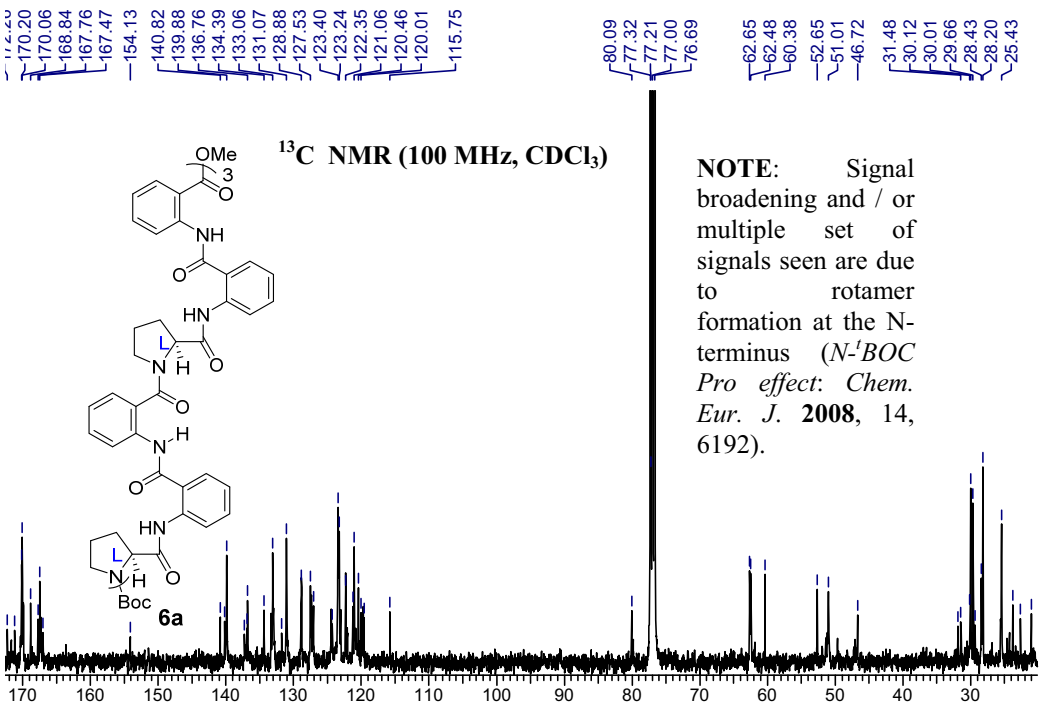

^{13}C NMR (100 MHz, $CDCl_3$)

NOTE: Signal broadening and / or multiple set of signals seen are due to rotamer formation at the N-terminus (*N-^{t}BOC Pro effect*: *Chem. Eur. J.* **2008**, 14, 6192).

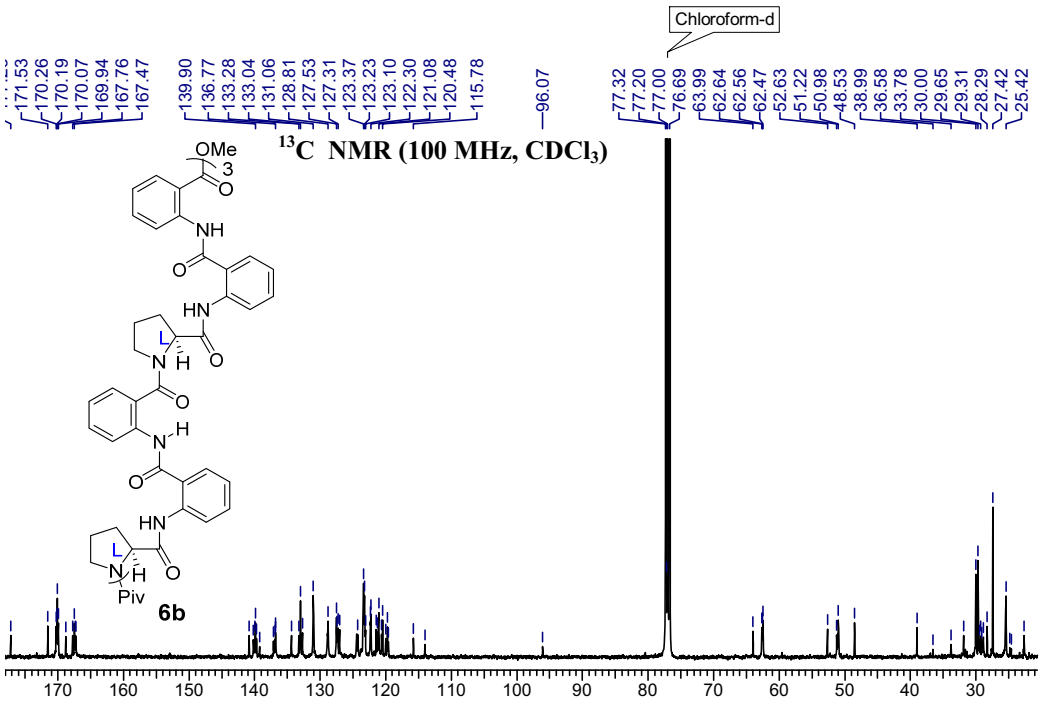
Chloroform-d
171.53
170.26
170.19
170.07
169.94
167.76
167.47
139.90
136.77
133.28
133.04
131.06
128.81
127.53
127.31
123.37
123.23
123.10
122.30
121.08
120.48
115.78
96.07
77.32
77.20
77.00
76.69
63.99
62.64
62.56
62.47
52.63
51.22
50.98
48.53
38.99
36.58
33.78
30.00
29.65
29.31
28.29
27.42
25.42
^{13}C NMR (100 MHz, CDCl$_3$)
OMe
NH
HN
Piv
6b
170
160
150
140
130
120
110
100
90
80
70
60
50
40
30

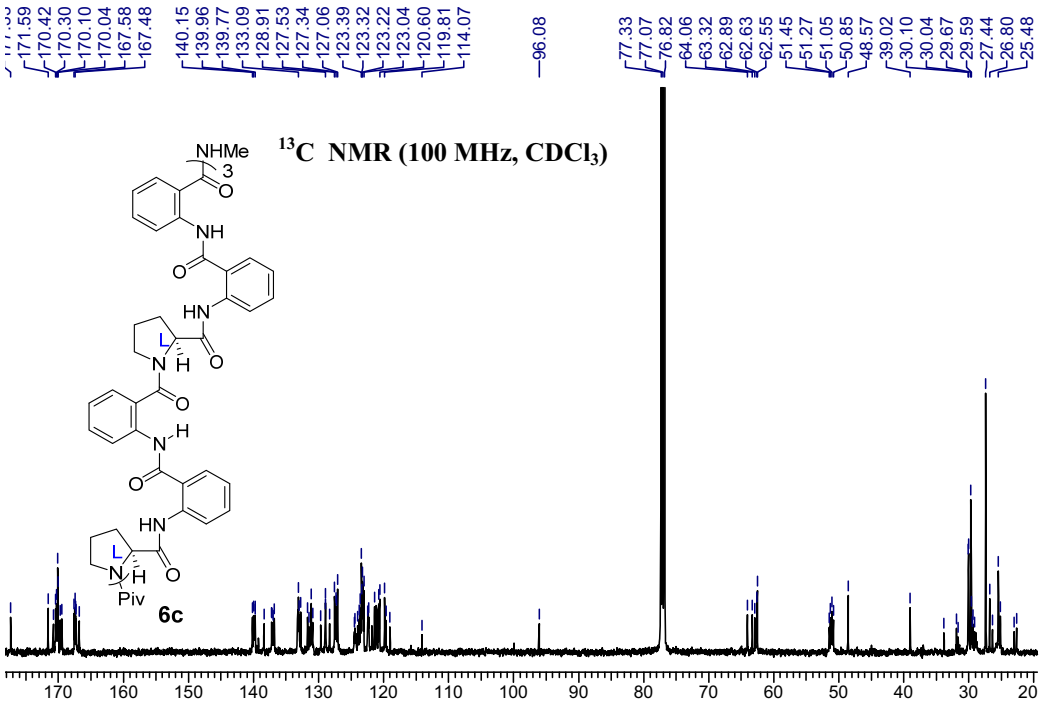
171.59
170.42
170.30
170.10
170.04
167.58
167.48
140.15
139.96
139.77
133.09
128.91
127.53
127.34
127.06
123.39
123.32
123.22
123.04
120.60
119.81
114.07
96.08
77.33
77.07
76.82
64.06
63.32
62.89
62.63
62.55
51.45
51.27
51.05
50.85
48.57
39.02
30.10
30.04
29.67
29.59
27.44
26.80
25.48
^{13}C NMR (100 MHz, CDCl$_3$)
NHMe
NH
HN
Piv
6c
170
160
150
140
130
120
110
100
90
80
70
60
50
40
30
20

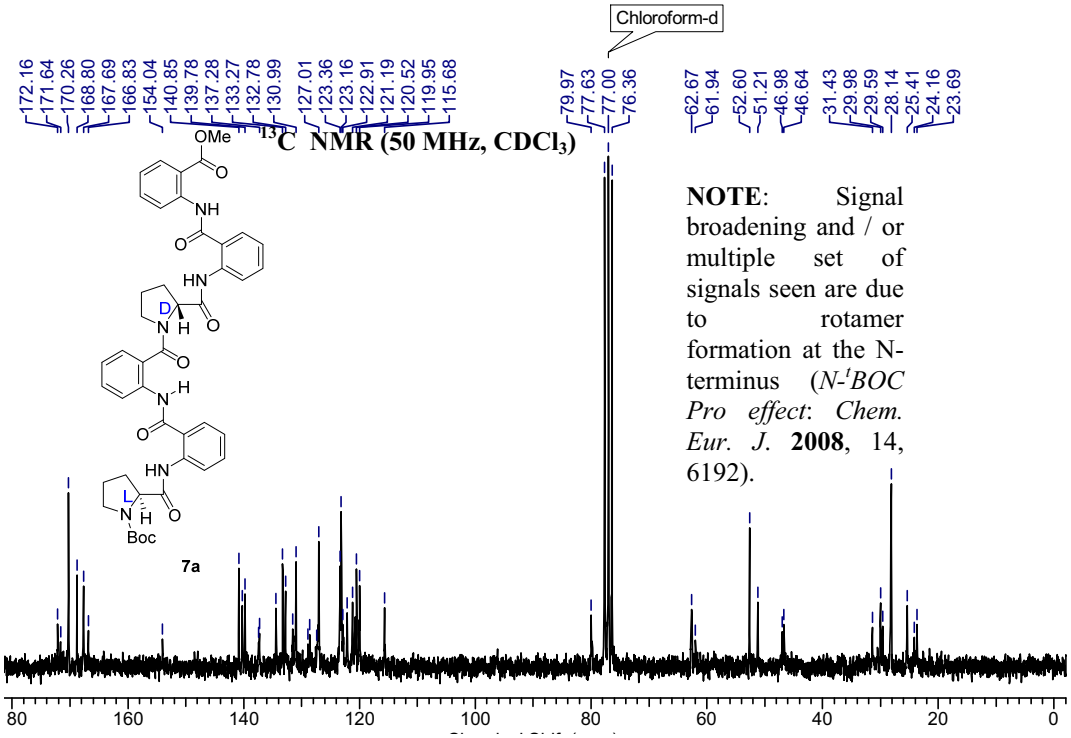

^{13}C NMR (50 MHz, CDCl$_3$)

NOTE: Signal broadening and / or multiple set of signals seen are due to rotamer formation at the N-terminus (*N-^{t}BOC Pro effect*: *Chem. Eur. J.* **2008**, 14, 6192).

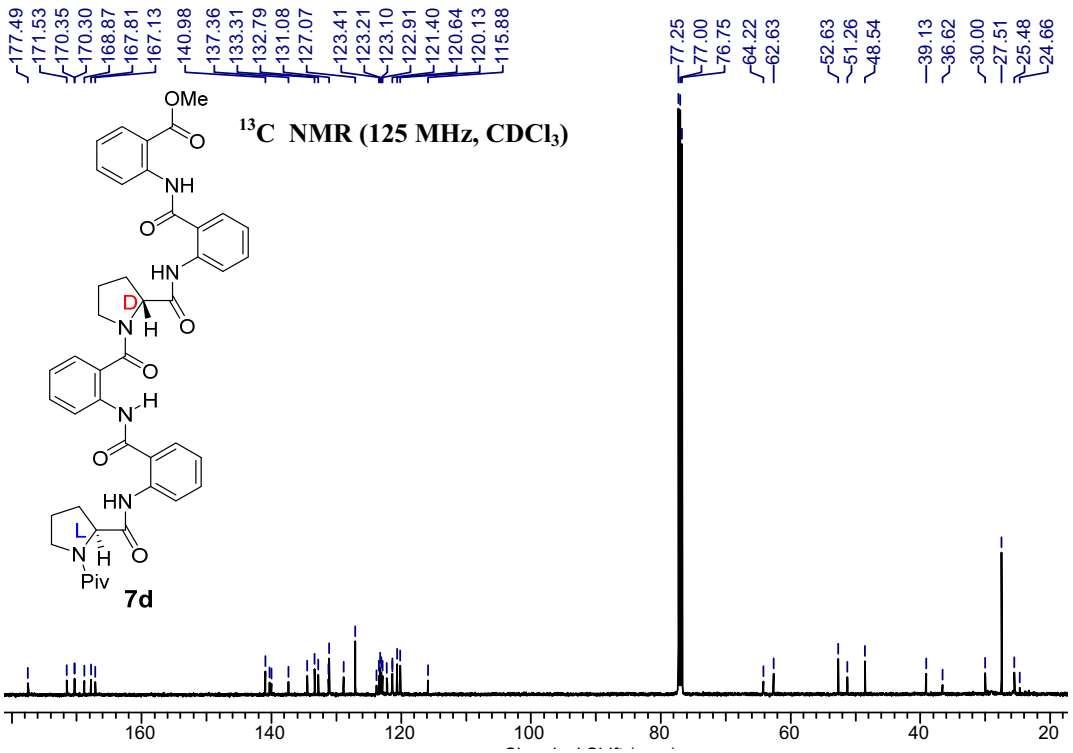

^{13}C NMR (125 MHz, CDCl$_3$)

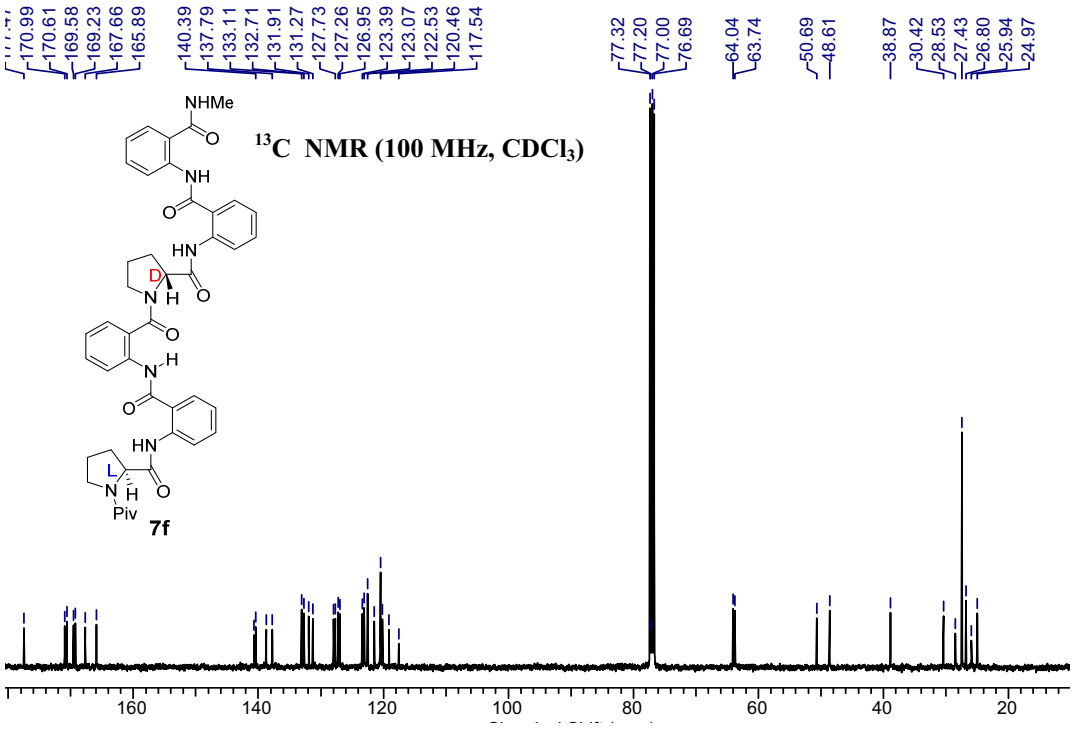
170.99
170.61
169.58
169.23
167.66
165.89
140.39
137.79
133.11
132.71
131.91
131.27
127.73
127.26
126.95
123.39
123.07
122.53
120.46
117.54
77.32
77.20
77.00
76.69
64.04
63.74
50.69
48.61
38.87
30.42
28.53
27.43
26.80
25.94
24.97
^{13}C NMR (100 MHz, CDCl$_3$)
7f
160
140
120
100
80
60
40
20

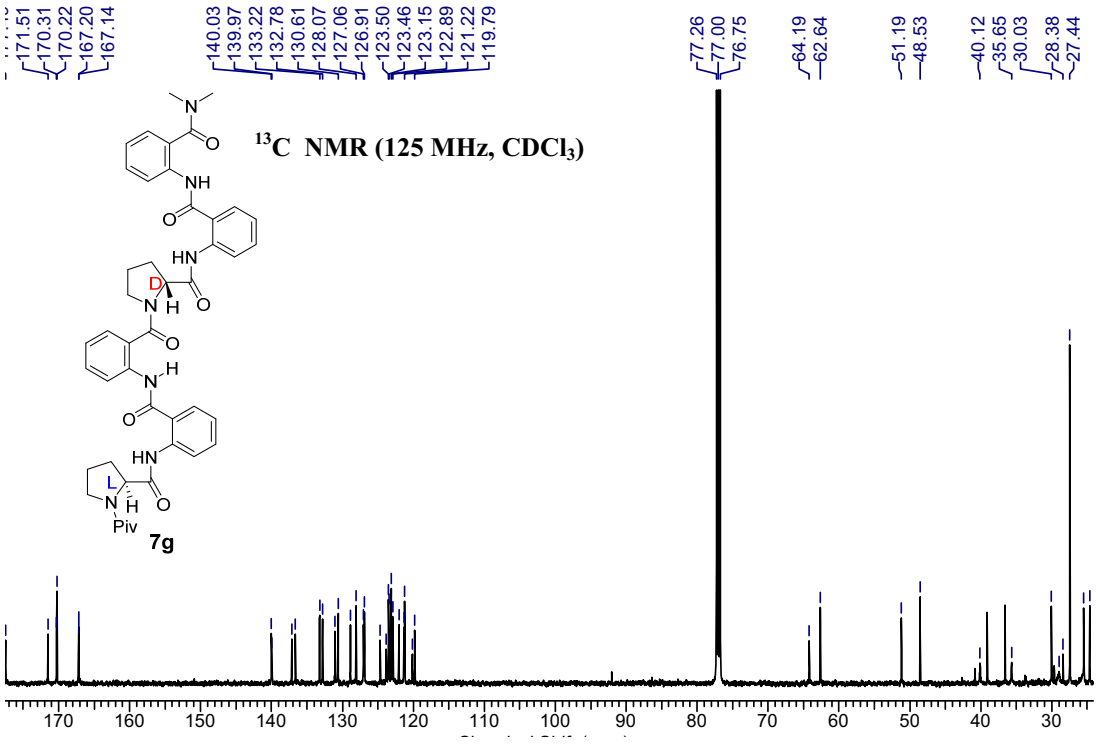
171.51
170.31
170.22
167.20
167.14
140.03
139.97
133.22
132.78
130.61
128.07
127.06
126.91
123.50
123.46
123.15
122.89
121.22
119.79
77.26
77.00
76.75
64.19
62.64
51.19
48.53
40.12
35.65
30.03
28.38
27.44
^{13}C NMR (125 MHz, CDCl$_3$)
7g
170
160
150
140
130
120
110
100
90
80
70
60
50
40
30

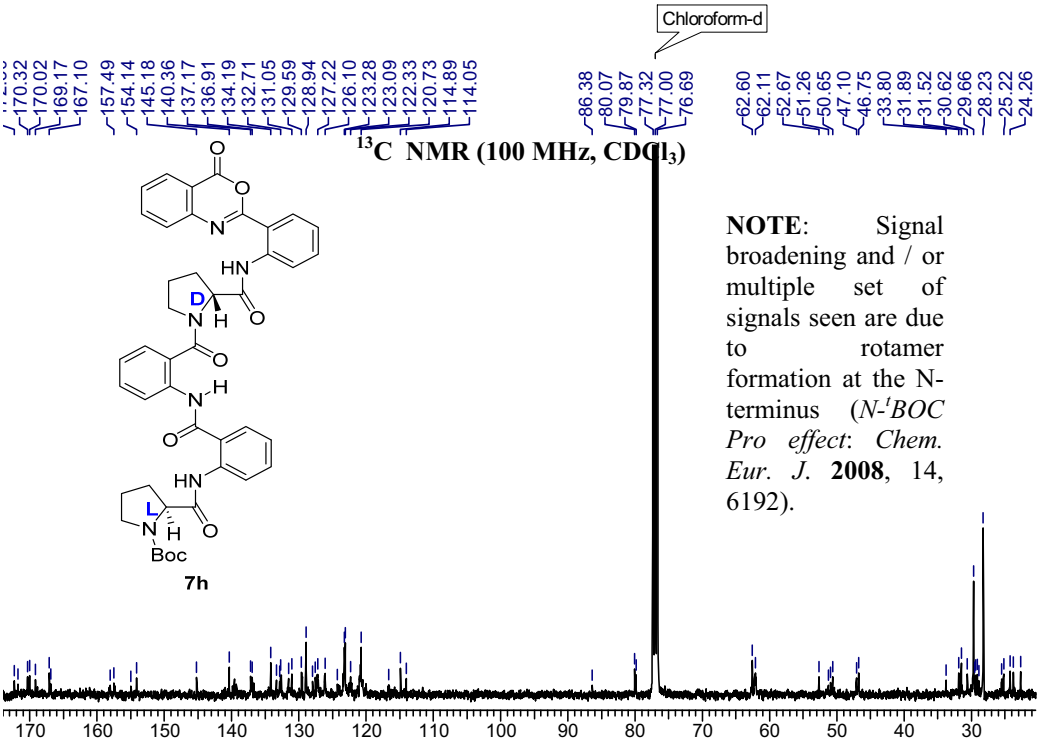

^{13}C NMR (100 MHz, CDCl$_3$)

7h

NOTE: Signal broadening and / or multiple set of signals seen are due to rotamer formation at the N-terminus (*N-^{t}BOC Pro effect*: *Chem. Eur. J.* **2008**, 14, 6192).

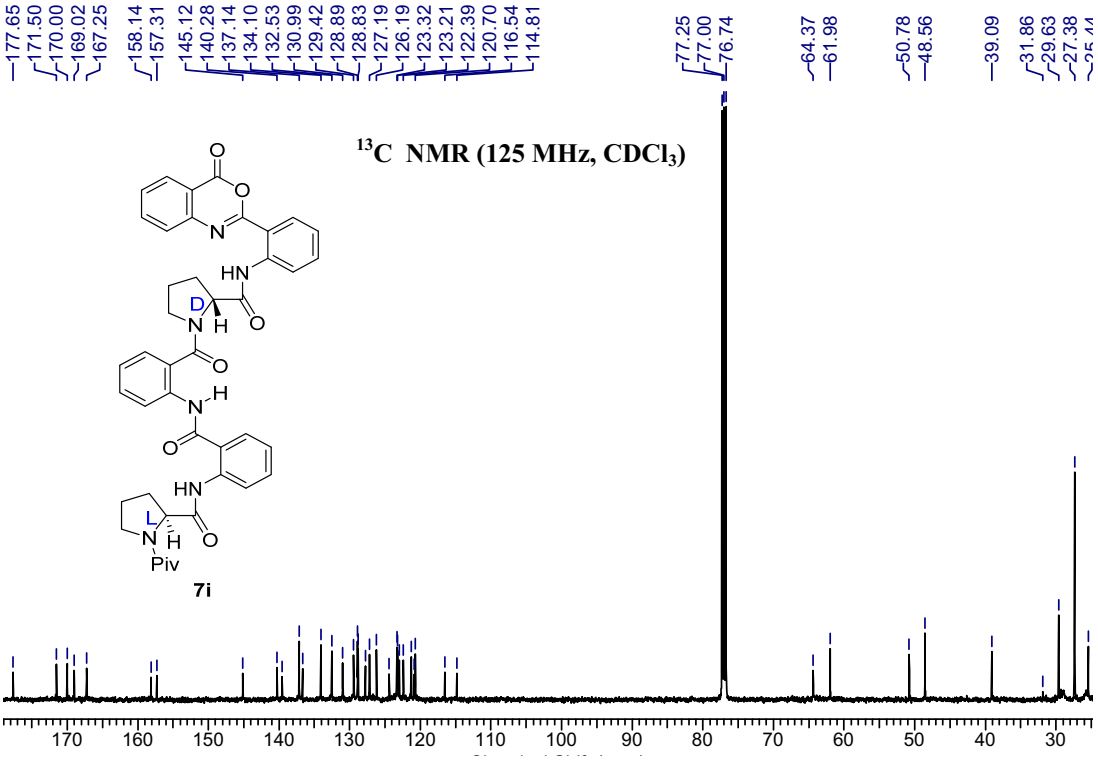

^{13}C NMR (125 MHz, CDCl$_3$)

7i

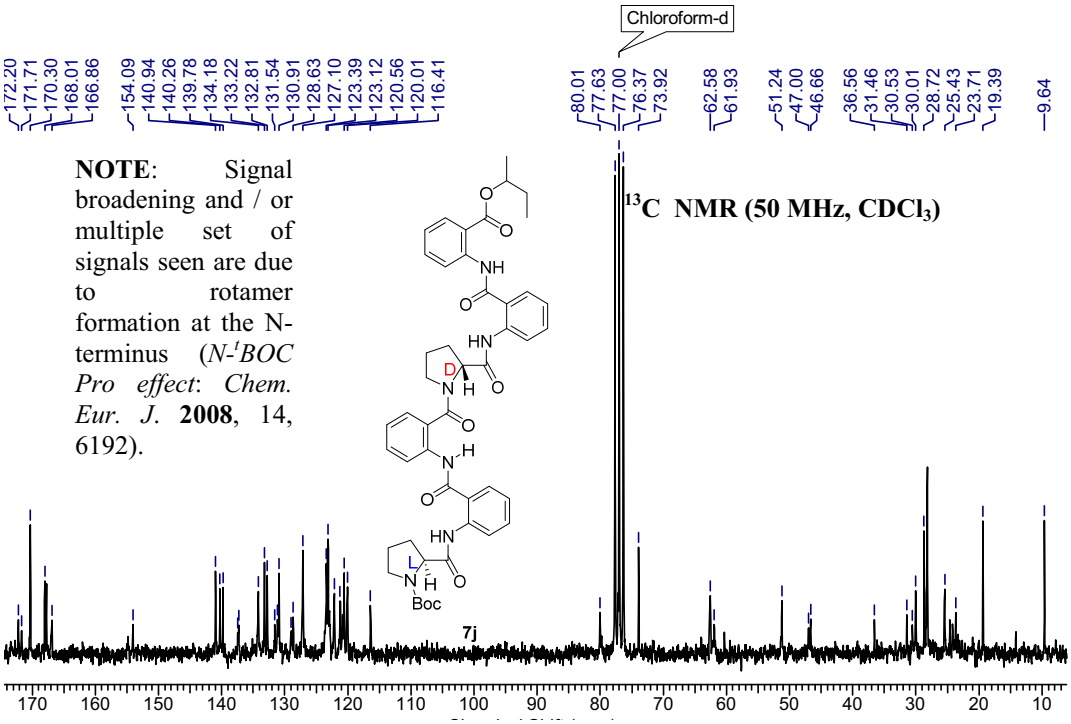
Chloroform-d
172.20
171.71
170.30
168.01
166.86
154.09
140.94
140.26
139.78
134.18
133.22
132.81
131.54
130.91
128.63
127.10
123.39
123.12
120.56
120.01
116.41
80.01
77.63
77.00
76.37
73.92
62.58
61.93
51.24
47.00
46.66
36.56
31.46
30.53
30.01
28.72
25.43
23.71
19.39
9.64
NOTE: Signal broadening and / or multiple set of signals seen are due to rotamer formation at the N-terminus (N-tBOC Pro effect: Chem. Eur. J. 2008, 14, 6192).
13C NMR (50 MHz, CDCl3)
7j
170
160
150
140
130
120
110
100
90
80
70
60
50
40
30
20
10

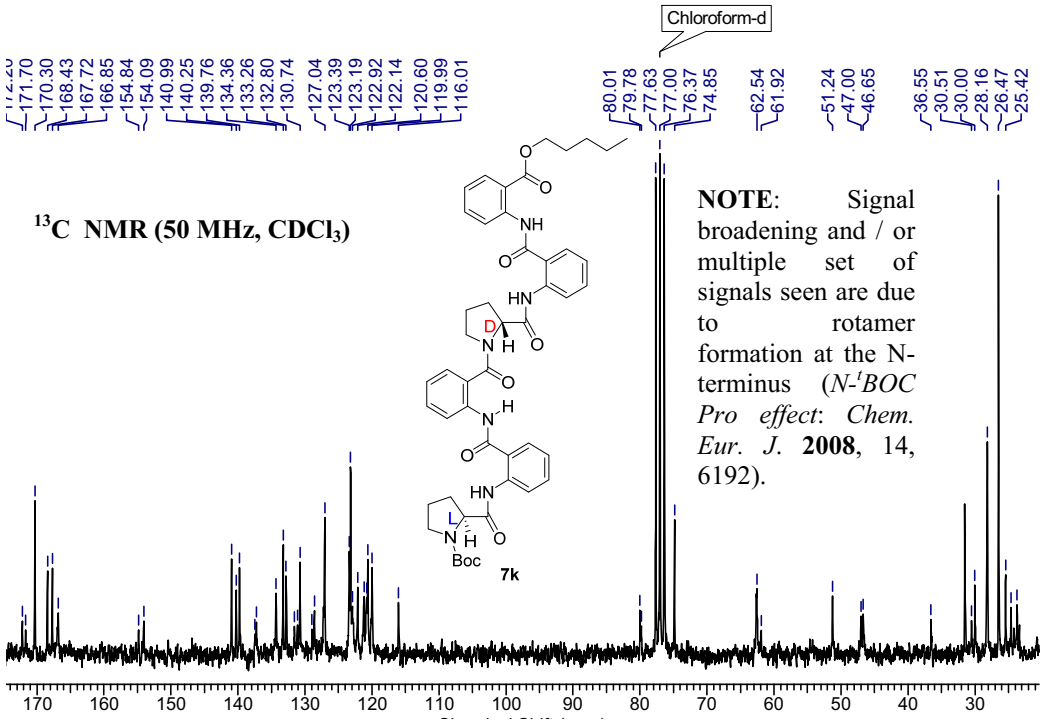
Chloroform-d
171.70
170.30
168.43
167.72
166.85
154.84
154.09
140.99
140.25
139.76
134.36
133.26
132.80
130.74
127.04
123.39
123.19
122.92
122.14
120.60
119.99
116.01
80.01
79.78
77.63
77.00
76.37
74.85
62.54
61.92
51.24
47.00
46.65
36.55
30.51
30.00
28.16
26.47
25.42
13C NMR (50 MHz, CDCl3)
NOTE: Signal broadening and / or multiple set of signals seen are due to rotamer formation at the N-terminus (N-tBOC Pro effect: Chem. Eur. J. 2008, 14, 6192).
7k
170
160
150
140
130
120
110
100
90
80
70
60
50
40
30

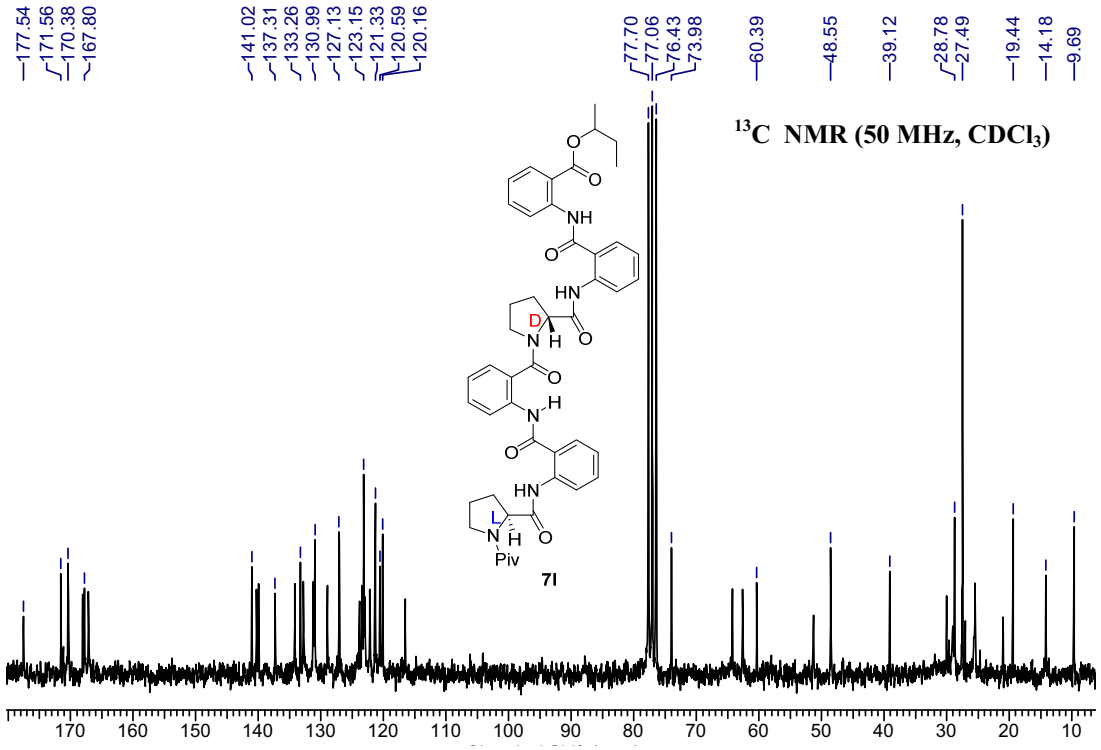
177.54
171.56
170.38
167.80
141.02
137.31
133.26
130.99
127.13
123.15
121.33
120.59
120.16
77.70
77.06
76.43
73.98
60.39
48.55
39.12
28.78
27.49
19.44
14.18
9.69
13C NMR (50 MHz, CDCl3)
Piv
7l

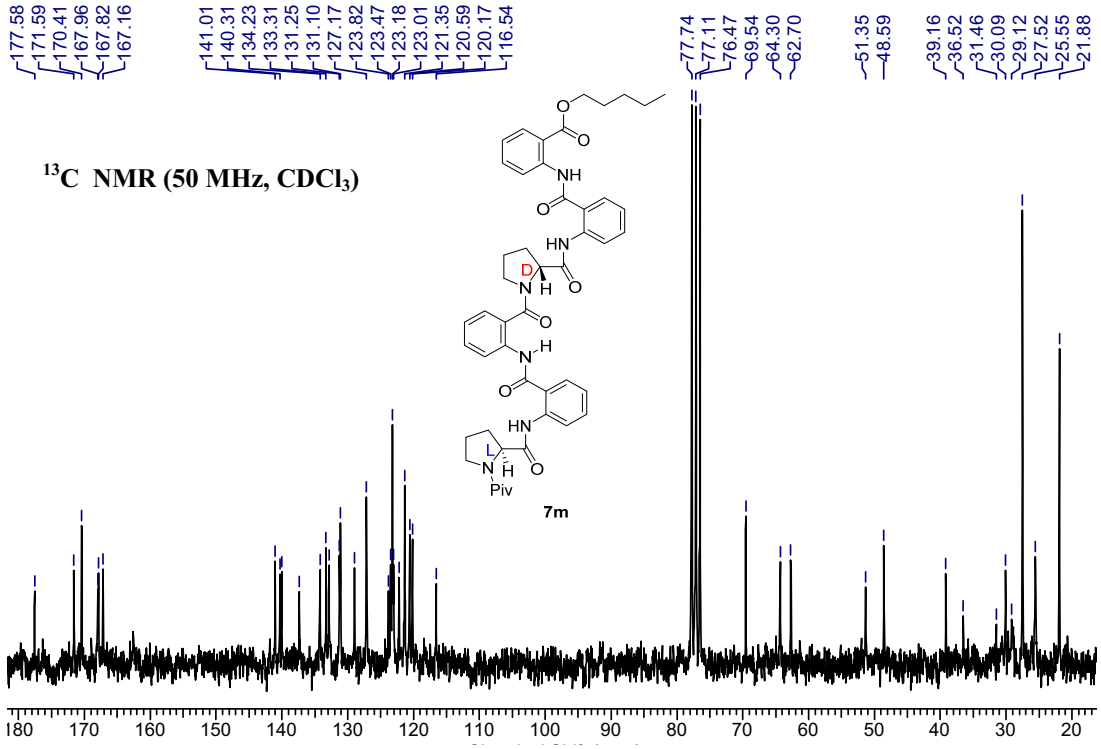
177.58
171.59
170.41
167.96
167.82
167.16
141.01
140.31
134.23
133.31
131.25
131.10
127.17
123.82
123.47
123.18
123.01
121.35
120.59
120.17
116.54
77.74
77.11
76.47
69.54
64.30
62.70
51.35
48.59
39.16
36.52
31.46
30.09
29.12
27.52
25.55
21.88
13C NMR (50 MHz, CDCl3)
Piv
7m

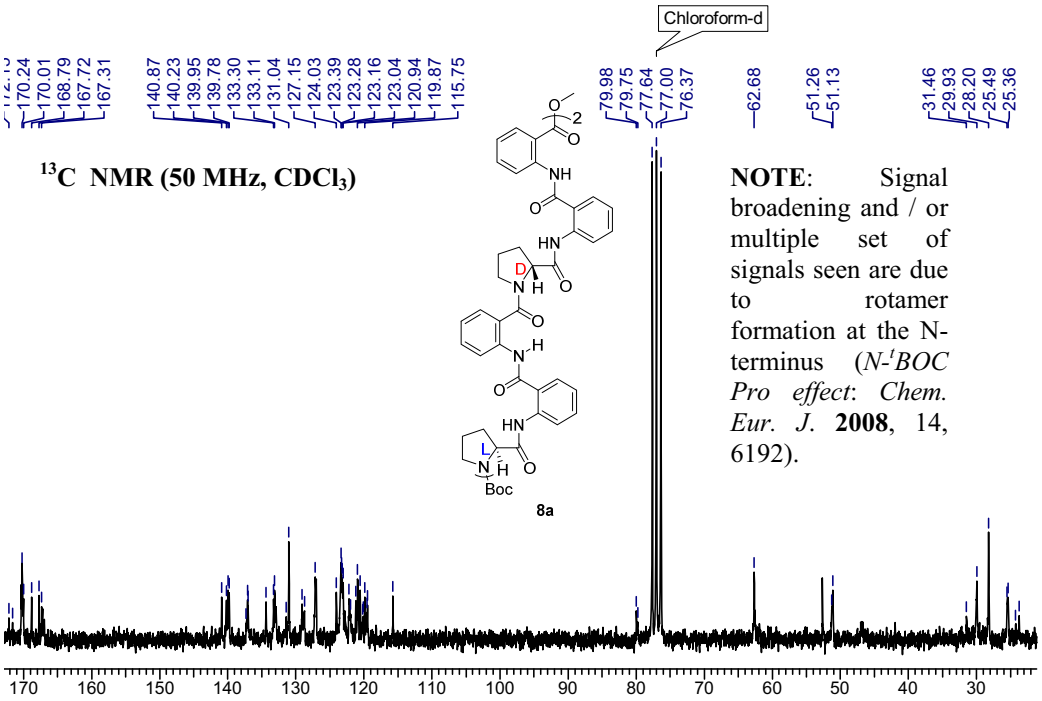

^{13}C NMR (50 MHz, $CDCl_3$)

8a

NOTE: Signal broadening and / or multiple set of signals seen are due to rotamer formation at the N-terminus (*N-^{t}BOC Pro effect*: *Chem. Eur. J.* **2008**, 14, 6192).

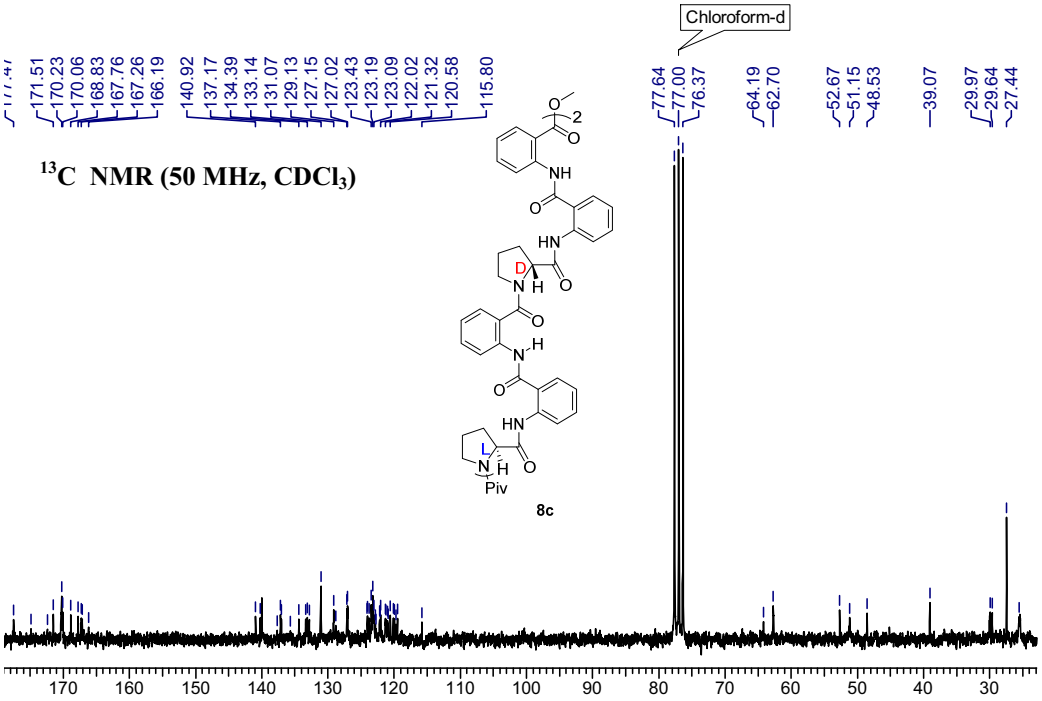

^{13}C NMR (50 MHz, $CDCl_3$)

8c

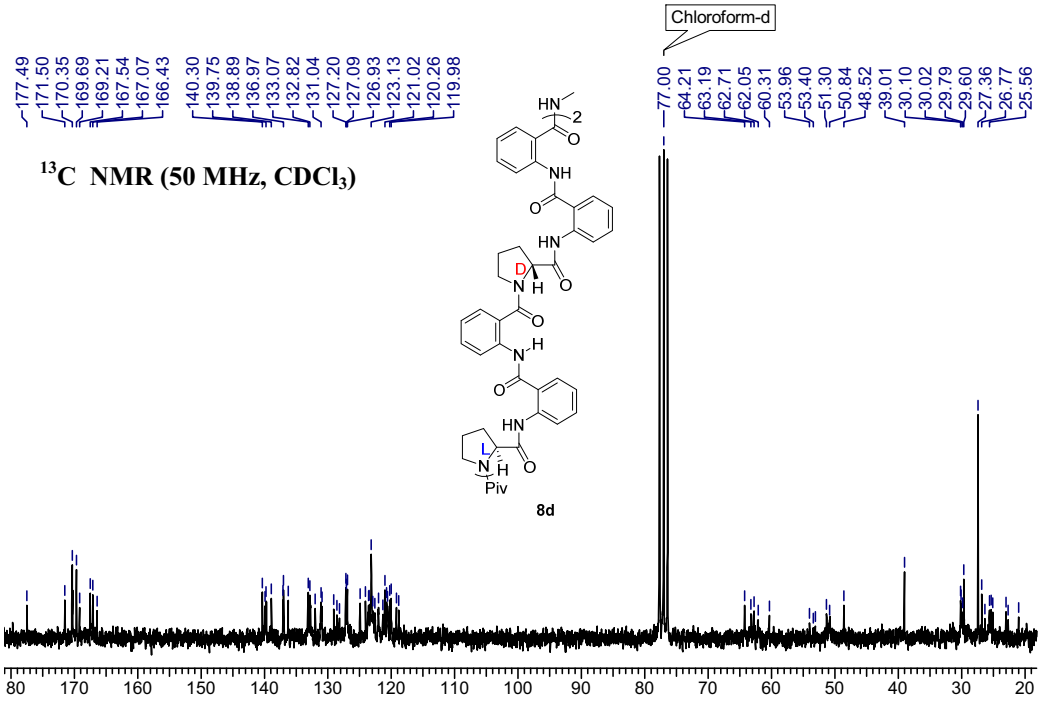
Chloroform-d
177.49
171.50
170.35
169.69
169.21
167.54
167.07
166.43
140.30
139.75
138.89
136.97
133.07
132.82
131.04
127.20
127.09
126.93
123.13
121.02
120.26
119.98
77.00
64.21
63.19
62.71
62.05
60.31
53.96
53.40
51.30
50.84
48.52
39.01
30.10
30.02
29.79
29.60
27.36
26.77
25.56
^{13}C NMR (50 MHz, CDCl$_3$)
8d
80 170 160 150 140 130 120 110 100 90 80 70 60 50 40 30 20

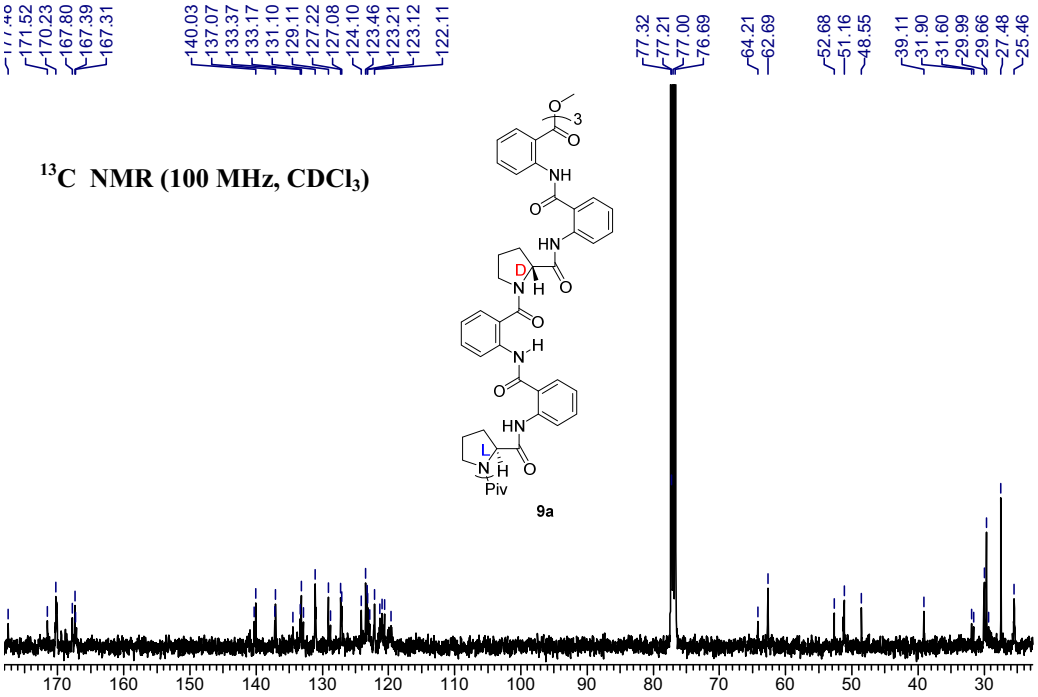
171.52
170.23
167.80
167.39
167.31
140.03
137.07
133.37
133.17
131.10
129.11
127.22
127.08
124.10
123.46
123.21
123.12
122.11
77.32
77.21
77.00
76.69
64.21
62.69
52.68
51.16
48.55
39.11
31.90
31.60
29.99
29.66
27.48
25.46
^{13}C NMR (100 MHz, CDCl$_3$)
9a
170 160 150 140 130 120 110 100 90 80 70 60 50 40 30

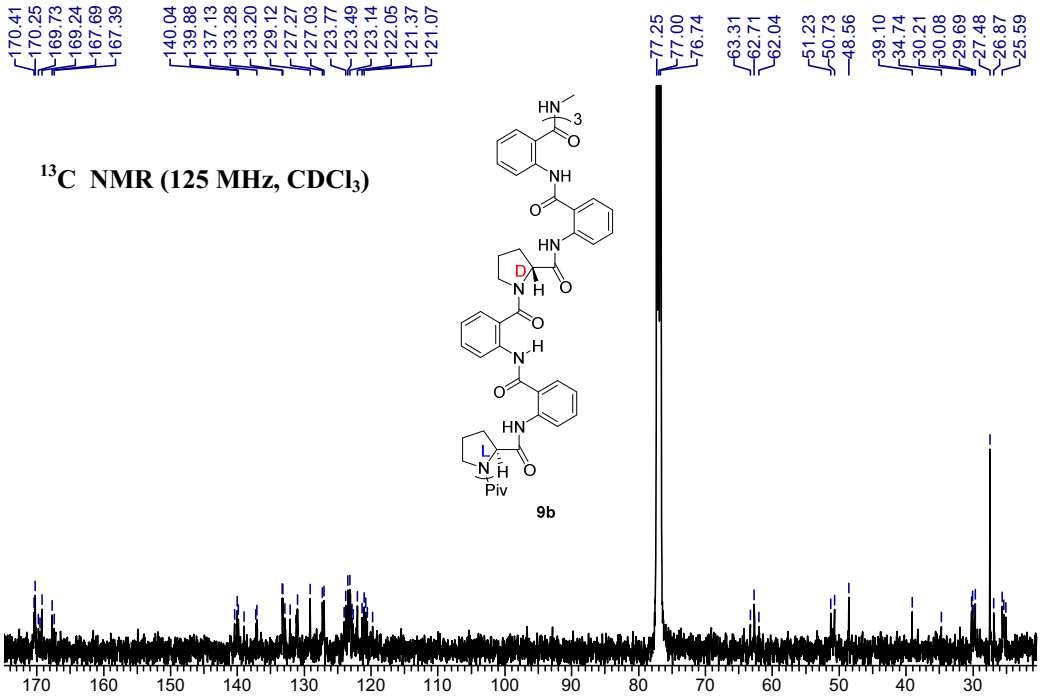
170.41
170.25
169.73
169.24
167.69
167.39
140.04
139.88
137.13
133.28
133.20
129.12
127.27
127.03
123.77
123.49
123.14
122.05
121.37
121.07
77.25
77.00
76.74
63.31
62.71
62.04
51.23
50.73
48.56
39.10
34.74
30.21
30.08
29.69
27.48
26.87
25.59
^{13}C NMR (125 MHz, CDCl$_3$)
9b
170
160
150
140
130
120
110
100
90
80
70
60
50
40
30

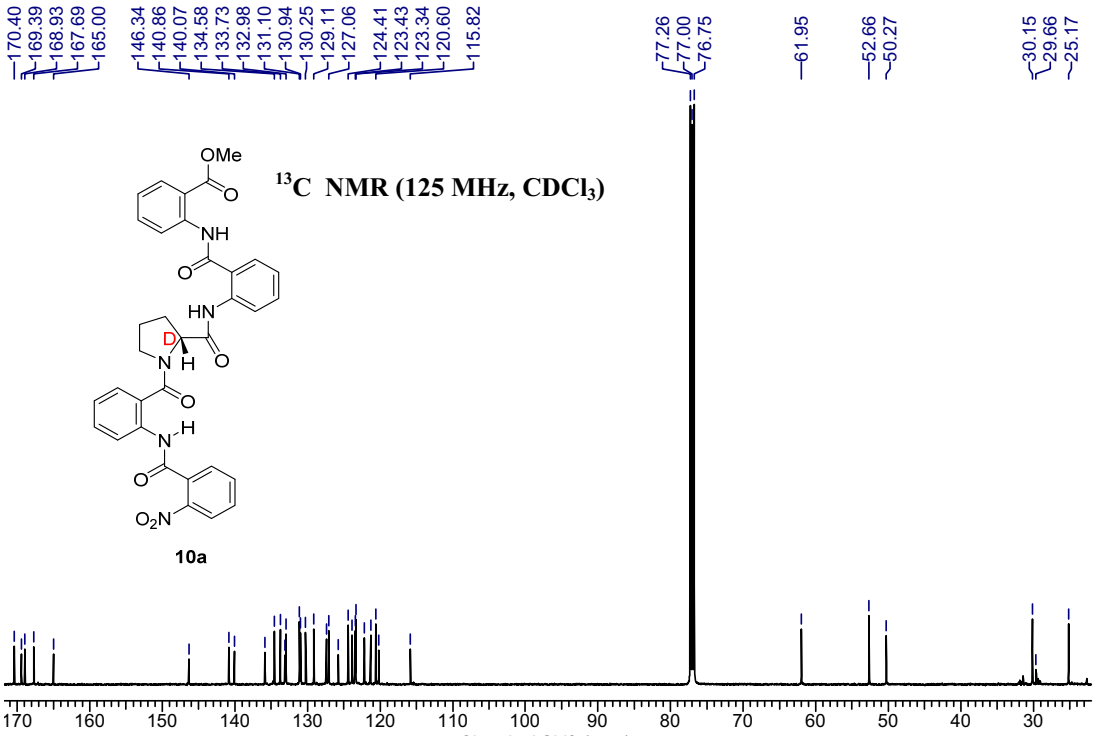
170.40
169.39
168.93
167.69
165.00
146.34
140.86
140.07
134.58
133.73
132.98
131.10
130.94
130.25
129.11
127.06
124.41
123.43
123.34
120.60
115.82
77.26
77.00
76.75
61.95
52.66
50.27
30.15
29.66
25.17
^{13}C NMR (125 MHz, CDCl$_3$)
10a
170
160
150
140
130
120
110
100
90
80
70
60
50
40
30

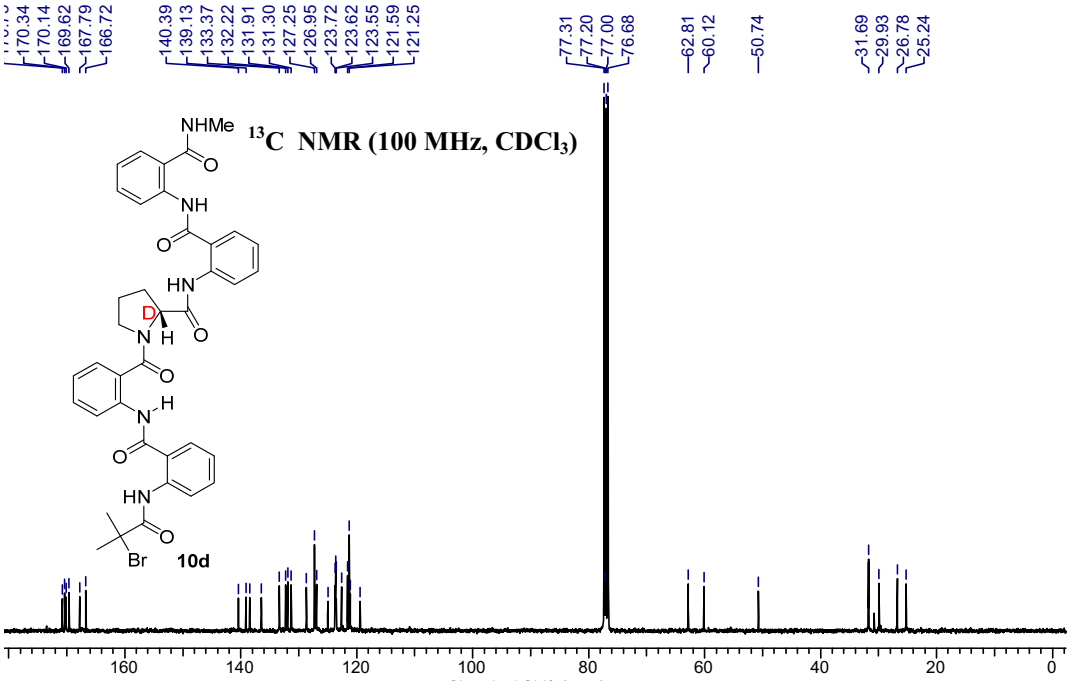
170.34
170.14
169.62
167.79
166.72
140.39
139.13
133.37
132.22
131.91
131.30
127.25
126.95
123.72
123.62
123.55
121.59
121.25
77.31
77.20
77.00
76.68
62.81
60.12
50.74
31.69
29.93
26.78
25.24
^{13}C NMR (100 MHz, CDCl$_3$)
NHMe
NH
HN
D
N H
N H
HN
Br
10d
160
140
120
100
80
60
40
20
0

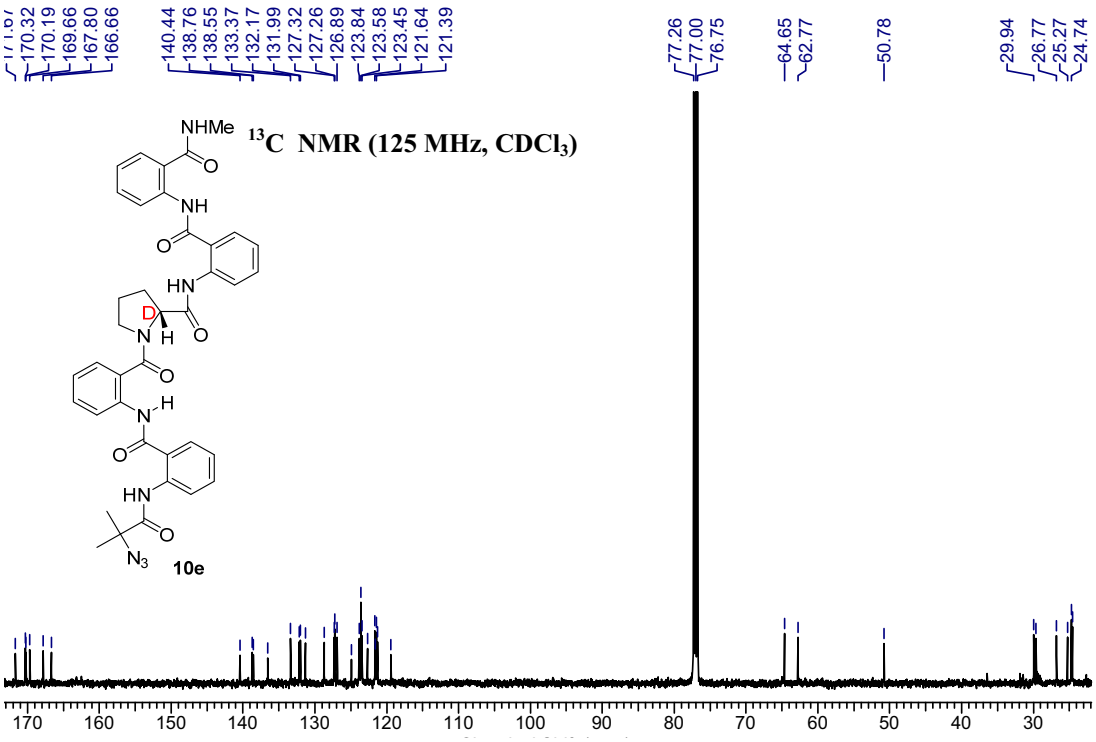
170.32
170.19
169.66
167.80
166.66
140.44
138.76
138.55
133.37
132.17
131.99
127.32
127.26
126.89
123.84
123.58
123.45
121.64
121.39
77.26
77.00
76.75
64.65
62.77
50.78
29.94
26.77
25.27
24.74
^{13}C NMR (125 MHz, CDCl$_3$)
NHMe
NH
HN
D
N H
N H
HN
N$_3$
10e
170
160
150
140
130
120
110
100
90
80
70
60
50
40
30

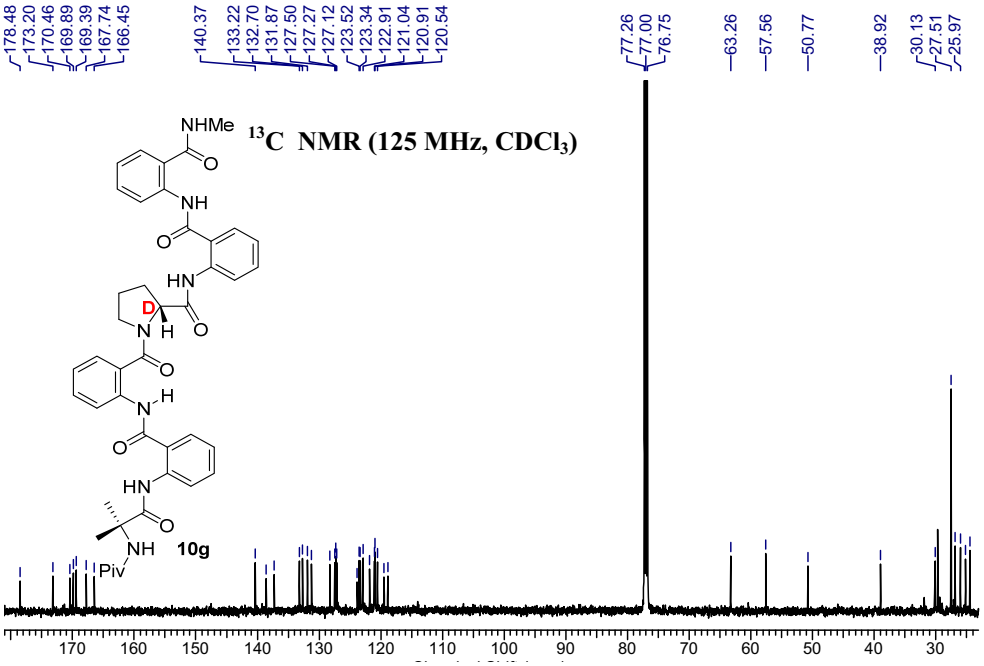
178.48
173.20
170.46
169.89
169.39
167.74
166.45
140.37
133.22
132.70
131.87
127.50
127.27
127.12
123.52
123.34
122.91
121.04
120.91
120.54
77.26
77.00
76.75
63.26
57.56
50.77
38.92
30.13
27.51
25.97
^{13}C NMR (125 MHz, CDCl$_3$)
NHMe
NH
HN
D
N H
N H
HN
NH
Piv
10g
170
160
150
140
130
120
110
100
90
80
70
60
50
40
30

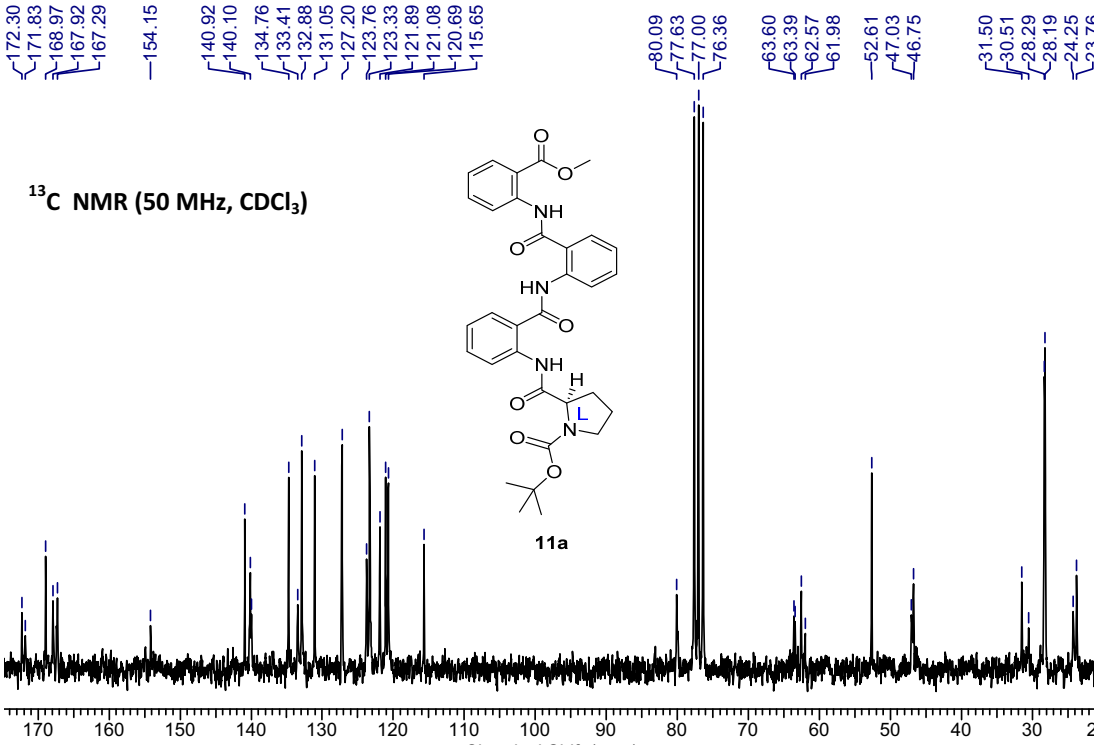
172.30
171.83
168.97
167.92
167.29
154.15
140.92
140.10
134.76
133.41
132.88
131.05
127.20
123.76
123.33
121.89
121.08
120.69
115.65
80.09
77.63
77.00
76.36
63.60
63.39
62.57
61.98
52.61
47.03
46.75
31.50
30.51
28.29
28.19
24.25
^{13}C NMR (50 MHz, CDCl$_3$)
NH
HN
NH
H
L
11a
170
160
150
140
130
120
110
100
90
80
70
60
50
40
30

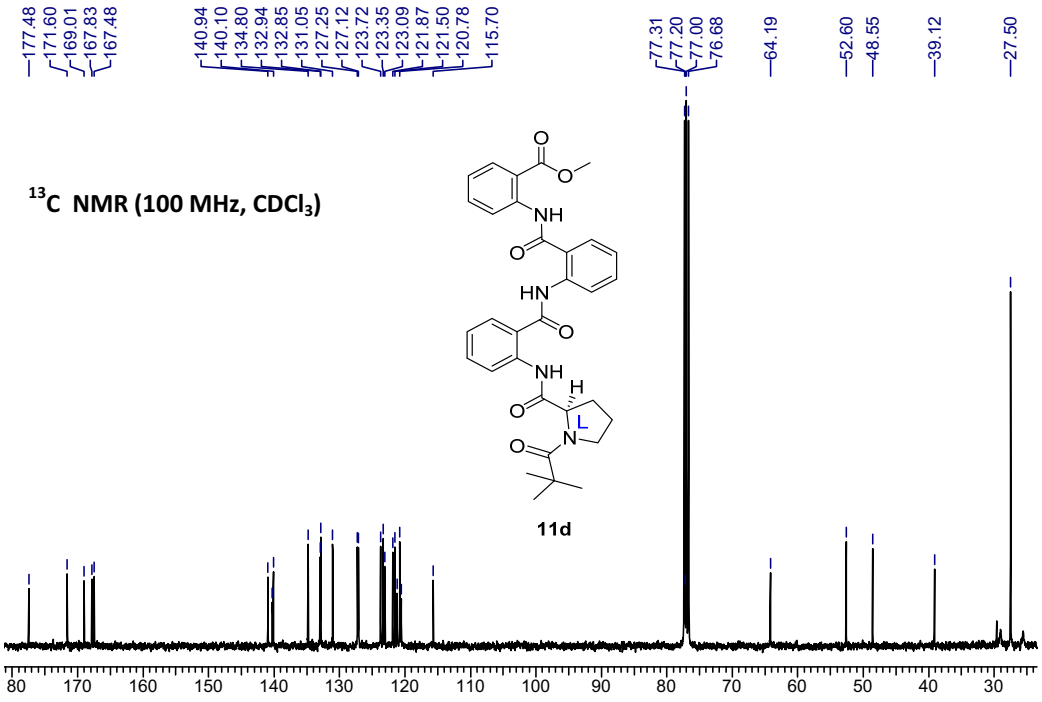
177.48
171.60
169.01
167.83
167.48
140.94
140.10
134.80
132.94
132.85
131.05
127.25
127.12
123.72
123.35
123.09
121.87
121.50
120.78
115.70
77.31
77.20
77.00
76.68
64.19
52.60
48.55
39.12
27.50
^{13}C NMR (100 MHz, CDCl$_3$)
11d

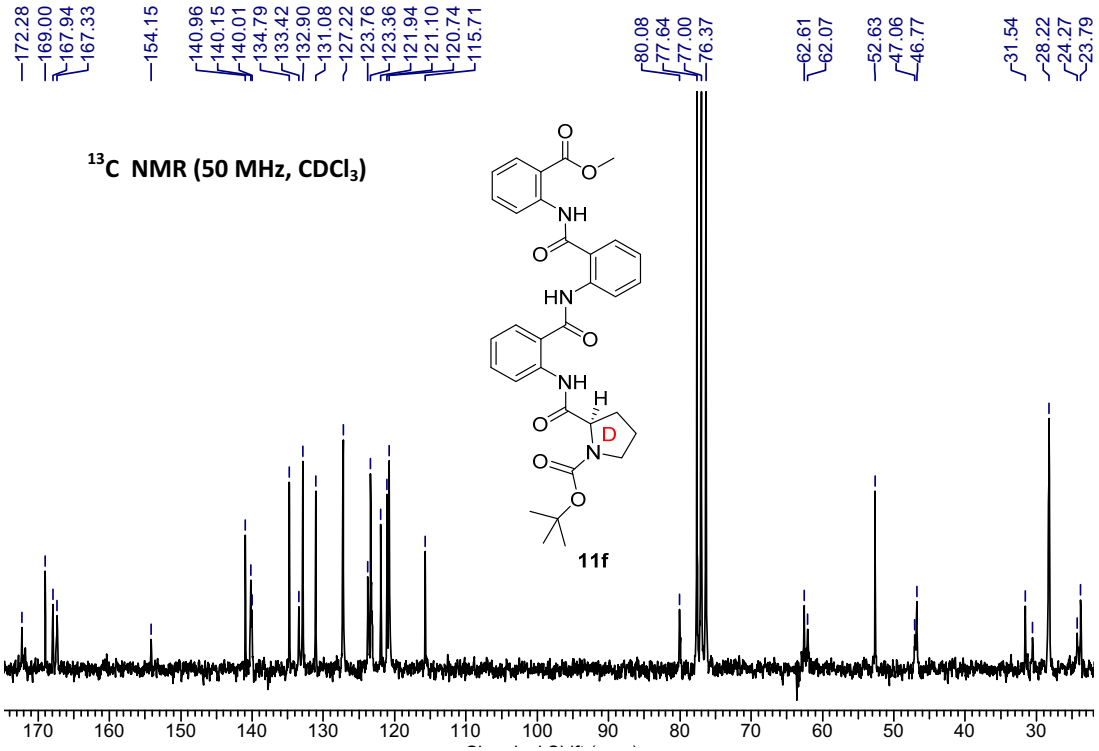
172.28
169.00
167.94
167.33
154.15
140.96
140.15
140.01
134.79
133.42
132.90
131.08
127.22
123.76
123.36
121.94
121.10
120.74
115.71
80.08
77.64
77.00
76.37
62.61
62.07
52.63
47.06
46.77
31.54
28.22
24.27
23.79
^{13}C NMR (50 MHz, CDCl$_3$)
11f

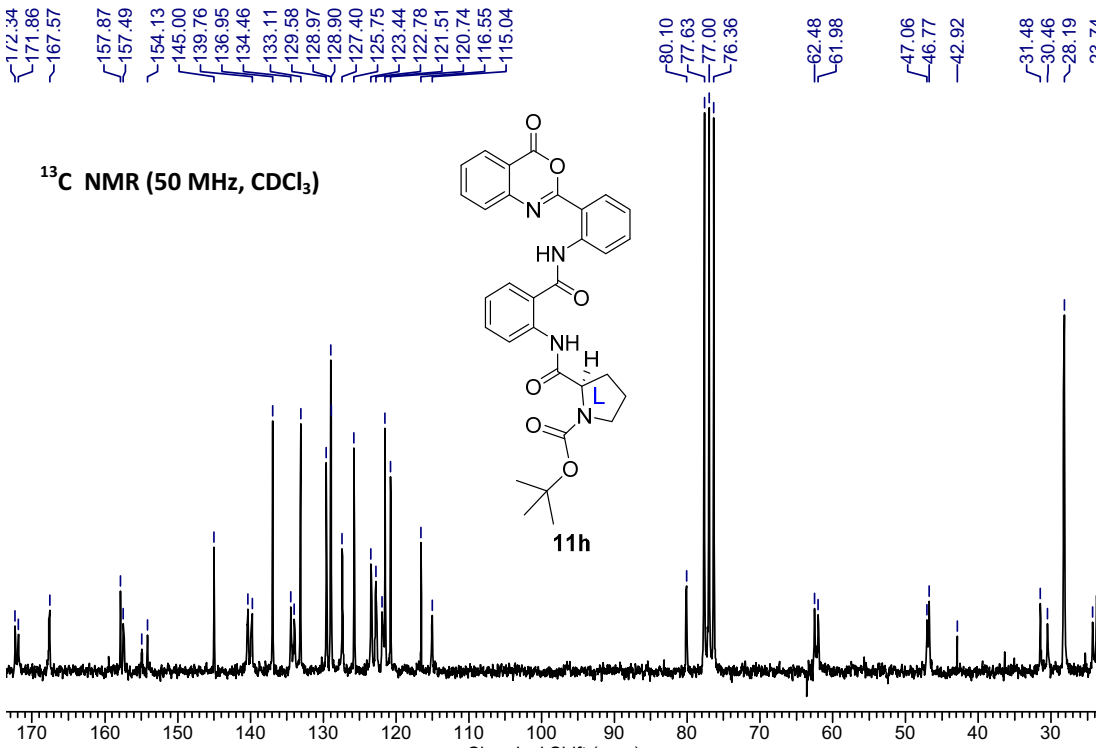
172.34
171.86
167.57
157.87
157.49
154.13
145.00
139.76
136.95
134.46
133.11
129.58
128.97
128.90
127.40
125.75
123.44
122.78
121.51
120.74
116.55
115.04
80.10
77.63
77.00
76.36
62.48
61.98
47.06
46.77
42.92
31.48
30.46
28.19
^{13}C NMR (50 MHz, CDCl$_3$)
11h

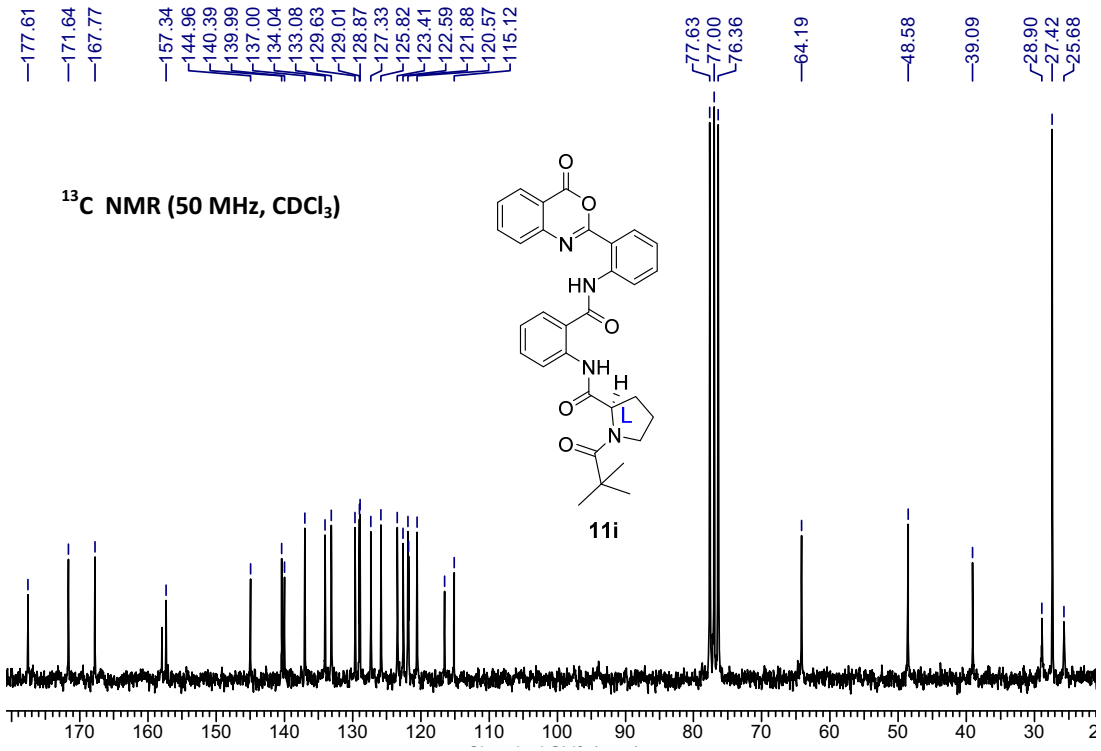
177.61
171.64
167.77
157.34
144.96
140.39
139.99
137.00
134.04
133.08
129.63
129.01
128.87
127.33
125.82
123.41
122.59
121.88
120.57
115.12
77.63
77.00
76.36
64.19
48.58
39.09
28.90
27.42
25.68
^{13}C NMR (50 MHz, CDCl$_3$)
11i

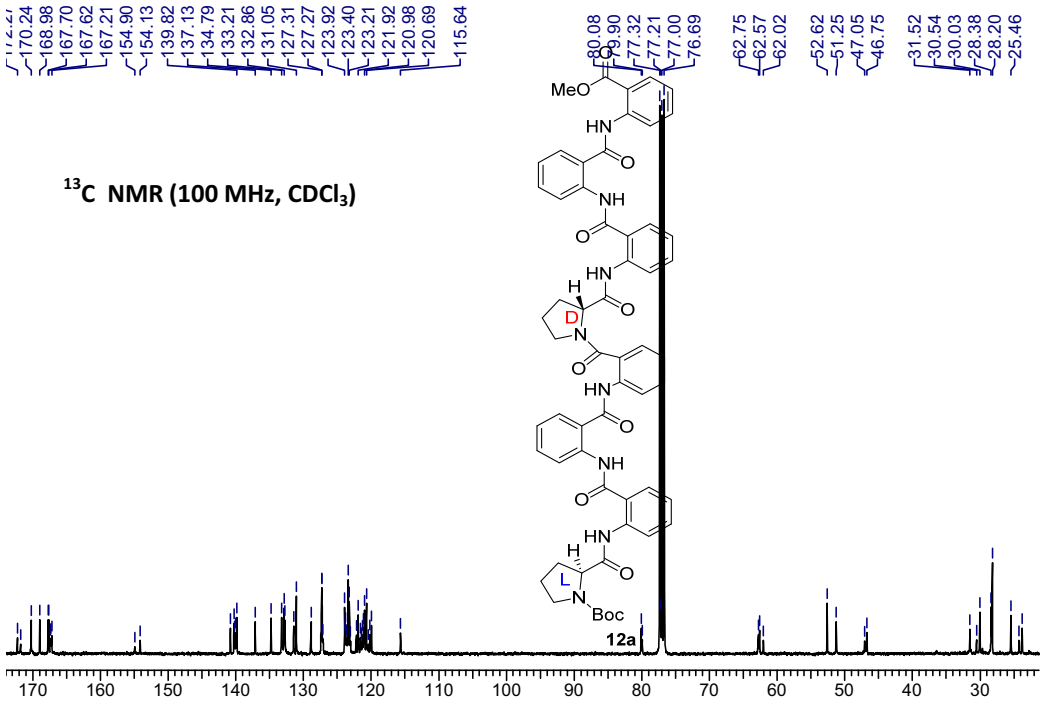

^{13}C NMR (100 MHz, $CDCl_3$)

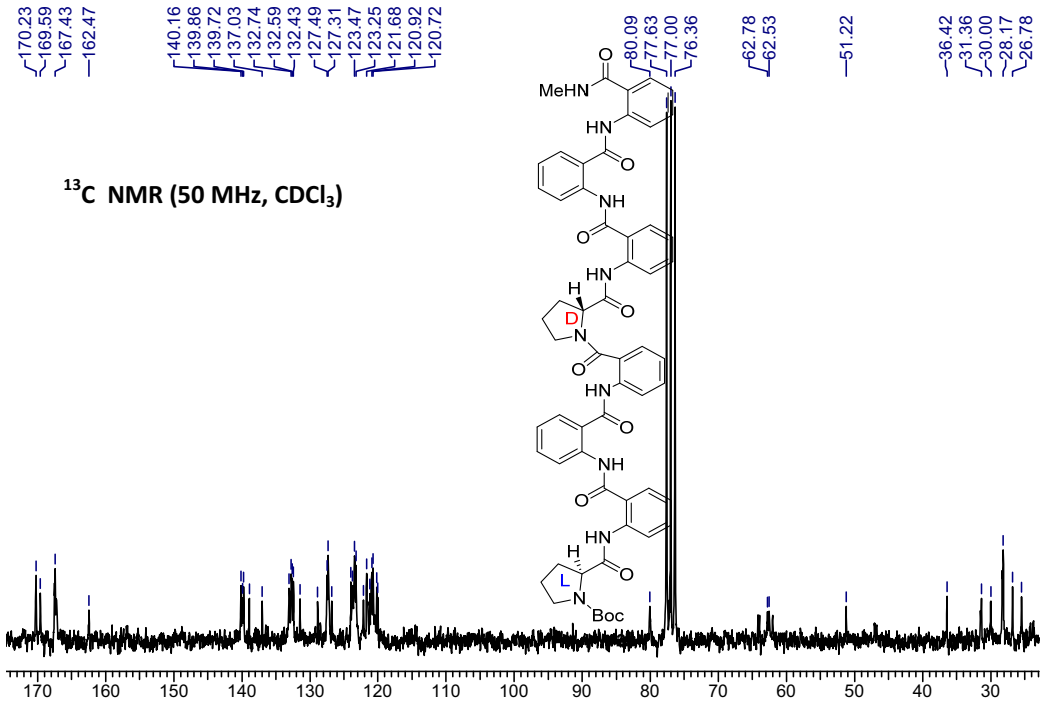

^{13}C NMR (50 MHz, $CDCl_3$)

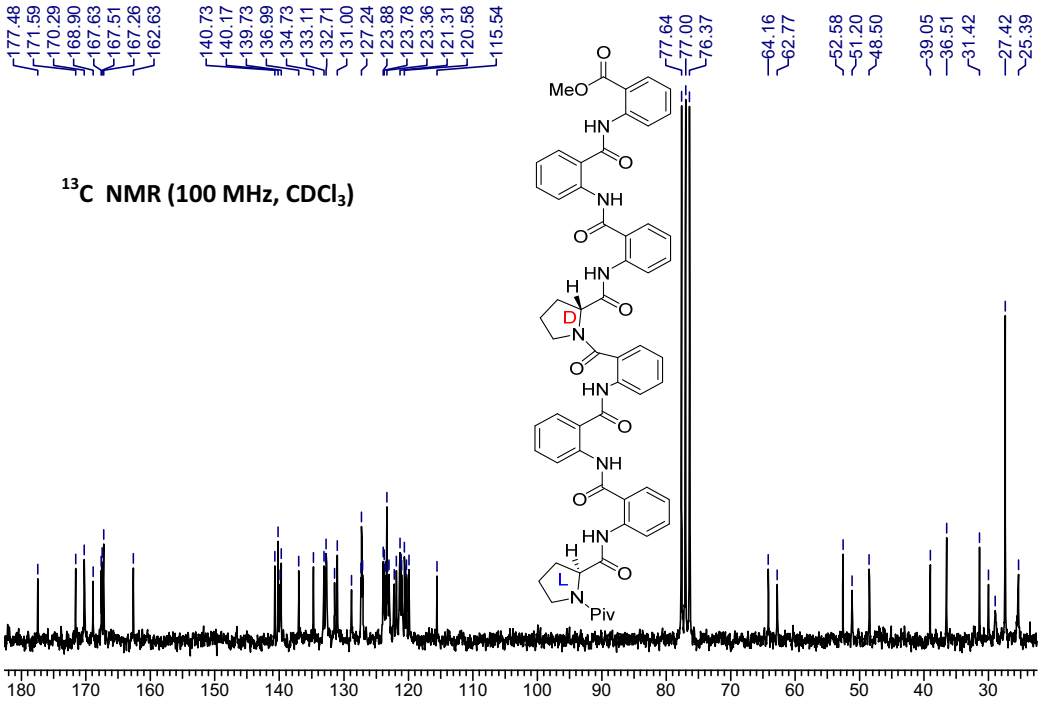
177.48
171.59
170.29
168.90
167.63
167.51
167.26
162.63
140.73
140.17
139.73
136.99
134.73
133.11
132.71
131.00
127.24
123.88
123.78
123.36
121.31
120.58
115.54
77.64
77.00
76.37
64.16
62.77
52.58
51.20
48.50
39.05
36.51
31.42
27.42
25.39
^{13}C NMR (100 MHz, CDCl$_3$)
MeO
HN
NH
D
L
Piv
180
170
160
150
140
130
120
110
100
90
80
70
60
50
40
30

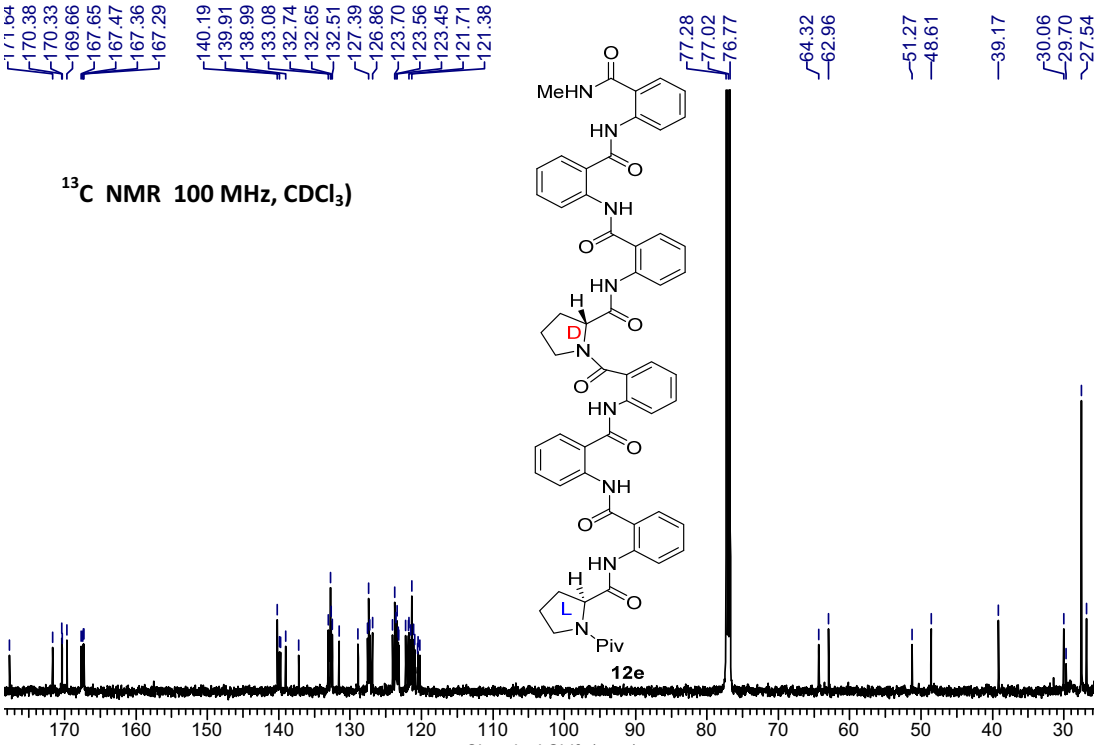
170.38
170.33
169.66
167.65
167.47
167.36
167.29
140.19
139.91
138.99
133.08
132.74
132.65
132.51
127.39
126.86
123.70
123.56
123.45
121.71
121.38
77.28
77.02
76.77
64.32
62.96
51.27
48.61
39.17
30.06
29.70
27.54
^{13}C NMR 100 MHz, CDCl$_3$)
MeHN
HN
NH
D
L
Piv
12e
170
160
150
140
130
120
110
100
90
80
70
60
50
40
30

Table 2. Titration study of hexapeptide **4h** in $CDCl_3$ (5mM) with DMSO-d_6 (volume of DMSO-d_6 used at each addition = 5 μl)

$V_{DMSO-d6}$ added (in μlit)	Chemical shift (in ppm)				
	δ_{NH5} (ppm)	δ_{NH6} (ppm)	δ_{NH2} (ppm)	δ_{NH3} (ppm)	δ_{NH7} (ppm)
0	12.27	12.02	11.18	10.32	7.25
5	12.23	12.08	11.18	10.35	7.28
10	12.21	12.13	11.18	10.36	7.39
15	12.18	12.17	11.18	10.37	7.49
20	12.16	12.20	11.17	10.38	7.56
25	12.14	12.23	11.16	10.38	7.62
30	12.11	12.25	11.15	10.38	7.67
35	12.09	12.27	11.14	10.37	7.72
40	12.07	12.29	11.12	10.37	7.76
45	12.05	12.30	11.11	10.36	7.79
50	12.03	12.31	11.09	10.35	7.83

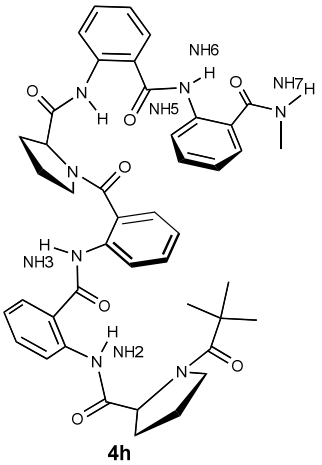

4h

Table 3. Titration study of hexapeptide **7d** in $CDCl_3$ (2mM) with DMSO-d_6 (volume of DMSO-d_6 used at each addition = 5 μl)

$V_{DMSO-d6}$ added (in μlit)	Chemical shift (in ppm)			
	δ_{NH5} (ppm)	δ_{NH6} (ppm)	δ_{NH2} (ppm)	δ_{NH3} (ppm)
0	12.08	11.93	11.45	10.63
5	12.06	11.92	11.43	10.61
10	12.05	11.91	11.41	10.59
15	12.03	11.89	11.38	10.58
20	12.01	11.88	11.36	10.56
25	12.0	11.86	11.34	10.54
30	11.98	11.85	11.32	10.53
35	11.96	11.83	11.29	10.51
40	11.95	11.81	11.27	10.49
45	11.93	11.80	11.25	10.47
50	11.91	11.78	11.23	10.46

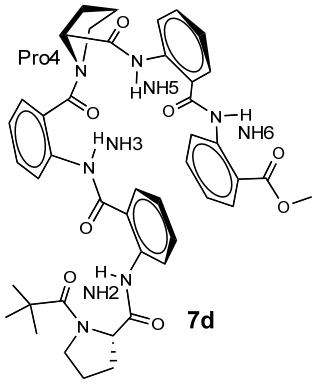

7d

Table 4. Titration study of hexapeptide **7f** in $CDCl_3$ (5mM) with DMSO-d_6 (volume of DMSO-d_6 used for each addition = 5 μl).

$V_{DMSO-d6}$ added (in μlit)	Chemical shift (in ppm)				
	δ_{NH5}	δ_{NH6}	δ_{NH2}	δ_{NH3}	δ_{NH7}
0	12.8	12.37	11.6	10.32	8.35
5	12.76	12.36	11.58	10.31	8.34
10	12.72	12.36	11.56	10.29	8.32
15	12.69	12.35	11.52	10.28	8.31
20	12.65	12.34	11.5	10.27	8.29
25	12.62	12.34	11.47	10.25	8.28
30	12.58	12.33	11.45	10.24	8.27
35	12.55	12.33	11.42	10.23	8.26
40	12.51	12.32	11.4	10.22	8.24
45	12.48	12.32	11.37	10.21	8.24
50	12.45	12.31	11.35	10.2	8.22

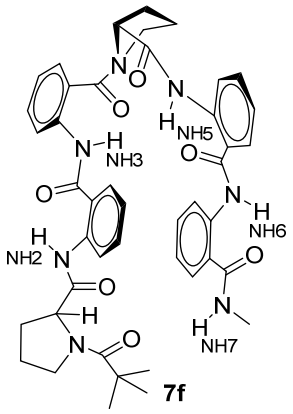

7f

Table 5. Titration study of hexapeptide **10g** in $CDCl_3$ (5mM) with DMSO-d_6 (volume of DMSO-d_6 used at each addition = 5 µl)

$V_{DMSO-d6}$ added (in µlit)	Chemical shift (in ppm)					
	δ_{NH5} (ppm)	δ_{NH6} (ppm)	δ_{NH2} (ppm)	δ_{NH3} (ppm)	δ_{NH7} (ppm)	δ_{NH1} (ppm)
0	12.53	12.23	11.76	10.36	7.51	6.28
5	12.49	12.25	11.74	10.37	7.57	6.32
10	12.45	12.28	11.72	10.38	7.66	6.35
15	12.41	12.3	11.71	10.39	7.72	6.37
20	12.38	12.31	11.69	10.39	7.76	6.38
25	12.33	12.33	11.67	10.38	7.8	6.39
30	12.31	12.25	11.65	10.38	7.84	6.4
35	12.29	12.27	11.63	10.38	7.86	6.405
40	12.26	12.29	11.61	10.37	7.89	6.41
45	12.23	12.3	11.59	10.36	7.91	6.41
50	12.2	12.31	11.56	10.36	7.93	6.41

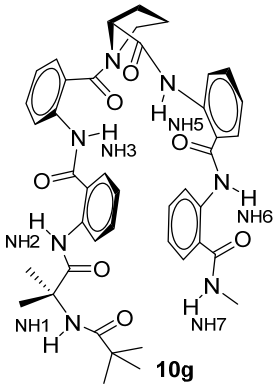

10g

Table 6. Titration study of octapeptide **12e** in $CDCl_3$ (5mM) with DMSO-d_6 (volume of DMSO-d_6 used at each addition = 5 µl)

$V_{DMSO-d6}$ added (in µlit)	Chemical shift (in ppm)						
	δ_{NH7} (ppm)	δ_{NH8} (ppm)	δ_{NH6} (ppm)	δ_{NH3} (ppm)	δ_{NH2} (ppm)	δ_{NH4} (ppm)	δ_{NH9} (ppm)
0	12.37	12.29	12.27	12.05	11.52	10.8	6.64
5	12.39	12.36	12.28	12.05	11.52	10.79	7.28
10	12.4	12.4	12.28	12.05	11.51	10.77	7.43
15	12.4	12.45	12.26	12.04	11.49	10.75	7.48
20	12.4	12.47	12.25	12.03	11.47	10.74	7.54
25	12.39	12.49	12.24	12.01	11.45	10.72	7.65
30	12.38	12.5	12.22	11.99	11.43	10.69	7.72
35	12.37	12.51	12.2	11.98	11.41	10.67	7.79
40	12.36	12.51	12.19	11.96	11.4	10.65	7.82
45	12.36	12.53	12.19	11.96	11.39	10.65	7.89
50	12.34	12.51	12.15	11.92	11.36	10.61	7.92

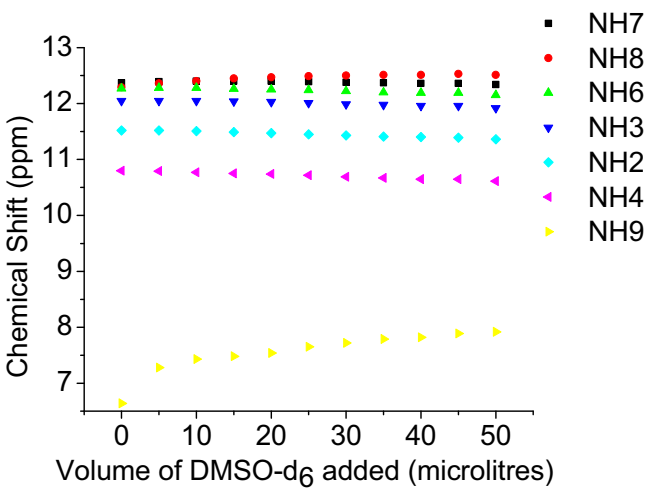

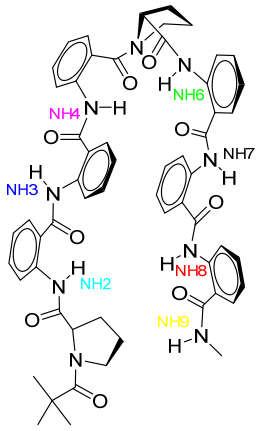

Table 7. Temperature variation study of hexapeptide **7f** (20 mmol, 400 MHz, $CDCl_3$)

Temperature (K)	Chemical shift (in ppm)				
	δ_{NH5}	δ_{NH6}	δ_{NH2}	δ_{NH3}	δ_{NH7}
218	12.98	12.38	11.71	10.4	8.74
223	12.97	12.38	11.71	10.4	8.72
228	12.96	12.38	11.71	10.4	8.71
233	12.95	12.38	11.71	10.39	8.68
238	12.94	12.38	11.7	10.39	8.67
243	12.93	12.38	11.7	10.39	8.65
248	12.92	12.38	11.69	10.38	8.63
253	12.91	12.38	11.68	10.38	8.61
258	12.9	12.38	11.67	10.37	8.59
263	12.89	12.38	11.66	10.36	8.58
268	12.88	12.38	11.65	10.35	8.57

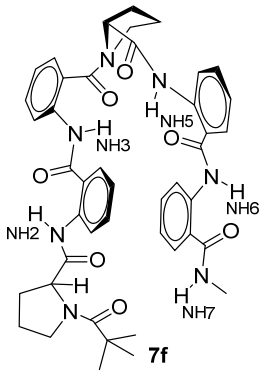

7f

Table 8. Temperature variation study of hexapeptide **7f** (20 mmol, 400 MHz, $CDCl_3$)

Temperature (K)	Chemical shift (in ppm)				
	δ_{NH5}	δ_{NH6}	δ_{NH2}	δ_{NH3}	δ_{NH7}
268	12.88	12.4	11.66	10.37	8.52
273	12.87	12.4	11.65	10.36	8.5
278	12.85	12.4	11.65	10.36	8.48
283	12.84	12.4	11.64	10.35	8.45
288	12.83	12.39	11.63	10.39	8.41
293	12.81	12.39	11.62	10.35	8.38
298	12.79	12.39	11.6	10.34	8.34
303	12.77	12.39	11.59	10.34	8.3
308	12.76	12.38	11.58	10.33	8.27
313	12.74	12.38	11.56	10.32	8.23
318	12.72	12.37	11.55	10.32	8.19

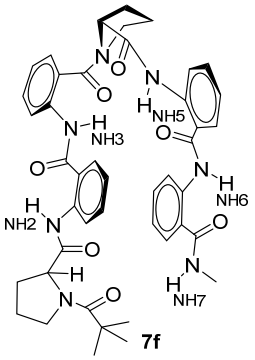

7f

^{1}H NMR NH/D exchange study of hexamer 7d in methanol-d$_4$

Deuterium exchange of the amide protons (NH/D) in the oligomer **7d** was studied at 400 MHz by dissolving the compound in $CDCl_3$ (0.4 ml) and methanol-(0.1 ml). The experiment was started immediately after the dissolution of compound using the following parameters: number of scans = 16, relaxation delay = 1 sec, flip angle = 30^o, spectral width = 8223. The ^{1}H NMR spectra were recorded then at different intervals at 296 K. A stacked plot at different time intervals is shown below.

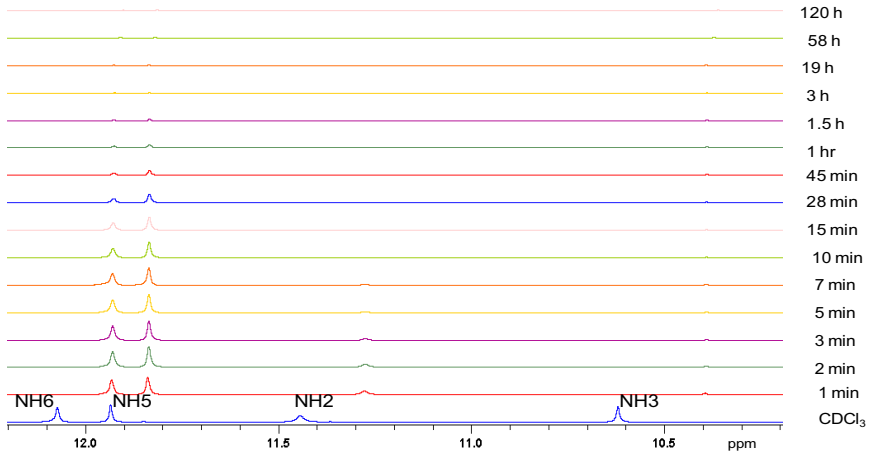

Figure 27. H/D Exchange of hexapeptide **7d** (400MHz, $CDCl_3$ + methanol-d_4).

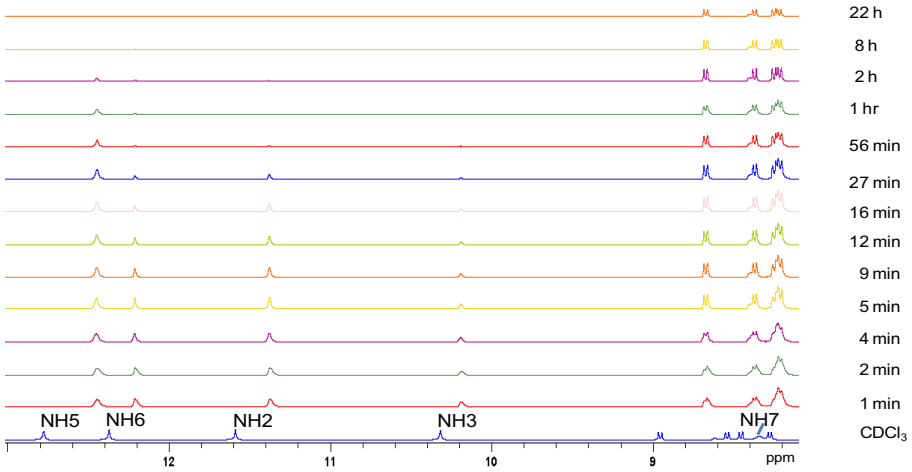

Figure 28. H/D Exchange of hexapeptide **7f** (400MHz, $CDCl_3$ + methanol-d_4).

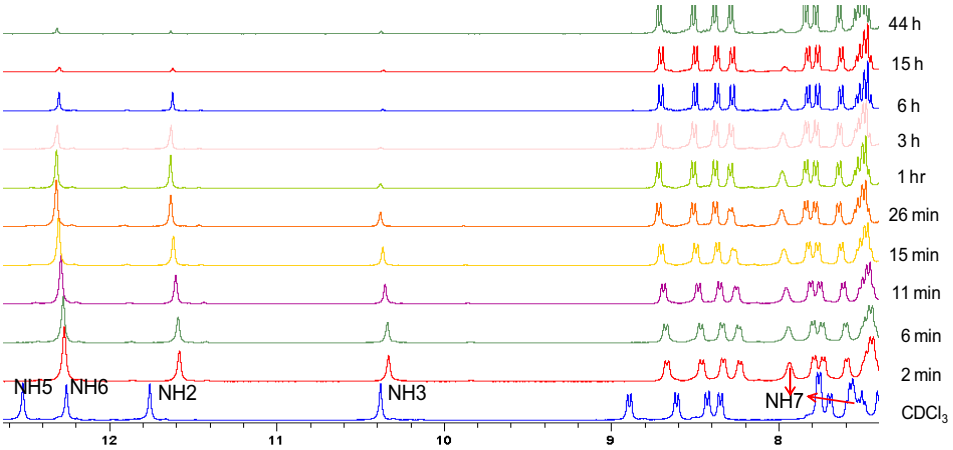

Figure 29. H/D Exchange of hexapeptide **10g** (400MHz, $CDCl_3$ + methanol-d_4).

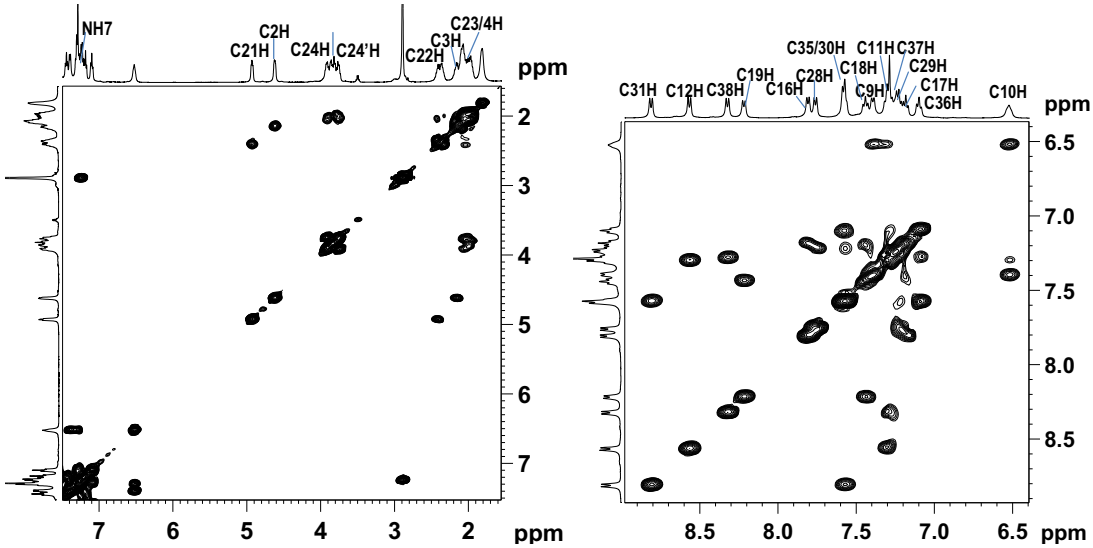

Figure 30. Partial COSY spectra of hexapeptide **4h** (500MHz, $CDCl_3$): Aliphatic (left) and aromatic region (right).

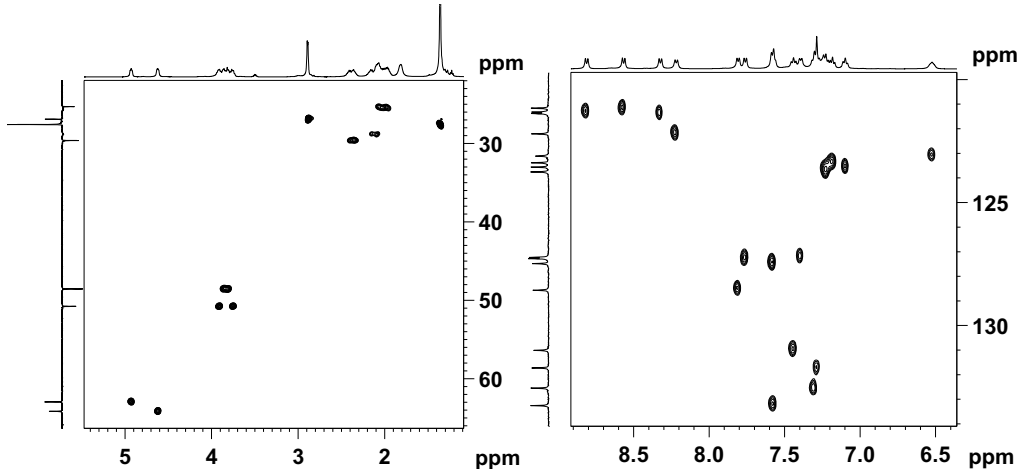

Figure 31. Partial HSQC spectra of hexapeptide **4h** (500MHz, CDCl3): Aliphatic (left) and aromatic regions (right).

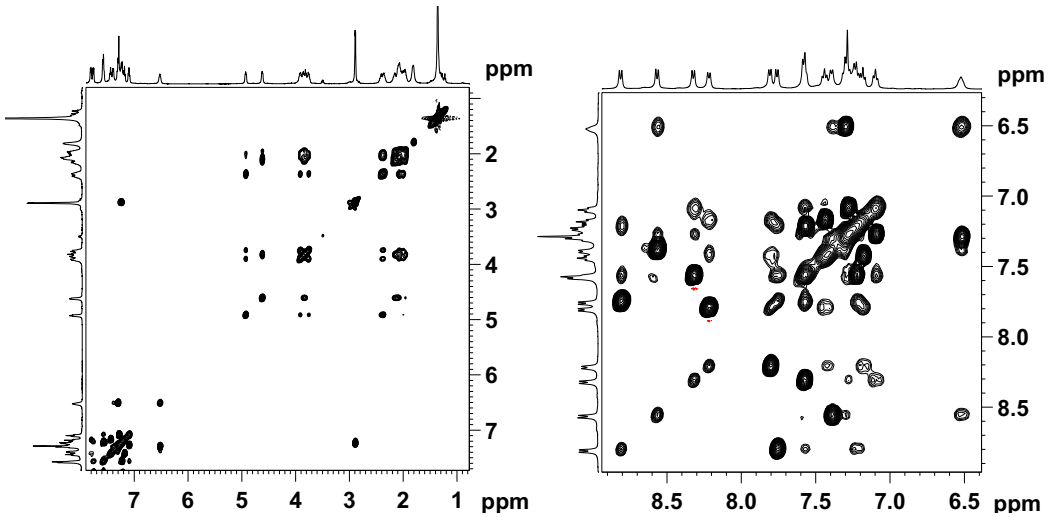

Figure 32. Partial TOCSY spectra of hexapeptide **4h** (500 MHz, CDCl3): Aliphatic (left) and aromatic regions (right).

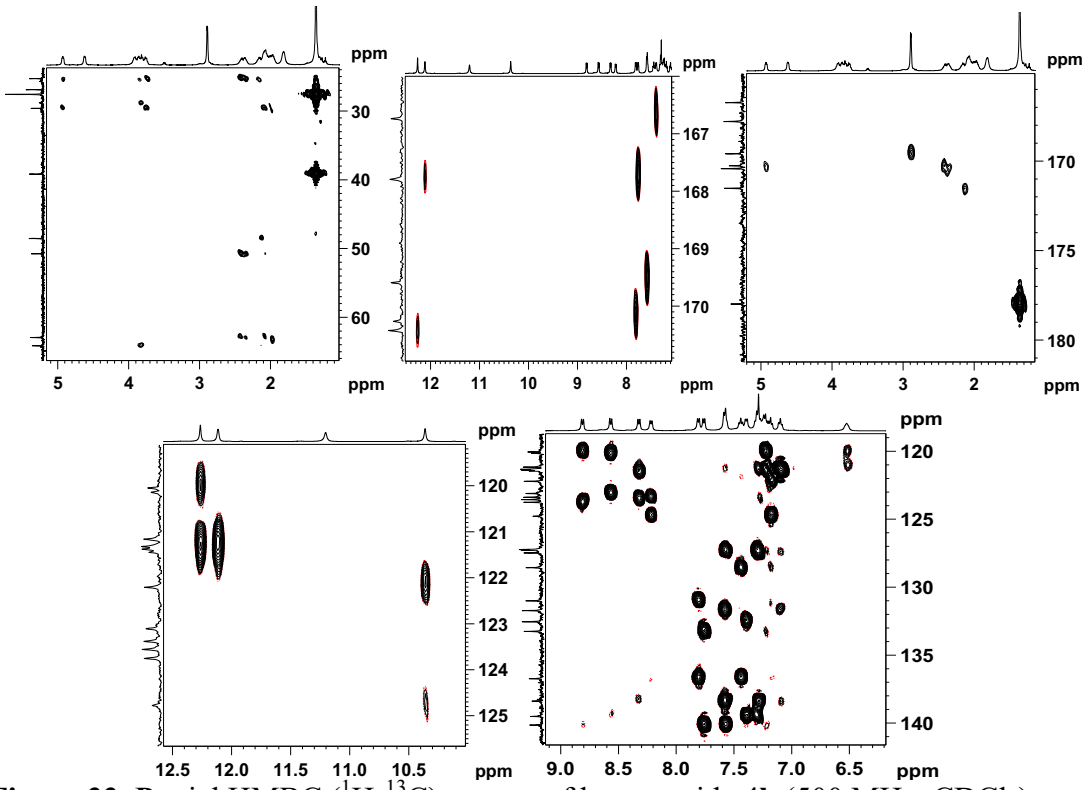

Figure 33. **P**artial HMBC (^{1}H-^{13}C) spectra of hexapeptide **4h** (500 MHz, $CDCl_3$).

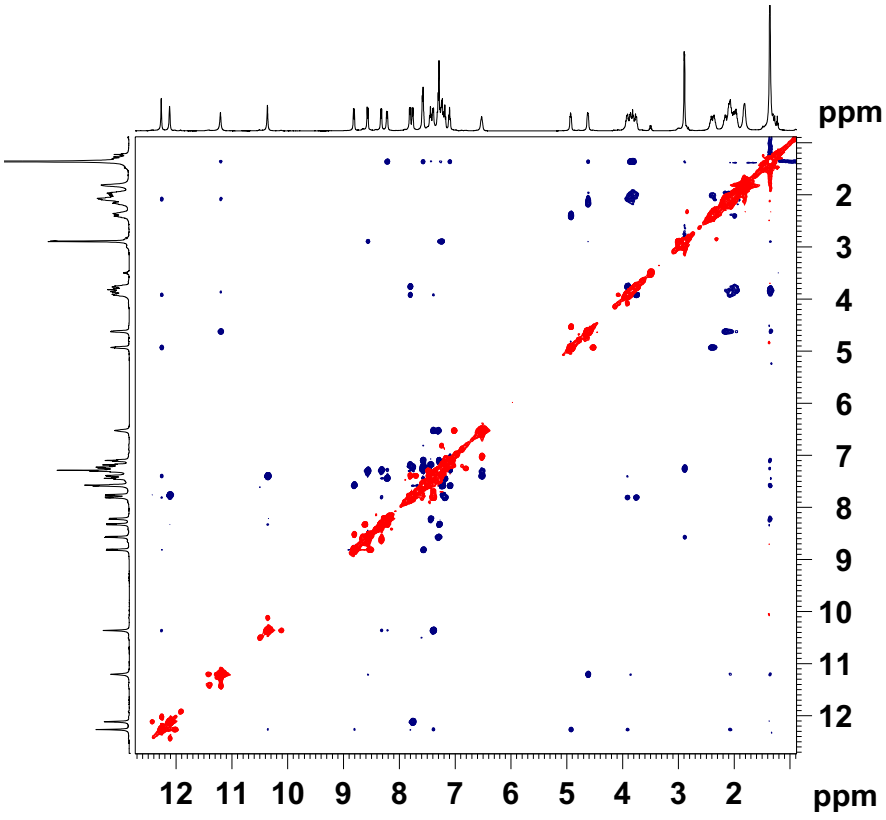

Figure 34. Full 2D NOESY spectrum of **4f** (500 MHz, $CDCl_3$).

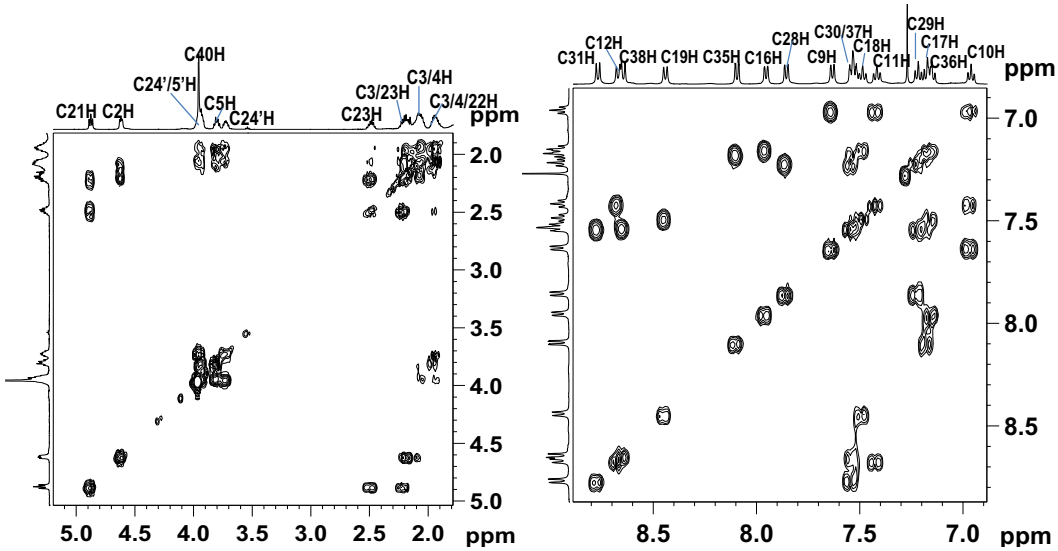

Figure 35. Partial COSY spectra of hexapeptide **7d** (500MHz, $CDCl_3$): Aliphatic (left) and aromatic region (right).

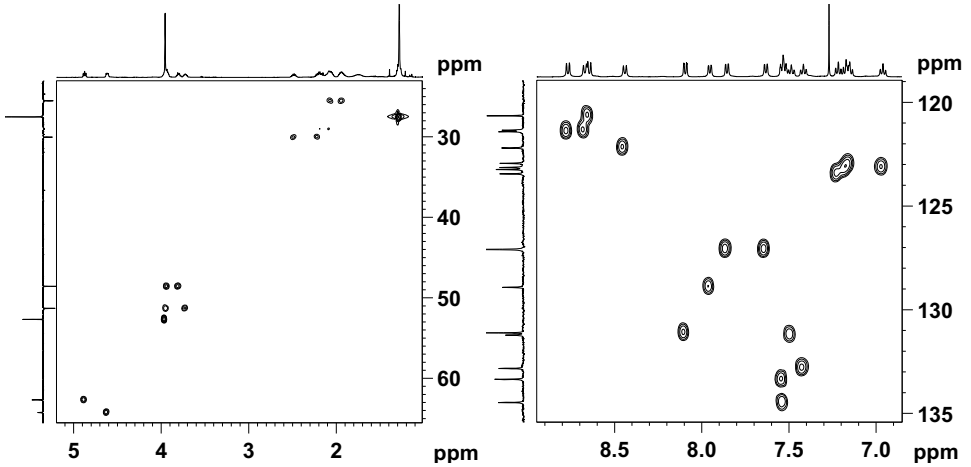

Figure 36. Partial HSQC spectra of hexapeptide **7d** (500MHz, $CDCl_3$): Aliphatic (left) and aromatic regions (right).

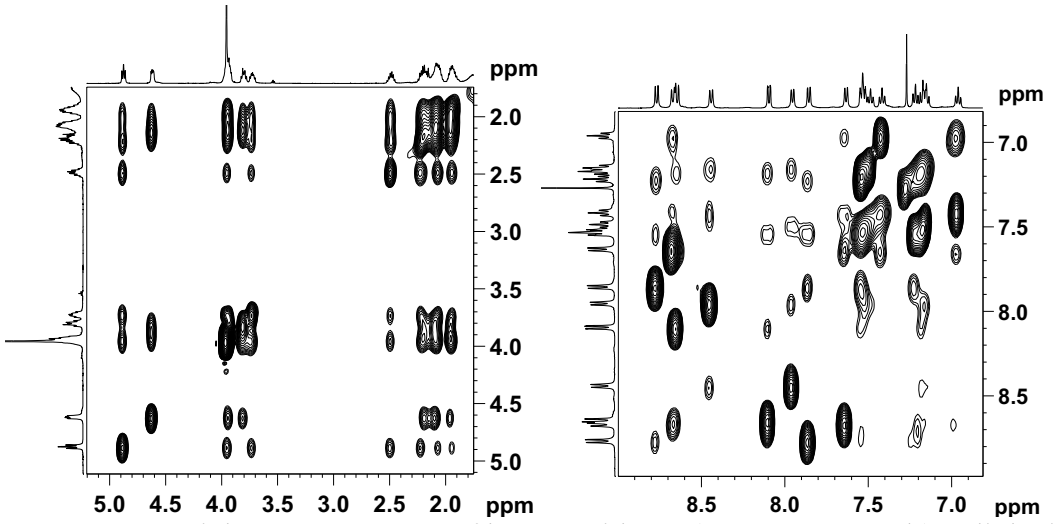

Figure 37. Partial TOCSY spectra of hexapeptide **7d** (500 MHz, $CDCl_3$): Aliphatic (left) and aromatic regions (right).

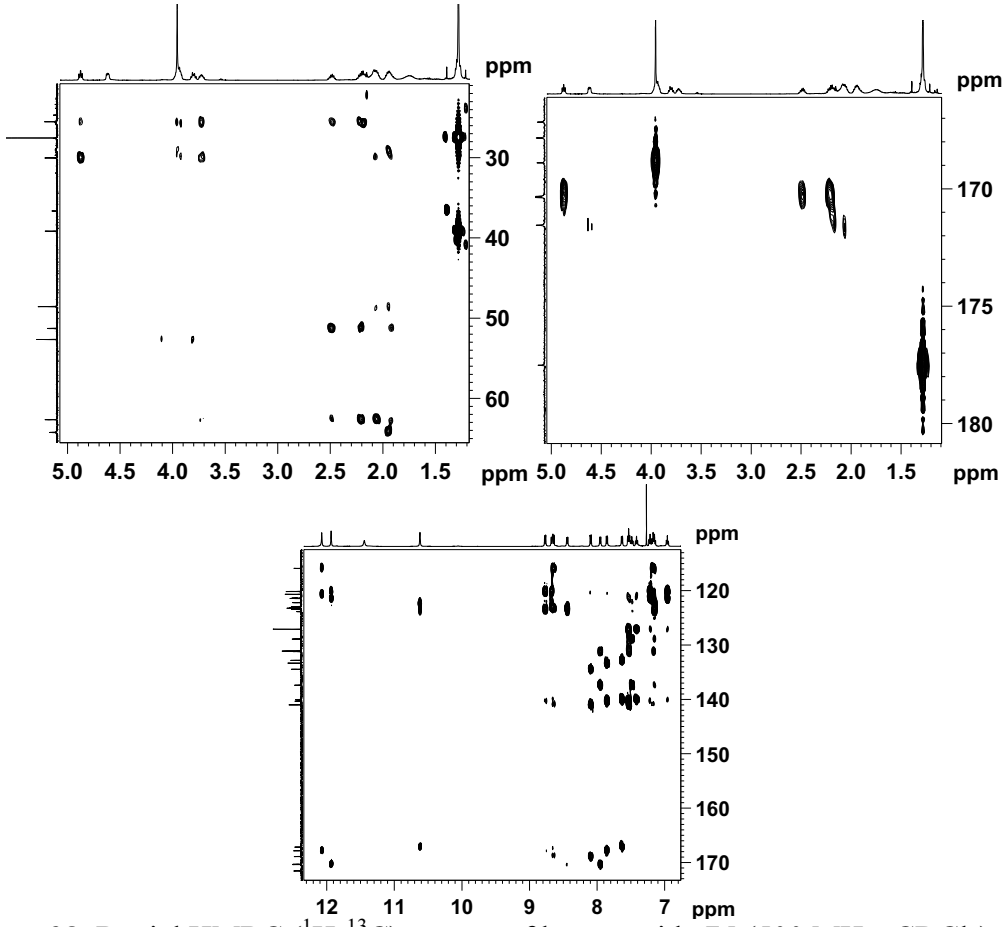

Figure 38. Partial HMBC (^{1}H-^{13}C) spectra of hexapeptide **7d** (500 MHz, $CDCl_3$).

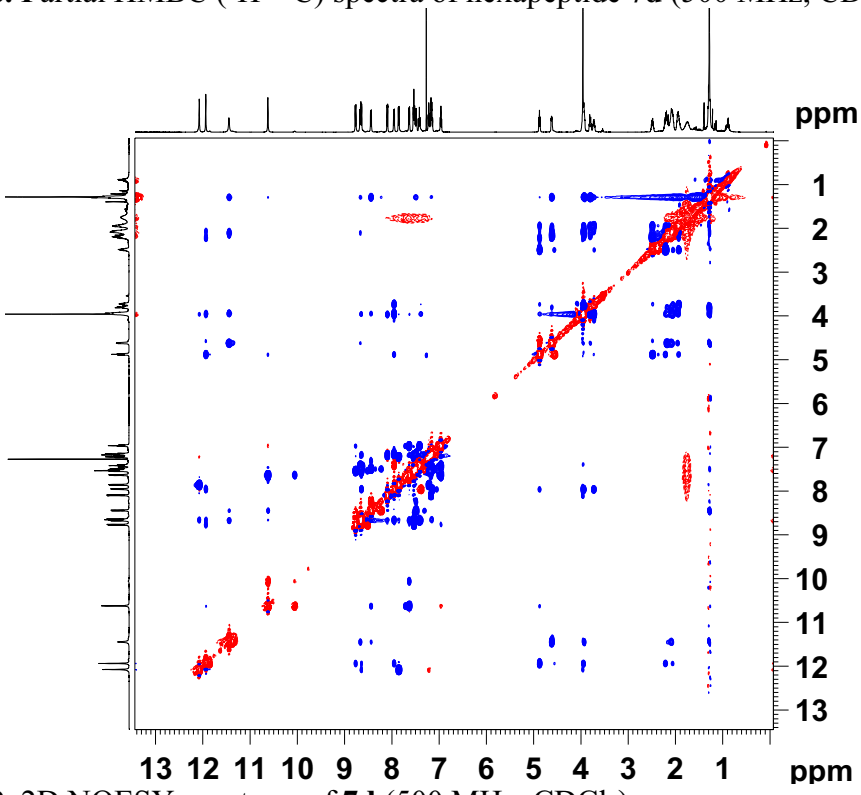

Figure 39. 2D NOESY spectrum of **7d** (500 MHz, $CDCl_3$).

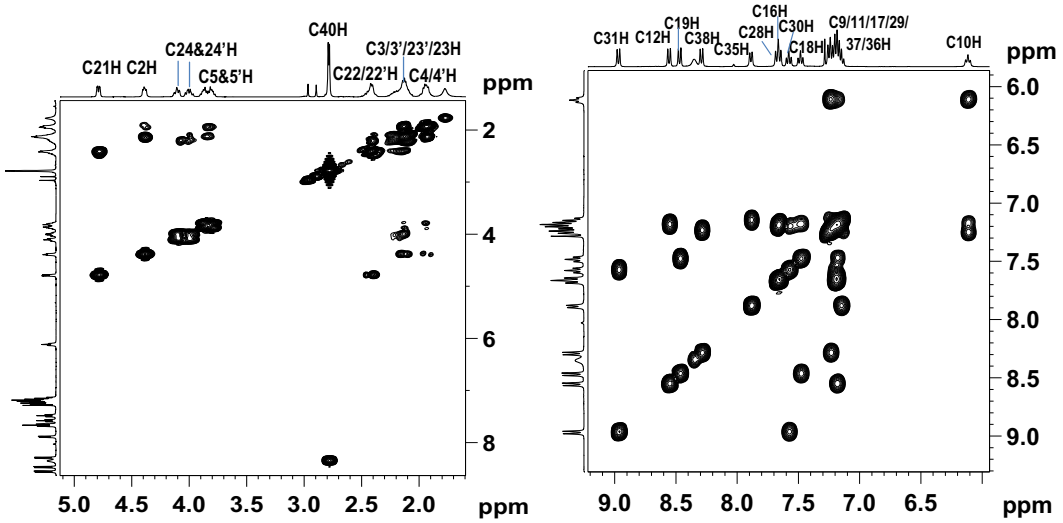

Figure 40. Partial COSY spectra of hexapeptide **7f** (400MHz, $CDCl_3$): Aliphatic (left) and aromatic region (right).

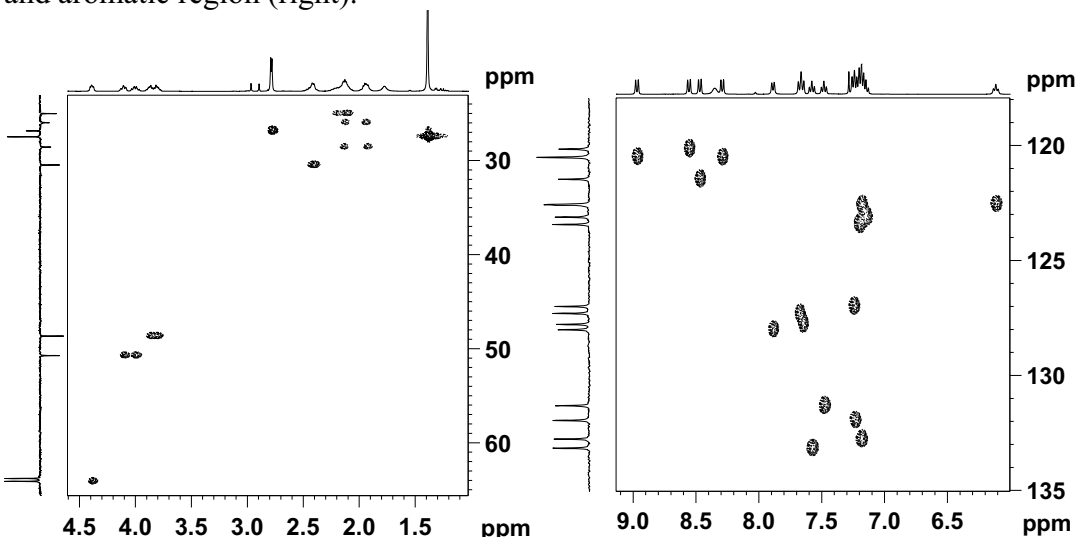

Figure 41. Partial HSQC spectra of hexapeptide **7f** (400MHz, $CDCl_3$): Aliphatic (left) and aromatic region (right).

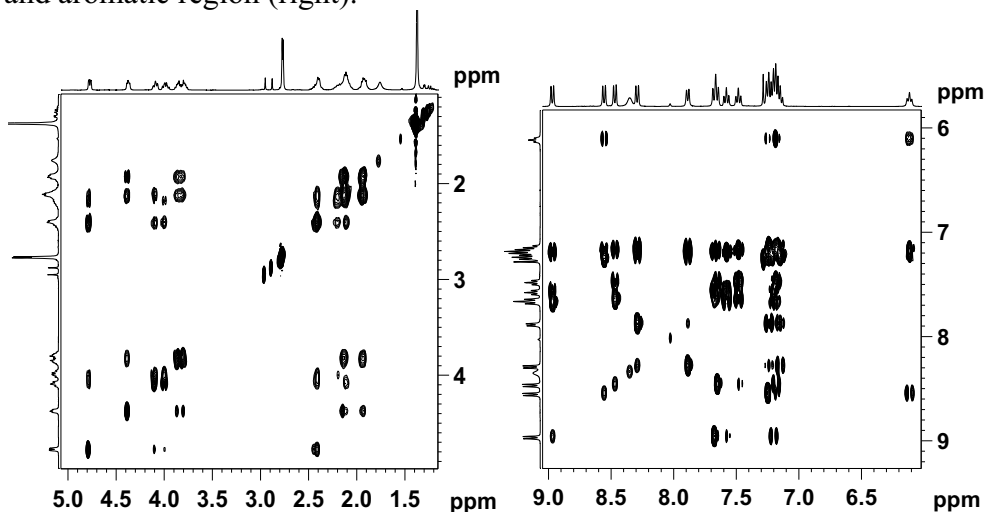

Figure 42. Partial TOCSY spectra of hexapeptide **7f** (400MHz, $CDCl_3$): Aliphatic (left) and aromatic region (right).

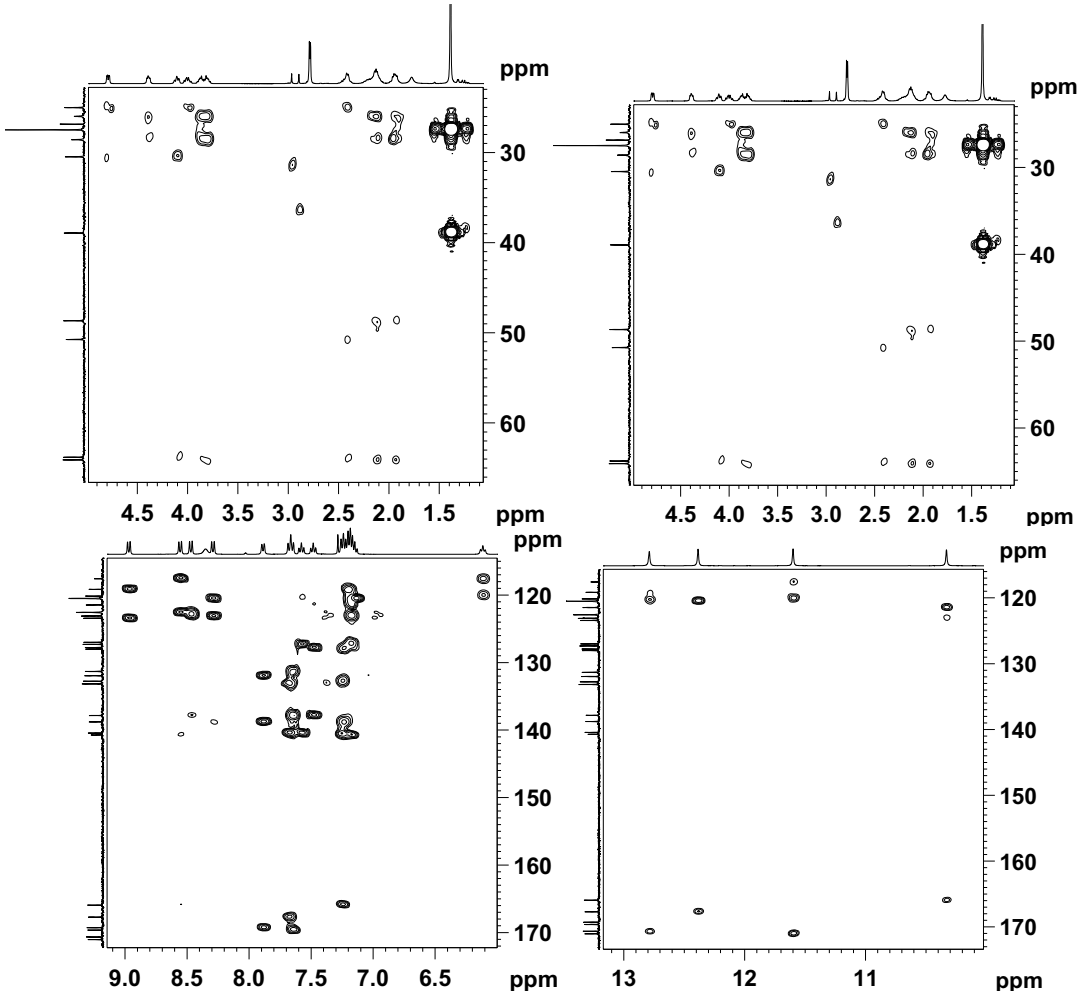

Figure 43. Partial HMBC (^{1}H-^{13}C) spectra of hexapeptide **7f** (400 MHz, $CDCl_3$).

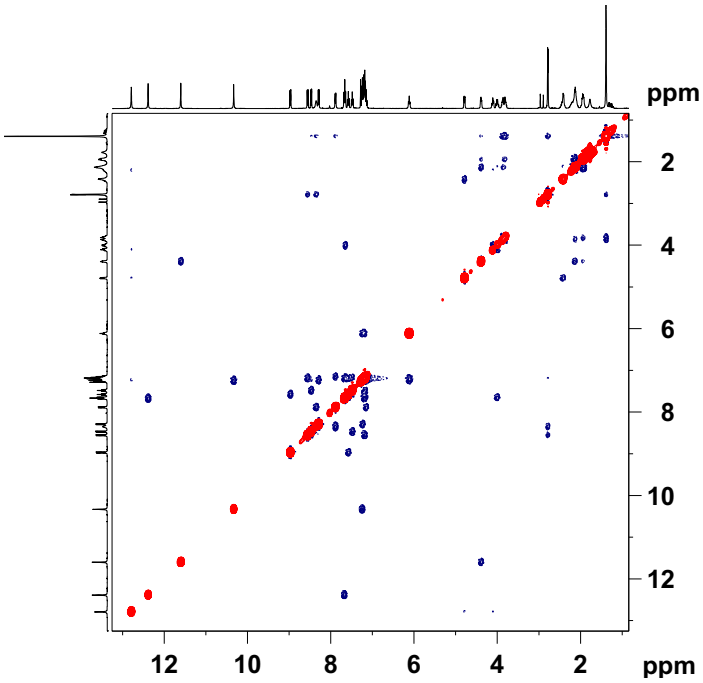

Figure 44. 2D NOESY spectrum of **7f** (400 MHz, $CDCl_3$).

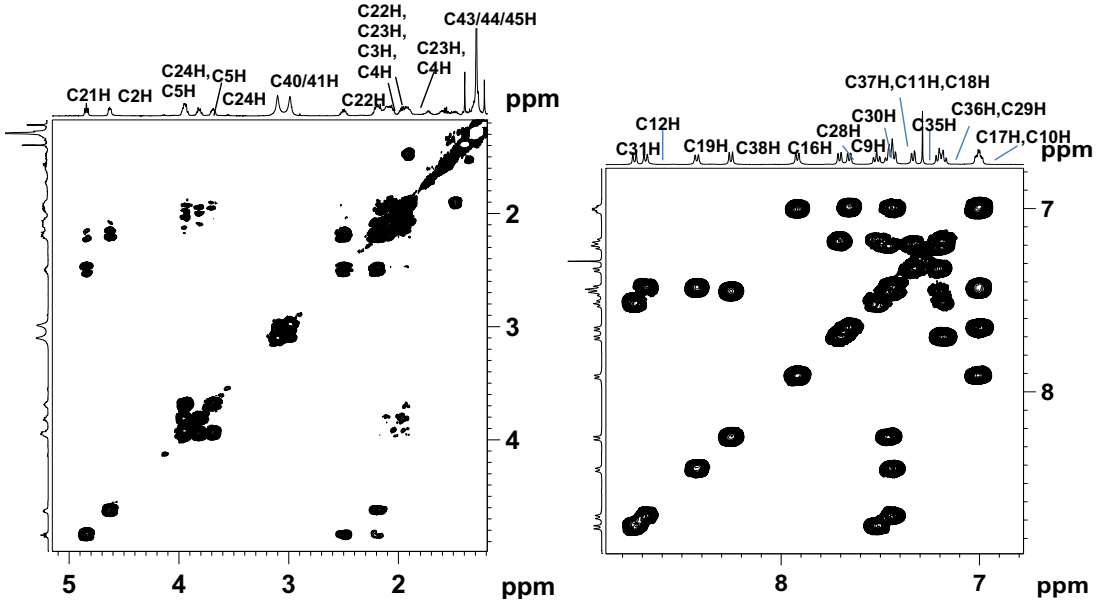

Figure 45. Partial COSY spectra of hexapeptide **7g** (500MHz, $CDCl_3$): Aliphatic (left) and aromatic region (right).

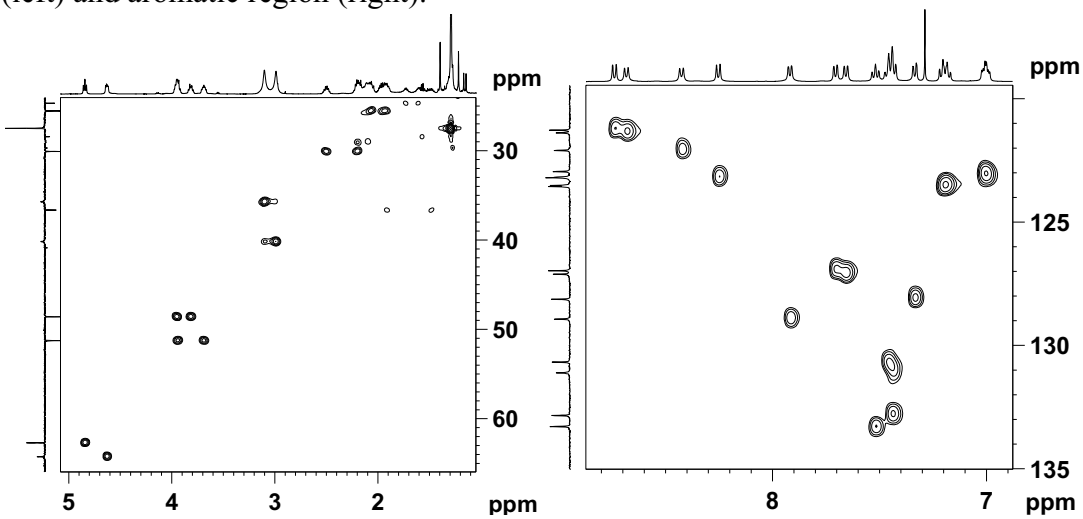

Figure 46. Partial HSQC spectra of hexapeptide **7g** (500MHz, $CDCl_3$): Aliphatic (left) and aromatic region (right).

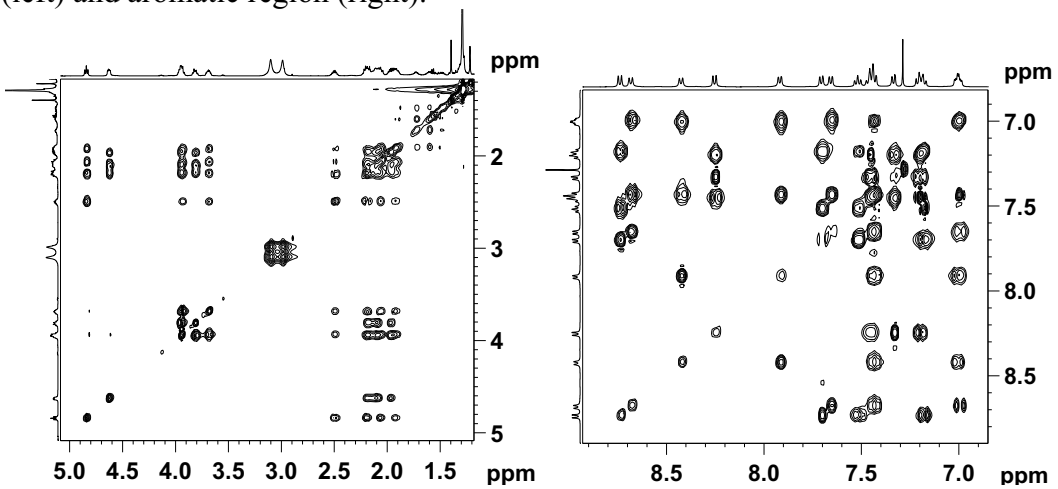

Figure 47. Partial TOCSY spectra of hexapeptide **7g** (500MHz, $CDCl_3$): Aliphatic (left) and aromatic region (right).

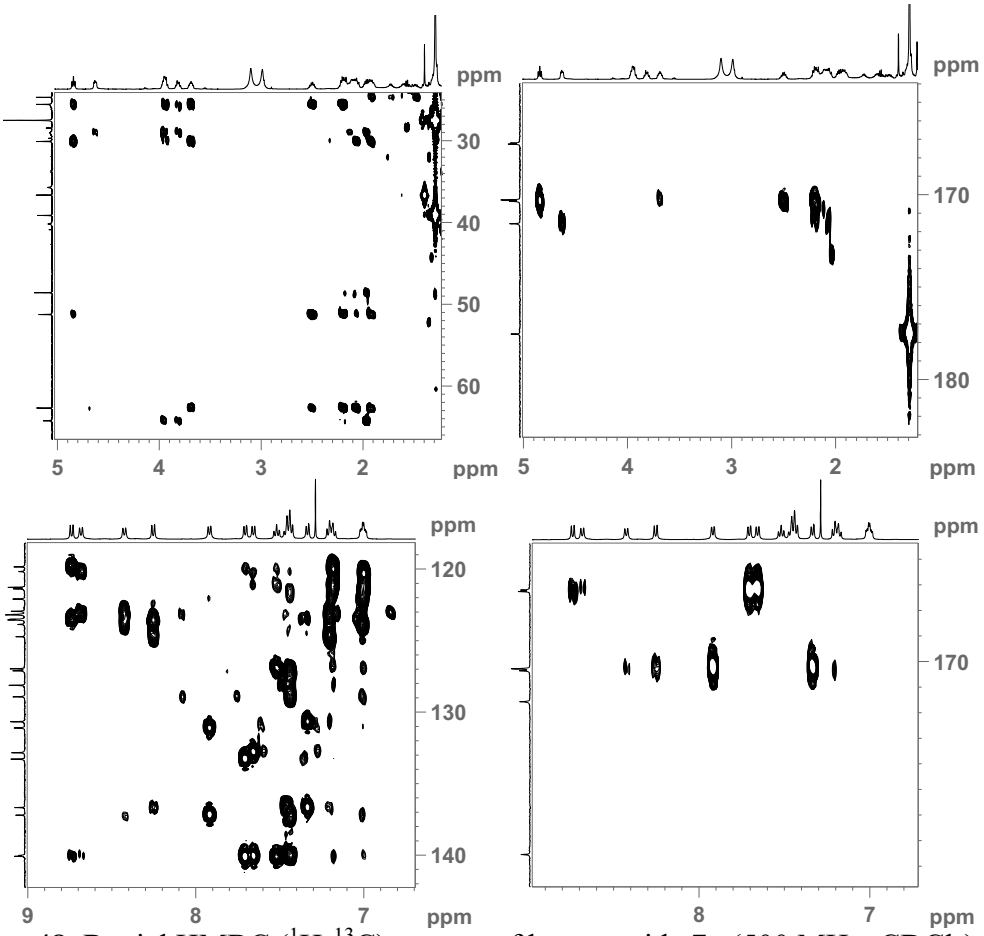

Figure 48. Partial HMBC (^{1}H-^{13}C) spectra of hexapeptide **7g** (500 MHz, $CDCl_3$): aliphatic **(a, b),** aromatic **(c,d)**.

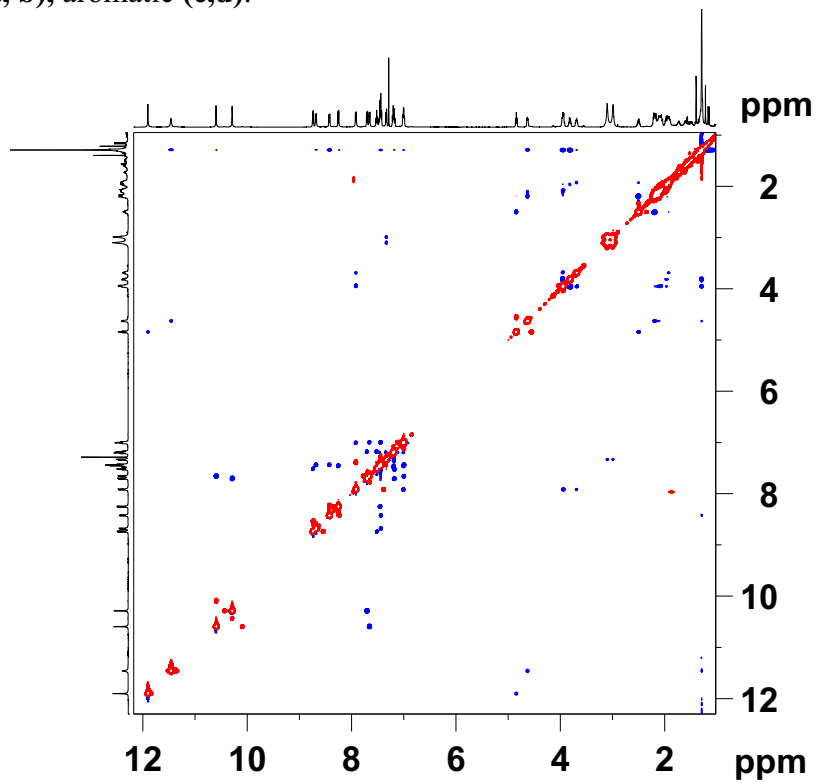

Figure 49. 2D NOESY spectrum of **7g** (500 MHz, $CDCl_3$).

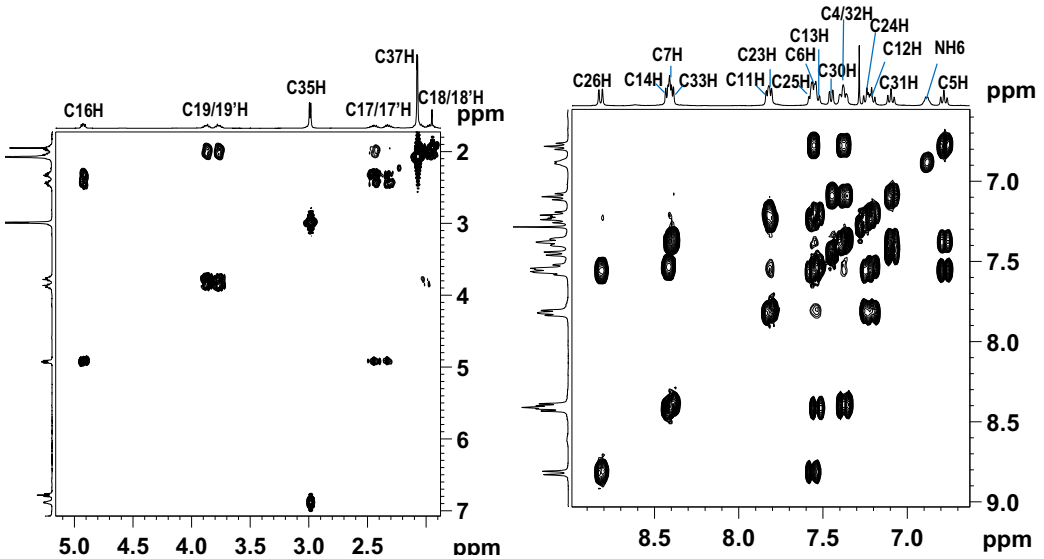

Figure 50. Partial COSY spectra of pentapeptide **10d** (500MHz, $CDCl_3$): Aliphatic (left) and aromatic region (right).

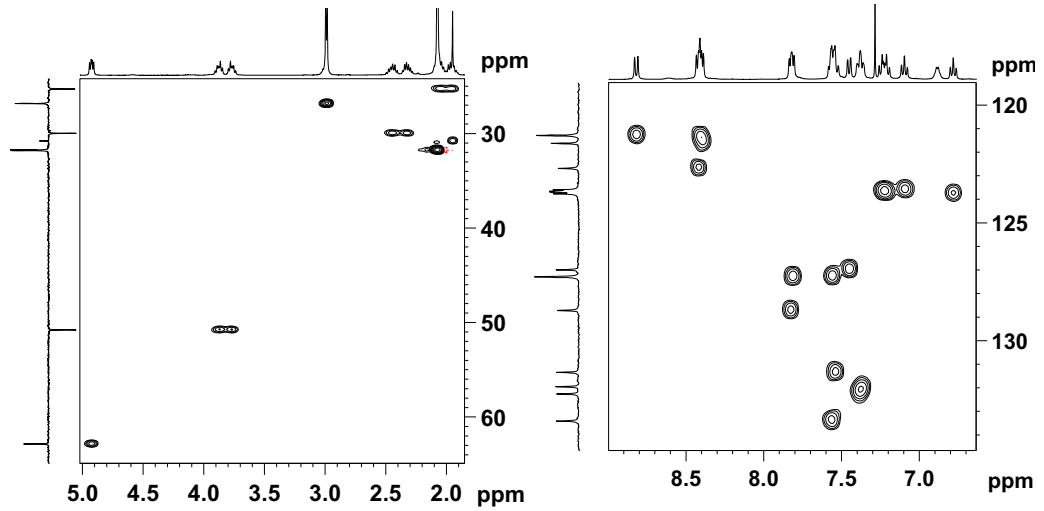

Figure 51. Partial HSQC spectra of pentapeptide **10d** (500MHz, $CDCl_3$): Aliphatic (left) and aromatic region (right).

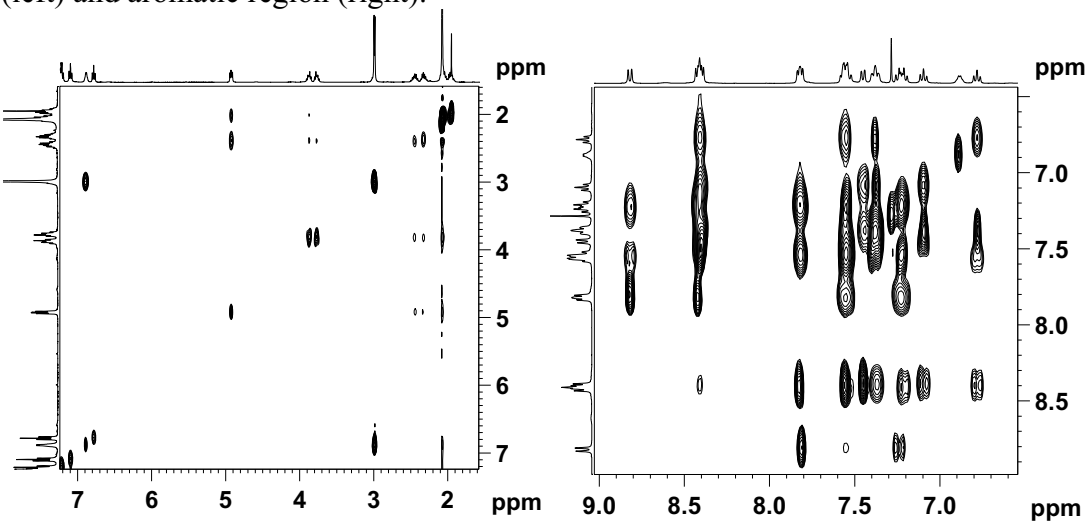

Figure 52. Partial TOCSY spectra of pentapeptide **10d** (500MHz, $CDCl_3$): Aliphatic (left) and aromatic region (right).

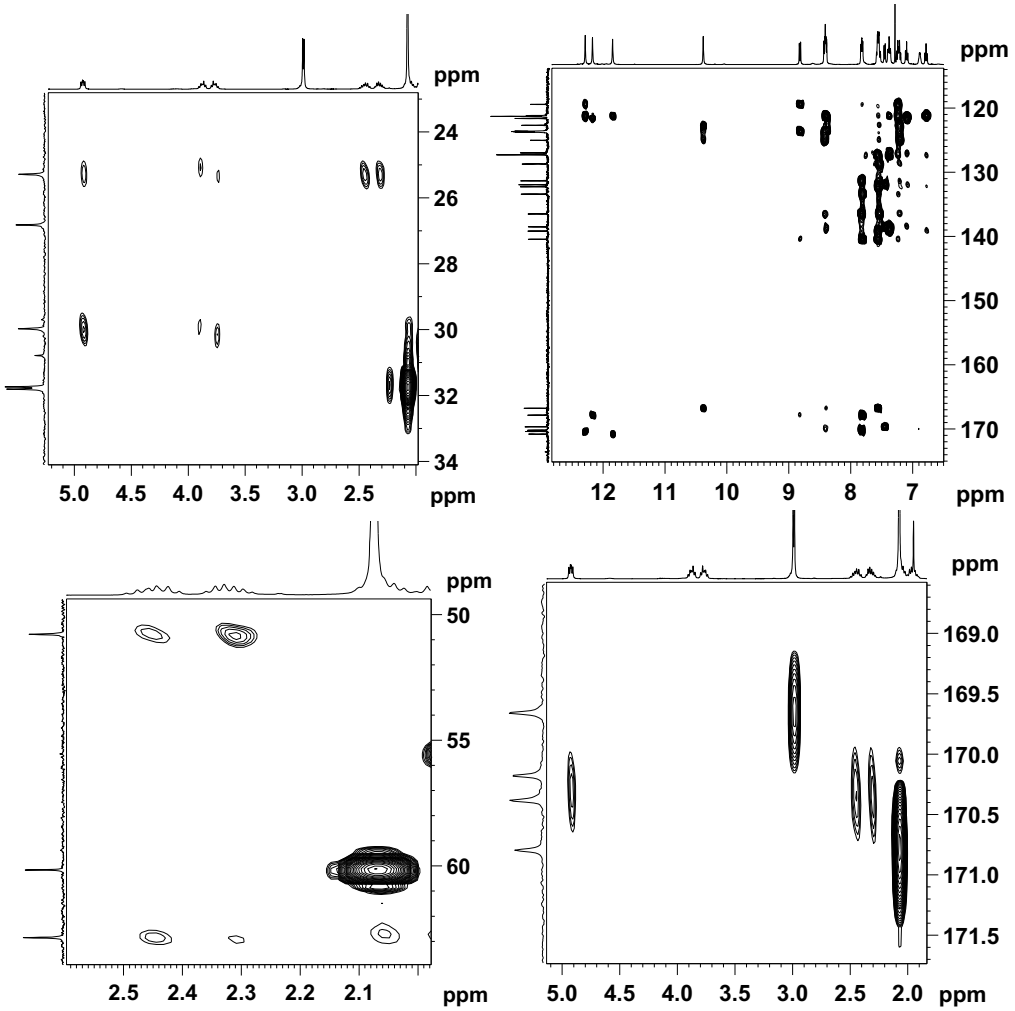

Figure 53. Partial HMBC (^{1}H-^{13}C) spectra of hexapeptide **10d** (500 MHz, $CDCl_3$): aliphatic **(a, b),** aromatic **(c,d)**.

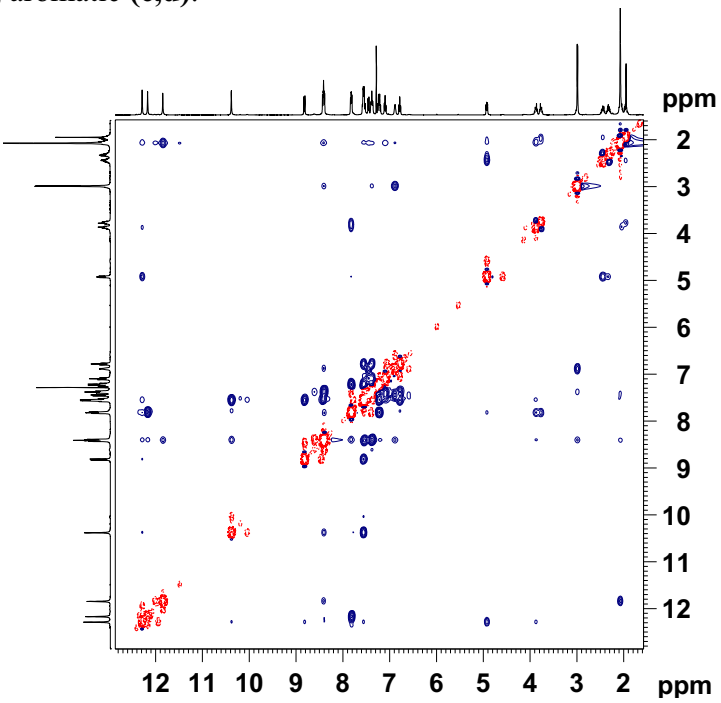

Figure 54. Full 2D NOESY spectrum of **10d** (500 MHz, $CDCl_3$).

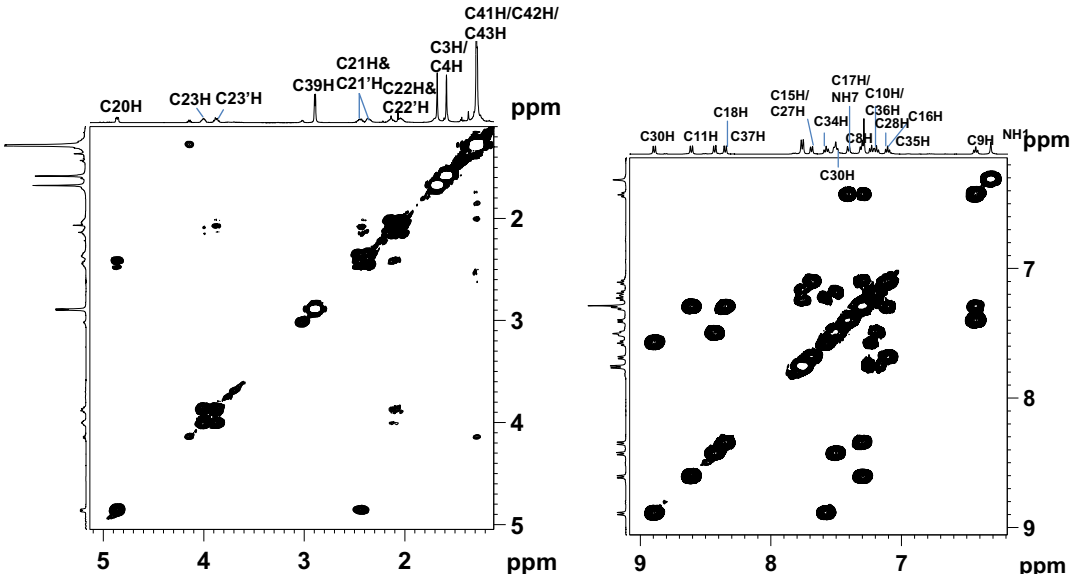

Figure 55. Partial COSY spectra of hexapeptide **10g** (500MHz, $CDCl_3$): Aliphatic (left) and aromatic region (right).

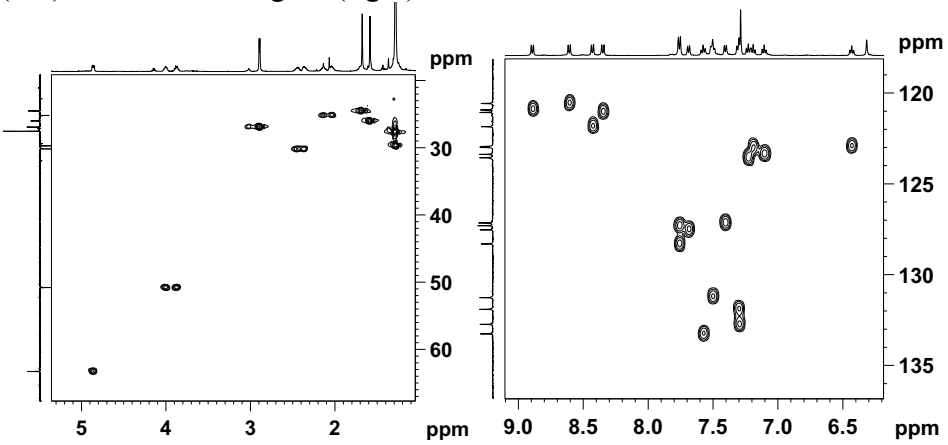

Figure 56. Partial HSQC spectra of hexapeptide **10g** (500MHz, $CDCl_3$): Aliphatic (left) and aromatic region (right).

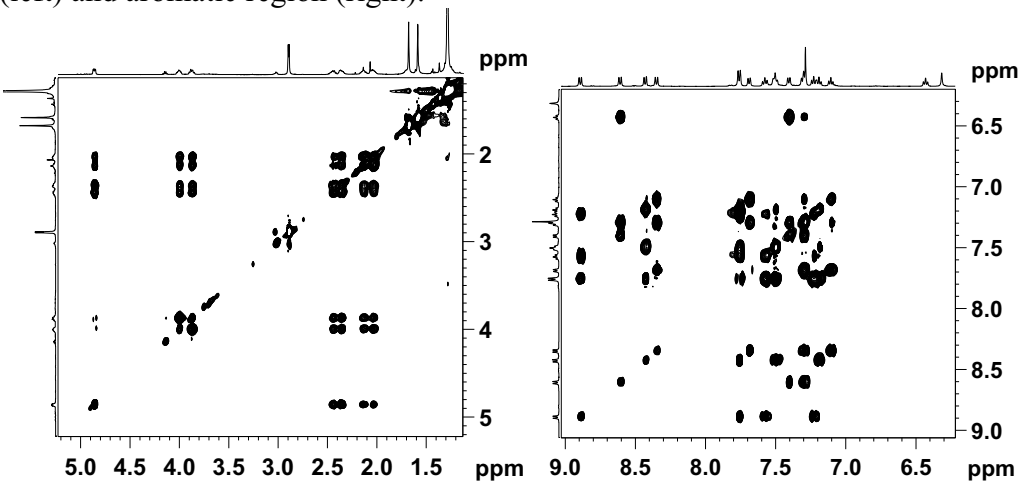

Figure 57. Partial TOCSY spectra of hexapeptide **10g** (500MHz, $CDCl_3$): Aliphatic (left) and aromatic region (right).

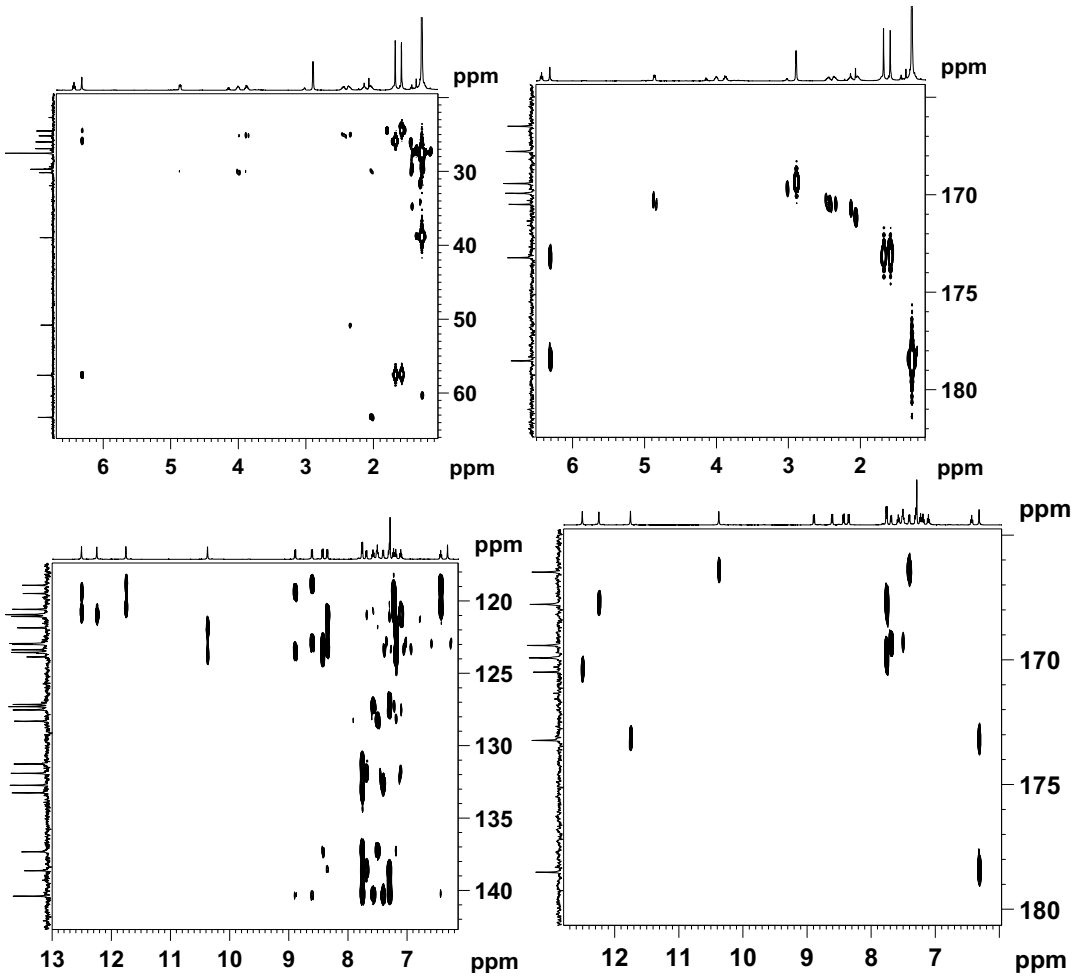

Figure 58. Partial HMBC (^{1}H-^{13}C) spectra of hexapeptide **10g** (500 MHz, $CDCl_3$): aliphatic **(a, b),** aromatic **(c,d)**.

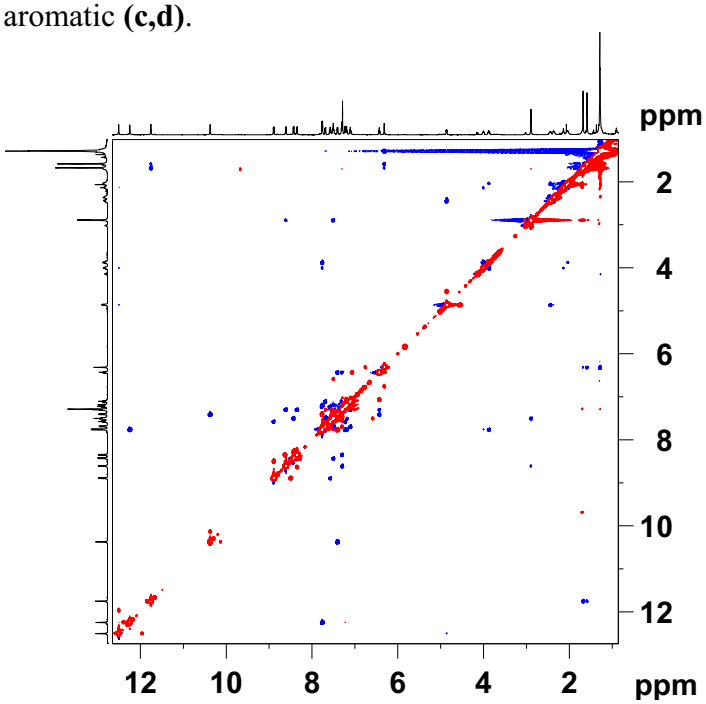

Figure 59. Full 2D NOESY spectrum of **10g** (500 MHz, $CDCl_3$).

2.16 References and Notes

(1) (a) Huc, I. & Cuccia, L. Foldamers Based on Local Conformational Preferences. in *Foldamers* 1-33 (Wiley-VCH Verlag GmbH & Co. KGaA, **2007**). (b) Horne, W.S.; Price, J. L.; Gellman, S.H. *Proc. Natl. Acad. Sci.* **2008**, *105*, 9151.

(2) (a) Gong, B. *Acc. Chem. Res.* **2012**. **DOI**: 10.1021/ar300007k. (b) Gonzalez-Rodriguez, D.; van Dongen, J. L. J.; Lutz, M.; Spek, A. L.; Schenning, A. P. H. J.; Meijer, E. W. *Nat. Chem.* **2009**, *1*, 151. (d) Etter, M. C. *Acc. Chem. Res.* **1990**, *23*, 120.

(3) (a) Klärner, F.-G.; Schrader, T. *Acc. Chem. Res.* 2012, 46, 967. (b) Waters, M. L. *Peptide Sci.* **2004**, *76*, 435. (d) Waters, M. L. *Curr. Opin. Chem. Bio.* **2002**, *6*, 736.

(4) (a) Kool, E. T. *Chem. Rev.* **1997**, *97*, 1473. (b) Jorgensen, W. L.; Pranata, J. *J. Am. Chem. Soc.* **1990**, *112*, 2008.

(5) (a) Erdmann, R. S.; Wennemers, H. *J. Am. Chem. Soc.* **2012**, *134*, 17117. (b) Erdmann, R. S.; Wennemers, H. *Angew. Chem., Int. Ed.* **2012**, *50*, 6835.

(6) Wimley, W. C. *Curr. Opin. Str. Biol.* **2003**, *13*, 404.

(7) (a) Kritzer, J. A.; Hodsdon, M. E.; Schepartz, A. *J. Am. Chem. Soc.* **2005**, *127*, 4118. (b) Liu, D.; Choi, S.; Chen, B.; Doerksen, R. J.; Clements, D. J.; Winkler, J. D.; Klein, M. L.; DeGrado, W. F. *Angew. Chem.*, *Int. Ed.* **2004**, *43*, 1158.

(8) Creighton, T. E. *Current Biology* **1995**, 5, 353.

(9) Hill, D. J.; Mio, M. J.; Prince, R. B.; Hughes, T. S.; Moore, J. S. *Chem. Rev.* **2001**, *101*, 3893.

(10) Garric, J.; Léger, J.-M.; Huc, I. *Angew. Chem., Int. Ed.* **2005**, *44*, 1954.

(11) (a) Gan, Q.; Ferrand, Y.; Bao, C.; Kauffmann, B.; Grélard, A.; Jiang, H.; Huc, I. *Science* **2011**, *331*, 1172. (b) Prabhakaran, P.; Priya, G.; Sanjayan, G. J. *Angew. Chem., Int. Ed.* **2012**, *51*, 4006.

(12) (a) Martinek, T. A.; Fulop, F. *Chem. Soc. Rev.* **2012**, *41*, 687. (b) Guichard, G.; Huc, I. *Chem. Commun.* **2011**, *47*, 5933. (c) Seebach, D.; Gardiner, J. *Acc. Chem. Res.* **2008**, *41*, 1366. (d) Chatterjee, S.; Roy, R. S.; Balaram, P. *J. R. Soc., Interface* **2007**, *4*, 587. (e) Horne, W. S.; Gellman, S. H. *Acc. Chem. Res.* **2008**, *41*, 1399. (f) Goodman, C. M.; Choi, S.; Shandler, S.; DeGrado,

W. F. *Nat Chem Biol* **2007**, *3*, 252. (g) Hill, D. J.; Mio, M. J.; Prince, R. B.; Hughes, T. S.; Moore, J. S. *Chem. Rev.* **2001**, *101*, 3893.

(13) (a) Zhang, D.-W.; Zhao, X.; Hou, J.-L.; Li, Z.-T. *Chem. Rev.* **2013**, *112*, 5271. (b) Li, Z.-T.; Hou, J.-L.; Li, C.; Yi, H.-P. *Chem. Asian J.* **2006**, *1*, 766. (c) Huc, I. *Eur. J. Org. Chem.* **2004**, *35*, 17.

(14) Kendhale, A.; Gonnade, R.; Rajamohanan, P. R.; Sanjayan, G. J. *Chem. Comm.* **2006**, *26*, 2756.

(15) Roy, A.; Prabhakaran, P.; Baruah, P. K.; Sanjayan, G. J. *Chem. Comm.* **2011**, *47*, 11593.

(16) (a) Brüggemann, J.; Bitter, S.; Müller, S.; Müller, W. M.; Müller, U.; Maier, N. M.; Lindner, W.; Vögtle, F. *Angew. Chem. Int. Ed.* **2007,** *46*, 254. (b) Feigel, M.; Ladberg, R.; Engels, S.; Herbst-Irmer, R.; Fröhlich, R. *Angew. Chem. Int. Ed.* **2006,** *45*, 5698.

(17) Hunter, C. A.; Spitaleri, A.; Tomas, S. Tailbiter: a new amide foldamer. *Chem. Comm.* **2005**, 3691.

(18) Ghosh, S.; Ramakrishnan, S. *Angew. Chem., Int. Ed.* **2004,** *43*, 3264.

(19) Delsuc, N.; Godde, F.; Kauffmann, B.; Le´ger, J.-M.; Huc, I. *J. Am. Chem. Soc.* **2007**, *129*, 11348.

(20) Cheng, P.-N.; Pham, J. D.; Nowick, J. S. *J. Am.Chem. Soc.* **2013**, *135*, 5477.

(21) Nowick, J. S.; Chung, D. M.; Maitra, K.; Maitra, S.; Stigers, K. D.; Sun, Y. *J. Am. Chem. Soc.* **2000**, *122*, 7654.

(22) Nowick, J. S. *Acc. Chem. Res.* **2008,** *41*, 1319.

(23) Gong, B. *Acc. Chem. Res.* **2012**, *45*, 2077.

(24) Yang, X.; Martinovic, S.; Smith, R. D.; Gong, B. *J. Am. Chem. Soc.* **2003**, *125*, 9932.

(25) Zeng, J.; Wang, W.; Deng, P.; Feng, W.; Zhou, J.; Yang, Y.; Yuan, L.; Yamato, K.; Gong, B. *Org. Lett.* **2011,** *13*, 3798.

(26) Cao, R.; Zhou, J.; Wang, W.; Feng, W.; Li, X.; Zhang, P.; Deng, P.; Yuan, L.; Gong, B. *Org. Lett.* **2010,** *12*, 2958.

(27) (a) Conn, M. M.; Rebek, J. *Chem. Rev.* **1997,** *97*, 1647. (b) Prins, L. J.; Reinhoudt, D. N.; Timmerman, P. *Angew. Chem., Int. Ed.* **2001,** *40*, 2382. (c) Cooke, G.; Rotello, V. M. *Chem. Soc. Rev.* **2002,** *31*, 275.

(28) Nelson, J. C.; Saven, J. G.; Moore, J. S.; Wolynes, P. G. *Science* **1997**, *277*, 1793.

(29) J.-M. Lehn, *Nature*, **2000,** *407*, 720.

(30) Zhao, Y.; Zhong, Z. *J. Am. Chem. Soc.,* **2005**, *127*, 17894.

(31) Lehn, J.-M.; Schmutz, M. *Chem.–Eur. J.,* **2000,** *6*, 1938.

(32) Salonen, L. M.; Ellermann, M.; Diederich, F. *Angew. Chem., Int. Ed.* **2011**, *50*, 4808.

(33) Gabriel, G. J.; Iverson, B. L. *J. Am. Chem. Soc.* **2002,** *124*, 15174.

(34) Zhang, W.; Horoszewski, D.; Decatur, J.; Nuckolls, C. *J. Am. Chem. Soc.* **2003**, *125*, 4870.

(35) (a) Sanchez-García, D.; Kauffmann, B.; Kawanami, T.; Ihara, H.; Takafuji, M.; Delville, M.-H.; Huc, I. *J. Am. Chem. Soc.* **2009**, *131*, 8642. (b) Sharma, G. V. M.; Chandramouli, N.; Choudhary, M.; Nagendar, P.; Ramakrishna, K. V. S.; Kunwar, A. C.; Schramm, P.; Hofmann, H.-J. *J. Am. Chem. Soc.* **2009**, *131*, 17335.

(36) (a) Choi, S. H.; Guzei, I. A.; Spencer, L. C.; Gellman, S. H. *J. Am.Chem. Soc.* **2009**, *131*, 2917. (b) Schmitt, M. A.; Choi, S. H.; Guzei, I. A.; Gellman, S.H. *J. Am. Chem. Soc.* **2006**, *128*, 4538.

(37) Gellman, S. H. *Acc. Chem. Res.* **1998**, *31*, 173.

(38) Guo, L.; Zhang, W.; Guzei, I. A.; Spencer, L. C.; Gellman, S. H. *Tetrahedron* **2012**, *68*, 4413.

(39) (a) Berlicki, Ł.; Pilsl, L.; Wéber, E.; Mándity, I. M.; Cabrele, C.; Martinek, T. A.; Fülöp, F.; Reiser, O. *Angew. Chem., Int. Ed.* **2012**, *51*, 2208. (b) Salwiczek, M.; Nyakatura, E. K.; Gerling, U. I. M.; Ye, S.; Koksch, B. *Chem. Soc. Rev.* **2012**, *41*, 2135. (c) Viso, A.; Fernandez de la Pradilla, R.; Tortosa, M.; Garcia, A.; Flores, A. *Chem. Rev.* **2011**, *111*, PR1. (d) Szakonyi, Z.; Fülöp, F. *Amino Acids* **2011**, *41*, 597. (e) Ramesh, V. V. E.; Roy, A.; Vijayadas, K. N.; Kendhale, A. M.; Prabhakaran, P.; Gonnade, R.; Puranik, V. G.; Sanjayan, G. J. *Org. Biomol. Chem.* **2011**, *9*, 367. (f) Roy, R. S.; Balaram, P. *J. Pep. Res.* **2004**, *63*, 279. (g) Johnson, S. W.; Jenkinson, S. F.; Angus, D.; Jones, J. H.; Watkin, D. J.; Fleet, G. W. J. *Tetrahedron: Asymmetry* **2004**, *15*, 3263. (h) Kotha, S. *Acc. Chem. Res.* **2003**, *36*, 342.

(40) Delsuc, N.; Godde, F.; Kauffmann, B.; Leger, J.-M.; Huc, I. *J. Am. Chem.Soc.* **2007**, *129*, 11348.

(41) Ramesh, V. V. E.; Priya, G.; Kotmale, A. S.; Gonnade, R. G.; Rajamohanan, P. R.; Sanjayan, G. J. *Chem. Commun.* **2012**, *48*, 11205.

(42) Prabhakaran, P.; Kale, S. S.; Puranik, V. G.; Rajamohanan, P. R.; Chetina, O.; Howard, J. A. K.; Hofmann, H.-J.; Sanjayan, G. J. *J. Am. Chem. Soc.* **2008**, *130*, 17743.

(43) (a) Hamuro, Y.; Geib, S. J.; Hamilton, A. D. *J. Am. Chem. Soc.* **1997**, *119*, 10587. (b) Hamuro, Y.; Geib, S. J.; Hamilton, A. D. *J. Am. Chem. Soc.* **1996**, *118*, 7529.

(44) (a) MacArthur, M, W.; Thornton, J. M. *J. Mol. Biol.* **1991**, *218*, 397. (b) Hurley, J. H.; Mason, D. A.; Matthews, B. W. *Biopolymers* **1992**, *32*, 1443.

(45) Chatterjee, B.; Saha, I.; Raghothama, S.; Aravinda, S.; Rai, R.; Shamala, N.; Balaram, P. *Chem. – Eur. J.* **2008**, *14*, 6192.

(46) (a) Deng, S.; Taunton, J. *J. Am. Chem. Soc*. **2002**, *124,* 916. (b) Nagel, M.; Kuemin, Y. A.; Schweizer, S.; Monnard, F. W.; Ochsenfeld, C.; Wennemers, H. *Angew. Chem. Int. Ed.* **2010**, *49*, 6324.

(47) S. M. El Rayes, I. A. I. Ali and W. Fathalla, ARKIVOC **2008**, *9*, 86.

(48) (a) Thorat, V. H.; Ingole, T. S.; Vijayadas, K. N.; Nair, R. V.; Kale, S. S.; Ramesh, V. V. E.; Davis, H. C.; Prabhakaran, P.; Gonnade, R. G.; Gawade, R. L.; Puranik, V. G.; Rajamohanan, P. R.; Sanjayan, G. J. *Eur. J. Org. Chem.* **2013**, *2013*, 3529. (b) Ref. 41.

(49) (a) Woody, R. W. *Methods. Enzymol.* **1995**, *246,* 34. (b) Greenfield, N. J. *Encyclopedia of Spectroscopy and Spectrometry*, **2009,** *130*, 153. (c) Eliel, E. L.; Wilen, S. H. "*Stereochemistry of Organic Compounds*" (Wiley, **1994**), 1000.

(50) (a) Kawamoto, T.; Hammes, B. S.; Haggerty, B.; Yap, G. P. A.; Rheingold, A. L.; Borovik, A. S. *J. Am. Chem. Soc.* **1996**, *118*, 285. (b) Huang, B.; Parquette, J. R. *J. Am. Chem. Soc*. **2001**, *123*, 2689.

(51) Tatko, C. D.; Waters, M. L. *J. Am. Chem. Soc.* **2002**, *124*, 9372.

(52) (a) Mathias, J. P.; Simanek, E. E.; Whitesides, G. M. *J. Am. Chem. Soc.* **1994**, *116*, 4326. (b) Damodaran, K.; Sanjayan, G. J.; Rajamohanan, P. R.; Ganapathy, S. Ganesh, K. N. *Org. Lett.* **2001**, *3*, 1921.

CHAPTER 3

Local Restraints in Conformational Proclivity of Peptides

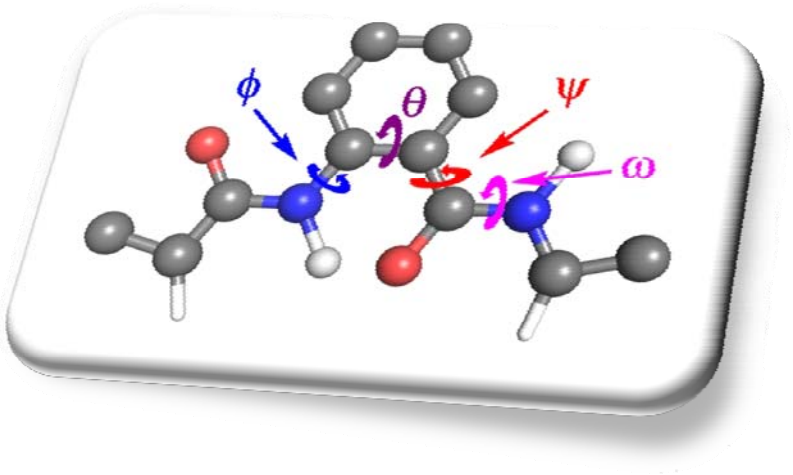

This chapter discusses a few instances where the local constraints of individual amino acids primarily contribute towards the conformational bias of the peptide chain. The first section deals with the investigations of the conformational behavior of -Aib-Ant-Pro- oligomer, in an effort to evaluate the effect of addition of constrained amino acid like "Aib" around the robust Ant-Pro motif. En route, peptide coupling related synthetic challenges were tackled by activation of the major side product: "benzoxazinone". The associated section features mild and successful amide bond formation using (thio)urea as catalyst. The subsequent section of the chapter also attempts to understand the role of local constraints through the conformational bias by swapping of the carboxamide with sulphonamide bond in certain peptide sequences.

"Science has nothing to do with any dogma. Science ceases to exist when there is a dogma."

— Jean-Marie Lehn

3.0 Preamble

The local (dihedral) constraints of individual amino acids contribute significantly towards orchestrating the structural architecture of peptide chains. Dihedral angles in a peptide backbone *viz*. ϕ, ψ, ω, describes rotation about the N-C(α), C(α)-C(O) and C(O)-N, respectively between three repeating bonds C(O)-N-C(α)-C(O), which are the main descriptors of local conformation. Although, the torsional parameters of individual amino acid define the relative orientation of the residues connected by the peptide backbone, they also significantly get influenced by the structural features, identity and conformational preferences of its adjacent residues.[1] Therefore, an accurate prediction of a protein's full three-dimensional structure from the given sequence of amino acids still remains as a formidable challenge for a structural biologist, as often modulated geometric preferences give rise to totally unprecedented assemblies. In order to simplify the understanding of peptide structuring phenomenon, diverse combinations and rearrangements of different natural/unnatural building blocks with distinct structural constraints has widened the scope of designing and developing novel molecular architectures. This exercise permits us to rationally identify the structure and function of biopolymers in depth.[2] The knowledge of stereochemical constraints of each residue not only assists us in achieving the desired molecular arrangement, but also increases our awareness about the synthetic hurdles faced during its synthesis. Though various ways to tackle the peptide related synthetic challenges have been formulated, there are still areas left unexplored.

Heterogeneity in peptide backbones has become a consistent practise in the area of foldamers.[3] Work carried out herein too is focussed towards development of heterogeneous aliphatic-aromatic hybrid peptides. This chapter deals with design, synthesis and investigations of structural characteristics of few peptide motifs featuring dissimilar conformationally constrained amino acids. Also, a part of the chapter discusses conformational outcome on swapping linkage form carboxamide to sulphonamide, which feature strikingly different hydrogen-bonding and geometrical preferences. Another facet of this work is related to resolving peptide coupling related synthetic challenges posed due to the formation of the undesired side product benzoxazinone, which emerges while synthesizing 2-(substituted amido)benzamides from *o*-aminobenzoic acid, using (thio)urea-mediated organocatalysis.

SECTION-I

Conformational Preferences of (Aib-Ant-^{L}Pro)$_n$ Hybrid Repeats

3.1 Conformational inclination of building blocks

Different amino acids possess fundamental proclivity to adopt helix or sheet structure depending on their dihedral restraints. The secondary structure propensity of peptides is well accounted in the form of Ramachandran maps (ϕ, ψ scatter plots) and Chou-Fasman parameters.[4] The torsional angle constraints are defined for each amino acid *i.e*. bond angle N-Cα-C can slightly change than its usual tetrahedral angle 109° in order to accommodate other strains in the structure.

The synthetic analogues of natural oligomers constructed utilising unnatural building blocks and their applications in peptide-based therapeutics have attracted great curiosity over decades. In order to improve the practical utility of peptides as drugs, enormous modifications of α-amino acids by several research groups has led to creation of a range of complex abiotic building blocks (refer chapter 1, Figure 3).[5]

Local conformational preferences are confined in case of aromatic building blocks wherein, the hybridisation in the aromatic residues stabilise the dihedral angles and restrict the peptide chain to a fixed orientation. Occasionally the non-covalently bound substituent rigidifies the structure and prefixes the structural pre-organisation.[6] This makes them tunable in comparison to its aliphatic counterparts with a rotationally restricted θ torsion angles (Figure 1).

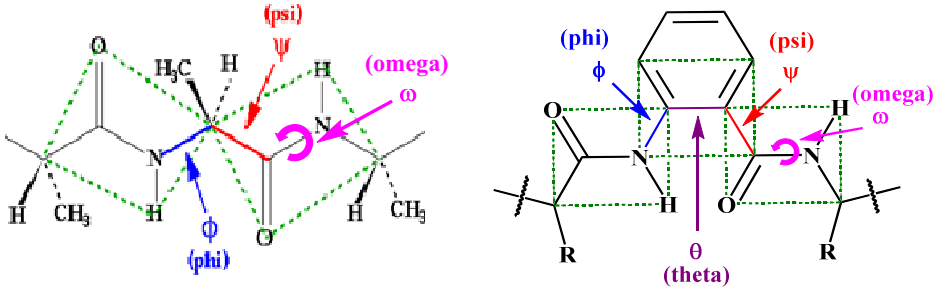

Figure 1: Peptide units defining the backbone torsion angles at α-amino acid residue (left) and *β*- aromatic amino acid residue (right) in a polypeptide chain.

Aromatic *homo*- and *hetero*-peptides too have been very well explored by various groups in the last two decades and a collection of shape persistent molecular structures have been produced.[7] Aromatic *homo*-oligomers exist in diverse secondary structures resembling strands as zig-zag ribbons,[8] or folded helices[9] *etc* by virtue of its

intrinsic hybridization induced planarity and locked dihedral angles. *o*-, *m*-, or *p*-substituted amino benzoic acid are the widely utilized among the aromatic amino acids, which have been used to generate a variety of structures like strands,[10] crescents and macrocycles,[11] *etc*. Substitution of groups like -OR, -F, -N *etc.,* deliver additional conformational rigidification to the aromatic amino acid residues as they act as H-bonding acceptors.[12] Many times, the kinks arising from aromatic amino acid residues can modulate the tuning of the curvature. [13] Recently, the concept of conformationally rigid two-dimensional aromatic frameworks is blossoming well, as they are rather conformationally ordered and often produce intriguing frameworks.[14]

3.2 Practice of heterogeneity in peptides and their implications in foldamers

Heterogeneity among peptides has been excercised with α-amino acids since long time, which can be clearly evidenced from Toniolo's work published in the early 1990s based on Aib-Pro repeats.[15] Proline oligomers (Figure 1A) are known to adopt compact PPI/PPII helical structures, totally devoid of any intramolecular H-bonding association. Aib (α-amino isobutyric acid) oligomers, on the contrary, adopt a highly compact 3_{10} helical structure (Figure 1B). However, their hybrid oligomer (Figure 1C) shows repeat β-bend conformation – a structural feature which is in stark contrast to the conformation of its corresponding homo-oligomers.

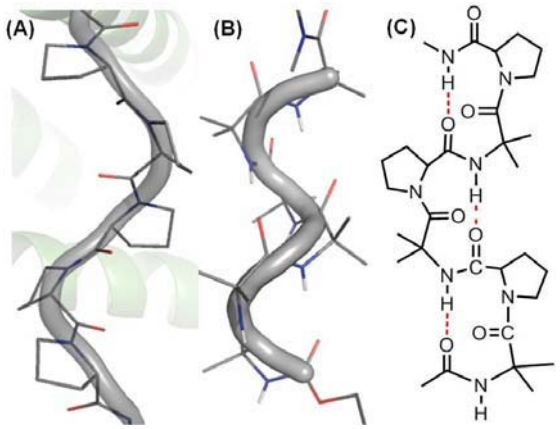

Figure 2. Crystal structure of PPII helix present in tetramerisation domain of acetylcholineesterase (pdb: 1VZJ) (A), crystal structure of Cbz-$(Aib)_6$-NHBn[16] (B), and the molecular structure of $(Aib\text{-}Pro)_n$ (C). Some atoms are omitted for clarity.

However, the introduction of the flexible α- amino acid residues and their homologated partners into natural peptide sequences introduces potential disparity into the peptide secondary structures wherein, helices with unusual number of atoms or mixed helices are very often obtained.[17]

3.3 Aliphatic-Aromatic foldamers

The addition of the characteristics of flexible aliphatic residue with rigid aromatic residues often results in unique structural architectures. Conjoining with aromatic planar aromatic residue, aliphatic amino acids offer directionality by virtue of its torsional restraints and chirality. In recent times, various interesting structures like knots, [18] tail biters,[19] pillars[20] *etc.,* have been reported using aliphatic-aromatic conjugates.

The folding propensities of oligomers get heavily modulated due to the adjacent residue in peptide chain. Introduction of aromatic amino dimethoxy benzoic acid (Adb) unit into Toniolo's Aib-Pro sequence abolished its periodic β-bend ribbon conformation and resulted in the formation of a very distinct helical secondary structure, displaying repeated β-turn network (Figure 3).[21] Another curious case is of the self-assembled sheet-like structures formed from Aib-Amb (3-amino-5-bromo-2-methoxy benzoic acid) repeats *via* extensive intermolecular hydrogen bonding interactions from the backbone amide groups.[22] The observation is in stark contrast to the general characteristic of Aib, a well-known sheet breaker, with conformation restraints largely lying in the region $\varphi = \pm 60°$ and $\psi = \pm 30°$. Not only it is possible to mimic helices or sheets, but also macrocycles have been obtained employing aliphatic-aromatic amino acid conjugates.

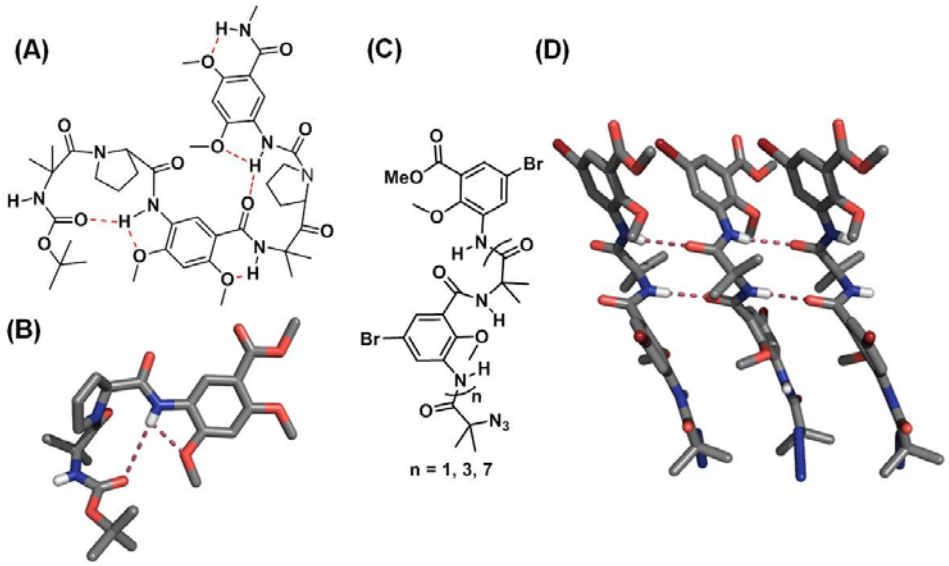

Figure 3. Molecular structure of Boc-Aib-Pro-Adb-Aib-Pro-Adb-NHMe oligomer (a), crystal structure of the monomer unit Boc-Aib-Pro-Adb-OMe (b), structure of Aib-Amb hybrid oligomer (c), and H-bond-mediated self-assembled structure of -Aib-Amb- tetramer (capped stick representation) (d).

Aliphatic amino acid like proline possesses strong conformational tendency to induce folding. Combining aromatic γ-amino acid like amino pyridine carboxylic acid with Proline resulted in the formation of macrocycle which displayed ionophoric properties as reported by Goddard *et al*.[23] Also, C_2 symmetric small and large bowls have been designed by Akazome and group using anthranilic acid and α-amino acid like leucine stabilised by bifurcated H-bonding interaction between the two anthranilic acid residues.[24]

3.4 Objective of the work

With the knowledge of the unprecedented folding and variable geometric tendencies of amino acids, our objective was to investigate the mutual effect of individual torsional preference on the overall conformational disposition in -Aib-Ant-^{L}Pro- unit repeats. Along these lines, we attempted to realize the structural influence of a constrained amino acid like Aib at the N-terminus of Ant-^{L}Pro motif and its repeats. The possible H-bonding contacts in -Aib-Ant-^{L}Pro- repeats are represented in figure 4.

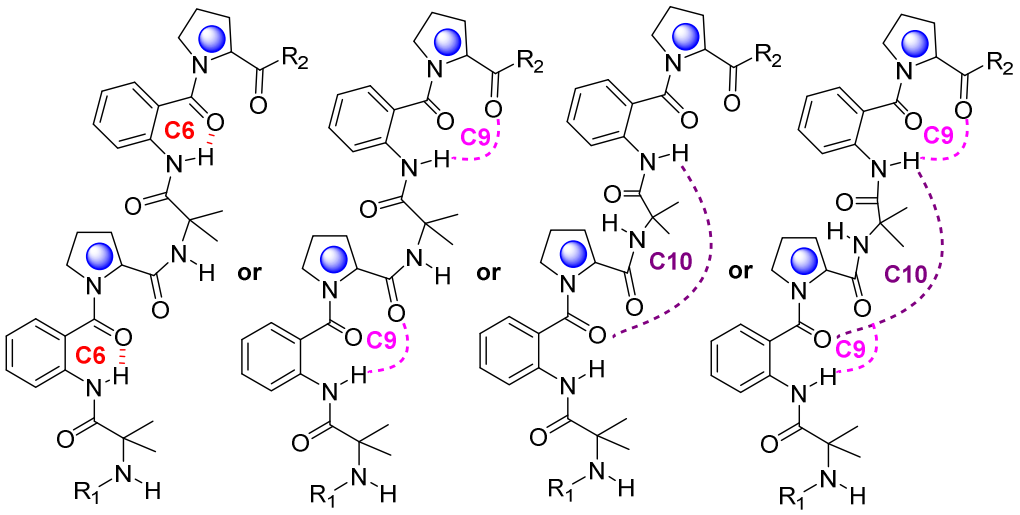

Figure 4: Designed oligomer representing plausible H-bonding patterns in R_1-(-Aib-Ant-^{L}Pro)$_2$-R_2

3.5 Design strategy

Ant-Pro motif is a robust reverse-turn inducer that forms a closed nine-membered H-bonding network involving just two amino acids (*pseudo-β*-turn)[25], which is shown to tolerate diverse structural and chirality perturbations in-and-around the turn

segment. On the other hand, (^{L}Pro-Aib)$_n$ (n = 3,4) sequential repeats are identified to adopt a right handed β-bend ribbon spiral structure,[15] stabilized by *intra*-molecular repeating 10-membered H-bonds, as reported by Toniolo *et al*. In addition to these, the inherent strong six-membered intra-residual hydrogen bonds in anthranilic acid also are estimated to compete with the other H-bonding networks.[26] Thus, a sequential repeat of -Aib-Ant-^{L}Pro- unit is anticipated to reveal one or more type of hydrogen-bonding patterns, on strategically placing the residues adjacent to each other (Figure 5). With these concepts in mind, we designed and developed -(Aib-Ant-^{L}Pro)- repeats.

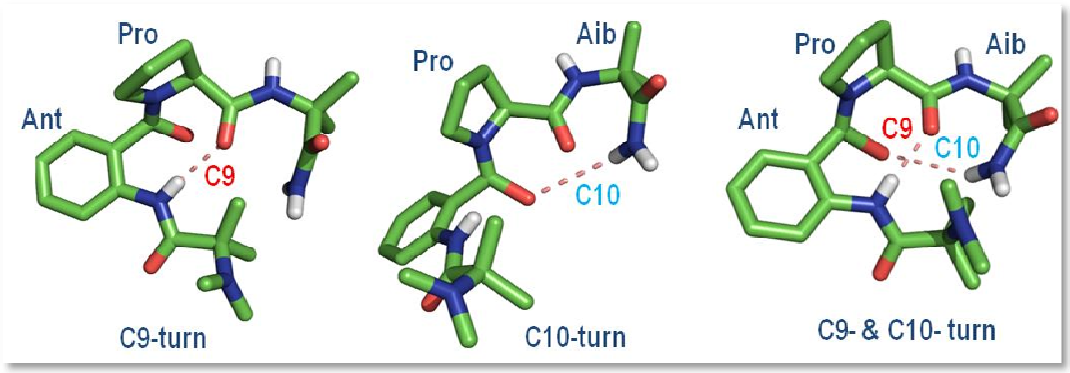

Figure 5: PyMOL generated models of plausible H-bonding patterns in R_1-(Aib-Ant-^{L}Pro)$_2$-R_2 showing: nine-membered H-bonding network formed by Ant-Pro motif (a), ten-membered H-bonding network formed between Pro-Aib (b), and simultaneous nine- and ten- membered H-bonding network (c).

3.6 Synthesis

Synthesis of the monomer unit was initiated by reacting α-bromoisobutyryl-bromide with anthranilic acid that afforded **2a**. Subsequently, bromo- functionality of **2a** was replaced to corresponding azide derivative **2b**. Its corresponding acid was prepared by cleaving ester group of **2c**. Several coupling attempts to attain trimer unit **3a** from **2c** suffered from poor yields because of formation of benozoxazinone as major side product.

After numerous efforts involving coupling agent and solvent variations, trimer unit **3a** was isolated with improved yield of 65% by coupling acid **2c** with HN-^{L}Pro-OBn using TBTU and DIEA in THF. Later for oligomerisation, azide group of **3a** was reduced to corresponding amine **3c** and the corresponding acid

counterpart **3b** generated was coupled using TBTU and DIEA in DCM to afford **4a** in 72% yield. **4a** was then converted into its corresponding methylamide derivative **4b**, which was isolated as fluffy white solid, by treating it with methanolic methylamine solution.

Scheme 3.1. Synthesis of hexapeptides **4a**,**b**

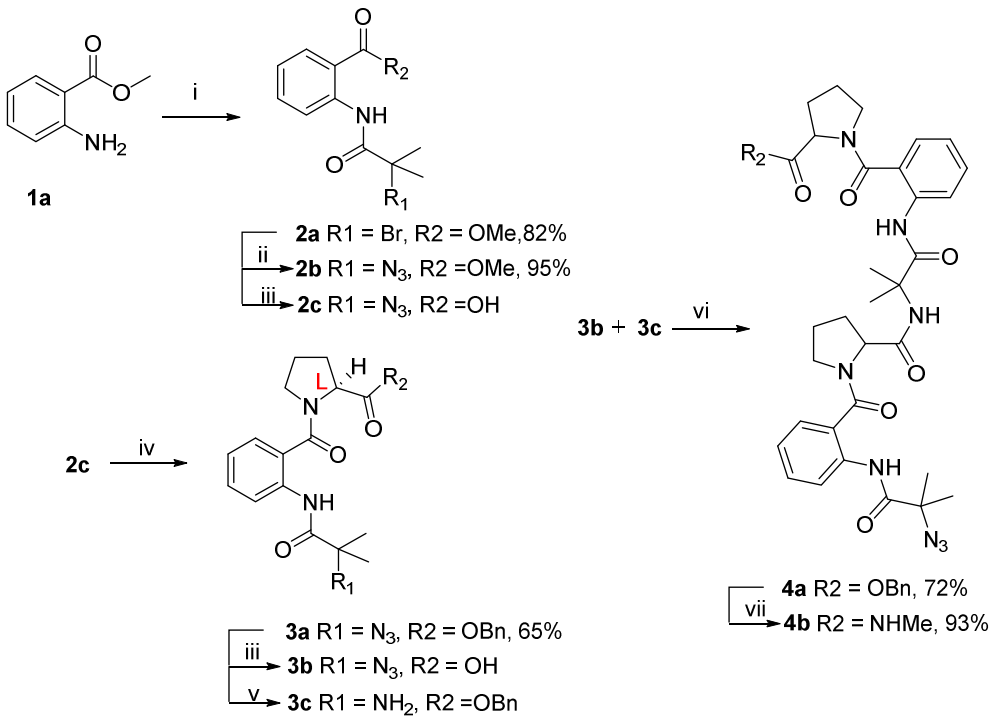

Scheme 1: *Reagents and conditions:* (i) α-bromo isobutyrylbromide, DIEA, DCM, 1h; (ii) NaN_3, LiCl, DMSO, 80 °C, 12h; (iii) $LiOH.H_2O$, MeOH, 12h; (iv) HN-^{L}Pro-OBn, TBTU, DIEA, THF, 12h; (v) PPh_3, MeOH, 2h; (vi) TBTU, DIEA, DCM, 12h; (vii) $MeNH_2$, MeOH, 1h.

3.7 Conformational analysis

The difficulty in crystal formation prompted us to investigate its conformation features employing solution-state studies.

3.7.1 NMR studies

NMR studies of the hexamer derivatives posed serious challenges due to the poor solubility and aggregation. The phenomenon of aggregation is well known to cause complications in solution-state investigations.[27] ^{1}H NMR spectrum revealed multiple set of signals in different concentrations in $CDCl_3$ (Figure 6). This can be attributed

to the existence of multiple conformations in solution-state due to exposed amide NHs that associat *inter*-molecularly and/or absence of any specific *intra*-molecular hydrogen bonding network in the peptide motif.[28]

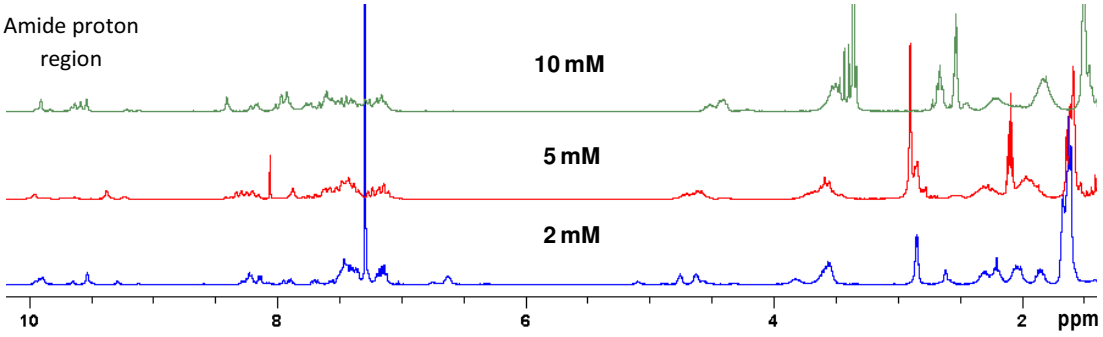

Figure 6: ^{1}H NMR spectral overlay of peptide **4b** at different concentrations in $CDC1_3$ (295 K, 400 MHz).

Variable temperature studies in $CDCl_3$ demonstrated the merging of signals and broadening of the peaks at higher temperatures (Figure 7). This observation confirmed the presence of multiple conformation of the peptide that gets arrested at lower temperatures.

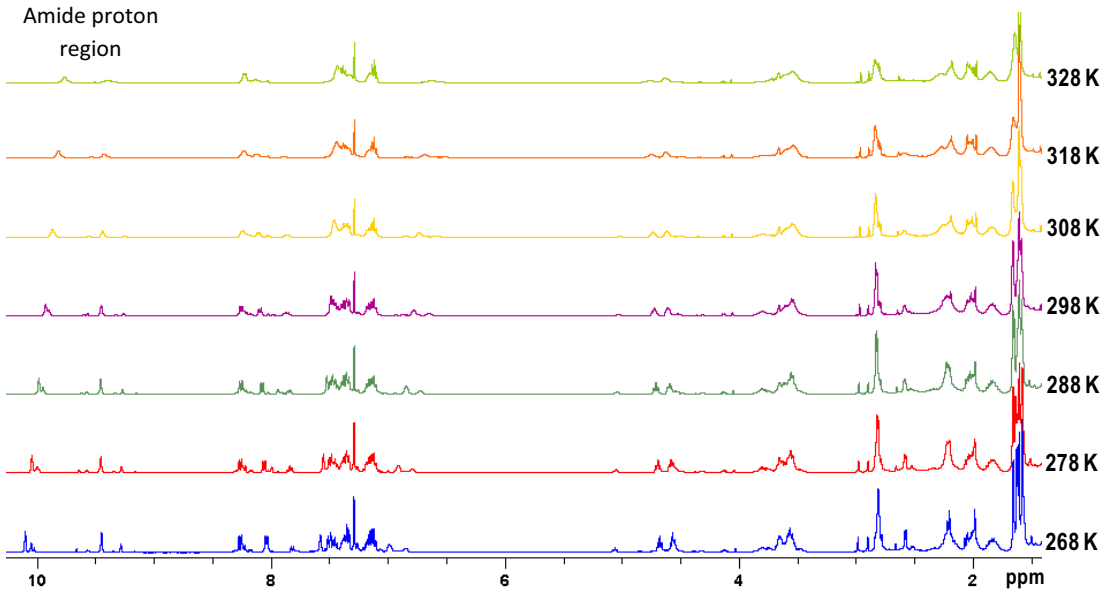

Figure 7: ^{1}H NMR spectral overlay of peptide **4b** at different temperatures (268-328 K).

Even when ^{1}H-NMR spectrum was recorded in polar solvents like acetone-d_6 and DMSO-d_6, similar characteristics with comparable patterns were observed due to signal multiplication (Figure 8). Good signal dispersion was not obtained in any of

the solvents. This created hurdles in structure elucidation *via* 2D-NMR and other solution-state studies.

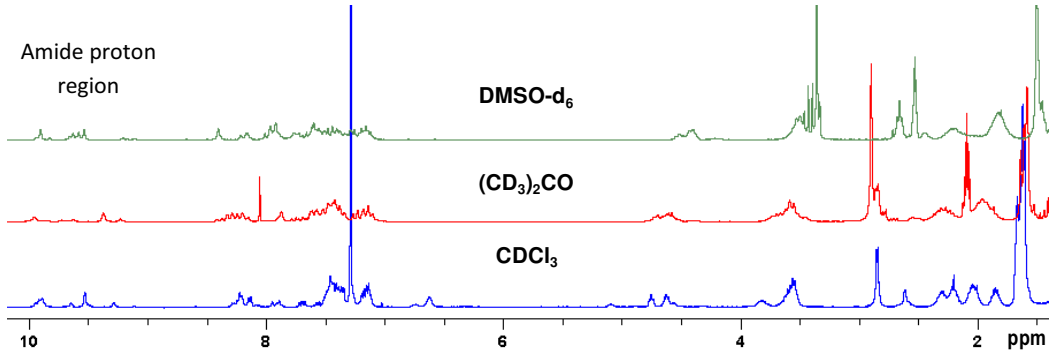

Figure 8: ^{1}H NMR spectral overlay of peptide **4b** in different solvents (295 K).

3.7.2 CD studies

CD spectrum recorded in acetonitrile revealed negative absorption ca. 190 nm, zero crossing at around 210 nm which ended at maxima around 217 nm. A strong negative absorption peak about 245 nm was observed, owing to the backbone aromatic electronic transitions in the oligomer.

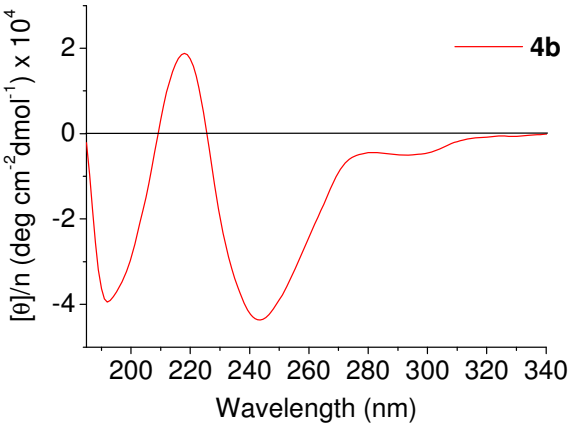

Figure 9: Representative CD spectrum of peptide **4b**. Spectrum was recorded at 293 K with a concentration of 0.1 mM in acetonitrile.

3.8 Conclusions

Oligomers of -(Aib-Ant-^{L}Pro)- sequence presumably adopt intermolecularly hydrogen-bonded extended conformations in both non-polar and polar solvents. This effect could be attributed to the presence of solvent exposed amide NHs available for intermolecular H-bonding association.

SECTION II

(Thio)urea-Mediated Benzoxazinone Opening: Mild Approach Towards Synthesis of 2-(acylamido)benzamides

3.9 Hassles in peptide synthesis

One of the major problems posed during carbonyl activation of α-amino acids generally during peptide coupling, is the immediate formation of side products like N-carboxyanhydride, diketopiperazine *etc*. This very often results in racemisation or degradation of the reactant/product, leading to difficulty in purification or drastic reduction in the yield of coupled product.[29] A very common cause of racemisation in peptides is the formation of the oxazolone intermediate when the terminal acid, which when reacts with a nucleophile, results in shuffling of the chiral centre. 1,3-benzoxazinone moiety is one such class of side products, which is quite often encountered while dealing with C-terminal segment activation of anthranilic acid derivatives. Benzoxazinones are formed due to the *intra*-molecular cyclization of the benzamide oxygen, which usually results in trace or no coupling in acylanthranils (Figure 10).[30] This generally forces the oligomerisation of synthetic peptides *via* reaction of N-terminus employing only mild conditions.

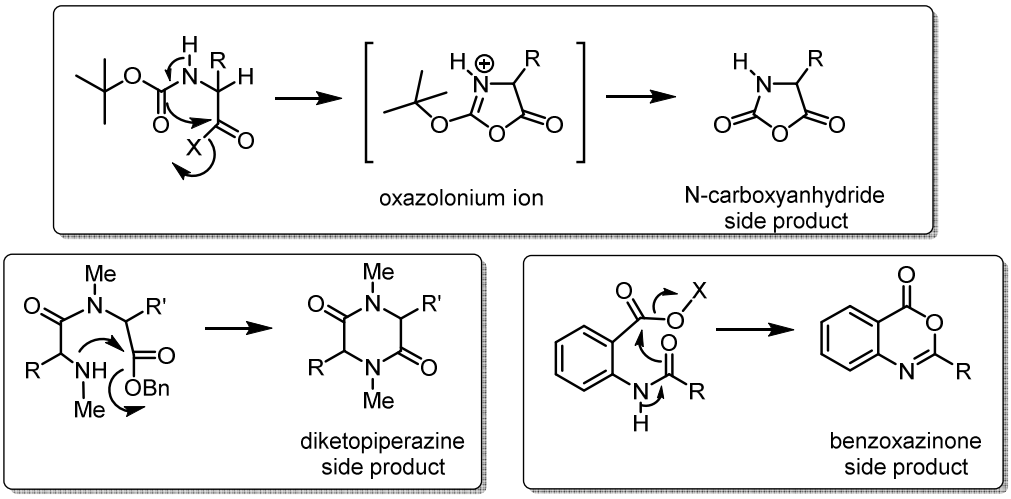

Figure 10: Mechanisms of formation of different side products in coupling reactions.

Detailed investigations about various acylanthranils were carried out by Errede *et al*. in the late 1970s. They explored stability of oxazinone moeity,[31] influence of steric factors on reactivity with amine, and different crucial factors responsible for the amide bond formation. Role of solvent was found to be one of the

very critical factors in the reaction pathway where, polar solvents were found to disfavour the amide bond formation. Also, the electron donating groups were shown to inhibit acetamidine intermediate formation that led to the formation of desired amide bonds.[32] With the literature precedence, and the knowledge about oxazinone reactivity, we set out to explore possibilities to achieve coupling by means of activation of benzoxazinone moiety.

3.10 Strategies meant to circumvent coupling side products

Side products obtained from the α-amino acid activation and the problems due to recemisation have been successfully addressed by development of numerous mild coupling reagents in past few years.[29] Strategies meant either to avert the formation of benzoxaninones *in situ* or to react it with the amine have been attempted in several ways, like heating with the reactants at elevated temperatures[33] and in presence of bases like pyridine, facilitating amine activation[33e] - but the former case often leads to quinozoline formation. So far, no strategies have been recognized meant to achieve coupling of aliphatic amino/imino acids with benzoxazinone moeity. Our group formerly utilized DBU as base and has successfully achieved coupling in different cases.[34] However, this strategy has not been consistent with certain systems. This prompted us to further explore different routes to achieve better coupling, thus we opted carbonyl activation method to achieve benzoxazinine activation and coupling with amines.

3.11 Activation of carbonyl group: (Thio)urea-mediated organocatalysis

(Thio)urea is a class of catalysts that utilizes *privileged explicit double hydrogen-bonding interactions* for substrate activation.[35] Schreiner's *N,N′*-bis[(3-fluoromethyl) phenyl]thiourea is a creditable achievement in this area because of requirement of low catalyst loading[36] and high competence.[37] The (thio)urea derivatives bear rigid hydrogen-bonding sites between the positively polarized *ortho* hydrogen atom and the Lewis-basic thiocarbonyl sulphur and the electron-deficient -CF_3 substitution at *meta*- or *para*- position of the phenyl ring (Figure 11). Schreiner's (thio)urea is stable in air and is water compatible.[38] Since its emergence, enhancement in reaction rates of numerous reactions was obtained like: Claisen rearrangements, Morita-Baylis-Hillman,[39] Diels-Alder and cycloaddition reactions *etc*.[40]

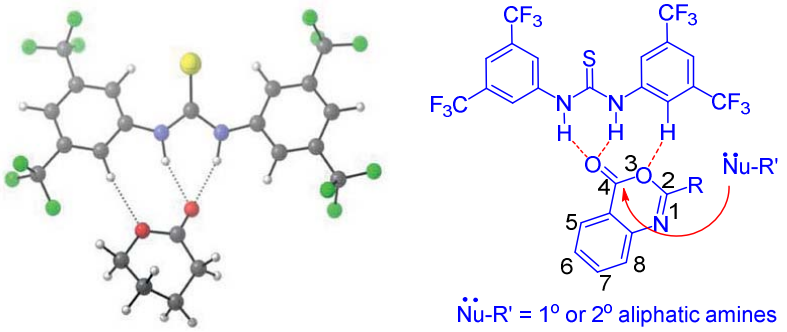

Figure 11: Binding interactions involving highly polar NH protons and *ortho*-protons with Lewis bases (left) and schematic representation of thio(urea)-mediated activation and nucleophilic attack (right).

Thiourea catalysts are synthetically accessible and act as modular catalysts for many organic reactions like Strecker synthesis, Mannich, Henry, Micheal reaction,[42] *etc*.[43] Also, this catalyst has been recently used as an agent for dynamic kinetic resolution of azlactones.[44] This further encouraged us to pursue the carbonyl activation of benzoxanzione carbonyl functionality, which was anticipated to facilitate attack of the nucleophile at its 4th position and achieve coupled product (Figure 11).

3.12 Objective of the work

As mentioned in the previous section of the chapter, several attempts made to couple N_3-Aib-Ant-OH with HN-^{L}Pro-OBn led to meagre yields of the product due to the formation of the [1,3]-benzoxazinone as prominent side product. In order to activate the benzoxazinone moiety and to increase yield of coupled products, various attempts were made including Lewis acid catalysis. Schreiner's (thio)urea involving explicit non-covalent double hydrogen-bonding donor based organocatalysis provided best results (Figure 12).

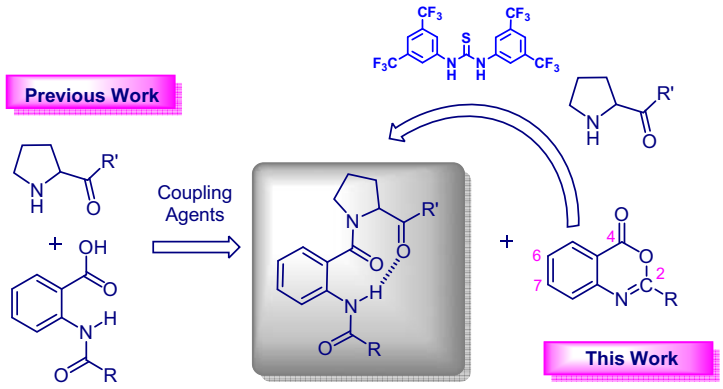

Figure 12: Schematic representation of the possible routes to achieve synthesis of *o*-(substituted amido)benzamide from 2-amino benzoic acid.

3.13 Synthesis

Syntheses of oxazinones employed for coupling were achieved by activation of the corresponding *o*-amino substituted anthranilic acids i.e. dipeptide analogues.

Scheme 3.2: Synthesis of oxazinones **5a-e**

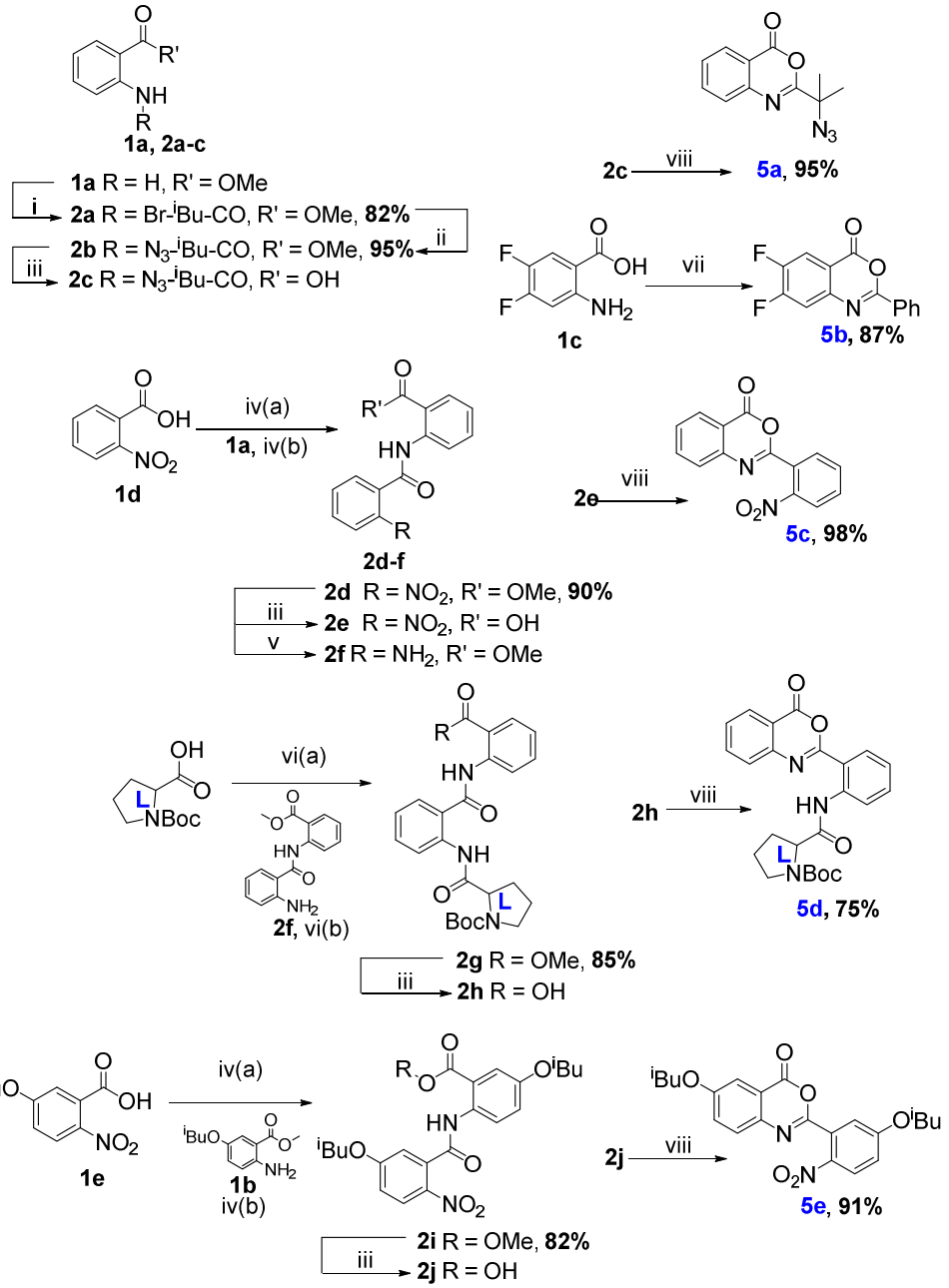

Scheme 2: *Reagents and conditions:* (i) α-bromo isobutyrylbromide, DIEA, DCM, 1h; (ii) NaN_3, LiCl, DMF, 0 °C - rt, 6h; (iii) aq. LiOH, MeOH, rt, 4 h; (iv) (a) $(COCl)_2$, DMF, DCM, 0 °C, 15 min. (b) 0 °C - rt, 1h; (v) Pd/C, H_2, 60psi, DMF, 6h; (vi) (a) ClCOOEt, Et_3N, THF, 0 °C - rt (b) 0 °C - rt- reflux, 6h; (vii) PhCOCl, Et_3N, 0 °C – rt, 4h; (viii) EDC.HCl, DCM, 0 °C - rt, 4h.

Oxazinones **5b** and **5c** were synthesized as per the reported procedure.[45,26] Oxazinone **5d** was synthesized in the similar way as given in chapter 2, **scheme 2.1**. Building block for **5a** i.e. acid **2c** was obtained as described in chapter 3, **scheme 3.1**. **2a** was activated using EDC.HCl in DCM to afford **5a** in 95% yield. Oxazinone **5e** was obtained by activation of its corresponding acid **2j**, which was obtained from **2i** by coupling 5-isobutyl-2-nitrobenzoic acid **1b** and methyl 2-amino-5-isobutylbenzoate **1e**.

3.14 Results and Discussion

Optimisation of catalyst loading and solvent to accomplish efficient coupling reaction has been discussed in the former segment of this section, and the latter part enlists its application to distinct oxazinones and amines.

3.14.1 Optimisation of solvent and catalyst loading

Our initial investigations began with the endeavours to achieve coupling of 2-(2-azido-2-methylpropanamido)benzoic acid with HN-^{L}Pro-OBn, as direct coupling furnished **6a** only in meagre yields. The by-product 2-(2- azidopropan-2-yl)-2H-benzo[d][1,3]oxazin-4-one **5a** was isolated by EDC.HCl-mediated activation of corresponding acid **2c**. Trials to activate the oxazinone and to facilitate nucleophilic attack at desired position, different conditions were attempted. In one of the trials, we refluxed oxazinone **3a** in toluene in the presence of amine H-^{L}Pro-OBn, but reaction underwent only partial conversion. Microwave assisted opening was also attempted in toluene and acetonitrile as solvents at 525W for 4 min, which afforded only trace conversion was observed. Lewis acid-catalysed carbonyl activation was also undertaken using $Ti(OiPr)_4$ and $Sc(OTf)_3$, but no coupling was observed.

Then, we diverted our attention towards Schreiner's (thio)urea organocatalyst that provides explicit non-covalent double hydrogen-bonding for effective carbonyl activation. To our surprise, completion of reaction was observed with mere 10% of catalyst loading in different solvents with no racemisation and without formation of any by-products. The reaction was then carried out in a range of solvents like toluene, DCM, acetonitrile, THF, DMF, DMSO, water *etc* (Table 1). Rate of the reaction revealed solvent polarity dependence, making polar solvents to be a better bet as it followed a trend: DMSO>DCM>toluene. However, contradictory to the

expectations, the reaction failed to reach completion in solvents like DMF, acetonitrile, THF *etc*. even on prolonged reaction time. The optimisation revealed DMSO to be the best solvent which provided best yields with just 10 mol% of the catalyst in 24h. Reaction was also carried out in water in which complete conversion was not achieved in similar time period, but, after 48 h, the product was isolated with improved yield of 67%. Same reaction carried out in slightly elevated temperature showed yield reduction, proving the optimum reaction temperature to be 25 °C in water as solvent.

Table 1. Organocatalytic ring opening of 2-(2-azidopropan-2-yl)-2H-benzo[d] [1,3]oxazin-4-one **5a** (1 equiv.) with H-^{L}Pro-OBn (1.5 equiv.).

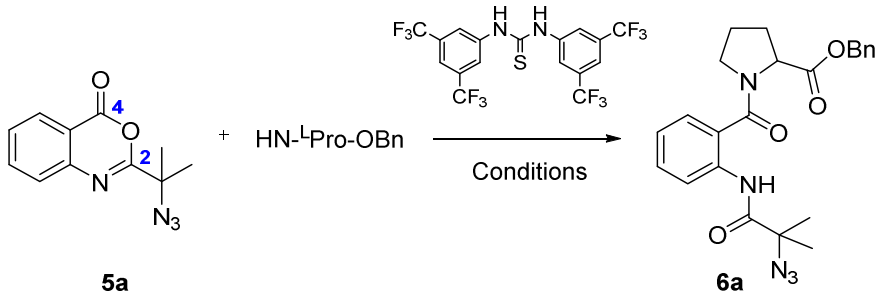

5a **6a**

	Catalyst (mol%)	Solvent	Time (h)	Inference Product (%)[a,c]
1	0	DMSO	24	0
2	10	DCM	36	76
3	10	Toluene	36	65
4	10	THF	48	30[c]
5	10	DMF	48	40[c]
6	10	ACN	48	36[c]
7	10	H_2O[d]	24	53
8	10	H_2O	48	67
9	5	DMSO	24	71
10	10	DMSO	0.5	48
11	**10**	**DMSO**	**24**	**81**
12	15	DMSO	24	79

[a]Yield refers to the column-purified product. [b]Unless specified, reaction was carried out at room temperature (25 °C). [c]Conversion calculated from NMR of crude reaction mixture (see experimental section, page 318-320). [d]Reaction was carried out at 40 °C.

3.14.2 Reactivity pattern of diverse oxazinones

After successful coupling of benzoxazinone **5a** with H-^{L}Pro-OBn, we further explored the reaction to a range of stable oxazinones that we often isolated during oligopeptide synthesis applying similar conditions (Table 2). Different aliphatic and aromatic 2-substituted [1,3]-oxazinones were subjected to thiourea-based ring opening like Boc-^{L}Pro- **5c**, 2-nitrophenyl **5d**, 6,7-difluoro-2-phenyl- **5b** *etc* which provided good to quantitative yields of coupled product. Different aliphatic and aromatic 2-substituted-[1,3]-oxazinones were subjected to (thio)urea-mediated ring opening, which provided good to quantitative yields. This study confirmed that the stability of the oxazinone has no great role to play in coupling tendency.

Table 2. Comparison of coupling of oxazinones **5a-e** with HN-^{L}Pro-OBn in DMSO.

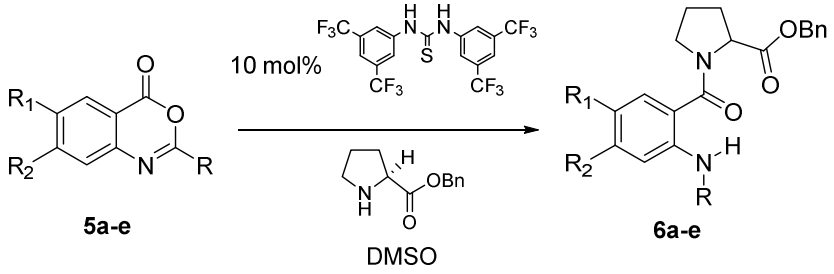

	-R	-R_1	-R_2	Time (h)	Conversion (%)	Yield (%)[a]
6a		H	H	24	100	81
6b		F	F	36	92	70[b]
6c		H	H	9	100	97
6d	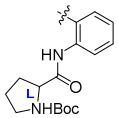	H	H	24	100	75
6e	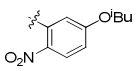	O^{t}Bu	H	48	52	91[c]

[a]Unless specified, reaction was carried out at 25 °C with oxazinone (1 equiv.) and H-^{L}Pro-OBn (1.5 equiv.). [b]Yield calculated after 8% oxazinone recovery. [c]Yield calculated after 48% oxazinone recovery.

According to the early investigations on acylanthranils, having electron withdrawing groups at 6th position or electron deficient phenyl rings were considered to disfavour *o*-acetamidobenzamide formation. This in turn increases the electrophilicity at the 2nd position, making it more preferable towards nucleophilic attack. Also, the presence electron donating groups at 6th position is shown to enhance the electron density at 2nd position.[32b]

However, it was observed that the activation by thiourea made 4th position of the oxazinone more electrophilic, driving the reaction more favourably to furnish desired product, as can be estimated from the observations obtained from reactivity which ranged in an order of **5c>5a>5d>5b>5e**.

3.14.3 Reactivity pattern with different amines

In all the above mentioned cases, reactions of different oxazinones were carried out with proline as amine, but proline itself is a well known catalyst for several reactions.[46] Thus in order to ensure any influence of proline, we assessed the reaction of the stable oxazinone **5d** with different chiral and achiral amine residues and also amino acids (Table 3).

Primary amines without any α-substitution like propylamine proceeded to completion very fast, affording 97% yield of the product **6j**. Chiral (S)-phenylethylamine also reacted smoothly within 10 min, revealing the hindrance at α-position doesn't affect reactivity drastically. This observation is in stark contradiction to the observations made by Errede *et al*, where the amines having alkyl chains with carbon number n<4 follow the pathway to form acetamidine intermediate that leads to formation of quinazolone moiety.[47]

Comparing primary and secondary amines, reaction rate was observed to be faster for the primary amine *i.e.* propylamine. Interestingly, with piperidine and (S)-phenyl-ethylamine, the reaction completed in less than 5 min providing excellent yields. When **5d** was reacted with hindered amino acid H-Aib-OMe (α-aminoisobutyric acid methyl ester), reaction proceeded sluggishly in 4 days but provided 82% (yield after 40% recovery of the reactant). Reaction was found to be poor in case of aromatic amines due to their reduced nucleophilicity. The reactivity of amines presumably is negatively influenced by methoxycarbonyl group.

Table 3. Comparison of coupling of different amines with oxazinone **5d**

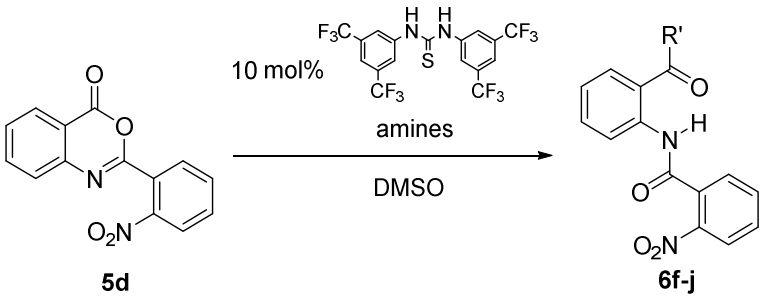

	-R	Time (h)	Conversion (%)	Yield (%)[a]
6f		0.5	100	94
6g		0.12	100	94
6h	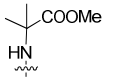	48	60	82[b]
6i	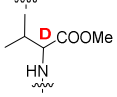	36	100	89
6j		0.05	100	97

[a]Unless specified, reaction was carried out at 25 °C with oxazinone (1 equiv.) and H-^{L}Pro-OBn (1.5 equiv.). [b]Yield calculated after 40% oxazinone recovery.

3.15 Conclusions

The inferences gained from these reactions authenticated that (thio)urea acts as a mild and efficient catalyst in activating benzoxazinone moiety, and assists in amide formation from C-terminal end. This method provides a convenient route to Ant (anthranilic acid) incorporated peptides, which are otherwise difficult to synthesize using the conventional method of peptide coupling. Employing mere 10% of the (thio)urea catalyst, the reactions were found to furnish good-to-excellent yields of coupled products at ambient conditions. This work presents one of the many facets of application of organocatalysis in the area of peptide coupling.

SECTION III

Conformational Predilection of Orthanilic Acid in Peptide Sequences

3.16 Sulphonamide linkage as *surrogate* of carboxamides: A critical perspective

Sulphonamide bond acts as an efficient isosteric replacement of carboxamide linkage due to their similar shape and electronic environment. In comparison with carboxamide, sulphonamide link is comparatively acidic making it a stronger hydrogen bonding donor with pK_a ~ l0-11. Presence of two H-bond acceptor oxygen atoms and limited rotation barrier about the S-N bond, along with the dihedral disparity of ω ~ 90° (compared to 180° of carboxamides), helps in rendering twists to the peptide chains.[48]These different aspects make sulphonamides as interesting candidates for generation of diverse synthetic peptides.[49]

Surprisingly, the twists obtained by the swapping of carboxamide with sulphonamide bond preserved the *pseudo-β*-turn, by assuming the highly deviated 'ω' = 163° ('ω' =165° of its carboxamide analogue) (Figure 13). This instance demonstrates that the fundamental torsional preference of ^{S}Ant can get dramatically modulated by the influence of adjoining residues.[50]

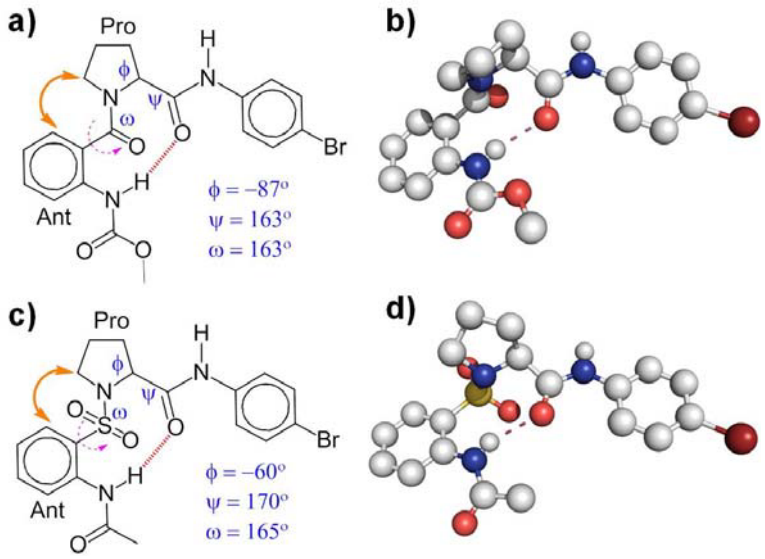

Figure 13. Comparable conformational features displayed by Ant-Pro and ^{S}Ant-Pro motifs. Molecular structures and corresponding crystal structures of Ant-Pro motifs linked *via*: (a,c) carboxamide and (b,d) sulphonamide, respectively. (Hydrogens, other than the polar amide hydrogens have been removed for clarity).

Orthanilic acid (2-aminobenzenesulfonic acid, ^{S}Ant) shares surprising structural similarity as discussed in the former case and revealed entirely dissimilar H-bonding pattern in Xaa-^{S}Ant-Yaa peptide sequence. Unlike the former case, this sequence featured a robust 11-membered-ring hydrogen-bonding formed in the backward direction, vindicating the efficiency of ^{S}Ant in promoting folding (Figure 14b).[51] Strangely, the oligomer of Pro-Xaa-Aib (Xaa = Ant/ ^{S}Ant) containing carboxamide and sulfonamides at regular intervals, in spite of different hydrogen-bonding patterns and helical handedness, revealed resembling conformational features (Figure 14). Solid-state structures confirmed that (Pro-^{S}Ant-Aib)$_n$ oligomers displayed 11-membered *intra*-molecularly hydrogen-bonded right-handed helical architecture whereas, the carboxamide oligomers (Pro-Ant-Aib)$_n$ display a periodically repeating six-membered intramolecular hydrogen-bonded left-handed helical structure.[52]

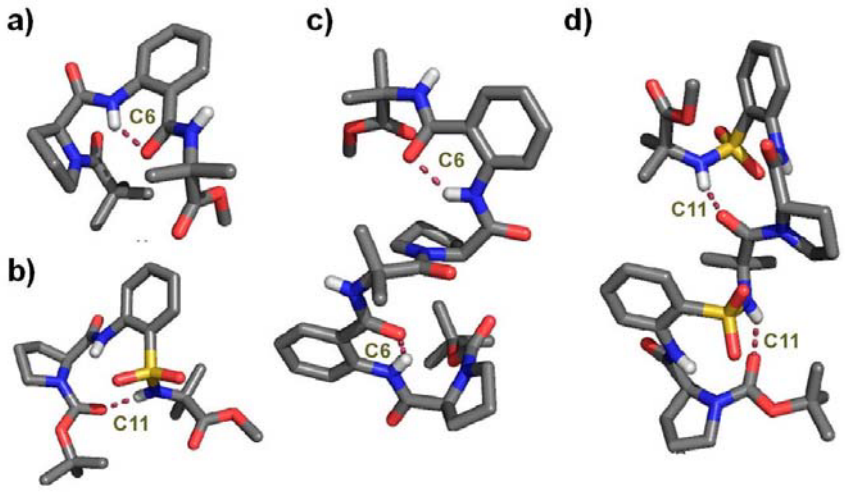

Figure 14. PyMOL-rendered crystal structures of: carboxamide monomer Piv-Pro-Ant-Aib-OMe (a), sulphonamide monomer Boc-Pro-^{S}Ant-Aib-OMe (b), carboxamide oligomer Boc-(Pro-Ant-Aib)$_2$-OMe (c), and sulfonamide oligomer Boc-(Pro-^{S}Ant-Aib)$_2$-OMe (d). Hydrogens, other than the polar amide hydrogens, have been removed for clarity.

3.17 Objective of the work

The aforementioned cases not only provide unambiguous evidence for strong turn inducing ability of ^{S}Ant, but also reveal the unprecedented modulation of its torsion angles. Swapping of carboxamides with sulphonamides brings about serious conformational effects on structure of oligomers. It was observed that on substitution

of constrained amino acid like α-amino isobutyric acid (Aib) at the N- terminus of ^{S}Ant-Pro dipeptide led to a twisted conformation and disengagement of C9-turn. Further, it was found that hexapeptide Boc-^{L}Leu-Aib-^{S}Ant-^{L}Pro-^{L}Leu-Aib-NHMe showed unusual and long range 15-membered H-bonding ring involving four amino-acid residues (Figure 15). The solid-state conformational analysis clearly indicated that the torsional constraint of the ^{S}Ant residue acted as the key to the folded conformation seen in the oligomer. Thus, our objective was to investigate the effect of substitution of different amino acids around the -^{S}Ant-^{L}Pro- turn segment in the hexapeptide sequence.

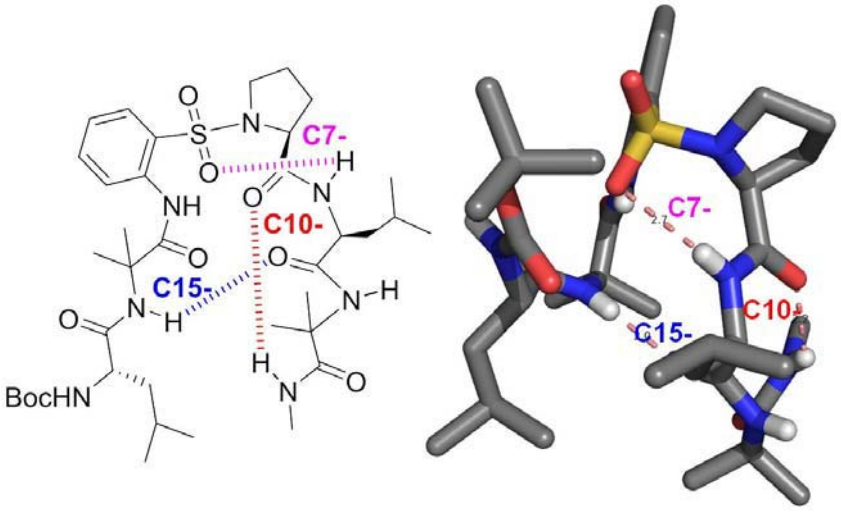

Figure 15. Molecular structure of hexapeptide Boc-^{L}Leu-Aib-^{S}Ant-^{L}Pro-^{L}Leu-Aib-NHMe (left) and its crystal structure (right), displaying simultaneous C7-, C10- and C15- H-bonding pattern.

3.18 Design strategy

^{S}Ant-Pro motif is also known to act as a reverse turn inducer featuring nine-membered H-bonding network. Some sequences containing orthanilic acid as a connecting entity were developed, which revealed unusual H-bonding preferences (Figure 15). Therefore, we designed hexapeptides comprising ^{S}Ant-Pro at the centre in order to assess the influence of substitution of constrained amino acid like Aib at both N- and C- termini i.e. Boc-^{L}Leu(1)-Aib(2)-^{S}Ant(3)-Pro(4)-Aib(5)-^{L}Leu(6)-NHMe in one sequence and the effect of flexible amino acid Leucine in another sequence i.e. Boc-Aib(1)-^{L}Leu(2)-^{S}Ant(3)-Pro(4)-^{L}Leu(5)-Aib(6)-NHMe.

3.19 Synthesis

To prepare the sequence Boc-^{L}Leu(1)-Aib(2)-^{S}Ant(3)-Pro(4)-Aib(5)-^{L}Leu(6)-NHMe **12b** possessing Aib at the N- and C- termini, **9a** was synthesised following the coupling of nitrobenzenesulfonyl chloride **7** with HN-^{L}Pro-OMe.HCl **8** in DCM using TEA as base. Nitro group of **9a** was then reduced by hydrogenation method and the amine **9b** obtained was subjected to react with α-bromoisobutyryl bromide to produce **10a**. **10a** was then subjected to azide- replacement to furnish **10b**, which on reduction gave amine **10c**. **10c** was coupled with Boc-Aib-OH in presence of EDC.HCl as coupling agent to afford the tetramer **11a** in 85% yield.

Scheme 3: Synthesis of hexapeptide **12b**

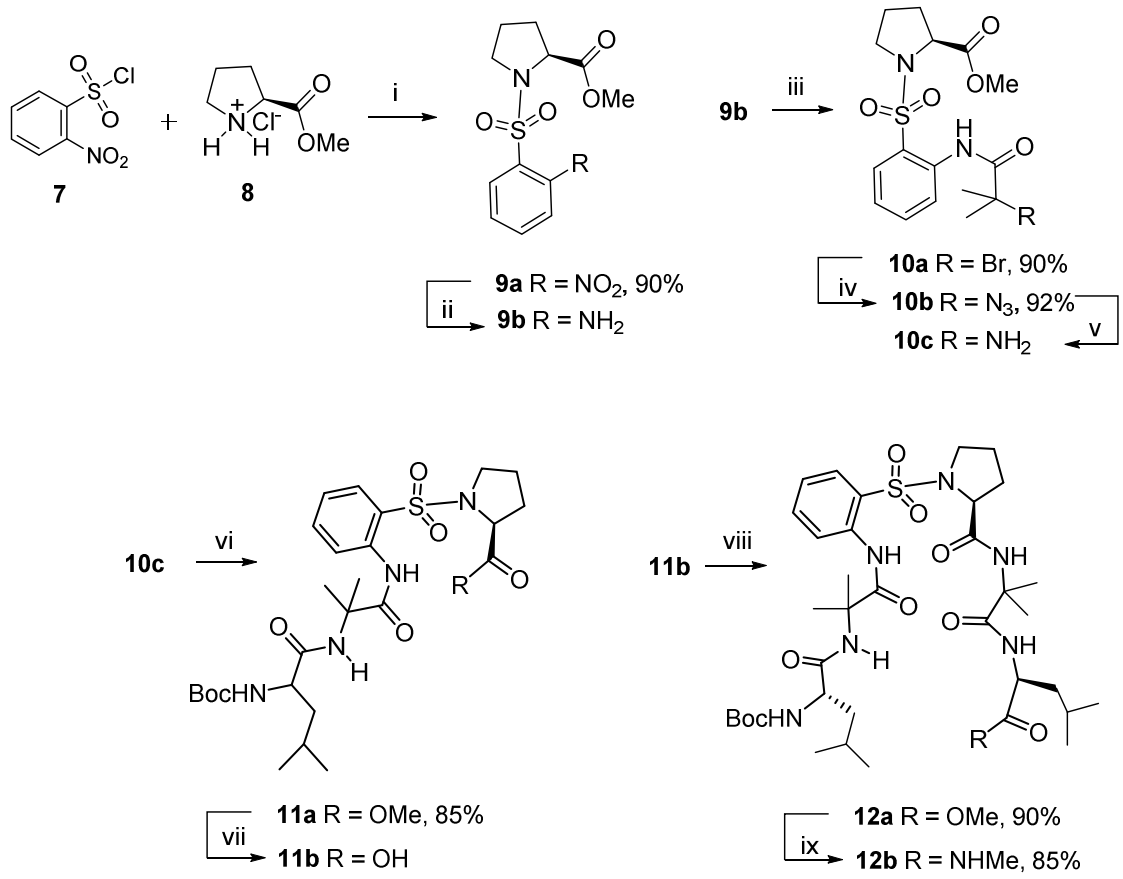

Scheme 3.3: *Reagents and conditions:* (i) Et_3N, DCM, 24 h; (ii) Pd/C, H_2. 60psi, 6h; (iii) α-bromoisobutyryl bromide, Et_3N, DCM, 24 h; (iv) NaN_3, DMF, 12h; (v) H_2, Pd/C, 60 psi, 10h; (vi) Boc-Leu-OH, EDC.HCl, HOBt, DCM, 12h; (vii) LiOH, MeOH, 4h; (viii) H_2N-Aib-^{L}Leu-OMe, EDC.HCl, HOBt, DCM; (ix) $MeNH_2$, MeOH.

Ester hydrolysis of the tetramer **11a** was followed by coupling of its free acid **11b** with the dipeptide amine H_2N-^{L}Leu-Aib-OMe, which produced hexamer **12a** in 90% yield. Treatment of which with methanolic $MeNH_2$ furnished the methyl amide analog **12b** in 85% yield.

Synthesis of sequence Boc-Aib(1)-^{L}Leu(2)-^{S}Ant(3)-Pro(4)-^{L}Leu(5)-Aib(6)-NHMe **15b** with ^{L}Leu at the N- and C- termini posed serious challenges. With great efforts, synthesis of Phth-^{L}Leu-^{S}Ant-^{L}Pro-OMe **13a** was achieved employing acid chloride method in meagre 33% yield. Amine obtained after deprotection of Phth-group was coupled with Boc-Aib-OH employing HBTU, DIEA in DMF to afford **14a**. Amine **14b** obtained by the deprotection of **14a** was coupled with H_2N-Aib-^{L}Leu-OMe to prepare **15a**. However, due to the presence of multiple peaks in the ^{1}H-NMR spectrum, further analysis couldn't be carried out for this hexapeptide analogue.

Scheme 4: Synthesis of hexapeptide **15b**

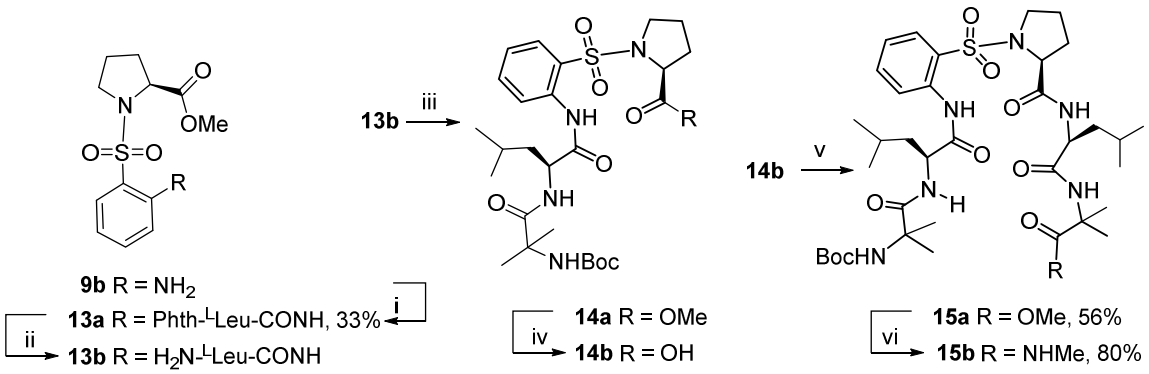

Scheme 3.4: *Reagents and conditions:* (i) Phth-^{L}Leu-COCl, DCM, 6h; (ii) diethylamine, DCM, 4h; (iii) Boc-Aib-OH, HBTU, DIEA, DMF, 12h; (iv) LiOH, MeOH; (v) H_2N-^{L}Leu-Aib-OMe, EDC.HCl, HOBt, DCM; (vi) $MeNH_2$, MeOH.

3.20 Conformational analyses

Solution-state NMR studies were undertaken to gain insights into the structural features of hexapeptide **12b**. But, peculiar broadening of peaks in proton NMR spectrum was observed in $CDCl_3$ suggesting presence of exposed amide NHs in the peptide. In order to evaluate the involvement of amide NHs in H-bonding networks in hexapeptide **12b**, DMSO-d_6 titration study was carried out (Figure 16). Four of the amide –NHs except NH1 and NH5, featured minimum chemical shift variations i.e. $\Delta\delta$ (NH6) < 0.01 ppm, $\Delta\delta$ (NH2) < 0.02 ppm, $\Delta\delta$ (NH7) < 0.2 ppm, and $\Delta\delta$ (NH3) <

0.05 ppm. This suggested their participation in *intra*-molecular H-bonding association.

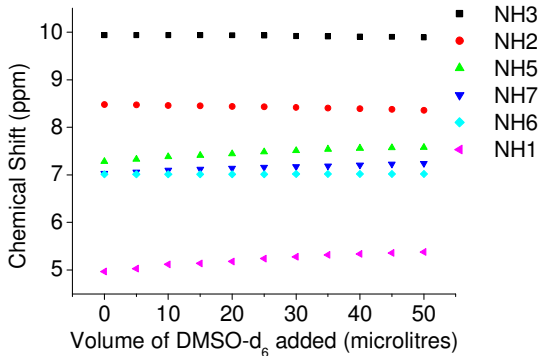

Figure 16: ^{1}H NMR DMSO-d_6 titration study (5 mM solution) of hexapeptide **12b** (volume of DMSO-d_6 used for each addition = 5 µl).

In order to substantiate this observation, elucidation of the conformational characteristics was attained by signal assignments and interpretation of 2D-NMR experiments, using a combination COSY, TOCSY, HSQC, HMBC and NOESY spectra (see experimental section, pages 331-333). Hexapeptide Boc-^{L}Leu(1)-Aib(2)-^{S}Ant(3)-Pro(4)-Aib(5)-^{L}Leu(6)-NHMe **12b** featured a perceptible C15- turn involving Aib(2)-^{S}Ant(3)-Pro(4)-Aib(5)-^{L}Leu(6)-residues, a C10- turn encompassing -Pro(4)-Aib(5)-^{L}Leu(6)-NHMe and a C7- turn between -^{S}Ant(3)-Pro(4)- residues.

Diagnostic nOes obtained in support of the characteristic *β*-turn were NH7/C18H, NH7/C21H, C33H/C18H *etc* (shown in Figure 17a,b,c, respectively). Due to the presence of ten-membered H-bonded ring, methylamide at the C-terminus gets drawn into proximity of third residue i.e. ^{S}Ant ring, which can be evidenced from the cross-peaks obtained between the aromatic protons C14H & C15H *vs* C33H and C15H *vs* C30H (Figures 17e,d, respectively)

Presence of a strong intra-residual six-membered H-bond was apparent from the ^{1}H-NMR chemical shift (appears at 9.1δ). Also extremely negligible shift for the corresponding amide proton was seen in DMSO-d_6 titration studies. Dipolar coupling between NH3 *vs* C18H and C21H (Figure 17f) also supported this observation. Presence of C15- H-bonding network between the carbonyl of Aib(2) and amide NH6 was evidenced from the dipolar coupling obtained between C9H and C10H protons with NH6 (Figure 17g).

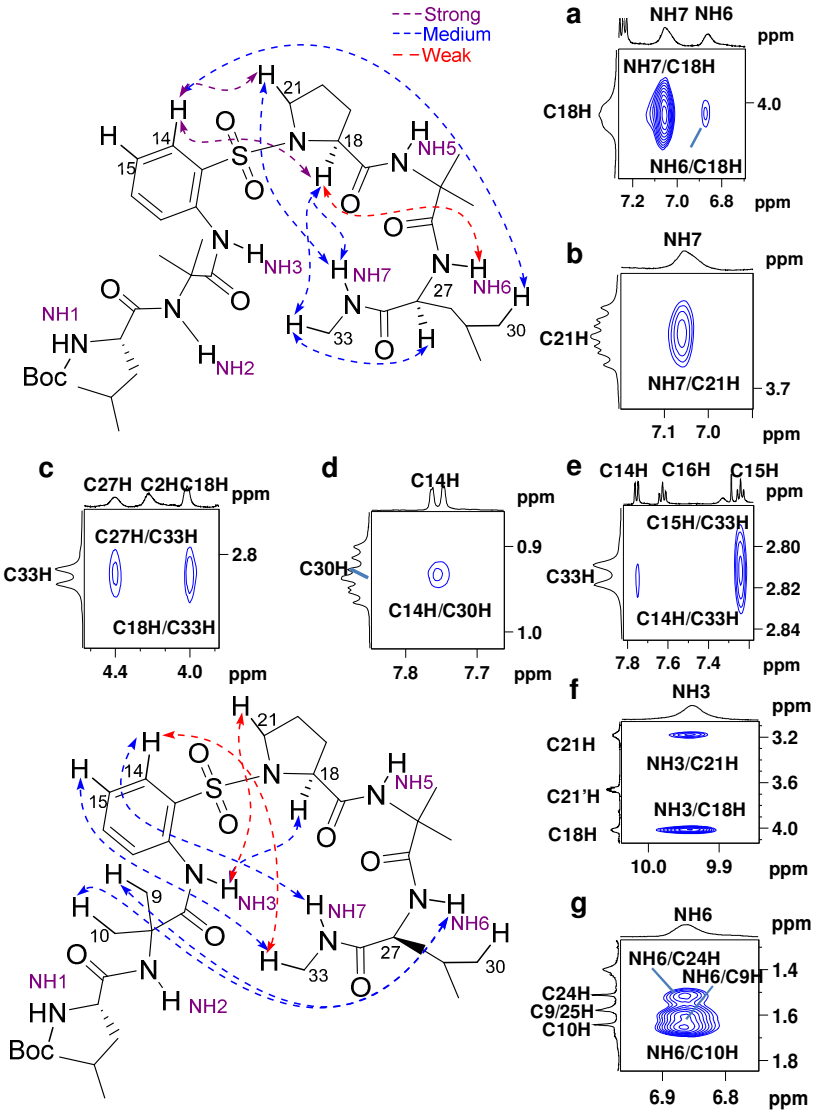

Figure 16: Selected NOE extracts from the 2D NOESY data of **12b** ($CDCl_3$, 500 MHz)**.** (a) $P_\alpha H$ *vs* NH-CH_3, (b) $P_\delta H$ region *vs* NH-CH_3, (c) NH-CH_3 *vs* $P_\alpha H$, (d) $L_\delta H$ *vs* Ar-H region,(e) NH-CH_3 *vs* Ar-H region, (f) $P_\alpha H$ and $P_\delta H$ *vs* NH region and (g) Aib *vs* NH region.

3.21 Conclusions

Oligomer sequence was synthesized and its elucidated structure revealed that substitution of constrained amino acid like Aib at both N- and C- termini around the ^{S}Ant-Pro segment, the folding pattern remained unperturbed. The oligomer retained the long range 15- and 10- membered H-bonded ring. These results further support the previously observed fact that orthanilic acid is a strong reverse-turn inducer.

3.22 Experimental section

methyl 2-(2-bromo-2-methylpropanamido)benzoate 2a:

To an ice cold solution of anthranilic methyl ester (10 g, 72.99 mmol, 1 equiv) and triethylamine, TEA (12.95 mL, 99.89 mmol, 1.1 equiv) in dry DCM (100 mL) bromo isobutyryl bromide (9.92 mL, 80.29 mmol, 1.2 equiv) was slowly added. The reaction mixture was stirred for 1 hr at room temperature. After completion, the reaction mixture was diluted with DCM (100 mL) and washed sequentially with saturated $NaHCO_3$, dil. HCl and brine solution. The organic layer was dried over Na_2SO_4, filtered and solvent was stripped off under reduced pressure. Column chromatographic purification (eluent: 10% AcOEt/pet. Ether, Rf: 0.3) of the residue afforded **2a** as a white solid (16.2g, 82%). mp: 44-45 °C; IR ($CHCl_3$) ν (cm^{-1}): 3264, 3020, 2927, 2400, 1685, 1590, 1528, 1451, 1381, 1272, 1088, 1048, 967; ^{1}H NMR (200 MHz, $CDCl_3$): 11.85 (s, 1H), 8.71-8.66 (dd, *J* = 1.01 Hz, *J* = 8.59 Hz, 1H), 8.06-8.01 (dd, *J* = 1.77 Hz, *J* = 8.08 Hz, 1H), 7.59-7.5 (m, 1H), 7.14-7.06 (m, 1H), 3.93 (s, 3H), 2.06 (s, 6H); ^{13}C NMR (50 MHz, $CDCl_3$): 170.6, 168.3, 140.9, 134.4, 130.8, 122.9, 120.1, 115.4, 60.1, 52.4, 31.7; Anal. Calcd. For $C_{12}H_{14}BrNO_3$: C, 48.02; H, 4.70; Br, 26.62; N, 4.67; Found: C, 48.10; H, 4.89; Br, 26.66; N, 4.29.

methyl 2-(2-azido-2-methylpropanamido)benzoate 2b:

To a solution of **2a** (10 g, 34.85 mmol, 1 equiv) in dry DMSO (60 mL) was added sodium azide (3.40 g, 52.28 mmol, 1.5 equiv) and catalytic amount of LiCl (0.15g, 3.48 mmol, 0.1 equiv), the reaction mixture was allowed to proceed at rt for 6h. After completion, the reaction mixture was added to water and the aqueous layer was extracted with DCM. The combined organic layer was washed repeatedly with water and brine solution. The organic layer was dried over Na_2SO_4, filtered and solvent was stripped off under reduced pressure. Column chromatographic purification (eluent: 10% AcOEt/pet. Ether, Rf: 0.3) of the residue afforded **2b** as a white solid (8 g, 88%). mp: 40-42 °C; IR ($CHCl_3$) ν (cm^{-1}): 3261, 3020, 2980, 2956, 2401, 1694, 1605, 1589, 1525. 1450, 1386, 1275, 1217, 1166, 1089, 967, 920; ^{1}H NMR (200 MHz, $CDCl_3$): 11.78 (s, 1H), 8.71-8.66 (d, *J* = 8.65 Hz, 1H), 8.04-8.0 (dd, *J* = 1.64 Hz, *J* = 7.96 Hz, 1H), 7.56-7.47 (m, 1H), 7.13-7.05 (m, 1H), 3.93 (bs, 3H), 1.6 (bs, 6H); ^{13}C NMR (50 MHz, $CDCl_3$): 171.5, 168.1, 140.5, 134.3, 130.8, 122.9, 120.2, 115.7, 64.7, 52.3, 24.5; Anal. Calcd. For $C_{12}H_{14}N_4O_3$: C, 54.96; H, 5.38; N, 21.36; Found: C, 54.81; H, 5.23; N, 21.38.

General Procedures for 2c, 3b, 2e, 2h, 2j, 9b** and **13b:

2-(2-azido-2-methylpropanamido)benzoic acid 2c:

To a solution of **2b** (6.97 g, 27.88 mmol, 1 equiv.) in methanol (25 mL) and water (10 mL), $LiOH{\cdot}H_2O.2H_2O$ (5.02 g, 8.64 mmol, 3 equiv.) was added and the reaction mixture was stirred for 18 hrs. The solvent was stripped off under reduced pressure. To the residue water (50 mL) was added and acidified with dilute HCl. The water layer was extracted with ethyl acetate (3 x 50 mL). The combined organic layer was washed with water and brine solution, dried over Na_2SO_4 and used for next reaction without further purification. Yield = 6.4 g (97.3%).

benzyl 1-(2-(2-azido-2-methylpropanamido)benzoyl)pyrrolidine-2-carboxylate 3a:

A solution containing **2c** (3 g, 12.36 mmol, 1 equiv.) and HN-^{L}Pro-OBn (3.8 g, 18.54 mmol, 1.5 equiv.) in dry THF (30 mL) was cooled to 0 °C. TBTU (4.76 g, 14.83 mmol, 1.2 equiv.) was added to the reaction mixture followed by DIEA (3.23 mL, 18.56 mmol, 1.5 equiv.). The reaction mixture was stirred at 0 °C for 10 min and at room temperature for 12 h and stripped off the solvent under reduced pressure, the residue was taken in DCM and the organic layer was washed sequentially with sat. $KHSO_4$ solution, sat. $NaHCO_3$ solution followed by water. The organic layer was dried over anhydrous Na_2SO_4 and evaporated under reduced pressure and the crude product was purified by column chromatography (eluent: 25% AcOEt/pet. Ether, R_f: 0.4) to furnish **3a** (81%) as a pale yellow glassy solid. $[\alpha]^{24.7}_{D}$: -67.56° (*c* 0.5, $CHCl_3$); IR ($CHCl_3$) ν (cm^{-1}): 3307, 2923, 2852, 2115, 1744, 1692, 1629, 1597, 1520, 1454, 1412, 1305, 1269, 1166; ^{1}H NMR (200 MHz, $CDCl_3$) δ: $10.12_{rotamer}$ (0.8H, amide), $9.59_{rotamer}$ (0.2H, amide), 8.39-8.35 (d, J = 8.34 Hz, 0.8H), 8.39-8.35 (d, J = 8.08 Hz, 0.2H), 7.50-7.38 (m, 6H), 7.19-6.56 (m, 2H), 5.26 (s, 2H), 5.04-4.72 (m, 1H), 3.94-3.78 (m, 0.4H), 3.73-3.54 (m,1.6H), 2.24-2.05 (m, 1H), 2.38-2.27 (m, 1H), 2.14-1.85 (m, 3H), 1.63 (s, 6H); ^{13}C NMR (50 MHz, $CDCl_3$) δ: 171.5, 171.2, 169.3, 168.5, 136.3, 135.6, 135.0, 131.1, 130.6, 128.5, 128.2, 128, 127.4, 126.4, 124.7, 123.3, 122.6, 121.9, 66.8, 64.5, 61.6, 59.2, 50.2, 46.6, 31.3, 29.1, 25.1, 24.5, 24.4; MALDI-TOF/TOF/TOF: 458.1152 ($M+Na^+$); 474.0970 ($M+K^+$); Anal. calcd for $C_{23}H_{25}N_5O_4$: C, 63.44; H, 5.79; N, 16.08. Found: C, 63.66; H, 5.98; N, 16.10.

benzyl (2-(2-(1-(2-(2-azido-2-methylpropanamido)benzoyl)pyrrolidine-2-carboxamido)-2-methylpropanamido)benzoyl)prolinate 4a:

Compound **4a** was synthesized from acid **3b** and amine **3c**, following the procedure for **3a.** The crude product was purified by column chromatography (eluent: 50% AcOEt/pet. Ether, R_f: 0.3) to furnish **4a** (72%) as a pale yellow glassy solid. $[\alpha]^{27.5}_D$: -71.652° (*c* 0.5, $CHCl_3$); IR ($CHCl_3$) ν (cm^{-1}): 3318, 2925, 2855, 2117, 1743, 1680, 1622, 1521, 1421, 1261, 1093, 1040, 847; ^{1}H NMR (200 MHz, $CDCl_3$) δ: 9.89 (s, 1H, amide), $9.70_{rotamer}$ (s, 0.2H, amide), $9.60_{rotamer}$ (s, 0.8H, amide), 8.24-8.12 (m, 2H), 7.71-7.36 (m, 12H), 7.18-7.11 (m, 2H), 7.19-6.56 (m, 2H), 5.22 (s, 2H), 4.72-4.66 (m, 2H), 3.60-3.55 (m, 4H), 2.41-2.12 (m, 4H), 2.07-1.89 (m, 4H), 1.63 (s, 3H), 1.57 (s, 9H); ^{13}C NMR (50 MHz, $CDCl_3$) δ: 173.3, 171.7, 171.3, 170.9, 169.3, 169.0, 136.1, 135.7, 135.5, 132.3, 132.2, 132.0, 131.1, 131.0, 128.7, 128.5, 128.3, 127.9, 127.1, 125.4, 125.3, 123.8, 123.5, 122.8, 122.3, 66.9, 64.5, 60.5, 59.2, 57.8, 50.8, 50.2, 29.3, 28.4, 26.3, 25.3, 25.1, 24.7, 24.1; MALDI-TOF/TOF/TOF: 748.5535 $(M+H)^+$, 760.4155 $(M+Na)^+$, 776.4878 $(M+K)^+$; Anal. calcd for $C_{39}H_{44}N_8O_7$: C, 63.57; H, 6.02; N, 15.21. Found: C, 63.36; H, 6.16; N, 15.34.

1-(2-(2-azido-2-methylpropanamido)benzoyl)-*N*-(2-methyl-1-((2-(2-(methyl carbamoyl)pyrrolidine-1-carbonyl)phenyl)amino)-1-oxopropan-2-yl)pyrrolidine-2-carboxamide 4b:

The ester **4a** (0.1g) was taken in saturated methanolic methylamine solution (2 mL) and stirred at room temperature for 2 h. The solvent was removed under reduced pressure, and the residue was purified by column chromatography (eluent: 5% MeOH/EtOAc, Rf: 0.4) to afford **4b** (0.085 g, 93%) as a fluffy white solid. mp: 115-117 °C; $[\alpha]^{23.5}_D$: -132.072° (*c* 0.5, $CHCl_3$); IR ($CHCl_3$) ν (cm^{-1}): 3317, 2979, 2927, 2116, 1664, 1624, 1522, 1453, 1419, 1303, 1244, 1161, 1045, 921; ^{1}H NMR (500 MHz, 295 K, $CDCl_3$) δ: 9.92-9.89 (m, 1H, amide), $9.58\text{-}9.55_{rotamer}$ (m, 0.2H, amide), $9.43_{rotamer}$ (s, 0.6H, amide), $9.30\text{-}9.24_{rotamer}$ (s, 0.6H, amide), 8.24-8.16 (m, 1H), $8.07\text{-}8.06_{rotamer}$ (m, 0.7H), $7.88\text{-}7.82_{rotamer}$ (m, 0.3H), 7.48-7.33 (m, 4H), 7.16-7.10 (m, 2H), $6.78_{rotamer}$ (broad, 0.6H, amide), $6.65_{rotamer}$ (broad, 0.4H, amide), $5.02\text{-}5.00_{rotamer}$ (m, 0.2H), $4.71\text{-}4.68_{rotamer}$ (m, 0.8H), $4.60\text{-}4.57_{rotamer}$ (m, 0.8H), $4.50\text{-}4.48_{rotamer}$ (m, 0.2H), 4.29 (broad, 1H, amide), 3.80-3.72 (m, 1H), 3.64-3.52 (m, 3H), $2.81\text{-}2.80_{rotamer}$ (m, 2.5H), $2.78\text{-}2.77_{rotamer}$ (m, 0.5H), 2.25-2.17 (m, 5H), 2.04-1.96 (m, 3H), 1.64-1.56 (m, 12H); ^{13}C NMR (125 MHz, $CDCl_3$) δ: 173.2, 172.1, 171.2, 170.7, 169.6, 169.4, 135.9, 135.8, 131.4, 131.2, 130.8, 130.5, 127.8, 127.5, 127.2, 126.2, 125.2, 124.5, 124.2, 123.9, 123.8, 123.6, 122.8, 122.6, 122.3, 64.6, 63.1, 60.6, 60.2, 29.9, 57.9, 57.7, 51.1, 50.7, 50.3, 47.1, 32.1, 29.6, 28.8, 28.3, 27.3, 26.4, 25.4, 25.3, 25.1, 24.8,

24.7, 24.6, 24.3, 24.1, 23.3, 23.0, 22.8; MALDI-TOF/TOF/TOF: 683.2515 $(M+Na)^+$, 699.3170 $(M+K)^+$; Anal. calcd for $C_{33}H_{41}N_9O_6$: C, 60.08; H, 6.26; N, 19.11. Found: C, 60.16; H, 6.10; N, 19.00.

General Procedures for 5a, 5d and 5e:

2-(2-azidopropan-2-yl)-4H-benzo[d][1,3]oxazin-4-one 5a:

To a solution of **3d** (3 g, 12.096 mmol, 1 equiv) in DCM, EDC.HCl (2.54 g, 13.306 mmol, 1.2 equiv) was added. The solution was allowed to stir for 2h. After the completion, reaction mixture was diluted with DCM (30 mL), the organic layer was combined and was washed with water, followed by $NaHCO_3$ solution and brine solution. The organic layer was then dried over Na_2SO_4 and was removed *in vacuo*. Colorless liquid was isolated with 94% yield. Characterization was difficult due to unstable nature of the oxazinone. IR ($CHCl_3$) ν (cm^{-1}): 3020, 2979, 2401, 2117, 1678, 1606, 1587, 1524, 1450, 1409, 1299, 1165, 1046, 1607, 1584, 1524, 1435, 1388, 1318, 1271, 1164, 1097, 927; ^{1}H NMR (200 MHz, $CDCl_3$): 8.22-8.18 (d, J = 1.01 Hz, J = 7.83 Hz, 1H), 7.88-7.79 (m, 1H), 7.68-7.64 (d, J = 7.58 Hz, 1H), 7.59-7.51 (m, 1H), 1.69 (s, 6H); ^{13}C NMR (50 MHz, CDCl3) δ 161.9, 158.8, 145.6, 136.6, 128.9, 128.5, 127.4, 116.8, 62.4, 24.8.

6,7-difluoro-2-phenyl-4H-benzo[d][1,3]oxazin-4-one 5b:
Compound **1b** was synthesized as per the reported procedure.[2]

2] A. A. Laeva, E. V. Nosova, G. N. Lipunova, A. V. Golovchenko, N. Yu. Adonin, V. N. Parmon, and V. N. Charushin. *Russ. J. Org. Chem.,* 2009*, **45**,* 913–920.

2-(2-nitrophenyl)-4H-benzo[d][1,3]oxazin-4-one 5c:
Compound **3c** was synthesized as per the reported procedure.[1]

1] Y. Hamuro, S. J. Geib and A. D. Hamilton, *J. Am. Chem. Soc.*, 1997, ***119***, 10587-10593.

6-isobutoxy-2-(5-isobutoxy-2-nitrophenyl)-4H-benzo[d][1,3]oxazin-4-one 5e:
The crude product was purified by column chromatography (eluent: 15% AcOEt/pet. Ether, R_f: 0.3) to furnish **1e** (98%) as a waxy solid. IR ($CHCl_3$) ν (cm^{-1}): 3480, 1771, 1635, 1609, 1531, 1470, 1349, 1219; ^{1}H NMR (200 MHz, $CDCl_3$) δ: 7.81-7.76 (d, J = 8.97 Hz, 1H), 7.32-7.31 (m, 1H), 7.14-7.08 (dd, J = 2.78 Hz, J = 9.09 Hz, 1H), 7.00-6.97 (dd, J = 2.78 Hz, J = 8.84 Hz, 1H), 3.58-3.53 (dd, J = 3.03 Hz, J = 6.57 Hz, 4H), 1.91-1.77 (m, 2H), 0.76-0.73 (dd, J = 3.16 Hz, J = 6.69 Hz, 6H); ^{13}C NMR (50 MHz, $CDCl_3$) δ 162.9, 159.6, 159.0, 153.7, 140.7, 140.1, 129.1, 128.7, 127.1, 126.1,

117.8, 116.5, 116.4, 105.6, 75.4, 75.1, 29.6, 28.1, 19.1, 19.0; LC-MS: 435.06 ($M+Na^+$); 467.08 ($M+K^+$);. Anal. calcd for $C_{22}H_{24}N_2O_6$: C, 64.07; H, 5.87; N, 6.79; Found: C, 64.21; H, 5.89; N, 6.80.

General Procedures for 6a-j:

To a solution of oxazinone (1 equiv) and amine (1.5 equiv) taken in DMSO (1 mL), 1,3-bis(3,5-bis(trifluoromethyl)phenyl)thiourea (10 mol%) was added. Completion of the reaction was constantly monitored by TLC. After the complete/maximum conversion of the oxazinone moiety, water (2 mL) was added to the reaction mixture. Compound was then extracted into DCM (3 x 5 mL) from the aqueous layer. Organic layer was pooled together and was washed with $KHSO_4$ solution followed by brine solution. The organic layer was then dried over Na_2SO_4 and was evaporated *in vacuo* to afford coupled product. Compounds were purified by silica gel column chromatography.

benzyl 1-(2-benzamido-4,5-difluorobenzoyl)pyrrolidine-2-carboxylate 6b:

The crude product was purified by column chromatography (eluent: 15% AcOEt/pet. Ether, R_f: 0.4) to furnish **6b** (70% after 8% recovery of starting material) as a pale yellow solid. mp: 78-80 °C;$[\alpha]^{25.84}_D$: -39.14° (*c* 1, $CHCl_3$); IR ($CHCl_3$) ν (cm-1): 3347, 2924, 1744, 1681, 1615, 1533, 1440, 1409, 1279, 1167; ^{1}H NMR (200 MHz, $CDCl_3$) δ: 10.4 (1H, amide), 8.65-8.54 (dd, *J* = 7.58 Hz, *J* = 12.88 Hz, 1H), 8.11-7.92 (m, 2H), 7.61-7.31 (m, 9H), 5.27- 5.12 (m, 2H), 4.78-4.72 (m, 1H), 3.70-3.61 (m, 2H), 2.41-2.27 (m, 1H), 2.09-1.91 (m, 3H); ^{13}C NMR (50 MHz, $CDCl_3$) δ: 171.4, 167.4, 165.4, 135.3, 134.8, 133.8, 133.4, 132.1, 130.0, 128.6, 128.4, 128.0, 127.4, 119.5, 116.3, 115.9, 111.7, 111.3, 67.0, 598.5, 50.5, 29.6, 29.0, 25.2; MALDI-TOF/TOF/TOF: 487.2480 ($M+Na^+$); 503.1575 ($M+K^+$); Anal. calcd for $C_{26}H_{22}F_2N_2O_4$: C, 67.23; H, 4.77; F, 8.18; N, 6.03. Found: C, 67.45; H, 4.84; F, 8.40; N, 6.0.

benzyl 1-(2-(2-nitrobenzamido)benzoyl)pyrrolidine-2-carboxylate 6c:

The crude product was purified by column chromatography (eluent: 40% AcOEt/pet. Ether, R_f: 0.3) to furnish 6**c** (90%) as a waxy solid. $[\alpha]^{25.86}_D$: -19.0687° (*c* 1, $CHCl_3$); IR ($CHCl_3$) ν (cm^{-1}): 2924, 2853, 1739, 1688, 1625, 1531, 1456, 1415, 1348, 1310, 1186; ^{1}H NMR (500 MHz, $CDCl_3$) δ: $9.43_{rotamer}$ (s, 0.9H, amide), $9.10_{rotamer}$ (s, 0.1H, amide), $8.50\text{-}8.49_{rotamer}$ (d, J = 8.24 Hz, 0.9H), $8.24\text{-}8.22_{rotamer}$ (m, 0.1H), 8.08-8.06

(d, J = 8.24 Hz, 0.9H), 8.01-7.99 (m, 0.1H), 7.73-7.65 (m, 2H), 7.58-7.55 (m, 1H), 7.51-7.48 (m, 1H), 7.41-7.14 (m, 7H), 5.07-4.98 (m, 2H), 4.71-4.69$_{rotamer}$ (m, 0.9H), 4.51-4.49$_{rotamer}$ (m, 0.1H), 3.64-3..6 (m, 1H), 3.51-3.47 (m, 1H), 2.37-2.27 (m, 1H), 2.01-1.86 (m, 3H); ^{13}C NMR (125 MHz, $CDCl_3$) δ: 172.1, 168.5, 164.9, 146.4, 135.5, 135.3, 133.7, 133.0, 130.9, 130.4, 129.1, 128.6, 128.4, 128.0, 126.6, 125.9, 124.3, 124.1, 122.3, 67.0, 58.9, 49.7, 29.2, 25.0; MALDI-TOF/TOF/TOF: 496.4159 ($M+Na^+$); 512.3204 ($M+K^+$); Anal. calcd for $C_{26}H_{23}N_3O_6$: C, 65.95; H, 4.90; N, 8.87;. Found: C, 65.74; H, 4.69; N, 8.95.

***tert*-butyl 2-((2-((2-(2-((benzyloxy)carbonyl)pyrrolidine-1-carbonyl)phenyl) carbamoyl)phenyl)carbamoyl)pyrrolidine-1-carboxylate 6d**:

The crude product was purified by column chromatography (eluent: 50% AcOEt/pet. Ether, R_f: 0.3) to furnish **2d** (75%) as a waxy solid. $[\alpha]^{25.6}_D$: -48.768° (*c* 0.5, $CHCl_3$); IR ($CHCl_3$) ν (cm^{-1}): 3276, 2925, 2853, 1742, 1694, 1626, 1585, 1520, 1449, 1411, 1298, 1216, 1165, 1121, 1089, 917; ^{1}H NMR (200 MHz, $CDCl_3$) δ: 11.68$_{rotamer}$ (0.6H, amide), 11.63$_{rotamer}$ (0.4H, amide), 10.37$_{rotamer}$ (0.6H, amide), 10.21$_{rotamer}$ (0.4H, amide), 8.65-8.61 (d, J = 8.34 Hz, 1H), 8.50-8.46$_{rotamer}$ (d, J = 7.83 Hz, 0.9H), 8.37-8.33$_{rotamer}$ (d, J = 8.08 Hz, 0.1H), 7.70-7.66 (m, 1H), 7.43-7.39 (m, 3H), 7.13-6.98 (m, 2H), 5.12 (s, 2H), 4.41-4.35 (m, 1H), 4.69-4.65$_{rotamer}$ (m, 0.4H), 4.25-4.18$_{rotamer}$ (m, 0.6H), 3.77-3.36 (m, 2H), 2.33-2.06 (m, 4H), 1.95-1.78 (m, 4H), 1.39$_{rotamer}$ (s, 3H), 1.27$_{rotamer}$ (s, 6H); ^{13}C NMR (50 MHz, $CDCl_3$) δ: 172.1, 171.6, 171.5, 169, 166.9, 154.8, 154.0, 139.7, 136.8, 135.3, 132.8, 131.5, 131.0, 128.4, 128.2, 127.8, 127.4, 127.3, 124.3, 123.1, 122.9, 121.9, 120.8, 120.2, 80.0, 79.8, 77.2, 66.8, 62.4, 61.8, 52.3, 50.4, 46.9, 46.6, 38.4, 36.5, 31.7, 31.3, 30.4, 29.5, 29.0, 28.1, 25.1, 24.5, 24.1, 23.6; MALDI-TOF/TOF/TOF: 663.4386 ($M+Na^+$); 679.4749 ($M+K^+$); Anal. calcd for $C_{36}H_{40}N_4O_7$: C, 67.48; H, 6.29; N, 8.74;. Found: C, 67.68; H, 6.16; N, 8.89.

benzyl 1-(5-isobutoxy-2-(5-isobutoxy-2-nitrobenzamido)benzoyl)pyrrolidine-2-carboxylate 6e:

The crude product was purified by column chromatography (eluent: 35% AcOEt/pet. Ether, R_f: 0.3) to furnish **6e** (91% after 48% recovery of starting material) as a waxy solidWaxy solid. $[\alpha]^{25.6}_D$: -48.768° (*c* 1, $CHCl_3$); IR ($CHCl_3$) ν (cm^{-1}): 3327, 3020, 2964, 2930, 2401, 1735, 1680, 1630, 1590, 1471, 1446, 1397, 1341, 1030; ^{1}H NMR (200 MHz, $CDCl_3$) δ: 8.94$_{rotamer}$ (0.9H, amide), 8.53$_{rotamer}$ (0.1H, amide), 8.34-8.30$_{rotamer}$ (d, J = 9 Hz, 0.9H), 8.12-8.07 (d, J = 9.22 Hz, 1H), 8.02-7.97$_{rotamer}$ (d, J = 9

Hz, 0.1H), 7.37-7.23 (m, 5H), 7.07-6.87 (m, 4H), 5.11-4.93 (2H), 4.71-4.64$_{rotamer}$ (m, 0.9H), 4.54-4.51$_{rotamer}$ (m, 0.1H), 3.83-3.80 (d, J = 6.57 Hz, 2H), 3.73-3.70 (d, J = 6.57 Hz, 2H), 3.65-3.42 (m, 2 H), 2.38-1.91 (m, 7H), 1.04-0.98 (dd, J = 2.65 Hz, J = 6.69 Hz, 4H); ^{13}C NMR (200 MHz, $CDCl_3$) δ: 172.1, 168.1, 165.0, 163.6, 155.7, 138.4, 135.7, 135.3, 128.5, 128.3, 128.0, 127.94, 127.9, 126.9, 124.1, 116.4, 115.4, 114.3, 112.4, 75.3, 74.8, 67.0, 58.8, 49.6, 29.6, 29.2, 28.2, 28.0, 24.9, 19.2, 19.0; MALDI-TOF/TOF/TOF: 640.8233 ($M+Na^+$); 656.9022 ($M+Na^+$); Anal. calcd for $C_{34}H_{39}N_3O_8$: C, 66.11; H, 6.36; N, 6.80;. Found: C, 66.34; H, 6.50; N, 6.85.

2-nitro-*N*-(2-(piperidine-1-carbonyl)phenyl)benzamide 6f:

The crude product was purified by column chromatography (eluent: 50% AcOEt/pet. Ether, R_f: 0.4) to furnish **6f** (94%) as a white solid. mp: 136-138°C; IR ($CHCl_3$) ν (cm^{-1}): 3230, 3004, 2938, 2857, 1678, 1615, 1600, 1531, 1436, 1348, 1310, 1287, 1257, 1125, 1003, 856; ^{1}H NMR (200 MHz, $CDCl_3$) δ: 9.3 (1H, amide), 8.27-8.23 (d, *J* = 8.21 Hz, 1H), 8.11-8.07 (d, *J* = 8.21 Hz, 1H), 7.76-7.57 (m, 3H), 7.52-7.43 (dt, *J* = 1.77 Hz, *J* = 8.46 Hz, 1H), 7.28-7.14 (m, 2H), 3.58 (bs, 4H), 1.67 (bs, 6H); ^{13}C NMR (50 MHz, $CDCl_3$) δ: 168.7, 164.5, 146.4, 135.9, 133.9, 132.8, 130.7, 130.6, 128.7, 127.2, 125.9, 124.7, 124.2, 124.0, 64.7, 43.6, 43.3, 29.7, 26.4, 25.6, 24.4; MALDI-TOF/TOF/TOF: 376.1107 ($M+Na^+$); 392.0699 ($M+K^+$); Anal. calcd for C19H19N3O4: C, 64.58; H, 5.42; N, 11.89;. Found: C, 64.69; H, 5.23; N, 11.87.

(*S*)-2-nitro-*N*-(2-((1-phenylethyl)carbamoyl)phenyl)benzamide 6g:

The crude product was purified by column chromatography (eluent: 40% AcOEt/pet. Ether, R_f: 0.3) to furnish **6g** (94%) as a white solid. $[\alpha]^{25.72}_D$: -0.612° (*c* 1, $CHCl_3$); IR ($CHCl_3$) ν (cm-1): 3251, 2924, 2853, 1681, 1600, 1531, 1437, 1348, 1287, 856; ^{1}H NMR (200 MHz, $CDCl_3$) δ: 11.61 (1H, amide), 8.65-8.61 (d, *J* = 8.21 Hz, 1H), 8.06-8.02 (m, 1H), 7.73-7.60 (m, 3H), 7.59-7.46 (m, 2H), 7.38-7.28 (m, 5H), 7.18- 7.10 (dt, *J* = 0.88 Hz, *J* = 7.58 Hz, 1H), 6.68 (bs, 1H), 5.29-5.15 (pentet, *J* = 7.07 Hz, 1H), 1.61-1.57 (d, *J* = 1.52 Hz, *J* = 6.82 Hz, 3H); ^{13}C NMR (50 MHz, $CDCl_3$) δ: 168.0, 164.4, 146.9, 142.5, 139.0, 133.7, 132.8, 132.7, 130.8, 128.8, 128.4, 127.6, 126.5, 126.0, 124.7, 123.7, 122.0, 120.8, 49.4, 29.7, 21.6; MALDI-TOF/TOF: 412.1174 ($M+Na^+$); 428.0916 ($M+K^+$); Anal. calcd for $C_{22}H_{19}N_3O_4$: C, 67.86; H, 4.92; N, 10.79. Found: C, 67.78; H, 4.69; N, 10.89.

methyl 2-methyl-2-(2-(2-nitrobenzamido)benzamido)propanoate 6h:

The crude product was purified by column chromatography (eluent: 40% AcOEt/pet. Ether, R_f: 0.4) to furnish **6h** (82% after 40% recovery of the starting material) as a white solid. mp: 125-126°C; IR ($CHCl_3$) ν (cm^{-1}): 3325, 2925, 2854, 1740, 1680, 1645, 1601, 1532, 1447, 1348, 1306, 1193, 1153, 904; ^1H NMR (200 MHz, $CDCl_3$) δ: 11.39 (1H, amide), 8.64-8.60 (d, *J* = 8.08 Hz, 1H), 8.07-8.03 (d, *J* = 8.08 Hz, 1H), 7.75-7.49 (m, 5H), 7.18-7.10 (t, *J* = 7.71 Hz, 1H), 6.99 (t, 1H), 3.71 (s, 3H), 1.61 (s, 6H); ^{13}C NMR (50 MHz, $CDCl_3$) δ: 174.7, 168.4, 164.4, 146.8, 138.9, 133.7, 132.9, 132.7, 130.8, 128.4, 16.8, 124.6, 123.6, 122.0, 120.9, 57.0, 52.7, 24.6; MALDI-TOF/TOF/TOF: 408.0110 ($M+Na^+$); 423.9817 ($M+K^+$); Anal. calcd for $C_{19}H_{19}N_3O_6$: C, 59.22; H, 4.97; N, 10.90. Found: C, 59.38; H, 4.69; N, 10.81.

(*R*)-methyl 3-methyl-2-(2-(2-nitrobenzamido)benzamido)butanoate 6i:

The crude product was purified by column chromatography (eluent: 40% AcOEt/pet. Ether, R_f: 0.4) to furnish **6i** (89%) as a pale yellow solid. mp: 145-146°C; $[\alpha]^{26.18}_D$: -7.336° (*c* 1, $CHCl_3$); IR ($CHCl_3$) ν (cm^{-1}): 3332, 2925, 2853, 1740, 1687, 1646, 1588, 1532, 1447, 1349, 1311, 1210; ^1H NMR (200 MHz, $CDCl_3$) δ: 11.46 (1H, amide), 8.72-8.68 (d, *J* = 8.21 Hz, 1H), 8.07-8.03 (d, *J* = 7.83 Hz, 1H), 7.76-7.53 (m, 5H), 7.23-7.15 (t, *J* = 7.71 Hz, 1H), 6.87-6.82 (d, *J* = 8.34 Hz, 1H), 4.68-4.62 (dd, *J* = 5.05 Hz, *J* = 8.46 Hz, 1H), 3.77 (s, 3H), 2.34-2.18 (m, 1H), 1.01-0.97 (dd, *J* = 1.14 Hz, *J* = 6.82 Hz, 6H); ^{13}C NMR (50 MHz, $CDCl_3$) δ: 172.0, 168.6, 164.3, 146.9, 139.1, 133.7, 133.1, 132.9, 130.7, 128.4, 126.7, 124.6, 123.7, 121.9, 120.2, 57.4, 52.4, 31.4, 18.9, 18.0; MALDI-TOF/TOF/TOF: 400.3518 ($M+H^+$); 422.3262 ($M+Na^+$); 438.2873 ($M+K^+$); Anal. calcd for $C_{20}H_{21}N_3O_6$: C, 60.14; H, 5.30; N, 10.52. Found: C, 60.01; H, 5.39; N, 10.85.

2-nitro-N-(2-(propylcarbamoyl)phenyl)benzamide 6j:

The crude product was purified by column chromatography (eluent: 35% AcOEt/pet. Ether, R_f: 0.3) to furnish **2j** (97%) as a white solid. mp: 167-169°C; IR ($CHCl_3$) ν (cm^{-1}): 3449, 2925, 1641, 1599, 1525, 1448, 1347; ^1H NMR (200 MHz, $CDCl_3$) δ: 11.72 (1H, amide), 8.70-8.65 (d, *J* = 8.21 Hz, 1H), 8.07-8.03 (d, *J* = 7.96 Hz, 1H), 7.73-7.49 (m, 5H), 7.18-7.10 (t, *J* = 7.83 Hz, 1H), 6.47 (s, 1H), 3.4-3.29 (m, 7.33 Hz, 3H); ^{13}C NMR (50 MHz, $CDCl_3$) δ: 168.8, 164.3, 139.1, 133.7, 133.0, 132.7, 130.7, 128.4, 126.4, 124.7, 123.6, 121.9, 120.8, 63.6, 63.1, 41.7, 29.7, 22.6, 11.4; MALDI-

TOF/TOF: 350.2100 ($M+Na^+$); 366.2022 ($M+K^+$); Anal. calcd for C17H17N3O4: C, 62.38; H, 5.23; N, 12.84. Found: C, 62.60; H, 5.21; N, 12.88.

methyl (2-((*S*)-1-((2-(2-((*S*)-2-((*tert*-butoxycarbonyl)amino)-4-methylpentanamido)-2-methylpropanamido)phenyl)sulfonyl)pyrrolidine-2-carboxamido)-2-methyl propanoyl)-L-leucinate 12a:

A solution of free acid **11b** (0.15 g, 0.25 mmol, 1 equiv.) and dimer amine H_2N-Aib-^{L}Leu-OMe (0.07 g, 0.31 mmol, 1.2 equiv.) in anhy. DCM was cooled to 0 °C. To this mixture EDC.HCl (0.073 g, 0.38 mmol, 1.5 equiv.) was added followed by HOBt (0.041 g, 0.31 mmol, 1.2 equiv.), and was stirred at 0 °C for 10 min followed by 12 h at room temperature. DCM (30 mL) was then added to the reaction mixture and the organic layer washed sequentially with sat. $NaHCO_3$, water, sat. $KHSO_4$ and brine, and concentrated under reduced pressure. The crude product was purified by column chromatography (eluent: 60% AcOEt/pet. Ether, R_f: 0.3) to furnish **12a** (90%) as a white solid. mp: 106-108 °C ; $[\alpha]^{26.1}_D$: -83.496° (*c* 1, $CHCl_3$); IR ($CHCl_3$) ν (cm^{-1}): 3226, 2958, 1662, 1521, 1436, 1367, 1337, 1246, 1152, 1019; ^{1}H NMR (200 MHz, $CDCl_3$) δ: 10.18 (s, 1H, amide), 8.58-8.54 (d, *J* = 8.46 Hz, 1H), 7.84-7.80 (dd, *J* = 1.52 Hz, *J* = 8.08 Hz, 1H), 7.61-7.52 (dt, *J* = 1.52 Hz, *J* = 8.59 Hz, 1H), 7.33 (broad, 1H, amide), 7.22-7.14 (m, 2H), 6.90-6.86 (d, *J* = 8.21 Hz, 1H), 5.28 (s, 1H), 5.21-5.17 (d, 8.08 Hz, 1H), 4.62-4.50 (m, 2H), 3.69 (s, 3H), 3.64-3.58 (m, 3H), 3.27-3.15 (m, 1H), 2.10-2.02 (m, 2H), 1.91-1.76 (m, 3H), 1.64 (s, 3H), 1.61-1.58 (5H), 1.53 (s, 3H), 1.50 (s, 3H), 1.47 (s, 3H), 1.64 (s, 3H), 1.40 (s, 9H), 0.91-0.85 (m, 12H); ^{13}C NMR (50 MHz, $CDCl_3$) δ: 173.7, 173.5, 172.9, 172.8, 170.8, 155.9, 137.2, 134.7, 129.8, 123.7, 123.3, 122.4, 80.1, 61.9, 57.6, 57.1, 52.9, 52.1, 50.8, 49.8, 41.3, 40.8, 30.8, 29.6, 28.2, 26.2, 25.5, 24.7, 24.6, 24.3, 24.0, 23.1, 22.7, 21.8; MALDI-TOF/TOF: 804.5322 $(M+Na)^+$; 820.6038 $(M+K)^+$; Anal. calcd for $C_{37}H_{60}N_6O_{10}S$: C, 56.90; H, 7.74; N, 10.76; Found: C, 56.69; H, 7.60; N, 10.59.

***tert*-butyl ((*S*)-4-methyl-1-((2-methyl-1-((2-(((*S*)-2-((2-methyl-1-(((*S*)-4-methyl-1-(methylamino)-1-oxopentan-2-yl)amino)-1-oxopropan-2-yl)carbamoyl) pyrrolidin-1-yl)sulfonyl)phenyl)amino)-1-oxopropan-2-yl)amino)-1-oxopentan-2-yl)carbamate 12b:**

Compound **12b** was synthesized from ester **12a**, following the procedure for **4b.** The crude product was purified by column chromatography (eluent: 85% AcOEt/pet. Ether, R_f: 0.2) to furnish **12b** (85%) as a fluffy white solid. mp: 182-184 °C; $[\alpha]^{25.1}_D$: -60.608° (*c* 1, $CHCl_3$); IR ($CHCl_3$) ν (cm^{-1}): 3335, 2958, 2925, 2872, 2853, 1661, 1582, 1524, 1466, 1366, 1334, 1220, 1153, 1024; ^{1}H NMR (500 MHz, $CDCl_3$) δ: 9.92

(broad, 1H, amide), 8.45-8.43 (m, 1H), 7.74-7.72 (d, *J* = 7.82 Hz, 1H), 7.63-7.59 (m,1H), 7.36 (broad,1H, amide), 7.25-7.21 (m,1H), 7.06 (broad,1H), 6.88 (broad, 1H), 5.07-5.06 (m,1H), 4.39 (broad,1H), 4.23-4.20 (m,1H), 3.99 (broad,1H), 3.67-3.62 (m,1H), 3.16-3.15 (m,1H), 2.80-2.79 (d, *J* = 4.65 Hz, 3H), 2.03-1.97 (m, 2H), 1.85-1.83 (m, 2H), 1.72-1.63 (m, 4H), 1.62 (s, 3H), 1.58 (s, 6H), 1.56-1.53 (m, 2H), 1.49 (s, 3H), 1.37 (s, 9H), 0.95-0.88 (m, 12H); ^{13}C NMR (125 MHz, $CDCl_3$) δ: 173.9, 173.3, 173.0, 172.8, 171.6, 156.0, 137.4, 135.1, 129.9, 124.0, 123.0, 80.2, 62.7, 57.6, 57.2, 53.1, 52.1, 49.9, 49.5, 40.6, 39.4, 30.9, 28.2, 27.2, 26.3, 25.7, 25.1, 24.7, 24.6, 23.5, 23.1, 21.8, 21.3; MALDI-TOF/TOF: 803.5760 $(M+Na)^+$; 819.6427 $(M+K)^+$; Anal. calcd for $C_{37}H_{61}N_7O_9S$: C, 56.98; H, 7.88; N, 12.57. Found: C, 56.79; H, 7.68; N, 12.52.

methyl ((2-((*S*)-2-(1,3-dioxoisoindolin-2-yl)-4-methylpentanamido)phenyl) sulfonyl)-L-prolinate 13a:

Phth-^{L}Leu-OH (0.4 g, 1.54 mmol, 1.5 equiv.) was converted to the corresponding acid chloride using oxalyl choride (0.14 mL, 1.84mmol, 1.8 equiv.) and catalytic amount of DMF in dichloromethane (10 mL) as the solvent. After 30 min, solvent and excess oxalyl chloride were removed under reduced pressure. The residue obtained was taken in dichloromethane (10 mL) and a solution containing amine **9b** (0.3 g, 1.02 mmol, 1 equiv.) and TEA (0.23 mL, 1.74 mmol, 1.7 equiv.) in DCM (5 mL) was added and the reaction mixture was allowed to stir for 12 h at room temperature. The solvent was removed under reduced pressure. The crude product was purified by column chromatography (eluent: 20% AcOEt/pet. Ether, R_f: 0.3) to furnish **13a** (33%) as a yellow sticky liquid that turned black on standing for a day. IR ($CHCl_3$) ν (cm^{-1}): 3063, 2959, 1720, 1661, 1532, 1453, 1417, 1384, 1247, 1153, 107; ^{1}H NMR (200 MHz, $CDCl_3$) δ: 10.28 (s, 1H, amide), 7.88-7.79 (m, 5H), 7.55-7.47 (m, 1H), 7.12-7.03 (m, 1H), 6.77-6.29 (m, 1H), 5.24-5.16 (dd, *J* = 4.42 Hz, *J* = 10.23 Hz, 1H), 4.55-4.4 (m, 1H), 3.70 (s, 3H), 3.72-3.64 (m, 2H), 3.46-3.37 (m, 2H), 2.58-2.45 (m, 1H), 2.19-1.81 (m, 5H), 1.62-1.47 (m, 1H), 1.01-0.96 (m, 6H); ^{13}C NMR (50 MHz, $CDCl_3$) δ: 167.7, 162.2, 134.4, 134.2, 131.7, 131.6, 130.3, 130.1, 123.7, 123.5, 121.7, 117.6, 116.9, 114.9, 60.0, 59.5, 53.0, 49.8, 48.6, 37.1, 30.9, 30.8, 25.1, 24.9, 24.8, 24.6, 23.1, 21.0; LC-MS: 550.03 $(M+Na)^+$, 566.00 $(M+K)^+$; Anal. calcd for $C_{26}H_{29}N_3O_7S$: C, 59.19; H, 5.54; N, 7.96. Found: C, 59.29; H, 5.69; N, 7.81.

methyl ((2-((*S*)-2-(2-((*tert*-butoxycarbonyl)amino)-2-methylpropanamido)-4-methylpentanamido)phenyl)sulfonyl)-L-prolinate 14a:

Amine **13b** was synthesized using standard phthalimide deprotection procedure with hydrazine hydrate in DCM:EtOH, which was used without any further purification. Compound **14a** was synthesized from acid Boc-Aib-OH and amine **13b**, following the procedure for **12a.** The crude product was purified by column chromatography (eluent: 30% AcOEt/pet. Ether, R_f: 0.3) to furnish **14a** (81%) as a waxy solid. $[\alpha]^{23.5}_D$: -60.752° (*c* 1, $CHCl_3$); IR ($CHCl_3$) ν (cm^{-1}): 3325, 2958, 1662, 1521, 1436, 1367, 1246, 1152, 1019; ^{1}H NMR (200 MHz, $CDCl_3$) δ: 9.91 (s, 1H, amide), 8.54-8.49 (dd, *J* = 0.88 Hz, *J* = 8.46 Hz, 1H), 7.92-7.87 (dd, *J* = 1.64 Hz, *J* = 7.96 Hz, 1H), 7.62-7.53 (m, 1H), 7.25-7.17 (m, 1H), 7.12- 7.08 (d, *J* = 7.83 Hz, 1H), 5.09 (s, 1H), 4.82-4.74 (m,1H), 4.49-4.43 (m,1H), 3.72 (s, 3H), 3.35-3.29 (t, *J* = 6.57 Hz, 2H), 2.18-2.05 (m, 2H), 1.95-1.85 (m, 3H), 1.77-1.67 (m, 3H), 1.62 (s, 3H), 1.52 (s, 3H), 1.43 (s, 9H), 0.99-0.92 (m, 6H); ^{13}C NMR (50 MHz, $CDCl_3$) δ: 175.0, 172.4, 171.6, 154.8, 136.5, 134.4, 129.8, 125.4, 123.7, 122.9, 80.1, 59.7, 56.9, 52.9, 52.7, 48.6, 41.5, 30.8, 29.6, 28.2, 26.1, 25.0, 24.7, 23.2, 21.6; MALDI-TOF/TOF: 605.2064 $(M+Na)^+$; 621.1768 $(M+K)^+$; Anal. calcd for $C_{27}H_{42}N_4O_8S$: C, 55.65; H, 7.27; N, 9.62; Found: C, 55.46; H, 7.21; N, 9.82.

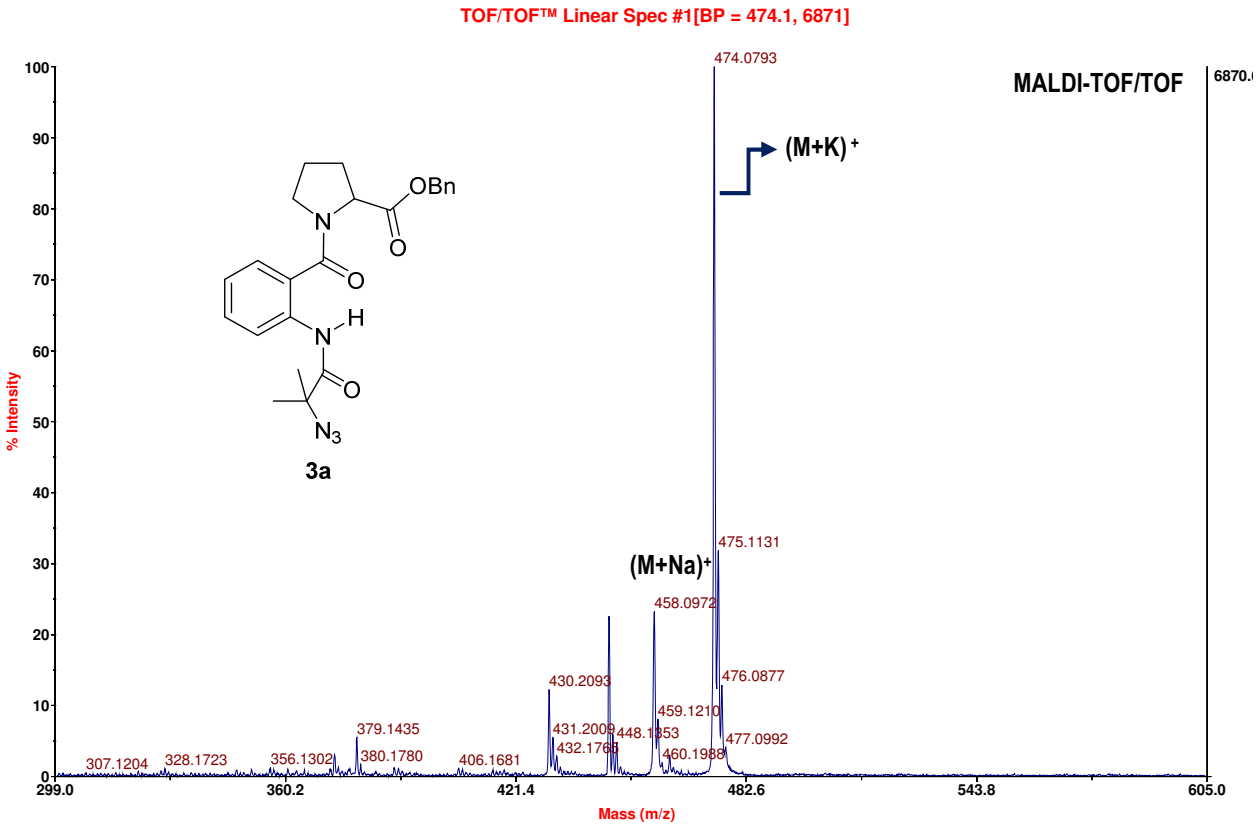
TOF/TOF™ Linear Spec #1[BP = 474.1, 6871]
MALDI-TOF/TOF
474.0793
(M+K)+
(M+Na)+
475.1131
458.0972
476.0877
430.2093
459.1210
477.0992
379.1435
431.2009
448.1353
432.1768
460.1988
307.1204
328.1723
356.1302
380.1780
406.1681
OBn
3a
% Intensity
Mass (m/z)

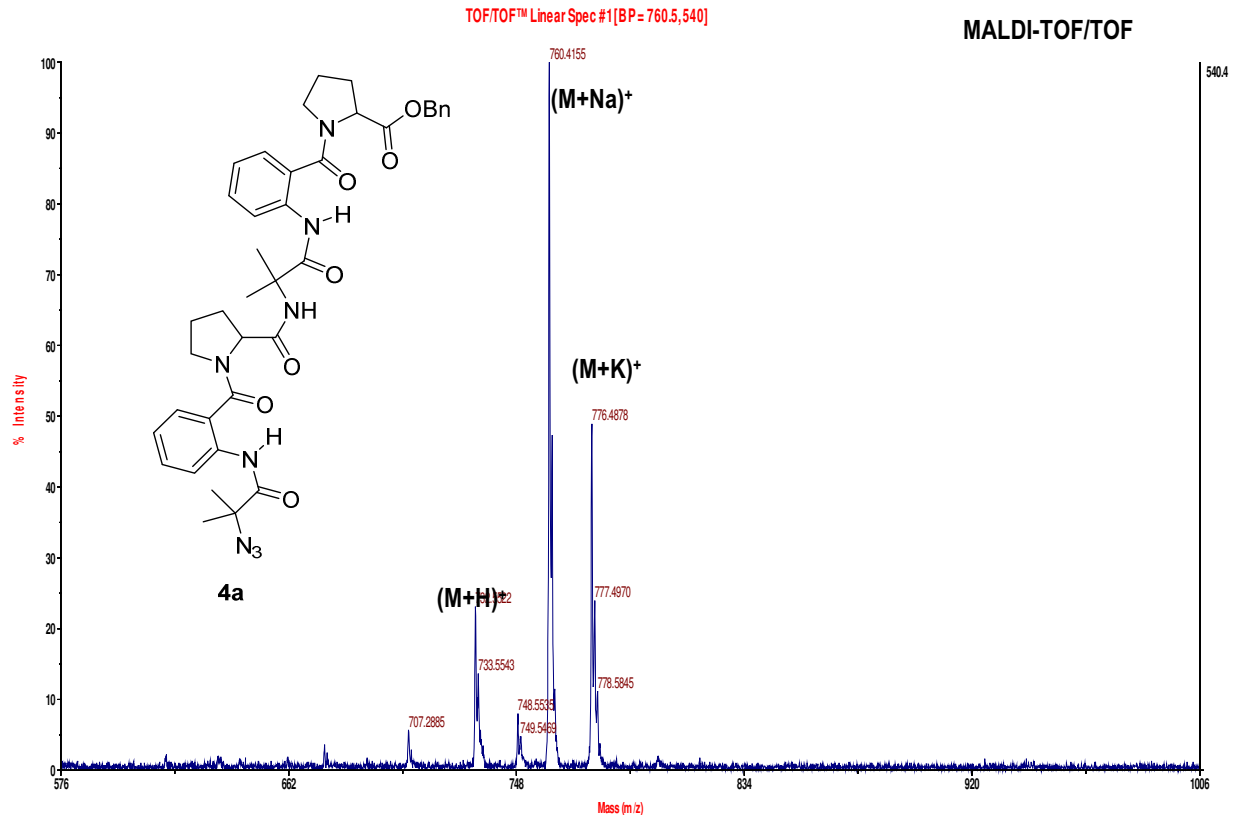
TOF/TOF™ Linear Spec #1[BP = 760.5, 540]
MALDI-TOF/TOF
760.4155
(M+Na)+
(M+K)+
776.4878
777.4970
778.5845
733.5543
707.2885
OBn
4a
% Intensity
Mass (m/z)

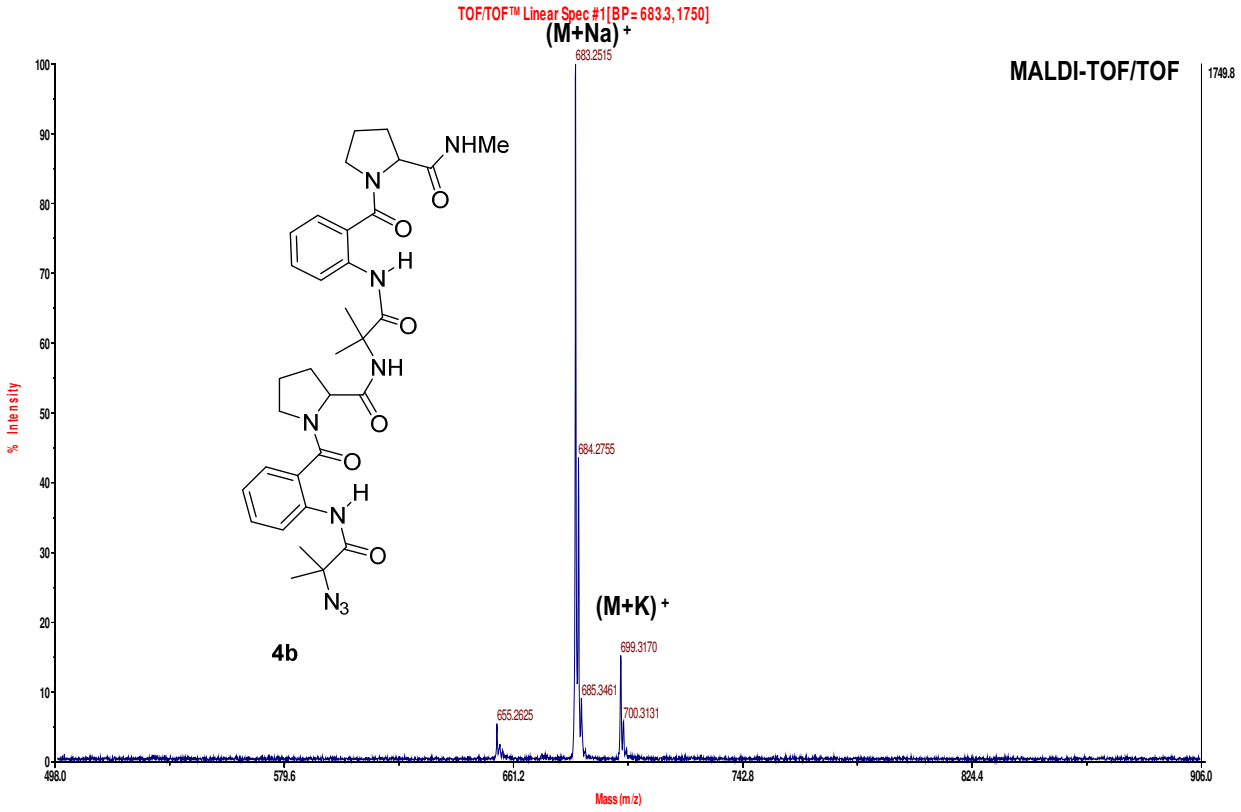
TOF/TOF™ Linear Spec #1[BP = 683.3, 1750]
(M+Na)+
683.2515
MALDI-TOF/TOF
1749.8
NHMe
NH
N3
4b
(M+K)+
684.2755
699.3170
685.3461
700.3131
655.2625
% Intensity
Mass (m/z)

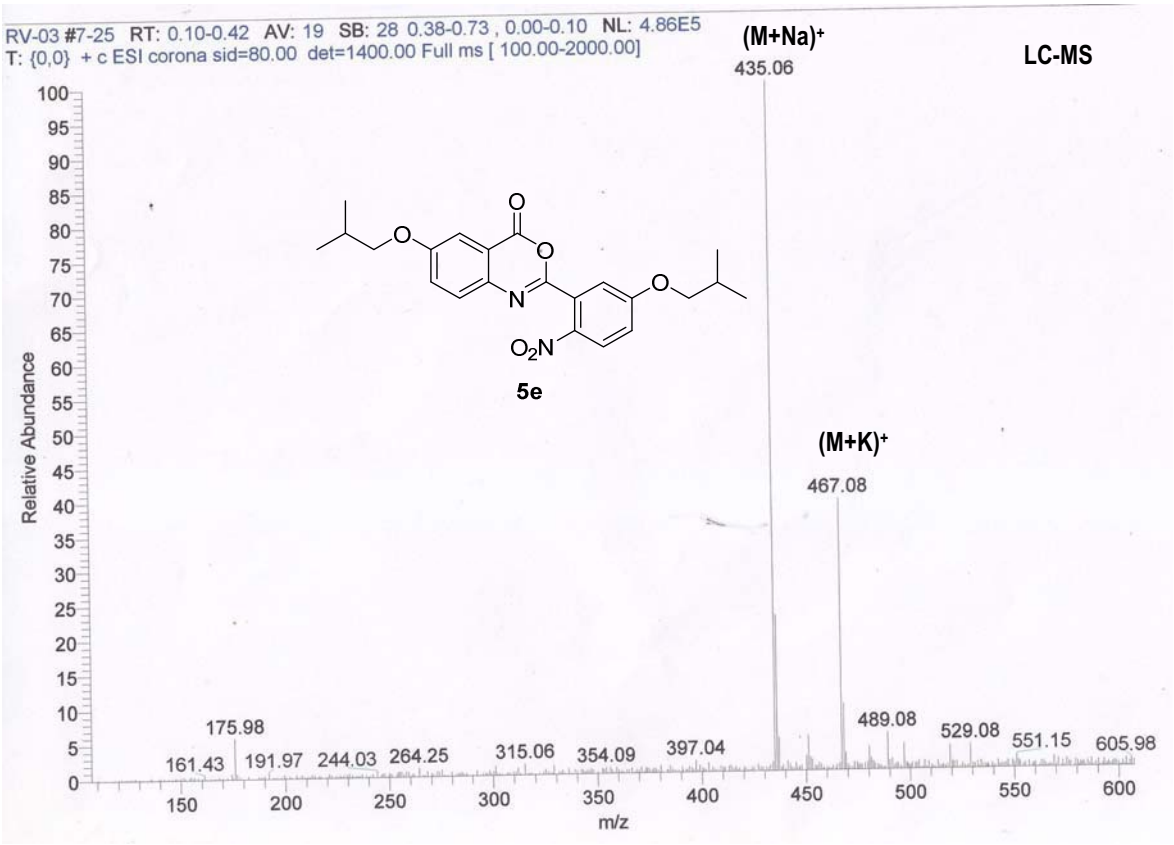
RV-03 #7-25 RT: 0.10-0.42 AV: 19 SB: 28 0.38-0.73 , 0.00-0.10 NL: 4.86E5
T: {0,0} + c ESI corona sid=80.00 det=1400.00 Full ms [100.00-2000.00]
(M+Na)+
435.06
LC-MS
O2N
5e
(M+K)+
467.08
Relative Abundance
175.98
161.43
191.97
244.03
264.25
315.06
354.09
397.04
489.08
529.08
551.15
605.98
m/z

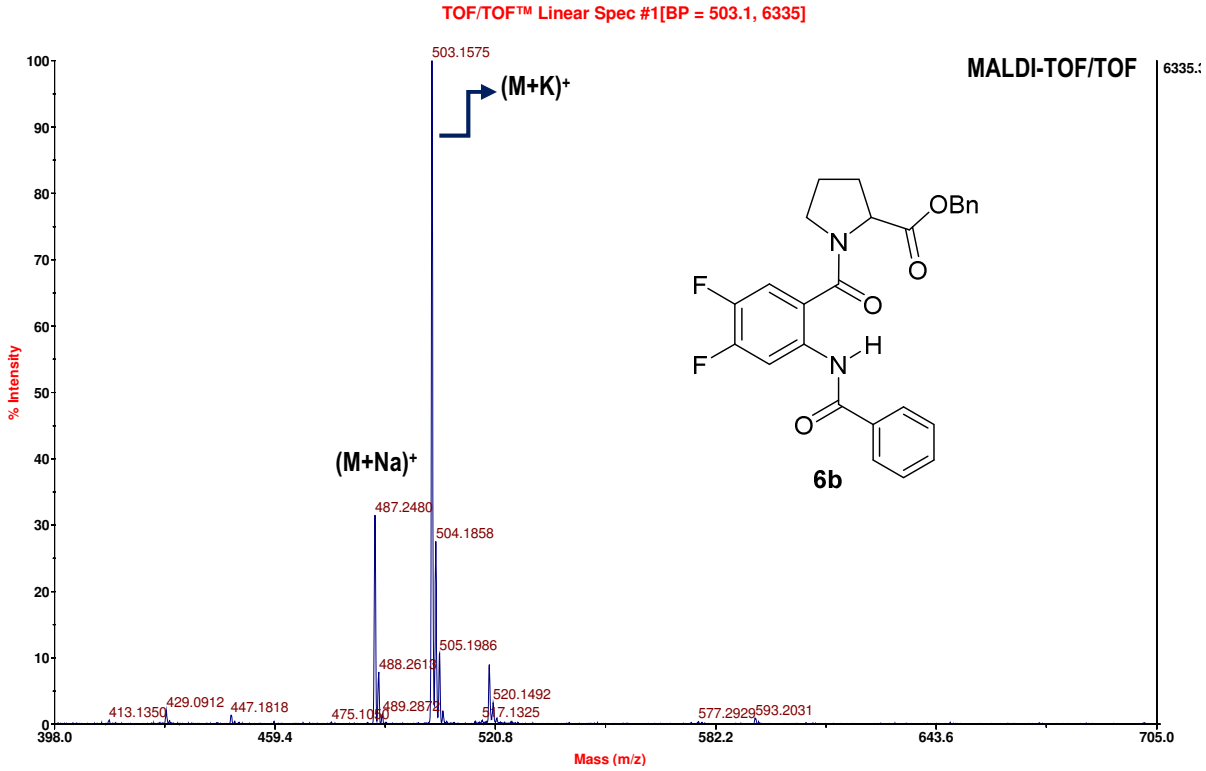
TOF/TOF™ Linear Spec #1[BP = 503.1, 6335]
MALDI-TOF/TOF
503.1575
(M+K)+
(M+Na)+
487.2480
504.1858
505.1986
488.2613
520.1492
413.1350
429.0912
447.1818
475.1050
489.2879
517.1325
577.2929
593.2031
OBn
N
O
F
F
H
6b
% Intensity
Mass (m/z)
100
90
80
70
60
50
40
30
20
10
0
398.0
459.4
520.8
582.2
643.6
705.0

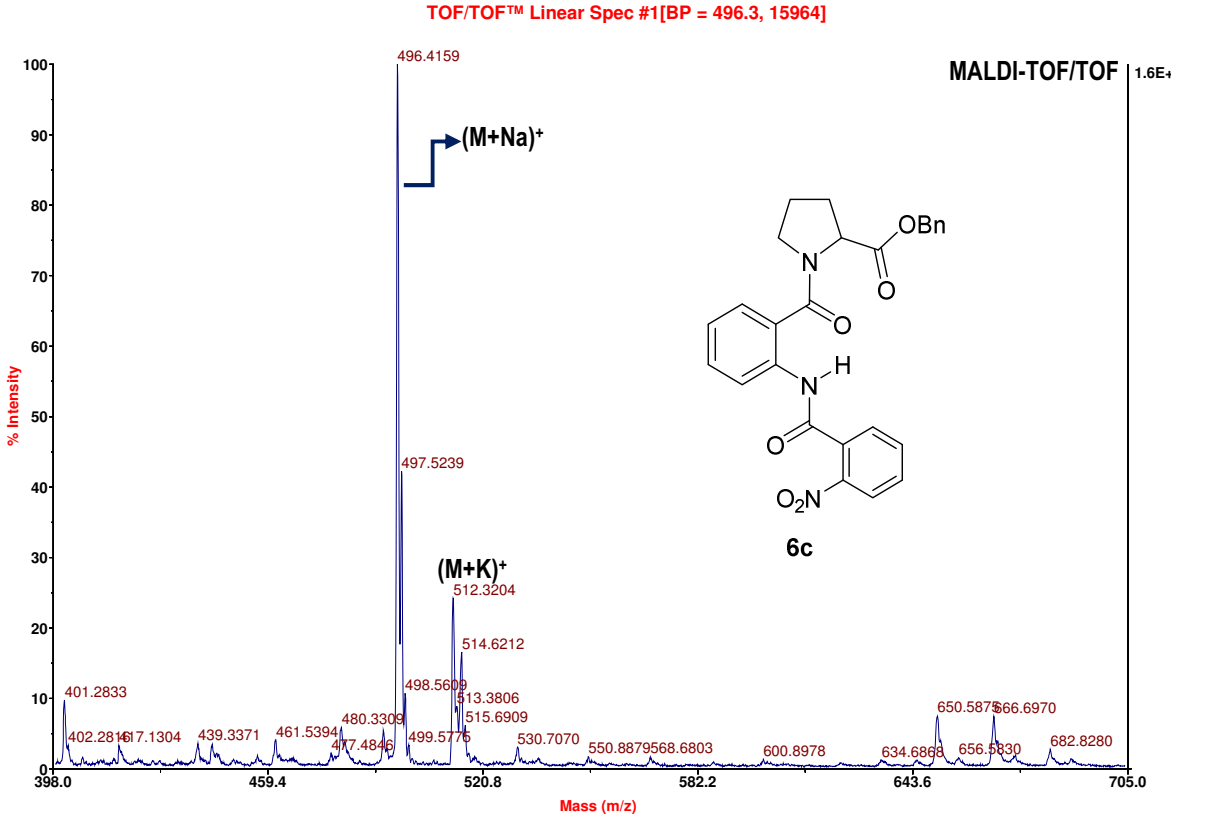
TOF/TOF™ Linear Spec #1[BP = 496.3, 15964]
MALDI-TOF/TOF
496.4159
(M+Na)+
497.5239
(M+K)+
512.3204
514.6212
498.5609
513.3806
515.6909
401.2833
402.2814
417.1304
439.3371
461.5394
480.3309
477.4846
499.5775
530.7070
550.8879568.6803
600.8978
634.6868
650.5875
656.5830
666.6970
682.8280
OBn
N
O
H
O2N
6c
% Intensity
Mass (m/z)
100
90
80
70
60
50
40
30
20
10
0
398.0
459.4
520.8
582.2
643.6
705.0

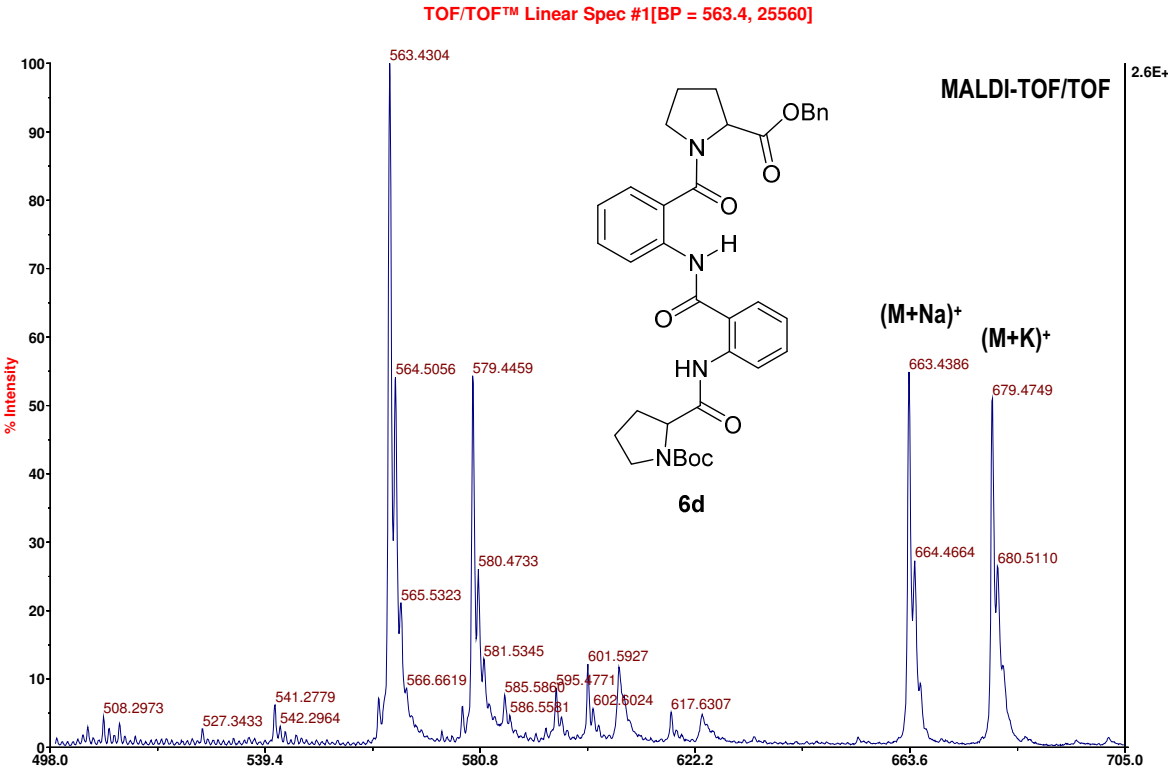
TOF/TOF™ Linear Spec #1[BP = 563.4, 25560]
MALDI-TOF/TOF
2.6E+
% Intensity
563.4304
564.5056
579.4459
580.4733
565.5323
581.5345
566.6619
601.5927
585.5865
595.4771
586.5581
602.6024
508.2973
527.3433
541.2779
542.2964
617.6307
(M+Na)+
(M+K)+
663.4386
679.4749
664.4664
680.5110
OBn
N
O
H
HN
NBoc
6d
100
90
80
70
60
50
40
30
20
10
0
498.0
539.4
580.8
622.2
663.6
705.0

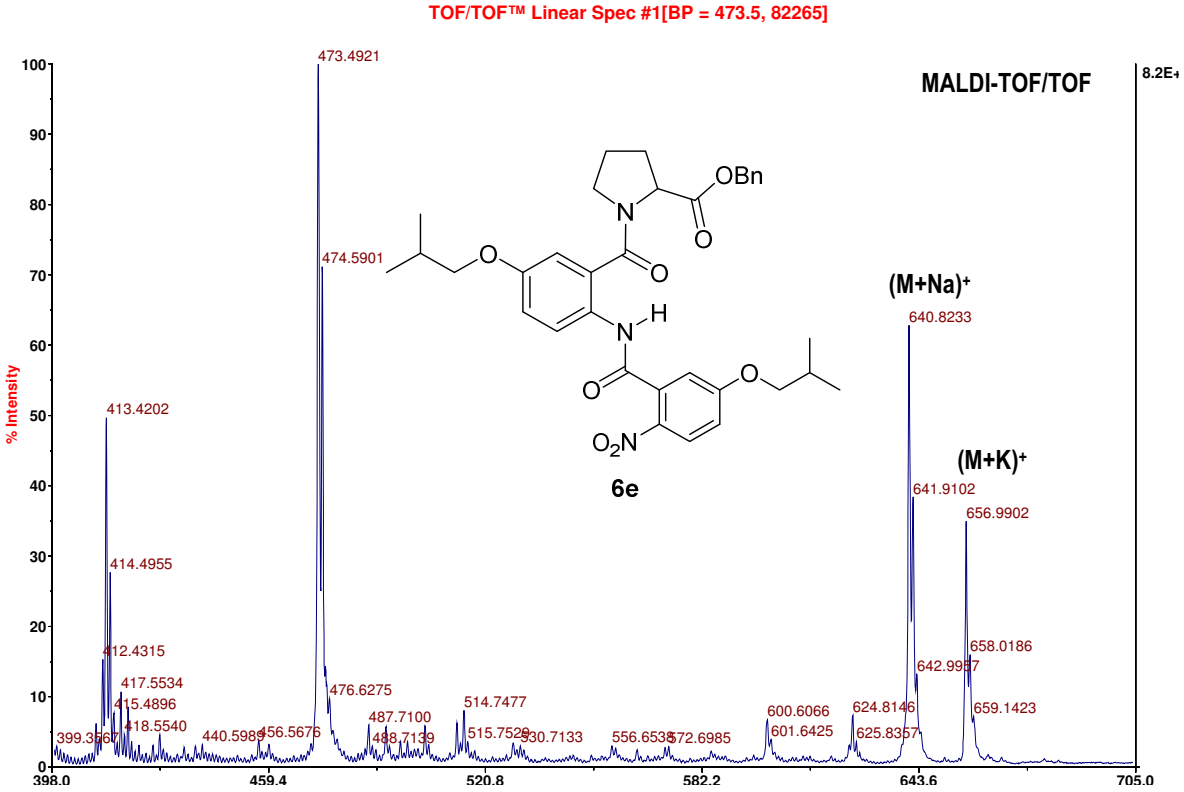
TOF/TOF™ Linear Spec #1[BP = 473.5, 82265]
MALDI-TOF/TOF
8.2E+
% Intensity
473.4921
474.5901
413.4202
414.4955
412.4315
417.5534
415.4896
418.5540
399.3567
440.5985
456.5676
476.6275
487.7100
488.7139
514.7477
515.7529
530.7133
556.6538
572.6985
600.6066
601.6425
624.8146
625.8357
640.8233
641.9102
656.9902
658.0186
642.9957
659.1423
(M+Na)+
(M+K)+
OBn
N
O
H
O2N
6e
100
90
80
70
60
50
40
30
20
10
0
398.0
459.4
520.8
582.2
643.6
705.0

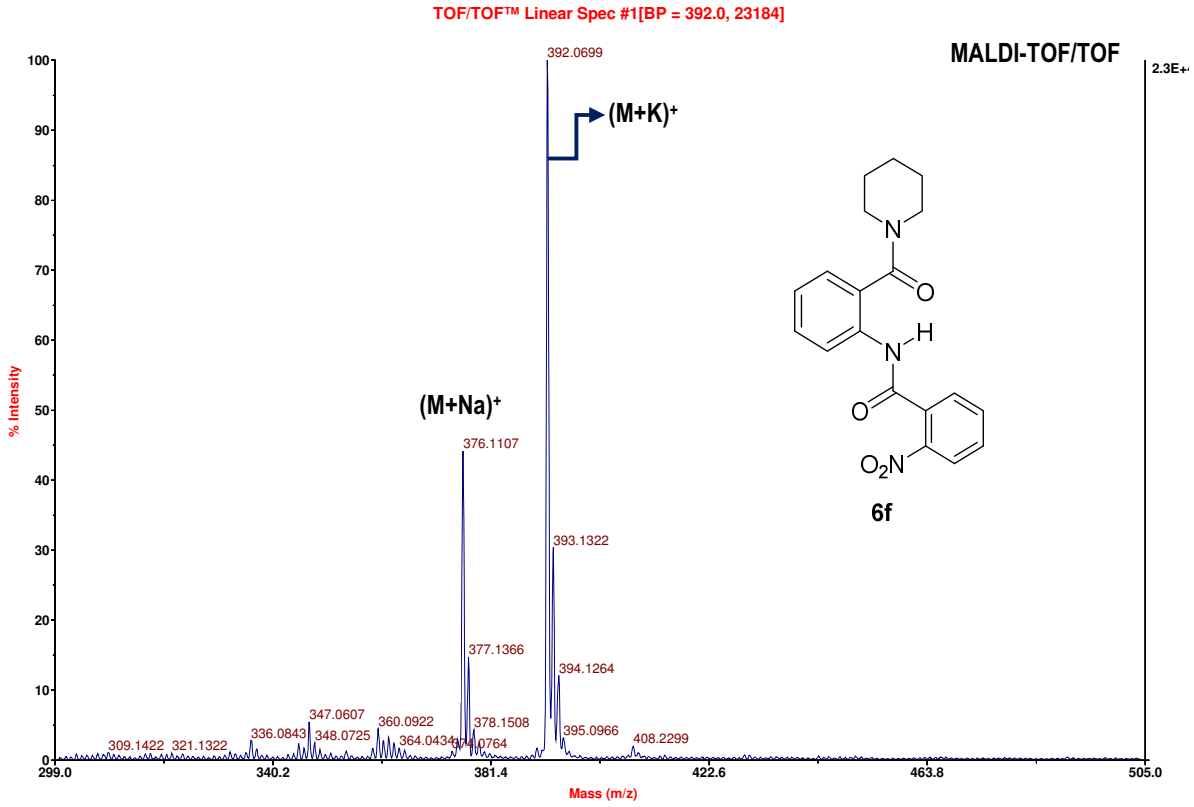
TOF/TOF™ Linear Spec #1[BP = 392.0, 23184]
MALDI-TOF/TOF
392.0699
(M+K)+
(M+Na)+
376.1107
393.1322
377.1366
394.1264
347.0607
360.0922
336.0843
348.0725
378.1508
395.0966
309.1422
321.1322
364.0434
374.0764
408.2299
% Intensity
Mass (m/z)
299.0
340.2
381.4
422.6
463.8
505.0
N
O
H
O2N
6f

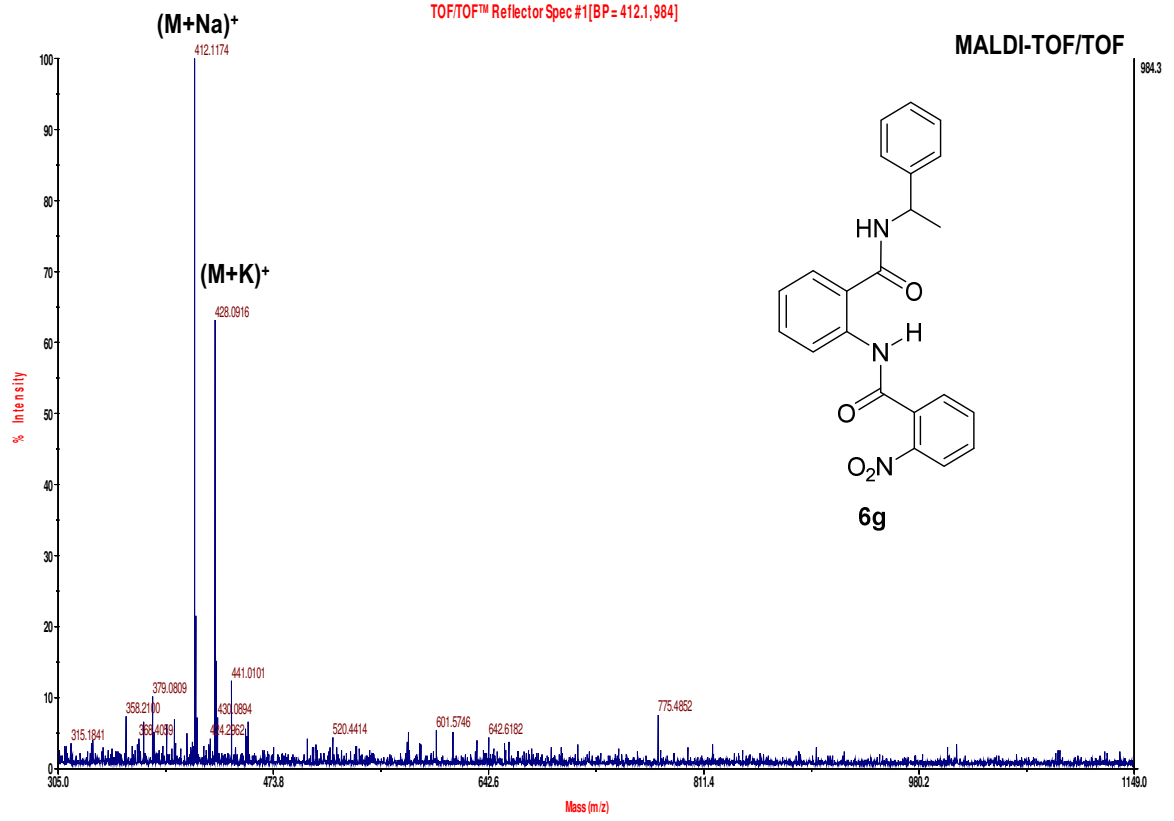
TOF/TOF™ Reflector Spec #1[BP = 412.1, 984]
MALDI-TOF/TOF
(M+Na)+
412.1174
(M+K)+
428.0916
441.0101
379.0809
358.2100
430.0894
315.1841
520.4414
601.5746
642.6182
775.4652
% Intensity
Mass (m/z)
305.0
473.8
642.6
811.4
980.2
1149.0
HN
O
N
H
O2N
6g

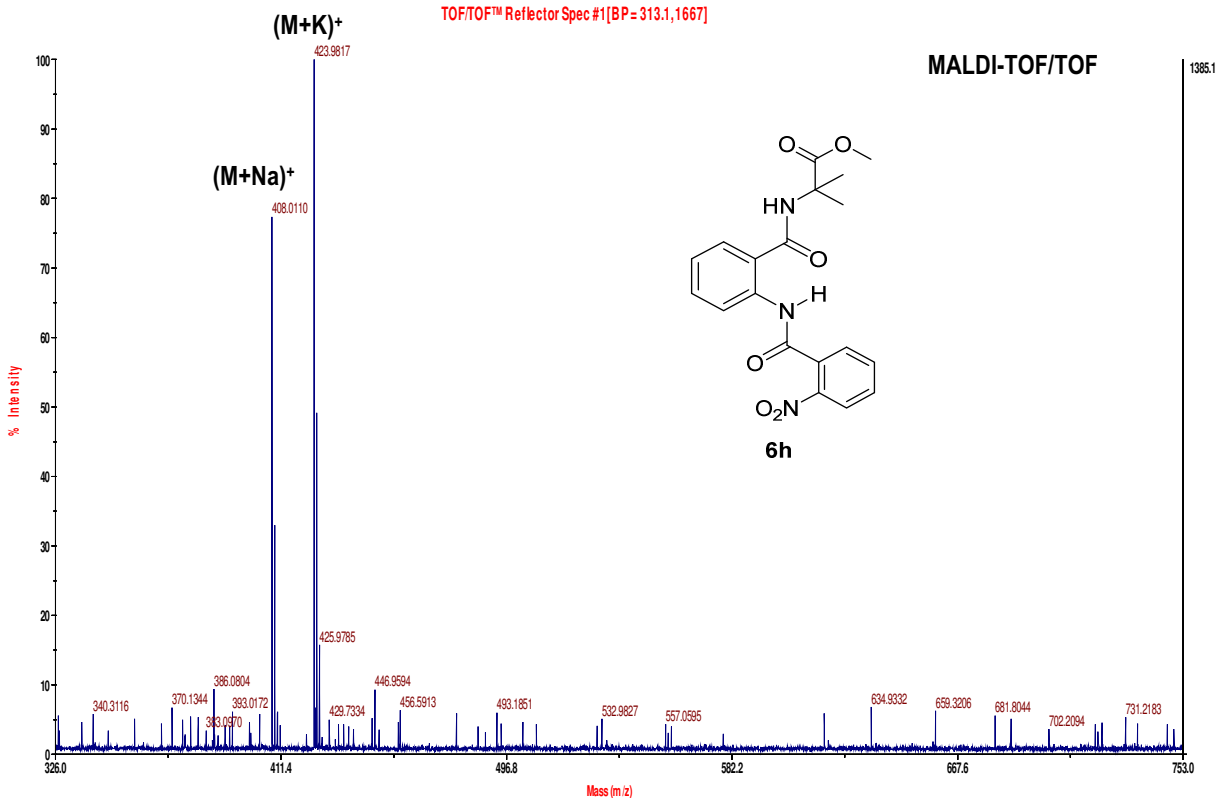
TOF/TOF™ Reflector Spec #1[BP = 313.1,1667]
MALDI-TOF/TOF
(M+K)+
423.9817
(M+Na)+
408.0110
425.9785
386.0804
446.9594
340.3116
370.1344
393.0172
429.7334
456.5913
493.1851
532.9827
557.0595
634.9332
659.3206
681.8044
702.2094
731.2183
1385.1
% Intensity
Mass (m/z)
6h

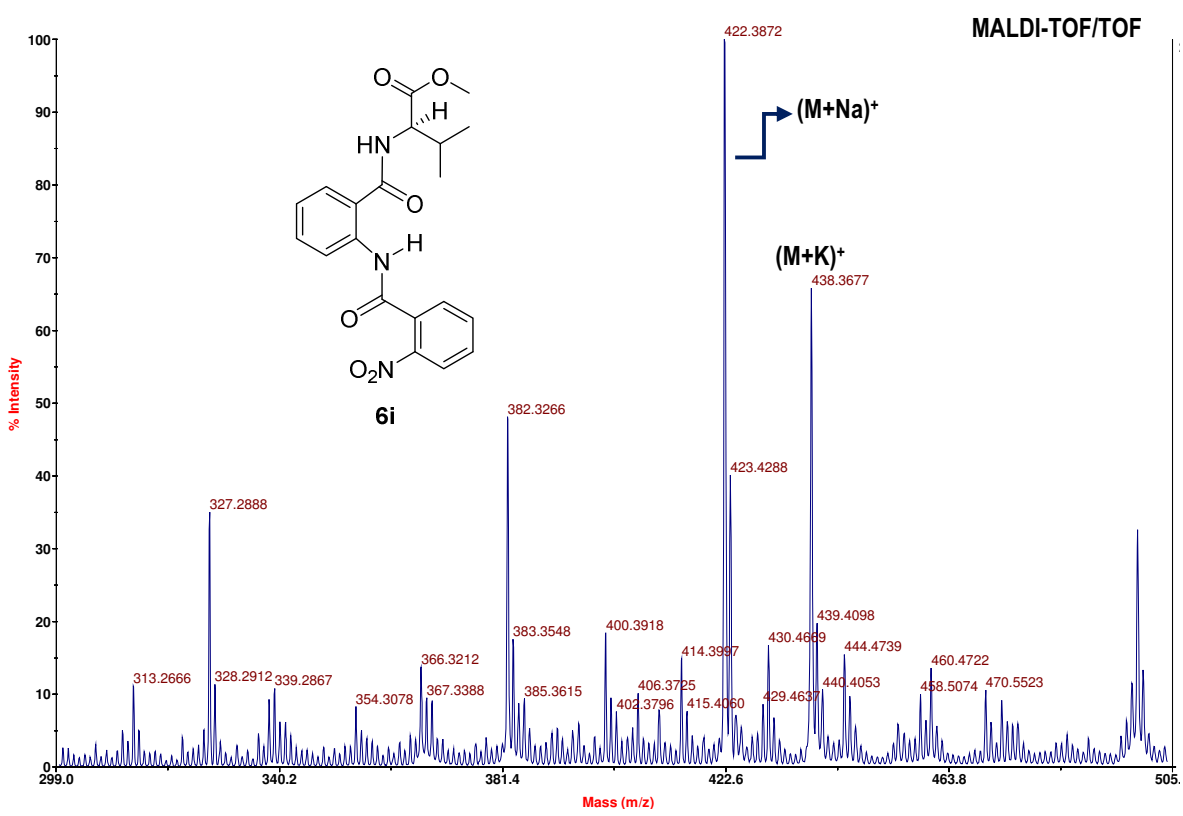
TOF/TOF™ Linear Spec #1[BP = 422.3, 26814]
MALDI-TOF/TOF
422.3872
(M+Na)+
(M+K)+
438.3677
382.3266
423.4288
327.2888
439.4098
383.3548
400.3918
444.4739
366.3212
414.3997
430.4669
460.4722
313.2666
328.2912
339.2867
354.3078
367.3388
385.3615
406.3725
402.3796
415.4060
429.4637
440.4053
458.5074
470.5523
% Intensity
Mass (m/z)
6i

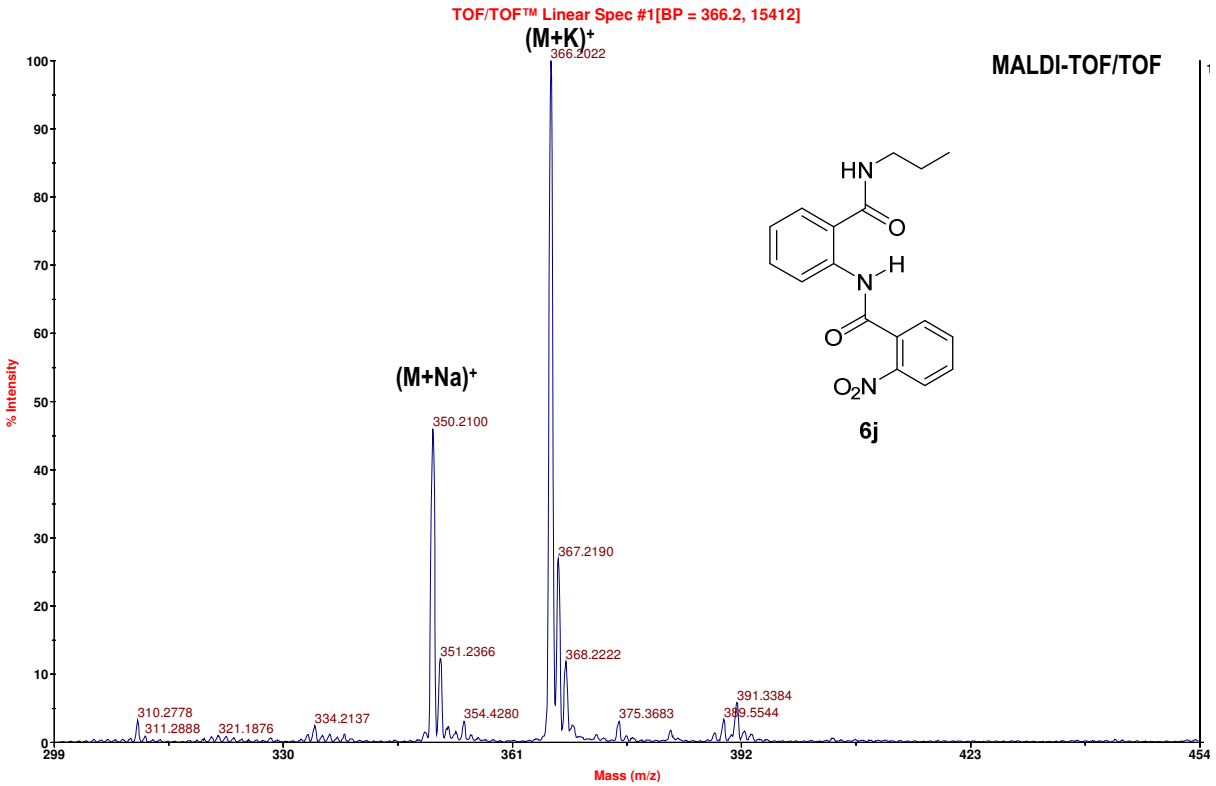
TOF/TOF™ Linear Spec #1[BP = 366.2, 15412]
(M+K)+
366.2022
MALDI-TOF/TOF
(M+Na)+
350.2100
367.2190
351.2366
368.2222
391.3384
310.2778
311.2888
321.1876
334.2137
354.4280
375.3683
389.5544
% Intensity
Mass (m/z)
HN
O
N
H
O
O2N
6j

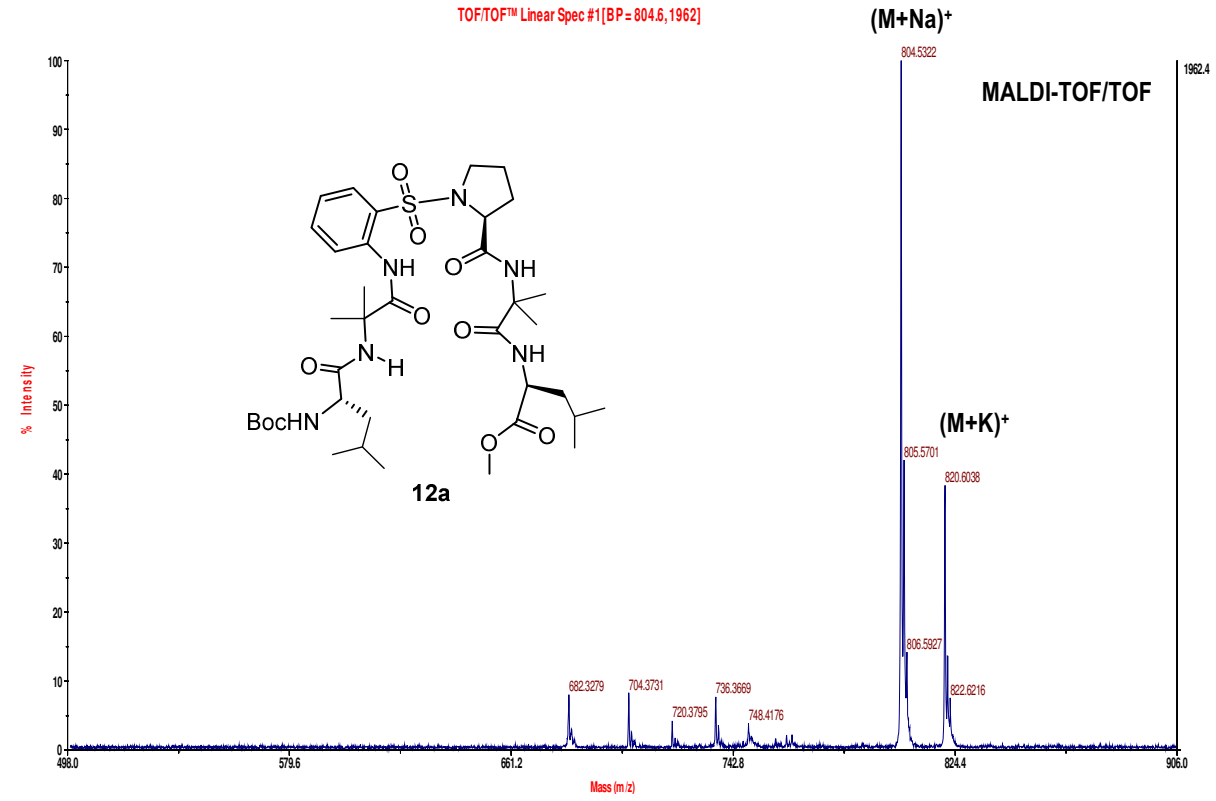
TOF/TOF™ Linear Spec #1[BP = 804.6, 1962]
(M+Na)+
804.5322
MALDI-TOF/TOF
(M+K)+
805.5701
820.6038
806.5927
822.6216
682.3279
704.3731
720.3795
736.3669
748.4176
% Intensity
Mass (m/z)
BocHN
12a

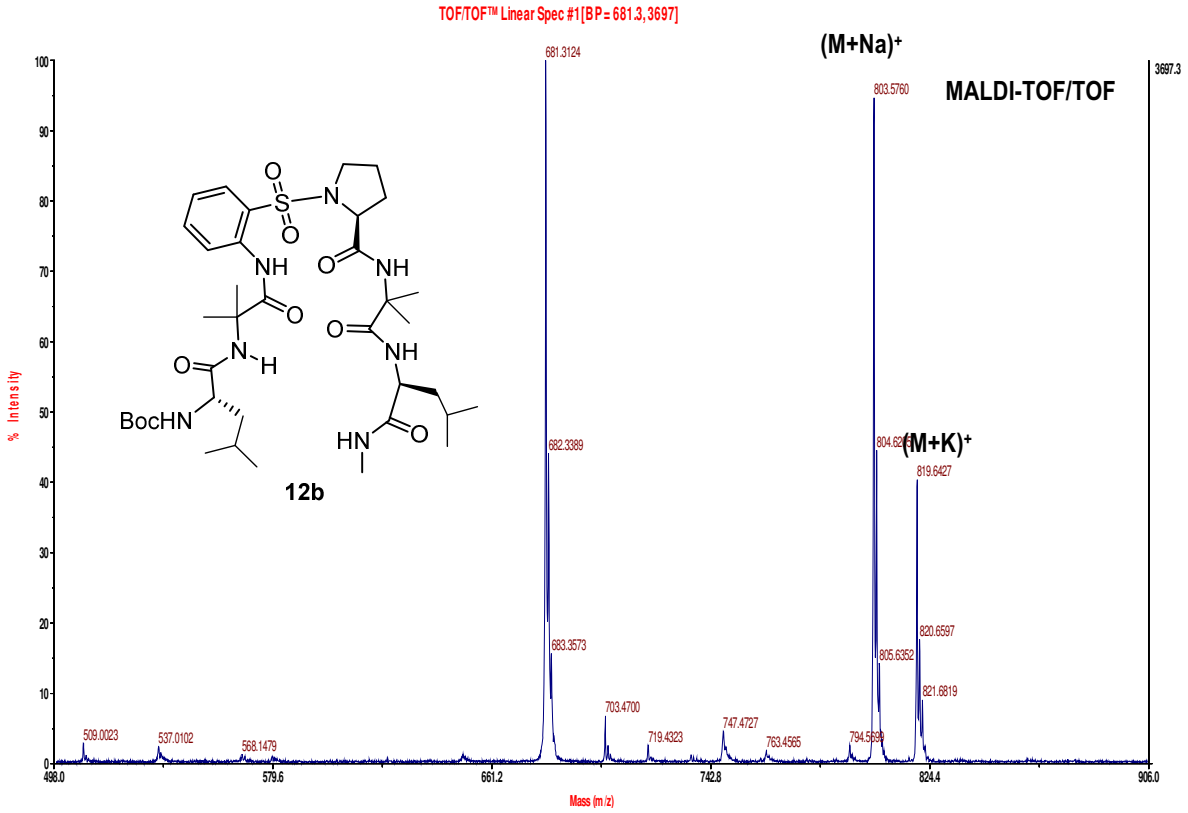
TOF/TOF™ Linear Spec #1[BP = 681.3, 3697]
(M+Na)+
MALDI-TOF/TOF
(M+K)+
12b
% Intensity
Mass (m/z)

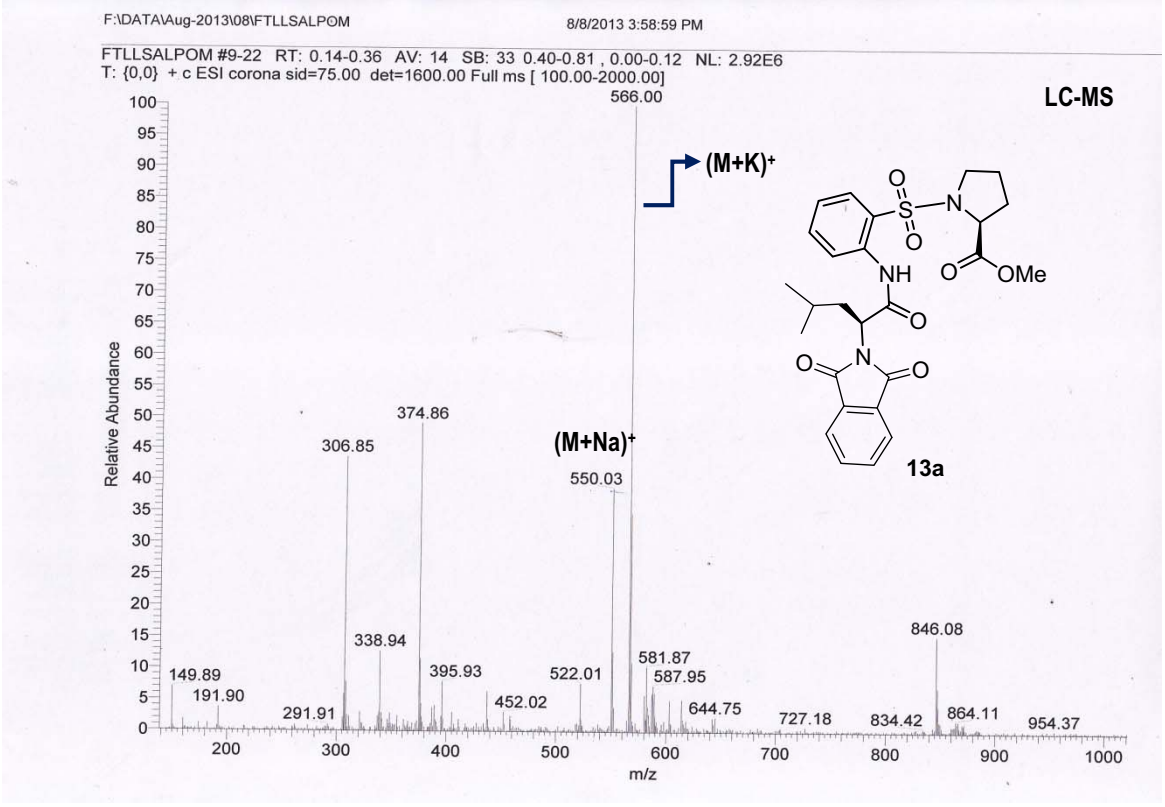
F:\DATA\Aug-2013\08\FTLLSALPOM
8/8/2013 3:58:59 PM
FTLLSALPOM #9-22 RT: 0.14-0.36 AV: 14 SB: 33 0.40-0.81 , 0.00-0.12 NL: 2.92E6
T: {0,0} + c ESI corona sid=75.00 det=1600.00 Full ms [100.00-2000.00]
LC-MS
(M+K)+
(M+Na)+
13a
Relative Abundance
m/z

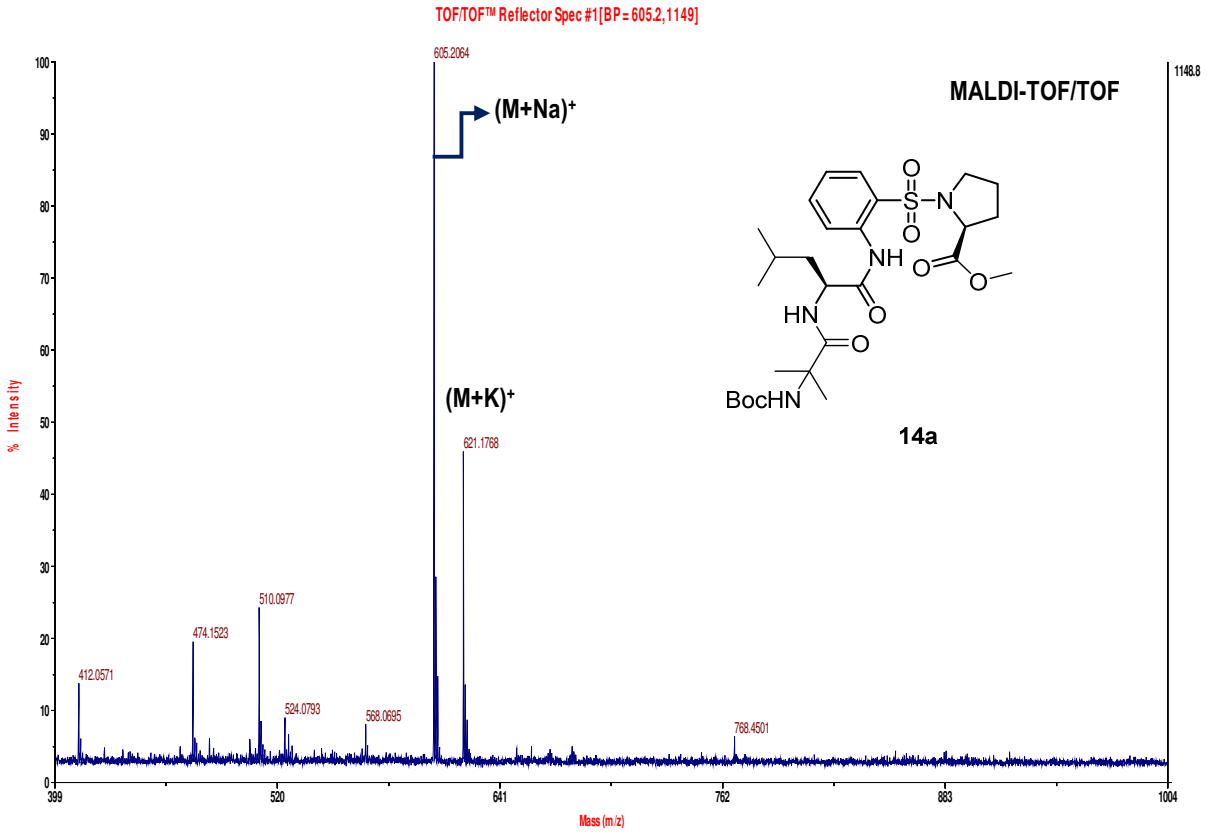
TOF/TOF™ Reflector Spec #1[BP = 605.2, 1149]
MALDI-TOF/TOF
(M+Na)+
(M+K)+
605.2064
621.1768
510.0977
474.1523
412.0571
524.0793
568.0695
768.4501
1148.8
% Intensity
Mass (m/z)
BocHN
14a

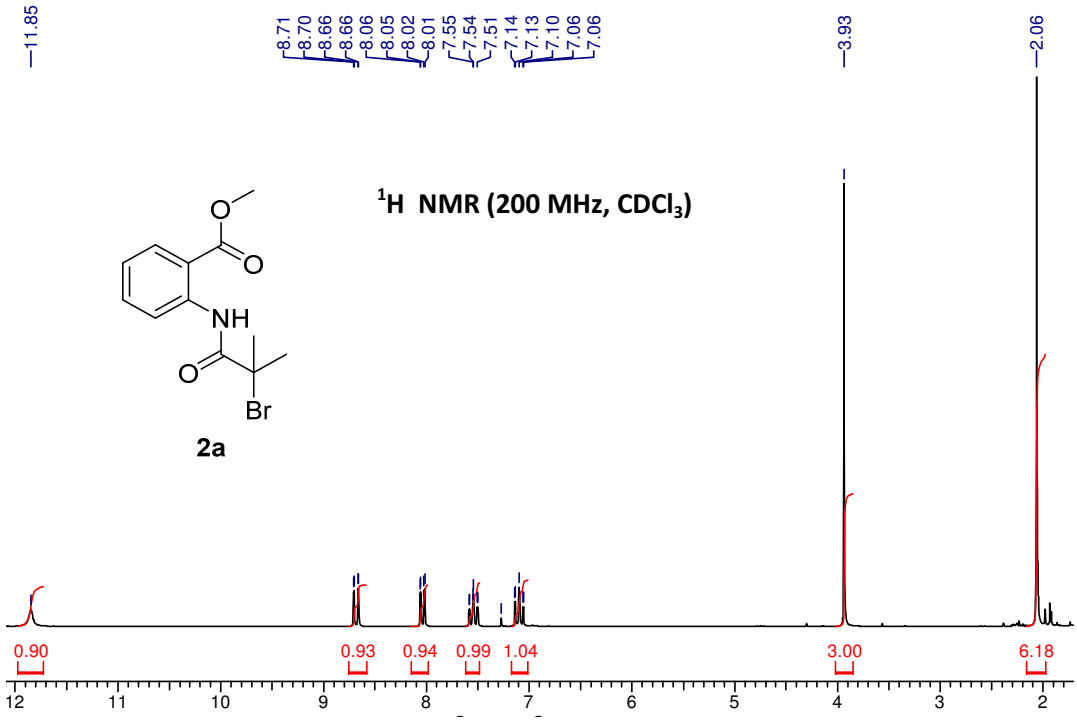
11.85
8.71
8.70
8.66
8.66
8.06
8.05
8.02
8.01
7.55
7.54
7.51
7.14
7.13
7.10
7.06
7.06
3.93
2.06
^{1}H NMR (200 MHz, CDCl$_3$)
O
O
NH
O
Br
2a
0.90
0.93
0.94
0.99
1.04
3.00
6.18
12
11
10
9
8
7
6
5
4
3
2

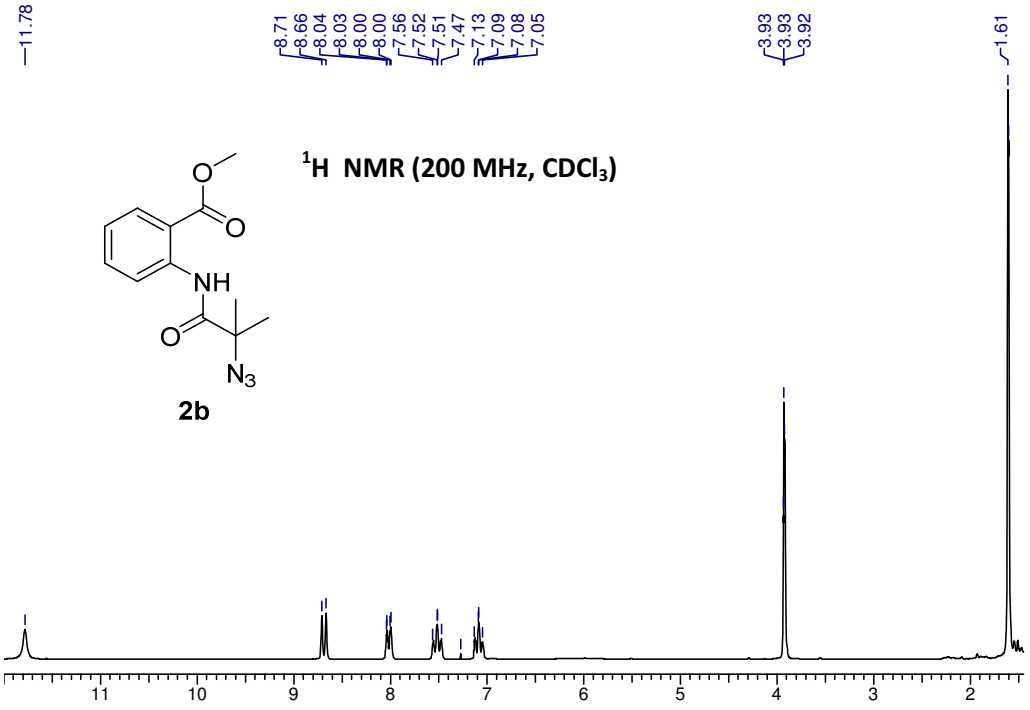
11.78
8.71
8.66
8.04
8.03
8.00
8.00
7.56
7.52
7.51
7.47
7.13
7.09
7.08
7.05
3.93
3.93
3.92
1.61
^{1}H NMR (200 MHz, CDCl$_3$)
O
O
NH
O
N$_3$
2b
11
10
9
8
7
6
5
4
3
2

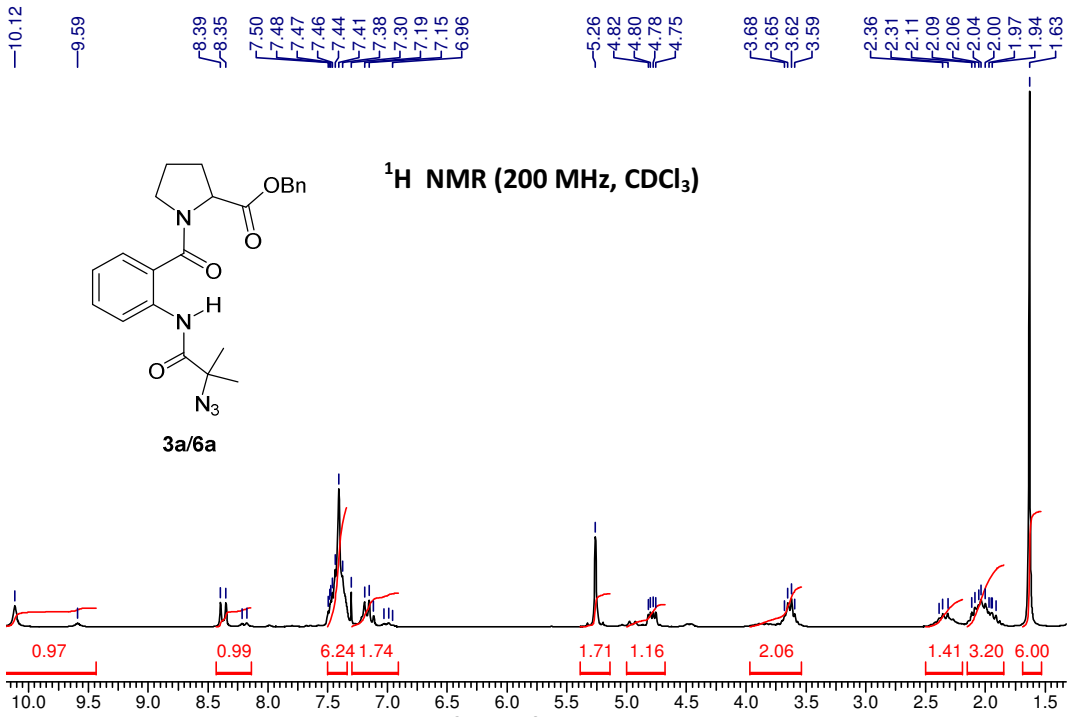
10.12
9.59
8.39
8.35
7.50
7.48
7.47
7.46
7.44
7.41
7.38
7.30
7.19
7.15
6.96
5.26
4.82
4.80
4.78
4.75
3.68
3.65
3.62
3.59
2.36
2.31
2.11
2.09
2.06
2.04
2.00
1.97
1.94
1.63
OBn
N
O
O
N
H
O
N3
3a/6a
1H NMR (200 MHz, CDCl3)
0.97
0.99
6.24
1.74
1.71
1.16
2.06
1.41
3.20
6.00
10.0
9.5
9.0
8.5
8.0
7.5
7.0
6.5
6.0
5.5
5.0
4.5
4.0
3.5
3.0
2.5
2.0
1.5

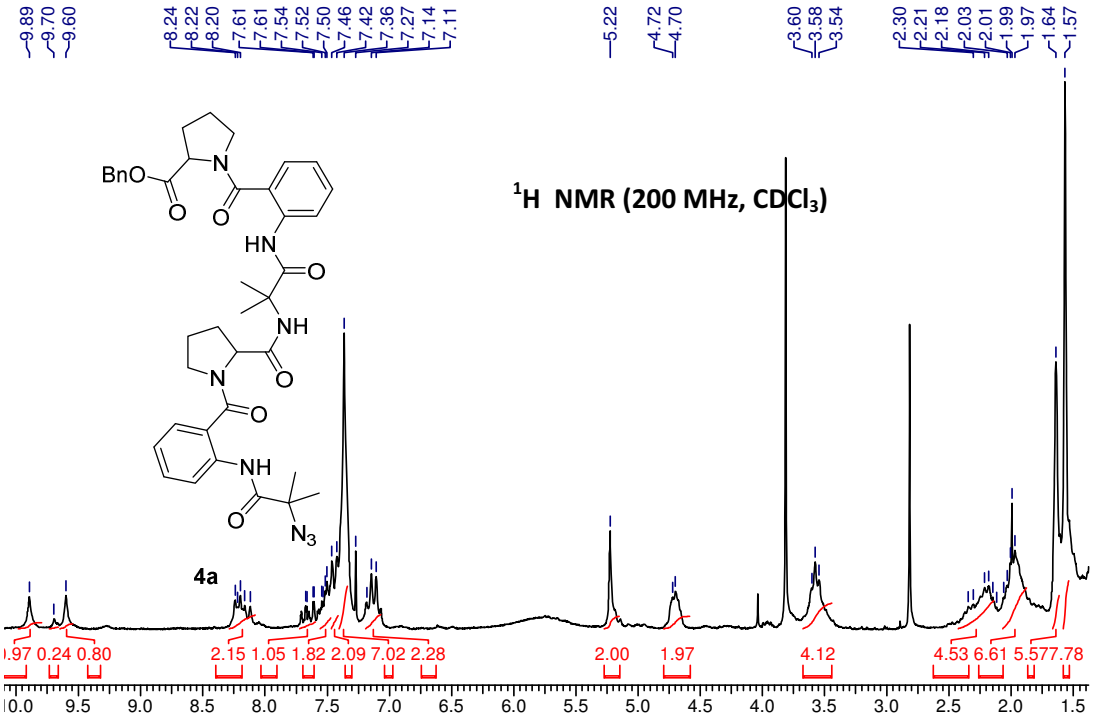
9.89
9.70
9.60
8.24
8.22
8.20
7.61
7.61
7.54
7.52
7.50
7.46
7.42
7.36
7.27
7.14
7.11
5.22
4.72
4.70
3.60
3.58
3.54
2.30
2.21
2.18
2.03
2.01
1.99
1.97
1.64
1.57
BnO
O
N
O
HN
O
NH
N
O
O
NH
O
N3
4a
1H NMR (200 MHz, CDCl3)
.97
0.24
0.80
2.15
1.05
1.82
2.09
7.02
2.28
2.00
1.97
4.12
4.53
6.61
5.57
7.78
10.0
9.5
9.0
8.5
8.0
7.5
7.0
6.5
6.0
5.5
5.0
4.5
4.0
3.5
3.0
2.5
2.0
1.5

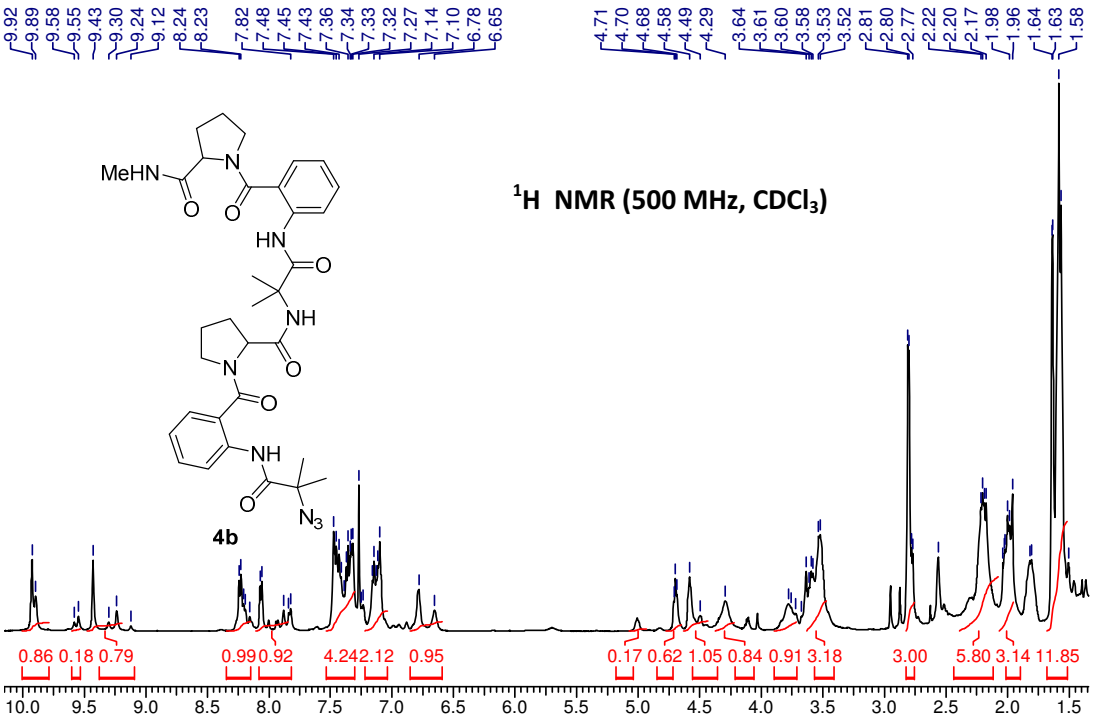
9.92 9.89 9.58 9.55 9.43 9.30 9.24 9.12 8.24 8.23 7.82 7.48 7.45 7.43 7.36 7.34 7.33 7.32 7.27 7.14 7.10 6.78 6.65
4.71 4.70 4.68 4.58 4.49 4.29 3.64 3.61 3.60 3.58 3.53 3.52 2.81 2.80 2.77 2.22 2.20 2.17 1.98 1.96 1.64 1.63 1.58
MeHN
HN
NH
NH
N3
4b
^{1}H NMR (500 MHz, CDCl$_3$)
0.86 0.18 0.79 0.99 0.92 4.24 2.12 0.95 0.17 0.62 1.05 0.84 0.91 3.18 3.00 5.80 3.14 11.85
10.0 9.5 9.0 8.5 8.0 7.5 7.0 6.5 6.0 5.5 5.0 4.5 4.0 3.5 3.0 2.5 2.0 1.5

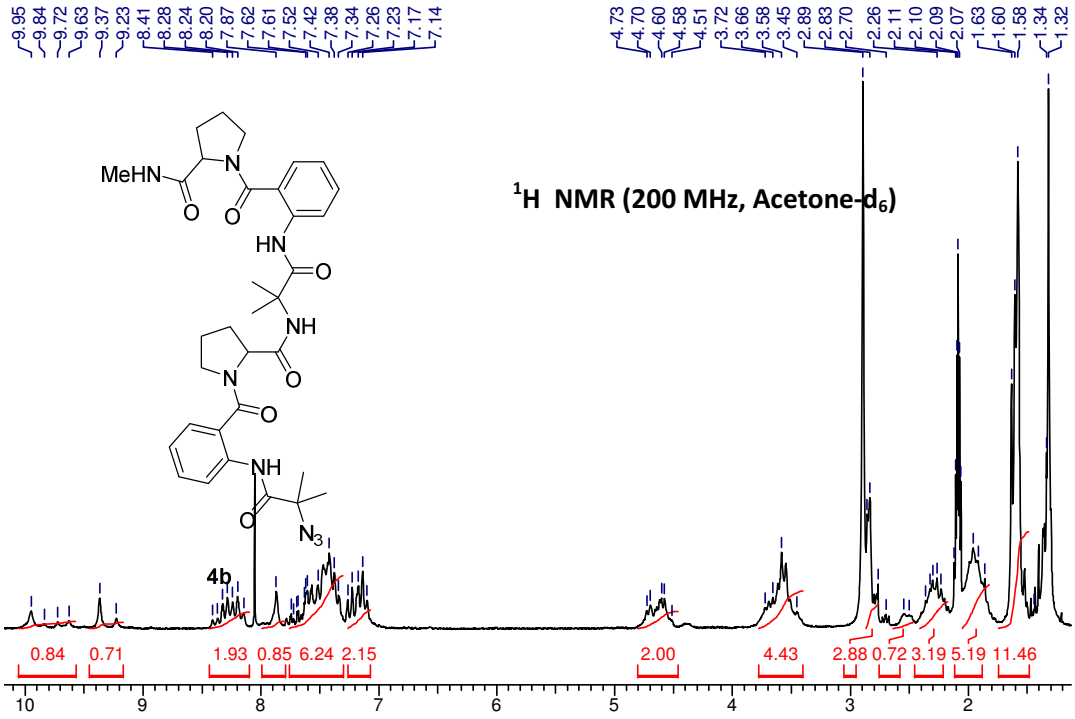
9.95 9.84 9.72 9.63 9.37 9.23 8.41 8.28 8.24 8.20 7.87 7.62 7.61 7.52 7.42 7.38 7.34 7.26 7.23 7.17 7.14
4.73 4.70 4.60 4.58 4.51 3.72 3.66 3.58 3.45 2.89 2.83 2.70 2.26 2.11 2.10 2.09 2.07 1.63 1.60 1.58 1.34 1.32
MeHN
HN
NH
NH
N3
4b
^{1}H NMR (200 MHz, Acetone-d$_6$)
0.84 0.71 1.93 0.85 6.24 2.15 2.00 4.43 2.88 0.72 3.19 5.19 11.46
10 9 8 7 6 5 4 3 2

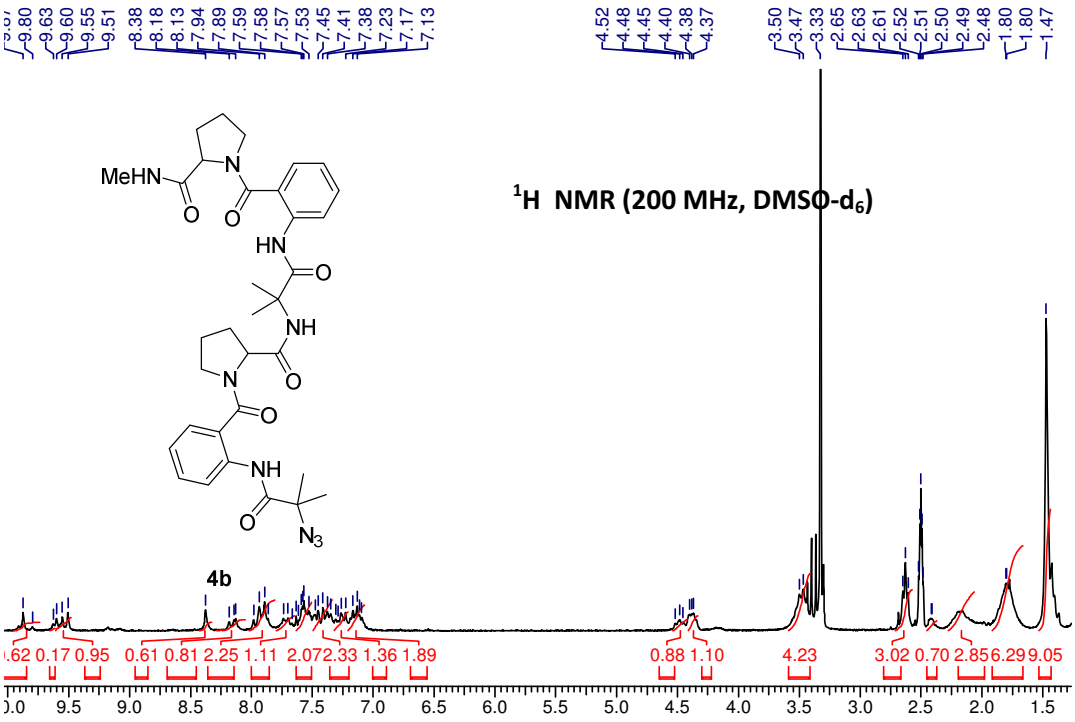
MeHN
HN
NH
NH
N_3
4b
^{1}H NMR (200 MHz, DMSO-d$_6$)

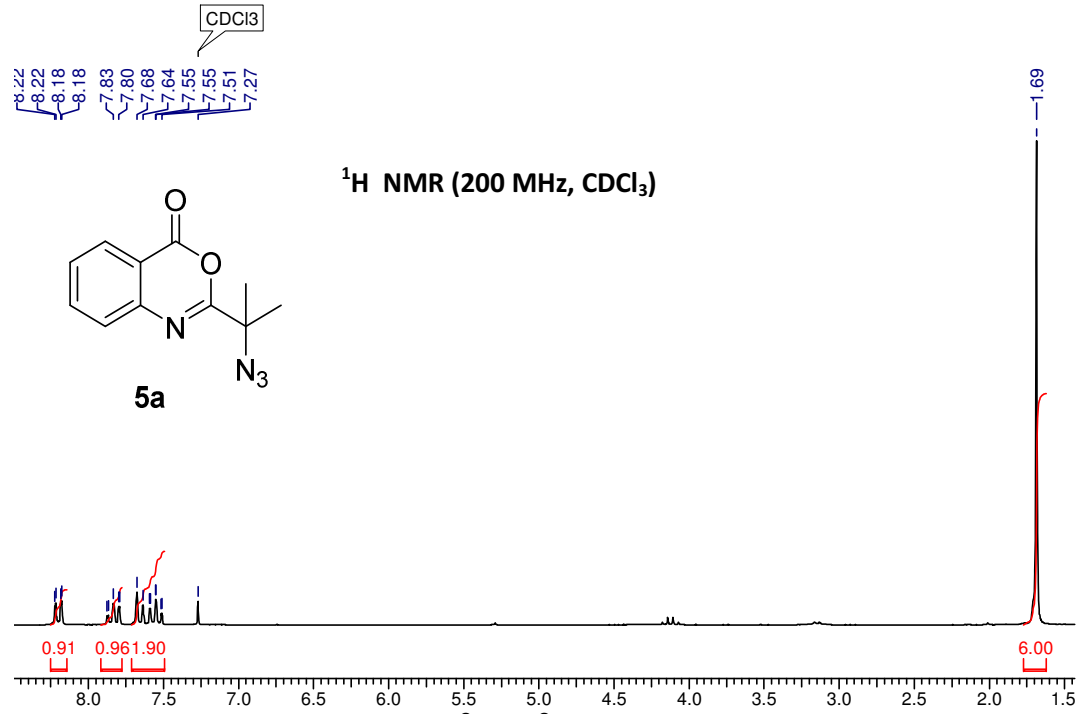
CDCl3
^{1}H NMR (200 MHz, CDCl$_3$)
N_3
5a

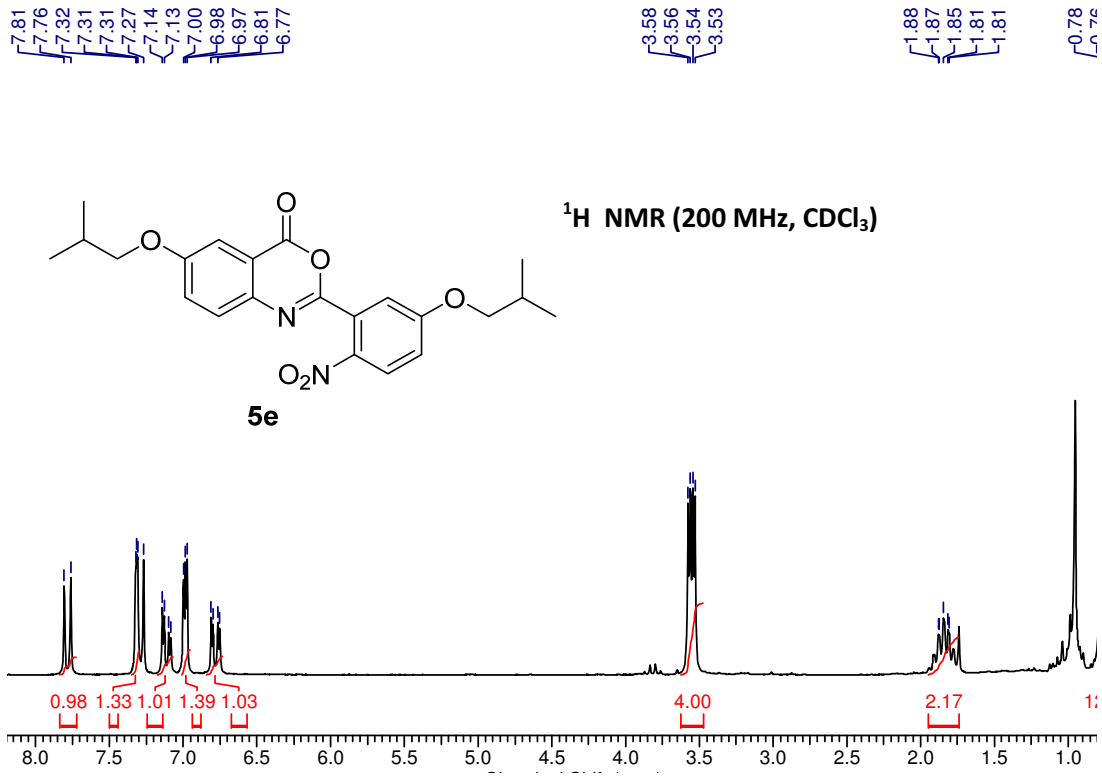
7.81
7.76
7.32
7.31
7.31
7.27
7.14
7.13
7.00
6.98
6.97
6.81
6.77
3.58
3.56
3.54
3.53
1.88
1.87
1.85
1.81
1.81
0.78
O
O
O
N
O
O2N
5e
1H NMR (200 MHz, CDCl3)
0.98 1.33 1.01 1.39 1.03
4.00
2.17
8.0 7.5 7.0 6.5 6.0 5.5 5.0 4.5 4.0 3.5 3.0 2.5 2.0 1.5 1.0

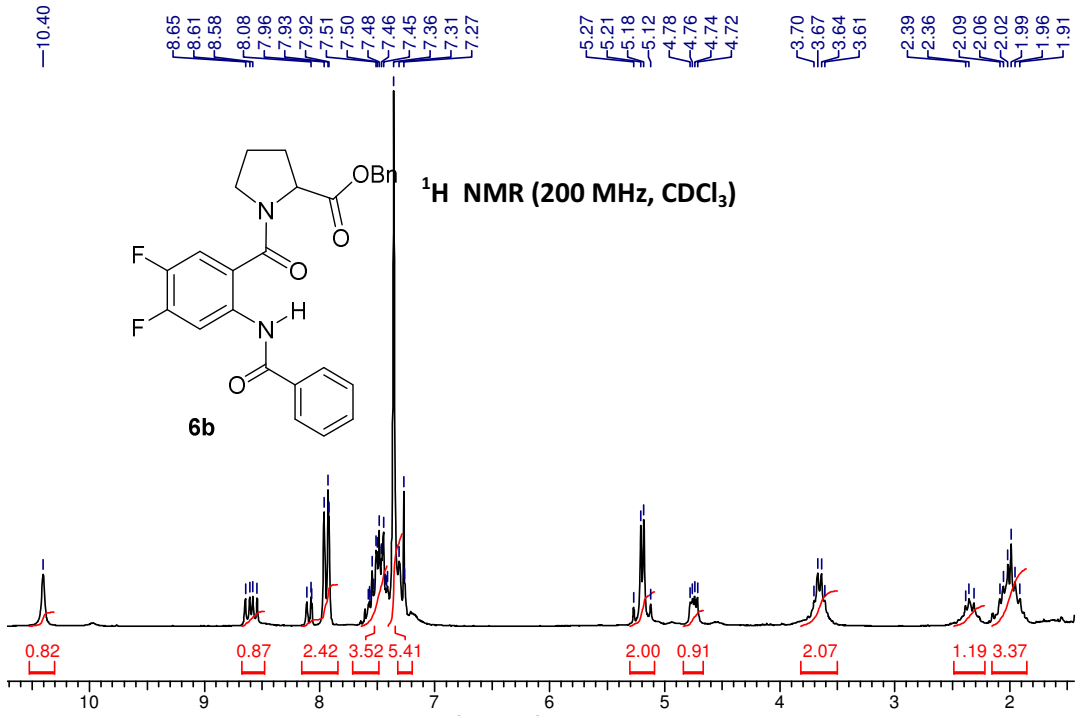
10.40
8.65
8.61
8.58
8.08
7.96
7.93
7.92
7.51
7.50
7.48
7.46
7.45
7.36
7.31
7.27
5.27
5.21
5.18
5.12
4.78
4.76
4.74
4.72
3.70
3.67
3.64
3.61
2.39
2.36
2.09
2.06
2.02
1.99
1.96
1.91
OBn
N
O
F
F
O
N
H
O
6b
1H NMR (200 MHz, CDCl3)
0.82
0.87
2.42
3.52
5.41
2.00
0.91
2.07
1.19
3.37
10 9 8 7 6 5 4 3 2

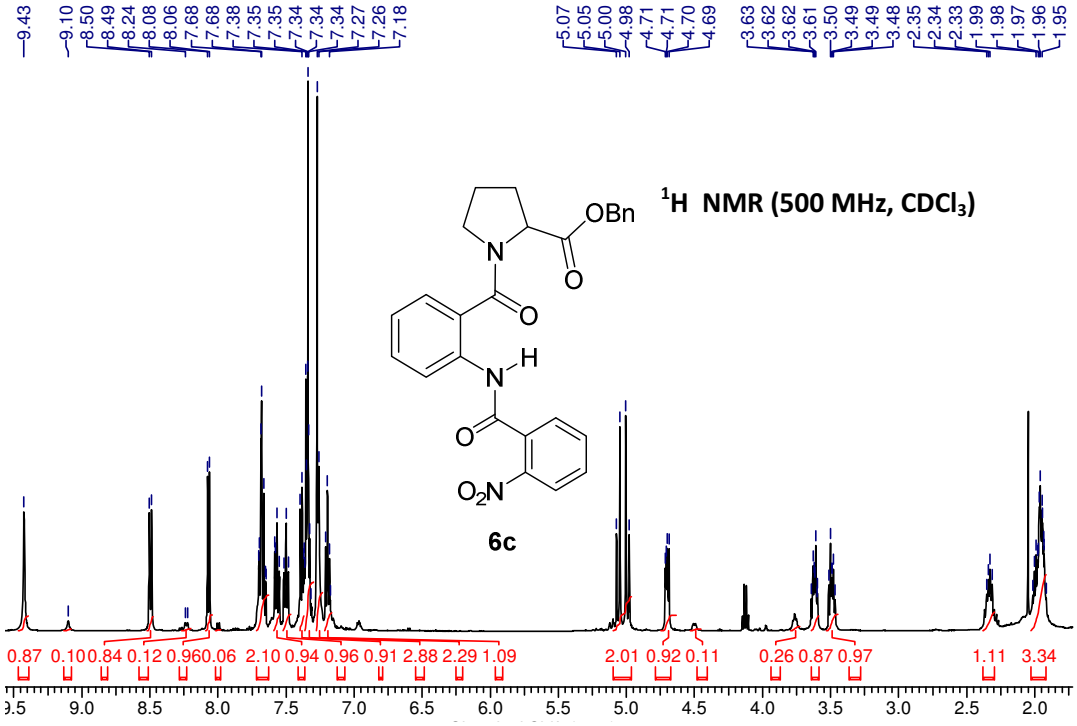
^{1}H NMR (500 MHz, CDCl$_3$)
OBn
N
O
O
N
H
O
N
O$_2$N
6c

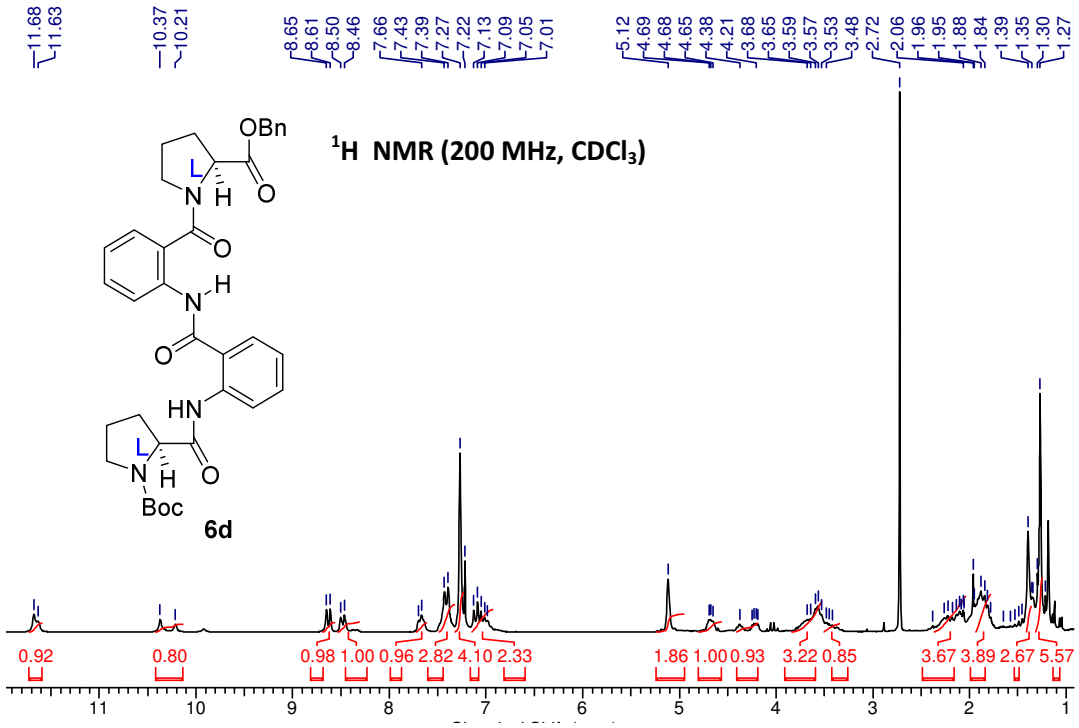
^{1}H NMR (200 MHz, CDCl$_3$)
OBn
L
N
H
O
O
N
H
O
HN
L
N
H
O
Boc
6d

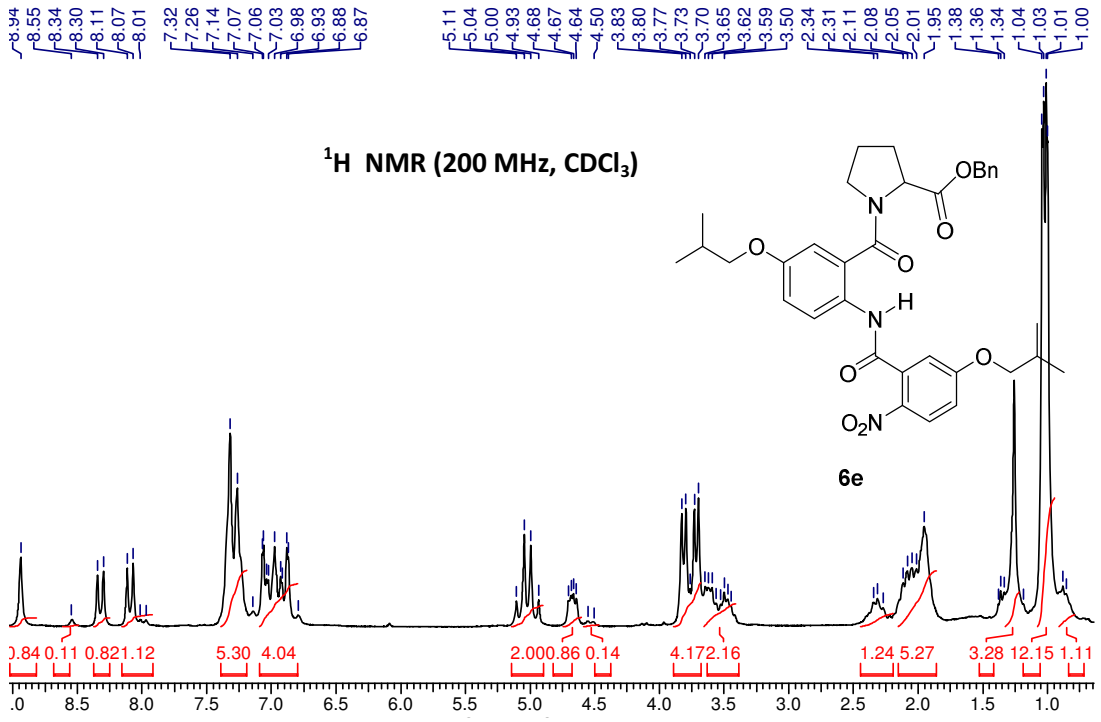
^{1}H NMR (200 MHz, CDCl$_3$)
OBn
O
N
O
O
N
H
O
O
O$_2$N
6e

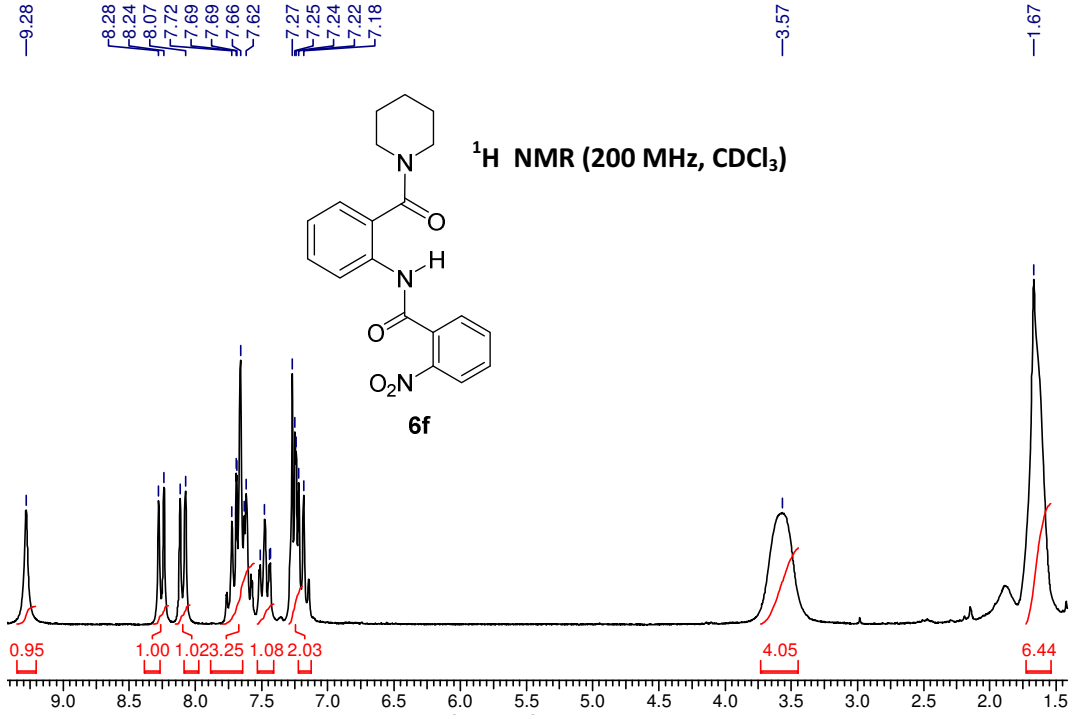
^{1}H NMR (200 MHz, CDCl$_3$)
O
N
H
O
O$_2$N
6f

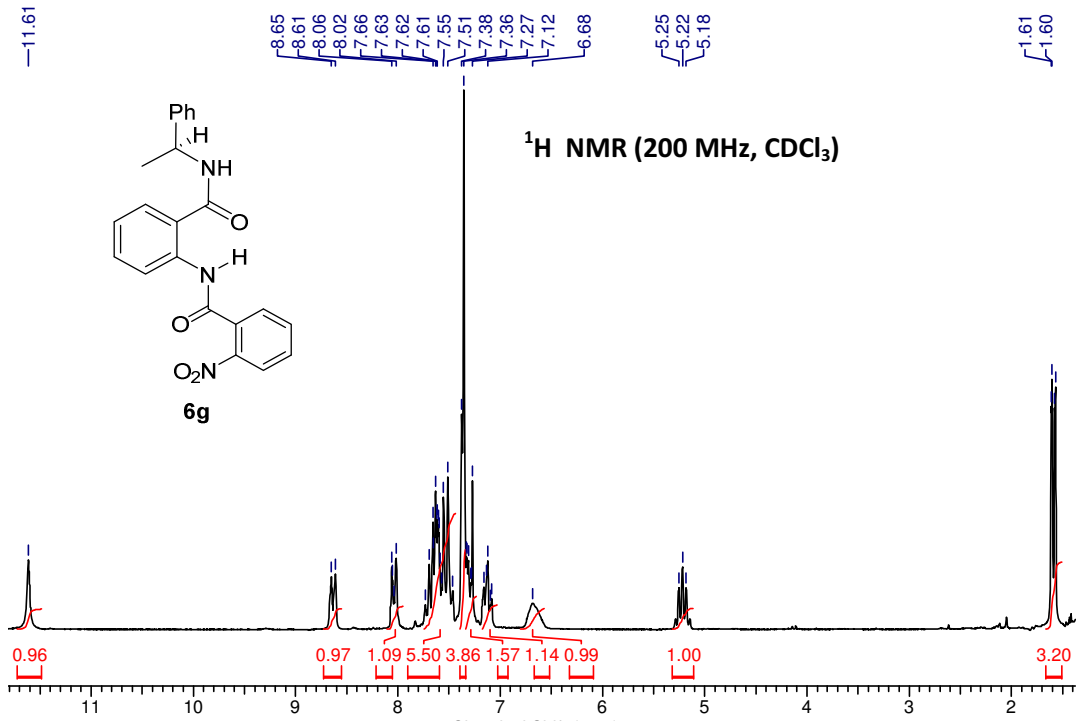
11.61
8.65
8.61
8.06
8.02
7.66
7.63
7.62
7.61
7.55
7.51
7.38
7.36
7.27
7.12
6.68
5.25
5.22
5.18
1.61
1.60
Ph
H
NH
O
N
H
O
O2N
6g
1H NMR (200 MHz, CDCl3)
0.96
0.97
1.09
5.50
3.86
1.57
1.14
0.99
1.00
3.20
11
10
9
8
7
6
5
4
3
2

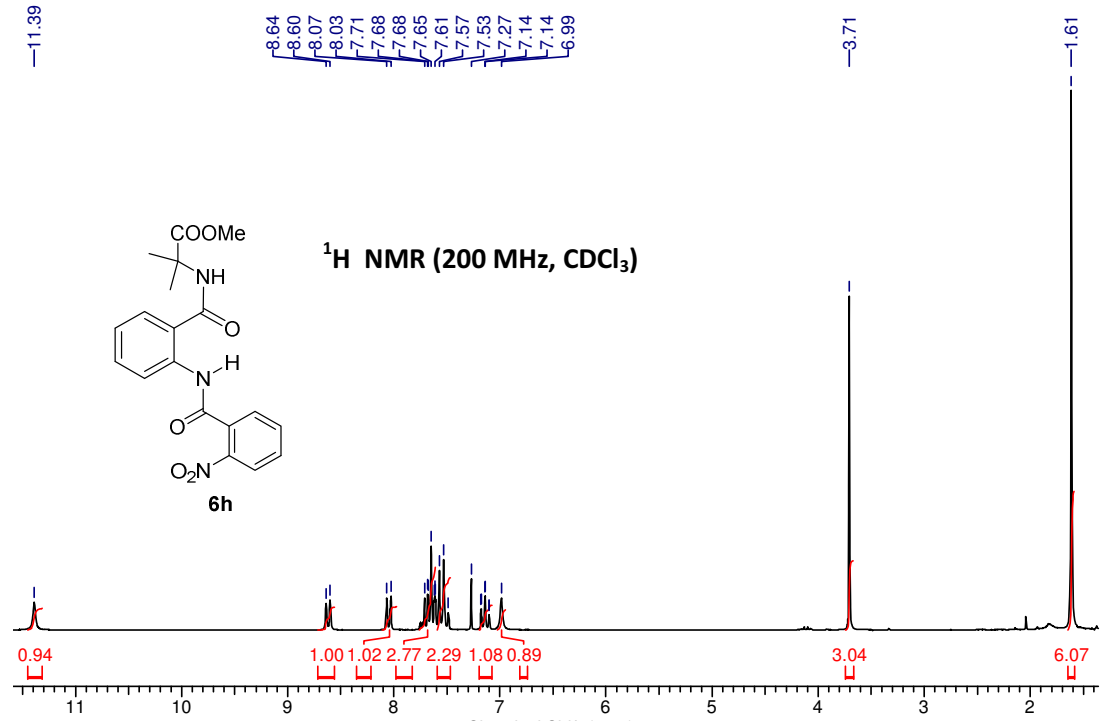
11.39
8.64
8.60
8.07
8.03
7.71
7.68
7.68
7.65
7.61
7.57
7.53
7.27
7.14
6.99
3.71
1.61
COOMe
NH
O
N
H
O
O2N
6h
1H NMR (200 MHz, CDCl3)
0.94
1.00
1.02
2.77
2.29
1.08
0.89
3.04
6.07
11
10
9
8
7
6
5
4
3
2

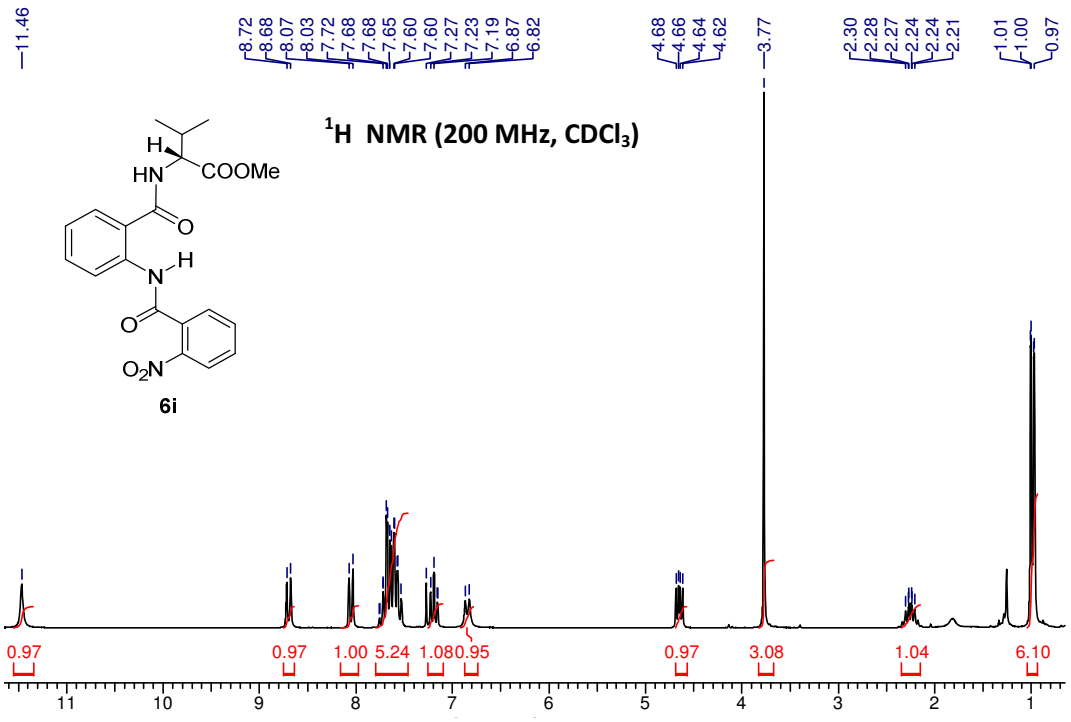
^{1}H NMR (200 MHz, CDCl$_3$)
6i

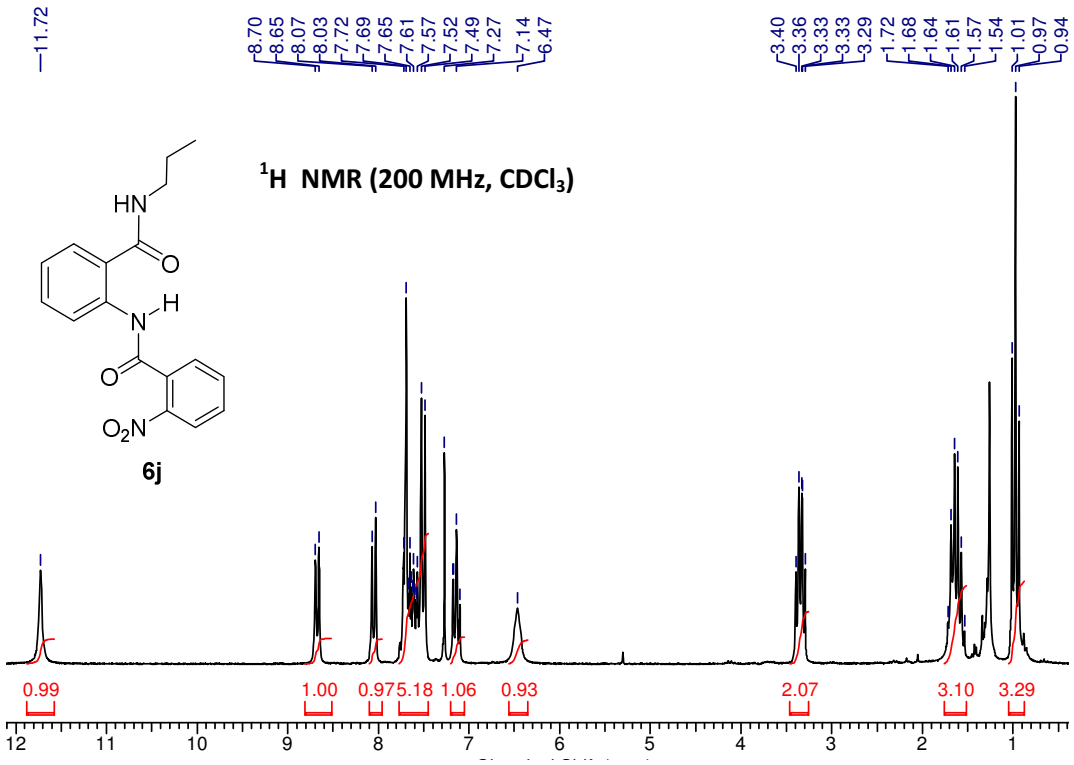
^{1}H NMR (200 MHz, CDCl$_3$)
6j

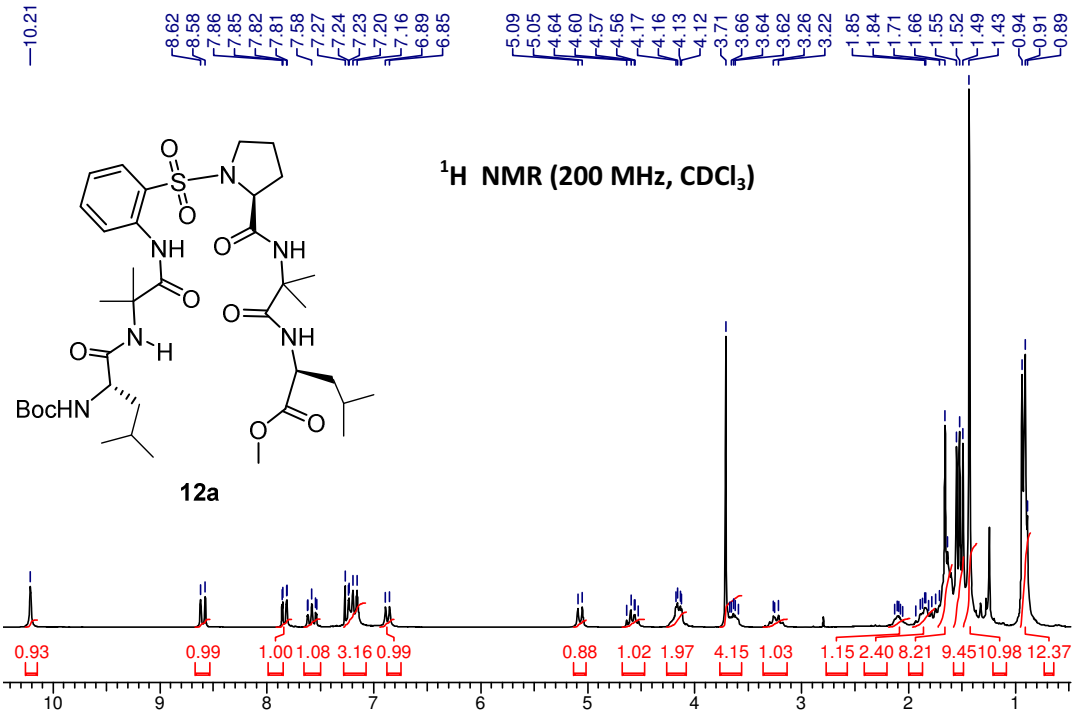
10.21
8.62 8.58 7.86 7.85 7.82 7.81 7.58 7.27 7.24 7.23 7.20 7.16 6.89 6.85
5.09 5.05 4.64 4.60 4.57 4.56 4.17 4.16 4.13 4.12 3.71 3.66 3.64 3.62 3.26 3.22
1.85 1.84 1.71 1.66 1.55 1.52 1.49 1.43 0.94 0.91 0.89
^{1}H NMR (200 MHz, CDCl$_3$)
12a
0.93 0.99 1.00 1.08 3.16 0.99 0.88 1.02 1.97 4.15 1.03 1.15 2.40 8.21 9.45 10.98 12.37
10 9 8 7 6 5 4 3 2 1

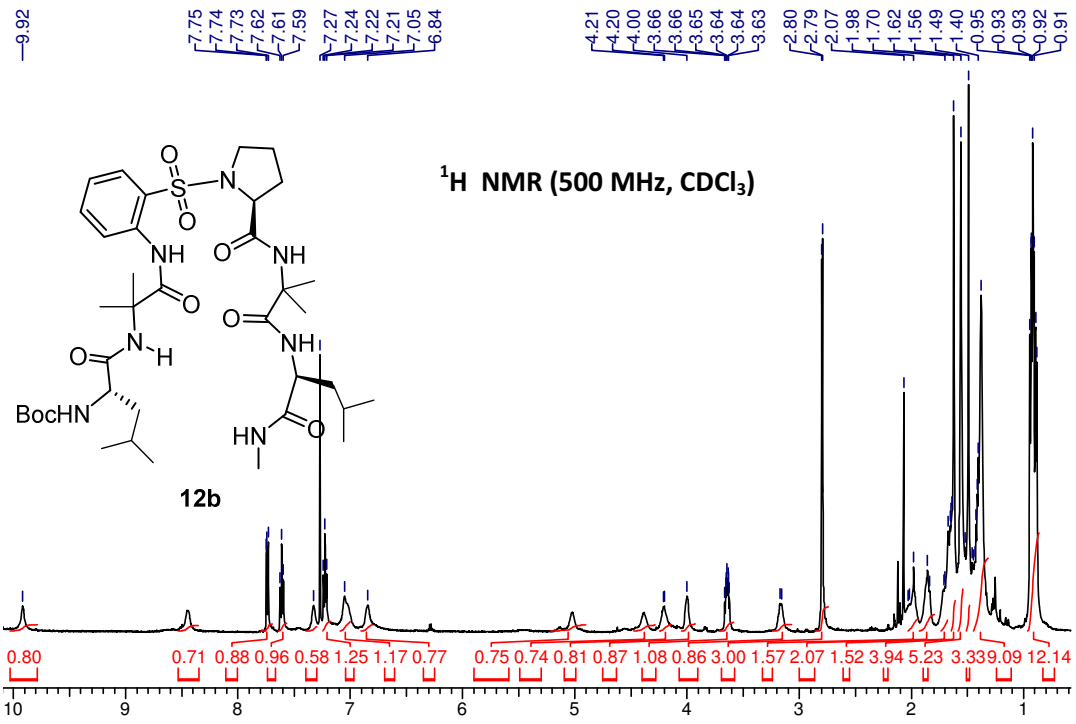
9.92
7.75 7.74 7.73 7.62 7.61 7.59 7.27 7.24 7.22 7.21 7.05 6.84
4.21 4.20 4.00 3.66 3.66 3.65 3.64 3.64 3.63 2.80 2.79 2.07 1.98 1.70 1.62 1.56 1.49 1.40 0.95 0.93 0.93 0.92 0.91
^{1}H NMR (500 MHz, CDCl$_3$)
12b
0.80 0.71 0.88 0.96 0.58 1.25 1.17 0.77 0.75 0.74 0.81 0.87 1.08 0.86 3.00 1.57 2.07 1.52 3.94 5.23 3.33 9.09 12.14
10 9 8 7 6 5 4 3 2 1

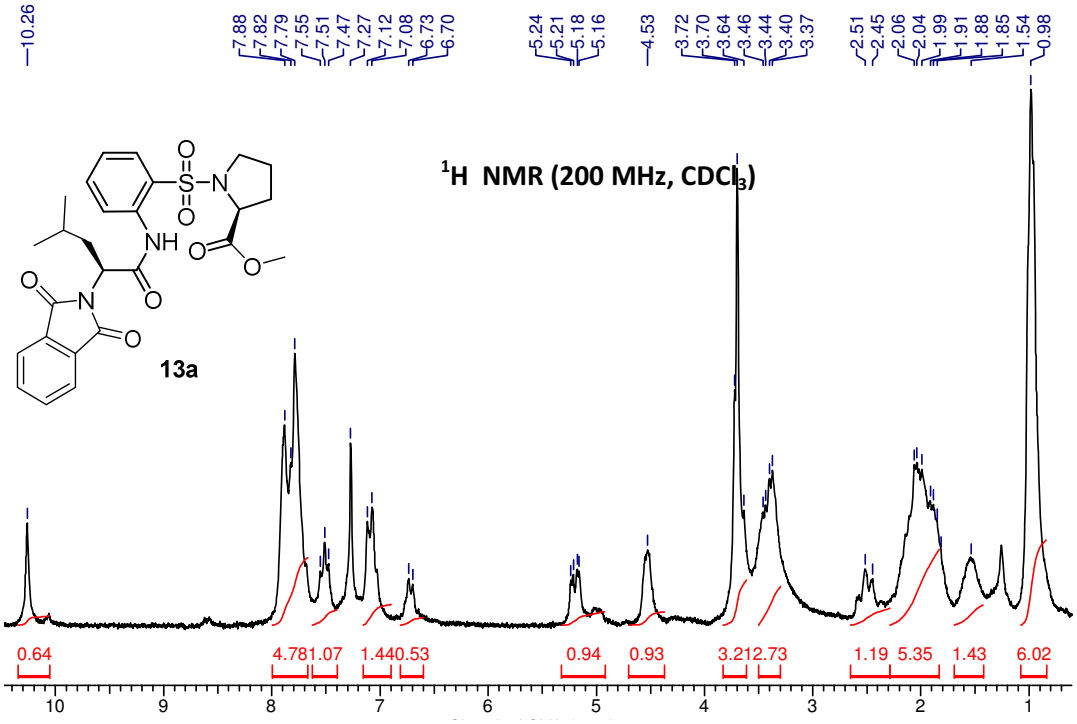
10.26
7.88
7.82
7.79
7.55
7.51
7.47
7.27
7.12
7.08
6.73
6.70
5.24
5.21
5.18
5.16
4.53
3.72
3.70
3.64
3.46
3.44
3.40
3.37
2.51
2.45
2.06
2.04
1.99
1.91
1.88
1.85
1.54
0.98
^{1}H NMR (200 MHz, CDCl$_3$)
13a
0.64
4.78
1.07
1.44
0.53
0.94
0.93
3.21
2.73
1.19
5.35
1.43
6.02

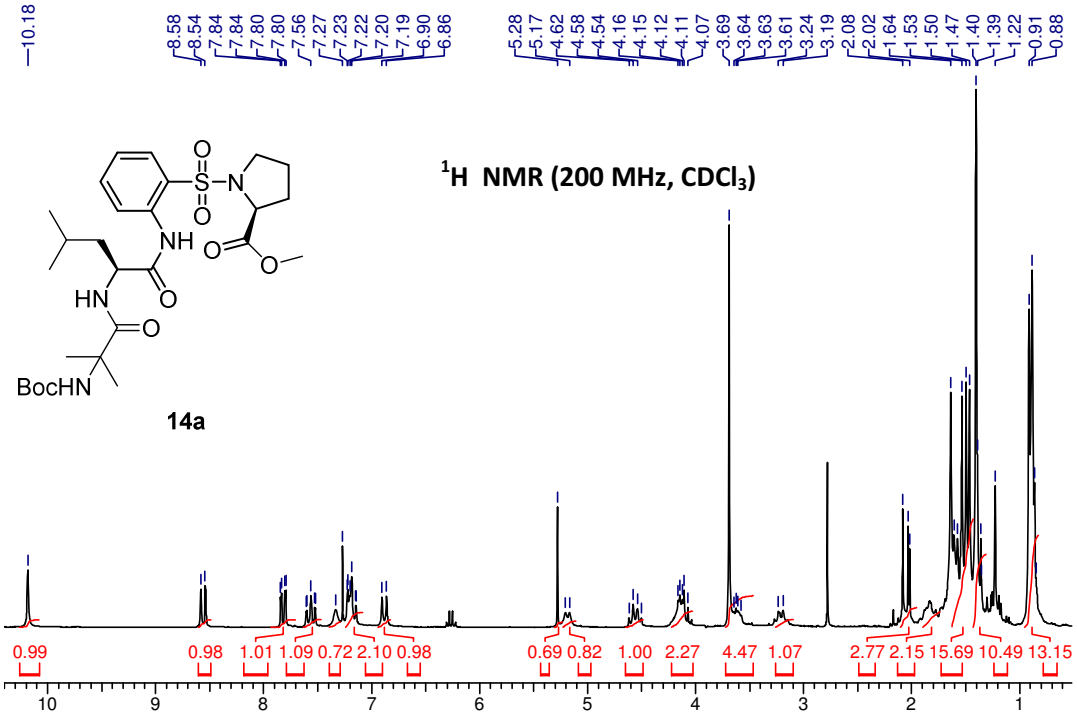
10.18
8.58
8.54
7.84
7.84
7.80
7.80
7.56
7.27
7.23
7.22
7.20
7.19
6.90
6.86
5.28
5.17
4.62
4.58
4.54
4.16
4.15
4.12
4.11
4.07
3.69
3.64
3.63
3.61
3.24
3.19
2.08
2.02
1.64
1.53
1.50
1.47
1.40
1.39
1.22
0.91
0.88
^{1}H NMR (200 MHz, CDCl$_3$)
14a
0.99
0.98
1.01
1.09
0.72
2.10
0.98
0.69
0.82
1.00
2.27
4.47
1.07
2.77
2.15
15.69
10.49
13.15

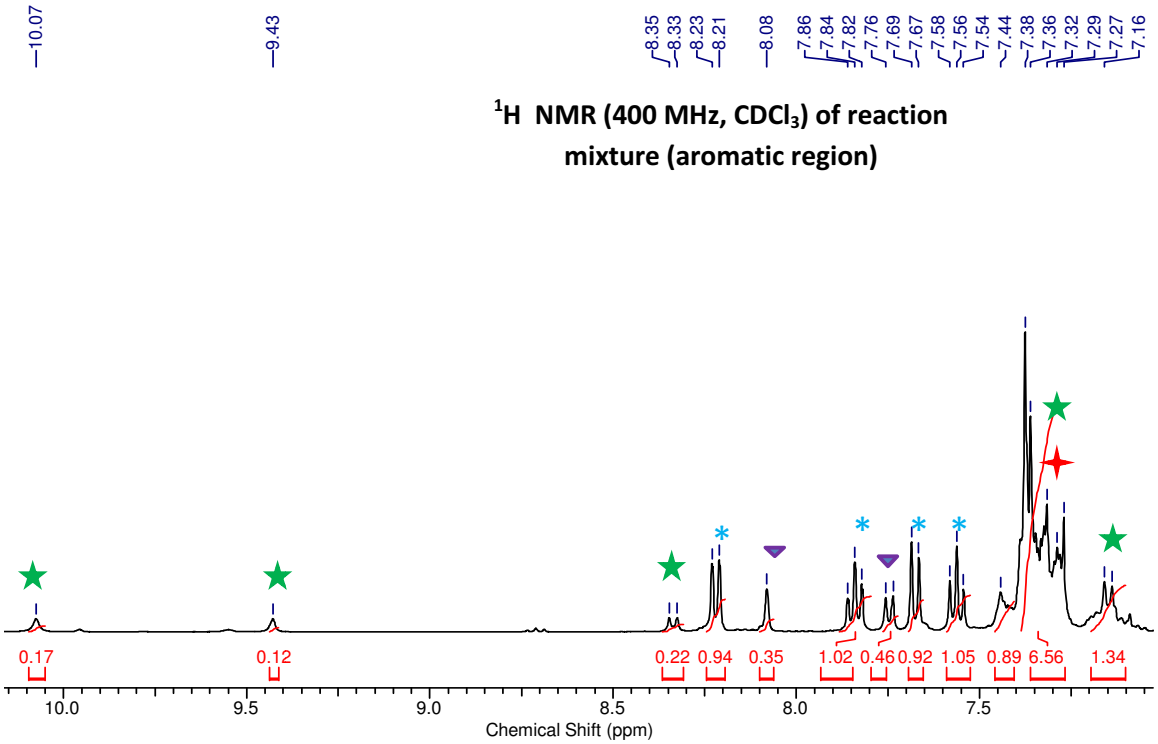

^{1}H NMR (400 MHz, $CDCl_3$) of reaction mixture (aromatic region)

Note: The compounds are labeled using different symbols, *i.e*. Product **2a** (★), Oxazinone **1a** (*), thiourea (▼) and H-^{L}Pro-OBn (✦).

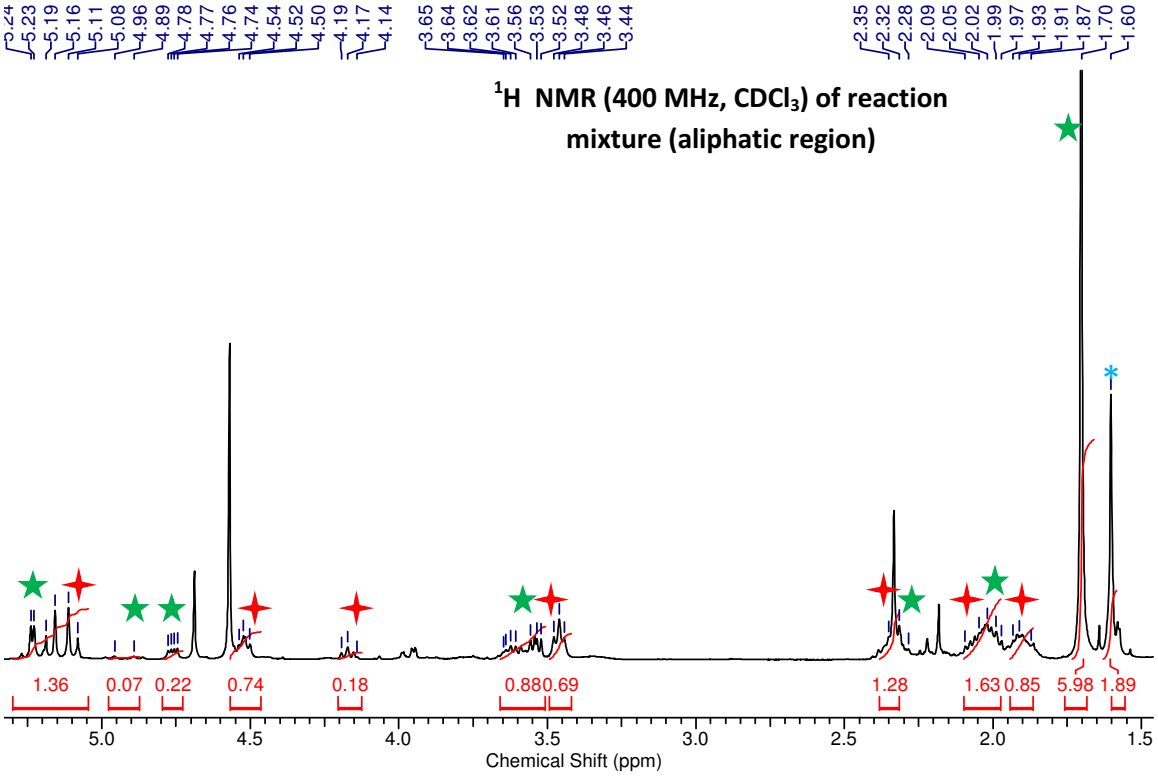

^{1}H NMR (400 MHz, $CDCl_3$) of reaction mixture (aliphatic region)

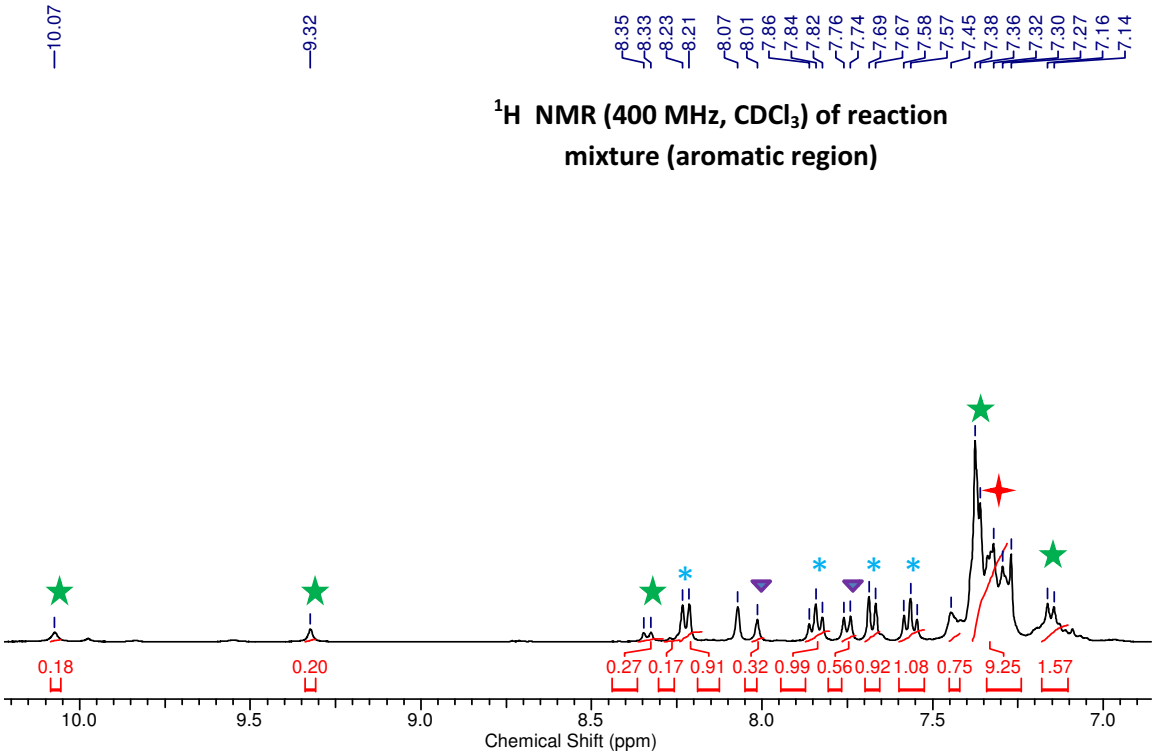

^{1}H NMR (400 MHz, $CDCl_3$) of reaction mixture (aromatic region)

Note: The compounds are labeled using different symbols, *i.e*. Product **2a** (★), Oxazinone **1a** (*), thiourea (▼) and H-^{L}Pro-OBn (✦).

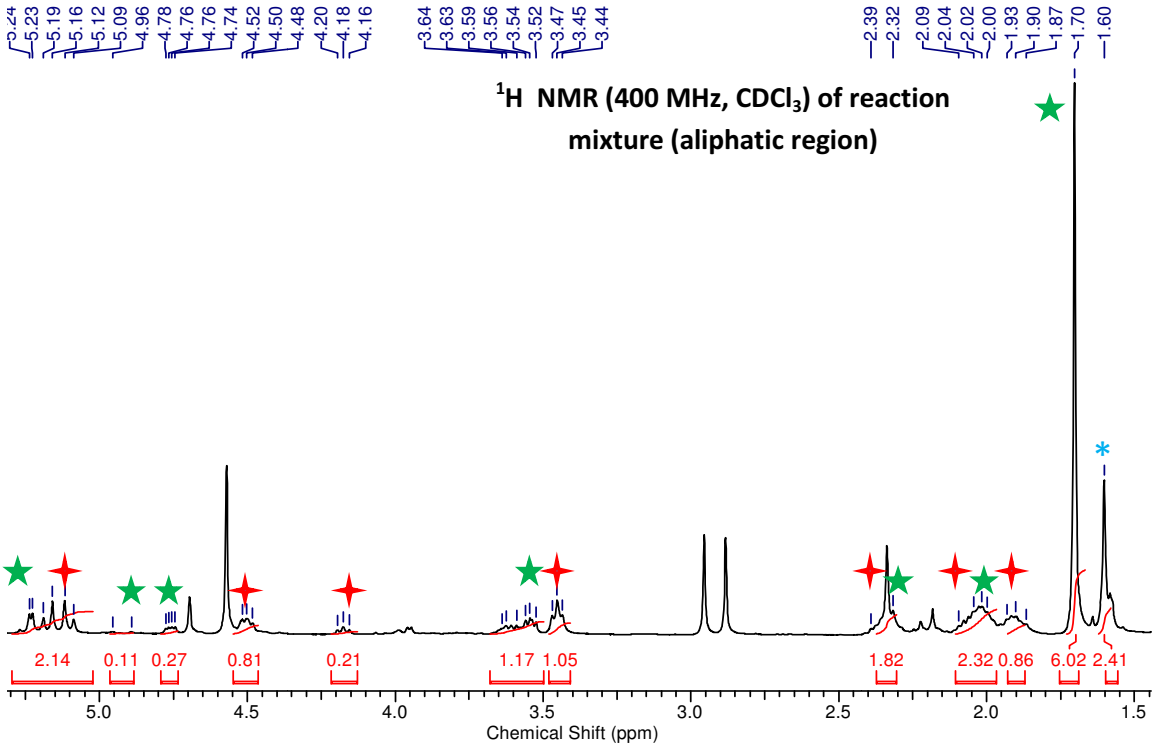

^{1}H NMR (400 MHz, $CDCl_3$) of reaction mixture (aliphatic region)

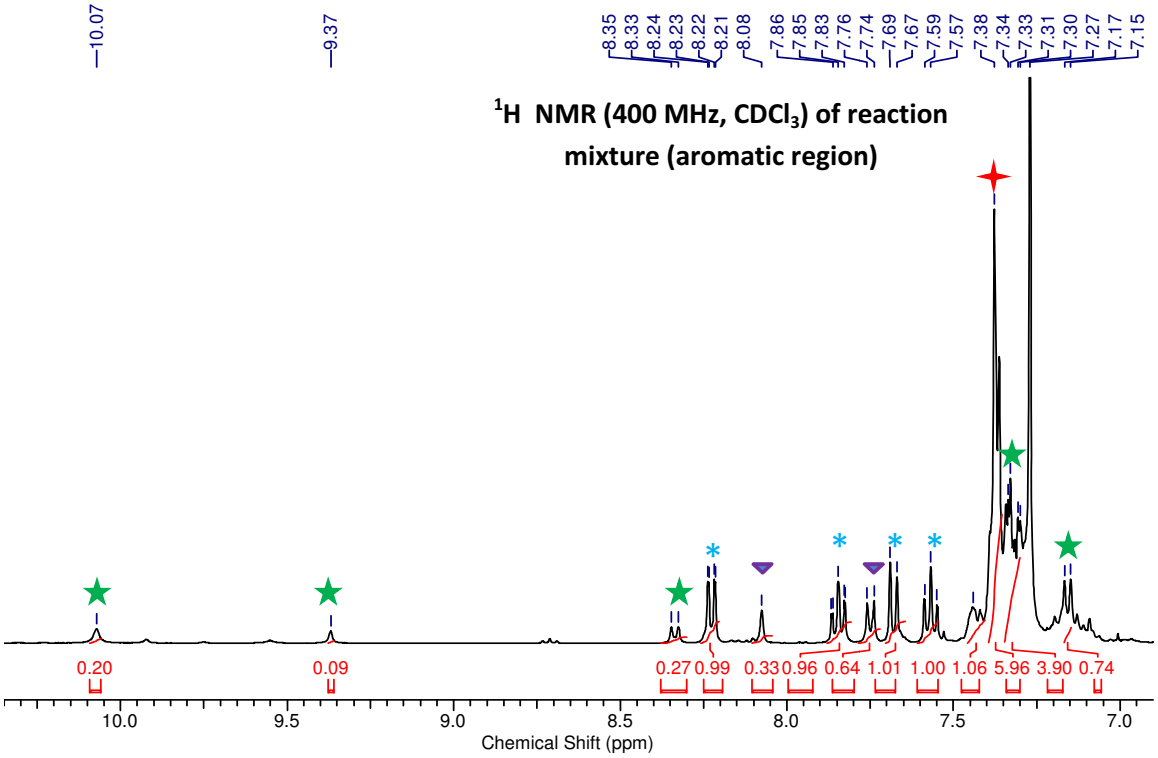

Note: The compounds are labeled using different symbols, *i.e*. Product **2a** (★), Oxazinone **1a** (*), thiourea (▼) and H-^{L}Pro-OBn (✦).

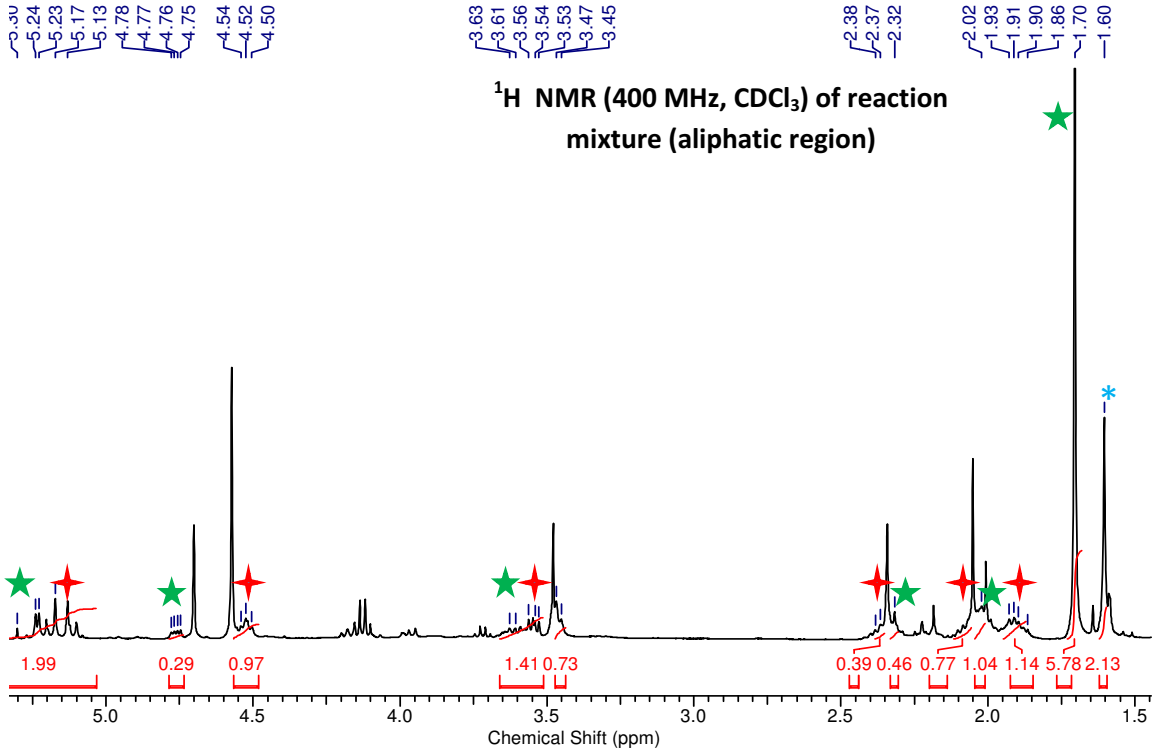

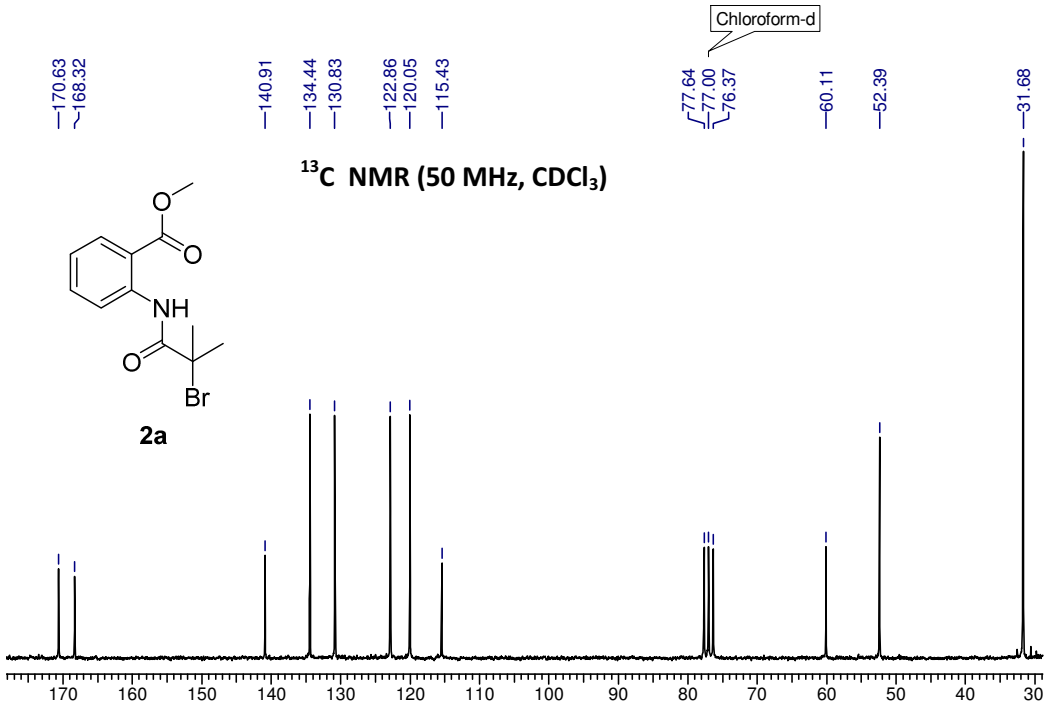
Chloroform-d
170.63
168.32
140.91
134.44
130.83
122.86
120.05
115.43
77.64
77.00
76.37
60.11
52.39
31.68
^{13}C NMR (50 MHz, CDCl$_3$)
O
O
NH
O
Br
2a
170
160
150
140
130
120
110
100
90
80
70
60
50
40
30

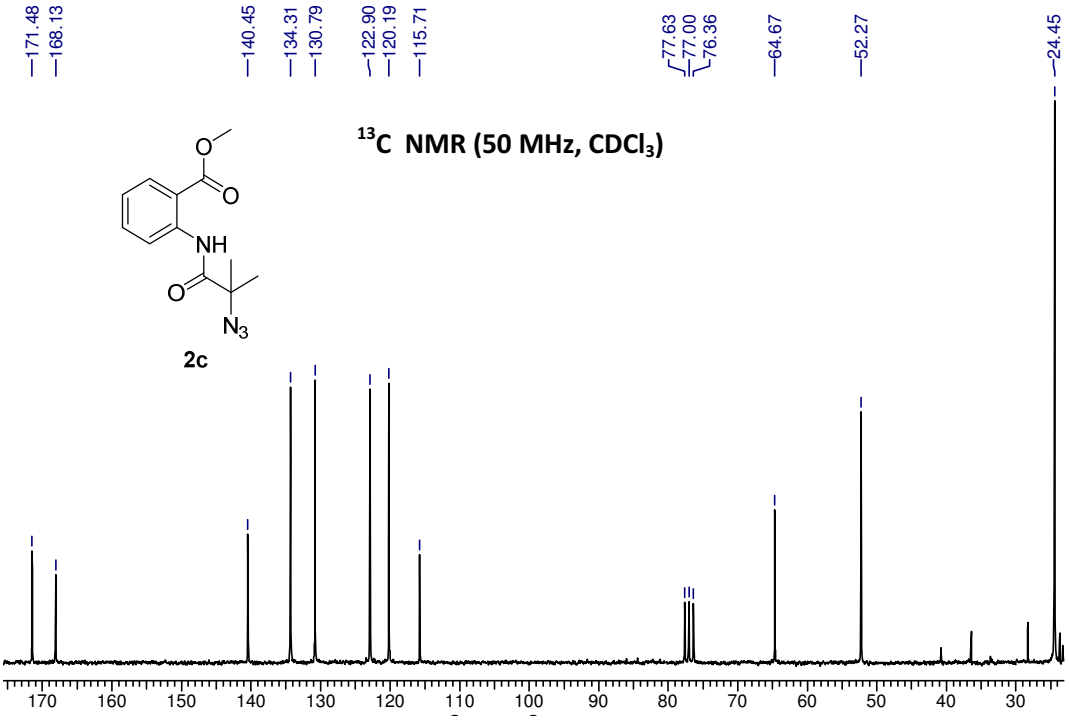
171.48
168.13
140.45
134.31
130.79
122.90
120.19
115.71
77.63
77.00
76.36
64.67
52.27
24.45
^{13}C NMR (50 MHz, CDCl$_3$)
O
O
NH
O
N$_3$
2c
170
160
150
140
130
120
110
100
90
80
70
60
50
40
30

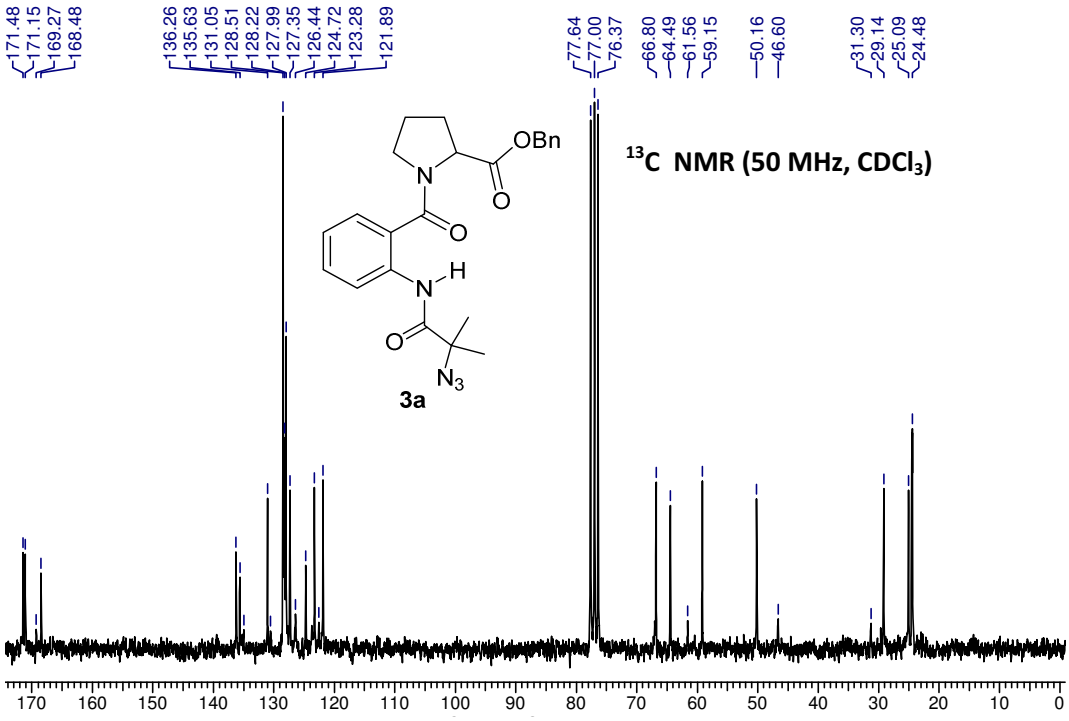
171.48
171.15
169.27
168.48
136.26
135.63
131.05
128.51
128.22
127.99
127.35
126.44
124.72
123.28
121.89
77.64
77.00
76.37
66.80
64.49
61.56
59.15
50.16
46.60
31.30
29.14
25.09
24.48
OBn
N
O
H
N_3
3a
^{13}C NMR (50 MHz, CDCl$_3$)
170 160 150 140 130 120 110 100 90 80 70 60 50 40 30 20 10 0

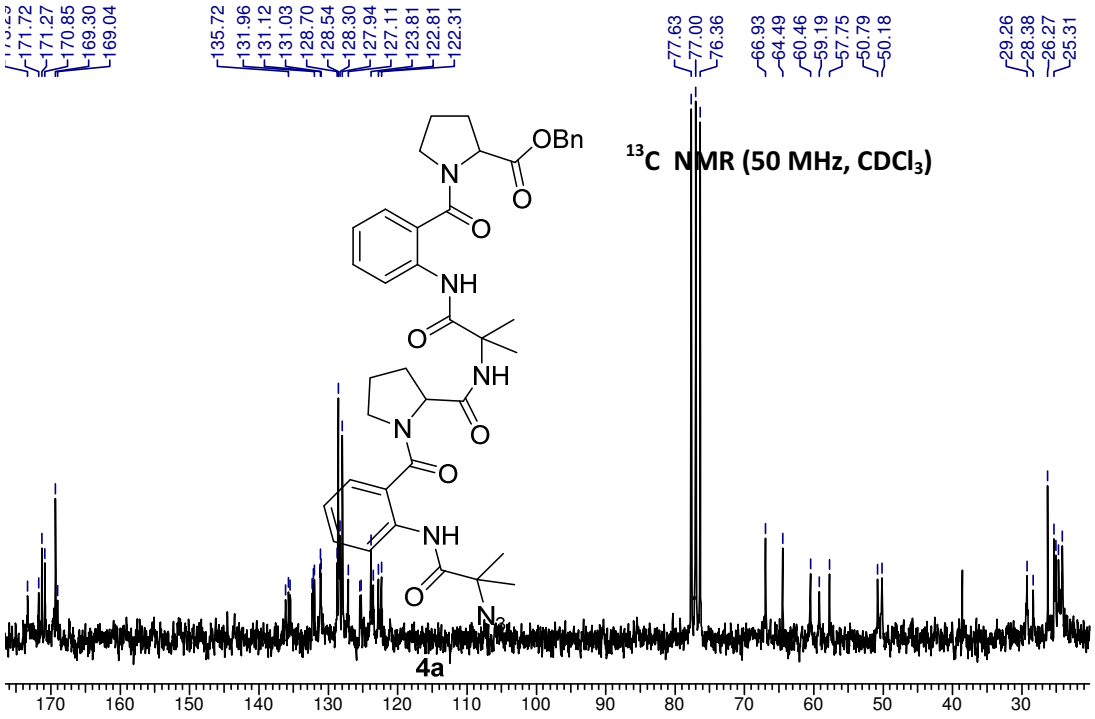
171.72
171.27
170.85
169.30
169.04
135.72
131.96
131.12
131.03
128.70
128.54
128.30
127.94
127.11
123.81
122.81
122.31
77.63
77.00
76.36
66.93
64.49
60.46
59.19
57.75
50.79
50.18
29.26
28.38
26.27
25.31
OBn
NH
NH
NH
N_3
4a
^{13}C NMR (50 MHz, CDCl$_3$)
170 160 150 140 130 120 110 100 90 80 70 60 50 40 30

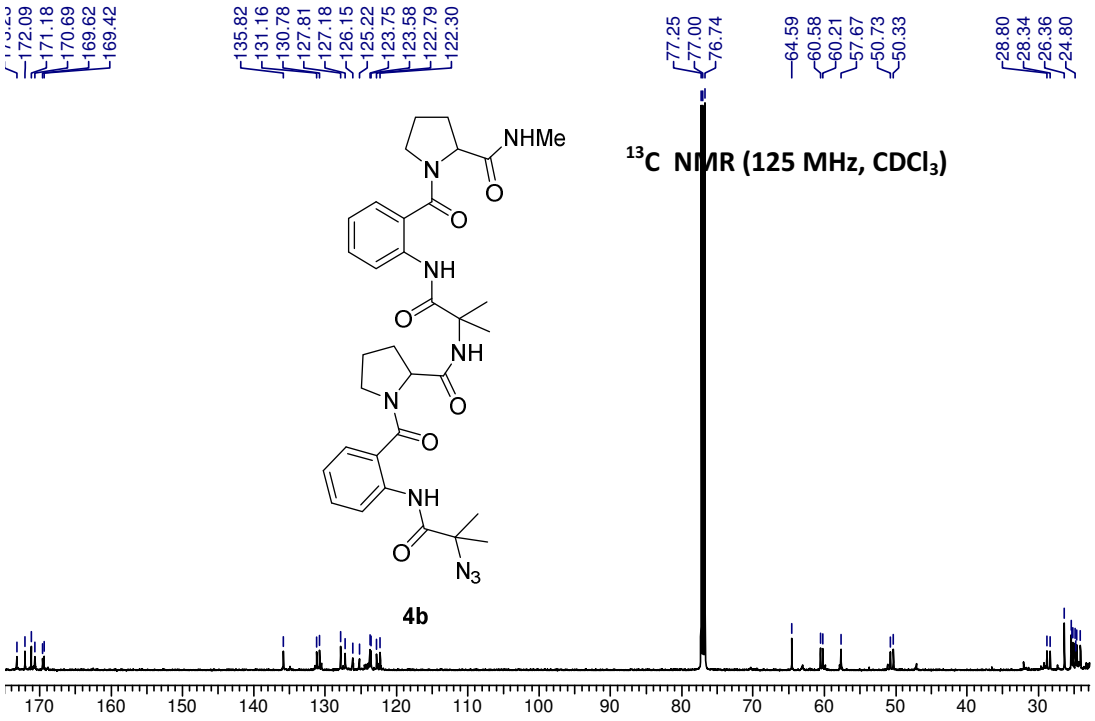
172.09
171.18
170.69
169.62
169.42
135.82
131.16
130.78
127.81
127.18
126.15
125.22
123.75
123.58
122.79
122.30
77.25
77.00
76.74
64.59
60.58
60.21
57.67
50.73
50.33
28.80
28.34
26.36
24.80
NHMe
NH
NH
NH
N3
4b
13C NMR (125 MHz, CDCl3)
170
160
150
140
130
120
110
100
90
80
70
60
50
40
30

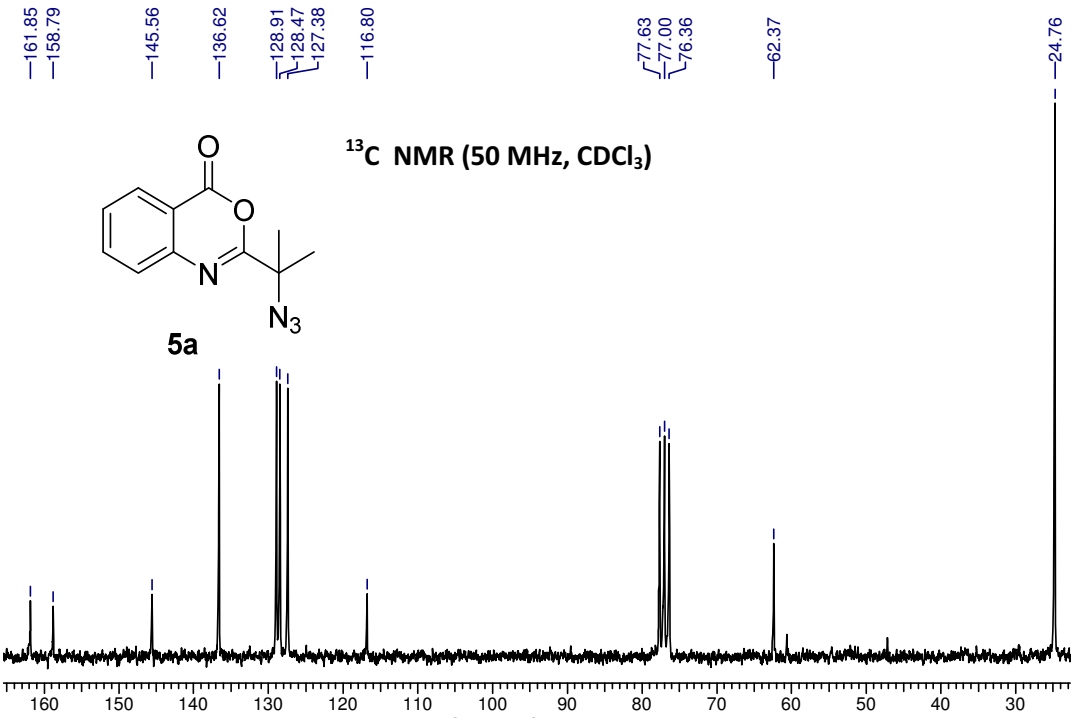
161.85
158.79
145.56
136.62
128.91
128.47
127.38
116.80
77.63
77.00
76.36
62.37
24.76
N3
5a
13C NMR (50 MHz, CDCl3)
160
150
140
130
120
110
100
90
80
70
60
50
40
30

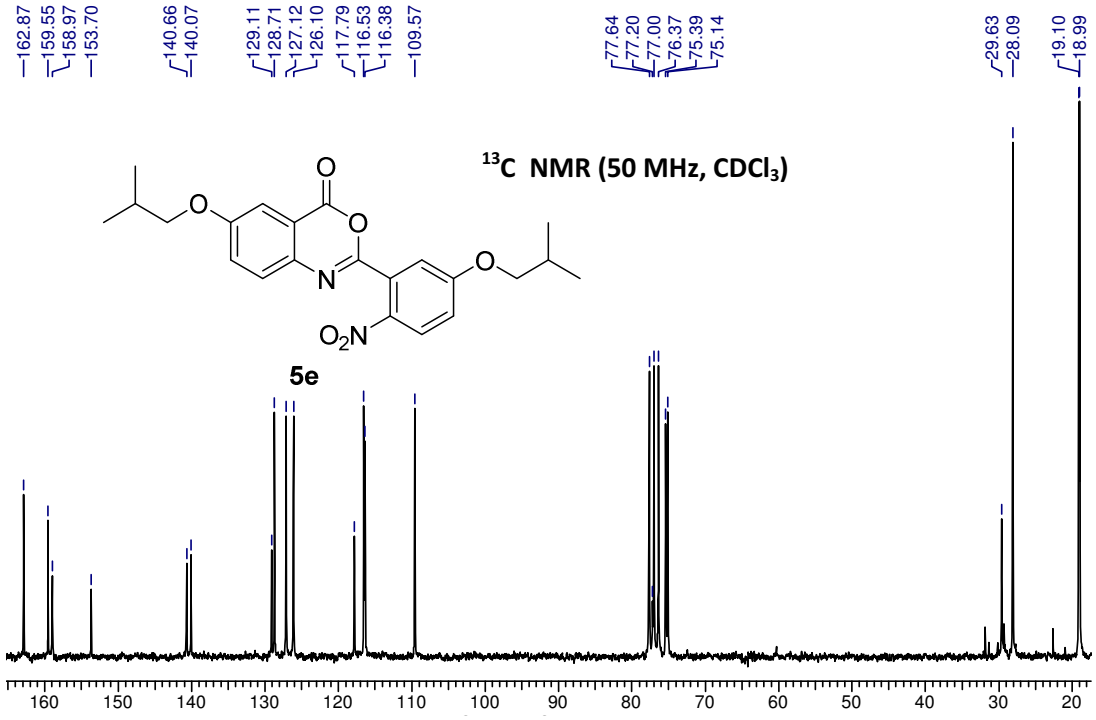
162.87
159.55
158.97
153.70
140.66
140.07
129.11
128.71
127.12
126.10
117.79
116.53
116.38
109.57
77.64
77.20
77.00
76.37
75.39
75.14
29.63
28.09
19.10
18.99
^{13}C NMR (50 MHz, CDCl$_3$)
5e
160
150
140
130
120
110
100
90
80
70
60
50
40
30
20

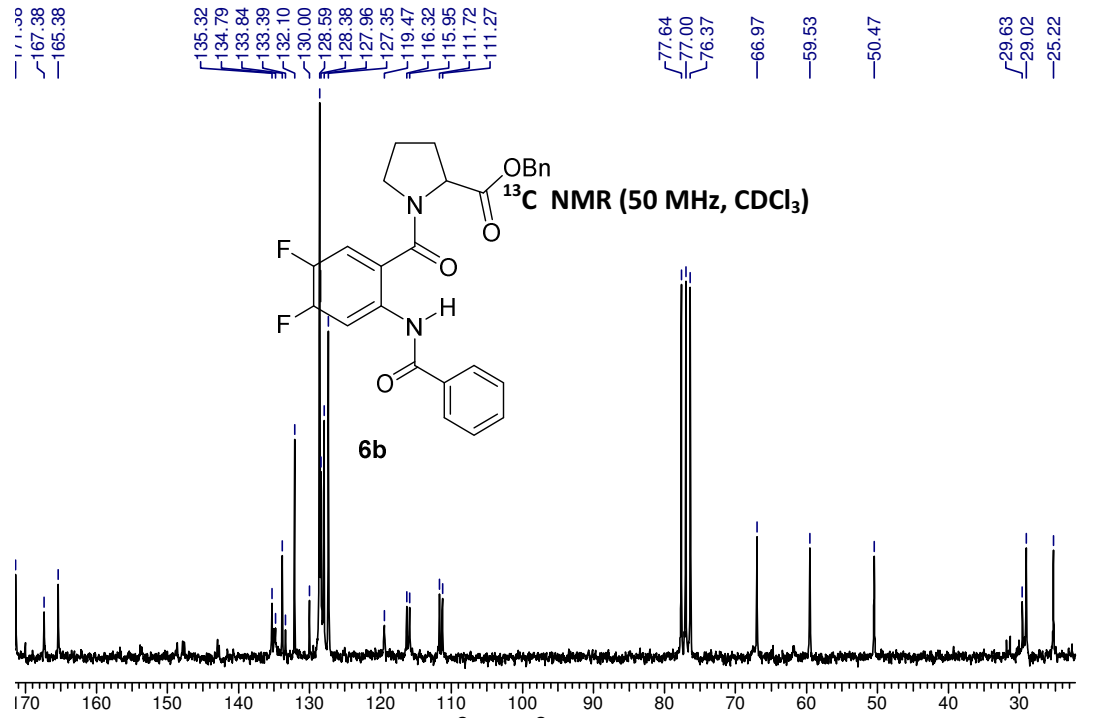
167.38
165.38
135.32
134.79
133.84
133.39
132.10
130.00
128.59
128.38
127.96
127.35
119.47
116.32
115.95
111.72
111.27
77.64
77.00
76.37
66.97
59.53
50.47
29.63
29.02
25.22
OBn
^{13}C NMR (50 MHz, CDCl$_3$)
6b
170
160
150
140
130
120
110
100
90
80
70
60
50
40
30

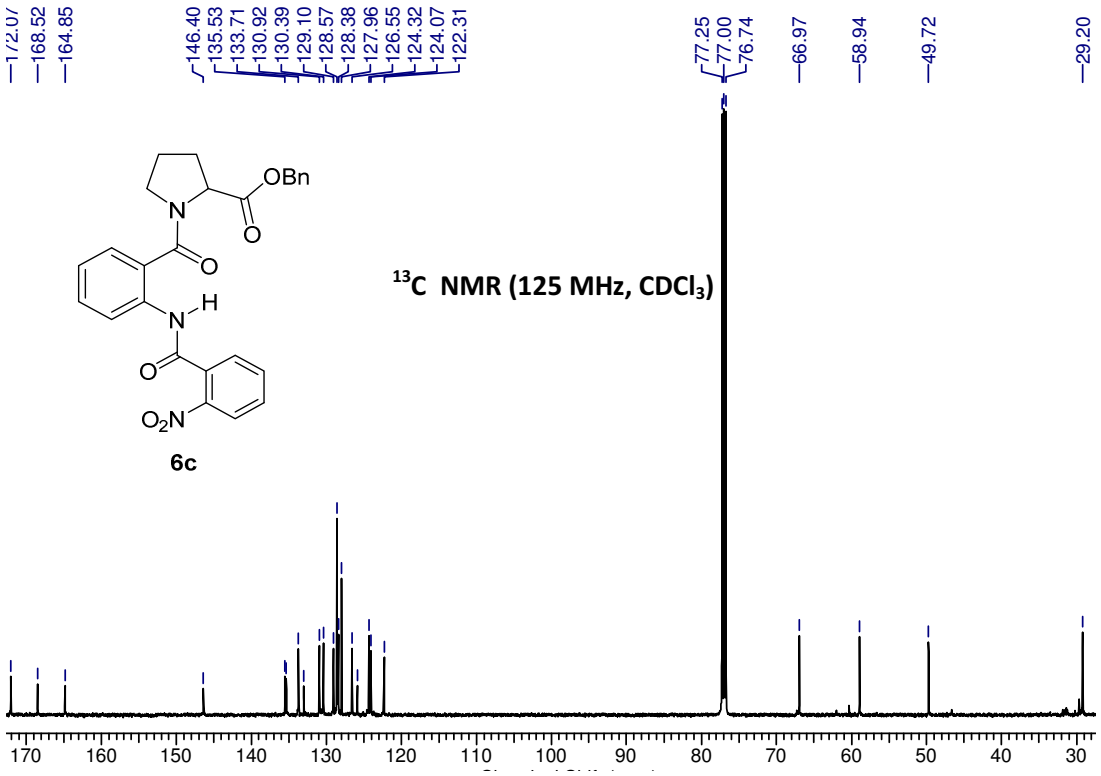
172.07
168.52
164.85
146.40
135.53
133.71
130.92
130.39
129.10
128.57
128.38
127.96
126.55
124.32
124.07
122.31
77.25
77.00
76.74
66.97
58.94
49.72
29.20
OBn
N
O
O
N
H
O
N
O2N
6c
13C NMR (125 MHz, CDCl3)
170
160
150
140
130
120
110
100
90
80
70
60
50
40
30

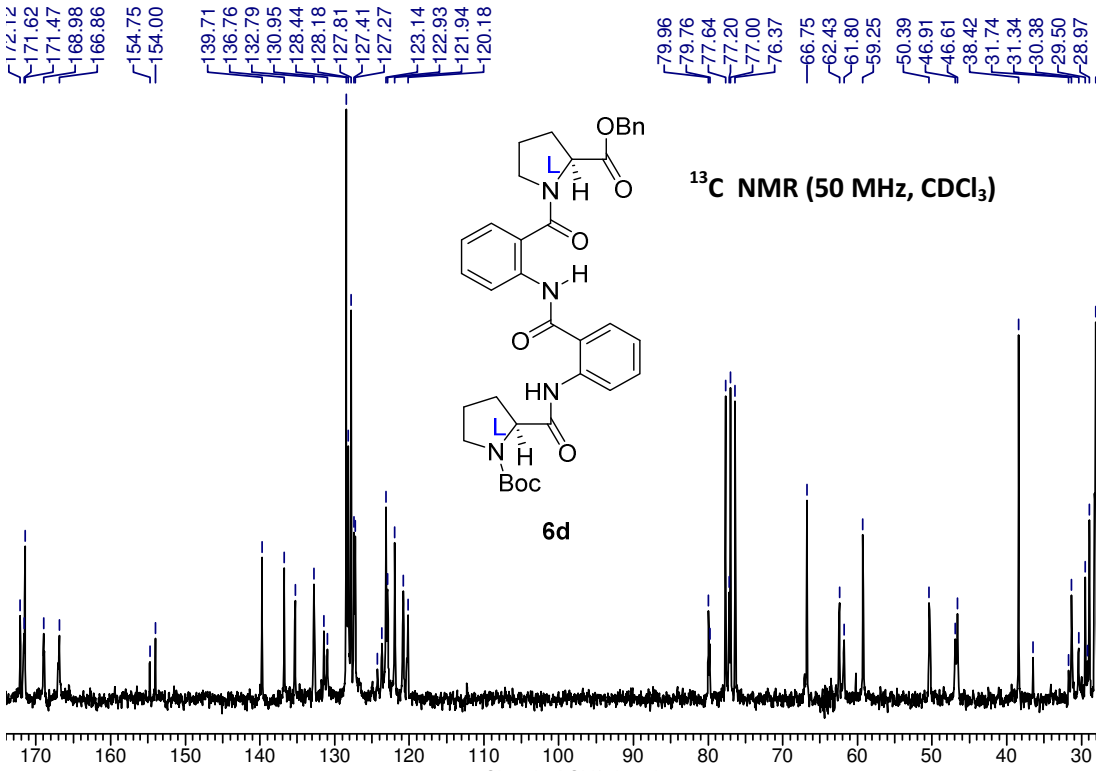
172.12
171.62
171.47
168.98
166.86
154.75
154.00
139.71
136.76
132.79
130.95
128.44
128.18
127.81
127.41
127.27
123.14
122.93
121.94
120.18
79.96
79.76
77.64
77.20
77.00
76.37
66.75
62.43
61.80
59.25
50.39
46.91
46.61
38.42
31.74
31.34
30.38
29.50
28.97
OBn
L
N H
O
O
N
H
O
HN
L
N H
O
Boc
6d
13C NMR (50 MHz, CDCl3)
170
160
150
140
130
120
110
100
90
80
70
60
50
40
30

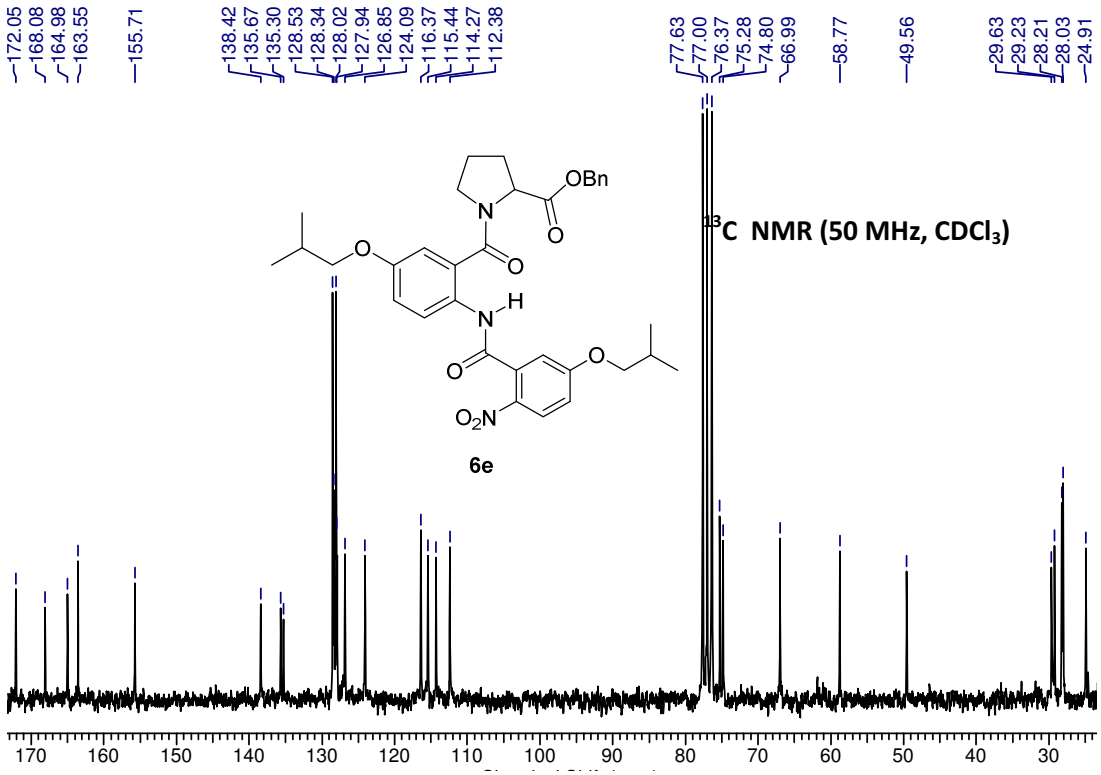
172.05
168.08
164.98
163.55
155.71
138.42
135.67
135.30
128.53
128.34
128.02
127.94
126.85
124.09
116.37
115.44
114.27
112.38
77.63
77.00
76.37
75.28
74.80
66.99
58.77
49.56
29.63
29.23
28.21
28.03
24.91
OBn
N
O
O
N
H
O
O
O
O_2N
^{13}C NMR (50 MHz, $CDCl_3$)
6e
170
160
150
140
130
120
110
100
90
80
70
60
50
40
30

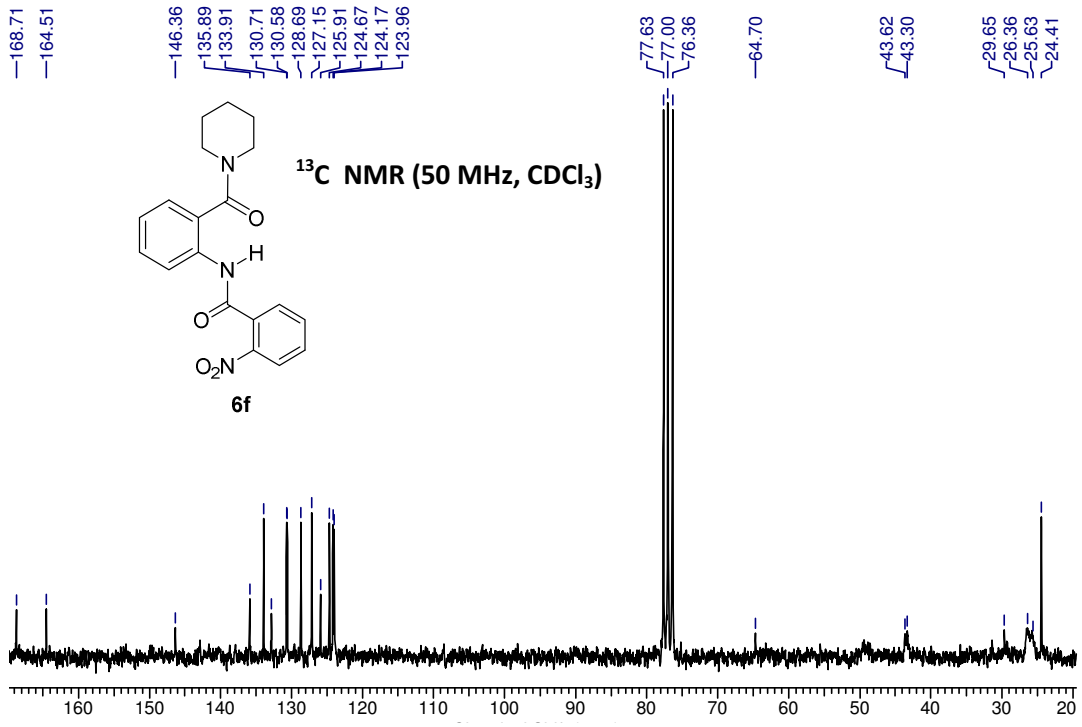
168.71
164.51
146.36
135.89
133.91
130.71
130.58
128.69
127.15
125.91
124.67
124.17
123.96
77.63
77.00
76.36
64.70
43.62
43.30
29.65
26.36
25.63
24.41
N
O
N
H
O
O_2N
^{13}C NMR (50 MHz, $CDCl_3$)
6f
160
150
140
130
120
110
100
90
80
70
60
50
40
30
20

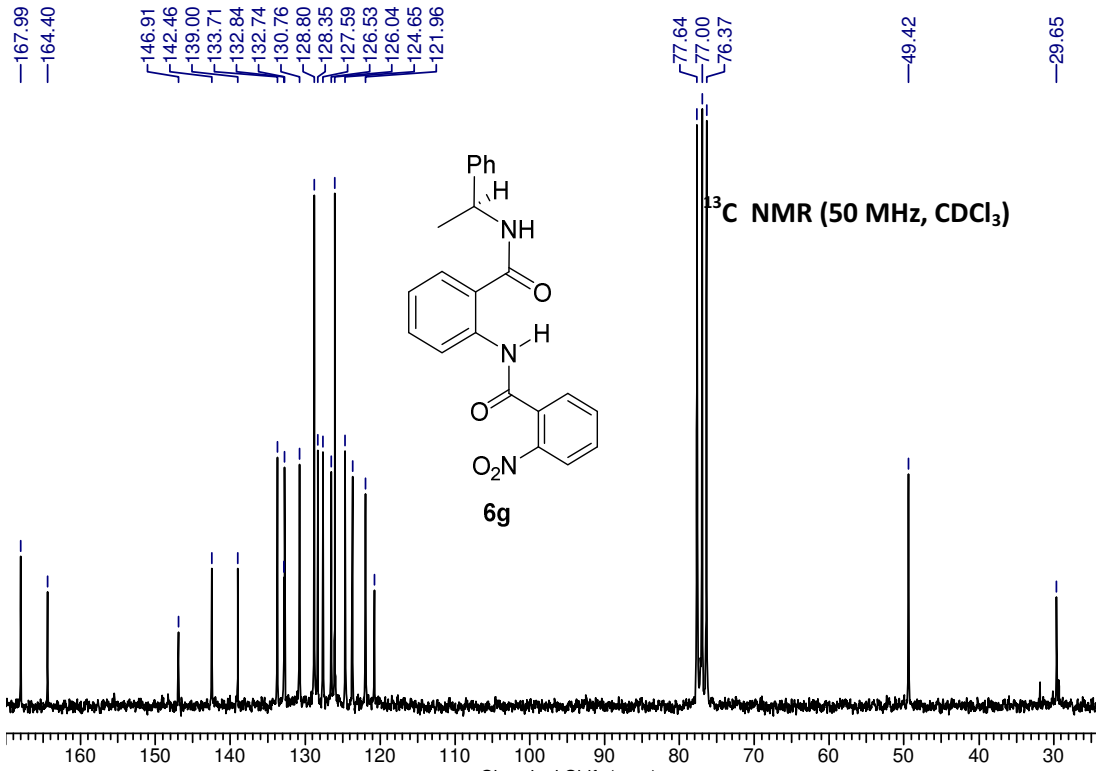
167.99
164.40
146.91
142.46
139.00
133.71
132.84
132.74
130.76
128.80
128.35
127.59
126.53
126.04
124.65
121.96
77.64
77.00
76.37
49.42
29.65
Ph
H
NH
O
H
N
O
O2N
6g
13C NMR (50 MHz, CDCl3)
160
150
140
130
120
110
100
90
80
70
60
50
40
30

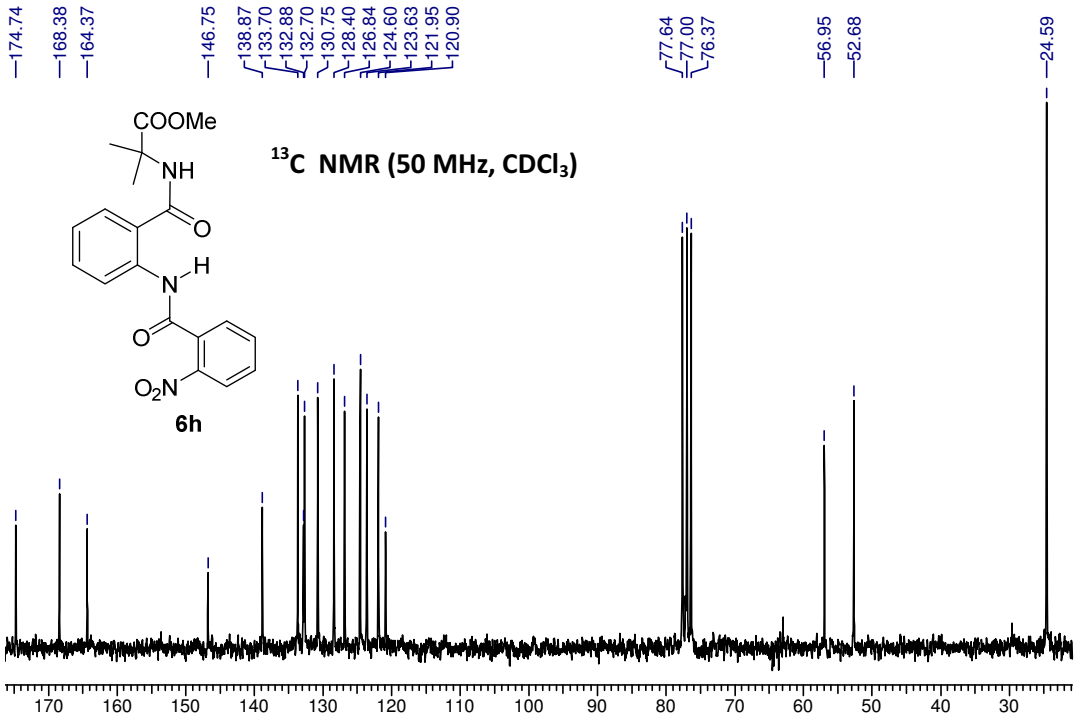
174.74
168.38
164.37
146.75
138.87
133.70
132.88
132.70
130.75
128.40
126.84
124.60
123.63
121.95
120.90
77.64
77.00
76.37
56.95
52.68
24.59
COOMe
NH
O
H
N
O
O2N
6h
13C NMR (50 MHz, CDCl3)
170
160
150
140
130
120
110
100
90
80
70
60
50
40
30

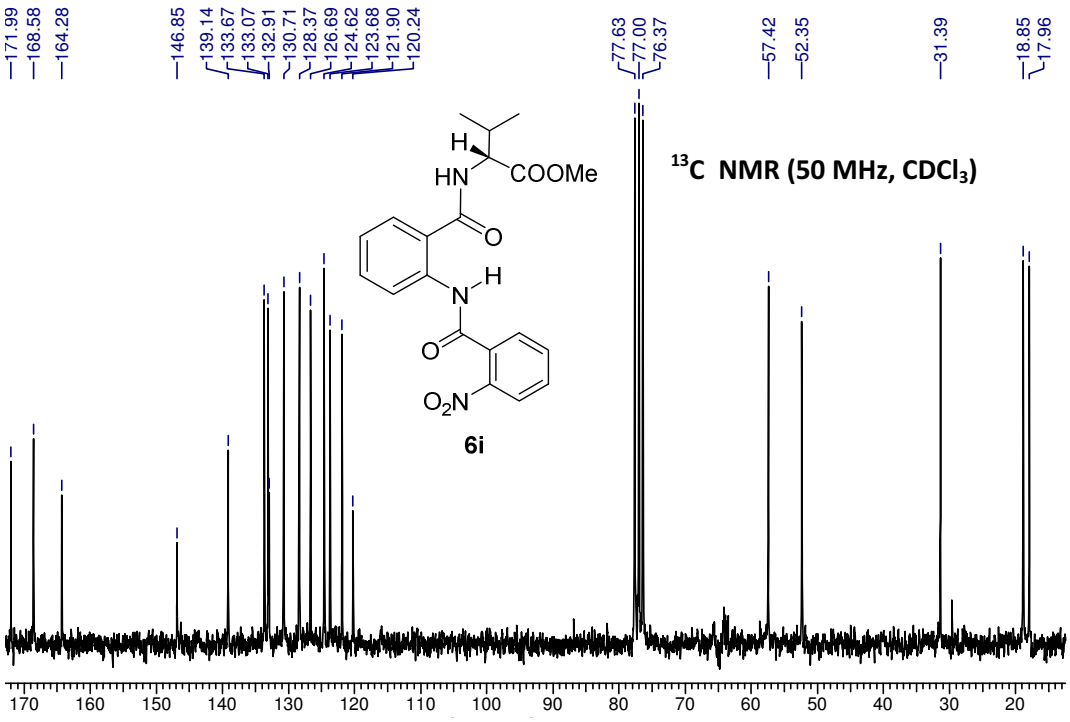
171.99
168.58
164.28
146.85
139.14
133.67
133.07
132.91
130.71
128.37
126.69
124.62
123.68
121.90
120.24
77.63
77.00
76.37
57.42
52.35
31.39
18.85
17.96
^{13}C NMR (50 MHz, CDCl$_3$)
6i
170 160 150 140 130 120 110 100 90 80 70 60 50 40 30 20

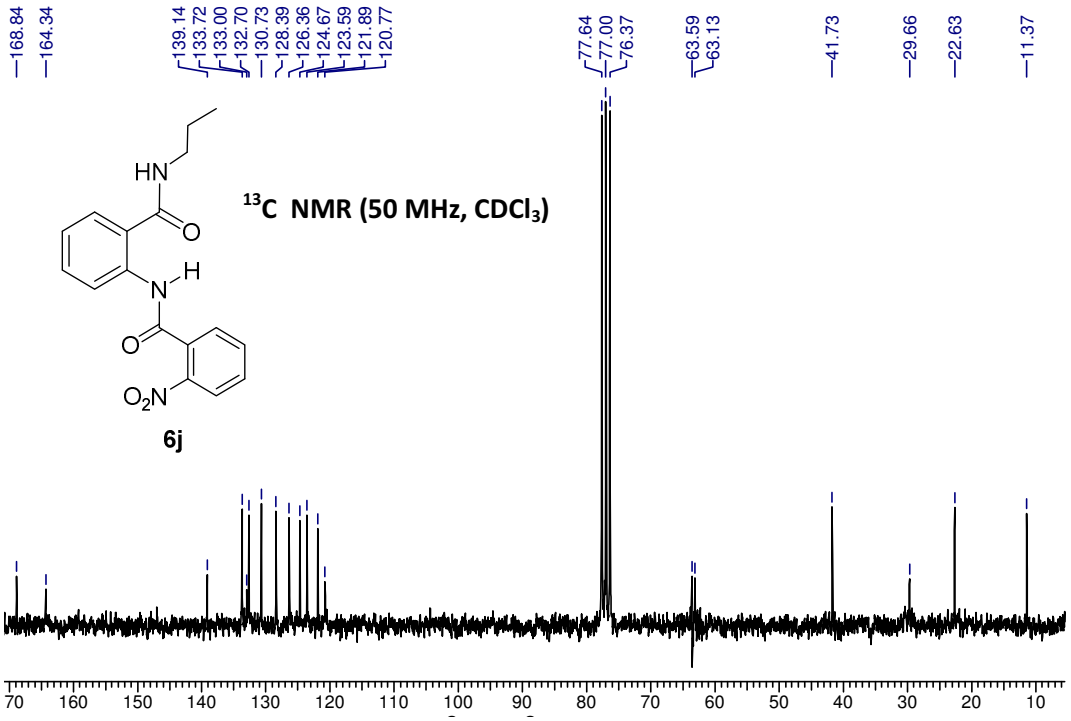
168.84
164.34
139.14
133.72
133.00
132.70
130.73
128.39
126.36
124.67
123.59
121.89
120.77
77.64
77.00
76.37
63.59
63.13
41.73
29.66
22.63
11.37
^{13}C NMR (50 MHz, CDCl$_3$)
6j
70 160 150 140 130 120 110 100 90 80 70 60 50 40 30 20 10

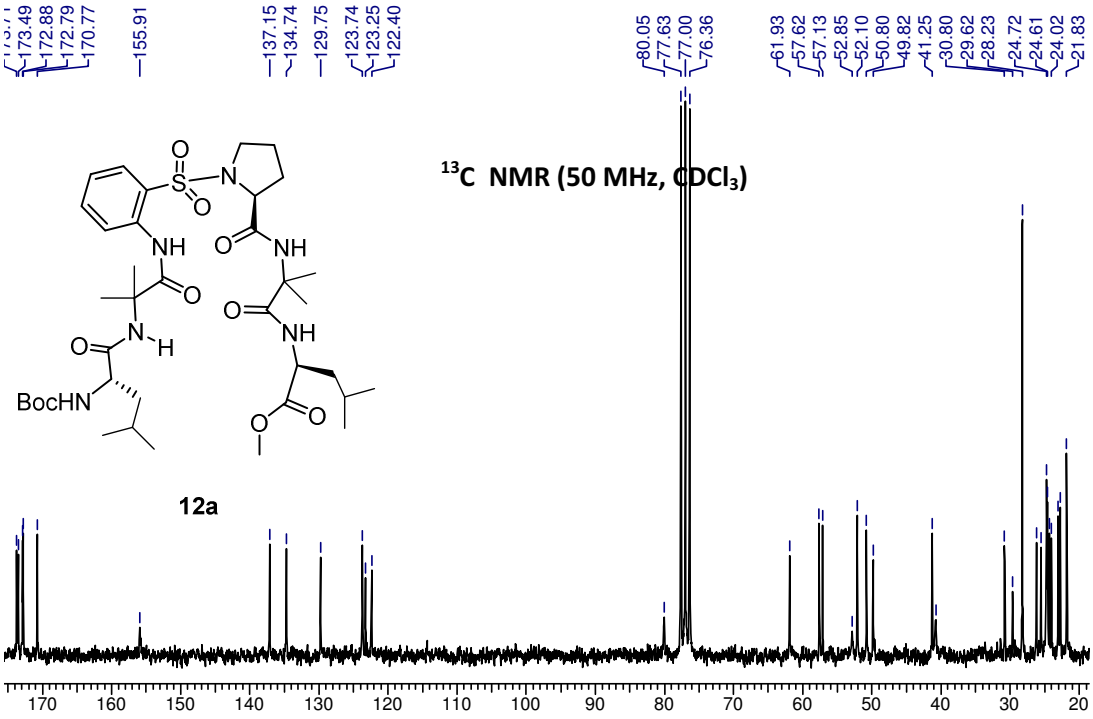
173.49
172.88
172.79
170.77
155.91
137.15
134.74
129.75
123.74
123.25
122.40
80.05
77.63
77.00
76.36
61.93
57.62
57.13
52.85
52.10
50.80
49.82
41.25
30.80
29.62
28.23
24.72
24.61
24.02
21.83
^{13}C NMR (50 MHz, CDCl$_3$)
BocHN
12a

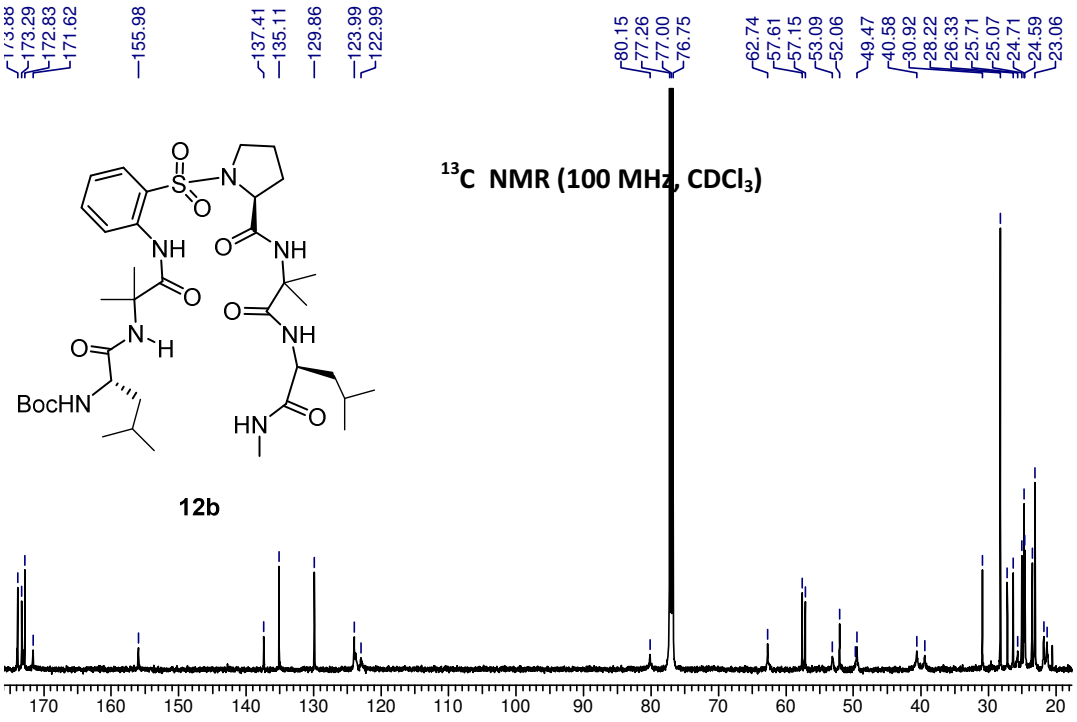
173.29
172.83
171.62
155.98
137.41
135.11
129.86
123.99
122.99
80.15
77.26
77.00
76.75
62.74
57.61
57.15
53.09
52.06
49.47
40.58
30.92
28.22
26.33
25.71
25.07
24.71
24.59
23.06
^{13}C NMR (100 MHz, CDCl$_3$)
BocHN
12b

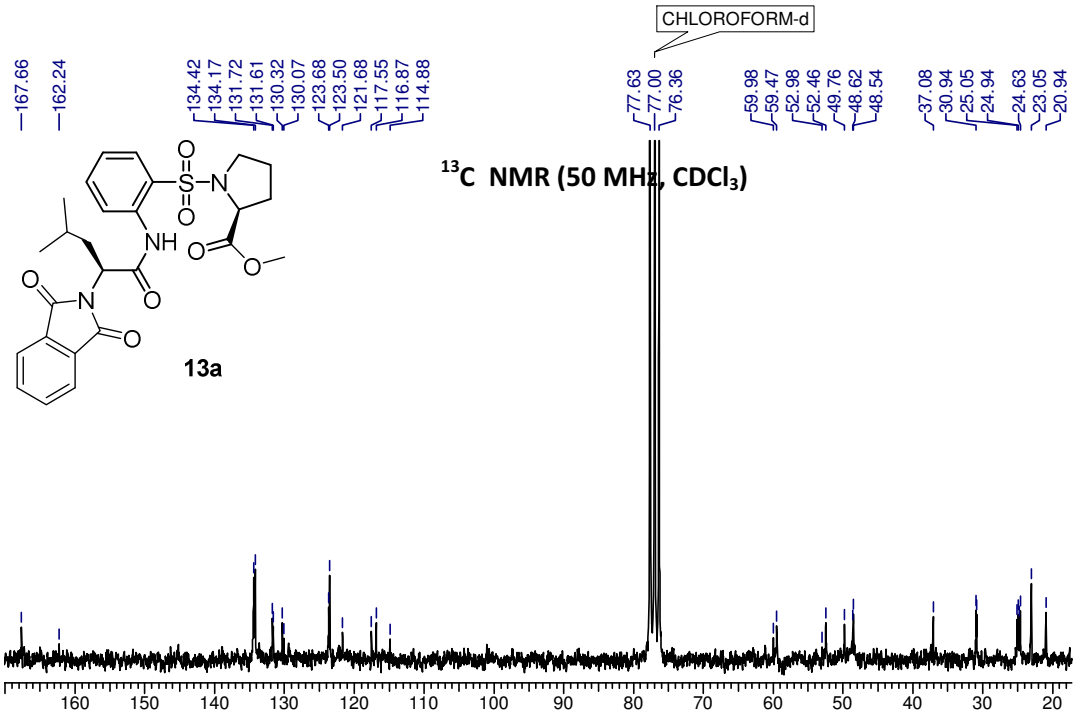
CHLOROFORM-d
167.66
162.24
134.42
134.17
131.72
131.61
130.32
130.07
123.68
123.50
121.68
117.55
116.87
114.88
77.63
77.00
76.36
59.98
59.47
52.98
52.46
49.76
48.62
48.54
37.08
30.94
25.05
24.94
24.63
23.05
20.94
^{13}C NMR (50 MHz, CDCl$_3$)
13a
160
150
140
130
120
110
100
90
80
70
60
50
40
30
20

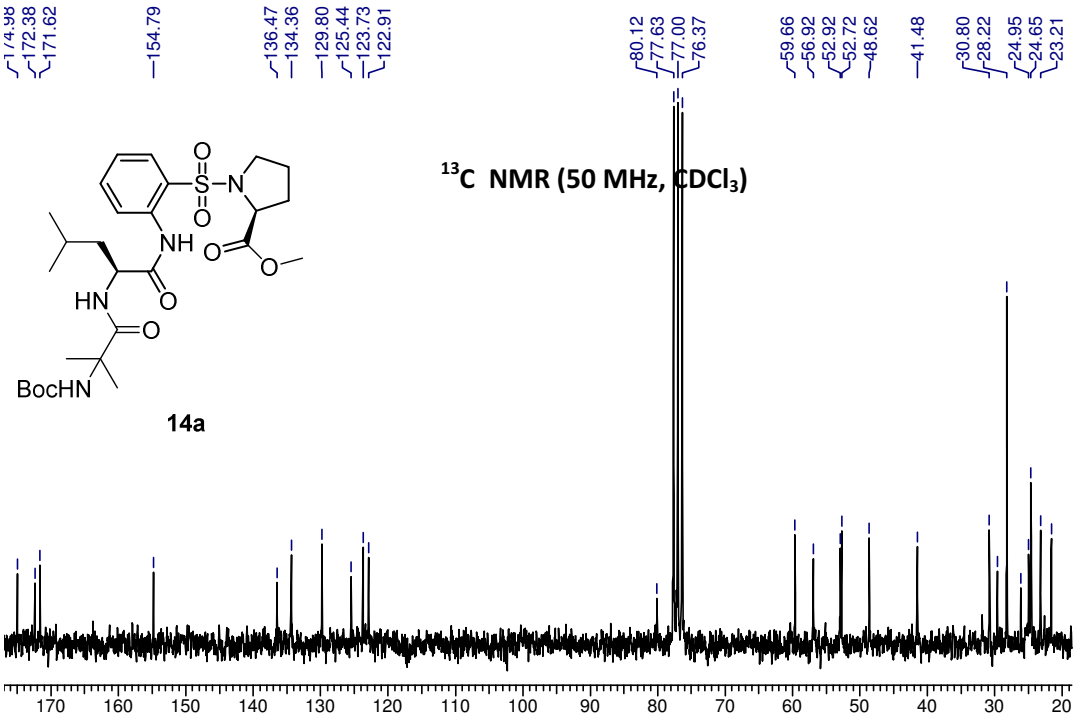
174.98
172.38
171.62
154.79
136.47
134.36
129.80
125.44
123.73
122.91
80.12
77.63
77.00
76.37
59.66
56.92
52.92
52.72
48.62
41.48
30.80
28.22
24.95
24.65
23.21
^{13}C NMR (50 MHz, CDCl$_3$)
BocHN
14a
170
160
150
140
130
120
110
100
90
80
70
60
50
40
30
20

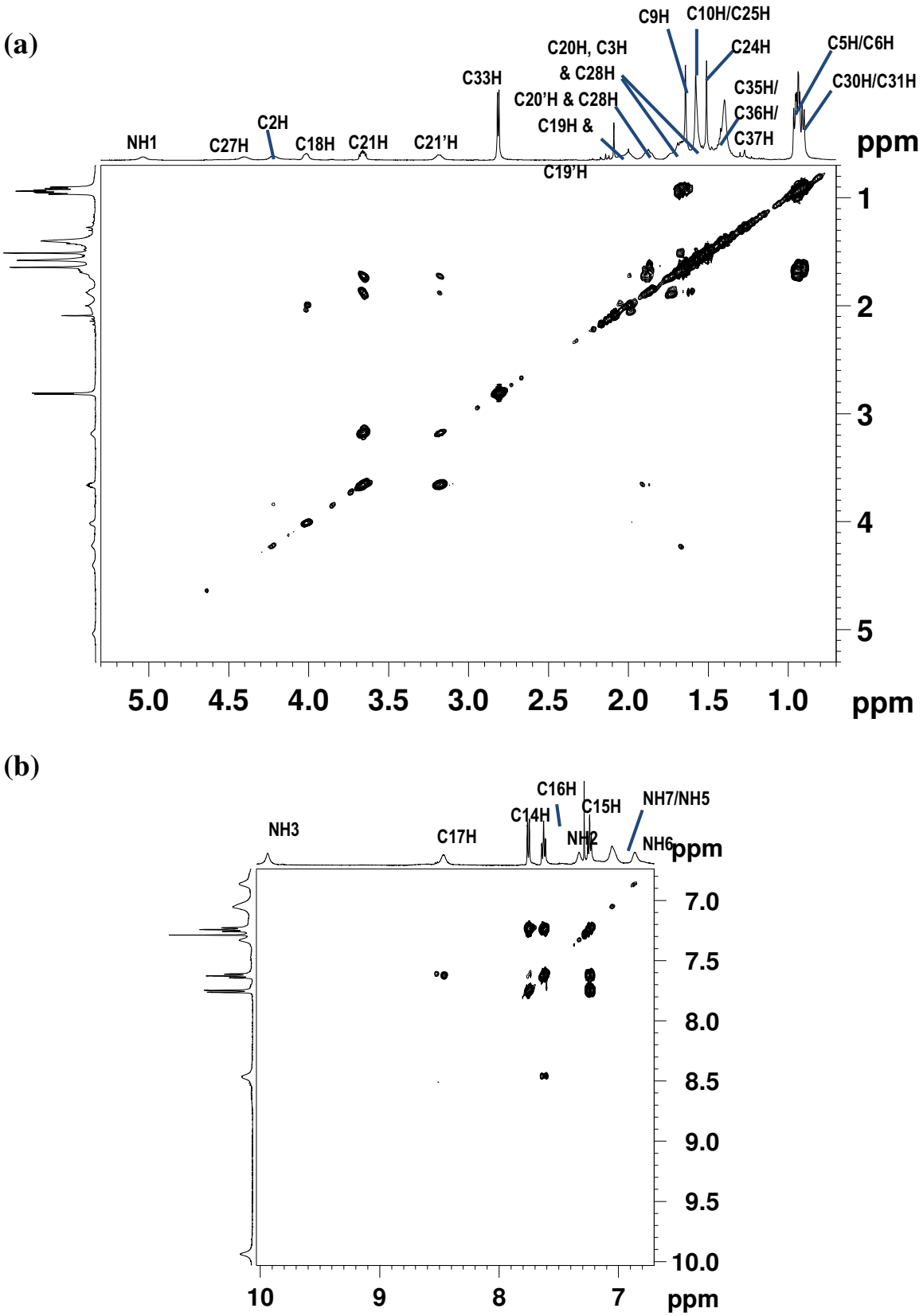

Figure 17. Partial COSY spectra of tetrapeptide **8** (500MHz, $CDCl_3$): Aliphatic **(a)** and aromatic regions **(b)**.

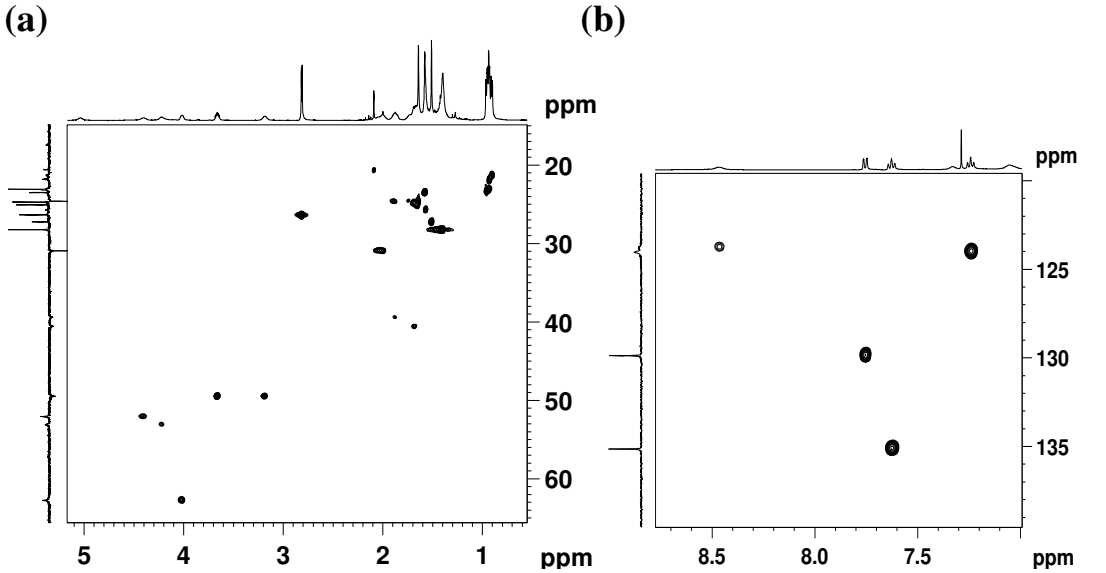

Figure 18. Partial HSQC spectra of hexapeptide **12b** (500MHz, $CDCl_3$): Aliphatic **(a)** and aromatic regions **(b)**.

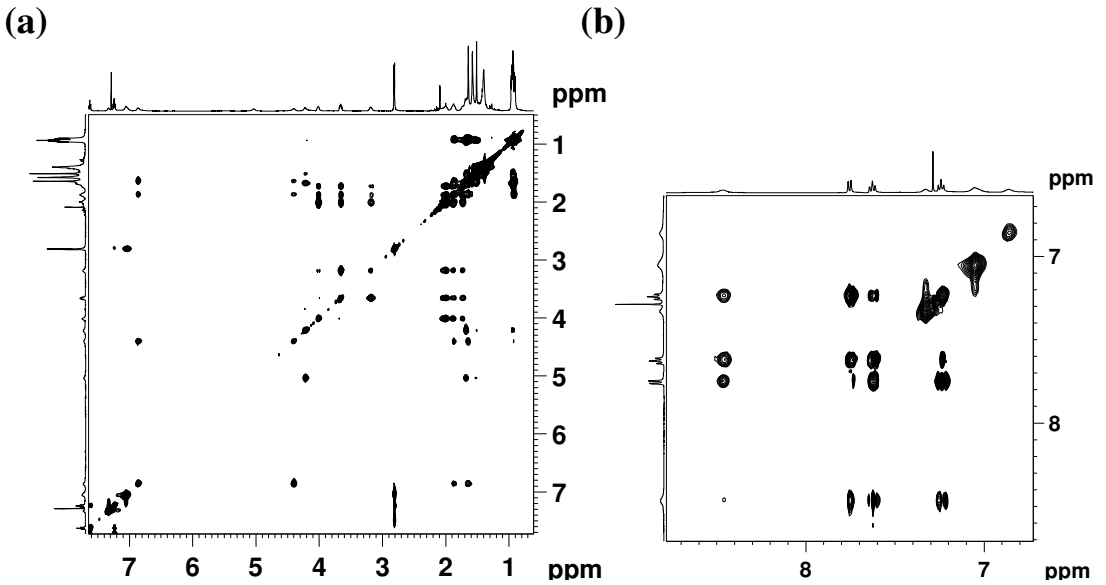

Figure 19. Partial TOCSY spectra of hexapeptide **12b** (500MHz, $CDCl_3$): Aliphatic **(a)** and aromatic regions **(b)**.

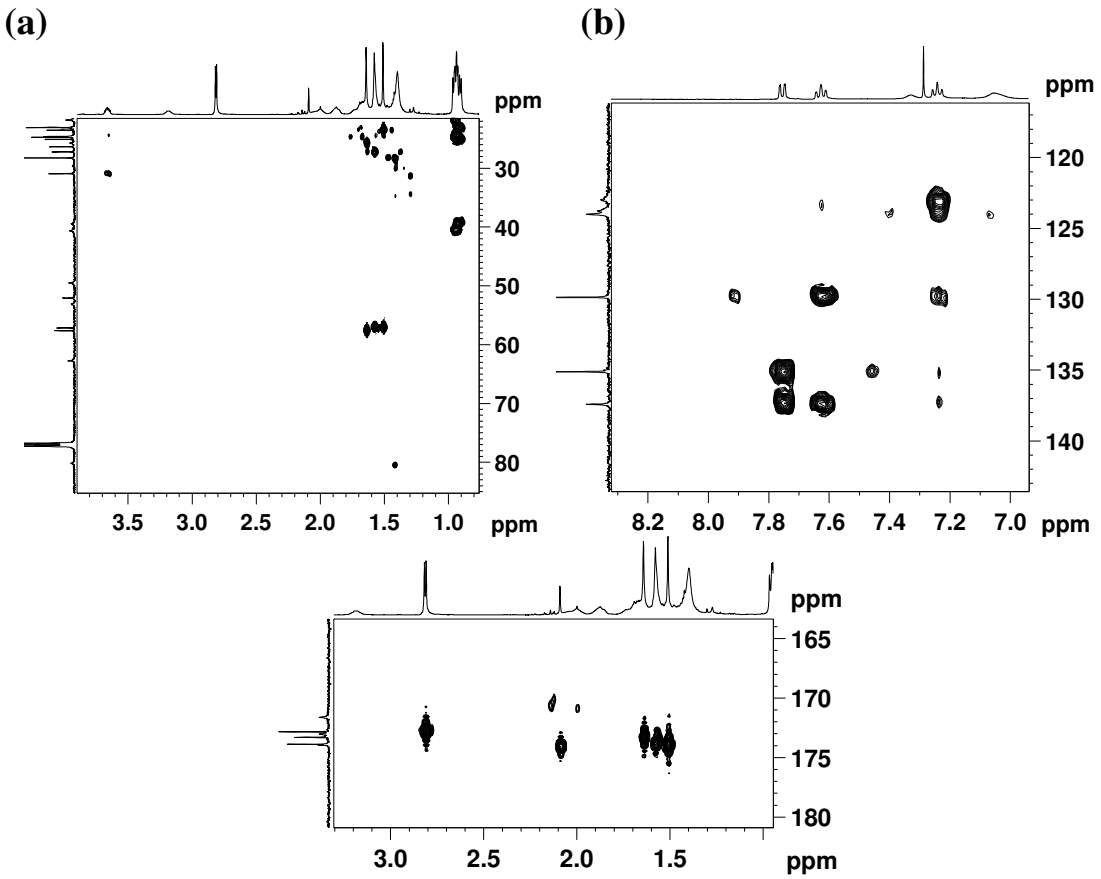

Figure 20. Partial HMBC spectra of hexapeptide **12b** (500MHz, $CDCl_3$): Aliphatic (**a**,**c**) and aromatic regions (**b**).

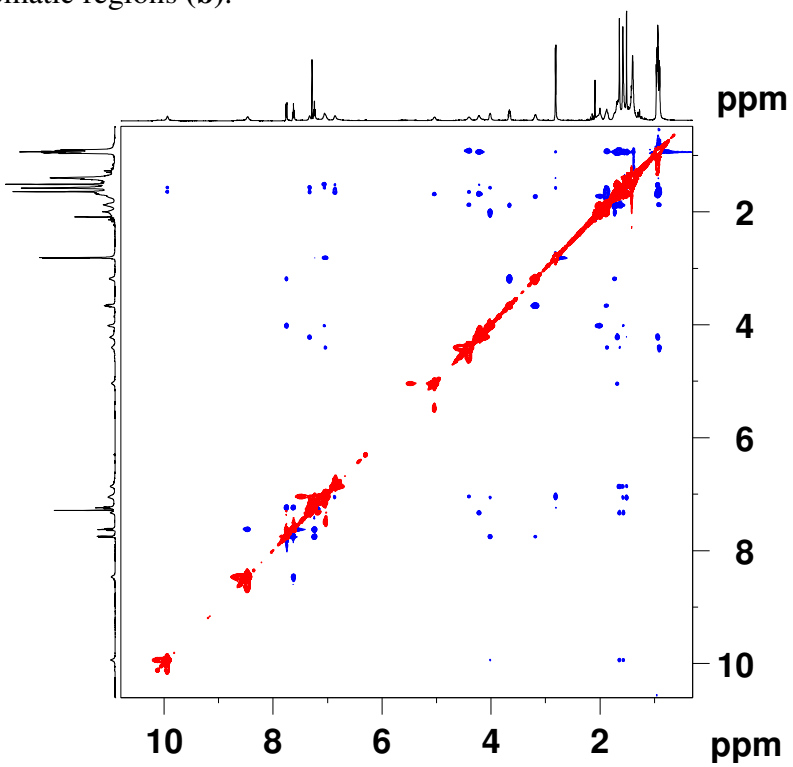

Figure 21. 2D NOESY spectrum of hexapeptide **12b** (500 MHz, $CDCl_3$).

3.23 References and Notes

(1) (a) Wood, M. J.; Hirst, J. D. *Proteins: Structure, Function, and Bioinformatics* **2005**, *59*, 476. (b) Lovell, S. C.; Word, J. M.; Richardson, J. S.; Richardson, D. C. *Proteins: Structure, Function, and Genetics* **2000**, *40*, 389.

(2) (a) Vasudev, P. G.; Chatterjee, S.; Shamala, N.; Balaram, P. *Chem. Rev.* **2011**, *111*, 657. (b) Horne, W. S.; Gellman, S. H. *Acc. Chem. Res.* **2008**, *41*, 1399. (c) Goodman, C. M.; Choi, S.; Shandler, S.; DeGrado, W. F. *Nat Chem Biol* **2007**, *3*, 252. (d) Hill, D. J.; Mio, M. J.; Prince, R. B.; Hughes, T. S.; Moore, J. S. *Chem. Rev.* **2001**, *101*, 3893.

(3) (a) Roy, A.; Prabhakaran, P.; Baruah, P. K.; Sanjayan, G. J. *Chem. Commun.* **2011**, *47*, 11593. (b) Guichard, G.; Huc, I. *Chem. Commun.* **2011**, *47*, 5933.

(4) (a) Gunasekaran, K.; Ramakrishnan, C.; Balaram, P. *J. Mol. Biol.* **1996,** 264,191. (b) Pal, D.; Chakrabarti, P. *Biopolymers* **2002,** *63*, 195. (c) Chou, P. Y.; Fasman, G. D. *Biochemistry* **1974**, *13*, 211.

(5) For more examples see chapter 1. (a) Salwiczek, M.; Nyakatura, E. K.; Gerling, U. I. M.; Ye, S.; Koksch, B. *Chem. Soc. Rev.* **2012**, *41*, 2135. (b) Szakonyi, Z.; Fülöp, F. *Amino Acids* **2011**, *41*, 597.

(6) (a) Huc, I. *Eur. J. Org. Chem.* **2004,** *35*, 17. (b) Rao, M. H. V. R.; Kumar, S. K.; Kunwar, A. C. *Tetrahedron Lett.* **2003,** *44*, 7369-7372.

(7) Zhang, W.; Moore, J. S. *Angew. Chem., Int. Ed.* **2006,** 45, 4416.

(8) Hamuro, Y.; Geib, S. J.; Hamilton, A. D. *J. Am. Chem. Soc.* **1997,** *119*, 10587.

(9) (a) Gong, B. *Acc. Chem. Res.* **2008,** *41*, 1376. (b) Prabhakaran, P.; Puranik, V. G.; Chandran, J. N.; Rajamohanan, P. R.; Hofmann, H.-J.; Sanjayan, G. J. *Org. Biomol. Chem.* **2009,** *7*, 2458.

(10) Rao, M. H. V. R.; Kumar, S. K.; Kunwar, A. C. *Tetrahedron Lett.* **2003,** *44*, 7369.

(11) (a) Yamato, K.; Kline, M.; Gong, B. *Chem. Commun.* **2012**, *48*, 12142. (b) Feng, W.; Yamato, K.; Yang, L.; Ferguson, J. S.; Zhong, L.; Zou, S.; Yuan, L.; Zeng, X. C.; Gong, B. *J. Am. Chem. Soc.* **2009**, *131*, 2629. (c) Yuan, L.; Sanford, A. R.; Feng, W.; Zhang, A.; Zhu, J.; Zeng, H.; Yamato, K.; Li, M.; Ferguson, J. S.; Gong, B. *J. Org. Chem*. **2005**, *70*, 10660.

(12) Li, Z.-T.; Hou, J.-L.; Li, C.; Yi, H.-P. *Chem. Asian J.* **2006,** 1, 766.

(13) (a) Kulikov, O. V.; Incarvito, C.; Hamilton, A. D. *Tetrahedron Lett.* **2011**, *52*, 3705. (b) Cummings, C. G.; Hamilton, A. D. *Curr. Opin. Chem. Biol.* **2010**, *14*, 341. (c) Saraogi, I.; Hamilton, A. D. *Chem. Soc. Rev.* **2009**, *38*, 1726. (d) Baruah, P. K.; Sreedevi, N. K.; Gonnade, R.; Ravindranathan, S.; Damodaran, K; Hofmann; H.-J.; Sanjayan, G. J. *J. Org. Chem*. **2007**, *72*, 636.

(14) (a) ThoŸ, M.; Seidel, R. d. W.; Feigel, M. *Tetrahedron* **2010**, *66*, 8503. (b) Prabhakaran, P.; Puranik, V. G.; Chandran, J. N.; Rajamohanan, P. R.; Hofmann, H.-J.; Sanjayan, G. J.; *Org. Biomol. Chem.*, **2009**, *7*, 2458. (c) Ramesh, V. V. E.; Roy, A.; Vijayadas, K. N.; Kendhale, A. M.; Prabhakaran, P.; Gonnade, R.; Puranik, V. G.; Sanjayan, G. J. *Org. Biomol. Chem.* **2011,** *9*, 367. (d) Srinivas,

D.; Gonnade, R.; Rajamohanan, P. R.; Sanjayan, G. J. *Tetrahedron Lett.* **2008**, *49*, 2139.

(15) Crisma, M.; Valle, G.; Bonora, G. M.; Toniolo, C.; Cavicchioni, G. *Int. J. Pept. Protein Res.* **1993,** *41*, 553.

(16) Dannecker-Dörig, I.; Linden, A.; Heimgartner, H. *Helv. Chim. Acta* **2011,** 94, 993

(17) Vasudev, P. G.; Chatterjee, S.; Shamala, N.; Balaram, P. *Chem. Rev.* **2011,** *111*, 657.

(18) (a) Böhmer, A.; Brüggemann, J.; Kaufmann, A.; Yoneva, A.; Müller, S.; Müller, W. M.; Müller, U.; Vergeer, F. W.; Chi, L.; De Cola, L.; Fuchs, H.; Chen, X.; Kubota, T.; Okamoto, Y.; Vögtle, F. *Eur. J. Org. Chem.* **2007**, 45. (b) Brüggemann, J.; Bitter, S.; Müller, S.; Müller, W. M.; Müller, U.; Maier, N. M.; Lindner, W.; Vögtle, F. *Angew. Chem. Int. Ed.* **2007,** *46*, 254. (c) Feigel, M.; Ladberg, R.; Engels, S.; Herbst-Irmer, R.; Fröhlich, R. *Angew. Chem. Int. Ed.* **2006,** *45*, 5698.

(19) Hunter, C. A.; Spitaleri, A.; Tomas, S. Tailbiter: a new amide foldamer. *Chem. Comm.* **2005**, 3691.

(20) (a) Ghosh, S.; Ramakrishnan, S. *Angew. Chem., Int. Ed.* **2004,** *43*, 3264. (b) (b) Zhang, W.; Horoszewski, D.; Decatur, J.; Nuckolls, C. *J. Am. Chem. Soc.* **2003**, *125*, 4870.

(21) Srinivas, D.; Gonnade, R.; Ravindranathan, S.; Sanjayan, G. J. *J. Org.Chem.* **2007**, *72*, 7022.

(22) Baruah, P. K.; Sreedevi, N. K.; Majumdar, B.; Pasricha, R.; Poddar, P.; Gonnade, R.; Ravindranathan, S.; Sanjayan, G. J. *Chem. Comm.* **2008**, 712.

(23) Kubik, S.; Goddard, R. *Eur. J. Org. Chem.* **2001,** *43*, 311.

(24) Akazome, M.; Enzu, M.; Takagi, K.; Matsumoto, S. *Chirality* **2011,** 23, 568.

(25) (a) Prabhakaran, P.; Kale, S. S.; Puranik, V. G.; Rajamohanan, P. R.; Chetina, O.; Howard, J. A. K.; Hofmann, H.-J.; Sanjayan, G. J. *J. Am. Chem. Soc.* **2008**, *130*, 17743. (b) Kale, S. S.; Kotmale, A. S.; Dutta, A. K.; Pal, S.; Rajamohanan, P. R.; Sanjayan, G. J. *Org. Biomol. Chem.* **2012**, *10*, 8426.

(26) Hamuro, Y.; Geib, S. J.; Hamilton, A. D. *J. Am. Chem. Soc*. **1996**, *118*, 7529.

(27) (a) Pysh, E. S.; Toniolo, C. *J. Am. Chem. Soc.* **1977**, *99*, 6211. (b) Meraldi, J. P.; Hruby, V. J. *J. Am. Chem. Soc.* **1976**, *98*, 6408. (c) Higashijima, T., Tasumi, M., Miyazawa, T. & Miyoshi, M. *Eur. J. Biochem.* **1978**, *89*, 543.

(28) (a) Iqbal, M.; Balaram, P. *Biopolymers* **1982**, *21*, 1427. (b) Iqbal, M.; Balaram, P. *Biochemistry* **1981**, *20*, 7278. (c) Venkataram Prasad, B. V.; Balaram, P. *Critical Reviews in Biochemistry* **1984**, *16*, 307.

(29) Han, S-Y.; Kim, Y-A. *Tetrahedron* **2004**, *60*, 2447.

(30) (a) El Rayes, S. M.; Ali, I. A. I.; Fathalla, W., ARKIVOC **2008**, *9*, 86. (b) Ref. 26.

(31) Errede, L. A.; Oien, H. T.; Yarian D. R., *J . Org. Chem.* **1977***, 42,* 12-18.

(32) (a) Errede, L. A.; McBrady, J. J.; Oien, H. T. *J . Org. Chem.* **1977***, 42,* 656. (b) Errede, L. A.; McBrady, J. J. *J. Org. Chem.* **1977***, 42,* 3863. (c) Errede, L. A. *J . Org. Chem.* **1978***, 43,* 1880.

(33) (a) Madkour, H.M.F., ARKIVOC **2004**, *1*, 36. (b) Yee, Y. K.;. Tebbe, A. L.; Linebarger, J. H.; Beight, D. W.; Craft, T. J.; Moore, D. G-; Goodson, Jr. T.; Herron, D. K.; Klimkowski, V. J.; Kyle, J.A.; Sawyer, J. S.; Smith, G. F.; Tinsley, J. M.; Towner, R. D.; Weir, L.; Wiley, M.R. *J. Med. Chem.* **2000,** *43,* 873. (c) Habib, O. M. O.; Hassan, H. M.; El-Mekabaty, A., *Am. J. Org. Chem.* **2012**, *2(3),* 45. (d) El-Hashash, M. A.; Rizk, S. A.; El-Bassiouny, F. A. *Chem. Proc. Eng. Res.* **2012**, *2*, 17. (e) Shibaa, S. A.; Madkoura, H. M. F.; Hamed, A. A.; Sayed H. M.; and Maher Abd El-aziz El-Hashash, *Eur. J. Chem*. **2011,** *2*, 200.

(34) (a) Lohmeijer, B. G. G.; Pratt, R. C.; Leibfarth, F.; Logan, J. W.; Long, D. A.; Dove, A. P.; Nederberg, F.; Choi, J.; Wade, C.; Waymouth, R. M.; Hedrick, J. L. *Macromolecules* **2006,** *39,* 8574. (b) Ramesh, V. V. E.; Priya, G.; Kotmale, A. S.; Gonnade, R. G.; Rajamohanan, P. R.; Sanjayan, G. J. *Chem. Commun.* **2012**, *48*, 11205.

(35) For selected reviews on thiourea in organocatalysis, see:
(a) Bernardi, L.; Fochi,M.; Franchini, M. C.; Ricci, A *Org. Biomol. Chem.* **2012**, *10*, 2911. (b) Schreiner, P. R. *Chem. Soc. Rev.* **2003**, *32*, 289. (c) Pihko, P. M. *Angew. Chem., Int. Ed.* **2004**, *43*, 2062. (d) Taylor M. S.; Jacobsen, E. N. *Angew. Chem., Int. Ed.* **2006**, *45*, 1520.

For lucid description of development in thiourea organocatalysis, refer:
Kotke M. Hydrogen-bonding (thio)urea organocatalysts in organic synthesis: State of the art and practical methods for acetalization, tetrahydropyranylation, and cooperative epoxide alcoholysis. *PhD Thesis*, University Giessen, Germany, **2009**, available online *via* the Electronic Library.

(36) Lippert, K. M.; Hof, K.; Gerbig, D.; Ley, D.; Hausmann, H.; Guenther, S.; Schreiner, P. R. *Eur. J. Org. Chem.* **2013**, 5919.

(37) (a) Weil, T.; Kotke, M.; Kleiner, C. M.; Schreiner, P. R. *Org. Lett.* **2008**, *10*, 1513. (b) Kotke, M.; Schreiner, P. R. *Synthesis* **2007**, *5*, 779. (c) Kotke, M.; Schreiner, P. R. *Tetrahedron* **2006***, 62*, 434. (d) Zuend, S. J.; Jacobsen, E. N. *J Am Chem Soc*. **2009** *131*, 15358.

(38) Kleiner C. M.; Schreiner P. R. *Chem. Comm.* **2006**, 4315.

(39) (a) Zhang, Z.; Lippert, K. M.; Hausmann, H.; Kotke, M.; Schreiner, P. R. *J. Org. Chem*. **2011**, *76*, 9764. (b) Reisman, S. E.; Doyle, A. G.; Jacobsen, E. N. *J. Am. Chem. Soc.* **2008**, *130*, 7198. (c) Gaunt, M. J.; Johansson, C. C. C.; McNally, A. Vo, N. T. *Drug Discovery Today* **2007**, *12*, 8. (d) Herrera, R. P.; Sgarzani, V.; Bernardi, L.; Ricci, A. *Angew. Chem., Int. Ed.* **2005**, *44*, 6576. (e) Okino, T.; Hoashi, Y.; Takemoto, Y. *J. Am. Chem. Soc*. **2003**, *125*, 12672. (f) M. S. Sigman, E. N. Jacobsen, *J. Am. Chem. Soc.* **1998**, *120*, 4901.

(40) (a) Wang, J.; Li, H.; Yu, X.; Zu, L.; Wang, W. *Org. Lett.* **2005**, *7*, 4293. (b) Sohtome, Y.; Tanatani, A.; Hashimoto, Y.; Nagasawa, K. *Tetrahedron Lett.* **2004**, *45*, 5589.

(41) (a) Curran, D. P.; Kuo, L. H. *Tetrahedron Lett.* **1995**, *36*, 6647. (b) Wittkopp, A. *Diploma Thesis*, University Göttingen, Germany, **1997**. (c) Gómez, D. E.; Fabbrizzi, L.; Licchelli, M.; Monzani, E. *Org. Biomol. Chem.* **2005**, *3*, 1495. (d) Blanco, J. L. J.; Bootello, P.; Benito, J. M.; Mellet, C. O.; Fernández, J. M. G. *J. Org. Chem.* **2006**, *71*, 5136. (e) Evans, D. A.; Chapman, K. T.; Bisaha, J. *J. Am. Chem. Soc.* **1984**, *106*, 4261. (f) Wittkopp, A. *PhD Thesis*, University Göttingen, Germany, **2001**, published online. (g) Schreiner, P. R. *Chem. Soc. Rev.* **2003**, *32*, 289.

(42) (a) Enders, D.; Urbanietz, G.; Hahn, R.; Raabe, G. *Synthesis* **2012**, *44*, 773. (b) Wang, W.-H.; Abe, T.; Wang, X.-B.; Kodama, K.; Hirose, T.; Zhang, G.-Y. *Tetrahedron: Asymmetry* **2010**, *21*, 2925. (c) Miyabe, H.; Tuchida, S.; Yamauchi, M.; Takemoto, Y. *Synthesis* **2006**, *19*, 3295. (d) Cao, C.-L.; Ye, M.-C.; Sun, X.-L.; Tang, Y. *Org. Lett.* **2006**, *8*, 2901. (e) Vakulya, B.; Varga, S.; Csàmpai, A.; Soós, T. *Org. Lett.* **2005**, *7*, 1967.

(43) (a) Wende, R.C.; Schreiner, P. R. *Green Chem.,* **2012**, *14*, 1821. (b) Takemoto, Y. *Org. Biomol. Chem*., **2005**, *3*, 4299. (c) Kotke, M.; Schreiner, P. R. in *Hydrogen Bonding in Organic Synthesis, ed. P. M. Pihko, Wiley-VCH, Weinheim*, **2009**, 141. (d) Connon, S. J. *Synlett* **2009**, 354. (e) Connon, S. J. *Chem. Commun*. **2008**, 2499. (f) Anastas, P. T.; Kirchhoff, M. M. *Acc. Chem. Res.*, **2002**, *35*, 686.

(44) (a) Berkessel, A.; Jurkiewicz, I., Mohan, R. *Chem. Cat. Chem.* **2011**, *3*, 319. (b) De, C. K.; Klauber, E. G.; Seidel, D. *J. Am. Chem. Soc.* **2009**, *131*, 17060. (c) Akiyama, T.; Itoh, J.; Fuchibe, K. *Adv. Synth. Catal.* **2006**, *348*, 999.

(45) A. A. Laeva, E. V. Nosova, G. N. Lipunova, A. V. Golovchenko, N. Yu. Adonin, V. N. Parmon, and V. N. Charushin. *Russ. J. Org. Chem.* **2009***, 45,* 913.

(46) El-Hamdouni, N.; Company, X.; Rios, R.; Moyano, A. *Chem. Eur. J.* **2010**, *16*, 1142.

(47) Errede, L. A.; Tiers, G. V. D. *J. Org. Chem.* **1978***, 43,* 1887.

(48) (a) J. L. Radkiewicz, M. A. McAllister, E. Goldstein and K. N. Houk, *J. Org. Chem.,* **1998**, *63,* 1419. (b) J. M. Langenhan, J. D. Fisk and S. H. Gellman, *Org. Lett.,* **2001,** *3,* 2559.

(49) (a) A.W. Hung, H. L. Silvestre, S. Wen, A. Ciulli, T. L. Blundell and C. Abell, *Angew. Chem. Int. Ed.,* **2009**, *48*, 8452. (b) M. G. Natchus et al., *J. Med. Chem.,* 2000**, 43***,* 4948. (c) J. Brouwer and R. M. J. Liskamp, *J. Org. Chem.* **2004**, *69*, 3662. (d) S. Turcotte, S. H. B. Gervais and W. D. Lubell, *Org. Lett.,* **2012**, *14*, 1318; (e) C. Giordano, G. Lucente, A. Masil, M. P. Paradisi, A. Sansone and S. Spisani, *Amino Acids*, **2007**, *33*, 477.

(50) Vijayadas, K. N.; Davis, H. C.; Kotmale, A. S.; Gawade, R. L.; Puranik, V. G.; Rajamohanan, P. R.; Sanjayan, G. J. *Chem. Commun.* **2012,** *48*, 9747.

(51) Kale, S. S.; Priya, G.; Kotmale, A. S.; Gawade, R. L.; Puranik, V. G.; Rajamohanan, P. R.; Sanjayan, G. J. **2013,** *49*, 2222.

(52) Ramesh, V. V. E.; Kale, S. S.; Kotmale, A. S.; Gawade, R. L.; Puranik, V. G.; Rajamohanan, P. R.; Sanjayan, G. J. *Org. Lett.* **2013,** *15*, 1504.